ACTA CHIMICA

ACADEMIAE SCIENTIARUM HUNGARICAE

TOMUS 109 FASCICULUS 1

AKADÉMIAI KIADÓ, BUDAPEST

1982

ACTA CHIM. ACAD. SCI. HUNG. ACASA2 109 (1) 1—110 (1982)

ACTA CHIMICA

A MAGYAR TUDOMÁNYOS AKADÉMIA KÉMIAI TUDOMÁNYOK OSZTÁLYÁNAK IDEGEN NYELVŰ KÖZLEMÉNYEI

Acta Chimica is a journal for the publication of papers on all aspects of chemistry in English, German, French and Russian.

Acta Chimica is published in 3 volumes per year. Each volume consists of 4 issues of varying size.

Manuscripts should be sent to

Acta Chimica
Budapest, P.O. Box 67, H-1450, Hungary

Correspondence with the editors should be sent to the same address. Manuscripts are not returned to the authors.

Hungarian subscribers should order from Akadémiai Kiadó, 1363 Budapest, P.O. Box 24. Account No. 215 11488.

Orders from other countries are to be sent to "Kultura" Foreign Trading Company (H-1389 Budapest 62, P.O. Box 149. Account No. 218 10990) or its representatives abroad.

ACTA CHIMICA

ACADEMIAE SCIENTIARUM HUNGARICAE

TOMUS 109

AKADÉMIAI KIADÓ, BUDAPEST

1982

ACTA CHIM. ACAD. SCI. HUNG.

ACTA CHIMICA

TOMUS 109

Fasciculus 1
Fasciculus 2
Fasciculus 3
Fasciculus 4

INDEX

Acta Chimica Academiae Scientiarum Hungaricae, Tomus 109 (1), pp. 1—3 (1982)

A NOVEL PHOTOCHEMICAL RING CONTRACTION IN THE DIHYDRO-1,2,4-TRIAZINE SERIES

(PRELIMINARY COMMUNICATION)

J. NAGY and J. NYITRAI*

(Department of Organic Chemistry, Technical University, Budapest)

Received September 30, 1981

Accepted for publication October 22, 1981

The di-π-methane and oxa-di-π-methane rearrangements have been thoroughly investigated in various systems including homocyclic compounds [1]. This type of photoreaction has, except in one case [2], not been observed in systems containing carbon-nitrogen double bonds. Therefore we intended to synthesize some six-membered *N*-heterocycles containing the aza-di-π-methane structure and to study their photochemical behavior.

First some 2,5(4,5)-dihydro-1,2,4-triazines (**1**—**3**) were synthesized by slight modification of published methods [3]. Compound **1** may theoretically exist in two annular tautomeric forms, **1a** and **1b**. According to the UV spectra of compounds **1**—**3**, the cross conjugated **1a**, which contains the aza-di-π-methane partial structure, is the predominant tautomeric form.

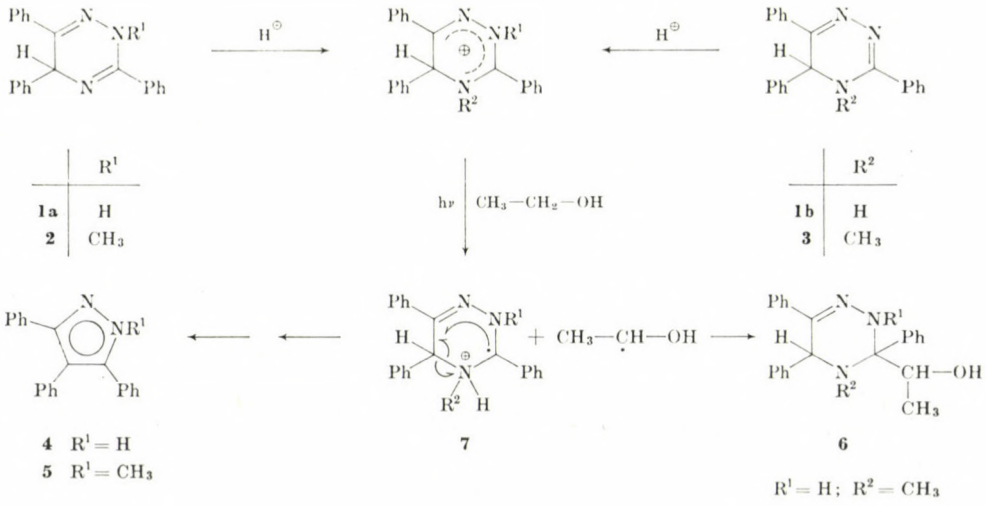

* To whom correspondence should be addressed

Compound **1** in ethanolic solution was insensitive to irradiation by a medium pressure mercury lamp (Philips, HPK, 125) through Pyrex. Since energy dissipation of the trivalent nitrogen atom was considered one possible reason for the photoinactivity of compound **1**, the monoprotonated conjugated acid of the latter (prepared by reaction with one equivalent of hydrogen chloride) was irradiated under similar conditions. The conjugated acid proved to be photoactive, and on irradiation it gave 3,4,5-triphenylpyrazole (**4**) as the main product in 25% yield; *i.e.* a novel photochemical ring contraction took place rather than an aza-di-π-methane rearrangement.

The protonated forms of compounds **2** and **3** have also been irradiated in ethanol, whereupon compounds **5** (yield: 30%) and **4**, (yield: 12%), respectively, were isolated; *i.e.* the nitrogen atom from position **4** of the 1,2,4-triazine ring was expelled.

Authentic **4** and **5** were prepared;by the method described in the literature [4].

A second product (**6**) was also obtained from the irradiation mixture of monoprotonated **3** in 21% yield besides of the expected pyrazol (**4**). It is suggested that **4** and **6** are formed *via* the same intermediate (**7**) which may become stabilized either by ring contraction or by photoaddition.

All new compounds described here gave satisfactory microanalyses. Their various spectra were in agreement with the assumed structures:

(*a*) UV spectra in ethanol [λ_{max} (log ε)]: **1**: 241 (4.34), 317 (3.85); **2**: 232 (4.30), 318 (3.89); **3**: 245 (4.05), 339 (3.86).

(*b*) ^{1}H—NMR spectra (δ, TMS): **1** (DMSO—d_6): 6.0 (s, 1, C*H*), 7.2—8.0 (m, 15, Ar*H*); **2** ($CDCl_3$): 3.35 (s, 3, N—CH_3), 5.94 (s, 1, C*H*), 7.1—8.0 (m, 15, Ar*H*); **3** ($CDCl_3$): 3.07 (s, 3, N—CH_3), 5.23 (s, 1, C*H*), 7.16—8.02 (m, 15, Ar*H*); **4** (DMSO—d_6): 7.3 (m, 15, Ar*H*); **5** ($CDCl_3$): 3.87 (s, 3, NCH_3), 6.9—7.5 (m, 15, Ar*H*); **6** (DMSO—d_6): 1.21 (d, 3, CH_3—CH), 2.54 (s, 3, N—CH_3), 4.1—4.3 (m, 1, CH_3—C*H*—OH), 4.87 (s, 1, C*H*), 6.9—7.5 (m, 15, Ar*H*).

(*c*) ^{13}C—NMR spectra (δ, TMS): **2** ($CDCl_3$): 41.60 (N—CH_3), 56.69 (*C*H), 126.51—140.70 (*Ar*H), 143.42 [C—*C*(Ph) = N—N], 154.01 [N = *C* (Ph)—N]; **3** ($CDCl_3$): 39.52 (N—CH_3), 57.63 (*C*H), 126.48—137.31 (*Ar*H), 148.22 [C—*C*(Ph) = N—N], 153.10 [N—*C*(Ph) = N]; **6** (DMSO—d_6): 18.73 (CH_3—CH), 59.22 (C5), 63.60 (C3), 66.35 (CH_3—*C*H)126.58—141.23 (*Ar*H), 145.53 [C—*C*(Ph)—*N* = *N*—].

(*d*) MS (70 eV, 150 °C) *m/e*: **3** 325 (M^+), 324, 310, 248, 222, 221, 178, 119, 118 (100%), 103, 77; **6** 371 (M^+), 326 (100%), 209, 208, 178, 167, 120, 119, 118, 104.

*

The authors are grateful to Mrs. I. Balogh—Batta and staff for the microanalyses and for the UV spectra, to Dr. P. Kolonits for the NMR, and to Mrs. A. Gergely and Dr. J. Tamás for the mass spectra.

REFERENCES

[1] HIXSON, S. S., MARIANO, P. S., ZIMMERMAN, H. E.: Chem. Revs., **73,** 531 (1973); ZIMMERMAN, H. E., TOLBERT, L. M.: J. Am. Chem. Soc., **97,** 5497 (1975); INGA-MAI TEGMO-LARSSON, GONZENBACH, H. U., SCHAFFNER, K.: Helv. Chim. Acta, **59,** 1376 (1976)
[2] NITTA, M., INOUE, O., TADA, M.: Chem. Lett., **1977,** 1065; NITTA, M., KASAHARA, I., KOBAYASHI, T.: Bull. Chem. Soc. Japan, **54,** 1275 (1981)
[3] ATKINSON, C. M., COSSEY, H. D.: J. Chem. Soc., **1962,** 1805; HEINZE, J., BAUMGAERTEL, H.: Chem. Ber., **102,** 1762 (1969)
[4] COMRIE, A. M.: J. Chem. Soc. (C), **1968,** 446; *ibid.*, **1971,** 2807

József NAGY
József NYITRAI } H-1521 Budapest, Gellért tér 4.

Acta Chimica Academiae Scientiarum Hungaricae, Tomus 109 (1), pp. 5—12 (1982)

DIELECTRIC RELAXATION STUDIES OF POLAR MOLECULES*

A. K. SHARMA and V. K. AGARWAL**

(Department of Physics, Institute of Advanced Studies, Meerut University, Meerut-250005, India)

Received September 24, 1980

Accepted for publication January 6, 1981***

Dielectric measurements on bromoform and 1-nitronaphthalene have been made in liquid state at two microwave frequencies (6.0 and 9.3 GHz) and in carbon tetrachloride solution at 9.3 GHz over the temperature range of 10 to 70 °C. Relaxation times, distribution parameters and thermodynamic parameters have been determined using the measured dielectric data for the pure liquid and in solution. The results indicate that bromoform in CCl_4 solution shows complex formation and a second dispersion region is expected for 1-nitronaphthalene in the mm and far infrared region in the pure state.

Introduction

From dielectric relaxation studies on dilute solutions of bromoform in cyclohexane, benzene, mesitylene, and 1,4-dioxane, BOULE [1] has shown complex formation between bromoform and mesitylene, and 1,4-dioxane. A literature survey shows that very little work on dielectric studies of bromoform in carbon tetrachloride has been reported. It would be interesting to check complex formation between bromoform and CCl_4. LEROY *et al.* [2] have reported dielectric relaxation studies on pure bromoform at 25 °C, but no temperature variation has been reported.

RAMPOLLA and SMYTH [3] have reported dielectric relaxation studies on 1-nitronaphthalene in the pure state at 60 °C and in dilute benzene solution at 20, 40 and 60 °C. The 1-nitronaphthalene molecule is rigid having a dipole moment of about 4 Debye. A temperature dependent dielectric relaxation study is likely to give information about dipolar interaction in the liquid state. A study of 1-nitronaphthalene in dilute CCl_4 solution and its comparison with the pure liquid may help understand solute-solvent interactions.

In view of the above facts the temperature dependence of dielectric relaxation in bromoform and 1-nitronaphthalene in the pure liquid state and in dilute CCl_4 solution are reported in this paper.

* This paper represents part of the work submitted by A. K. SHARMA to the Meerut University in partial fulfillment of the requirements for the degree of Doctor of Philosophy

** To whom correspondence should be addressed

*** In final form accepted May 13, 1981

Experimental

The chemicals used in the present study are commercially available with sufficient purity. All chemicals except 1-nitronaphthalene were fractionally distilled. 1-Nitronaphthalene was recrystallized from diethyl ether. The sources of chemicals, their boiling points and refractive indices are summarized in Table I.

Table I

Source, quality, boiling point, melting point and refractive index of the substances used

Substances	Source and quality	Boiling point (°C)		Refractive index at 20 °C	
		Observed	Literature*	Observed	Literature*
Bromoform	E. Merck, Extra pure	148.5	149.5	1.6000	1.5976
1-Nitronaphthalene	High purity chemicals, extra pure	M.P. 57.5	58.5+	—	—
Carbon tetrachloride	BDH, ANALAR	76	76.54	1.4590	1.4601

* Handbook of Physics and Chemistry (The Chemical Rubber Co., Cleveland, Ohio), (1972—73).
+ Beilstein

Dielectric permittivities and losses of bromoform and 1-nitronaphthalene in the liquid state were measured at frequencies of 6.0 and 9.3 GHz in the temperature range of 10 to 50 °C (bromoform) and 60 to 70 °C (1-nitronaphthalene). The dielectric permittivities and losses are evaluated using POLEY's [4] method. The dielectric permittivity (ε_0) was determined at 1 MHz, using a "Wayne—Kerr bridge" type B602; refractive indices were also measured at the above temperatures.

The distribution parameter (α) of 1-nitronaphthalene in benzene is about 0.1 [3], while for bromoform in dilute solution it is nearly zero [1], so that the single frequency concentration variation method can be successfully used for the determination of relaxation times. The dielectric measurements on dilute solutions of bromoform and 1-nitronaphthalene in CCl_4 have been made at 9.3 GHz at 20, 35 and 50 °C. SMYTH's [5] method has been used for the evaluation of ε' and ε''. The dielectric permittivity (ε_0) at 100 KHz and refractive indices of the solution at the above temperature were also measured. The accuracy of measurements at all frequencies were the same as described earlier [6].

Results

The measured values of dielectric permittivity (ε'), dielectric loss (ε''), static dielectric permittivity (ε_0), and the high frequency dielectric permittivity ($\varepsilon_\infty = n_D^2$) for bromoform and 1-nitronaphthalene for the pure liquid state and in carbon tetrachloride solution at different temperatures are given in Tables II and III respectively.

Analysis of experimental data

The data for the pure liquid state of bromoform and 1-nitronaphthalene were examined in terms of COLE-COLE arc plots [7]. All these plots are of DEBYE type with symmetric distribution of relaxation. Representative curves

Table II

Dielectric permittivity (ε'), dielectric loss (ε''), static dielectric permittivity (ε_0), extrapolated permittivity on the high frequency side (ε_∞), square of refractive index (n_D^2), distribution parameter (α) and relaxation time (τ) of bromoform and 1-nitronaphthalene

Temp. °C	$f = 6.0$ GHz		$f = 9.3$ GHz						
	ε'	ε''	ε'	ε''	ε_0	ε_∞^*	n_D^2	α	$\tau \times 10^{12}$ (sec)
			Bromoform						
10.5	3.61_2	0.66_3	3.27_2	0.60_3	4.48_8	2.82	2.57_8	0.22	32.2
20	3.63_9	0.57_8	3.40_2	0.76_7	4.41_8	2.78	2.56_0	0.29	24.4
35	3.74_7	0.68_8	3.42_1	0.78_6	4.25_9	2.66	2.53_1	0.17	18.2
50	3.67_1	0.37_5	3.50_8	0.69_3	4.13_2	2.73	2.50_2	0.27	13.3
			1-Nitronaphthalene						
60	6.70_6	4.92_0	5.56_7	4.17_3	20.50_0	3.83	2.69_4	0.31 (0.23)**	103 (69.5)**
65	6.30_0	4.83_1	5.37_0	5.18_7	19.90_0	3.62	2.67_7	0.36	99.6
70	6.12_6	4.75_5	5.50_7	3.80_0	19.38_2	3.78	2.66_9	0.24	90.8
75	6.46_3	5.12_0	6.15_8	3.58_8	18.85_1	3.60	2.65_9	0.30	81.7

* Obtained from COLE-COLE plots
** Ref. [3]

at 10.5 °C for bromoform and at 60 °C for 1-nitronaphthalene are shown in Fig. 1. The relaxation times (τ), distribution parameters (α), and extrapolated permittivities on the high frequency side (ε_∞), obtained from COLE-COLE arc

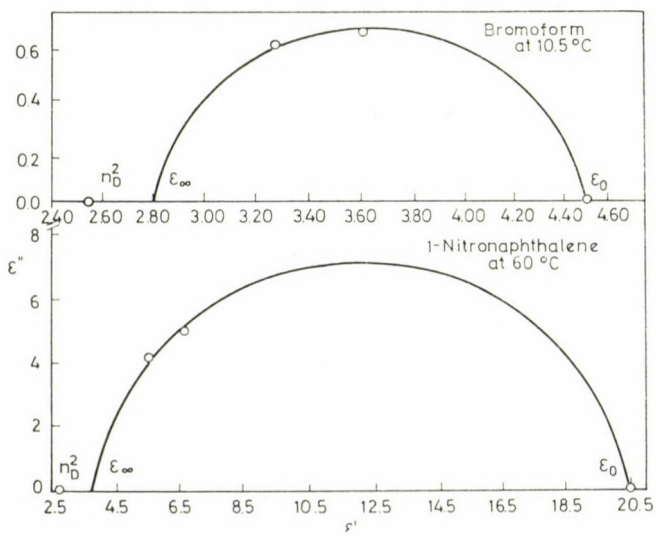

Fig. 1. COLE-COLE plots for bromoform and 1-nitronaphthalene

Acta Chim. Acad. Sci. Hung. 109, 1982

Table III

Variation of dielectric permittivity (ε'), dielectric loss (ε''), static dielectric permittivity (ε_0) and high frequency dielectric permittivity ($\varepsilon_\infty = n_D^2$) with concentration ($x_2$) of bromoform and 1-nitronaphthalene in carbon tetrachloride solution

x_2 (mole fraction)	20 °C				35 °C				50 °C			
	ε_0	ε'	ε''	ε_∞	ε_0	ε'	ε''	ε_∞	ε_0	ε'	ε''	ε_∞
Bromoform in carbon tetrachloride												
0.0285	2.23_6	2.28_6	0.01_8	2.14_1	2.20_3	2.25_3	0.01_7	2.11_4	2.16_9	2.22_6	0.01_4	2.08_8
0.0501	2.27_6	2.32_5	0.02_9	2.14_8	2.23_7	2.28_8	0.02_4	2.12_2	2.20_4	2.25_8	0.02_3	2.09_5
0.0669	2.30_8	2.33_9	0.03_0	2.15_5	2.26_4	2.30_8	0.03_4	2.12_8	2.23_2	2.28_6	0.03_0	2.10_2
0.0972	2.36_4	2.37_4	0.05_5	2.16_6	2.31_1	2.34_1	0.04_7	2.13_9	2.28_0	2.31_5	0.04_2	2.11_3
0.1106	2.38_8	2.39_4	0.05_5	2.17_1	2.33_2	2.36_6	0.05_0	2.14_4	2.30_1	2.34_0	0.04_8	2.11_7
1-Nitronaphthalene in carbon tetrachloride												
0.0045	2.30_1	2.30_2	0.03_9	2.13_4	2.26_5	2.27_2	0.03_8	2.11_1	2.20_1	2.25_4	0.03_8	2.08_5
0.0090	2.38_5	2.33_6	0.08_2	2.14_1	2.34_5	2.31_6	0.07_5	2.11_7	2.30_0	2.29_6	0.07_4	2.09_4
0.0174	2.56_0	2.38_8	0.13_9	2.14_6	2.50_5	2.37_9	0.14_6	2.12_3	2.44_7	2.36_5	0.14_6	2.09_8
0.0271	2.75_4	2.45_0	0.17_1	2.15_5	2.68_5	2.44_4	0.18_5	2.13_1	2.62_0	2.44_1	0.18_6	2.10_6

plots for bromoform and 1-nitronapthalene in the pure liquid state are also given in Table II.

SMYTH *et al.* [5] have observed experimentally for dilute solutions of a polar solute in non-polar solvents that the dielectric permittivity (ε') and loss (ε'') are proportional to the solute concentration:

$$\varepsilon' = \varepsilon_1 + a' x_2 \tag{1a}$$

$$\varepsilon'' = a'' x_2 \tag{1b}$$

$$\varepsilon_0 = \varepsilon_{10} + a_0 x_2 \tag{1c}$$

and

$$\varepsilon_\infty = \varepsilon_{1\infty} + a_\infty x_2 \tag{1d}$$

Here ε_∞ is the dielectric permittivity of the solution at infinite frequency, which is taken equal to the square of refractive index ($\varepsilon_\infty = n_D^2$). Subscript 1 refers to the solvent (CCl_4). The coefficients in Eq. (1), a', a'', a_0 and a_∞, which are called "slopes", are obtained by plotting ε', ε'', ε_0 and the square of the refractive index (n_D^2) of the solutions against the concentration x_2 in mole fraction.

For a system with a single relaxation time, the DEBYE equation for dilute solutions [8] can be written in the following form

$$a' = a_0 - \tau(\omega a'') \tag{2}$$

and

$$a' = a_\infty + (a''/\omega)\, 1/\tau \tag{3}$$

Equation (2) has been used for calculating τ in view of the fact that ε_∞ cannot be measured correctly as these rigid molecules show a far infrared absorption.

The GUGGENHEIM [9] equation has been used for calculating the dipole moment (μ) in the solution state. The values of a_0, a', a'', a_∞ and μ are given in Table IV.

Discussion of results

The relaxation time (τ) for bromoform at 35 °C was about 25% higher than the reported value of chloroform [10] at 30 °C. The higher values of τ in bromoform, as compared to chloroform, may be attributed to the higher viscosity and moment of inertia of bromoform. The relaxation time for 1-nitronaphthalene at 60 °C was about 50% higher than the reported value [3]. This may be due to the different purity of the sample used by us, as our value of ε_0 at 60 °C is about 10% higher than the reported value [3].

Table IV

Values of a_0, a', a'', a_∞, τ and μ for bromoform and 1-nitronaphthalene in carbon tetrachloride

Temp. °C()	a_0	a'	a''	a_∞	$\tau \times 10^{12}$ (sec)	$\mu \times 10^{18}$ (D)
Bromoform in CCl_4						
20	1.86	1.25	0.48	0.37	21.8 (9.2)*	1.12 (0.98)*
35	1.58	1.26	0.42	0.36	13.3	0.97
50	1.63	1.33	0.43	0.36	12.0	1.01
1-Nitronaphthalene in CCl_4						
20	20.0	6.36	5.45	0.92	42.8 (22.8)*	3.99 (4.0)*
35	18.6	7.59	6.26	0.88	29.9	3.97
50	17.5	8.27	6.23	0.85	25.3	4.08

* Refs [1] and [3]

The relaxation times (τ) at 20 °C for bromoform and 1-nitronaphthalene in dilute solution of carbon tetrachloride are higher than in benzene, as shown in Table IV. This may be due to the higher viscosity of CCl_4 than C_6H_6. The dipole moment (μ) of bromoform and 1-nitronapthalene in CCl_4 are comparable to the reported values [1, 3] in C_6H_6. BOULE [1] has made dielectric measurements of relaxation times on dilute solutions of bromoform in cyclohexane, benzene, mesitylene and 1,4-dioxane, and found the ratios of relaxation times for complexes to the relaxation times of bromoform in cyclohexane to be as follows: 1.3 for bromoform-benzene, 3.3 for bromoform-mesitylene, and 2.6 for bromoform 1,4-dioxane. From this, he has concluded on complex formation of bromoform with mesitylene and 1,4-dioxane. We have calculated the ratios of reduced relaxation times (τ/η) of bromoform in various solvents with cyclohexane, using the data of BOULE. These are as follows: bromoform-benzene 1.7; bromoform-mesitylene 3.5; and bromoform-1,4-dioxane 1.7. Our measurements on $CHBr_3$ in CCl_4 give this ratio to be 2.96, which indicates complex formation of bromoform in carbon tetrachloride (reduced relaxation times for $CHBr_3$ in cyclohexane have been taken from BOULE's data). For bromoform and 1-nitronapthalene in pure liquid and solution state, the relaxation time decreases with increasing temperature (Tables II and IV). The decrease of relaxation time (τ) with increasing temperature in pure liquid and solution is partly due to the decrease of viscosity. A similar behaviour has been observed by many workers [3, 11—14].

The extrapolated dielectric permittivity at the high frequency end of the COLE-COLE plot is much larger than the square of the refractive index

(Table II). This indicates that a second dispersion region exists at mm and far infrared region. LEROY *et al.* [2] have already reported the absorption and dispersion of bromoform at 25 °C. It is expected that 1-nitronaphthalene in the liquid state will also show a similar behaviour.

The thermodynamic parameters for dipole orientation of bromoform and 1-nitronaphthalene in pure liquid and in solution for the activated state have been calculated using EYRING's theory [15] of chemical rate process. These parameters are given in Table V. The free energy of activation (ΔF) increases

Table V

Thermodynamic parameters for bromoform and 1-nitronapthalene in pure liquid and solution

Compound	Temperature (°C)	ΔF (kJ/mol)	ΔS (J/mol K)	ΔH (kJ/mol)
Bromoform	10.5	12.4	8.41	
	20	12.2	8.87	
	35	12.2	8.41	14.8
	50	12.0	8.41	
Bromoform in Carbon tetrachloride	20	11.9	6.70	
	35	11.4	8.12	13.9
	50	11.8	6.49	
1-Nitronaphthalene	60	18.2	−17.2	
	65	18.4	−17.6	
	70	18.5	−17.4	12.5
	75	18.5	−17.3	
1-Nitronapthalene in carbon tetrachloride	20	13.6	−11.7	
	35	13.5	−10.9	10.1
	50	13.8	−11.4	

with the size of the molecules, *i.e.* on going from bromoform to 1-nitronaphthalene. This amounts to saying that the increase in molecule size increases the amount of energy required for dipole orientation [16]. The increase in ΔF also decreases the probability of a jump from one orientation to another with a consequent increase in the relaxation time. The most probable enthalpies of activation (ΔH) for 1-nitronaphthalene in pure liquid and in solution are found to be less than the corresponding free energy of activation (ΔF), but for bromoform in pure liquid and in solution the values of ΔH are found to be greater than the corresponding values of ΔF. The entropy of activation (ΔS), both in pure liquid and in solution, is found to be negative for 1-nitronaphthalene and positive for bromoform. The small values of ΔS prohibit the determination of the exact sign because $\Delta H \simeq \Delta F$. The value of ΔS should be negative because the activated state should be more ordered. However, if there is complex formation and in the activated state the dipole can disengage itself

from the complex than it may have more freedom and random state available, giving rise to a positive ΔS [17]. Since this is happening in bromoform in which evidence for complex formation had clearly been shown [1], the positive value may not be due to experimental uncertainity alone.

Conclusions

From the above study the following conclusions have been drawn.

(i) Bromoform in carbon tetrachloride solution shows complex formation.

(ii) A second dispersion region is expected for 1-nitronaphthalene in the mm and far infrared region in the pure state.

*

The authors are grateful to Dr. Abhai MANSINGH (University of Delhi) for many helpful suggestions and one of us (AKS) is thankful to the Department of Atomic Energy, India for providing financial assistance.

REFERENCES

[1] BOULE, P.: J. Chem. Phys., **57,** 5285 (1972)
[2] LEROY, Y., CONSTANT, E., ABBAR, C., DESPLANQUES, P.: Advan. Mol. Relaxation Processes, **1,** 273 (1967—68)
[3] RAMPOLLA, R. W., SMYTH, C. P.: J. Am. Chem. Soc., **80,** 1057 (1958)
[4] POLEY, J. P.: Appl. Sci. Res., **134,** 337 (1955)
[5] HESTON, Jr., W. M., FRANKLIN, A. D., HENNELLY, E. J., SMYTH, C. P.: J. Am. Chem. Soc., **72,** 3443 (1950)
[6] SHARMA, A. K.: Acta Chim. Acad. Sci. Hung., **97,** 407 (1978)
[7] COLE, K. S., COLE, R. H.: J. Chem. Phys., **9,** 341 (1941)
[8] HIGASI, K.: Bull. Chem. Soc. Japan, **39,** 2157 (1966)
[9] GUGGENHEIM, E. A.: Trans. Faraday Soc., **45,** 714 (1949)
[10] GOPALAN, T. V., KADABA, P. K.: J. Phys. Chem. **72,** 3676 (1968)
[11] HILL, N. E., VAUGHAN, W. E., PRICE, A. H., DAVIES, M.: Dielectric Properties and Molecular Behaviour. Van Nostrand Reinhold, London, New York 1969
[12] KRISHNAJI, MANSINGH, A.: J. Chem. Phys., **42,** 2503 (1965)
[13] MANSINGH, A., MCLAY, D. B.: J. Chem. Phys., **54,** 3322 (1971)
[14] MARTIN, G. D., WALKER, S.: Can. J. Chem., **50,** 707 (1972)
[15] EYRING, H.: J. Chem. Phys., **4,** 283 (1936); GLASSTONE, S., LAIDLER, K. J., EYRING, H.: Theory of Rate Processes. McGraw-Hill Book Co. Inc., New York 1941
[16] BRANIN, Jr. F. H., SMYTH, C. P.: J. Chem. Phys., **20,** 1121 (1952)
[17] SRIVASTAVA, K. K.: J. Phys. Chem., **74,** 152 (1970)

Ashok K. SHARMA
Vinod K. AGARWAL
Department of Physics, Institute of Advanced Studies, Meerut University, Meerut-250005, India

Acta Chimica Academiae Scientiarum Hungaricae, Tomus 109 (1), pp. 13—20 (1982)

DITHIOCARBAMATO DERIVATIVES OF DICHLOROBIS-(π-CYCLOPENTADIENYL)-TITANIUM(IV) AND ZIRCONIUM(IV)

S. KUMAR and N. K. KAUSHIK*

(Department of Chemistry, University of Delhi, Delhi—110007, India)

Received November 4, 1980

Accepted for publication January 27, 1981

Titanium(IV) and zirconium(IV) dithiocarbamato complexes of the types-$[Cp_2M(S_2CNRR')Cl]$ and $[CpM(S_2CNRR')_3]$ where M = Ti(IV) or Zr(IV) and R = H, R′ = $-C_5H_9$ (cyclopentyl) or $-C_7H_{13}$ (cycloheptyl) or R = $-C_2H_5$ (ethyl), R′ = $-C_6H_4CH_3$ (*m*-tolyl) groups have been prepared by the reaction of dichlorobis-(cyclopentadienyl) titanium(IV) or zirconium(IV) with sodium salts of *N*,*N*′-ethyl, *m*-tolyl or *N*-cyclopentyl or *N*-cycloheptyl dithiocarbamic acid in refluxing dichloromethane. All these complexes have been characterized by elemental analysis, electrical conductance, magnetic susceptibility measurements, molecular weight determination and spectral (infrared, electronic and proton nmr) data. These compounds are found to be monomeric nonelectrolytes in which dithiocarbamate behaves as a bidentate ligand. Therefore coordination numbers of "five" and "seven" have been assigned to the metals in these complexes. Proton magnetic resonance studies support the findings of the i.r. spectral studies.

Introduction

A number of transition metal dithiocarbamates have been synthesized and characterized in the recent years [1—3]. In view of the interesting synthetic and structural aspects of these complexes, interest in the study of dithiocarbamate complexes continues to increase. However, only a few dithiocarbamato complexes of organometallic derivatives have been studied [4, 5]. The special interest in the study of metal dithiocarbamates aroused because of the diversified application of dithiocarbamates. They can be used as accelerators in vulcanization, as high pressure lubricants in industry, and also as fungicides and pesticides. Further, dithiocarbamate ligands have been known to stabilize the higher coordination states of metals due to their low charge and their relatively small "bites" (2.8—2.9Å). Also the organometallic compounds of titanium and zirconium have been found capable of activating molecular nitrogen [6, 7]. Hence, it was considered worthwhile to investigate dithiocarbamato complexes of types $[Cp_2M(S_2CNRR')Cl]$ and $[CpM(S_2CNRR')_3]$ with various R, R′ groups since any change in the groups attached to nitrogen may affect the spectral properties of the complexes.

* To whom correspondence should be addressed

Experimental

Materials and methods

Sodium dithiocarbamates NaS_2CNRR' were prepared by the method reported by KLOPPING and KERK [8] and dried in vacuum over phosphorus pentoxide. Dichlorobis-(π-cyclopentadienyl)titanium(IV) and zirconium(IV) were prepared by reacting titanium(IV) or zirconium(IV) tetrachloride with sodium cyclopentadienide in THF [9, 10]. Dichloromethane was dried by refluxing it for 24 hrs over calcium hydride. Nitrobenzene was purified for conductance measurements by the method of FAY *et al.* [11]. All operations were carried out under anhydrous condition.

Titanium and zirconium were determined gravimetrically as oxides, and chloride as AgCl. Nitrogen was estimated by Kjeldahl's method and sulphur as barium sulphate.

Molecular weights were determined ebullioscopically in benzene using a Gallenkemp (U.K.) ebulliometer. Conductance measurements were made in nitrobenzene at 30° using a Beckmann conductivity Bridge Model No. RC-18A. Solid state infrared spectra were recorded (KBr Pellets) in the 4000–200 cm^{-1} region on a Perkin–Elmer 621 grating spectrometer. Magnetic measurements were performed by Gouy's method using mercury(II) tetrathiocyanatocobaltate(II) as a calibrant. The electronic spectra of the complexes were run on a Perkin–Elmer 4000 Å instrument in the 400–750 nm range. The proton nmr spectra of the ligands (in D_2O) and of the complexes (in $CDCl_3$) were recorded on a Perkin–Elmer R-32 spectrom-

Table I

Analytical data of the compounds

Compounds	Mol. wt. Found (Calc.)	Percentage: Found (Calc.)					
		C	H	N	S	M	Cl
$Cp_2Ti(S_2CNRR')^aCl$	370.0 (373.4)	51.0 (51.4)	5.0 (5.3)	3.5 (3.7)	17.0 (17.1)	12.6 (12.8)	9.2 (9.5)
$CpTi(S_2CNRR')_3^a$	590.0 (592.9)	46.2 (46.5)	5.6 (5.9)	6.8 (7.0)	32.2 (32.4)	7.8 (8.0)	—
$Cp_2Zr(S_2CNRR')^aCl$	415.0 (416.72)	45.7 (46.0)	4.6 (4.8)	3.2 (3.3)	15.0 (15.3)	21.8 (21.9)	8.2 (8.5)
$CpZr(S_2CNRR')_3^a$	635.0 (636.22)	43.0 (43.4)	5.2 (5.5)	6.5 (6.6)	29.8 (30.1)	14.1 (14.3)	—
$Cp_2Ti(S_2CNRR')^bCl$	400.0 (401.4)	53.6 (53.8)	5.9 (6.0)	3.2 (3.5)	15.5 (15.9)	11.7 (11.9)	8.5 (8.8)
$CpTi(S_2CNRR')_3^b$	675.0 (676.9)	51.0 (51.4)	6.8 (6.9)	6.0 (6.2)	28.0 (28.4)	6.8 (7.0)	—
$Cp_2Zr(S_2CNRR')^bCl$	444.0 (444.72)	48.2 (48.6)	5.2 (5.4)	3.0 (3.1)	14.0 (14.4)	20.3 (20.5)	7.8 (8.0)
$CpZr(S_2CNRR')_3^b$	718.0 (720.22)	48.0 (48.3)	6.2 (6.5)	5.5 (5.8)	26.4 (26.6)	12.6 (12.7)	—
$Cp_2Ti(S_2CNRR')_3^cCl$	420.0 (423.4)	56.0 (56.6)	5.0 (5.2)	3.0 (3.3)	14.8 (15.1)	11.0 (11.3)	2.3 (2.4)
$CpTi(S_2CNRR')_3^c$	740.0 (742.9)	56.0 (56.5)	5.0 (5.5)	5.1 (5.6)	25.5 (25.8)	6.3 (6.4)	—
$Cp_2Zr(S_2CNRR')^cCl$	465.0 (466.72)	51.0 (51.4)	4.0 (4.7)	2.8 (3.0)	13.3 (13.7)	19.2 (19.5)	7.0 (7.6)
$CpZr(S_2CNRR')_3^c$	784.00 (786.22)	53.0 (53.4)	5.0 (5.2)	5.0 (5.3)	24.2 (24.4)	11.2 (11.6)	—

[a] where R = H, R′ = $-C_5H_9$; [b] where R = H, R′ = $-C_7H_{13}$ and [c] where R = $-C_2H_5$, R′ = $C_6H_4CH_3$

eter at a sweep width of 900 Hz. The magnetic field sweep was calibrated with a standard sample of H_2O and TMS (1%) in D_2O and also with a standard sample of $CHCl_3$ and TMS (1%) in $CDCl_3$.

Preparation of the complexes

All these complexes were prepared in a similar manner. Dichlorobis (π-cyclopentadienyl)titanium(IV) and zirconium(IV) were refluxed separately in CH_2Cl_2 ($\sim$100 mL) with anhydrous sodium *N*,*N'*-ethyl, *m*-tolyl or sodium *N*-cyclopentyl or sodium *N*-cycloheptyl dithiocarbamates in 1 : 1 or 1 : 3 metal to ligand molar ratio for 18—24 hrs. The solution was then filtered and its volume was reduced to *ca.* 20 mL. Yellow orange or white crystals appeared on the addition of petroleum ether *ca.* 30 mL to the concentrated filtrate and allowing the mixture to stand overnight. The product was filtered and dried under vacuum at room temperature.

Results and Discussion

Dichlorobis-(π-cyclopentadienyl)titanium(IV) and zirconium(IV) react with the sodium dithiocarbamates in refluxing dichloromethane in both 1 : 1 and 1 : 3 molar ratios. The reaction with 1 : 2 molar ratio have also been performed but in such cases too only 1 : 1 product could be isolated. The methods used for preparing and isolating these complexes yield materials of good purity. The titanium(IV) dithiocarbamato complexes are yellowish orange in colour whereas zirconium(IV) complexes are white. They are soluble in benzene, dichloromethane, chloroform, nitrobenzene, carbon disulphide, dimethyl formamide and dimethyl sulphoxide. They are quite stable as solids in air but their solution hydrolyze rather rapidly. Electrical conductance data in nitrobenzene indicate that they are nonelectrolytes. Molecular weight determinations in benzene indicate that all complexes are monomeric.

Magnetic moments and electronic spectra

Magnetic susceptibility values at room temperature show that these complexes are diamagnetic. The electronic spectra of all the dithiocarbamato complexes of dichlorobis-(π-cyclopentadienyl)titanium(IV) and zirconium(IV) were recorded in chloroform and acetone. All complexes show a single band in the region 24700—24300 and 25000—24400 cm^{-1}, respectively, for titanium(IV) and zirconium(IV) complexes which can be assigned to the charge transfer band [12] and is in accordance with their $(n-1)d^{\circ}\, ns^{\circ}$ electronic configuration.

Infrared spectral study

Infrared spectral studies have not been carried out in detail, since, it is quite difficult to assign all of the bands because most of them are highly coupled. The main aim for the preparation of these compounds is their stereochemistry, which is closely related to the nature of attachment of the dithiocarbamate

ligand to the metal. The different resonance structures of dithiocarbamate can be represented as

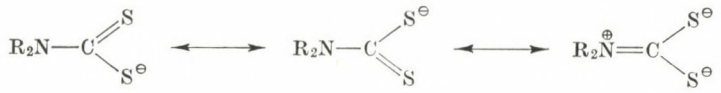

(a) (b) (c)

NAKAMOTO [13] reported that resonance form (*c*) does contribute to the structure to a considerable extent. If all these dithiocarbamate ligands are bidentate, as in $Mo(NO)((S_2CNR_2)_3$ (R = Me [14] or *n*-Bu [15]) and the cyclopentadienyl group occupies one coordination site, coordination number "five" and "seven" can be assigned to $[Cp_2M(S_2CNRR')Cl]$ and $[CpM(S_2CNRR')_3]$ M = Ti(IV) or Zr(IV), respectively. FAY *et al.* [16] have reported on the X-ray diffraction of $[CpZr\{S_2CN(CH_3)_2\}_3]$ in which because of the relatively small size of the cyclopentadienyl group it is considered to occupy single *axial* coordination site in a pentagonal bipyramidal structure. By this analogy, it is assumed that cyclopentadienyl group in the compounds reported in this communication occupies a single coordination site. However, the more common coordination number of six would result in 1 : 3 complexes if one of the dithiocarbamate ligands behaves as an S-bonded monodentate ligand, as in $[Ru(NO)\ (S_2CNR_2)_3]$ (R = Me [14]). The two bonding possibilities can be distinguished by i.r. spectroscopy [17]. The $[Sn(S_2CN\ Et_2)_4]$ which has been shown by X-ray analysis to be a 6-coordinate complex having two monodentate $S_2CN\ Et_2$ groups [18], exhibits two C—N bands (1512 and 1471 cm^{-1}) and two C—S bands (1008 and 989 cm^{-1}) [19] while the 8-coordinate $[Ti(S_2CN\ Et_2)_4]$ shows only one C—N band (1503 cm^{-1}) and one C—S band (1001 cm^{-1}) [19, 20].

Important i.r. bands for all the complexes prepared are given in Table II. The "thiureide" band (C···N) near 1500 cm^{-1} is very characteristic of dithiocarbamates. The frequency of this band lies between that for C—N (1250—1350 cm^{-1}) and C=N (1640—1690 cm^{-1}), which suggests that this bond has some double bond character [22]. In all these complexes this band shifts to higher frequency (~10—15 cm^{-1}) indicating the bidentate behaviour of the ligand [22] which is further supported by the appearance of a single C—S band. Coordination through sulphur has been confirmed by the appearance of new bands in the far i.r. region *ca.* 370—385 and 360—370 cm^{-1} in the titanium(IV) and zirconium(IV) complexes, respectively, which can be assigned to ν(M—S). In the monochloro-bis(π-cyclopentadienyl)titanium(IV) and zirconium(IV) complexes additional bands for M—Cl mode appear in the region 385—400 and 380—390 cm^{-1}, respectively. Further, the absorption bands occuring at ~3100 cm^{-1}, (C—H stretching) ~1430 cm^{-1} (asymmetric ring

Table II

Characteristic i.r. bands (cm^{-1})

Compound	ν(C···N)	ν(C···S)	ν(M—S)	ν(M—Cl)	ν(C—H)	ν(C—C) asym	ν(C—H) inplane	(C—H) out-of-plane (def.)	ν(C—N—C)
$Cp_2Ti(S_2CNRR')^aCl$	1500s	1005s	375w	395m	3105m	1445m	1025s	815vs	1150m
$Cp\ Ti(S_2CNRR')_3^a$	1495s	1000s	370w	—	3105m	1440m	1015s	810vs	1140m
$Cp_2Zr(S_2CNRR')^aCl$	1505s	995s	365w	385w	3100m	1440m	1020s	810vs	1145m
$Cp\ Zr(S_2CNRR')_3^a$	1500s	1000s	360w	—	3105m	1440m	1020s	810vs	1145m
$Cp_2Ti(S_2CNRR')^bCl$	1485s	1010s	380w	395w	3110m	1450m	1025s	815vs	1142m
$Cp\ Ti(S_2CNRR')_3^b$	1490s	1005s	375w	—	3105m	1430m	1025s	825vs	1148m
$Cp_2Zr(S_2CNRR')^bCl$	1490s	1015s	362w	380m	3105m	1425m	1025s	825vs	1142m
$CpZr\ (S_2CNRR')_3^b$	1490s	1000s	360w	—	3115m	1430m	1015m	810vs	1145m
$Cp_2Ti(S_2CNRR')^cCl$	1480s	1020s	385w	400m	3095m	1440m	1020s	820vs	1140m
$CpTi\ (S_2CNRR')_3^c$	1490s	1015s	375w	—	3100m	1450m	1020s	820vs	1145m
$Cp_2Zr(S_2CNRR')^cCl$	1495s	1000s	370w	390m	3110m	1430m	1015s	825vs	1145m
$Cp\ Zr(S_2CNRR')_3^c$	1495s	1010s	365w	—	3105m	1445m	1015s	815vs	1150m

[a] where R = H, R′ = $-C_5H_9$; [b] where R = H, R′ = $-C_7H_{13}$ and [c] where R = $-C_2H_5$, R′ = $C_6H_4CH_3$; vs = very strong, s = strong, m = medium and w = weak.

breathing), ~1030 cm^{-1} (C—H deformation of C_5H_5 ring) and ~815 cm^{-1} (C—H bending out-of-plane deformation) indicate [23] the presence of π-bonded cyclopentadienyl ring in all the complexes.

From the above discussion it is evident that in these complexes, the three new dithiocarbamate ligands, chosen for the present study, act as bidentate ligands and coordination to metal takes place through sulphur. Therefore, five- and seven-coordinate structure are proposed for the compounds $[Cp_2M(S_2CNRR')Cl]$ and $[CpM(S_2CNRR')_3]$, respectively.

^1H nmr spectral study

^1H nmr spectral studies of the ligands and the complexes were carried out in D_2O and $CDCl_3$, respectively, simply because of difference in their solubility. The intensity of the resonance signals were determined by planimetric integration. The integrated proton ratios correspond to $[Cp_2M(S_2CNRR')Cl]$ and $[CpM(S_2CNRR')_3]$ stoichiometries, where M = Ti(IV) or Zr(IV); R = H, R′ = $-C_5H_9$ or C_7H_{13} or R = $-C_2H_5$, R′ = $C_6H_4.CH_3$ and Cp = $-C_5H_5$ groups. Chemical shifts for the protons in different chemical environments are presented in Table III. A general low field shift in the values of δ ppm for R, R′ protons in all these complexes in comparison to the δ ppm values for the respective protons in the ligand indicate that on coordination with the

Table III

^1H nmr chemical shifts data (δ ppm)

Compounds	C_5H_5	C_6H_4	NH	—CH_3	Cycloalkyl C_5H_9 or C_7H_{13}
$Cp_2Ti(S_2CNRR')^aCl$	6.5b	6.95t, 7.15d, 7.2s	—	2.25s, 1.2t, 4.25q	—
$Cp\ Ti(S_2CNRR')_3^a$	6.5s	7.0b, 7.15b, 7.25d	—	2.3d, 1.15m, 4.3m	—
$Cp_2Zr(S_2CNRR')^aCl$	6.22s	7.0t, 7.2d, 7.3s	—	2.28s, 1.25t, 4.3q	—
$Cp\ Zr(S_2CNRR')_3^a$	6.45s	7.2b, 7.22b, 7.3d	—	2.32d, 1.2m, 4.28m	—
$Cp_2Ti(S_2CNRR')^bCl$	6.4s		4.65s		1.85b
$Cp\ Ti(S_2CNRR')_3^b$	6.6s		4.70s		1.85d
$Cp_2Zr(S_2CNRR')^bCl$	6.42s		4.68s		1.8b
$Cp\ Zr(S_2CNRR')_3^b$	6.35s		4.7s		1.9d
$Cp_2Ti(S_2CNRR')^cCl$	6.5s		5.0s		1.65b
$Cp\ Ti(S_2CNRR')_3^c$	6.65s		5.05s		1.7b, 1.3s
$Cp_2Zr(S_2CNRR')^cCl$	6.6s		5.0s		1.7b
$Cp\ Zr(S_2CNRR')_3^c$	6.55s		5.0s		1.72d
$NaS_2CNRR'^a$			4.62s		2.0Sh, 1.6b
$NaS_2CNRR'^b$			4.95s		1.75b, 1.43s
$NaS_2CNRR'^c$		6.92t, 7.12d, 7.22s		2.22s, 1.05t, 4.20q	—

[a] where R = $-C_2H_5$, R′ = $C_6H_4CH_3$; [b] where R = H, R′ = C_4H_9 and [c] where R = H, R′ = $-C_7H_{13}$; S = Singlet, d = doublet, t = triplet, q = quadruplet, m = multiplet, Sh = shoulder and b = broad.

metals, the R, R′ protons become less shielded due to the movement of the electron clouds towards the concerned metal atom in the complex molecule. The spectra of the complexes of the type $[Cp_2M(S_2CNRR')Cl]$ favour a trigonal bipyramidal [5] structure (with the two cyclopentadienyl groups in *trans* positions). Further, it is not possible to explain the stereochemical rigidity or nonrigidity in the dithiocarbamate part of the complexes due to the symmetry involved in the above structures, since the same number of resonance signals for R, R′ groups will be observed whether the S_2 C—N bond rotation is slow or fast. In the case of complexes of the type $[CpM(S_2CNRR')_3]$ two distinct resonance signals for each set of R, R′ protons are observed due to (*a*) protons on R, R′ groups of the two S_2CNRR' moiety *trans* to each other (similar magnetic environment) and (*b*) one S_2CNRR' moeity *trans* to π-C_5H_5 ring (different magnetic environment in comparison to the other two mentioned above) with relative intensities 2 : 1. The appearance of a single sharp cyclopentadienyl resonance is attributed to rapid rotation of the ring around the metal ring axis. Thus, the seven-coordinate complexes $[CpM(S_2CNRR')_3]$ have pentagonal bipyramidal structures. The structure is slightly distorted due to the presence of a cyclopentadienyl group in the molecule.

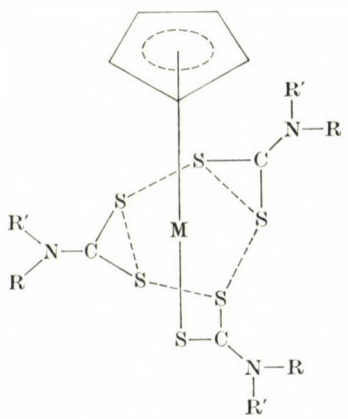

M = Ti (IV) or Zr (IV)

*

One of the authors (S. K.) is thankful to the Council of Scientific and Industrial Research, New Delhi (India) for the award of a Junior Research Fellowship.

REFERENCES

[1] THORN, G. D., LUDWIG, R. A.: "The Dithiocarbamates and Related Compounds", Elsevier, New York, 1962

[2] COUCOUVANIS, D.: "Progress in Inorganic Chemistry", Vol. XI, Interscience, 1970, pp 233

[3] WILLEMSE, J., CRAS, J. A., STEGGARDA, J. J., KIEJERS, C. P.: "Structure and Bonding" Vol. XXVIII, Springer Verlag, 1976, pp 83
[4] COUTTS, R. S. P., WAILES, P. C.: Aust. J. Chem., **27,** 2483 (1974); J. Organomet. Chem., **84,** 47 (1975); COUTTS, R. S. P., WAILES, P. C., KINGSTON, J. V.: Aust. J. Chem., **23,** 463 (1970)
[5] KAUSHIK, N. K., BHUSHAN, B., CHHATWAL, G. R.: Transition Metal Chem., **3,** 215 (1978); Synth. React. Inorg. Metalorg. Chem., **8,** 467 (1978)
[6] VOLPIN, M. E., SHUR, V. B.: Nature, **209,** 1236 (1966); VAN TAMELEN, E. E., SEELEY, D., SCHNELLER, S., RUDLER, M., CRETNEY, W.: J. Am. Chem. Soc., **92,** 5251 (1970)
[7] GRAY, D. R., BRUBAKER, C. H.: Chem. Commun., **1969,** 1239
[8] KLÖPPING, H. L., VAN DER KERK, G. J. M.: Rec. Trav. Chim., **70,** 917 (1951)
[9] WILKINSON, G., BIRMINGHAM, J. M.: J. Am. Chem. Soc., **76,** 4281 (1954)
[10] JOLLY, W. L.: "Synthetic Inorganic Chemistry" Prentice Hall, New Delhi, 176 (1965)
[11] FAY, R. C., LOWRY, R. N.: Inorg. Chem., **6,** 512 (1967)
[12] DORAIN, P. B., PATTERSON, H. H., JORDON, P. C.: J. Chem. Phys., **49,** 3845 (1968); DUNN, T. M., NYHOLM, R. S., YAMAD, S.: J. Chem. Soc., **1962,** 1564
[13] NAKAMOTO, K., FUJITA, J., CONDRATE, R. A., MORIMOTO, Y.: J. Chem., Phys., **39,** 423 (1963)
[14] JOHNSON, B. F. G., AL OBAIDI, K. H., MCCLEVERTY, J. A.: J. Chem. Soc. (A), **1969,** 1668
[15] BRENMAN, F. T., BERNAL, I.: Chem. Commun, **1970,** 138; Inorg. Chim. Acta, **7,** 283 (1973)
[16] BRUDER, H. A., FAY, R. C., LEWIS, F., SAYLER, A. A.: J. Am. Chem. Soc., **98,** 6932 (1976)
[17] BONATI, F., UGO, R.: J. Organomet. Chem., **10,** 257 (1967)
[18] HARRELD, C. S., SCHLEMPER, E. O.: Acta Crystallogr. Sec. B, **27,** 1964 (1971)
[19] ALYEA, E. C., RAMASWAMY, B. S., BHAT, A. N., FAY, R. C.: Inorg. Nucl. Chem. Lett., **9,** 399 (1973)
[20] COLAPIETRO, M., VACIAGO, A., BRADLEY, D. C., HURTSHOUSE, M. B., RANDALL, I. F.: Chem. Commun., **1970,** 743; J. Chem. Soc. Dalton Trans., **1972,** 1052
[21] BRADLEY, D. C., GITLITZ, M. H.: Chem. Commun., **1965,** 289; J. Chem. Soc. (A), **1969,** 1152
[22] CHATT, J., DUNCANSON, L. A., VENANZI, L. M.: Soumen Kemi, **B29,** 75 (1956); Nature, **177,** 1042 (1956); O'CONNOR, D. C., GILBERT, J. D., WILKINSON, G.: J. Chem. Soc. (A), **1969,** 84
[23] FRITZ, H. P.: Adv. Organomet. Chem., **1,** 279 (1964)

Shyam KUMAR
Narender K. KAUSHIK
Department of Chemistry, University of Delhi, Delhi-110007 India

Acta Chimica Academiae Scientiarum Hungaricae, Tomus 109 (1), pp. 21—27 (1982)

TRANSITION METAL COMPLEXES WITH α-(1,3-DIOXOINDANE-2-YL)-ETHYLIDENE-*p*-TOLUIDINE

M. A. QURAISHI,* B. KUMAR** and D. SHARMA***

(Department of Chemistry, Government Science College, Jabalpur, M. P., India)

Received December 1, 1980

Accepted for publication January 27, 1981

Reaction products of α-(1,3-dioxoindane-2-yl)-ethylidene-*p*-toluidine with Ni^{2+}, Co^{2+}, Mn^{2+}, Zn^{2+}, UO_2^{2+} and Th^{4+} are reported. The ligand, HL, forms complexes of the type $ML_2.2CH_3OH$(M = Ni^{2+}, Co^{2+} and Mn^{2+}), ZnL_2 $UO_2(L)Cl.CH_3OH$ and $ThL_2.Cl_2$. These metal chelates were characterized on the basis of elemental analysis, molecular weight, electrical conductivity, IR, far-IR, electronic spectra and magnetic susceptibility measurements. Infrared spectral measurements revealed the monoprotic bidentate nature of the ligand coordinating through azomethine nitrogen and enolic oxygen. The magnetic susceptibility data of the complexes at 300 K suggested the paramagnetic nature of Ni^{2+}, Co^{2+} and Mn^{2+} complexes and the diamagnetic nature of Zn^{2+}, UO_2^{2+}, and Th^{4+} complexes. The electronic spectral assignments consistent with the tetrahedral stereochemistry for Zn^{2+} complexes and the octahedral environment for the rest of the metal chelates. The complexes are monomers and nonelectrolytes.

Introduction

A perusal of literature revealed that a lot of matter is available pertaining to the transition metal complexes of anils [1—7] but there is no report about the synthesis of metal chelates of α-(1,3-dioxoindane-2-yl)-ethylidene--*p*-toluidine. In this paper we wish to report a few hitherto unknown Ni^{2+}, Co^{2+}, Mn^{2+}, Zn^{2+}, UO_2^{2+} and Th^{4+} complexes of a bidentate ON donor ligand α-(1,3-dioxoindane-2-yl)-ethylidene-*p*-toluidine. The ligand is capable of existing in the keto-enol tautomeric form [8] **I** and **II** as the later form produces

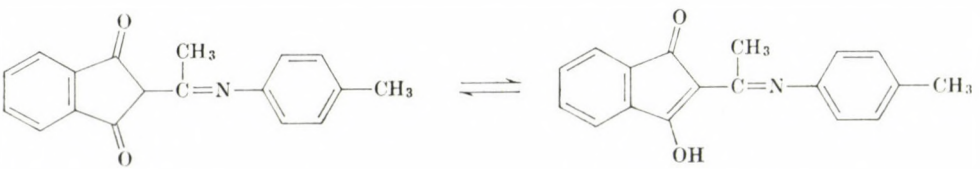

I **II**

* To whom correspondence should be addressed: Department of Chemistry, Kurukshetra University, Kurukshetra-132119, Haryana, India

** Present address: E-243, ET Hostel, Sector III. BHEL, Hardwar, India

*** Present address: Department of Chemistry, D. J. College, Baraut, Meerut (U. P.), India

the metal chelates by loosing enolic proton. The precursor of Schiff base 2-acyl-1,3-indanediones have been tested as a blood coagulant [9]. Hence the metal chelates of this ligand may be of biophysical and biological interest.

Experimental

Materials

Nickel acetate tetrahydrate, cobalt acetate monohydrate, manganese acetate tetrahydrate, zinc acetate dihydrate, anhydrous dioxouranium dichloride and anhydrous thorium tetrachloride used were the products of BDH.

Physical Measurements

Nickel was determined gravimetrically as bis(dimethyglyoximato)nickel(II). The metal content of the complexes of Co^{2+}, Mn^{2+} and Zn^{2+} was determined by EDTA titrations using Xylenol Orange or Eriochrome Black-T as an indicator. Thorium and uranium contents were determined as their respective oxides, ThO_2 and U_3O_8, gravimetrically. The chloride analysis was performed by VOLHARD's method. Microanalyses were obtained from the analytical services of Delhi University, Delhi. The molecular weight measurements were done ebullioscopically by a Gallenkamp type CM.82T was used for conductivity measurements. The infrared and far infrared spectra were recorded in nujol mull on a Beckman IR-20 infrared spectrophotometer from Kurukshetra University, Kurukshetra. The elektronic spectra were recorded on a Beckman DU spectrophotometer. The magnetic susceptibility of the complexes were measured by the GOUY method using mercury(II)-tetrathiocyanocobaltate(II) as a calibrant.

Preparation of the ligand

2-acetyl-1,3-indanedione (1.88 g, 0.01 mole) and *p*-toluidine (1.05 g, 0.01 mole) were dissolved in absolute ethanol (20 mL) and the mixture was refluxed in the presence of a catalytic amount of acetic acid on a water bath for 3 hrs. On cooling a green solid compound separated out which crystallized from ethanol in the form of green needles (yield 62%, m.p. 140°).

Preparation of the complexes

Appropriate metal salts (0.01 mole) dissolved in 50 mL methanol and the ligand (0.02 mole) dissolved in 30 mL methanol were refluxed on a water bath for 3–4 hrs. The solid compounds were obtained on partial evaporation of the solvent at room temperature. The compounds were suction filtered, washed and recrystallized from methanol and dried in vacuo. (Yield: 40–50%, appearance: yellowish green to brown.) The results of elemental analysis are given in Table I.

Results and Discussion

The elemental analyses (Table I) indicate a 1 : 2 (metal to ligand) stoichiometry for the Ni^{2+}, Co^{2+}, Mn^{2+}, Zn^{2+} and Th^{4+} and a 1 : 1 stoichiometry for the UO_2^{2+} complexes. These compounds are insoluble in water and benzene but soluble in methanol, ethanol and acetone. The electrical conductance data for methanol indicate that all the complexes are nonelectrolytes. The molecular weight data indicate the monomeric nature of the complexes.

Infrared Spectra

The Ni^{2+}, Co^{2+}, Mn^{2+} and UO^{2+} complexes form associates with methanol as evidenced by the existence of a broad band ν(OH) strecth and ν(C—O)CH_3OH at around 3400 cm^{-1} and 990—1000 cm^{-1} respectively [10—

Table I

Elemental analysis molecular weight, electrical conductance of complexes of α-(1,3-*dioxoindane-2-yl*)-*ethylidene-p-toluidine*

Compound	Mol. formula	Mol. Wt. Calcd. (found)	Colour	Conductance Λ^{-1} mol^{-1} cm^2	Elemental analysis, Calcd. (Found)				
					C%	H%	N%	M%	Cl%
DET	$C_{18}H_{15}NO_2$	277 (275)	Green	—	77.98 (78.20)	5.42 (5.29)	5.05 (4.89)	—	—
Ni(II)$(DET)_2$.2 CH_3OH	$C_{38}H_{36}N_2O_6Ni$	674.7 (671)	Yellow-Green	10.5	67.59 (67.32)	5.34 (5.56)	4.15 (4.01)	8.70 (8.51)	—
Co(II)$(DET)_2$.2 CH_3OH	$C_{38}H_{36}N_2O_6Co$	674.9 (671)	Yellow	8.7	67.57 (67.80)	5.33 (5.02)	4.15 (4.43)	8.73 (8.97)	—
Mn(II)$(DET)_2$.2 CH_3OH	$C_{38}N_{36}N_2O_6Mn$	670.8 (681)	Brown	3.5	67.97 (67.56)	5.37 (5.30)	4.17 (4.35)	8.18 (8.37)	— —
Zn(II)$(DET)_2$.	$C_{36}H_{28}N_2O_4Zn$	617.4 (602)	Light-Green	11.8	69.97 (69.51)	4.54 (4.63)	4.54 (4.30)	10.59 (10.88)	—
UO_2(VI)Cl(DET).CH_3OH	$C_{18}H_{18}NO_5UCl$	601.5 (600)	Brown	7.4	35.91 (36.23)	2.99 (3.31)	2.32 (2.11)	39.57 (39.28)	5.90 (6.11)
Th(IV)$Cl_2(DET)_2$	$C_{36}H_{28}N_2O_4ThCl_2$	855 (852)	Yellow-Green	8.3	50.53 (50.30)	3.27 (3.10)	3.27 (3.54)	27.13 (27.58)	8.30 (8.59)

* DET = α-(1,3-dioxoindane-2-yl)-ethylidene-*p*-toluidene

11]. In the present complexes the downward shift of ν(C—O) band of CH_3OH occurring at 1034 cm^{-1} further confirmed the coordination of methanol in the complexes [12—13]. The complexes do not loose weight on heating at 120 °C for 3—4 hrs and this also confirms the coordination of CH_3OH to Ni^{2+}, Co^{2+}, Mn^{2+} and UO_2^{2+} ions.

In the infrared spectra of the ligand two bands were observed one at 1690 cm^{-1} and another at 1650 cm^{-1} assignable to ν(C=O). In all the metal chelates this former band persists at the same position but the second band disappears and a new band at 1230—1240 cm^{-1} is observed. The existence of the former band reveals the nonparticipation in coordination of the keto group. The appearance of the band in the later region suggests that the coordination takes place *via* deprotonation of enolized oxygen of the ligand.

The medium intensive ν(C=N) stretch of the ligand occurs at 1620 cm^{-1}. This band is decreased by 5—15 cm^{-1} in all the complexes along with changes in deformation, wagging and rocking azomethine vibrations and these suggest that the metals are coordinated through the azomethine nitrogen atom. In the far-IR spectra the bands assigned to ν(Ni—N), ν(Co—N), ν(Mn—N) and ν(U—N) at 460, 435, 305 and 300 cm^{-1} in the complexes also confirmed the mode of metal-nitrogen linkage [14—16].

The complex of dioxouranium(VI) exhibits a strong band at 900 cm^{-1} characteristic of ν_{as} (OUO) and the ν_s (OUO) occurs at around 810 cm^{-1} also compatible with the earlier work [17—19]. The region 290—325 cm^{-1} is characteristic of metal-oxygen stretching vibrations [20]. The weak band

Table II

Important assignments of IR, far-IR, magnetic susceptibility and electronic spectra of the transition metal compounds

Compound	ν(C=O) (cm^{-1})	ν(C=N) (cm^{-1})	ν(C—OH) enolic (cm^{-1})	ν(M—O) (cm^{-1})	ν(M—N) (cm^{-1})	μ_{eff} B.M. (300 K)	ν_{max} (cm^{-1})
DET	1690	1620	—	—	—	—	—
Ni(II)(DET)$_2$.2 CH_3OH	1690	1590	1235	430	460	3.26	25,000
				300			15,600
							9,400
Co(II)(DET)$_2$.2 CH_3OH	1690	1590	1230	415	435	4.85	20,500
				290			18,000
							8,000
Mn(II)(DET)$_2$.2 CH_3OH	1690	1600	1235	425	305	5.90	29,850
				295			33,000
Zn(II)(DET)$_2$.	1690	1595	1230	325	—	Diamag.	—
UO_2(VI)Cl(DET)$_2$.CH_3OH	1690	1580	1235	—	300	Diamag.	22,000
Th(IV)Cl$_2$(DET)$_2$.	1690	1590	1230	480	—	Diamag.	—

observed at 300, 290, 195 and 325 cm^{-1} in the spectra of respective metal complexes may be assigned as ν(Ni—O), ν(Co—O), ν(Mn—O), and ν(Zn—O) stretch [21—22]. In the thorium(IV) complex the weak band appeared at 480 cm^{-1} is due to combined frequency of ν(Th—O) and ν(Th—N) stretch [23]. Another set of new bands appear in the region 415—460 cm^{-1} [21] and the complexes of Ni^{2+}, Co^{2+} and Mn^{2+} exhibit at 430, 415, 425 cm^{-1}, respectively. They are originated from metal oxygen stretching linkages [24].

The far-infrared spectral measurements indicated the presence of a medium intensive band at 230 and 245 cm^{-1} in the UO_2^{2+} and Th^{4+} complexes respectively. This band has been assigned to M—Cl stretching vibrations and shows direct coordination of Cl^- to the metal atom as reported by earlier workers [25—26].

Magnetic and Spectral Studies

The magnetic moments at 300 K for Ni^{2+}, Co^{2+} and Mn^{2+} complexes are 3.26, 4.85, 5.90 B.M., respectively. The values are within the range postulated for high-spin complexes of the respective metal [27—28]. The values indicate octahedral stereochemistry. The magnetic moment of the high spin octahedral Co^{2+} complex is higher than the spin-only value due to very large orbital contribution arising from orbitally degenerated ground states. The high-spin Mn^{2+} complex has an orbitally nondegenerated 6_S ground term [29]. The complexes of Zn^{2+} are diamagnetic. This is expected for a $3d^{10}$ system. This complex is tetracoordinated and a tetrahedral structure with sp^3 hybridization is suggested to this complex. The magnetic susceptibility measurements indicate that the complexes of UO_2^{2+} and Th^{4+} are diamagnetic as expected for the $5f^0$ system.

Electronic Spectra

The electronic spectra of Ni^{2+}, Co^{2+} and Mn^{2+} complexes were recorded in their 0.001 mole solution in 10 mL methanol.

Nickel(II) complex

Ni^{2+} complex exhibits the following absorption bands for the corresponding assignments: 25,000, 15,600, 9,400 cm^{-1} for $3A_{2g} \rightarrow 3T_{1g}(P)$, $3A_{2g} \rightarrow$ $\rightarrow 3T_{1g}(F)$ and $3A_{2g} \rightarrow 3T_{2g}$, respectively. This confirms coordination number six with an octahedral structure [30—32].

Cobalt(II) complex

Co^{2+} complex shows the following electronic absorption bands: 20,500, 18,000, 8,000 cm^{-1} for the corresponding assignments of $4T_{1g}(F) \rightarrow 4T_{1g}(P)$

(ν_3), $4T_{1g} \rightarrow 4A_{2g}$ (ν_2), $4T_{1g} \rightarrow 4T_{2g}(F)$ (ν_1). This suggests hexa-coordination and octahedral environment for Co^{2+} [33—36].

Manganese(II) complex

The weak absorptions for this complex were observed in the electronic spectrum indicating the presence of only sextet level $6A_{1g}$ with the lowest configuration $t_{2g}^3 e_g^2$. No higher lying sextet is present and hence the transition is spin forbidden. However, due to spin orbital interaction these transitions appear as very weak absorption bands. The weak band observed at 29,850 cm^{-1} and 33,000 cm^{-1} correspond to $^6A_{1g} \rightarrow {}^4E_g(D)$ and $^6A_{1g} \rightarrow {}^4T_{1g}(P)$ transitions, respectively [37].

Dioxouranium(VI) complex

The complex exhibits an electronic spectral band at around 22,000 cm^{-1} and this is attributed to $^1E_g^+ \rightarrow 3\pi_u$ transition which is a typical for OUO symmetric stretch for the first excited state [38].

*

One of the authors (M.A.O.) is thankful to UGC, New Delhi for the financial support.

REFERENCES

[1] McKenzie, S. F. S.: Inorg. Chim. Acta, **26,** L-49 (1978)
[2] Cassity, R. P., Taylor, L. T.: J. Coord. Chem., **9,** 7 (1979)
[3] Deshmukh, K. G., Bhobe, R. A.: J. Incrg. Nucl. Chem., **40,** 135 (1978)
[4] Titus, S. J. E., Barr, W. M., Taylor, L. T.: Inorg. Chim. Acta, **32,** 103 (1979)
[5] Consiglio, M., Maggio, F., Pizzino, T., Romano, V.: Inorg. Nucl. Chem. Lett., **14,** 135 (1978)
[6] Maley, L. E., Mellor, D. P.: Nature, **159,** 370 (1947)
[7] Yamada, S.: Coord. Chem. Rev., **1,** 415 (1966)
[8] Gupta, S. C., Quraishi, M. A., Ihawan, S. N.: Indian J. Chem., **18,** 547 (1979)
[9] Shapiro, L., Geiger, K., Freedman, L.: J. Org. Chem., **25,** 1860 (1960)
[10] Lindoy, L. F., Linvingstone, S. E.: Inorg. Chem., **2,** 1149 (1968)
[11] Nakamoto, K.: Infrared Spectra of Inorganic and Coordination Compounds, 220 p. Wiley Intersicence, New York, 1969
[12] Herzberg, G.: Molecular Spectra and Molecular Structure, Nostrand D. V., Vol. **II,** 335 p, New York 1959
[13] Adams, D. M.: Metal Ligand and Related Vibrations, Arnold, E., London 1967
[14] Sengupta, S. K., Sahni, S. K., Kapoor, R. N.: Acta Chim. Acad. Sci. Hung., **104,** 89 (1980)
[15] Kundu, P. C., Beru, A. K.: Indian J. Chem., **18A,** 62 (1979)
[16] Hutchinson, B., Takemoto, J., Nakamoto, K.: J. Am. Chem. Soc., **92,** 3335 (1970)
[17] Hsieh, A. T. T., Sheahan, R. M., West, B. O.: Aust. J. Chem., **28,** 885 (1975)
[18] Jones, M. M.: J. Chem. Phys., **23,** 2105 (1955); Comyns, A. E., Gatehouse, B. M., Watt, E.: J. Chem. Soc., **1958,** 4055
[19] McGlynn, S. P., Smith, J. K., Neely, W. C.: J. Chem. Phys., **35,** 105 (1961)
[20] Reedijk, J.: Inorg. Chim. Acta, **5,** 687 (1971)
[21] Sangal, S. K., Rana, V. B.: Acta Chim. Acad. Sci. Hung., **104,** 29 (1980)
[22] Adams, R. W., Martin, R. L., Winter, G.: Aust. J. Chem., **20,** 773 (1967)
[23] Sharma, C. L., Singh, A. K., Pandey, S. P.: J. Indian Chem. Soc., **L—VI,** 28 (1979)

[24] MIKAMI, M., NAKAGAWA, I., SHIMANOUCHI, T.: Spectrochim. Acta, **23A**, 1037 (1967); **25A**, 365 (1969)
[25] VIJAY, R. G., TANDON, J. P.: Indian J. Chem., **17 A**, 188 (1979)
[26] DASH, K. C., MOHANTA, H.: Transition Metal Chem., **2**, 6 (1977)
[27] COTTON, F. A., WILKINSON, G.: Advanced Inorg. Chem., 752 p. Interscience Publishers, Inc., New York, 1962
[28] FLUKUDA, Y., SONE, K.: J. Inorg. Nucl. Chem., **34**, 2315 (1972); **37**, 455 (1975)
[29] SAHNI, S. K., RANA, V. B.: Indian J. Chem., **15A**, 890 (1977)
[30] SINGH, P. P., SRIVASTAVA, A. K., PATHAK, L. P.: J. Coord. Chem., **9**, 67 (1979)
[31] FERNELIUS, W. C., MANCH, W.: J. Chem. Educ., **38**, 192 (1961)
[32] MICHAEL, J., WALTON, T. A.: J. Inorg. Nucl. Chem., **37**, 71 (1975)
[33] CLARK, R. J. H., WILLIAMS, C. S.: J. Chem. Soc., **A, 1966**, 1425
[34] LEVER, A. B. P., LEWIS, J., NYHOLM, R. S.: J. Chem. Soc., **1962**, 1235
[35] GOODWIN, H. A., SYLVA, R. N.: Aust. J. Chem., **20**, 217 (1967)
[36] LEVER, A. B. P.: J. Chem. Educ., **45**, 711 (1968)
[37] CHAUDHURY, G. R., DASH, K. C.: Indian J. Chem., **17A**, 364 (1979)
[38] MCGLYNN, S. P., SMITH, J. K.: J. Mol. Spectrosc., **6**, 164 (1961)

M. A. QURAISHI
B. KUMAR
D. SHARMA

Department of Chemistry, Government Science College, Jabalpur, M.P., India

Acta Chimica Academiae Scientiarum Hungaricae, Tomus 109 (1), pp. 29—37 (1982)

FLUORESCENCE, TRANSMITTANCE AND LIGHT SCATTERING STUDIES ON SOLUBILIZATION OF ANTHRAQUINONE

R. C. BHARDWAJ, V. N. MISHRA and R. C. KAPOOR*

(Department of Chemistry, University of Jodhpur, Jodhpur, Raj., India)

Received September 2, 1980

Accepted for publication February 4, 1981

The solubilization action of surfactants on anthraquinone has been studied with the help of fluorescence and transmittance spectroscopy. The fluorescence peak heights at 385 and 405 nm increase on increasing the concentration of surfactant solution reaching limiting values. The solubilization phenomenon was also confirmed by light scattering measurements, since a large decrease in scattering flux occurred on increasing the concentration of surfactants. The results have been attributed to micelle formation action of surfactants.

Introduction

Solubilization caused by surfactant micelles had been reviewed earlier by KLEVENS [1] and MCBAIN [2]. The process of solubilization caused by surface-active agents has also been investigated by ELWORTHY and coworkers [3]. Solubilization of proteins, water insoluble hydrocarbons and some phenolic compounds by surfactants has been studied by HSIN-CHOU CHAING [4], FRIBERG [5], DONBROW [6] and coworkers. OGINO and coworkers [7] studied the solubilizing action of some anionic surfactants. KAPOOR and MISHRA [8, 9] have studied the solubilization of 9,10-diphenylanthracene in surfactant solutions employing a fluorescence technique and have interpreted their results in terms of micells formation. Solubilization of anthracene by surfactant solutions have recently been investigated by MISHRA and coworkers [10]. HAUTALA [11], SCHORE [12], GEIGER [13] and coworkers have employed naphthalene, pyrene and indole lumophore as fluorescent probes to examine the structure and dynamics of solutions of common micelle-forming detergents.

We report here investigations on the solubilization of anthraquinone occurring in the presence of surfactant solutions, employing fluorescence and transmittance measurements and light scattering studies.

Experimental

Fluorescence studies were made on a Perkin-Elmer Spectrofluorimeter model 204A with a xenon lamp as the light source. The slit width for the excitation and emission spectra was kept at 10 nm and a cell of 1 cm path length was used. The transmittance in ultraviolet

* To whom correspondence should be addressed

and visible regions was recorded with a Specord UV-Vis (range 50,000 to 12,500 cm^{-1}) instrument made by Carl Zeiss Jena, with a deuterium lamp D2E and tungsten filament lamp 6V30W as light source for the UV and visible spectral regions, respectively. Quartz cells of 1 cm path length were used. The transmittance was recorded as a function of wavenumber.

Light scattering studies were carried out with a Brice-Phoenix light scattering photometer (USA) Model 2000A with an attached multiflex galvanometer. A mercury lamp was used as the light source with a blue interference filter of 436 nm for the incident light; measurements were made at 90° angle to the incident light.

The stock solution of analytically pure anthraquinone (SISCO Chem.) was prepared in pure ethanol. All the experiments were carried out at room temperature (23 to 28 °C) in 5% ethanolic medium, keeping the final concentration of anthraquinone at 5×10^{-6} *M*.

The following surfactants were used for the study.

(A) ANIONIC:
- (i) Dodecyl benzene sodium sulfonate (DBSS).
- (ii) Dioctyl sodium sulfo succinate (DSSS).

(B) CATIONIC:
- (iii) Cetyltrimethylammonium bromide (CTAB)
- (iv) Cetyldimethylbenzylammonium chloride (CDBAC)
- (v) Cetylpyridinium bromide (CPB)

(C) NONIONIC:
- (vi) Polyoxyethylene teroctyl phenol (Eq-10) (Tx-100)
- (vii) Polyoxyethylene sorbitan monopalmitate (Tween-40)
- (viii) Polyoxyethylene sorbitan monosterate (Tween-60)
- (ix) Polyoxyethylene sorbitan mono-oleate (Tween-80)
- (x) Polyoxyethylene (E_{23}) lauryl ether (Brij-35).

All surfactants were "Sigma" USA product, except Brij-35 which was a BDH product, and were used as such. The purity of surfactants was checked by determining their cmc values by surface tension measurements employing the drop weight method.

Results

Fluorescence studies

The excitation spectrum of anthraquinone gave peaks at 356 and 375 nm. The emission spectrum caused by excitation at 356 nm in solution containing 5% ethanol showed two peaks, at 385 and 405 nm.

All the nonionic and anionic surfactants caused enhancement in fluorescence intensity, while cationic surfactants showed an increase during initial addition only. Subsequently at higher concentration a decrease in fluorescence intensity was observed. Observations made with nonionic, anionic and cationic surfactants are given in Figs 1—3 respectively.

In 5% ethanolic medium the peak heights at 385 and 405 nm increased on increasing the concentration of nonionic and anionic surfactants and reached a limiting value. On the other hand with the cationic surfactant CTAB the decrease in fluorescence intensity started to occur at .008% and reached a minimum value at 0.12% concentration. Readings could not be taken at higher concentrations with some cationic and anionic surfactants due to their limited solubility at room temperature. Therefore, the limiting values of fluorescence peak heights could not be reached with these surfactants.

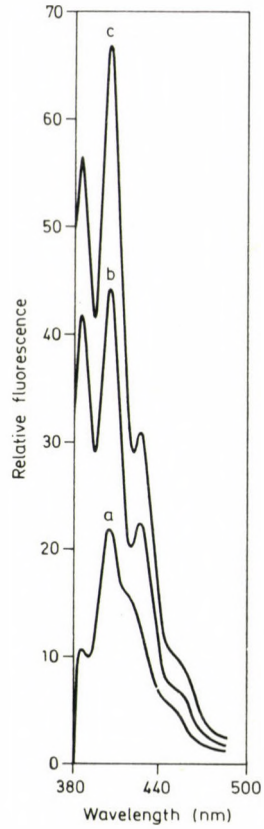

Fig. 1. Emission spectra; a. anthraquinone (5×10^{-6} *M*), b. anthraquinone + 0.10% Tween-80, c. anthraquinone + 0.22% Tween-80; $\lambda_{ex} = 356-358$ nm

Effect of ethanol

Enhancement in fluorescence intensity was also observed on adding ethanol to the solution of anthraquinone. The peaks heights at 385 and 405 nm increased on increasing the concentration of ethanol and reached their maximum values in the presence of 80% ethanol. Enhancement in fluorescence intensity on increasing the concentration of ethanol from 10 to 80% is given in Fig. 4. The influence of varying the concentration of ethanol on the peak heights of anthraquinone are given in Table I.

Transmittance studies

The transmittance spectrum of anthraquinone gave four peaks, at 340, 356, 375 and 392 nm. The addition of nonionic, anionic and cationic surfactants resulted in a decrease in transmittance, disappearance of the peak at

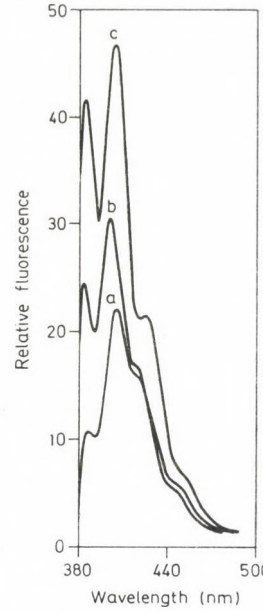

Fig. 2. Emission spectra; a. anthraquinone (5×10^{-6} *M*), b. anthraquinone + 0.01% DSSS, c. anthraquinone + 0.25% DSSS; $\lambda_{ex} = 356-358$ nm

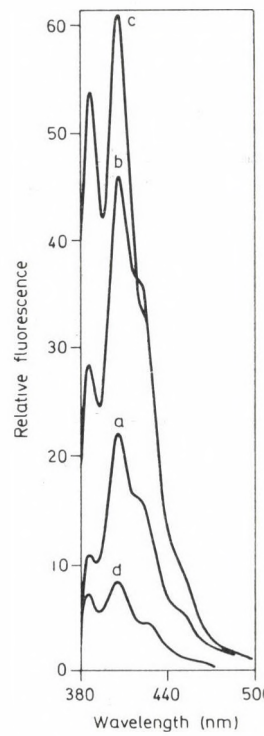

Fig. 3. Emission spectra; a. anthraquinone (5×10^{-6} *M*), b. anthraquinone + 0.004% CPB, c. anthraquinone + 0.016% CPB, d. anthraquinone + 0.16% CPB; $\lambda_{ex} = 356$ nm

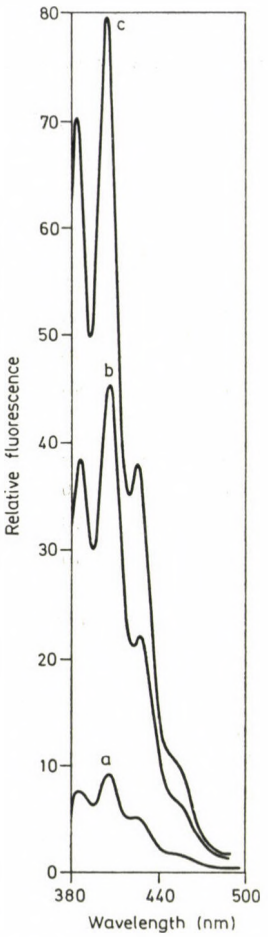

Fig. 4. Emission spectra; a. anthraquinone (5×10^{-6} *M*) in 5% ethanolic medium, b. anthraquinone in 30% ethanolic medium, c. anthraquinone in 80% ethanolic medium; $\lambda_{ex} = 356$ nm

392 nm and increase in peak heights at 340, 356 and 375 nm. A red shift of 2—3 nm was observed in all the peaks. The changes observed during addition of nonionic (Tween-60, Tx-100), anionic (DBSS, DSSS) and cationic (CTAB, CPB) surfactants are illustrated in Figs 5—7.

Light scattering studies

The scattering intensity was measured in terms of a galvanometer deflection. It was observed that the galvanometer deflection decreased and reached a minimum value in each case on progressive addition of each surfactant. The observations made with Tween-80 (nonionic), DBSS (anionic) and

Table I

Variation of fluorescence intensity vs. ethanol concentration

No.	% of Ethanol	Fluorescence intensity (arbitrary units)	
		385 nm	405 nm
1.	5	8	9
2.	10	9	11
3.	20	12	14
4.	30	39	45
5.	40	42	47
6.	50	45	53
7.	60	56	67
8.	70	63	73
9.	80	70	80
10.	90	70	80
11.	100	70	80

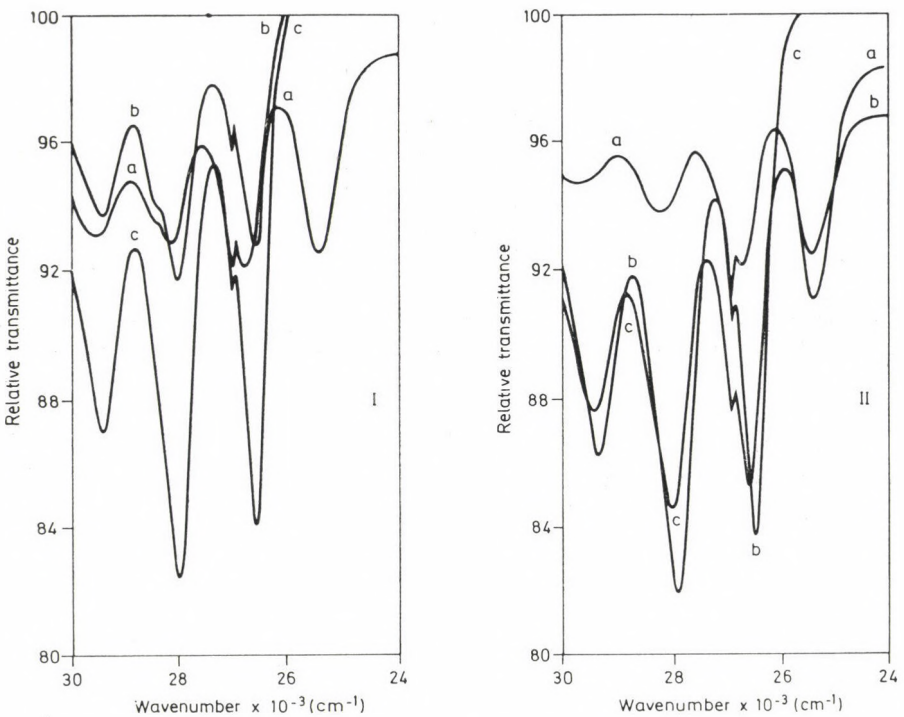

Fig. 5. Transmittance spectra; (I) a. anthraquinone (5×10^{-6} *M*), b. anthraquinone + 0.02% Tween-60, c. anthraquinone + 0.10% Tween-60. (II) a. anthraquinone (5×10^{-6} *M*), b. anthraquinone + 0.02% TX-100, c. anthraquinone + 0.05% TX-100; $\lambda_{ex} = 356$ nm

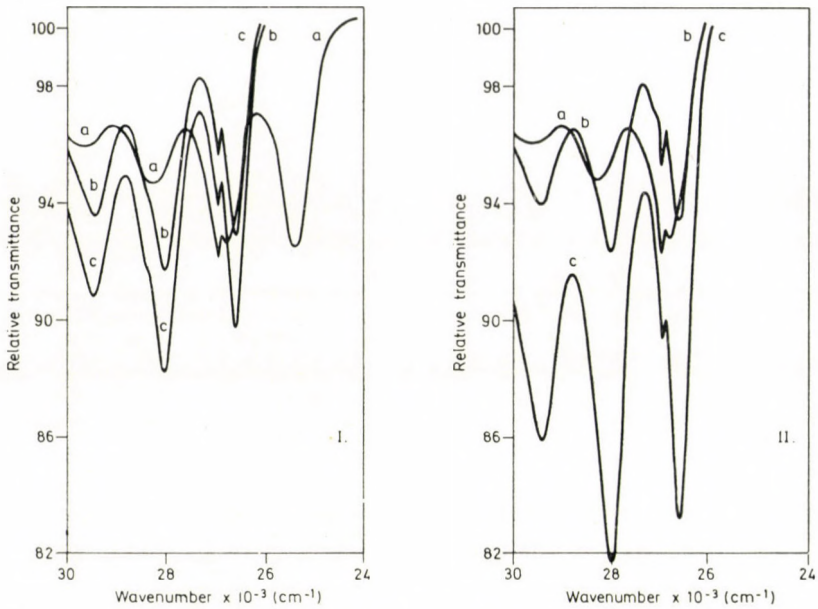

Fig. 6. Transmittance spectra; (I) a. anthraquinone (5×10^{-6} *M*), b. anthraquinone + 0.20% DSSS, c. anthraquinone + 0.35% DSSS. (II) a. anthraquinone (5×10^{-6} *M*), b. anthraquinone + 0.05% DBSS, c. anthraquinone + 0.10% DBSS

CTAB (cationic) are given in Fig. 8. It was noted that after centrifuging the solution at 16,000 RPM for twenty minutes, the galvanometer deflection reached zero value which was initially 100 before centrifuging the same solution. This clearly indicates that the deflection was due to insoluble particles present in the solution of anthraquinone which were later removed by centrifuging.

Discussion

These observations can be explained on the basis of the solubilizing action of the surfactants. The enhancement in the fluorescence intensity and the disappearance of the peak at 392 nm in the transmittance spectrum appears to be due to the solubilization of suspended particles of anthraquinone in surfactant micelles. This is also supported by light scattering studies since the scattering of incident light by suspended particles decreases on addition of surfactants (measured as galvanometer deflection). It is notable that the same concentration of surfactant was needed for (i) disappearance of the peak from the transmittance spectrum, (ii) for light scattering to reach a minimum level and (iii) for fluorescence intensities to reach their maximum value. The solubilization action is also confirmed by observing the effect of ethanol on

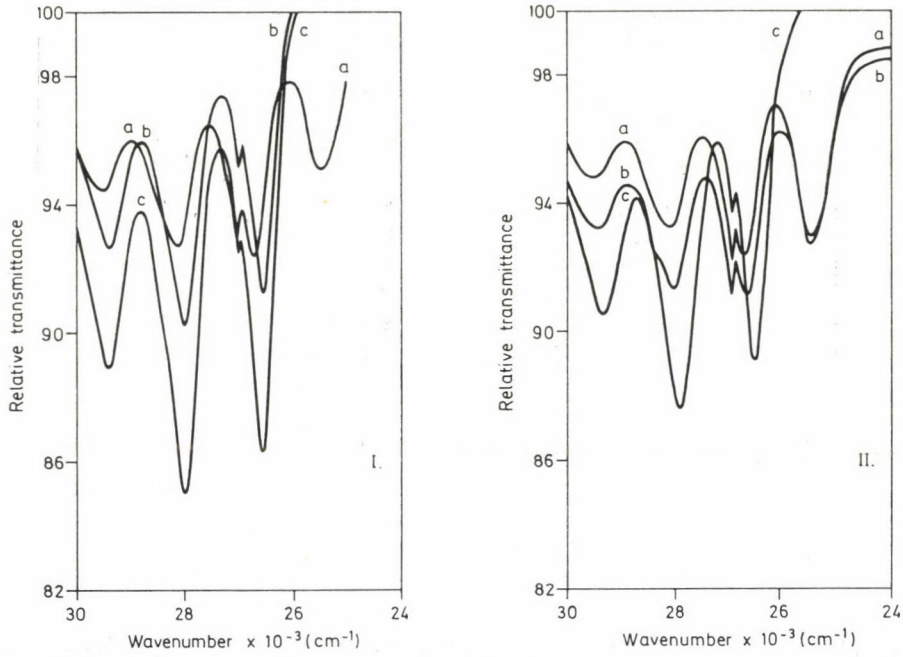

Fig. 7. **Transmittance spectra; (I) a. anthraquinone (5×10^{-6} *M*), b. anthraquinone + 0.08% CTAB, c. anthraquinone + 0.10% CTAB. (II) a. anthraquinone (5×10^{-6} *M*), b. anthraquinone + 0.02% CPB, c. anthraquinone + 0.08% CPB**

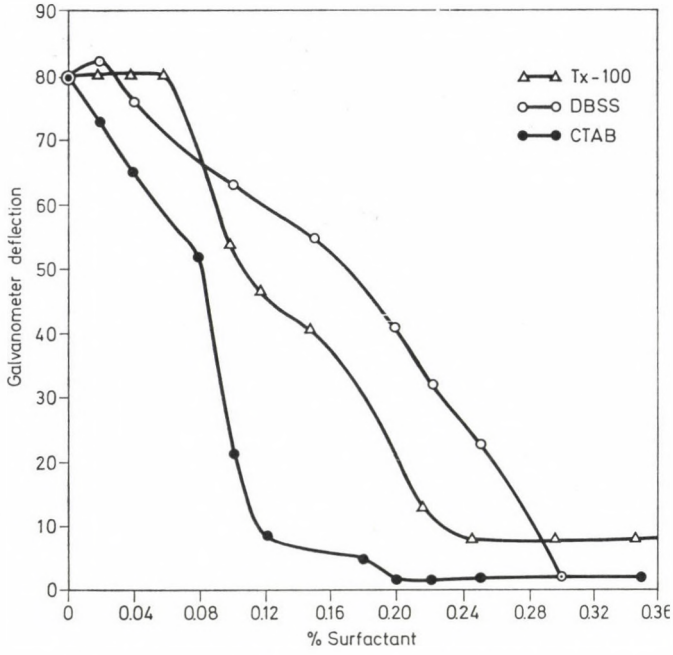

Fig. 8. **Plot of % Surfactant *vs.* scattering intensity**

the fluorescence of anthraquinone. The peak heights increased on the addition of ethanol in a manner similar to that observed with the surfactants. In 80% ethanol anthraquinone appeared to be fully solubilized at the concentration employed.

It is apparent that anthraquinone is not fully solubilized in 5% ethanolic medium. The suspended particles of anthraquinone solubilize on addition of surfactants or on increasing the ethanol concentration. The disappearance of the peak at 392 nm in transmittance spectrum is also due to the solubilization of the suspended particles. Thus there appears to be a straightforward correlation between solubilizing action and enhancement in fluorescence emission. The value of the limiting concentration of each surfactant is found to be higher than its critical micelle concentration.

*

Thanks are due to University Grants Commission for the grant of a project under which this work was made possible and for the award of a Junior Research Fellowship to one (RCB) of the authors.

REFERENCES

[1] KLEVENS, H. B.: Chem. Rev., **47**, 1 (1950)
[2] MCBAIN, J. W., HUTCHINSON: Solubilization and Related phenomena, Academic Press, New York 1955
[3] ELWORTHY, P. H., FLUORENCE, A. T., MACFARLANE, C. B.: Solubilization by Surface Active Agents, Chaucer Press Ltd., Bungay, Suffolk Great Britain 1968
[4] CHOU CHAING, H., AARON, L.: J. Phys. Chem., **79**, 1935 (1975)
[5] FRIBERG, S., BURACZEWSKA, I., RAVEY, J. C.: Proc. Int. Symp. 1976 (Pub. 1977) **2**, 901, Ed. MITTAL, K. L., Plenum Press, New York
[6] DONBROW, M., AZAZ, E.: J. Colloid Interfac. Sci., **57**, 20 (1976)
[7] OGINO, K., ABE, M.: J. Am. Oil. Chem. Soc., **52**, 465 (1975)
[8] KAPOOR, R. C., MISHRA, V. N.: Indian J. Chem., **14A**, 123 (1976)
[9] MISHRA, V. N., BHARDWAJ, R. C., KAPOOR, R. C.: Cellulose Chem. Technol, **14**, 801 (1980)
[10] KAPOOR, R. C., MISHRA, V. N.: J. Indian Chem. Soc., **56**, 735 (1979)
[11] HAUTALA, P. R., SCHORE, N. E., TURRO, N. J.: J. Am. Chem. Soc., **95**, 5508 (1973)
[12] SCHORE, N. E., TURRO, N. J.: J. Am. Chem. Soc., **97**, 2488 (1975)
[13] GEIGER, M. W., TURRO, N. J.: Photochem., **22**, 273 (1975)

R. C. BHARDWAJ
V. N. MISHRA
R. C. KAPOOR

Department of Chemistry, University of Jodhpur, Jodhpur (Rajasthan) India

[*Acta Chimica Academiae Scientiarum Hungaricae, Tomus 109 (1), pp. 39—49 (1982)*

STEREOCHEMICAL STUDIES, XLVIII* SATURATED HETEROCYCLES, XXVII**

CRYSTAL AND MOLECULAR STRUCTURE OF 2-(*p*-NITROPHENYL)-*cis*-5,6--TETRAMETHYLENE-2,3,5,6-TETRAHYDRO-1,3-OXAZINE AND 2-(*p*-NITROPHENIL-*cis*-4,5-TETRAMETHYLENE-2,3,4,5-TETRAHYDRO-1,3-OXAZINE

Gy. ARGAY,[1] A. KÁLMÁN,[1] F. FÜLÖP[2] and G. BERNÁTH[2]***

([1]Central Research Institute for Chemistry, Hungarian Academy of Sciences, Budapest and [2]Institute of Pharmaceutical Chemistry, University Medical School, Szeged)

Received January 13, 1981

Accepted for publication February 4, 1981

The structures of the title compounds have been established by X-ray crystallography from diffractometer data. Crystals of **1** are monoclinic, space group $P2_1/c$ with cell dimensions $a = 685.6$ (1), $b = 2106.3$ (1), $c = 1044.9$ (1) pm, $\beta = 117.82$ (1)°, $Z = 4$. Crystals of **2** are also monoclinic, space group $P2_1/c$ with cell dimensions $a = 658.5$ (4), $b = 1250.7$ (6), $c = 1605.4$ (6) pm, $\beta = 91.61$ (2)°, $Z = 4$. Both structures were solved by direct methods and refined by least-squares calculations to R values of 0.033 for 1730 reflexions for **1** and 0.076 for 1633 reflexions for **2**. The characteristic features of the conformations of these compounds in comparison with those of the analogous compounds reported hitherto are discussed.

Introduction

The synthesis and stereochemistry of bicyclic saturated heterocycles with condensed skeleton containing two heteroatoms have been the subject of our study for a long time. The main aims of our work can be summarized in the following: *a*, Synthetic work including the investigation of the ring closure of alicyclic 1,3-bifunctional compounds and the study of some reactions of the products; *b*, Conformational analysis by spectroscopic (IR, NMR) measurements and X-ray diffraction; *c*, A pharmacological screening of the synthesized compounds.

In Table I are collected the types of compounds investigated. A large number of stereoisomeric homologous and analogous derivatives were synthesized, therefore, a comparative evaluation was also possible.

Continuing this work, now we report the results of X-ray analysis of 2-(*p*-nitrophenyl)-*cis*-5,6-tetramethylene-2,3,5,6-tetrahydro-1,3-oxazine (**1**) and 2-(*p*-nitrophenyl)-*cis*-4,5-tetramethylene-2,3,4,5-tetrahydro-1,3-oxazine (**2**). The synthesis and spectroscopic study of **1** and **2** was reported earlier [1].

* Part XLVII: G. BERNÁTH, F. FÜLÖP, Gy. ARGAY, A. KÁLMÁN, P. SOHÁR: Tetrahedron Letters **22**, 3797 (1981)

** XXVI: L. Fodor, J. Szabó, G. Bernáth, L. Párkányi, P. Sohár: Tetrahedron Letters, **22**, 5077 (1981)

*** To whom correspondence should be addressed

Table I

Types of the investigated heterocycles

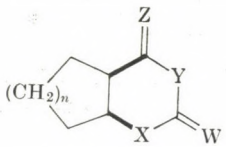

$n = 1, 2, 3$

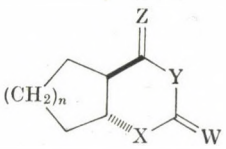

$n = 2, 3$

X	Y	W	Z	References	
				Synthesis Spectroscopy	X-ray
O	NH	Ar, H	H_2	[1, 2]	This work
NH	O	Ar, H	H_2	[1, 2]	This work
O	NH	O	H_2	[3, 4]	
NH	O	O	H_2	[3, 4]	
O	N	Ar	H_2	[5]	[5]
N	O	Ar	H_2	[5]	[5, 10]
N	NH	Ar	O	[6]	[11—13]
O	NH	Ar, H	O	[7]	[14, 15]
O	NR*	Ar, H	H_2	[8, 9]	
NR*	O	Ar, H	H_2	[8, 9]	

*R = CH_3, $CH_2C_6H_5$

X-Ray analysis

Crystal data

1: From single crystal diffractometry using monochromated CuK_α radiation ($\lambda = 154.18$ pm) $a = 685.6$ (1), $b = 2106.3$ (1), $c = 1044.9$ (1) pm, $\beta =$ $= 117.82$ (1)°, $Z = 4$, $D_c = 1.305$ Mg m^{-3}, space group $P2_1/c$ from systematic absences.

2: From Weissenberg and precession photographs taken with Ni-filtered CuK_α radiation ($\lambda = 154.18$ pm), $a = 658.5$ (4), $b = 1250.7$ (6), $c = 1605.4$ (6) pm, $\beta = 91.61$ (2)°, $Z = 4$, $D_c = 1.317$ Mg m^{-3} space group $P2_1/c$ from systematic absences.

Intensity data, structure determinations and refinements

1: Intensities of 2816 independent reflexions were collected in the range $2\Theta \leq 154°$ by a $\omega - 2\Theta$ scan on an Enraf-Nonius CAD-4 diffractometer with graphite-monochromated CuK_α radiation. Cell constants were determined by

least squares from the setting angles of 25 reflexions. After data reduction 1730 reflexions with $I - 3.0\sigma(I) > 0$ were taken as observed. No absorption correction was applied. The structure was solved with program MULTAN [16] by use of 244 normalized structure factors with $E \geq 1.8$. An E map computed from a phase set with the best consistency gave the positions of all non-hydrogen atoms ($R = 0.27$). Full-matrix least squares refinement of positional and vibrational parameters reduced R to 0.092. At this stage H positions were located from a difference Fourier map. Further anisotropic refinement of heavy atom positions including an extinction coefficient with fixed H coordinates gave $R = 0.043$. In the last three cycles of refinement the assigned H positions were also refined with fixed individual isotropic temperature factors. The final R was then 0.033 for 1730 observed reflexions ($R_w = 0.043$). Scattering factors were taken from *International Tables for X-ray Crystallography* [17].

2: Intensity data were collected on a Stoe semi-automatic two-circle (Weissenberg) diffractometer. After setting the crystal and the counter in an equi-inclination arrangement, the intensities of each two-dimensional reciprocal layer (0kl → 6kl) were measured automatically, but independently (for details see [18]). Cell constants were refined from Buerger precession photographs. 1648 independent reflexions were collected. No absorption correction was applied. The phase problem for 239 reflexions with $E \geq 1.25$ was solved by program SHELX [19]. The E-map computed from the solution with the best figure of merit revealed all the non-hydrogen atoms. Full-matrix isotropic and anisotropic refinement together with seven scale factors for 0kl → 6kl reduced R to the final value of 0.076 ($R_w = 0.119$) for 1633 reflexions. Prior to the refinement, all H atoms were generated from assumed geometries with X—H constrained to 108 pm. The positions of these generated H atoms were checked in a difference Fourier synthesis. A bonded H-atom scattering factor was employed [20] with complex neutral scattering factors for the remaining atoms [21, 22].

Discussion of the molecular structures

The final coordinates for non-hydrogen atoms of both isomers are given in Table II, the parameters for H atoms in Table III, and bond distances and angles in Tables IV and V. The atomic numbering, identical with that applied in the case of the corresponding partially saturated derivatives [5] is given in Fig. 1. The corresponding bond lengths and angles agree with each other within experimental error (3σ). As the results of the saturation of the C(2)—N(3) bonds of **12** and **14** [5] the C(2)—O(1) [C(sp^2)—O] bond lengths 136.2 (4) and 136.7 (5) pm increased up to 142.5 (2) and 142.1 (4) pm, respectively. The even more pronounced lengthening of the saturated C(2)—N(3) bonds [123.8

Table II

Fractional coordinates ($\times 10^4$) *for non-hydrogen atoms*
E.s.d.'s are in parentheses

	1			2		
	x/a	*y/b*	*z/c*	*x/a*	*y/b*	*z/c*
O(1)	3086(1)	1142 (1)	4886 (1)	−334 (3)	3816 (2)	1759 (1)
C(2)	1370 (2)	681 (1)	4276 (2)	1627 (4)	3343 (3)	1815 (2)
N(3)	−816 (2)	946 (1)	3578 (1)	2893 (4)	3775 (2)	2495 (1)
C(4)	−1185 (2)	1394 (1)	4519 (2)	1934 (4)	3664 (3)	3306 (2)
C(5)	668 (2)	1881 (1)	5236 (2)	−248 (5)	4139 (3)	3269 (2)
C(6)	2871 (2)	1528 (1)	5946 (2)	−1412 (5)	3670 (3)	2517 (2)
C(7)	662 (3)	2388 (1)	4197 (2)	−221 (5)	5358 (3)	3244 (2)
C(8)	2641 (3)	2831 (1)	4894 (2)	1124 (5)	5835 (3)	3950 (2)
C(9)	4773 (3)	2460 (1)	5520 (2)	3289 (5)	5373 (3)	3947 (2)
C(10)	4849 (3)	1966 (1)	6584 (2)	3249 (5)	4160 (3)	3985 (2)
C(11)	1788 (2)	284 (1)	3230 (1)	2641 (4)	3454 (2)	993 (2)
C(12)	287 (2)	− 184 (1)	2420 (2)	4647 (4)	3113 (3)	930 (2)
C(13)	639 (3)	− 563 (1)	1480 (2)	5635 (5)	3216 (3)	192 (2)
C(14)	2524 (2)	− 468 (1)	1348 (2)	4598 (5)	3642 (2)	− 485 (2)
C(15)	4022 (2)	− 5 (1)	2103 (2)	2618 (5)	3975 (3)	− 444 (2)
C(16)	3657 (2)	365 (1)	3056 (2)	1622 (5)	3872 (3)	304 (2)
N(17)	2928 (2)	− 871 (1)	352 (1)	5648 (5)	3755 (3)	−1269 (2)
O(18)	4625 (2)	− 795 (1)	262 (1)	7466 (5)	3579 (3)	−1274 (2)
O(19)	1532 (2)	−1272 (1)	− 356 (1)	4678 (5)	4030 (3)	−1887 (2)

(4) → 143.8 (2) and 126.8 (5) → 145.9 (4) pm] in both structures is accompanied by a significant closure of the bond angle at C(2) [126.7 (3)° → 114.2 (2)° and 126.6 (3)° → 113.1 (4)°]. Consequently, as shown by the *puckering parameters* [23] listed in Table VI in both isomers the conformation of the hetero-ring changed from a more or less distorted sofa [5] (envelope/half chair, [24] 5*E*, 5*E*/5*H*6) shape to an almost perfect chair form (Fig. 2). These alterations hardly influence, however, the nearly identical conformation of the unsaturated and saturated isomer pairs around the *cis*-junction depicted in the Newman projections (Fig. 3). In these two pairs of isomers the hetero atom O(1) or N(3) is *axial*, while the methylene group bound to C(5) is *equatorial* as inferred from ^{1}H NMR studies [1].

This arrangement is violated only in two related compounds, 2-*p*-(chlorophenyl)-*cis*-4,5-pentamethylene-4,5-dihydro-1,3-oxazine [10] and 2-*p*-(chlorophenyl)-*cis*-5,6-pentamethylene-2,3,5,6-tetrahydro-1,3-oxazin-4-one [15] the fused carbocycle of which is seven-membered. In both cases the twofold axis

Table III

Fractional coordinates ($\times 10^3$ *for* **1**) *and* ($\times 10^4$ *for* **2**) *of hydrogen atoms*
E.s.d.'s are in parentheses

	1			2		
	x/a	*y/b*	*z/c*	*x/a*	*y/b*	*z/c*
H(2)	148 (2)	40 (1)	511 (2)	1431 (4)	2508 (3)	1966 (2)
H(3)	−105 (2)	115 (1)	276 (1)	4359 (4)	4141 (2)	2411 (1)
H(41)	−255 (2)	162 (1)	392 (2)	1793 (4)	2823 (3)	3449 (2)
H(42)	−136 (2)	114 (1)	525 (2)			
H(5)	46 (2)	209 (1)	599 (2)	−1020 (5)	3928 (3)	3831 (2)
H(61)	286 (2)	124 (1)	670 (1)	−2874 (5)	4057 (3)	2455 (2)
H(62)				−1626 (5)	2824 (3)	2619 (2)
H(71)	69 (2)	215 (1)	336 (2)	361 (5)	5612 (3)	2653 (2)
H(72)	− 68 (2)	261 (1)	390 (2)	−1753 (5)	5652 (3)	3304 (2)
H(81)	248 (3)	308 (1)	564 (2)	454 (5)	5653 (3)	4540 (2)
H(82)	266 (3)	318 (1)	427 (2)	1201 (5)	6691 (3)	3871 (2)
H(91)	611 (2)	274 (1)	598 (2)	4138 (5)	5674 (3)	4482 (2)
H(92)	492 (2)	226 (1)	473 (2)	4018 (5)	5620 (3)	3384 (2)
H(101)	622 (2)	171 (1)	688 (1)	2665 (5)	3923 (3)	4579 (2)
H(102)	484 (2)	219 (1)	744 (2)	4782 (5)	3866 (3)	3932 (2)
H(12)	−105 (2)	− 25 (1)	254 (1)	5437 (4)	2778 (3)	1468 (2)
H(13)	− 41 (2)	− 87 (1)	87 (2)	7193 (5)	2958 (3)	147 (2)
H(15)	534 (2)	7 (1)	196 (2)	1828 (5)	4310 (3)	−982 (2)
H(16)	462 (3)	68 (1)	355 (2)	63 (5)	4131 (3)	349 (2)

of the energetically most stable twist-chair form of the cycloheptane ring [25] bisects one of the carbons of the *cis*-junction. Accordingly, the substituents of this carbon atom are *isoclinal*.

In the first case the *isoclinal* methylene group is accompanied by an *equatorial* N(3) (unusual conformation) while in the second case the hetero-atom O(1) is *isoclinal* and the methylene group is, as expected, *equatorial*.

It is worth noting that the theoretically so flexible *cis*-junction in the structures possessing six-membered fused rings (the title compounds, their partially saturated forms [5] and another related compound, 2-phenyl-*cis*-5,6-tetramethylene-5,6-dihydropyrimidin-4(3*H*)-one [12, 13]) exhibit rather limited torsional changes in crystalline state (Fig. 3). Somewhat different amount of rotation around the *cis*-junction can be seen in the trimethylene derivatives (in which the hetero-ring is fused with a cyclopentane ring) [14] or the already discussed pentamethylene derivative [10, 15]. To summarize, the present work, along with those reported previously, corroborates the noteworthy fact that

Table IV

Bond lengths (pm) for **1** *and* **2**
E.s.d.'s are in parentheses

	1	**2**
O(1)—C(2)	142.5 (2)	142.1 (4)
O(1)—C(6)	143.7 (1)	143.8 (4)
C(2)—N(3)	143.8 (2)	145.9 (4)
C(2)—C(11)	150.7 (2)	150.2 (4)
N(3)—C(4)	146.7 (2)	146.9 (4)
C(4)—C(5)	153.0 (2)	155.4 (5)
C(5)—C(6)	152.8 (2)	152.9 (5)
C(5)—C(7)	152.1 (2)	152.5 (5)
C(7)—C(8)	152.3 (2)	153.9 (5)
C(8)—C(9)	151.1 (2)	153.8 (5)
C(9)—C(10)	150.5 (2)	151.9 (5)
C(10)—C(4)	—	150.7 (5)
C(10)—C(6)	151.3 (2)	—
C(11)—C(12)	139.0 (2)	139.4 (4)
C(11)—C(16)	138.6 (2)	138.0 (4)
C(12)—C(13)	137.2 (2)	137.4 (4)
C(13)—C(14)	137.7 (2)	137.5 (4)
C(14)—C(15)	136.9 (2)	137.2 (5)
C(15)—C(16)	137.7 (2)	139.0 (4)
C(14)—N(17)	146.6 (2)	146.0 (4)
N(17)—O(18)	122.1 (2)	121.7 (4)
N(17)—O(19)	123.1 (2)	121.5 (4)

the predominant conformation of the isomers discussed in the crystalline state is practically identical with that in solution.

The substituents of the C(2)-sp^3 atom may assume either *axial* or *equatorial* conformations. In accord with our earlier observation [1, 8], the aryl (4-nitro-phenyl) group, in both structures, is linked *equatorially* (*e.g.* C(4)—N(3)—C(2)—C(11) torsion angles are *antiperiplanar* [26], *i.e.* —173.5 (2)° and —179.4 (5)°, resp.). The fairly coplanar phenyl rings [max dev. from the best plane ($-0.1692X - 0.6574Y - 0.7343Z = -1.7363$) for **1** 0.9 pm, for **2** ($-0.3043X - 0.9142Y - 0.2677Z = -4.8837$) 0.8 pm] assume *synperiplanar* positions relative to the O(1) atoms [O(1)—C(2)—C(11)—C(16) are 4.0 (2)° and —5.5(5)°]. This can presumably be attributed to a weak C(16)—H(16)...O(1) interaction and the repulsion between H(3) and H(12) atoms

Table V

Bond angles for **1** *and* **2**
E.s.d.'s are in parentheses

	1	2
C(2)—O(1)—C(6)	111.8 (2)°	111.3 (4)°
O(1)—C(2)—N(3)	114.2 (2)	113.1 (4)
O(1)—C(2)—C(11)	107.9 (2)	109.4 (4)
N(3)—C(2)—C(11)	110.8 (2)	111.4 (4)
C(2)—N(3)—C(4)	112.0 (2)	112.2 (4)
N(3)—C(4)—C(5)	113.3 (2)	110.5 (4)
N(3)—C(4)—C(10)		110.5 (4)
C(5)—C(4)—C(10)		112.5 (5)
C(4)—C(5)—C(6)	108.5 (2)	109.0 (5)
C(4)—C(5)—C(7)	113.3 (2)	111.8 (5)
C(6)—C(5)—C(7)	111.1 (2)	111.6 (5)
O(1)—C(6)—C(5)	109.6 (2)	111.8 (5)
O(1)—C(6)—C(10)	106.9 (2)	
C(5)—C(6)—C(10)	113.4 (2)	
C(5)—C(7)—C(8)	112.5 (2)	112.0 (5)
C(7)—C(8)—C(9)	110.8 (2)	111.5 (5)
C(8)—C(9)—C(10)	111.8 (2)	111.0 (5)
C(9)—C(10)—C(4)		113.1 (5)
C(9)—C(10)—C(6)	112.4 (2)	
C(2)—C(11)—C(12)	119.9 (2)	118.7 (5)
C(2)—C(11)—C(16)	121.7 (2)	121.4 (5)
C(12)—C(11)—C(16)	118.4 (2)	119.9 (5)
C(11)—C(12)—C(13)	121.4 (2)	120.4 (5)
C(12)—C(13)—C(14)	118.3 (2)	118.8 (5)
C(13)—C(14)—C(15)	122.2 (2)	122.1 (5)
C(13)—C(14)—N(17)	118.9 (2)	118.8 (5)
C(15)—C(14)—N(17)	118.9 (2)	119.1 (5)
C(14)—C(15)—C(16)	118.7 (2)	119.0 (5)
C(15)—C(16)—C(11)	121.0 (2)	119.8 (5)
C(14)—N(17)—O(18)	118.7 (2)	118.5 (5)
C(14)—N(17)—O(19)	118.2 (2)	118.7 (5)
O(18)—N(17)—O(19)	123.1 (2)	122.7 (6)

Table VI

Puckering parameters (Q, φ, ϑ) *and the mean endocyclic torsion angles* $(\bar{\varepsilon}_i)$

	Q	φ	ϑ	$\bar{\varepsilon}_i$
H1	**53.7 pm**	**130.0°**	**172.2°**	**54.4°**
I1	**53.7**	**9.4**	**175.9**	**53.1**
H2	**54.5**	**33.0**	**1.9**	**55.2**
I2	**54.3**	**20.9**	**177.0**	**53.2**

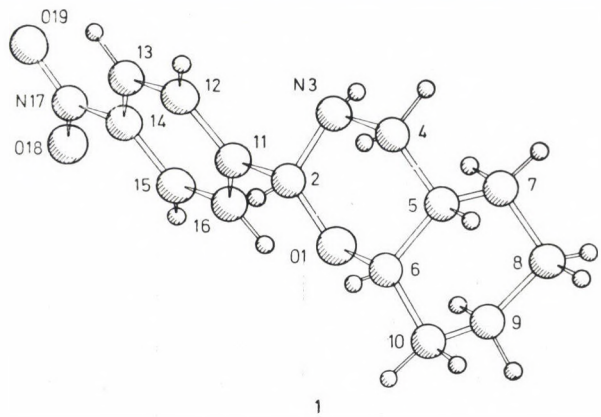

1

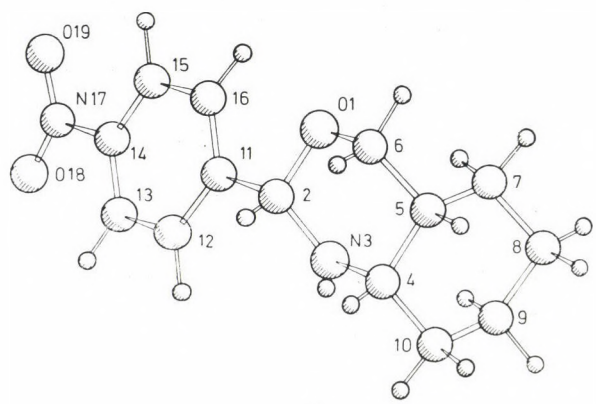

2

Fig. 1. A perspective view of molecules 1 and 2 with atomic numbering. Atoms are carbon unless indicated otherwise. The numbering of the hydrogen atoms follow those of the non-hydrogen atoms

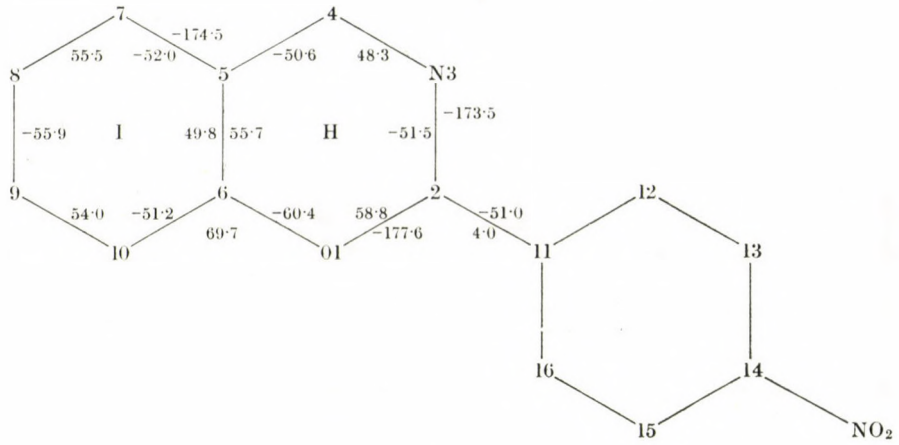

1

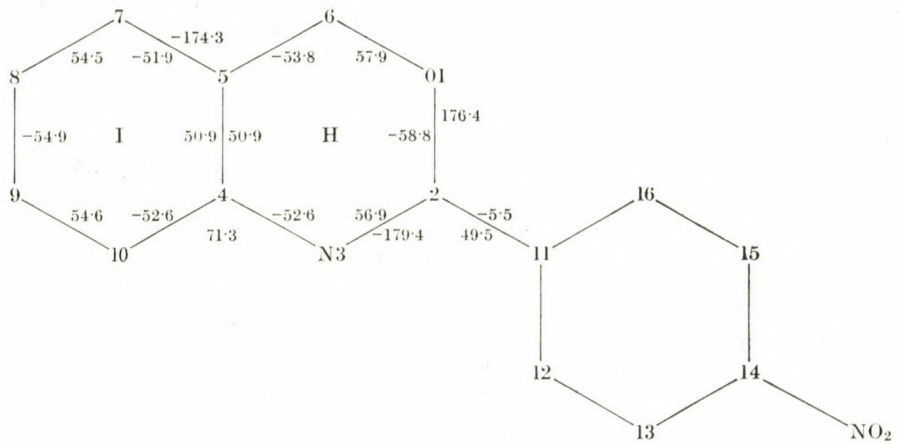

Fig. 2. Endocyclic and some relevant exocyclic torsion angles. The bare numbers are for carbon atoms unless indicated otherwise

[N(3)—C(2)—C(11)—C(12) torsion angles are *synclinal*, −51.0 (2)° and 49.5 (5)°, respectively]. The coplanar *para*-nitro moiety lies in the plane of the phenyl ring in **1**, while in **2** is slightly (by 8°) twisted out of it. The C(14)—N(17) bond lengths [146.6 (2) and 146.0 (4) pm] are significantly longer than *e.g.* in 2-methyl-4-nitro-imidazole [27] in which there is a strong interaction between the NO_2 group and the endocyclic sp^2-N atom. The significant differences in the internal angles of the *para*-disubstituted benzene rings can be attributed to the superposition of the independent inductive and resonance effects [28]. By use of the angular substituent parameters for NO_2 and CH_3

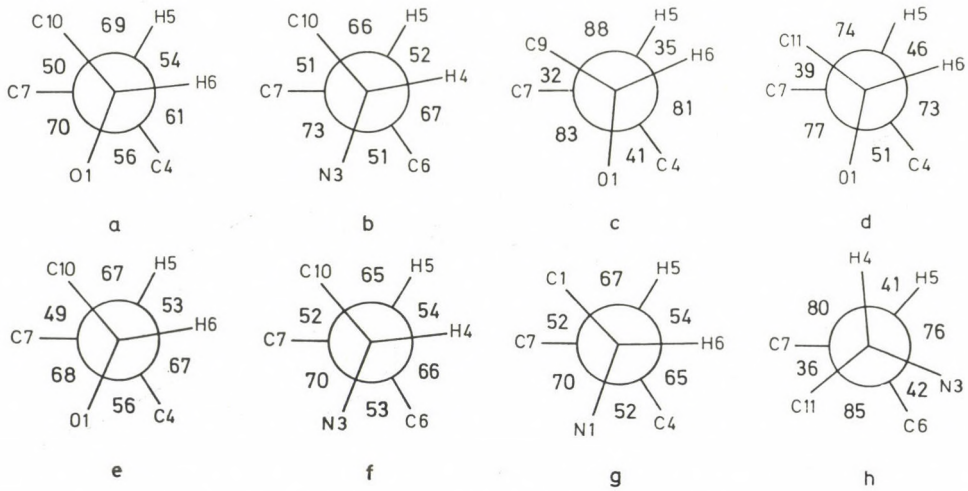

Fig. 3. Newman projections perpendicular to the *cis*-junctions. *a:* title compound 1; *b:* title compound 2; *c:* compound, possessing a five-membered carbocyclic moiety, reported in [14]; *d:* compound, having a seven-membered carbocyclic moiety, reported in [15]; *e, f:* compounds 12 and 14 reported in [5]; *g:* compound reported in [12—13]; h: compound with seven-membered carbocyclic moiety reported in [10]

(the latter is for C(2)) moieties suggested by DOMENICANO and MURRAY—RUST we obtained a very good agreement for the more accurately determined **1** structure:

	Calculated	Observed
at C(11) Θ_1	118.5°	118.4 (2)°
C(12) & C(16) Θ_2	121.3°	⟨121.2 (2)°⟩
C(13) & C(15) Θ_3	118.5°	⟨118.5 (2)°⟩
C(14) Θ_4	122.1°	122.2 (2)°

The less accurately determined structure **2** exhibits some deviation from the suggested values.

REFERENCES

[1] BERNÁTH, G., LÁNG, K. L., KOVÁCS, K., RADICS, L.: Acta Chim. Acad. Sci. Hung., **73,** 81 (1972)
[2] BERNÁTH, G., GÖNDÖS, Gy., GERA, L., TÖRÖK, M., KOVÁCS, K.: Acta Phys. et Chem. Szeged, **19,** 147 (1973)
[3] BERNÁTH, G., GÖNDÖS, Gy., KOVÁCS, K., SOHÁR, P.: Tetrahedron, **29,** 981 (1973)
[4] SOHÁR, P., BERNÁTH, G.: Org. Magnetic Resonance, **5,** 159 (1973)
[5] BERNÁTH, G., FÜLÖP, F., GERA, L., HACKLER, L., KÁLMÁN, A., ARGAY, Gy., SOHÁR, P.: Tetrahedron, **35,** 799 (1979)
[6] BERNÁTH, G., GERA, L., GÖNDÖS, Gy. ECSERY, Z., HERMANN, J., SZENTIVÁNYI, M., JANVÁRY, E.: Brit. Pat. 1,559,985, Jan. 30, 1980.

[7] BERNÁTH, G., FÜLÖP, F., JERKOVICH, Gy., SOHÁR, P.: Acta Chim. Acad. Sci. Hung., **101**, 61 (1979)
[8] SOHÁR, P., GERA, L., BERNÁTH, G.: Org. Magnetic Resonance, **14**, 204 (1980)
[9] GERA, L., BERNÁTH, G., SOHÁR, P.: Acta Chim. Acad. Sci. Hung., **105**, 293 (1980)
[10] RIBÁR, B., LAZAR, D., KÁLMÁN, A., SASVÁRI, K., BERNÁTH, G., HACKLER, L.: Cryst. Struct. Comm., **6**, 671 (1977)
[11] RIBÁR, B., PETROVIC, D., GÖNDÖS, Gy., BERNÁTH, G.: Cryst. Struct. Comm., **8**, 671 (1979)
[12] KAPOR, Á., RIBÁR, B., ARGAY, Gy., KÁLMÁN, A., BERNÁTH, G.: Cryst. Struct. Comm., **9**, 343 (1980)
[13] KAPOR, Á., RIBÁR, B., ARGAY, Gy., KÁLMÁN, A., BERNÁTH, G.: Cryst. Struct. Comm., **9**, 347 (1980)
[14] ARGAY, Gy., KÁLMÁN, A., RIBÁR, B., LAZAR, D., BERNÁTH, G.: Cryst. Struct. Comm., **9**, 335 (1980)
[15] ARGAY, Gy., KÁLMÁN, A., RIBÁR, B., LAZAR, D., BERNÁTH, G.: Cryst. Struct. Comm., **9**, 341 (1980)
[16] GERMAIN, G., MAIN, P., WOOLFSON, M. M.: Acta Cryst., **A27**, 368 (1971)
[17] "International Tables for X-ray Crystallography", Vol. **III**, Birmingham, Kynoch Press (1962)
[18] KÁLMÁN, A., SIMON, K., SCHAWARTZ, J., HORVÁTH, G.: J.C.S. Perkin II, **1974**, 1849
[19] SHELDRICK, G. M.: SHELX. Program for crystal structure determination. Univ. of Cambridge, England (1976)
[20] STEWART, R. F., DAVIDSON, E. R., SIMPSON, W. T.: J. Chem. Phys., **42**, 3175 (1965)
[21] CROMER, D. T., LIBERMAN, D.: J. Chem. Phys., **53**, 1891 (1970)
[22] CROMER, D. T., MANN, J. B.: Acta Cryst., **A24**, 321 (1968)
[23] CREMER, D., POPLE, J. A.: J. Am. Chem. Soc., **97**, 1354 (1975)
[24] BOEYENS, J. C. A.: J. Cryst. Mol. Struct., **8**, 317 (1978)
[25] HENDRICKSON, J. B.: J. Am. Chem. Soc., **89**, 7047 (1967)
[26] KLYNE, W., PRELOG, V.: Experientia, **16**, 521 (1960)
[27] KÁLMÁN, A., van MEURS, F., TÓTH, J.: Cryst. Struct. Comm., **9**, 709 (1980)
[28] DOMENICANO, A., MURRAY-RUST, P.: Tetrahedron Lett., **1979**, 2283

Gyula ARGAY
Alajos KÁLMÁN } H—1525 Budapest, P.O. Box 17.

Ferenc FÜLÖP
Gábor BERNÁTH } H—6720 Szeged, Eötvös u. 6.

Acta Chimica Academiae Scientiarum Hungaricae, Tomus 109 (1), pp. 51—56 (1982)

ÜBER DEN OXIDATIONSMECHANISMUS UND DIE FORMALPOTENTIALE VON REDOXANEN

N. V. TROFIMOV,[1] A. I. BUSEV[1] und P. NENNING[2]*

([1]Chemische Fakultät der Lomonossov-Universität Moskau und [2]Sektion Chemie der Karl-Marx-Universität Leipzig)

Eingegangen am 31. März 1980

Revidiert 19. Januar 1981

Zur Veröffentlichung angenommen am 9. Februar 1981

Anhand spektrofotometrischer Messungen wird der Oxidationsmechanismus der Leukobase von Redoxan III diskutiert, sowie der Einfluß des pH-Wertes auf das Formalpotential des Reagenzes. Die Einstellung des Potentialgleichgewichtes wird bestimmt durch die Umwandlungsgeschwindigkeit der Farbstofformen ineinander. Die Änderung des Formalpotentials der Redoxane in wäßrig-organischen Lösungsmitteln entspricht den Protonisierungs- und Hydrolysekonstanten von Leukobase und Farbstoff in diesen Lösungen.

Bis-(2,3-dimethyl-1-phenylpyrazol-5-on-4-yl)methane (Diantipyrilmethane, Redoxane) sind gut eingeführte analytische Reagenzien. Bevorzugt werden sie verwendet zur Bestimmung von Mikromengen Cer [1—3], Vanadin (4, 5], Gold [6], Palladium [7], Cobalt [8] und anderen Elementen, die leicht veränderbare Wertigkeit haben. Es ist von Interesse, die elektrochemischen Eigenschaften der Diantipyrilmethane zu untersuchen, wobei die Bestimmung ihrer Redoxpotentiale und Halbstufenpotentiale im Vordergrund steht.

Als Beispiel wird Bis-(2,3-dimethyl-1-phenylpyrazol-5-on-4-yl)-4-dimethylaminophenylmethan (4-Dimethyl-aminophenyldiantipyrilmethan, Redoxan III) ausgesucht, das nach [9] hergestellt wird.

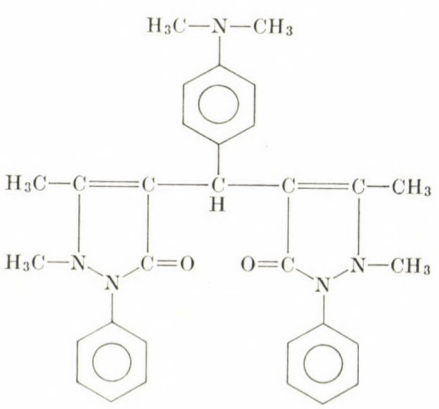

Leukobase

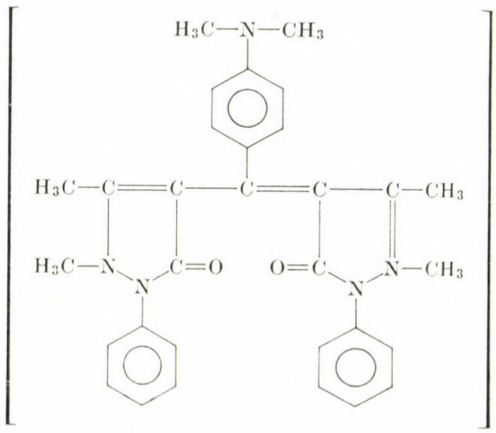

Farbstoff

* Korrespondenz bitte an diesen Autor richten

Der pH der Lösung wird mit einer Glaselektrode/gesättigte Kalomel elektrode gemessen, die Formalpotentiale mit einer Platinelektrode als Indikatorelektrode und einer gesättigten Kalomelelektrode als Bezugselektrode am Potentiometer pH-340. Spektrofotometrische Messungen im UV und sichtbaren Bereich werden am SF 4 A bzw. SF 10 durchgeführt. Nachdem die potentiometrische Titration äquimolarer Gemische von Leukobase und Farbstoff mit Säure und mit Alkali ein Absinken des Potentials bei pH $> 0{,}5$

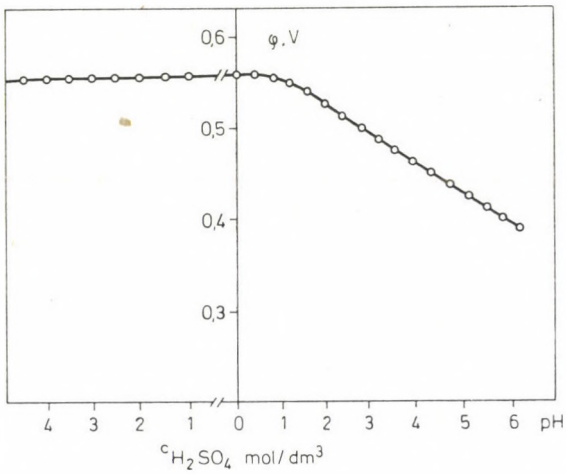

Abb. 1. **Abhängigkeit des Formalpotentials vom pH-Wert im System Farbstoff/Leukobase des Bis(2,3-dimethyl-1-phenyl-pyrazol-5-on-4-yl)-4-dimethylaminophenyl-methans**

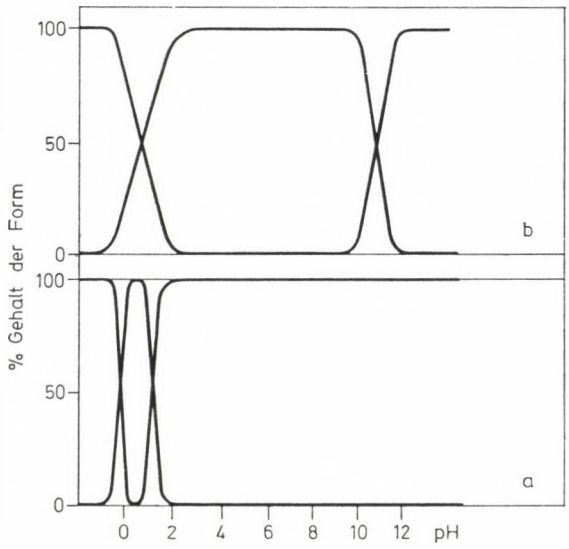

Abb. 2. **Existenzform von Leukobase (a) und Farbstoff (b) des Bis(2,3-dimethyl-1-phenyl-pyrazol-5-on-4-yl)-4-dimethylaminophenyl-methans in Lösung in Abhängigkeit vom pH**

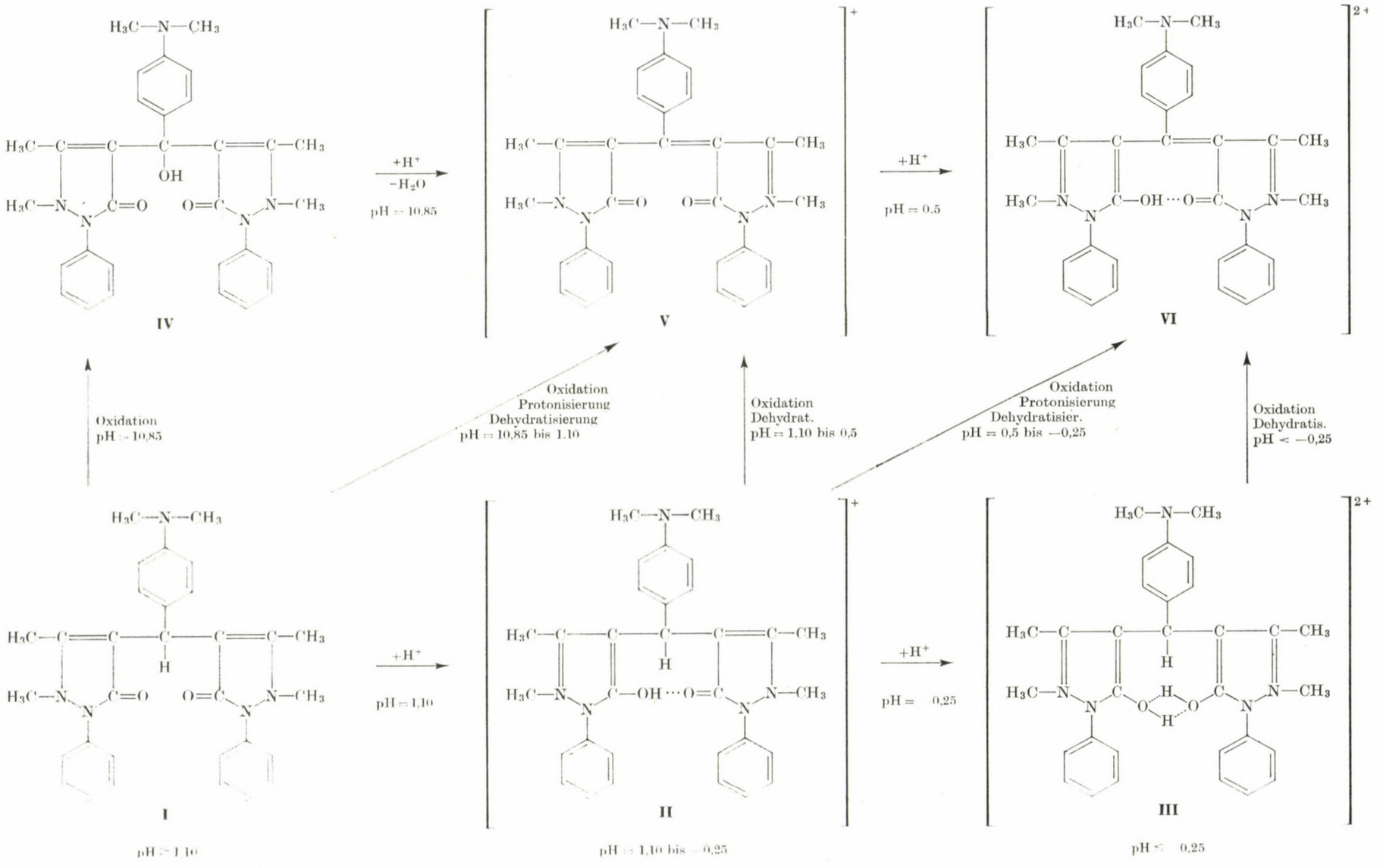

Abb. 3. Schema der Existenzformen des Bis-(2,3-dimethyl-1-phenyl-pyrazol-5-on-4-yl)-4- dimethylaminophenyl-methans in Lösung

anzeigte (Abb. 1), ergab die spektrofotometrische Untersuchung, daß die Leukobase von Redoxan III sich in molekularer, ein- und zweifach protonisierter Form in Lösung befindet (Abb. 2a). Der Farbstoff tritt in Abhängigkeit vom pH-Wert entgegen der in [9] vertretenen Auffassung in 3 Formen auf (Abb. 2b). Durch Elektrophorese haben wir festgestellt, daß bei pH > 11 der Farbstoff molekular vorliegt, bei pH < 11 als Kation. Die molekulare Form (pH > 11) ist mit $CHCl_3$ gut extrahierbar. Bei pH 0,5—11 wird der Farbstoff mit $CHCl_3$ nur in Anwesenheit von ClO_4^-, SCN^- oder J^- extrahiert. Das Verhältnis der Komponenten in den extrahierten Assoziaten ist 1 : 1, das Farbstoffkation ist also einfach geladen. Bei pH $< 0,5$ wird der Farbstoff zum zweiwertigen Kation protonisiert. Mit $CHCl_3$ läßt er sich jetzt nur bei mindestens 2.000-fachem Reagenzüberschuß extrahieren. Das erklärt sich daraus, daß die Bildung eines neutralen Ionenassoziates, das chloroformextrahierbar ist, sterisch ungünstig ist.

Unsere Untersuchungen gestatten das Aufstellen eines Schemas über das Vorliegen von Leukobase und Farbstoff in Lösung bei verschiedenen pH-Werten (Abb. 3).

Die Oxidation der Leukobase kann man sich wie folgt vorstellen.

Oxidation der zweifach protonisierten Form der Leukobase

In stark saurem Medium wird die molekulare Form **I** zweifach protonisiert (Abb. 2,3).

$$\mathbf{I} + 2\ H^+ \rightarrow \mathbf{III}$$

Wirkt ein Oxidationsmittel ein [z. B. Ce(IV)], wird in der Form **III** der Leukobase der methanständige Wasserstoff oxidiert.

$$\mathbf{III} + 2\ Ce^{4+} + \mathbf{H_2O} \rightarrow \mathbf{VII} + 2\ Ce^{3+} + 2\ H^+$$

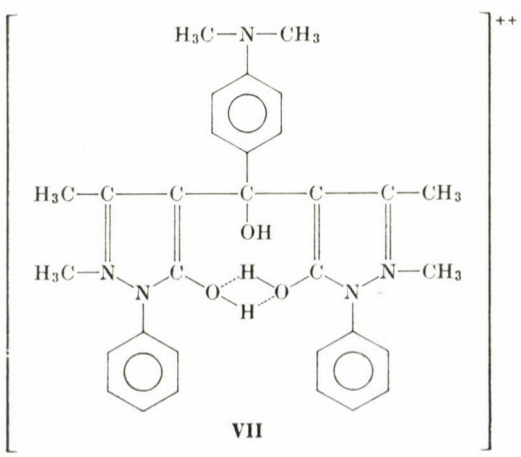

VII

In dieser Form ist die Verbindung aber nicht beständig (Abb. 2). Es wird H_2O abgespaltet und die Verbindung **VI** entsteht.

$$\mathbf{VII} \rightarrow \mathbf{VI} + H_2O$$

Bei der Oxidation werden 2 Protonen frei, aber diese werden für die Protonisierung der Leukobase **I** verbraucht und haben keinen Einfluß auf den pH der Lösung.

Oxidation der einfach protonisierten Form der Leukobase

In mäßig saurer Lösung wird die molekulare Form **I** protonisiert (Abb.2,3).

$$\mathbf{I} + H^+ \rightarrow \mathbf{II}$$

Wirken Oxidationsmittel ein, wird der methanständige Wasserstoff oxidiert.

$$\mathbf{II} + 2\ Ce^{4+} + H_2O \rightarrow \mathbf{VIII} + 2\ Ce^{3+} + 2\ H^+$$

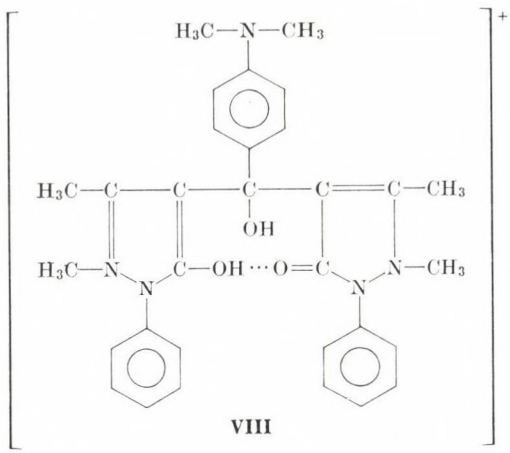

VIII

Wie aus Abb. 2 ersichtlich, ist dieses Kation nicht beständig, es dehydratisiert in Abhängigkeit vom pH zu Form **V** (bei pH = 1,10 bis 0,5)

$$\mathbf{VIII} \rightarrow \mathbf{V} + H_2O$$

oder zu Form **VI** (pH < 0,5):

$$\mathbf{VIII} + H^+ \rightarrow \mathbf{VI} + H_2O$$

Bei der Oxidation werden 2 Protonen frei, im erstgenannten Fall wird eines verbraucht zur Protonisierung der Leukobase, durch das andere aber wird

das Protonengleichgewicht gestört. Im zweiten Fall wird eines zur Dehydratisierung verbraucht, das zweite wie o.a. zum Protonisieren der Leukobase, so daß das Gesamtgleichgewicht erhalten bleibt.

Oxidation der molekularen Form der Leukobase

In schwach saurem Medium (Abb. 2,3) ist die molekulare Form der Leukobase beständig. Oxidationsmittel wirken auf den methanständigen Wasserstoff.

$$\mathbf{I} + 2\ Ce^{4+} + H_2O \rightarrow \mathbf{IV} + 2\ Ce^{3+} + 2\ H^+$$

Wenn die Oxidation im pH-Existenzbereich der Form **IV** stattfindet, ist sie damit beendet. Bei pH $<$ 11 erfolgt Wasserabspaltung zur Form **V**.

$$\mathbf{IV} + H^+ \rightarrow \mathbf{V} + H_2O$$

In diesem Fall ist die Protonenbalance gestört, denn es werden mehr H^+ frei als verbraucht.

Aus den erörterten Leukobasenoxidationsprozessen wird das Potentialverhalten bei pH-Änderung der Lösung erklärt. Das Formalpotential, das zu 0.57 V bestimmt wurde, ist *dann* nicht vom pH der Lösung abhängig, wenn im Oxidationsprozess die Protonenbalance nicht gestört wird, wie es bei der Oxidation der protonisierten Leukobasenform beobachtet wird. Die Oxidation der molekularen Form der Leukobase führt zur Protonenfreisetzung, was mit einer Verringerung des Formalpotentials bei steigendem pH der Lösung verbunden ist (Abb. 1). Die Existenzgrenzen der einzelnen Formen von Leukobase und Farbstoff sind durch deren Protonisierungs- und Hydrolysekonstanten fixiert, folglich ist der Einfluß des pH-Wertes der Lösung auf die Größe des Formalpotentials durch diese Konstanten (Abb. 3) bestimmt ($pK_{H^+} = -1{,}10$; $pK_{H_2^{2+}} = 0{,}25$; $pK_{Hydr} = 10{,}85$).

Aus dem Oxidationsgleichungen geht hervor, daß die früher festgestellte [10] langsame Einstellung des Gleichgewichtspotentials der Redoxane bedingt ist durch die Umwandlungsgeschwindigkeit der Farbstoff-Formen ineinander. Die Geschwindigkeit hängt ab von der Natur des Substituenten am zentralen Phenylrest und schwankt sehr stark [11].

In organischen Lösungsmitteln ändern sich die Hydrolysekonstante der Farbstoffe [12] und die Protonisierungskonstante der Leukobase [13] erheblich. Das bedingt eine Verringerung der Formalpotentiale in diesen Fällen [siehe auch 10].

LITERATUR

[1] Kanaev, N. A.: Z. anal. Chem. (UdSSR), **18,** 575 (1963)
[2] Zhivopistsev, V. P., Parkačeva, V. V.: Lehrmaterial der Universität Perm (russ.), **25,** 104 (1963)

[3] KANAEV, N. A., KLIMOVA, O. N., TROFIMOV, N. V.: Physikalisch-chemische Analysenmethoden für Metalle, Legierungen und Elektrolytbäder (russ.), Moskau, ONTI VIAM, 1975, S. 5
[4] PODČAINOVA, V. N., DOLGOREV, A. V., DERGAČEV, V. J.: Z. anal. Chem. (UdSSR), **21,** 53 (1966)
[5] KANAEV, N. A., TROFIMOV, N. V.: Verwendung organischer Reagenzien in der chemisch-analytischen Qualitätskontrolle, Teil 1, Moskau, MDNTP Dshershinski, 1967, S. 134
[6] KANAEV, N. A.: Spektrofotometrische Methoden der Materialanalyse, Moskau, MDNTP Dshershinski, 1966, S. 134
[7] KANAEV, N. A., TROFIMOV, N. V.: Z. anal. Chem. (UdSSR), **23,** 1851 (1968)
[8] TROFIMOV, N. V., KANAEV, N. A., BUSEV, A. I.: Z. anal. Chem. (UdSSR), **29,** 2001 (1974)
[9] PORAI-KOŠIC, A. E., GINSBURG, O. F., PORAI-KOŠIC, B. A.: Z. allgem. Chemie (UdSSR), **17,** 1752 (1947)
[10] TROFIMOV, N. V.: Untersuchung von Diantipyrilmethanderivaten (Redoxanen) als analytische Redoxreagentien, Dissertation VIAM Moskau 1975
[11] SSINEV, V. V., GINSBURG, O. F., KVJAT, E. I.: Z. allgem. Chemie (UdSSR), **38,** 112 (1968)
[12] GINSBURG, O. F.: Z. allgem Chemie (UdSSR), **23,** 1677 (1953)
[13] AKIMOV, V. K., BUSEV, A. I., JEMELJAKOVA, I. A.: Z. allgem. Chemie (UdSSR), **41,** 196 (1971)

N. V. TROFIMOV, A. I. BUSEV } Moskau V-234, Lomonossov-Universität, Chemische Fakultät

P. NENNING Sektion Chemie der Karl-Marx-Universität, 701 Leipzig, Liebigstraße 18, DDR

Acta Chimica Academiae Scientiarum Hungaricae, Tomus 109 (1), pp. 57—65 (1982)

INVESTIGATION OF NUCLEOTIDE-METAL ION SYSTEMS, II

THE ATP—Co^{2+} SYSTEM

L. KISS and J. CSÁSZÁR*

(Department of General and Physical Chemistry, József Attila University of Sciences Szeged)

Received January 21, 1980

In revised form September 15, 1980

Accepted for publication February 12, 1981

The system Co^{2+}—ATP-5′ has been studied both in solution and solid phase. Titrimetric, conductometric, magnetochemical and spectroscopic investigations have shown that the Co^{2+} ions are attached primarily to the β,γ-phosphate groups, but the formation of a hydrogen bond between the N_7 atom and the Co^{2+} ion is also possible. Isolated $CoATPH_2 \cdot 4H_2O$ has distorted octahedral structure; water elimination and the increase of pH promotes a partial octahedral → tetrahedral transition.

Introduction

It has been pointed out in our previous paper [1] that although the literature of metal-adenosine-triphosphate (ATP-5′) systems is extremely rich, the role of metal ion in the activity of ATP and the position and nature of metal ion — ATP bond are far from being clear (*e.g.* [2—5]). The published data pertain almost exclusively to mixtures of components in various stoichiometric ratios; very little attention has been paid to the isolation of metal-nucleotide complexes, and the investigation of crystalline products [6, 7].

This paper deals primarily with the preparation of crystalline Co-ATP-5′ complex and the results obtained by the physico-chemical investigation of this compound, thereby contributing to the better understanding of its properties and structure.

Results

Na_4ATP-5′ and $CoCl_2 \cdot 6\,H_2O$ in amounts corresponding to a molar ratio of 1 : 1 were reacted at 5 °C in concentrated aqueous solution, and then cooled acetone was added under steady stirring. The suggested composition of the filtered product, washed with alcohol and dried over P_2O_5, is $CoATPH_2 \cdot \cdot 4\,H_2O$; $d_{25} = 1.6823$ kg · dm^{-3} [1]. Under different conditions Indian authors [6] isolated a product of composition $Na_2CoATP \cdot 2\,H_2O$ from a solution of pH = 7 (adjusted by NaOH) by means of precipitation with alcohol.

* To whom correspondence should be addressed

The formation of 1 : 1 complex is proved by literature data [8, 9] as well as by our pH-metric titration results. When titrating a 1 : 1 mixture, the first pH jump characteristic of Na_2ATP does not appear. The buffer range extending to the addition of two equivalents of alkali shifts to lower pH values, and the second pH jump characteristic of Na_2ATP appears at two equivalents. The same titration curve is obtained when the aqueous solutions prepared from the above crystalline product are titrated with akali.

The composition suggested by us is also proved by conductometric data. The aqueous solution of the complex behaves as a weak 1 : 2 electrolyte; at 25 °C in a 1.2×10^{-3} mol/dm^3 solution $\Lambda_M = 168\ \Omega^{-1}\,m^2\,mol^{-1}$ (Table I), which is in good agreement with the literature date [6].

Table I

The molar specific conductivity of solutions with various concentration

$\sqrt{c}$	$\Lambda_M(\Omega^{-1}\,m^2\,mol^{-1})$
0.034	168
0.0525	154
0.0725	133
0.1195	112
0.164	97
0.263	83

The effect of complex formation is unambiguously reflected in the polarographic behaviour, too. The $Co^{2+} \rightarrow Co$ reduction wave (0.002 mol/dm^3 $CoCl_2$:$E_{1/2} = -1.166$ mV) is shifted in the presence of Na_2ATP towards more negative voltage (0,002 mol/dm^3 $CoCl_2$ + 0.002 mol/dm^3 Na_2ATP:$E_{1/2} = -1.217$ mV), its upper region is distorted, and the wave characteristic of Na_2ATP ($E_{1/2} = -1.36$ mV) is superimposed on it. The current *vs.* voltage curves suggest an irreversible electrode process.

The magnetic moment of $\mu_{BM} = 4.93$ measured in solid state indicates the formation of a high-spin hexacoordinated Co^{2+}-complex with significant orbital contribution.

In the UV spectrum of the aqueous solution of the substance the bands of the free ligand [10] remain practically unchanged ($\lambda_1 = 208$ nm, $\log \varepsilon = 4.27$; $\lambda_2 = 260$ nm, $\log \varepsilon = 4.12$). The visible spectra measured in solution and in solid state are hardly different (Fig. 1 and Table II). The three d—d bands characteristic of the high-spin Co^{2+}-complexes appear at 8300, 17500 and 20000 cm^{-1}. It is significant that the colour of the solution turns violet upon the effect of more than two equivalents of alkali, and blue at a pH of *ca.* 10.5. The colours of the solid samples isolated from solutions of pH = 7, 8,

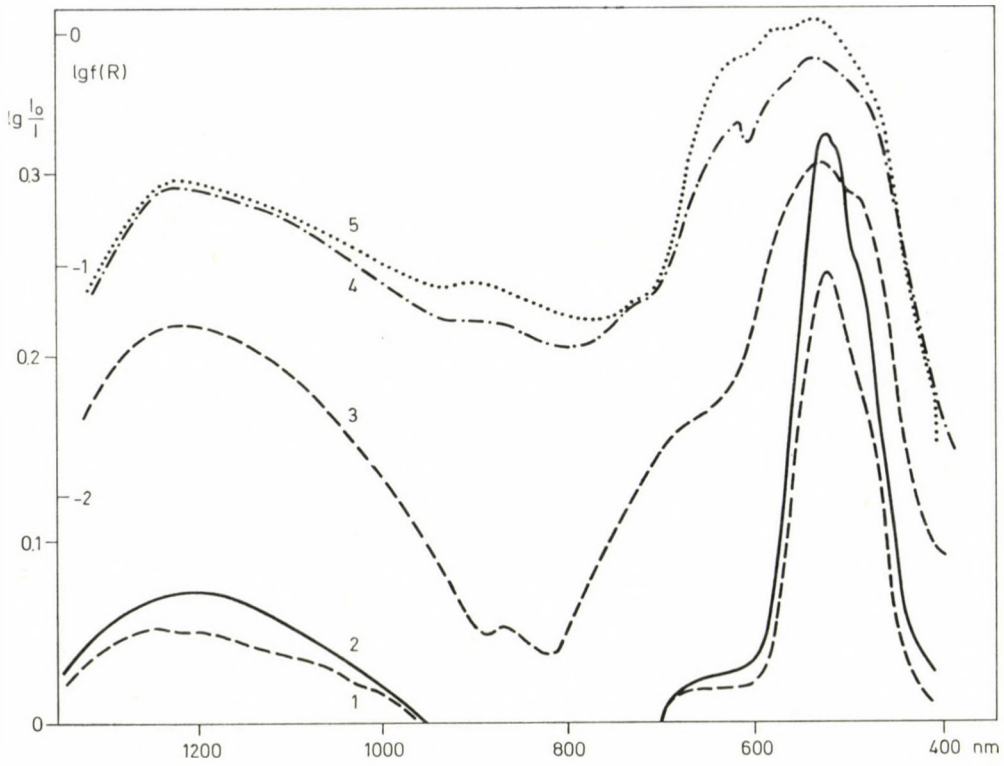

Fig. 1. 1: 1 : 1 mixture of the aqueous solutions of $CoCl_2$ and Na_2ATP, $[Co^{2+}] = 2\times10^{-2}$ mol/dm³; 2: aqueous solution of Co-ATP, $c = 2\times10^{-2}$ mol/dm³; 3: the reflection spectrum of the metal salt; 4: the same after 24 hours and 5: the same after 96 hours of drying

Table II

Measured and calculated spectroscopic data of the Co^{2+} *complex*

	Solution	Reflection
ν_1	8,300 cm^{-1}	8,250 cm^{-1}
ν_2	17,500 cm^{-1}	17,700 cm^{-1}
ν_3	20,100 cm^{-1}	20,300 cm^{-1}
Δ	9,700 cm^{-1}	9,500 cm^{-1}
B	846 cm^{-1}	883 cm^{-1}
β	0,76 cm^{-1}	0,79 cm^{-1}
δ	332 cm^{-1}	370 cm^{-1}
LFSE	7,760 cm^{-1}	7,600 cm^{-1}

9 and 10 change accordingly; the corresponding magnetic moments are 4.68, 4.60, 4.52 and 4.41 BM. The spectrum of the aqueous solution of the complex shows characteristic changes between pH = 2 and 10 (Fig. 2 and Table III);

Table III

Variation of extinction with pH

pH	$E_{20,000}$	$E_{17,000}$
2.40	0.536	0.046
3.30	600	048
4.45	740	050
5.45	780	060
6.40	795	085
7.90	850	110
9.00	930	480
10.00	995	1.300

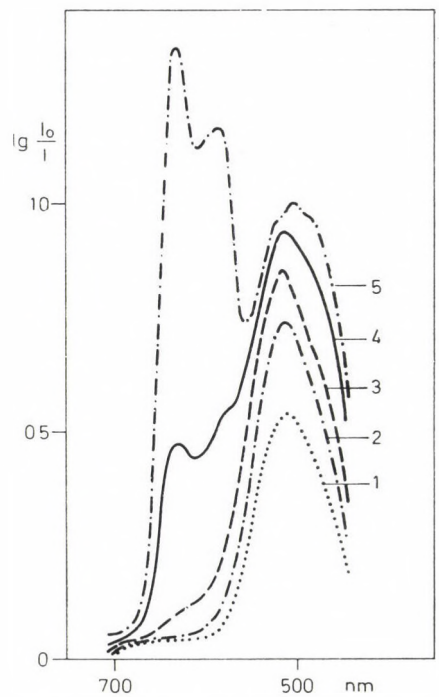

Fig. 2. The spectra of the aqueous solution of CoATP. pH = 2.4 (1), 4.5 (2), 7.9 (3), 9.0 (4), 10.0 (5)

with increasing pH a strong band develops at about 17000 cm^{-1}, and it is characteristic of the blue, tetrahedral Co^{2+} derivatives.

The infrared spectra of Na_2ATP and $CoATPH_2 \cdot 4\ H_2O$ are hardly different in the 4000—400 cm^{-1} region investigated. The $\nu_{as}(P-O-P)$ band appears at 902 cm^{-1}, the $\nu(P-O + C-O)$ band at 1080 cm^{-1}, and the $\nu(P=O)$ band at 1260 cm^{-1}. We assign the band at 1698 cm^{-1} — in agreement with literature data [11] — to the C=N group (Table IV).

Table IV

Infrared bands and their assignment

$ATP.Na_2$	Co^{2+}—ATP	Assignment
3360 s	3350 s	antisymm. H_2O
3165 s	3150 s	NH stretch
1714 s	—	
1562 m	1968 s	C=N stretch
1616 m	1618 w	skeletal vibrations of the aromatic ring
1560 w	1570 w	
1500 w	1519 m	
1418 w	1432 w	
1259 s	1222 s	P=O stretch
1110 s	1080 s	P—O + C—O stretch
902 m	920 m	P—O—P vibration
816 w	824 w	
641 m	636 w	
520 m	520 m	
495 m	—	

s: strong, m: medium, w: weak band

Discussion

The method described could be used to prepare a reproducible crystalline product with a composition of $CoATPH_2 \cdot 4\ H_2O$ as determined by C, H, N, Co and H_2O analyses [1]. Formation of complexes other than 1 : 1 could not be detected *e.g.* by pH-metric titration, and the composition of the isolated product was always the same, with no regard to the stoichiometry of the reagents or the type of Co^{2+} salt. The identical composition of the dissolved and solid isolated complexes is proved, among others, by the polarographic data; the

half-wave potentials measured in the solution mixture and in the aqueous solution of the product are practically the same (0.002 mol/dm^3 Co · $ATPH_2$ · 4 H_2O: $E_{1/2} = -1.213$ mV).

The results of spectroscopic investigations indicate a very weak ligand-metal interaction, the spectrum of the aqueous solution of Na_2ATP is hardly changed by complex formation. The two strong bands may be assigned unambiguously to the $\pi - \pi^*$ transitions of the adenine, since neither the ribose nor the phosphate part have significant absorption in this region, and the spectra of adenine and its phosphates are practically the same. (The spectra of guanine and cytosine and their phosphates show similar property.)

On the basis of ligand field theory [12, 13], and assuming octahedral coordination,the three bands observed in the visible spectrum may be assigned to the following transitions:

$$\nu_1 = {}^4T_{2g}(F) \leftarrow {}^4T_{1g}(F), \quad \nu_2 = {}^4A_{2g}(F) \leftarrow {}^4T_{1g}(F) \text{ and } \nu_3 = {}^4T_{1g}(P) \leftarrow {}^4T_{1g}(F).$$

The weak ν_2 band corresponding to a two-electron transition may be found on the low energy side of ν_3 (Fig. 1).

The diffuse reflectance spectrum of the crystalline substance is hardly different from the spectrum of the aqueous solution (Table II). The mixture of the aqueous solutions of $CoCl_2$ and Na_2ATP has the same spectrum as the aqueous solution of the crystalline substance. The visible region of the spectra does not change upon standing, the intensity of the 260 nm band slightly decreases, due presumably to hydrolysis.

The structure of absorption spectra indicates the presence of hexacoordinated, distorted octahedral Co^{2+} ion, and the same is suggested by the magnetic moment of 4.93 BM corresponding to three unpaired electrons and a significant orbital contribution. On the basis of the RACAH parameter B calculated from the spectroscopic data (*e.g.* Ref. [13]) under the assumption of octahedral coordination, the bonds in the compound have 76—80% ionic character, very close to 76%, calculated for the hydrated ion. Consequently, (a) ATP-5′ is close to H_2O in the nephelauxethic series, and (b) the Co—O bonds dominate in the molecule; the ratio of Co—N bonded species is smaller, but their presence may not be excluded.

The splitting of ${}^4T_{1g}$(F) level due to spin-orbit coupling is $\delta \approx 330-370$ cm^{-1}, LFSE is 7600—7800 cm^{-1}. The rule of mean environment yields $\Delta =$ $= 10\,100$ cm^{-1} for ATP, which is close to $\Delta = 9500$ cm^{-1} of $[Co(H_2O)_6]^{2+}$.

On varying the pH of the aqueous solution of Co-ATP between 2 and 10, a pink → violet → blue transition may be observed (see page 58), and this is accompanied by a characteristic change in the absorption spectrum (Table III). The limiting curve was obtained around pH = 10 (Fig. 2). Even at this alkalinity no precipitation occurs, indicating the high stability of the blue species, which is presumably a binuclear hydroxo-compound: $[CoATP(OH)]_2^{6-}$.

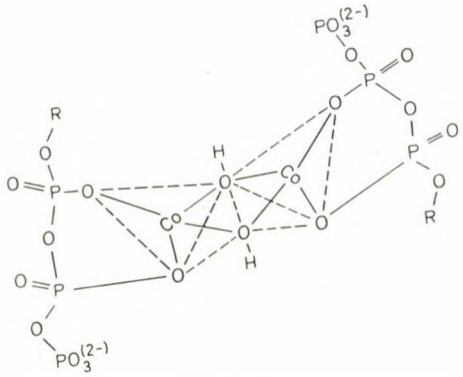

Fig. 3

It is known that $[Co(OH)_4]^{2-}$ is a stable species [14], its absorption at 16 kK is close to the band measured by us. The spectrum measured at high pH is characteristic of the tetrahedral Co^{2+} compounds; the probable structure of this species is shown in Fig. 3. It is to be noted that the pH *vs.* extinction diagram has a step at the same pH as the titration curve. The octahedral → tetrahedral transition with increasing pH is also reflected in the behaviour of magnetic moment mentioned before. The magnetic moment of the products isolated at higher pH drops to *ca.* 4.5 BM from 4.93 BM owing to the decreasing orbital contribution, and this is characteristic of tetrahedral Co^{2+} compounds.

The infrared spectra of the ligand and the complex are very similar and extremely rich in bands (Table IV).

The medium band at 902 cm^{-1} corresponds to the antisymmetric stretching of P—O—P bonds; in the presence of metal salt this band appears at 20 cm^{-1} higher wavenumber [15]. The overlapping bands of P—O and C—O vibrations were observed at 1110 and 1080 cm^{-1} for the ligand and the Co derivative, respectively. The P=O stretching frequency of 1260 cm^{-1} decreases by about 40 cm^{-1} in the presence of metal salt. The frequency assigned to the C=N bond of the adenine rings is shifted from 1652 to 1698 cm^{-1} in the presence of Co^{2+} ions, due probably to the change on the $C=\overset{+}{N}$ group [15]. The NH_2 stretching vibrations can be found at about 3370 cm^{-1}. The weak bands in the low wavenumber region are hard to assign; the spectrum in this region is generally structureless in the presence of metal salt.

On the basis of molecular models and the experimental results discussed, the following assumptions may be made on the structure of the compound. Three types of linkages (Structures **I**—**III**) may be assumed. Primarily for steric reasons, structure **I** is hardly probable, and the spectroscopic data also contradict it. In solid phase structure **II** appears probable which has been *e.g.* on the basis of ^1H NMR studies [16], too. In this case a water molecule

links atom N_7 and the Co^{2+} ion by hydrogen bond. In aqueous solutions structures **II** and **III** are equally probable, on the basis of our results they cannot be distinguished.

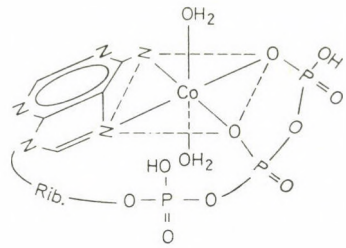

I

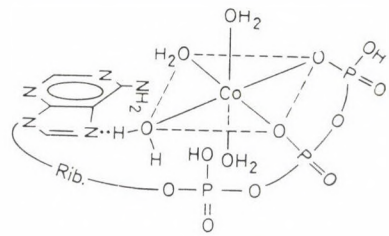

II

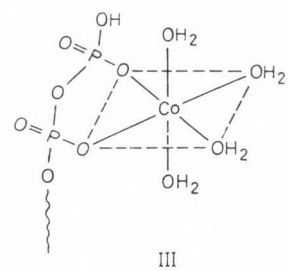

III

Experimental

For the preparative work chemicals of analytical grade were used. The composition of the isolated product was determined by the analysis of C, H, Co (photometric and titrimetric methods), Cl^- and H_2O (the analytical data were given in our previous paper [17]).

The magnetic measurements were carried out by the method of Gouy at 298 K; $Hg[Co(SCN)_4]$ was used as a calibrant. The diamagnetic correction was calculated on the basis of literature data [14].

Absorption and reflection spectra were measured with BECKMAN DU and SPECORD UV VIS spectrophotometers. The reference for reflection measurements was MgO. The infrared spectra were taken in KBr pellets with a UNICAM SP-100 spectrophotometer.

pH-metric titrations were performed in solutions of 5×10^{-2} mol/dm^3 concentration with a RADELKISZ OP 205 titrimeter and a combined glass electrode of type OP 807.

Polarographic investigations were carried out with a V 301 polarograph in thermostated KALOUSEK vessel at 298 K. Supporting electrolyte was 0.1 mol/dm³ KNO_3. The half-wave potentials were determined in a three-electrode system with an OP 205 pH-meter against normal calomel electrode.

Conductivity measurements were performed at 298 K, in a concentration range of 1.4×10^{-3} to 7.1×10^{-2} mol/dm³ with an OK 102 instrument.

*

The authors feel indebted to CHINOIN Works for the financial support.

REFERENCES

[1] CSÁSZÁR, J., KISS, L.: Acta Chim. Acad. Sci. Hung. (in press)
[2] SPICER, S. S.: J. Biol. Chem., **199,** 301 (1952)
[3] HERS, H. G.: Biochim. Biophys. Acta, **8,** 424 (1952)
[4] IZATT, R. M., CHRISTENSEN, J. J., RYTTING, J. H.: Chem. Rev., **71,** 439 (1971)
[5] PHILLIPS, R. S. J.: Chem. Rev., **66,** 501 (1966)
[6] BHATTACHARYYA, R. G., BHADURI, I.: J. Inorg. Nucl. Chem., **40,** 733 (1978)
[7] BRIGANDO, J., COLAITIS, D.: Bull. Soc. Chim. France, **1969,** 3440, 3445, 3449, 3453
[8] See [5] and the references cited therein
[9] COTTON, F. A., WILKINSON, G.: Advanced Inorganic Chemistry, 2nd Ed., Wiley New York, 1969
[10] BOCK, R. M., LING, N., MORELL, S. A., LIPLON, S. H.: Arc. Biochem. Biophys., **62,** 253 (1956)
[11] EPP, A., RAMASARMA, T., WETTER, L. R.: J. Amer. Chem. Soc., **80,** 724 (1958)
[12] BALLHAUSEN, C. J.: Introduction to Ligand Field Theory, McGraw-Hill, New York, 1962
[13] CSÁSZÁR J., BÁN M.: Optikai színkép, ligandumtér-elmélet, komplex szerkezet. Akad. Kiadó, Budapest, 1972
[14] GOODGAME, D. M. L. *et al.:* Inorg. Chem., **4,** 139 (1965); J. Amer. Chem. Soc., **83,** 1780 (1961)
[15] LEWIS, J., WILKINS, R. G.: Modern Coordination Chemistry, Intersci. Publ., New York, 1960
[16] GLASSMAN, T. A., COOPER, C., HARRISON, L. W., SWIFT, T. J.: Biochem., **10,** 843 (1971)

László KISS
József CSÁSZÁR } H—6701 Szeged, Rerrich B. tér 1.

Acta Chimica Academiae Scientiarum Hungaricae, Tomus 109 (1), pp. 67—69 (1982)

REACTION OF THIOLSULFONATES WITH SODIUM CYANIDE AND HALOGEN CYANIDES IN ACETONITRILE

(SHORT COMMUNICATION)

J. LÁZÁR* and E. VINKLER

(Pharmaceutical Chemical Department, Medical University, Szeged)

Received May 20, 1980

In revised form November 25, 1980

Accepted for publication February 12, 1981

The reactions of thiosulfonates with sodium cyanide in aqueous media have been investigated by several researchers [1—4]. FOOTNER and SMILES [1] mentioned first that thiolsulfonates (**I**) are converted by sodium cyanide into sodium sulfinate (**II**) and the appropriate thiocyanate (**III**).

$$\underset{\mathbf{I}}{Ar + SO_2{-}S{-}Ar} + NaCN \rightarrow \underset{\mathbf{II}}{Ar{-}SO_2Na} + \underset{\mathbf{III}}{Ar{-}SCN}$$

KLAYMAN and MILNE [2] employed the above reaction for the preparation of 2-aminothiazol.

KICE *et al.* [3, 4] made reaction kinetic examinations of the reactions of aromatic thiolsulfonates with sodium cyanide in the presence of hydrogen cyanide buffer in aqueous dioxane.

OAE *et al.* [5] allowed to react 1,2-dithiaacenaphthene-*S*-*S*-dioxide with sodium cyanide in methanol, however, instead of the expected cleavage products, disulfide and sodium cyanate were detected in the reaction mixture. In the case of *p*-tolyl thiolsulfonate, disulfide was formed again in a significant amount, besides the products of splitting.

The reaction can thus proceed in different ways, depending on the solvent and the structure of the thiolsulfonate, and reduction may also take place in addition to splitting.

On the basis of the work of KLAYMAN and MILNE [2], we assumed a possible preparative importance of this reaction, therefore it was attempted to find such reaction conditions which ensure higher yields and eliminate the occurrence of side-reactions (*e.g.*, reduction).

Aqueous medium was considered unsuitable, because of the alkaline reaction of sodium cyanide. Similarly, alcohols were rejected because of the possibility of reduction.

* To whom correspondence should be addressed

After several unsuccessful experiments, acetonitrile was found to be the most suitable solvent, since both the thiocyanate and sodium sulfinate could be isolated in almost the theoretical yields on processing the reaction mixture.

After the successful reaction with sodium cyanide, the effecting of the cleavage was tried with cyanogen bromide. Special interest was attached to these reactions, since the splitting of thiolsulfonates with cyanogen bromide has not been described in the literature.

The reaction was effected in acetonitrile solution by heating with a calculated amount of cyanogen bromide. The products of splitting, *i.e.*, the corresponding sulfonyl bromide and thiocyanate, were obtained in satisfactory yields on processing the reaction mixture.

In addition to splitting with cyanogen bromide, the reaction was tried with cyanogen chloride and cyanogen iodide, in view of the fact that, owing to the different electron affinities of halogens, in the reaction of cyanogen chloride with Grignard reagent nitriles are obtained, while cyanogen bromide and iodide react with the formation of alkyl halides [6—10]. The experiments failed, since the splitting reaction did not take place with cyanogen chloride in acetonitrile — tetrachloromethane solution at 120 °C, even when employing heating in a closed vessel for several days. Cyanogen iodide suffered decomposition under the conditions of the reation, and the large amount of iodine formed prevented the processing of the reaction mixture in the manner described. above. After the removal of iodine, only thiocyanate and unchanged thiolsulfonate could be isolated.

Experimental

M.p.'s were determined on a Boetius (Franz Küstner, Dresden) melting point determining apparatus and are uncorrected.

Reaction of *p*-tolyl thiolsulfonate with sodium cyanide

p-Tolyl thiolsulfonate (13.9 g; 0.05 mole) was dissolved in acetonitrile (25 cm^3) and added to a solution of finaly powdered sodium cyanide (2.5 g; 0.05 mole) in acetonitrile (75 cm^3). The mixture was refluxed on an oil bath at 100 °C for 12 h, with stirring. After cooling, the crystalline precipitate was filtered off, washed with acetonitrile and dried (8.9 g; 100%). The product was *p*-tolylsulfinic acid sodium salt.

In order to characterize the product, the iron salt was prepared. The crystals were dissolved in water (30 cm^3) and 20% iron(III) chloride solution was added to the solution under continuous shaking, until no more precipitate was formed. The precipitate was allowed to thicken, filtered off on a Büchner funnel, and washed with water. The dry, orange-red substance was iron(III) *p*-tolylsulfinate (7.55 g; 87%). The acetonitrile solution was evaporated to dryness and the residual oil (7.45 g: 100%) was distilled, to obtain *p*-tolylthiocyanate (7 g; 93%) as a colourless, strongly refractive oil with characteristic smell resembling coconut oil.

B.p.$_{303Pa}$ 115 °C.
IR:2160 cm^{-1} SCN
n_D^{23} 1.5652.

Reaction of *p*-tolyl thiolsulfonate with cyanogen bromide

p-Tolyl thiolsulfonate (13.9 g; 0.05 mole) was dissolved in acetonitrile (100 cm^3), cyanogen bromide (5.02 g; 0.05 mole) was added, and the mixture was refluxed on an oil bath at 80 °C for 20 h. After removal of the acetonitrile by distillation, the residue was recrystallized twice from *n*-hexane (10.2 g; 86%); m.p. 94 °C; *p*-tolylsulfonyl bromide. For characterization, the product was dissolved in ether, ammonia gas was passed into the solution, the precipitate which separated was filtered off, washed with water to remove ammonium bromide, and recrystallized from ethanol; m.p. 136 °C; *p*-tolylsulfonamide.

The combined *n*-hexane solutions were evaporated to dryness and the residue was distilled in vacuum.

$B.p._{303Pa}$: 115 °C, 5.6 g (73%); *p*-tolyl thiocyanate.

Reaction of *p*-tolyl thiolsulfonate with cyanogen iodide

p-Tolyl thiolsulfonate (13.9 g; 0.05 mole) was dissolved in acetonitrile (100 cm^3) and refluxed with cyanogen iodide (8.16 g; 0.055 mole) in an oil bath at 80 °C for 24 h. The acetonitrile was evaporated, the residue dissolved in benzene and extracted repeatedly with 10% sodium thiosulfate to remove iodine. The benzene was evaporated. the residue treated with petroleum ether and the insoluble fraction was filtered off to obtain *p*-tolyl thiolsulfonate (3.75 g; 27% of the amount allowed to react), m.p. 76 °C. Evaporation of the petroleum ether and distillation of the residue in vacuum gave *p*-tolyl thiocyanate, $b.p._{303Pa}$: 115 °C (4.55 g, 61%).

REFERENCES

[1] Footner, H. B., Smiles, S.: J. Chem. Soc., **127,** 2667 (1925)
[2] Klayman, D. L., Milne, G. W. A.: J. Org. Chem., **31,** 2349 (1966)
[3] Kice, J. L., Rogers, T. E., Warheit, A. C.: J. Am. Chem. Soc., **96,** 8020 (1974)
[4] Chau, M. M., Kice, J. L.: J. Org. Chem., **43,** 914 (1978)
[5] Tamagaki, S , Hirota, H., Oae, S.: Bull. Chem. Soc. Japan, **47,** 2075 (1974)
[6] Houben-Weyl: Methoden der Organischen Chemie. **VIII.** Sauerstoffverbindungen, **III,** p.93. Georg Thieme Verlag, Stuttgart 1952
[7] Grignard, V.: Compt. rend., **152,** 388 (1911)
[8] Grignard, V., Bellett. E.: Compt. rend. **155,** 44 (1912); **158,** 457 (1914)
[9] Grignard, V., Courtot, Ch.: Compt. rend., **154,** 361 (1912)
[10] Grignard, V., Bellett, E., Courtet, Ch.: Ann. **4,** 28 (1915); **12,** 364 (1919)

János Lázár
Elemér Vinkler } H—6701 Szeged P.O.B. 121.

Acta Chimica Academiae Scientiarum Hungaricae, Tomus 109 (1), pp 71—82 (1982)

STEROIDS, XXVII*
NEIGHBOURING GROUP PARTICIPATION, IV**

PREPARATION OF 16α-HYDROXYMETHYLANDROST-5-ENE-3β,17α-DIOL

Gy. SCHNEIDER,[1]*** I. VINCZE,[1] A. VASS,[2] L. HACKLER[1] and Gy. DOMBI[1]

([1]Department of Organic Chemistry, József Attila University, Szeged,

[2]Research Institute for Heavy Chemical Industries, Veszprém)

Received October 14, 1980

Accepted for publication February 12, 1981

Reduction of 16-acetoxymethylene-17-oxo-5-androstene-3β-ol 3-acetate (**1b**) with complex metal hydrides yielded a mixture of three stereoisomeric 16-hydroxymethyl-5-androstene-3β,17-diol 3-acetates: 16α,17β(**3a**), 16β,17β(**4a**) and 16β,17α(**5a**). The fourth isomer, 16α,17α(**6a**), was prepared from the **3e** acetate-*p*-toluenesulfonate by solvolysis in acetic acid or dimethyl sulfoxide in the presence of potassium acetate, through neighbouring group participation.

To confirm the participation of the 16α-acetoxymethyl group in the reaction, comparative solvolytic investigations were carried out on 5-androstene-3β,17β-diol 3-acetate 17-*p*-toluenesulfonate (**14b**).

16-Hydroxymethyl-17-hydroxysteroids are suitable starting materials for the preparation of steroids with heterocyclic ring E. The former compounds can be obtained by the reduction of the relatively readily accessible 16-formyl-17-ketones.

KNOX prepared the 16-hydroxymethyl-17-ketone by catalytic hydrogenation of 16-hydroxymethylene-17-keto-5α-androstane-3β-ol; the product was then reduced with $LiAlH_4$ to obtain 16-hydroxymethyl-5α-androstane-3β,17-diol [1].

In the case of the androstene derivatives investigated by us catalytic hydrogenation would also affect the C-5 double bond; therefore, such a reduction method has to be chosen which leaves this bond intact, further, does not convert the vicinal formyl ketones into methyl ketones [2, 3].

According to our earlier observation, the reduction of 16-hydroxymethylene-17-keto-5-androstane-3β-ol (**1a**) with complex metal hydrides, such as $LiAlH_4$ in tetrahydrofuran or $NaBH_4$ in alcoholic medium, yielded a mixture of isomeric 16-hydroxymethyl-5-androstene-3β,17-diols without by-products [4]. The 16α,17β(**3a**) and 16β,17β(**4a**) epimers were isolated in

* XXVI: Gy. SCHNEIDER, L. HACKLER, Gy. DOMBI: J. Chem. Soc. Chem. Comm., **1980**, 891

** III: Gy. SCHNEIDER, I. VINCZE, A. VASS: Acta Chim. Acad. Sci. Hung., **99** (1), 51 (1979)

*** To whom correspondence should be addressed

nearly identical amounts, while the third isomer (**5a**) was obtained in a significantly smaller quantity. The ratio of **5a**, having 16β,17α configuration, could not be increased above 5% by varying the conditions of the reduction. The best result was achieved when carrying out the reduction with $NaBH_4$ in ethanol solution in the presence of 2 equivalents of $CaCl_2$. Under such conditions the enolacetate-diol **2a** could be isolated. This compound suffered partial hydrolysis and was further reduced to a mixture of **3b**, **4b** and **5b**. The 16α,17α isomer could not be detected even in traces.

In an earlier work we reported the preparation of the 16β,17αisomer (**5a**) by the conversion of the 16β,17βisomer (**4a**) [5].

In the possession of 16α-hydroxymethyl-5-androstene-3β,17β-diol 3-acetate (**3b**), now an attempt was made to convert it in to the missing fourth isomer (**6a**) with configuration 16α,17α. On selective acetylation **3b** gave the 16α-acetoxymethyl derivative **3c**, which was converted to the mixed acetate-tosylate **3e**. Solvolytic conversion of **3e** afforded then the missing member of the series with configuration 16α,17α (**6a**).

Solvolytic experiments

The acetolysis of 16α-acetoxymethyl-5-androstene-3β,17β-diol 3-acetate 17-*p*-toluenesulfonate (**3e**) was effected at 0.1 mole concentration in anhydrous acetic acid, in the presence of 1 equivalent of acetic anhydride and 0.12 mole of potassium acetate, at the boiling temperature of the mixture. Similar solvolytic experiments were made in both aqueous acetic acid and in dimethyl sulfoxide solution at 160 °C.

Comparative solvolysis experiments were performed with **14b** *p*-toluenesulfonate under similar conditions.

The reactions were monitored by TLC, the products separated by column chromatography, and identified on the basis of their ^{1}H-NMR, ^{13}C-NMR and IR spectra.

Solvolysis of **3e** in anhydrous acetic acid gave the **6b** triacetate (41%) by inversion, and the **3d** triacetate by retention, as the main products. The unsaturated 18-nor-derivative **10b** was also formed (33%) through a WAGNER-MEERWEIN rearrangement.

The ^{1}H-NMR spectrum of **6b** has a doublet at 5.05 ppm (C-17 H) with a coupling constant of 5.6 Hz, due to the α,α (*cis*) position of the C-16, C-18 substituents [6].

The structures of compounds **10** are given on the basis of their spectra. The structure of **10b** is verified by the doublet due to the C-17 methyl group in the ^{1}H-NMR spectrum. The position of the methyl group remaining in β orientation is in accordance with the "principle of least displacement" [8].

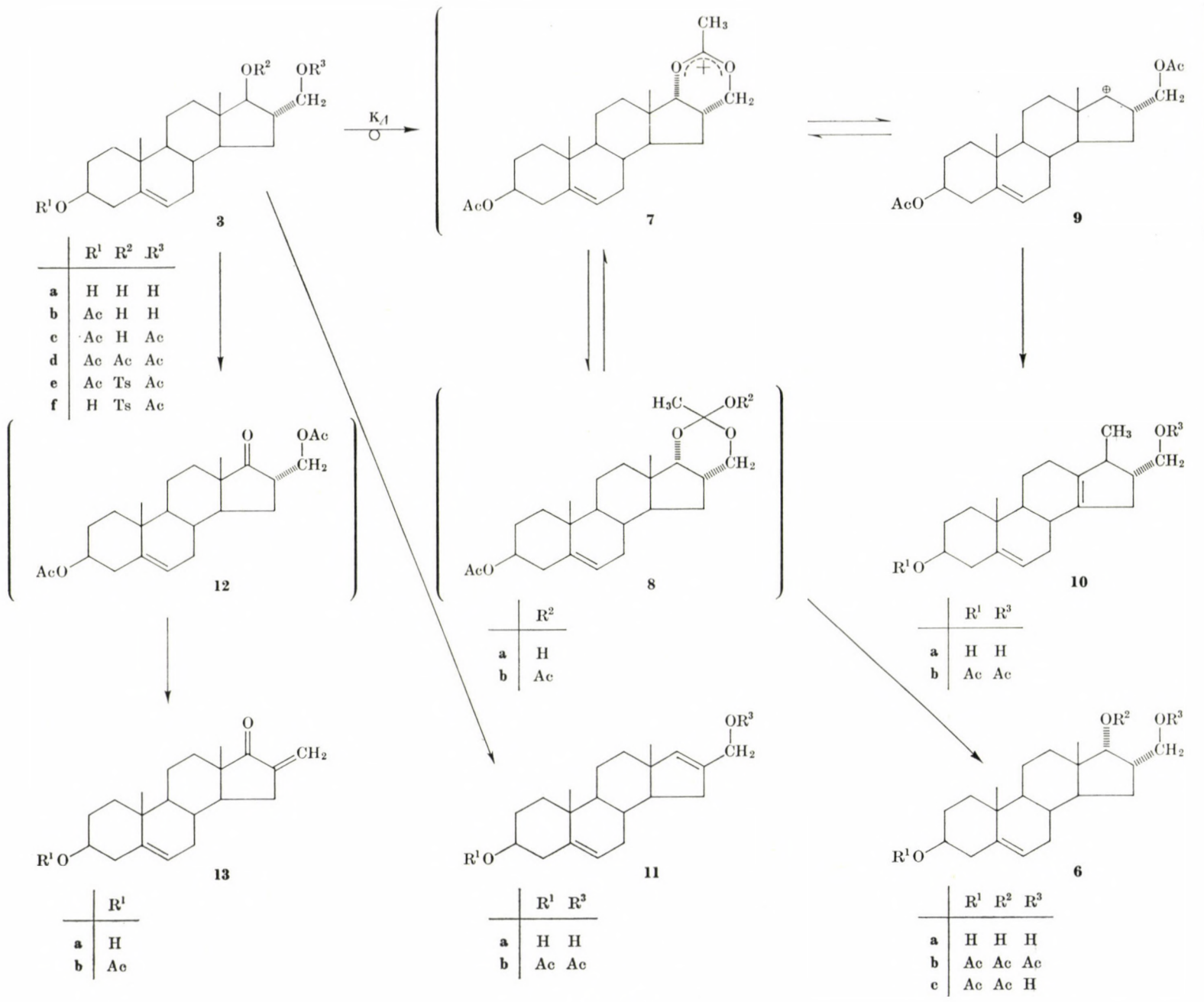

	R^1	R^2	R^3
a	H	H	H
b	Ac	H	H
c	Ac	H	Ac
d	Ac	Ac	Ac
e	Ac	Ts	Ac
f	H	Ts	Ac

	R^2
a	H
b	Ac

	R^1	R^3
a	H	H
b	Ac	Ac

	R^1
a	H
b	Ac

	R^1	R^3
a	H	H
b	Ac	Ac

	R^1	R^2	R^3
a	H	H	H
b	Ac	Ac	Ac
c	Ac	Ac	H

Fig. 1

The C-16 acetoxymethyl group did not take part in the rearrangement, so retained its original configuration. The ^{13}C-NMR spectrum shows, besides the C-5 and C-6 carbon atoms, two further atoms in sp^2 hybridized state, which can be C-13 and C-14.

In the acetolysis of **3e** in 95% aqueous acetic acid, one single diacetate **6c** formed (67%) with inversed configuration; **10b** could also be isolated (31%).

From the solvolysis of **3e** in dimethyl sulfoxide, **6b** was obtained in 58% yield, and **10b** was also formed (21%). Besides these, 16-methylene (**13b**) (10%) and 16-unsaturated-17-unsubstituted (**11b**) (8%) derivatives were also isolated from the reaction mixture.

The physical constants of compound **13b** are identical with the literature data [14].

Compound **11a** was prepared by GERALY *et al.* [12] through the $LiAlH_4$ reduction of 16-formylandrosta-5,16-diene-3β-ol. Its acetylated derivative was identical with our **11b**.

The *p*-toluene-sulfonate **14b** containing us functional group at C-16, gave on solvolysis in acetic acid rearranged products only, the known **15b** [9] and the 13(17)-unsaturated **16b**, as an inseparable mixture. In the ^{13}C-NMR spectrum of the mixture the signals of the C-5, C-6 and C-13 atoms appear twice, while C-14 and C-17 gives one signal each. Compounds **15b** and **16b** are present in nearly identical amounts, their ration being 55 : 45. In the ^{1}H-NMR spectrum the C-17-methyl group appears as a doublet at 0.88 ppm with a coupling constant of 6.8 Hz, while in **16b** it is a singlet at 1.52 ppm.

The **15b** derivative was described by WESTPHAL *et al.* in connection with the nucleophilic substitution of 3β-acetoxy-17-chloro-5-androstene [9]. The melting point (75 °C) measured by WESTPHAL is lower than that of our mixture (**15b**, **16b**: 98—102 °C). The optical rotation values also differ, the published value is $[\alpha]_D$ +68° (etanol), which is quite uncommon for androstene derivatives having generally negative optical rotation. Our results is $[\alpha]_D$ —140° (chloroform).

Solvolysis of **14b** in dimethylsulfoxide gave, besides the mixture of **15b** and **16b** (22%), the diacetate **17b** (51%) as well as **18b** (25%).

Discussion

In order to explain the partial inversion observed during the solvolysis of **3e** in anhydrous acetic acid, it was assumed that the 16α-acetoxymethyl group with a favourable steric position affects the substitution of the β-oriented *p*-toluenesulfonyloxy group. First a six-membered acetoxonium ion (**7**) is formed by inversion, which gives an ortho ester anhydride **8b** with the acetate ion by ion association in a kinetically controlled reaction. The compound is

Table I

^{1}H-NMR data of compounds

Compound	Substituents at			Chemical				
	C-3	C-16	C-17	H-3	H-6	Me-18	Me-19	17H
2a	βAcO	=CHOAc	OH	4.5	5.3	0.71	1.05	4.01
2b	βAcO	=CHOAc	OAc	4.5	5.3	0.76	1.04	5.2
3c	βAcO	αCH_2OAc	βOAc	4.5	5.35	0.82	1.04	3.32
3e	βAcO	αCH_2OAc	βOTs	4.5	5.3	0.83	0.98	4.18
3f	βOH	αCH_2OH	βOTs	3.3	5.3	0.82	0.96	4.25
3g	βOAc	αCH_2OTs	βOTs	4.45	5.25	0.76	0.95	4.05
6b	βOAc	αCH_2OAc	αOAc	4.5	5.4	0.85	1.04	5.05
10a	βOH	αCH_2OH	βCH_3	3.5	5.38	—	0.82	—
10b	βOAc	αCH_2OAc	βCH_3	4.6	5.36	—	1.01	—
11a	βOH	CH_2OH	Δ16.17	3.5	5.38	0.82	1.05	5.74
11b	βOAc	CH_2OAc	Δ16.17	4.6	5.39	0.12	1.06	5.76
14a	βOAc	—	βOH	4.5	5.35	0.76	1.04	3.6
14b	βOAc	—	βOTs	4.5	5.35	0.8	1.00	4.18
15a	βOH	—	βCH_3	3.5	5.3	—	0.92	—
15b	βOAc	—	βCH_3	4.45	5.3	—	0.92	—
16a	βOH	—	CH_3	3.5	5.3	—	0.85	—
16b	βOAc	—	CH_3	4.4	5.35	—	0.85	—
17b	βOH	—	αOH	3.35	5.25	0.65	0.98	3.65
18a	βOAc	—	=O	4.5	5.26	0.85	1.0	—

* Reaction with trichloroacetyl isocyanat (TAI) resulting formation of the trichloroacetylcarbamoyl derivative (TAC) [18]

unstable under the experimental conditions and transforms into the thermodynamically more stable triacetate in an intramolecular reaction. During this intramolecular transformation, the acetate ion can attack at either the C-17 or the C-16-CH_2-site. The attack at C-17 is accompanied by inversion and thus the double inversion occurring the reactions results in the triacetate (**3d**) whose configuration is identical with that of the starting compound. On the other hand, the attack at C-16-CH_2- does not affact the chiral centres, thus **6b** with 16α, 17α configuration is obtained. Since the formation of this com-

2, 3, 6, 10 *and* 14—18

shifts δ (ppm) other signals	TAI-reaction*	Coupling const., J (Hz)
2.02 and 2.12 AcO; 7.15 16 = CH—OAc	5.3 17β-H; 8.51 NH	—
2.00 and 2.10 and 2.10 AcO; 6.95 16 = CHOAc	—	—
2.02 and 2.06 AcO; 4.07 16α-CH_2OAc	4.68 17α-H; 8.7 NH	$J_{17\alpha H,\ 16\beta H} = 7$ Hz
2.00 and 2.00 AcO; 2.4 CH_3Ar; 3.7 and 3.85 CH_2OAc; 7.3 and 7.75 aromatic protons	—	$J_{17\alpha H,\ 16\beta H} = 7$ Hz
2.4 CH_3Ar; 3.5 16α-CH_2OH; 7.25 and 7.75 aromatic protons	4.15 16α-CH_2; 4.6 3αH, 8.35 and 9.1 NH	$J_{17\alpha H,\ 16\beta H} = 7$ Hz
1.98 AcO; 2.4 CH_3Ar; 3.8 16α-CH_2OTs; 7.25 and 7.75 aromatic protons	—	$J_{17\alpha H,\ 16\beta H} = 7$ Hz
2.02 and 2.04 and 2.06 AcO; 4.09 16α-CH_2OAc	—	$J_{17\beta H,\ 16\beta H} = 5.05$ Hz
1.03 17βCH_3; 3.61 16α-CH_2OH; 1.9 OH	4.5 3α-H; 4.15 16α-CH_2; 8.9 NH	—
2.03 and 2.06 AcO; 4.03 16α-CH_2OAc; 1.05 17β-CH_3	—	$J_{17H,\ CH_2} = 6.5$ Hz
4.16 16-CH_2OH; 1.57 OH	4.5 3α-H; 4.1 16α-CH_2; 8.7 NH	—
2.04 and 2.08 AcO; 4.58 16-CH_2OAc	—	—
2.01 AcO	4.55 17α-H; 8.45 NH	—
2.00 AcO; 2.4 CH_3Ar; 7.25 and 7.75 aromatic protons	—	$J_{17\alpha H,\ 16H} = 8$ Hz
0.88 17β-CH_3	4.5 3αH; 8.6 NH	$J_{17CH_3,\ 17H} = 6.7$ Hz
0.88 17β-CH_3; 2.02 AcO	—	$J_{17CH_3,\ 17H} = 6.8$ Hz
1.52 17 CH_3	4.5 3αH; 8.7 NH	—
1.50 17 CH_3; 2.05 AcO	—	—
—	4.55 3αH; 4.85 17β-H; 8.35 NH	$J_{17\beta H,\ 16H} = 5.5$ Hz
1.97 AcO	—	—

pound can be explained by the attack at the sterically less hindered 16-CH_2-group, its appearance in the reaction mixture in larger amount can readily be understood.

The origin of **10b** can be explained by both the formation of the cyclic acetoxonium ion (**7**) and the S_N1 dissociation of the C-17-*p*-toluenesulfonyloxy group. According to the first hypothesis, the acetoxonium ion **7** isomerizes to cation **9** which is stabilized through migration of the neighbouring methyl group and deprotonation. Cation **9** can also be formed through the direct

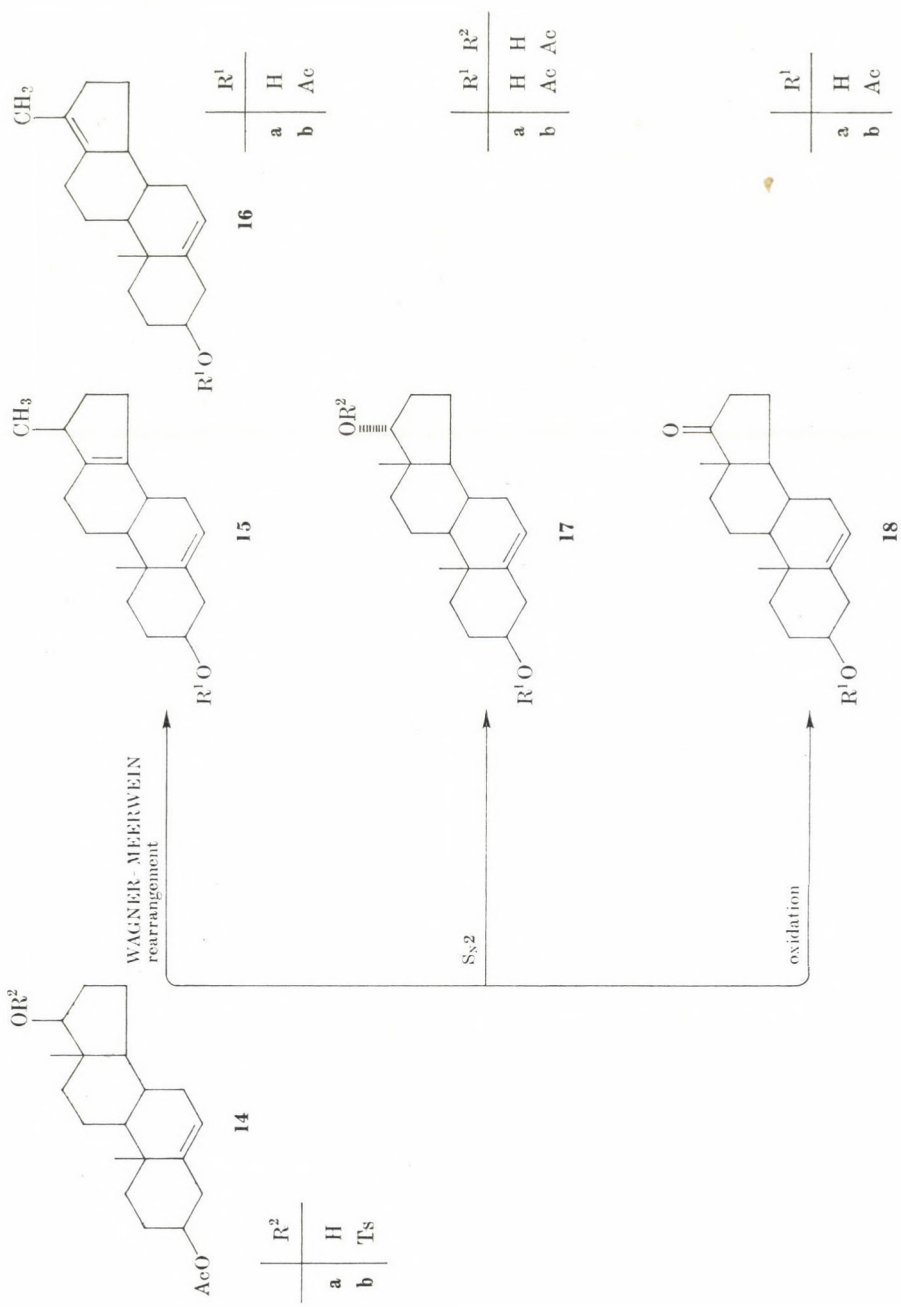
OR²
AcO
14
R² | H | Ts
a | b
WAGNER–MEERWEIN rearrangement
S_N2
oxidation
CH₃
R¹O
15
OR²
R¹O
17
O
R¹O
18
CH₂
R¹O
16
R¹ | H | Ac
a | b
R¹ R² | H H | Ac Ac
a | b
R¹ | H | Ac
a | b

Fig. 2

S_N1 fission of the toluenesulfonyloxy group from **3e**. It is known [7] that the probability of the S_N1 transformation increases with increasing order of the carbon atom, but in this case the *-I* effect of the C-16 acetoxy group does not favour the ionization of the C-17-*p*-toluenesulfonyloxy group.

It was assumed that in the solvolysis of **3e** in anhydrous acetic acid compounds **6b** was formed with one single inversion, while **3d** apparently with retention through double inversion. In order to confirm this route of the above transformations and to suppress the formation of **3d**, the solvolysis was carried out in aqueous acetic acid. One single diacetate (**6c**) was obtained, and **3d** did not form. This can be explained by the formation of an unstable ortho acid semiester (**8a**) in the reaction with water of the acetoxonium ion **7** formed by inversion followed by spontaneous isomerization to gives **6c**.

The formation of **10b** during this reaction can be interpreted in the same way as in anhydrous acetic acid.

The solvolysis of **14b** is faster than that of **3e**; it yielded in one hour a mixture of **15b** and **16b** through WAGNER—MEERWEIN rearrangement and no substitution took place. The relatively fast reaction was attributed to the absence of the C-16 acetoxymethyl group, thus ionization of the *p*-toluenesulfonyloxy group was not reduced by its *-I* effect. Stabilization by rearrangement indicates the pure S_N1 nature of the solvolytic process.

Solvolytic conversion of **3e** was also effected in dimethyl sulfoxide at 160 °C in the presence of potassium acetate. The transformation was significantly faster. Besides the expected **6b** (58%) and **10b** (21%), the earlier not observed acetoxymethyl drivative **11b** (8%) and methylene compound **13b** (10%) were isolated.

The formation of **6b** can be interpreted by the opening of the acetoxonium ion (**7**) formed by S_N1 reaction or by an S_N2 exchange of the C-17β-*p*-toluenesulfonyloxy group favoured in the dipolar aprotic dimethyl sulfoxide. Compound **10b** (21%) can arise through the opening and rearrangement of the acetoxonium ion **7**, while **11b** through the elimination of the *p*-toluenesulfonyloxy group. Concerning the formation of **13b** we supposed, on the basis of literary analogies [10], that the *p*-toluenesulfonyloxy group of **3e** was oxidized into the 17-ketone in the dimethyl sulfoxide/potassium acetate system, and **12** decomposed into the corresponding methylene ketone derivative (**13b**) at the temperature employed.

Solvolysis of the reference compound **14b** in dimethyl sulfoxide produced the rearranged products **15b** and **16b** only in 22.4%, in contrast with the 100% conversion in acetolysis. The main product of this solvolysis was the diacetate **17b**; its formation was explained by the S_N2 reaction of the 17-*p*-toluenesulfonyloxy group. 3β-Hydroxy-5-androsten-17-one 3-acetate (**18b**), formed by oxidation of the C-17-*p*-toluenesulfonyloxy group, was also detected in the reaction mixture.

Experimental

M. p.'s were determined on a Kofler block and are uncorrected.

Specific rotations were measured with a Lippich polarimeter. The error of the rotation values is $\pm 2°$.

The ^{1}H-NMR measurements were effected with a 60 MHz instrument (JEOL, C-60 HL Tokyo), the ^{13}C-FT-NMR spectra were recorded with a PS-100/PFT-100 (JEOL, Tokyo) instrument at 25.15 MHz the Fourier transformation technique.

In both cases the spectra were obtained in $CDCl_3$, using TMS internal standard. The data are given on the δ scale in ppm values.

The IR spectra were recorded with a UNICAM SP 200 instrument in KBr pellets.

The thin-layer chromatograms were made on Kieselgel-G (Merck) layers of 0.25 mm thickness. The following developing solvent systems were employed: I. acetone : benzene : petroleum ether, 30 : 35 : 35; II. methanol : benzene, 1 : 99; III. methanol : benzene, 5 : 95; IV. glacial acetic acid : chloroform, 10 : 90.

The spots were detected by spraying with 50% aqueous phosphoric acid followed by heating at 100—120 °C for 15 min. The R_f values were determined in UV light of 365 nm wavelength.

In the column chromatographic separation Al_2O_3 of activity III—IV, standardized according to Brockmann, was used.

The dimensions of the chromatographic columns used were the following:

Size I: lengt 30 cm; diameter 4.5 cm; Al_2O_3 370 g.

Size II: length 25 cm; diameter 2.5 cm; Al_2O_3 110 g.

Size III: length 25 cm; diameter 2.0 cm; Al_2O_3 50 g.

16-Acetoxymethylene-5-androstene-3β,17ξ-diol 3-acetate (2a)

Finely powdered 16-acetoxymethylene-3β-acetoxy-5-androsten-17-one [5] (**1b**) (2 g; 0.005 mole) was suspended in ethanol (50 mL) in which anhydrous $CaCl_2$ (1.1 g; 0.01 mole) had been dissolved. The reaction mixture was cooled to 0 °C, then $NaBH_4$ (0.75 g; 0.02 mole) was added. After 2 h the reaction mixture was saturated with water, the precipitate was filtered off, washed with water and dried over P_2O_5 in a vacuum desiccator. Recrystallization from a mixture of benzene and petroleum ether gave **2a** (1.80 g; 89.5%), m.p. 193—195 °C; $[\alpha]_D$ —148° ($c = 1$; chloroform). (*Lit.* [11] m.p. 116—118 °C), R_f: 0.20 (solvent system II).

$C_{23}H_{34}O_5$ (402.53). Calcd. C 71.61; H 8.51. Found C 71.30; H 8.75%.

IR: 3500 (OH), 1735, 1250 cm^{-1} (OCO).

16-Acetoxymethylene-5-androstene-3β,17ξ-diol 3,17-diacetate (2b)

Compound **2a** (0.40 g; 0.001 mole) was dissolved in a mixture of pyridine (2 mL) and acetic anhydride (2 mL), allowed to stand for 12 h, then diluted with water. The precipitate was filtered off, washed and recrystallized from a mixture of acetone and water to obtain **2b** (0.380 g, 85.5%), m.p. 173—175 °C; $[\alpha]_D$ —126° ($c = 1$, chloroform). R_f: 0.60 (solvent system II).

$C_{26}H_{36}O_6$ (444.57). Calcd. C 70.25; H 8.16. Found C 70.05; H 8.35%

16α- and 16β-Hydroxymethylandrost-5-ene-3β,17β-diol 3-acetate and 16β-hydroxymethyl-5-androstene-3β,17α-diol 3 acetate (3b, 4b, 5b)

Finely powdered **1b** (20 g; 0.05 mole) was suspended in ethanol (500 mL) in which $CaCl_2$ (11 g; 0.1 mole) had been dissolved. The reaction mixture was cooled to 0 °C, then $NaBH_4$ (7.5 g; 0.2 mole) was added to it in small portions. The mixture was allowed to stand at room temperature for 24 h, then additional (3.7 g; 0.1 mole) $NaBH_4$ was added. After the evolution of gas had ceased, the reaction mixture was saturated with water, acidified to pH 4 with dilute hydrochloric acid and the precipitate was filtered off and washed until free from acid. The solid was then dried over P_2O_5 in a vecuum desiccator.

The isomeric mixture obtained (**3b**, **4b**, **5b**) was dissolved in chloroform (200 mL) and chromatographed on an alumina (column of Size I; 16×250 mL of with benzene-chloroform (1 : 1) eluted first entirely pure **4b** (9.2 g; 50.8%), m.p. 199—201 °C (*lit.* [5] m.p. 199—201 °C).

Continued elution with 8×250 mL fractions of a benzene-chloroform mixture (1 : 1) afforded, after evaporation, a mixture of **3b** and **4b** (0.45 g; 2.4%), then 8×250 mL of chloroform yielded pure **3b** (7 g; 38.6) m.p. 242—244 °C.

Thereafter, 2000 mL of methanol eluted pure **5b** (0.950 g; 5.2%), m.p. 223—225 °C; $[\alpha]_D$ −58° (c = 0.5, ethanol); R_f 0.50 (solvent system I).

$C_{22}H_{34}O_4$ (362.51). Calcd. C 72.88; H 9.45. Found C 72.75; H 9.38%.

IR: 3500 (OH), 1730, 1250 cm^{-1} (OCO).

Finally, elution with acetone-methanol (1 : 1) gave the deacetylated derivatives (**3a**, **4a**, **5a**) amounting to 3% of the mixture to be separated.

16α-Acetoxymethyl-5-androstene-3β,17β-diol 3-acetate (3c)

16α-Hydroxymethyl-5-androstene-3β,17β-diol 3-acetate (**3b**) (3.62 g; 0.01 mole) was dissolved in pyridine (40 mL), and acetic anhydride (1.2 g; 0.012 mole) dissolved in pyridine (10 mL) was added dropwise, while cooling in ice. The reaction mixture was stirred at 0 °C for 6 h, then poured into ice water. The precipitate was filtered off, dissolved in benzene and the benzene solution was dried and chromatographed on alumina (column size III).

Benzene-petroleum ether (1 : 1) eluted **3c** (3.2 g; 79.2%), m..p 141—142 °C; $[\alpha]_D$ −80° (c = 1, chloroform). R_f: 0.75 (solvent system III).

$C_{24}H_{36}O_5$ (404.54). Calcd. C 71.26; H 8.97. Found C 71.45; H 8.63%.

IR: 3540 (OH), 1735, 1250 cm^{-1} (OCO).

16α-Acetoxymethyl-5-androstene-3β,17β-diol 3-acetate 17-*p*-toluenesulfonate (3e)

16α-Acetoxymethyl-5-androstene-3β,17β-diol 3-acetate (**3c**) (4.04 g; 0.01 mole) was dissolved in pyridine (40 mL), and a solution of *p*-toluenesulfonyl chloride (1.9 g; 0.01 mole) dissolved in pyridine (10 mL) was added dropwise while cooling in ice. The reaction mixture was allowed to stand at room temperature for 24 h, then saturated with water. The precipitate was filtered off, washed and dried. The product was crystallized from chloroform-petroleum ether to obtain 5.2 g, (93.2%) of **3e**, m.p. 142—144 °C; $[\alpha]_D$ −84° (c = 1, chloroform). R_f: 0.40 (solvent system II).

$C_{31}H_{42}O_7S$ (558.74). Calcd. C 66.64; H 7.57. Found C 66.75; H 7.65%.

IR: 1735, 1250 cm^{-1} (OCO).

16α-Hydroxymethyl-5-androstene-3β,17β-diol 17-*p*-toluenesulfonate (3f)

16α-Acetoxymethyl-5-androstene-3β,17β-diol 3-acetate 17-*p*-toluenesulfonate (**3e**) (0.558 g; 0.001 mole) was dissolved in methanol (30 mL) containing $NaOCH_3$ (0.1 g). The reaction mixture was allowed to stand for 24 h, then diluted with water. The precipitate was filtered off, washed and dried. The product was crystallized from acetone-water to obtain 0.430 g (90.7%) of **3f**, m.p. 198—200 °C; $[\alpha]_D$ −78° (c = 1, pyridine). R_f: 0.35 (solvent system I).

$C_{27}H_{38}O_5S$ (474.67). Calcd. C 68.33; H 8.07. Found C 68.48; H 8.35%.

IR: 3580 cm^{-1} (OH).

^{13}NMR: δ32.6 (C_{12}); δ46.1 (C_{13}); δ38.9 (C_{16}); δ16.8 (C_{18}) [13].

Acetolysis of 3e in anhydrous acetic acid

Acetic anhydride (1 mL; 0.01 mole) and potassium acetate (1.92 g; 0.012 mole) were refluxed in anhydrous acetic acid (100 mL) for 1 h. Compound **3e** (5.58 g; 0.01 mole) was added, and the solution was maintained at the boiling temperature for 120 h. The reaction mixture was then diluted with water, and the oil which separated was extracted with benzene (3 × 200 mL). The benzene solution was washed with $NaHCO_3$ and then with water until neutral, dried and evaporated to dryness. The residual brown oil was chromatographed on alumina (column size II).

In the chromatographic procedure, 100 mL fractions were collected.

8 × 100 mL of benzene-petroleum ether (5 : 95) eluted a mixture of **10b** and **11b** (1.27 g; 3.3%);

2 × 100 mL of benzene-petroleum ether (10 : 90) contained a mixture of compounds;

2 × 100 mL of benzene-petroleum ether (20 : 80) and

8 × 100 mL of benzene-petroleum ether (30 : 70) afforded a mixture of **3b** and **6b**.

From a methanolic solution of the **10b** and **11b** mixture, 16-acetoxymethylandrosta-5,16-diene-3β-ol 3-acetate (**11b**) crystallized (0.350 g; 27.5%), m.p. 133—135 °C $[\alpha]_D$ −91° (c = 1, chloroform; *lit.* [12] m.p. 135—137 °C); $[\alpha]_D$ −83° (chloroform); R_f: 0.85 (solvent system II).

$C_{24}H_{34}O_4$ (386.53). Calcd. C 74.57; H 8.86. Found C 74.80; H 8.96%.
IR:1735, 1250 cm^{-1} (OCO).

The methanolic mother liquor was saturated with water, whereupon a precipitate separated; this was filtered off and recrystallized from acetone-water to obtain pure **10b** (0.870 g; 6.8%), m.p. 89—91 °C; $[\alpha]_D$ −110° ($c = 1$, chloroform). R_f: 0.85 (solvent system II).
$C_{24}H_{34}O_4$ (386.53). Calcd. C 74.64; H 8.93. Found C 74.35; H 8.80%.
IR: 1735, 1250 cm^{-1} (OCO).

16-Hydroxymethylandrosta-5,16-diene-3β-ol (11a)

Compound **11b** (0.190 g; 0.0005 mole) was hydrolyzed as described in the case of **3f**. The mixture was allowed to stand overnight, diluted with water, made neutral with 1*N* HCl and the precipitate which separated was filtered off, washed with water and dried. The product was crystallized from acetone—water (0.130 g; 86%); m.p. 173—175 °C. $[\alpha]_D$ −75° ($c = 1$, chloroform). (*Lit.* [12] m.p. 170—173 °C; $[\alpha]_D$ −82° (chloroform). R_f: 0.80 (solvent system I).
$C_{20}H_{30}O_2$ (302.46). Calcd. C 79.42; H 9.99. Found C 79.50; H 9.85%.
IR: 3300 cm^{-1}, broad (OH).

16α-Hydroxymethyl-17β-methyl-18-norandrosta-5,13-diene-3β-ol (10a)

Compound **10b** (0.380 g; 0.001 mole) was hydrolyzed as described for **3f**. The product (0.270 g; 89.4%) had m.p. 153—156 °C; $[\alpha]_D$ −126° ($c = 1$, chloroform). R_f: 0.80 (solvent system I).
$C_{20}H_{30}O_2$ (302.46). Calcd. C 79.42; H 9.99. Found C 79.22; 9.76%.
IR: 3500 cm^{-1}, broad (OH).

16α-Hydroxymethyl-5-androstene-3β,17β-diol (3a) and 16α-hydroxymethyl-5-androstene-3β,17α-diol (6a)

The mixture of **3b** and **6b** (2.87 g; 64.5%), obtained in the chromatographic separation procedure, was dissolved in methanol (50 mL) and 1*N* $NaOCH_3$ (2 mL) was added. The reaction mixture was allowed to stand overnight. Compound **6a** separated in the form of hard crystals (1.82 g; 41%), while **3a** remained in solution. M.p. 277—278 °C. R_f: 0.55 (solvent system IV).
$C_{20}H_{32}O_3$ (320.45). Calcd. C 74.94; H 10.07. Found C 74.80; H 10.25%.
The mother liquor was saturated with water, neutralized with 1*N* HCl, the precipitate was filtered off, washed and dried, and the product was crystallized from acetone-water to obtain **3a** (1.04 g; 23.5% [5]).

16α-Acetoxymethyl-5-androstene-3β,17α-diol 3,17-diacetate (6b)

Compound **6a** (1.6 g; 0.005 mole) was suspended in a mixture of acetic anhydride (10 mL) and pyridine (10 mL) and warmed on a water bath at 45 °C for 6 h. After saturation with water, the precipitate was filtered off, washed with water and dried. Compound **6b** (2.1 g; 94.1%) was crystallized from aqueous methanol; m.p. 119—120 °C; $[\alpha]_D$ −46° ($c = 1$, chloroform). R_f: 0.50 (solvent system II).
$C_{26}H_{38}O_6$ (446.56). Calcd. C 69.93; H 8.45. Found C 69.85; H 8.63%
IR: 1730, 1250 cm^{-1} (OCO).

Acetolysis of 3e in aqueous acetic acid]

Potassium acetate (1.92 g; 0.012 mole) was dissolved in a mixture of acetic acid (95 mL) and water (5 mL); **3e** (5.58 g; 0.01 mole) was added to the solution and was refluxed for 120 h.

The reaction mixture was then diluted with water and the oil which separated was extracted with benzene (3 × 200 mL). The benzene layer was washed with dilute $NaHCO_3$ solution and with water until neutral, dried and evaporated to dryness.

The residue was chromatographed as described in the case of the acetolysis of **3e**; **10b** (1.2 g; 31%) and (**6c** 2.98 g; 67%) were eluted.

Solvolysis of 3e in dimethyl sulfoxide

Potassium acetate (3.84 g; 0.024 mole) was dissolved in dimethyl sulfoxide (100 mL), then **3e** (11.16 g; 0.02 mole) was added. The reaction mixture was heated at 160 °C for 24 h. After cooling, benzene (500 mL) was added and dimethyl sulfoxide was removed by washing with water. The benzene layer was dried, evaporated to dryness, and the brownish-red oily residue was dissolved in methanol (200 mL), 1*N* $NaOCH_3$ solution (5 mL) was added, and the mixture was allowed to stand for 24 h, wherupon homogeneous **6a** separated in the form of a hard crystal crust (3.7 g; 58%).

The methanolic mother liquor was neutralized with 1*N* HCl, evaporated to dryness, and chromatographed on alumina (column size II); 4×100 mL of chloroform-benzene (1 : 3) eluted **13a** (0.60 g; 10%) m.p. 183–184 °C; $[\alpha]_D$ −56° (*c* = 1, chloroform); (*lit.* [13] m.p. 160–165 °C). R_f: 0.80 (solvent system I).

$C_{20}H_{28}O_2$ (300.44). Calcd. C 79.97; H 9.39%. Found C 79.68; H 9.34%.

6×100 mL of chloroform-benzene (1 : 1) eluted then **11a** (0.48 g; 8%).

Next, 10×100 mL of chloroform-benzene (2 : 1) eluted **10a** (1.26 g; 21%).

5-Androstene-3β,17β-diol 3-acetate (14a)

3β-Hydroxy-5-androsten-17-one 3-acetate (6.6 g; 0.02 mole) was dissolved in methanol (100 mL) and $NaBH_4$ (3.7 g; 0.1 mole) was added in small portions, while cooling in ice. The pH of the solution was maintained between 5 and 6 by the addition of alcoholic acetic acid solution in the presence of Bromothymol Blue indicator. The reaction mixture was allowed to stand overnight, diluted with water, and acidified with dilute hydrochloric acid. The precipitate was filtered off, washed until free from acid, and dried. The product (**14a**) was recrystallized from benzene-petroleum ether (6.1 g; 91.8%), m.p. 148–150 °C; $[\alpha]_D$ −62° (*c* = 1, chloroform; *lit.* [15] m.p. 144–145 °C; $[\alpha]_D$ −56°, ethanol). R_f: 0.60 (solvent system III).

$C_{21}H_{32}O_3$ (332.48). Calcd. C 75.88; H 9.70; Found C 75.73; H 9.64%.

IR: 1735, 1250 cm^{-1} (OCO).

5-Androstene-3β,17β-diol 3-acetate 17-*p*-toluene-δ-sulfonate (14b)

Compound **14a** (6.64 g; 0.02 mole) was esterified as described for **3e**. Compound **14b** was crystallized from methanol (9.2 g; 94.6%), m.p. 165–166 °C; $[\alpha]_D$ −70° (*c* = 1, chloroform). (*Lit.* [16] m.p. 162–164 °C; $[\alpha]_D$ −72°, ethanol). R_f: 0.60 (solvent system II).

$C_{28}H_{38}O_5S$ (486.68). Calcd. C 66.32; H 7.90. Found C 66.30; H 7.65%.

IR: 1730, 1250 cm^{-1} (OCO).

Acetolysis of 14b in anhydrous acetic acid

Potassium acetate (1.92 g; 0.006 mole) and **14b** (2.43 g; 0.005 mole) were dissolved in anhydrous acetic acid (50 mL). The reaction mixture was kept at its boiling temperature for 6 h. Benzene (200 mL) was added to the solution, and the acetic acid was removed by washing with water. The benzene layer was evaporated to dryness and the residue chromatographed on alumina (column size III). 5×100 mL of benzene-petroleum ether (1 : 1) eluted a mixture of **15b** and **16b** (1.50 g; 95.5%), m.p. 98–102 °C; $[\alpha]_D$ −140° (*c* = 1, chloroform). (*Lit.* [9] m.p. 75 °C; $[\alpha]_D$ +68°, ethanol). R_f: 0.85 (solvent system II).

$C_{21}H_{30}O_2$ (314.47). Calcd. C 80.21; H 9.62. Found C 80.43; H 9.75%.

IR: 1730, 1250 cm^{-1} (OCO).

^{13}NMR: δ138.8 (C_5); δ122.3 (C_6); δ136.6 (C_{13}); δ138.3 (C_{14}).

^{13}NMR: δ140.0 (C_5); δ122.7 (C_6); δ136.1 (C_{13}); δ54.1 (C_{14}) δ127.4 (C_{17}).

17β-Methyl-18-norandrosta-5,13-diene-3β-ol (15a) and 17-methyl-18-norandrosta-5,13(17)-diene-3β-ol (16a)

The mixture of **15b** and **16b** (1.57 g; 0.005 mole) was hydrolyzed as described for **3f**. The product was crystallized from acetone-water (0.98 g; 72%), m.p. 136–138 °C; $[\alpha]_D$ −155° (*c* = 1, chloroform). R_f: 0.55 (solvent system III).

$C_{19}H_{28}O$ (272.43). Calcd. C 83.78; H 10.36; Found C 83.65; H 10.56%.
IR: 3500 cm^{-1} (broad, OH).

Solvolysis of 14b in dimethyl sulfoxide

Potassium acetate (1.92 g; 0.012 mole) and **14b** (4.86 g; 0.01 mole) were dissolved in dimethyl sulfoxide (100 mL) and the mixture was kept at 100 °C for 6 h. The reaction mixture was worked up as in the solvolysis of **3e**.

Compound **18a** (0.72 g; 25%) was eluted with 6×100 mL of benzene-petroleum ether (1 : 3); m.p. 141–142 C°; $[\alpha]_D$ +3° (c = 1, chloroform). R_f: 0.70 (solvent system III). (*Lit.* [17] m.p. 140 °C; $[\alpha]_D$ +2° (chloroform)).

4×100 mL of benzene-petroleum ether (1 : 1) and 2×100 mL of benzene-petroleum ether (3 : 1) eluted then a mixture of **15a** and **16a** (0.610 g; 22.4%).

Finally, 4×100 mL of benzene eluted (**17a**) (1.42 g; 41%), m.p. 197 °C; $[\alpha]_D$ −56° (c = 1, chloroform). (*Lit.* [17] m.p. 180 °C; $[\alpha]_D$ 61° (chloroform-ethanol, 9 : 1)).

*

The authors' thanks are due to the Chemical Works of Gedeon Richter Ltd., Budapest, for supporting this research. The authors acknowledge the assistance of Dr. G. ENGELHARDT (Akademie der Wissenschaften der DDR, Zentralinstitut für physikalische Chemie, Berlin-Adlershof) in recording the ^{13}C-NMR spectra. Thanks are due to Mr. J. KISS for the IR spectra, to Dr. K. LAKOS–LÁNG, Dr. G. BARTÓK–BOZÓKI for the microanalyses, and to Miss Cs. HORVÁTH for technical assistance.

REFERENCES

[1] KNOX, L. H.: U. S. Pat. 3,088,954; Chem. Abstr., **59,** 11613 g (1965)
[2] KNOX, L. H., VELARDE, E.: J. Org. Chem., **27,** 3925 (1962)
[3] COUNSELL, D. E. KUNSTRA, P. O.: J. Med. Chem., **6,** 736 (1967)
[4] SCHNEIDER, Gy., W. VINCZE, L.: Kémiai Közlemények, **31,** 383 (1969)
[5] SCHNEIDER, Gy., VINCZE, I., VASS, A.: Acta Chim. Acad. Sci. Hung., **99,** 51 (1979)
[6] SCHÖNECKER, B., TRESSELT, D., DRAFFEHN, J., PONSOLD, K., ENGELHARDT, G., ZEIGAN, D., SCHNEIDER, Gy., W. VINCZE, I., DOMBI, Gy.: J. prakt. Chem., **319,** 419 (1977)
[7] PRITZKOW, W., SCHÖPPLER, H.: Chem. Ber., **95,** 834 (1962)
[8] HINE, J.: J. Org. Chem., **31,** 1236 (1966)
[9] WESTPHAL, V., WANG, Y. L., HELLMANN, H.: Chem. Ber., **6,** 1233 (1939)
[10] EPSTEIN, W. W., SWEAT, F. W.: Chem. Rev., **67,** 247 (1967)
[11] GERALI, G., IUS, A., PARINI, C., SPORTOLETTI, G. C.: Il Farmaco, **24,** 2 (1969)
[12]GERALI, G., SPORTOLETTI, G.C., PARINI, C., IUS, A., CORBELLINI, A.: Il Farmaco, **23,** 679 (1961)
[13] ENGELHARDT, G., SCHNEIDER, Gy., WEISZ-VINCZE, I., VASS, A.: J. prakt. Chem., **316,** 391 (1974)
[14] JULIAN, P. L., MAYER, E. W., MEYER, P. L., PRINTY, H. C.: J. Am. Chem. Soc., **70,** 3872 (1948)
[15] WESTPHAL, V., WANG, Y.-L., HELLMANN, H.: Ber., **72,** 1233 (1939)
[16] MADAEVA, O. S., LURI, F. A.: Doklady Akad. Nauk. USSR, **84,** 713 (1952)
[17] BARTON, D. H. R., COX, J. D.: J. Chem. Soc., **1948,** 783
[18] GOODLETT, V. W.: Anal. Chem., **37,** 431 (1965)

Gyula SCHNEIDER
Irén VINCZE
László HACKLER
György DOMBI
H–6720 Szeged, Dóm tér 8.

András VASS
H–8201 Veszprém

Acta Chimica Academiae Scientiarum Hungaricae, Tomus 109 (1), pp. 83—91 (1982)

THE ACIDITY OF PICROLONIC ACID AND THE CONDUCTANCE OF ITS SODIUM, POTASSIUM AND RUBIDIUM SALTS IN WATER AND DIMETHYL SULFOXIDE

M. M. OSMAN,* A. M. HAFEZ, M. A. MAKHYOUN and A. B. TADROS

(Chemistry Department, Faculty of Science, Alexandria University, Alexandria, EGYPT)

Received October 16, 1980

In revised form January 15, 1981

Accepted for publication February 12, 1981

The acidity of picrolonic acid in 5% ethyl alcohol solution was studied by spectrophotometric and potentiometric methods. The strong acid character was attributed, on the basis of the i.r. spectra of the acid and its alkali metal salts with sodium, potassium and rubidium, to the active methine group. The conductance of these salts were studied at 25 ± 0.02 °C in water and in dimethyl sulfoxide. The alkali metal picrolonates were found to be non-associated electrolytes. The conductance at infinite dilution, the contact distance and the association constants were determined and explained in terms of solvation. The ionic conductance of the rubidium ion in DMSO at 25 °C was found to be 15.96 ohm^{-1} cm^2.

Introduction

A substantial amount of work has been done on the application of picrolonic acid in analytical chemistry [1—7]. Complex formation of picrolonic acid with some alkaline earth and transition metal ions has also been studied by conductometric methods [8]. However, no appreciable work has been done on the acid itself or on its alkali metal salts. The present work is an attempt to study the acidity of picrolonic acid related to its structure and also the conductance of sodium, potassium and rubidium picrolonates in water and in dimethyl sulfoxide.

Experimental

Solutes. Picrolonic acid was obtained by twice recrystallising a commercial sample (Fluka AG) from ethyl alcohol and drying it in vacuum (P_2O_5) to a constant weight. The acid content of the compound was determined potentiometrically and was found to be 99.82%.

Sodium, potassium and rubidium picrolonates were prepared by addition of individual solutions of A.R. sodium hydroxide, potassium hydroxide and rubidium chloride (10 mmole each) in a least amount of water to a hot solution of picrolonic acid (10 mmole) in 20 cm^3 ethyl alcohol. The separated yellow crystalline products were filtered, washed with hot alcohol and ether. Further purification of the salts was done by recrystallisation from water-alcohol and drying to a constant weight for four days in vacuum (P_2O_5).

Analysis. Calc. for $NaC_{10}H_7N_4O_5$: Na, 8.04%; C, 41.96%; N, 19.58%. Found: Na, 8.02%; C, 41.80%, N, 19.20%. Calc. for $KC_{10}H_7N_4O_5$: K, 12.93%; C, 39.73%; N, 18.54%.

* To whom correspondence should be addressed.

Found: K, 12.89%; C, 39.70%; N, 18.20%. Calc. for $RbC_{10}H_7N_4O_5$: Rb, 24.52%; C, 34.45% N, 16.07%. Found: Rb, 24.47; C, 34.70%; N, 16.50%.

Solvents. Double distilled, CO_2-free water was generally used for the preparation of the solutions. Conductivity water was obtained by passing ordinary distilled water through a 60-cm long Elgastat deionizer and guarded against contamination with atmospheric CO_2. It had a specific conductivity of $5-7\times10^{-7}$ ohm^{-1} cm^{-1}.

DMSO was purified as described by BRUNO *et al.* [9] and had the following physical properties at 25 ± 0.02 °C: specific conductance $= 3-5\times10^{-5}$ ohm^{-1} cm^{-1}, density $=$ 1.09562 g · cm^{-3} and viscosity $= 1.99657\times10^{-2}$ Pa s. These values of density and viscosity are in excellent agreement with those reported in literature [10].

Solutions. A stock solution of 0.02 *M* picrolonic acid was prepared in ethyl alcohol and standardized potentiometrically with standard carbonate-free potassium hydroxide. Aqueous solutions of the same concentration of sodium, potassium and rubidium picrolonates were prepared. The dilute solutions were prepared from these solutions by accurate dilution.

An accurate 0.1 *M* solution of potassium hydroxide was prepared by the dilution of a standard 1.00 *M* solution (BDH volumetric reagents).

Physical measurements. The electronic spectra were recorded on a Pye-Unicam SP 1800 recording spectrophotometer.

The pH-measurements were carried out on a Unicam pH-meter, model 291 MK. The apparatus was calibrated by the titration of a 10^{-3} *M* HCl solution [11]. The measurements were carried out under purified nitrogen [12].

The i.r. spectra were recorded on a Beckman 4220 infra-red spectrophotometer in potassium bromide pellets.

The electrical conductances were measured in borosilicate glass Erlenmeyer conductivity cell having rigid bright platinum electrodes. A Beckman conductivity bridge, model 18A was used to measure the resistance of the solution at 3 Kc/S. All solutions were prepared by the addition of weighed amount of stock solution to a known weight of the solvent in the cell; a current of dry, purified nitrogen was passed over the solution during the addition.

Density measurement was performed in a 20 cm^3 pycnometer. Viscosities were measured using a modified Ub Belohde suspended level viscosimeter.

Results and Discussion

The electronic spectra of 2×10^{-5} *M* solution (5% ethyl alcohol) of picrolonic acid at 25 °C and at different pH-values (between 2.08 and 10.8) are shown in Fig. 1. All spectra exhibit only one absorption peak at 338 nm. The absorbance is also pH independent indicating the presence of only one absorbing species irrespective of the neutralisation degree of the acid.

The electronic spectra of 2×10^{-5} *M* solution each of sodium picrolonate, potassium picrolonate and rubidium picrolonate were recorded in the same wavelength range chosen for picrolonic acid. The spectra show identical bands in position and absorbance, which are as well identical with that of the acid itself. We can accordingly suggest that picrolonic acid behaves as a strong acid.

The potentiometric titration of picrolonic acid at 25 °C in 5% ethyl alcohol solution gives further evidence for the strong acidic character of this acid. Figure 2 shows the titration curve of 10^{-3} *M* solution of picrolonic acid compared with that of HCl of the same concentration, and solvent composition.

The protonation degree $\bar{p}$, defined as $[HP]/[HP]_{tot.}$ [11, 13] was also calculated at different pH values and is given in Table I.

$$\bar{p} = \frac{[HP]_{tot.} - [KOH] - [H^+] + [OH^-]}{[HP]_{tot.}} . \qquad (1)$$

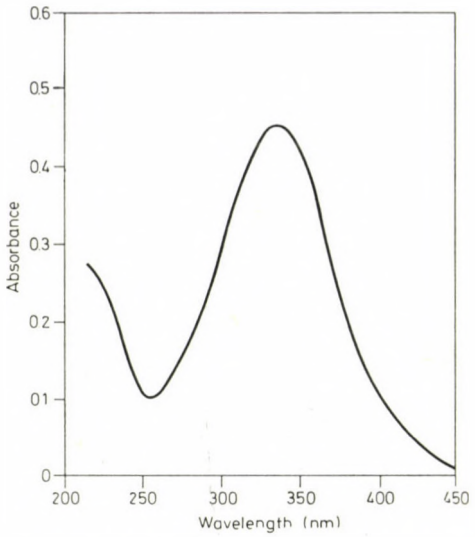

Fig. 1. Electronic spectra of picrolonic acid in 5% ethanol solution at 25 °C and at different pH values (2.08—10.3)

Table I

Protonation degree of picrolonic acid in 5% ethyl alcohol solution at 25 °C

$10^4 C_{HP}$	$pH_{calc.}$	$pH^*_{exper.}$	$\bar{p}$
8.5	3.071	3.087	−0.018
8.0	3.097	3.097	0.000
7.5	3.125	3.127	0.004
7.0	3.155	3.157	0.003
6.5	3.187	3.187	0.000
6.0	3.222	3.217	−0.007
5.5	3.260	3.257	−0.003
5.0	3.301	3.307	0.007
4.5	3.347	3.347	0.000
4.0	3.398	3.407	0.008
3.5	3.456	3.437	−0.016
3.0	3.477	3.517	0.004
2.5	3.602	3.597	−0.003
2.0	3.699	3.697	−0.001

* Corrected pH

The values of $\bar{p}$ were found to deviate very slightly from zero, thus supporting the strong acid character of picrolonic acid.

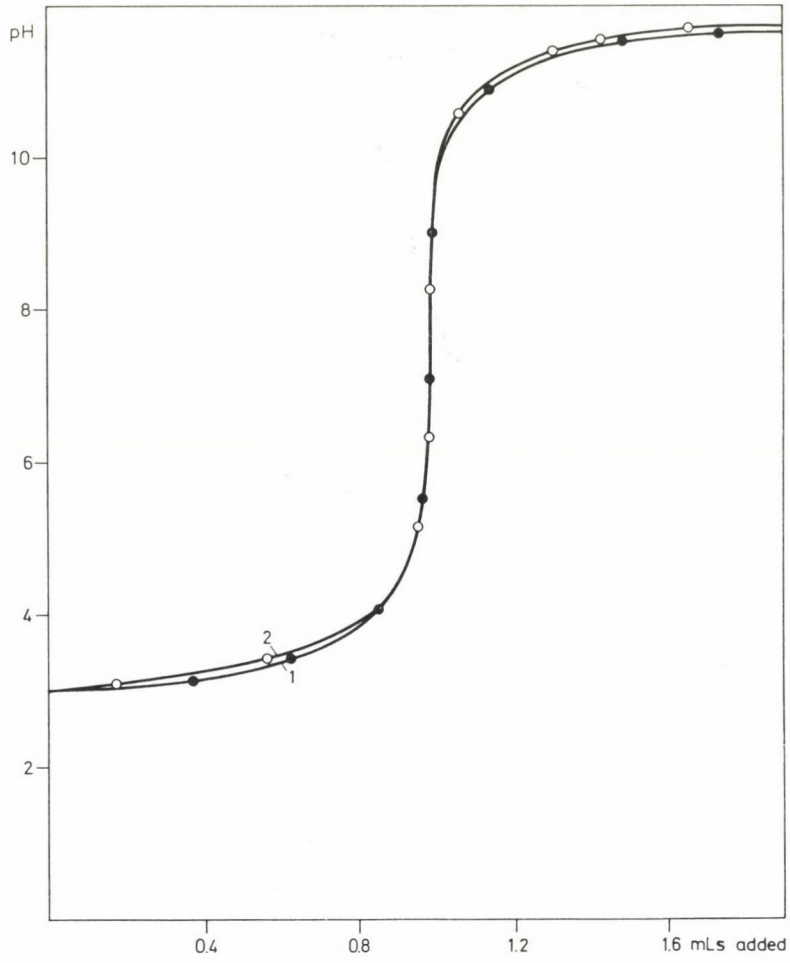

Fig. 2. Potentiometric titration curves of 10^{-3} *M* solutions (5% ethanol) at 25 °C of (1) picrolonic acid and (2) HCl

It has been reported that picrolonic acid exists in two tautomeric forms [7].

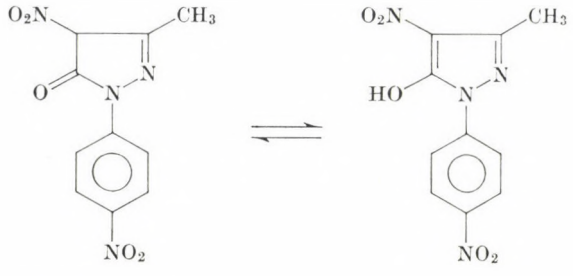

The electron-attracting character of the nitro group, adjacent to the carbonyl group, together with the resonance effect will be reflected on the enhanced acidity of picrolonic acid. The deprotonation of the acid will normally be expected to take place from the enol form. We thought, however, that the strong acidity of the compound could not be achieved through deprotonation of the enol group. The proton should more probably be released from the active methine group in position 4. This assumption is consistent with the i.r. spectra of picrolonic acid and its alkali metal salts (Table II). The absence of any absorption due to ν(OH) frequency and the presence of ν(C=O) fre-

Table II

Characteristic i.r. frequencies of picrolonic acid and its sodium, potassium and rubidium salts

HP	NaP	KP	RbP	Assignment
1660 s	1660 s	1660 s	1660 s	ν(C=O)
1610 w	1610 sh	1610 sh	1605 sh	ν(C=N)
1600 m	1600 m	1600 m	1595 m	ν(C=C)
1500 s	1500 s	1505 s	1500 s	ν(C=C) + $\nu(NO_2)_{as.}$
1445 m	1440 m	1440 m	1440 m	ν(C=C) + $\nu(CH_3)$
1350 s	1345 m	1345 m	1345 m	$\nu(NO_2)_{s.}$
1355 m	1360 w	1360 w	1360 w	ν(C–N)
1250 m	1250 s	1250 s	1250 m	ν(N–N)

P, picrolonate ion; s, strong; m, medium; w, weak; sh, shoulder; as., asymmetric; s., symmetric

quency at 1660 cm^{-1} suggest only the acid keto form. The ν(C=O) is assigned by comparison with similar compounds reported by LEONARD *et al.* [14]. The position of the strong ν(C=O) frequency of the acid remains unchanged in sodium picrolonate, potassium picrolonate and rubidium picrolonate. This indicates that the picrolonate ion also exists only in the keto form.

The conductance parameters: the conductance at infinite dilution Λ_0, contact distance a^0 and association constant K_A were calculated for the sodium picrolonate, potassium picrolonate and rubidium picrolonate by applying the conductivity equations for these 1 : 1 electrolytes.

The conductance data of the alkali metal picrolonates in water and in DMSO are summarized in Tables III and IV, respectively, where Λ (ohm^{-1} cm^2 mole^{-1}) is given at several concentrations C in moles per liter of solution.

In order to obtain an accurate value for Λ_0 and the association constant K_A, the FUOSS–ONSAGER's equation [15]:

$$\Lambda = \Lambda_0 - S(C\gamma)^{1/2} - EC\gamma \log C\gamma + JC\gamma - K_A C\gamma f^2 \Lambda - F\Lambda_0 C\gamma \qquad (2)$$

Table III

Conductance of alkali metal picrolonates in water at 25 °C

NaP		KP		RbP	
$10^4 C$	Λ	$10^4 C$	Λ	$10^4 C$	Λ
11.1990	74.166	18.6480	97.464	14.0100	100.971
8.9083	74.556	15.9190	97.707	11.8170	101.075
8.0755	74.706	10.5470	98.303	8.3490	101.587
5.8238	75.092	8.5237	98.610	7.2608	101.790
4.1018	75.547	6.6505	98.844	6.1664	102.269
2.7508	76.040	5.0348	99.057		
2.1509	76.163				

Table IV

Conductance of alkali metal picrolonates in dimethyl sulfoxide at 25 °C

NaP		KP		RbP	
$10^4 C$	Λ	$10^4 C$	Λ	$10^4 C$	Λ
25.5860	24.218	15.6640	25.166	15.1660	26.549
21.7270	24.427	13.8620	25.266	13.3020	26.659
17.1680	24.686	10.5600	25.404	10.8880	26.829
13.006	24.930	7.8330	25.907	8.2488	27.137
9.6573	25.183	6.0882	26.194	6.3396	27.365
7.2793	25.375			5.0076	27.596
5.8415	25.483			3.9164	27.911

was used. A preliminary value of Λ_0 was estimated from the FUOSS—KRAUS—SCHEDLOVSKY equation [16]:

$$1/\Lambda S_{(Z)} = 1/\Lambda_0 + C\Lambda S_{(Z)} f^2 / K\Lambda_0^2 \tag{3}$$

where the SCHEDLOVSKY function $S_{(Z)}$ has been tabulated by DAGGETT [17],

$$Z = (\alpha/\Lambda_0^{3/2})(C\gamma)^{1/2} \tag{4}$$

and α is the limiting tangent and K the dissociation constant. All the symbols in equations 2—4 have their usual meaning; the necessary equations and constants have been summarized elsewhere [18, 19]. Figures 3 and 4 show the FKS plots for sodium, potassium and rubidium picrolonates in water and DMSO. Tables V and VI summarize the derived constants, which were obtained by a computer program [20] on an IBM (1620) machine. The accuracy in these computation are ± 0.02 for Λ_0, ± 20 for $J > 200$ and ± 5 for $J < 200$.

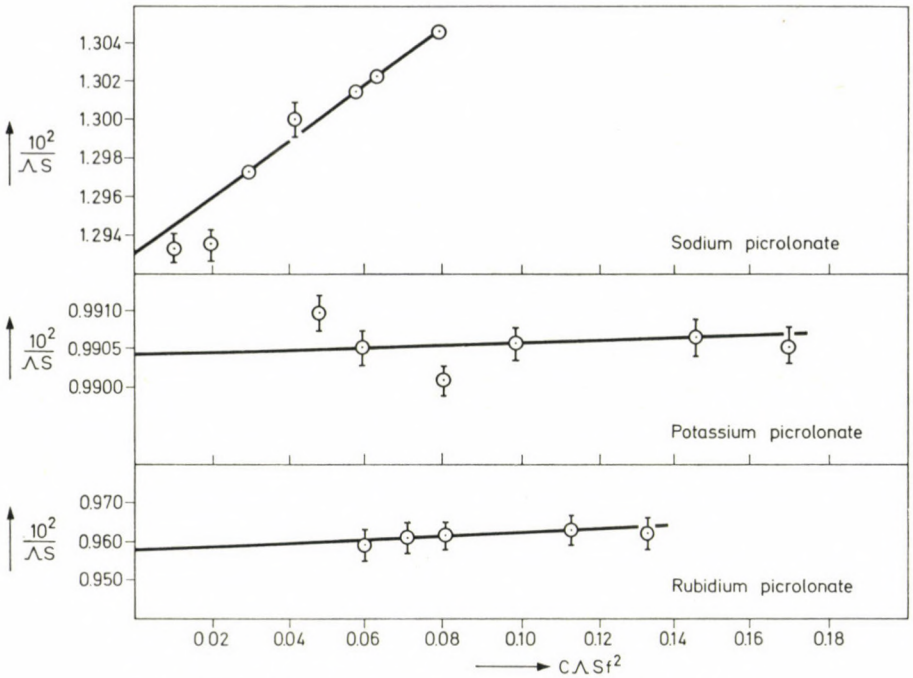

Fig. 3. (FKS) plots of alkali metal picrolonates in water at 25 °C

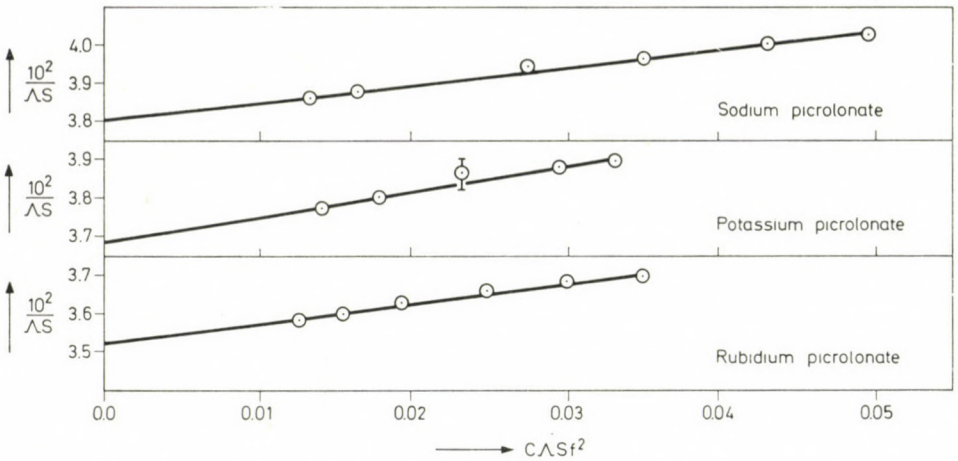

Fig. 4. (FKS) plots of alkali metal picrolonates in dimethyl sulfoxide at 25 °C

In water, it can be seen from Table V, that Λ_0 for sodium picrolonate, potassium picrolonate and rubidium picrolonate increases while a^0 decreases with an increase in the cation size. This behaviour can be attributed to solvation. Owing to the successive decrease of the charge density from Na^+ to

Table V

Constants derived from conductance data for the picrolonate salts in water at 25 °C

Salt	Λ_0	J	$a°$	$\lambda°_-$	K_A
NaP	77.45	254.1	6.5	27.35	0.12
KP	100.96	240.0	6.06	27.46	0.95
RbP	104.33	222.5	4.5	27.13	3.76
				($\lambda°_{-av} = 27.23$)	

$\lambda°_{Na^+} = 50.1$ (15), $\lambda°_{K^+} = 73.50$ (15), $\lambda°_{Rb^+} = 77.20$ (15)

Table VI

Constants derived from conductance data for the picrolonate salts in dimethyl sulfoxide at 25 °C

Salt	Λ_0	J	$a°$	$\lambda°_-$	K_A
NaP	26.20	224.6	7.57	12.50	30.60
KP	27.14	215.8	6.90	12.64	47.34
RbP	28.53	170.4	4.9		46.04
				($\lambda°_{-av} = 12.57$)	
				($\lambda°_{Rb^+} = 15.96$)	

$\lambda°_{Na^+} = 13.7$ (23), $\lambda°_{K^+} = 14.5$ (23)

Rb^+, a smaller number of water molecules should be immobilized to a considerable extent around the ion to form a solvation sheath. In other words, the solvation decreases in the order $Na^+ > K^+ > Rb^+$ and hence the ionic mobility will increase in the reverse order.

The values of K_A for the alkali metal picrolonates in aqueous solution are all very small indicating that these salts in water are of the non-associated type. This finding is in accordance with our previous conclusion based on the spectrophotometric measurements. If one compares, however, these small K_A values, it is obvious that a slight increase of K_A occurs with an increase in the cation size of the alkali metal ion. This suggests that the size of the solvated cation becomes the essential factor in controlling the extent of ion-pair formation, since the solvation of the picrolonate ion is assumed to be constant for the three salts.

The same behaviour for Λ_0, K_A and a^0 was observed for alkali metal chlorates in water [21]. The authors explained their results in a similar way in terms of the degree of solvation. Further evidence for these findings were observed in the case of alkali halides in the hydrogen-bonded solvents; methanol, ethanol and *n*-propanol [22].

The derived constants for the alkali metal picrolonates in DMSO are listed in Table VI. Again Λ_0 increases and a^0 decreases with an increase in the cation size. This behaviour is in accordance with that found in water and may similarly be explained in terms of solvation. The same trend of Λ_0 and a^0 was reported for alkali metal perchlorates in ethylene glycol [24]. KEMPA and LEE [25] also found that the value of the solvation number for the alkali metal ions in ethylene carbonate supports the increase of ionic conductance along the series $Na^+ < K^+ < Rb^+$. The conductance of the alkali picrolonates in DMSO also leads to the calculation of the ionic conductance of rubidium in this solvent having a value of 15.96 ohm^{-1} cm^2 at infinite dilution. The association constants of the picrolonate salts in DMSO are higher than those in water, which is normally expected due to electrostatic effects.

REFERENCES

[1] VOGEL, A. I.: "A Textbook of Macro- and Semimicro Quantitative Inorganic Analysis", Longmans, London, 1959, p. 305
[2] KOLARIK, Z.: Coll. Czech. Chem. Comm., **26,** 2009 (1961)
[3] BECHERECU, D.: Bull. Stiint. Technic., Inst. Politechnik, Timisoara, **1956** (21), 1, 281
[4] GUNTHER, R. C., KOLTHOFF, I. M.: J. Biol. Chem., **147,** 705 (1953)
[5] DUPUIS, Th., DUVAL, Cl.: Anal. Chem. Acta, **3,** 589 (1949)
[6] PETROV, A. E.: Spiridonov-Izvest. Timoryazev Sel Skakhoz. Akad., **1,** 236 (1960)
[7] BECHERESCU, D.: Ser. Stiinte Chim., **6,** 115 (1959)
[8] JOSHI, D. P., JAIN, D. V.: J. Indian. Chem. Soc., **41,** 711 (1964)
[9] BRUNO, P., MONICA, M. D.: J. Phys. Chem., **176,** 1049 (1972)
[10] COWIE, J. M. G., TAPOROWSKI, P. M.: Can. J. Chem., **39,** 2240 (1961)
[11] OSMAN, M. M., SALEM, T. M., ELEZABY, M. S.: J. Chem. Soc. (A), **1971,** 1401
[12] HONIGSCHMIDT, O.: Z. anorg. Chem., **78,** 163 (1927)
[13] OSMAN, M. M.: Helv. Chim. Acta, **55,** 239 (1972)
[14] LEONARD, N. J., SENTZ, R. C.: J. Am. Chem. Soc., **74,** 1704 (1952)
[15] ROBINSON, R. A., STOKES, R. H.: "Electrolyte Solution", Butterworths, London 1961
[16] FUOSS, R. M., KRAUS, C. A.: J. Am. Chem. Soc., **55,** 476 (1933); FUOSS, R. M.: *ibid.*, **57,** 488 (1935); FOUSS, R. M., SCHEDLOVSKY, T.: *ibid.*, **71,** 1496 (1949)
[17] DAGGETT, H. M.: J. Am. Chem. Soc., **73,** 4977 (1951)
[18] LIND, J. E., ZWOLENIK, J. J., FUOSS, R. M.: J. Am. Chem. Soc., **81,** 1557 (1959)
[19] FUOSS, R. M., ACCASCINA, F.: "Electrolytic Conductance", Interscience, N. Y., 1959
[20] HAFEZ, A. M.: Ph. D. Thesis, Chemistry Department, Faculty of Science, Alexandria, 1972
[21] DAPRANO, A., DANATO, I. D.: Electrochimica Acta, **17,** 1175 (1971)
[22] KAY, R. L.: J. Am. Chem. Soc., **82,** 2099 (1959)
[23] ATLANI, C., JUSTICE, J. C.: J. Solution Chem., **4,** 962 (1975)
[24] FERNANDES-PRINI, R., URRUTIA, G.: J. Chem. Soc., Faraday Trans., **1976,** 637
[25] KEMPA, R. F., LEE, W. H.: J. Chem. Soc., **1961,** 100

Maher Mohamed OSMAN
Amina Mohamed HAFEZ
Mohamed Abd-Allah MAKHYOUN
Aida Botros TADROS

Chemistry Department, Faculty of Science, Alexandria Univ., Alexandria, Egypt

Acta Chimica Academiae Scientiarum Hungaricae, Tomus 109 (1), pp. 93—101 (1982)

PYRIDINE AND ANILINE COMPOUNDS OF COMPLEX HALOACIDS OF THE IIB GROUP METALS

TH. F. ZAFIROPOULOS, S. P. PERLEPES, J. K. KOUÏNIS and A. G. GALINOS*

(Department of Inorganic Chemistry, University of Patras, 231 Korinthou str., Patras, Greece)

Received September 18, 1980

Accepted for publication February 17, 1981

The preparation of nine new pyridine and aniline compounds of complex haloacids of Zn(II), Cd(II) and Hg(II) is reported.

Analytical, conductometric, spectral (infrared and ultraviolet) and X-ray data were used for the characterization of the complexes. Pseudotetrahedral and pyramidal structures are proposed for the Zn(II)- and Hg(II)-complexes, respectively. The structure of the Cd(II) complexes, in the solid state, cannot be deduced with certainty.

Introduction

Although a large number of salts of the type $R^+[MX_3]^-$ (where R^+ is usually a large organic cation and M is zinc, cadmium or mercury) are known, and have been extensively investigated, the situation with respect to the parent acids is far from clear. The study of haloacids is of special interest, since some of them are used in certain Friedel—Crafts reactions. The catalytic action of the etherate $HAlCl_4 \cdot 2\ Et_2O$ (Et_2O = diethyl ether) has been studied [1].

Compounds of simple and mixed complex tri-haloacids of Zn(II), Cd(II) and Hg(II) with Lewis organic bases, have been prepared and studied [2—9]. Very recently, we established the preparative conditions and studied the complex compounds $HCdI_3 \cdot 3B$ and $H_2CdI_4 \cdot nB$ (B = Et_2O, Pyridine, Aniline and n = 4, 5) [10]. As a continuation of the interest of our laboratory in the complex haloacids and their compounds, we report here the preparation and study of nine pyridine and aniline compounds of complex haloacids of Zn(II), Cd(II) and Hg(II).

Experimental

Materials

High purity reagents were used for the preparation of the complex compounds. Diethyl ether was treated for the removal of peroxides and moisture, by standard methods. Pyridine (Py) and aniline (An) were doubly distilled under atmospheric pressure. Ethanol, used for the ultraviolet spectra, was of spectroscopic quality (Merck). For the conductometric measurements

* To whom correspondence should be addressed

as solvents were used absolute C_2H_5OH (Merck, *L*, conductance = 0.5 μS), CH_3COCH_3 (Carlo Erba, >99.8%, $L = 0.7$ μS), DMF (Carlo Erba, >99.5%, $L = 2.0$ μS) and CH_3NO_2; the last compound was purified by drying it over anhydrous $CaSO_4$ and then retaining the fraction 101—102 °C of the distillate ($L = 2.4$ μS).

Preparation of the complexes

Method A

To a definite (*ca.* 2g) amount of freshly prepared etherate compound of the complex haloacid, a small excess of Py or An was added dropwise and under continuous stirring. The ensuing reaction was vigorous, exothermic and was accompanied by the evolution of vapours. The solidification of the whole system commenced immediately after the addition of the organic base; the addition of more base caused complete dissolution of the solid product and formation of a clear solution. The reaction vessel was placed in a vacuum desiccator over concentrated H_2SO_4. The final, crystalline product was obtained by repeated pumping. The product was washed with small portions of absolute Et_2O and heated at 35 °C for 30 min.

Method B

A definite amount (*ca.* 2g) of freshly prepared etherate compound was suspended in *ca.* 50 mL *absolute* Et_2O. To the suspension was added 100% excess Py or An. The oily etherate complex was dissolved while simultaneously a precipitate formed. The addition of 50 mL Et_2O caused the formation of more precipitate. The precipitated complex was filtered through a G4 sintered crucible and washed repeatedly with Et_2O. It was dried in a vacuum desiccator over P_4O_{10}.

The salts PyHX and AnHX (X = Cl, Br, I) were, also, prepared according to previously published methods [11], so that these salts can be used for comparative spectroscopic studies.

Analyses

The acidic hydrogen (H^+) of the complexes was determined potentiometrically with a standard 0.1 *N* KOH solution, after dissolving them in DMSO [12]. A Radiometer Copenhagen pH-meter NV. Type PHM 26 c was employed with glass and calomel electrodes; the saturated aqueous KCl solution of the calomel electrode was replaced by a methanolic one. The content of An and Py was determined by dissolving the complexes in glacial CH_3COOH and potentiometric titration with a standard 0.1 *M* $HClO_4$ solution in CH_3COOH, using the above potentiometer [13]; a small amount of 6% $(CH_3COO)_2Hg$ solution in CH_3COOH was added to the samples being analyzed. Zinc and cadmium were determined volumetrically with a standard 0.05 *M* EDTA solution and Eriochrome Black T as indicator by dissolving the compounds in a warm, 20% aqueous solution, of C_2H_5OH. Mercury was determined gravimetrically as HgS, by the addition of small excess of 5% CH_3CSNH_2 solution to solutions of complexes **4**, **8** and **9** in hot 5 *M* CH_3COOH and to the solution of **7** in 2 *N* HNO_3. For the halogen determination, the Zn(II)- and Cd(II)-compounds were decomposed in 2 *N* HNO_3. The quantity of total halogen was determined by the VOLHARD method, the iodide in the presence of chloride or bromide ions by the $PdCl_2$ method [14] and chloride or bromide in the presence of each other by potentiometric titration with a standard 0.1 *N* $AgNO_3$ solution, using a Corning-Eel, model 12, potentiometer with calomel and selective sulfide electrodes [15]. The halogen determination in the mercury complexes was performed in the filtrate obtained from the gravimetric determination of mercury, described above. Thus the filtrate, to which the washings had been added, was boiled gently, until all H_2S was expelled. The complete removal of H_2S was ascertained with $(CH_3COO)_2Pb$ paper. The halides were, subsequently, determined exactly as in the case of Zn(II)- and Cd(II)-compounds.

Physicochemical measurements

The melting points of the complexes were obtained in a Büchi 510 apparatus. Conductance measurements were carried out at 25 °C in an Ehrhardt—Metzger Nachf. (type L21) conductivity bridge previously calibrated with standard KCl solution. The cell constant was found 1.02 cm^{-1}, the concentrations of the solutions used were of the order of 1×10^{-3} *M* (the compounds were assumed monomeric in solution) and the measurements were taken

Table I

Analytical results (%)[a], method of preparation, yields, colours and melting points of the complexes

No.	Complex	Method of preparation	Acidic hydrogen	M	Cl	Br	I	B	Yield[b] [%]	Colour	M.P. [°C]
1	$HZnI_2Cl \cdot 3Py$	*A*	0.15	11.21	5.44		42.42	40.59	72	chestnut brown	121
			(0.17)	(11.03)	(5.98)		(42.80)	(40.02)			
2	$HZnI_2Br \cdot 3Py$	*A*	0.16	10.41		13.06	37.82	38.18	80	beige	131
			(0.16)	(10.26)		(12.53)	(39.82)	(37.23)			
3	$HCdCl_2I \cdot 3Py$	*B*	0.17	20.87	12.01		23.84	41.55	75	white	98—104d
			(0.18)	(20.49)	(12.92)		(23.13)	(43.26)			
4	$HHgBr_2I \cdot 2Py$	*A*	0.15	31.80		24.01	20.40	23.38	81	yellow	68
			(0.15)	(31.03)		(24.72)	(19.63)	(24.47)			
5	$HCdCl_2Br \cdot 3An$	*B*	0.20	19.89	13.47	15.18		53.08	82	cream	108—112d
			(0.19)	(20.68)	(13.04)	(14.70)		(51.40)			
6	$HCdI_2Br \cdot 3An$	*A*	0.15	14.88		11.85	32.56	39.56	68	gray	77—80
			(0.14)	(15.47)		(11.00)	(34.93)	(38.46)			
7	$HHgBr_3 \cdot 2An$	*B*	0.17	32.17		38.03		28.81	32	chestnut brown	140—150d
			(0.16)	(31.96)		(38.19)		(29.68)			
8	$HHgBr_2I \cdot 2An$	*A*	0.15	29.91		22.99	20.01	27.40	83	chestnut brown	112
			(0.15)	(29.74)		(23.69)	(18.81)	(27.61)			
9	$HHgI_2Br \cdot 2An$	*B*	0.13	28.04		11.49	34.62	25.19	39	white	150—160d
			(0.14)	(27.80)		(11.07)	(35.17)	(25.81)			

[a] The calculated values in parentheses. [b] Based on the metal. d = decomposition; B = Py, An; M = Zn, Cd, Hg

ca. 15 min after the preparation of the solution. The UV spectra (400—210 nm) of the complexes were recorded in a Bausch Lomb—Shimadzu Spectronic 210 UV double beam spectrophotometer with a deuterium lamp. The concentration of the ethanolic solutions was between 5×10^{-5} and 5×10^{-4} *M*. The IR spectra of the complexes, in the 4000—250 cm^{-1} region were recorded on Perkin-Elmer 457 and 577 spectrophotometers, calibrated with a polystyrene film. The samples were used in the form of KBr pellets; the spectra were also taken in the form of Nujol and hexachlorobutadiene mulls between CsI crystals. For the complexes **1** and **2**, the 250—180 cm^{-1} region was also scanned on a Perkin-Elmer 580 spectrophotometer (Nujol mulls supported between polyethylene sheets). The X-ray powder spectra, for some of the complexes, were taken on a Philips diffractometer which operated at a power of 700 W. As an X-ray primary beam source a Cu anticathode ($\lambda_{CuKa_1} = 1.5418$ Å) was employed. These spectra covered the region of the angle 2θ from 3° to 60°.

Results and Discussion

General

The pyridine and aniline compounds are formed by the complete substitution of the Et_2O molecules in the etherate complexes with Py or An molecules, since the latter are stronger Lewis bases than Et_2O. The complexes are crystalline solids and stable in the normal laboratory atmosphere, over a long period of time. The complex **8**, on standing, loses its original crystalline form. The complexes **1**, **2**, **3**, **5**, **6** and **7** are insoluble in nonpolar solvents, somewhat soluble in H_2O and alcohols, and soluble in CH_3COCH_3, CH_3NO_2, *N*,*N*-dimethyl formamide (DMF) and dimethyl sulfoxide (DMSO); they are easily decomposed by dilute mineral acids. The analytical results, methods of preparation, yields, colours and melting points (uncorrected) are given in Table I.

Conductometric measurements

The molar conductance (Λ_M) values are shown in Table II. From the Λ_M values obtained, it is concluded that all complexes behave in C_2H_5OH, CH_3COCH_3 and CH_3NO_2 as 1 : 1 electrolytes [16]. The somewhat larger Λ_M value of the complexes in DMF and the fact that the L of the solution increases with time arise chiefly from the strong donor capacity of DMF, which leads to partial displacement of anionic ligands and change of electrolyte type.

Ultraviolet spectra

The UV spectra of the *pyridine complexes* show absorption maxima at 238, 244, 251, 257 and 263 nm. These maxima are attributed to $\pi \rightarrow \pi^*$ and $n \rightarrow \pi^*$ electronic transitions of the pyridine ring [17]. The spectra of **1**, **2** and **3** show three additional maxima at about 220, 290 and 358 nm, which require some additional discussion. The 220 nm maximum is due to a charge-transfer transition between the I^- ion and the solvent (charge transfer to solvent C.T.T.S.) [18].

Table II

Λ_M values for ca. 10^{-3} M solutions at 25 °C

Complex	Λ_M[S cm² mol⁻¹]			
	C_2H_5OH	CH_3COCH_3	CH_3NO_2	DMF[b]
1	41	133	83	a
2	43	137	83	a
3	46	123	72	a
4	40	142	89	a
5	a	77	86	101
6	35	137	77	a
7	33	75	51	150
8	47	129	90	127
9	a	129	67	121

[a] No data. [b] The conductances of the solutions increase significantly with time

The two absorptions at 290 and 358 nm are assigned to the $\sigma_g \rightarrow \sigma_u^*$ and $\pi_g \rightarrow \sigma_u^*$ transitions of the I_3^- ion, respectively [19].

The maxima at 233 and 285 nm, in the spectra of all *aniline complexes*, are due to electronic transitions of the aniline molecule, since they appear also in the spectra of An, AnHX and coordination compounds of aniline [20]. The successive shoulders, which appear in the 265—254 nm region are attributed to the presence of the AnH^+ ion in solution [8—10].

The 298 band in the spectrum of **9** was assigned, tentatively, to the $[HgI_2Br]^-$ ion, since *a)* the $[HgI_3]^-$ ion gives a maximum at 305 nm in C_2H_5OH [21], which is due to a iodide-to-mercury charge-transfer transition and *b)* the positions of bands of this kind show a successive blue shift $I^- < Br^- < Cl^-$ [22].

Infrared spectra of the pyridine complexes

Some characteristic and of diagnostic value IR frequencies (cm^{-1}) of the pyridine complexes are given in Table III.

The two or three weak bands in the 3220—3100 cm^{-1} region, in the spectra of all pyridine complexes, are attributed to $\nu(N^+H)$ and are due to the PyH^+ ion [23]; their low intensity indicates that the PyH^+ ion is involved in hydrogen bridging [23]. The appearance of a weak, broad band below 3000 cm^{-1}, in positions different from that of the corresponding intense broad band of the salts PyHX, is a strong indication of hydrogen bonding, not of the cation-anion type, N^+——H---X^- [11, 23]. The presence of the PyH^+ ion is also indicated by the bands at *ca.* 1630, 1600, 1525, 1480, 1325, 1235 and 1190 cm^{-1} [24].

Table III

IR spectral assignments of some absorption bands of diagnostic value for the pyridine complexes

Complex	Ring vibrations	$\nu(MCl)_t$	$\nu(MBr)_t$	$\nu(MI)_t$	$\nu(MN)$
1[a]	632s 420s, 413sh	325w, 307s, 286w		194m	223vs
2[a]	633s 421s, 413sh		252s	187m	220vs
3	632s 419s	<250		<250	<250
4	603m 380w		<250	<250	—

[a] There are data in the 250—180 cm^{-1} region. s = strong, m = medium, w = weak, sh = shoulder, vs = very strong

The spectra of **1**, **2** and **3** show two bands at 1570 and 1445 cm^{-1} as well as strong ones at 1217, 1150, 1065, 1040, 1010, 750 and 685 cm^{-1}, which are due to vibrational modes of coordinated pyridine [24]. The strong bands at 632 and 420 cm^{-1} are shifts of the bands at 604 cm^{-1} (an in-plane ring deformation) and 405 cm^{-1} (an out-of-plane ring deformation) of free pyridine. The shift of these bands to higher frequencies indicates coordinated pyridine [25]; consistent with this is the splitting of the 420 cm^{-1} band in the spectra of **1** and **2** [25]. The very strong bands at 223 and 220 cm^{-1} in the spectra of **1** and **2**, respectively, are assigned to the Zn—N stretching vibration [26], since they appear at the same frequency and for both complexes. From the spectrum of **4**, all bands, characteristic of coordinated pyridine, are absent.

Careful examination of the spectra of all prepared pyridine complexes clearly shows the absence of characteristic bands of free pyridine; hence, they contain no lattice pyridine of crystallisation [27].

The frequencies of Zn—X terminal stretching vibrations $\nu(ZnX)_t$ (Table III) show that **1** and **2** have tetrahedral structures [25, 26]. No band, which would be assigned to a Cd—Cl stretching mode, is observed for **3** above 250 cm^{-1} (the low frequency limit of the instrument used).

IR spectra of the aniline complexes

The spectra of all aniline complexes show two strong and very broad bands at *ca.* 2900 and 2580 cm^{-1}, which are indicative of the AnH^+ ion involved in hydrogen bridging [11]. The weak bands in the region 2550—1650 cm^{-1} are, mainly, combination bands and overtones. The assignments in the region 1620—1500 cm^{-1} are difficult, since bands in this region are due to stretching vibrations of the benzene ring and bending vibrations of the $-NH_3^+$ group [11]. In the remaining region the spectra are complicated by cation bands. The most outstanding feature of the IR spectra of **5** and **6** in the rock salt region is observed in the 3μ region.

In the free aniline the N—H antisymmetric and symmetric stretching vibrations occur at 3440 and 3360 cm^{-1}, respectively. In complexes **5** and

6 these bands occur at *ca.* 130 cm^{-1} lower than the corresponding ones in the free ligand. This shift of the N—H stretching bands to lower frequencies is explained by the weakening of the N—H bonds, resulting from the electron drainage from the nitrogen atom on account of its coordination to the cadmium atom [28]. In the region 450—270 cm^{-1} appears only one strong absorption band in the spectra of An (390 cm^{-1}), AnHX (*ca.* 385 cm^{-1}), **7** (391 cm^{-1}), **8** (371 cm^{-1}) and **9** (393 cm^{-1}). In the same region, there are two or three bands, in the spectra of **5** and **6**, which are attributed to Cd—N stretching vibrations or, more probably, to vibrational modes of aniline; the latter have shifted or become IR active upon the coordination of aniline [28, 29]. The absence of lattice aniline is also certain.

A medium band at 255 cm^{-1}, in the spectrum of **5**, is probably due to a Cd—Cl terminal stretching vibration [30]. Absorption bands due to Cd—Br, Cd—I, Hg—Br and Hg—I stretching vibrations in the monomeric and polymeric complexes of Cd(II) and Hg(II) appear below 250 cm^{-1} [31, 32]. So in the aniline complexes the coordination geometry has not been clarified.

X-ray powder spectra

The X-ray powder patterns of the pyridine complexes **1** and **2** are similar; consequently, these compounds are isomorphous. The complexes **5** and **6** have different patterns. All patterns suggest, by the multitude of the reflections, that the crystals formed are of low symmetry [10].

Conclusions

The complexes, with regards to solubility, behave as typical ionic compounds; they also behave as 1 : 1 electrolytes in four solvents. The UV spectra show the presence of the AnH^+ and, probably, $[HgI_2Br]^-$ ions in C_2H_5OH. From the IR spectral analysis, in the solid state, it is concluded that *a)* the complexes **1**, **2**, **3**, **5** and **6** contain at least one molecule of coordinated organic base, *b)* in all complexes the PyH^+ and AnH^+ ions are involved in hydrogen bonding, not of the cation-anion type, *c)* none of the complexes contain lattice pyridine or aniline and *d)* the zinc complexes are tetrahedral monomers. On the basis of all the aforementioned data, we can predict the stereochemical environment of some of the prepared complexes:

1, 2. $[ZnI_2XPy]^-$ $[Py---H---Py]^+$, pseudotetrahedral structure, X = Cl, Br

4, 8, 9. $[HgX_2Y]^-$ $[B---H---B]^+$, pyramidal anions probably C_s symmetry, B = Py, An and X, Y = Br, I.

7. $[HgBr_3]^-$ $[An---H---An]^+$, pyramidal anions probably C_{3v} symmetry.

The symbol --- represents a hydrogen bridge between the protonic hydrogen and two nitrogen atoms of two molecules of the organic base in the outer sphere of the complexes; such a hydrogen bond has been established for numerous compounds of complex haloacids [3—10].

For the complexes of Cd(II) there is a possible monomeric pseudotetrahedral structure, even though a polymeric octahedral one cannot be ruled out; complexes of Cd(II), having, in addition to others, halogens as ligands, show a notable and much varied structural behaviour [30, 31, 33, 34]. Weak bromine bridging interactions are present in $[Me_4N]$ $[HgBr_3]$, (Me— = CH_3—) the crystal structure of which is known [35]. The structure may be described as containing near-trigonal anions with one further fairly close bromine-mercury contact from a neighbouring anion resulting in a "two-anion" asymmetric unit. For the prepared complexes of Hg(II) the probability of halogen-bridged structures cannot be ruled out; for salts containing the complex anions $[HgX_3]^-$, a distinction between essentially monomeric anionic structures and halogen-bridged associated anions is possible with the aid of far IR and Raman spectra as far as 50 cm^{-1} [30, 32, 36, 37].

REFERENCES

[1] Galinos, A.: Bull. Soc. Chim. France, **1962,** 284
[2] Galinos, A. G.: Angew. Chem., **69,** 507 (1957)
[3] Galinos, A. G.: J. Am. Chem. Soc., **82,** 3032 (1960)
[4] Galinos, A. G.: J. Inorg. Nucl. Chem., **19,** 69 (1961)
[5] Galinos, A. G.: Bull. Soc. Chim. France, **1962,** 1592
[6] Galinos, A. G., Papadimitriou, A.: Mh. Chem., **105,** 1228 (1974)
[7] Galinos, A. G., Perlepes, S. P.: Z. Naturforsch., **32b,** 850 (1977)
[8] Galinos, A. G., Perlepes, S. P.: Bull. Soc. Chim. France, **1979,** I-46
[9] Galinos, A. G., Kouinis, J. K., Ioannou, P. V., Zafiropoulos, Th. F., Perlepes, S. P.: Z. Naturforsch., **34b,** 1101 (1979)
[10] Galinos, A. G., Perlepes, S. P., Kouinis, J. K.: Mh. Chem., **111,** 829 (1980)
[11] Chenon, B., Sandorfy, C.: Canad. J. Chem., **36,** 1181 (1958)
[12] Barnes, K. K., Mann, C. K.: Anal. Chem., **36,** 2502 (1964)
[13] Fritz, J. S.: "Acid-Base Titrations in Nonaqueous Solvents", Boston, Allyn and Bacon Inc., pp. 122—127 (1973)
[14] Vogel, A. I.: "A Text-Book of Quantitative Inorganic Analysis", 3rd ed., London, Longmans, pp. 568, 569 (1961)
[15] Bazzelle, W. E.: Anal. Chim. Acta, **54,** 29 (1971)
[16] Geary, W. J.: Coord. Chem. Rev., **7,** 81 (1971)
[17] Rao, C. N. R.: "Ultra-Violet and Visible Spectroscopy", 2nd ed., London, Butterworths, pp. 15—17, 60, 77—79 (1967)
[18] Smith, M., Symons, M. C. R.: Trans. Faraday Soc., **54,** 338 (1958)
[19] Andrews, L., Prochaska, E. S., Loewenschuss, A.: Inorg. Chem., **19,** 463 (1980)
[20] Misra, C. H., Parmar, S. S., Shukla, S. N.: J. Inorg. Nucl. Chem. **28,** 147 (1966)
[21] Deacon, G. B., West, B. O.: J. Chem. Soc., **1961,** 3929
[22] Gunter, J. D., Schreiner, A. F., Evans, R. S.: Inorg. Chem., **14,** 1589 (1975)
[23] Nuttall, R. H., Sharp, D. W. A., Waddington, T. C.: J. Chem. Soc., **1960,** 4965
[24] Mitchell, P. C. H.: J. Inorg. Nucl. Chem., **21,** 382 (1961)
[25] Clark, R. J. H., Williams, C. S.: Inorg. Chem., **4,** 350 (1965)
[26] Postmus, C., Ferraro, J. R., Wozniak, W.: Inorg. Chem., **6,** 2030 (1967)
[27] McColm, I. J.: J. Inorg. Nucl. Chem., **32,** 1461 (1970)
[28] Key, D. L., Larkworthy, L. F., Salmon, J. E.: J. Chem. Soc. (A), **1971,** 2583

[29] AHUJA, I. S., BROWN, D. H., NUTTALL, R. H., SHARP, D. W. A.: J. Inorg. Nucl. Chem., **27**, 1105 (1965)
[30] BARR, R. M., GOLDSTEIN, M.: J. Chem. Soc. Dalton Trans., **1974**, 1180
[31] MARCOTRIGIANO, G.: Z. Anorg. Allg. Chem., **417**, 75 (1975)
[32] BARR, R. M., GOLDSTEIN, M.: J. Chem. Soc. Dalton Trans., **1976**, 1593
[33] GOLDSTEIN, M., HUGHES, R. J.: Inorg. Chim. Acta, **37**, 71 (1979)
[34] BELL, N. A., DEE, T. D., GOLDSTEIN, M., NOWELL, I. W.: Inorg. Chim. Acta, **38**, 191 (1980)
[35] WHITE, J. G.: Acta Cryst., **16**, 397 (1963)
[36] HOOPER, M. A., JAMES, D. W.: Aust. J. Chem., **24**, 1331 (1971)
[37] PERLEPES, S. P., ZAFIROPOULOS, TH. F., KOUINIS, J. K., GALINOS, A. G.: accepted for publication in Z. Naturforsch.

TH. F. ZAFIROPOULOS
S. P. PERLEPES
J. K. KOUÏNIS
A. G. GALINOS

Department of Inorganic Chemistry, University of Patras, 231 Korinthou str., Patras, Greece

RECENSIONES

M. H. GUTCHO: *Microcapsules and Other Capsules — Advances Since* 1975

Chemical Technology Review No. 135

Noyes Data Corp., Park Ridge, New Jersey, USA, 1979, 340 pages

Microcapsulation processes, discovered in the thirties as a coacervation method in colloidal sense, have been widely and successfully used in the last 20 years in several fields of practical life. The manufacturing technology of microcapsules has undergone a long process of development from the discovery of the method up to our days. In the period from the initial simple coacervation operation to the present large-scale industrial microcapsule manufacture, several processes and coating materials have been used. Today the method can be employed with good results for the preparation of certain products of the pharmaceutical and dye industries, of agriculture and of the food industry, particularly when the primary task is the protection of chemical compounds against heat, light. oxygen and moisture. The handling of microcapsulated products become easier and safer, because the wall of the capsule, whether flexible or hard, prevents the contact of the contents with external environment. Thus, *e.g.* in the case of toxic or volatile liquids, a possible poisoning can be prevented. In addition to the protection of the active substance, the microcapsulated products of the pharmaceutical industry can provide also for the covering of odour and taste and possibly for prolonged action.

The literature of microcapsulation has been reviewed according to several aspects. The book by GUTCHO on the patent literature of microcapsulation fills a gap and one can get a great deal of information which cannot be found in periodicals. In addition to critical observations, it calls attention to technological potentialities which have not yet been sufficiently utilized, though, in his opinion, they would be promising fields for research and development.

In his work the author gave up with the conventional form of former publications, and attempted to give an up-to-date survey of the whole field. One of the greatest advantages of the examples collected in the book is their direct utilizability in practical work.

The grouping of the patents and the Content itself can be considered as a subject index, including the following subjects: complex coacervation, microcapsulation with synthetic film-formers, other encapsulation techniques of drugs and other medicinal products, foodstuffs, detergents and pressure-sensitive copying systems. At the end of the book other possible fields of application of the products made by means of the process are presented.

Processes particularly utilizable in pharmaceutical practice are contained in the fourth chapter, where problems of the preparation of systems with controlled release are discussed. For instance, the possible preparation of systems containing eyedrops and the microcapsulation processes of active substances are shown by means of actual examples. This chapter also deals with the presentation of methods applicable in the field of cosmetic preparations.

The last chapter selects an interesting theme. It covers the applicability of microcapsulation in fields not listed so far. This part gives, besides listing a series of uses in connection with catalysts, pigments, thermoplastic resins, *etc.*, the patent description of the preparation of hydrogen microspheres applicable as laser fusion target.

The patent collection in the book is followed by an alphabetical listing of firms engaged in microcapsulation and by a list of the patent numbers. This makes possible detailed orientation in the patent literature for all those who interested in the subject, and gives informations on the source of supply of the substances.

The book will be useful first of all to experts working in the pharmaceutical, chemical and food industries, but it can also be recommended to university teachers, lecturing on similar subjects, and to their students.

I. RÁCZ

M. M. SCHUMACHER: *Enhanced Recovery of Residual and Heavy Oils*

Noyes Data Corp., Park Ridge, New Jersey, 1980, 378 pages

The book surveys the enhanced recovery methods of oils. All the material is based on research reports and studies prepared between 1973 and 1979 by various industrial, university and other research groups commissioned by American federal organs. Most frequently the work was done at the request of organs of high authority, such as the Energy Research and Development Administration (ERDA), Federal Energy Administration (FEA), Bureau of Mines (BM), Environmental Protection Agency (EPA).

The author grouped and systematized the studies and the information contained in them, however, without adding his personal evaluation or opinion.

The book deals in detail with the following enhanced recovery methods:

- miscible displacement by liquid hydrocarbons;
- displacement of petroleum with carbon dioxide,
- with aqueous polymer solutions,
- with the joint application of micellar and polymer solutions,
- with alkaline solutions;
- thermal processes injection of steam or hot water, *in situ* combustion.

For each method the technological principle of the process is described, the production data and the profit-centered economical results of the more important industrial applications or experiments are given, and further problems to be solved in conjunction with the method, as well as research directions are indicated. From all this, conclusions are drawn on the prospective applicability of the method. Generally, these forecasts can be considered valid up to the middle of the eighties or the beginning of the nineties.

Two separate chapters deal with the approach of oil bearing rocks by shaft sinking, conventionally used in solids mining. Following this, the rocks are raised and oil is recovered at the surface, or alternatively, the hydrocarbons are recovered *in situ*, through a network of flooding and production wells, established in the shaft system.

Among the production methods of heavy oils, the description of rock blasting by the conventional method and subsequent flooding with solvents deserves special attention.

The book contains a detailed technological and economic analysis on the mining of oil shale and oil sand by the open-cut method, and the methods of *in situ* oil recovery after the removal of gangue.

A brief but interesting chapter deals with the basic principles of yield enhancing processes by nuclear explosion.

For industrial experts the most interesting part of the book is thought to be the chapter showing how to select for the given parameters (using 17 parameters) of a given petroleum reservoir an enhanced recovery method, which can be considered optimal from the technical-economical aspect. The correctness of the selection is proved by actual case histories from production, or by the profit-centered economic analysis of plant experiments.

Useful chapters of the book discuss the problems of oil recovery from the aspects of environmental protection, accident prevention and corrosion prevention.

Those engaged in the practical work of petroleum production will find in the book a great deal of useful information, applicable also in Hungary. In spite of this, from the aspect of world oil production the book is somewhat restricted, because it contains exclusively data from the USA. The sole exception is the brief chapter already mentioned on the application of nuclear explosion, the data of which arise from Soviet source. Moreover, it follows from the character of the book that in certain fields there is an overlap in the subject-matter between the different chapters, and even contradictory data can be found. In spite of these small insufficiencies, a valuable book is available, which will be useful reading also to Hungarian experts, particularly at present, when the introduction and industrial application of enhanced oil recovery methods is the order of the day also in Hungary.

J. TÓTH

Giuseppe DEL RE, Gaston BERTHIER and Josiane SERRE: *Electronic States of Molecules and Atom Clusters — Foundations and Prospects of Semiempirical Methods*

Lecture Notes in Chemistry, No. 13,

Springer-Verlag, Berlin, 1980. pp. 177.

In this book the authors present a survey on semiempirical quantum chemical methods placing emphasis on the mathematical and physical background and on the justification of the theories. Computational details are not treated. A vast amount of questions are discussed and many answers are given. Relations and applications to solid state physics are demonstrated.

The book consists of five chapters. Chapter 1 introduces the principal models and concepts applied in molecular quantum theory. Chapter 2 treats general mathematical formulation (second quantization, matrix formalism, *etc.*). Further on, a detailed critical, theoretical analysis of different methods can be found. Chapter 3 describes the non-SCF one-electron schemes, the Hückel and Extended Hückel methods. Chapter 4 treats the SCF one-electron methods (PPP and NDO models) and it gives some insight into the correlation problem (PCILO method). Theoretical description of excited states is also outlined. Finally, the fifth chapter is devoted to the basis set problem (hybridization, localization, nonorthogonality, etc.).

The value of the book is that it outlines a concise philosophy of semiempirical theories. The guiding principle is that semiempirical methods are respectable as models for physical interpretation of chemical effects. As a consequence, they are not expected to give unquestionable facts or excellent quantitative agreement with experiments. Indeed, they can suggest trends corresponding to effects in the model involved. This whole philosophy is different from that of computational quantum chemists who are accustomed to calculate physical constants with the highest accuracy.

The readers of this book are supposed to be familiar, at least to some extent, with the topics mentioned, *i.e.* it cannot be used as a textbook. It may be best recommended to specialists who are interested in the foundations of semiempirical MO theories.

P. R. SURJÁN

Steady-State Flow-Sheeting of Chemical Plants (Chemical Engineering Monographs 12.) P. BENEDEK (editor)

Coedition of Akadémiai Kiadó (Budapest) and Elsevier Scientific Publishing Co.

(Amsterdam—Oxford—New York) 1980, 410 pp. figs.

This book is a significantly completed and further developed edition of the work already published in Hungarian and German by the authors G. ALMÁSY, P. BENEDEK, M. FARKAS, I. PALLAI, F. SIMON, P. SZEPESVÁRY and T. SZTANÓ. (This edition contains two more chapters and numerous additional examples as compared to the preceding edition.)

The book contains 12 chapters. In Chapter 0, which was intended for an introduction by the authors, they report clearly and correctly on their thoughts about mathematical modelling, simulation, about their concepts, about the success and failure of their ideas. These thoughts and results, which are important and interesting for the reader as well, cannot and must not be forced into the Procrustes-bed of an introduction. Therefore, it was right that the authors rised all this onto the niveau of a separate chapter, and summarize it in "Chapter 0". The reviewer is obliged to tell his opinion in most detail on this chapter, as it concerns such important basic principles which are of considerable interest for the whole work.

After reading this chapter, the reader sees clearly the concept of a unit operation in an up-to-date, systems theoretical formulation, which is necessary for the understanding of the further chapters.However, the definition of a complex operation (= chemical plant) has certain difficulties, which are probably caused by the fact that in the whole hierarchy this is the step where the character of the surroundings of the system in question is different from that of simple and combined units.

The sub-chapter "Idea, conception, realization" is very illuminating, it contains the 5 main principles applied by the elaboration of the SIMUL system. Three of them concern

the chemical engineering side of the problem, the other two deal with the computational methods.

These main principles are the following:

— principle of the component independence
— principle of the independence of processing equipment
— principle of the network independence
— principle of the automatic execution of calculations
— principle of the independent simulation language.

The consequent application of the first two principles raised a number of problems, which resulted in some concessions owing to rational reasons. The authors did not stick rigidly to these principles, which is not a fault, rather a merit of the book. Thus, *e.g.* the principle of the independence of processing equipment is applied in such a way that for the same unit operation more models are elaborated, of which a choice can be made according to the purpose of application. (It is clear that in the physico-chemical sense a less exact model is usable, if enough information is available on unit operations already functioning, in possession of which the parameters can be determined with a satisfactory accuracy.)

The task for the preparation of simulation is the processing and refining of information, the analysis of the technological flow-sheet and the elaboration of the process program of simulation by successive abstraction.

Chapter 1 sticks to technology, it analyzes, orders and selects the pieces of information. It also describes a simple example of the production (the catalytic isomerization of butane).

Chapter 2 deals with the number of characterizing parameters, the definition of the stream type, the interpretation of the stream vector and the calculation of physical and chemical properties. With regard to the last point it has to be emphasized that the authors did not strive for the application of the most accurate methods available in the literature, but chose which correspond best to the character of the SIMUL system within the accuracy required in simulation calculations, and at the same time represent a relatively economical computation procedure.

Chapter 3 contains the description of the conventions of equipment boxes and their graphic representation, the rules for the elaboration of these boxes, and the description of the equipment boxes. In addition to boxes generally applicable, special boxes are also presented, some of these are used later on in the examples. The most significant extension of this chapter is represented by the distributed parametral model of the single or multiphase unit operation (box "dipa"), which can be used extensively for the solution of different tasks.

In Chapter 4 the description of the networks of unit operations, definitions in connection with them, and the mathematical and organizing procedures and boxes are contained.

Chapter 5 shows the course of process simulation calculations on the example of butane isomerization, and the results are discussed in detail, however, the detailed treatment of control and optimization is left for further chapters. This way of treatment can only be approved of, because thus every question remains easy to survey. This chapter also contains the classification of the definitions separately, and describes the symbols and notations of the operation-order flow-sheets.

In chapter 6 the recycle, the control, the solution of system of equations, and calculation of feed-back are described. This content seems at the first glance to be very heterogeneous, in reality, however, there is a close relation between the sub-chapters: recycles and control circuits also mean a feed-back from the point of view of information flow. These mean, at the same time, also the solution of non-linear equation systems, as the mathematical models are in general non-linear. For solving the equation systems the SIMUL system applied the direct iteration and the NEWTON—RAPHSON method.

Chapter 7 deals with optimization. In the SIMUL system two boxes are available for this purpose: one of them optimizes with the sequential simplex method, the other one with the dynamic optimization method of BELLMAN.

Chapter 8 contains the description of the organizing program. It shortly discusses also the computer used by the authors, because this is necessary for the understanding of the character and structure of their organizing program.

The simple model built up by the authors (isomerization of butane) is an excellent method for leading the reader successively through the task and for helping to understand the subject. Also the examples quoted in the individual chapters are very useful from the point of view of practical application. They show solutions of partial problems or the simulation of simple or combined unit operations.

In Chapter 9 (which is fully new in this edition) the flow-sheeting with the SIMUL system is shown on a more complex example taken from practice, namely the gas separation plant of a naphta cracker.

Chapter 10 discusses the computer-aided process design by means of the SIMUL system, on an also quite complicated practical example, in the case of the production of acetic anhydride. This is a revised and significantly completed version of the same chapter in the preceding edition.

Chapter 11 is also new, which finishes the book with the discussion of the "state-of-the-art".

The authors succeded in presenting the SIMUL system with an unbroken tracing and in a well arranged manner. The language of the book is clear and correct. It is worth reading also for those, who are not directly interested in the practical applications, but want to keep up with the development in the application of computer science in chemistry, chemical engineering and chemical technology.

M. BAKOS

Endre BERECZ: *Physical Chemistry*

Tankönyvkiadó, Budapest 1980, 691 pages

Physical chemistry is an important discipline in university teaching of natural sciences and engineering. Inspite of this, we have missed for many years a modern handbook of physical chemistry, satisfying the demands in conjunction with the education of university students at various faculties, and the post-graduate training of specialists. Thus, the work of the author, head of the Department of General and Physical Chemistry at the Technical University for Heavy Industries, Miskolc, fills in the strictest sense of the word a gap.

The handbook is divided into three main chapters. The first, chemical thermodynamics, describes the basic concepts, methods and fundamental laws of thermodynamics. This knowledge is lucidly applied by the author for the interpretation and calculation of the properties of concrete material systems, and of the direction and equilibrium of physical chemical processes. The second main chapter deals with the laws of reaction kinetics, *i.e.* with the rate and mechanism of the proceeding of physico-chemical processes and with transport processes directly connected with the former. The third chapter covers electrochemistry, the physical chemistry of systems with electric charge.

The author discusses material systems in the broadest sense, from the single-component simple molecular gas systems, through single- and multi-component vapour and condensed systems up to macroscopic systems, consisting of individual colloidal or larger particles with their own surface.

A great merit of the work besides the assertion of didactical aspects is the purposeful and application-centered summarization of the fundamental principles and methods of physical chemistry in a closed system. The book covers a concise and large subject. Descriptive explanations are relatively rare, it is actually a compact guide line for both the lecturer and the student as well as specialists.

The organization of the book permits the suitable and selective choosing of the subject, and makes at the same time possible the formation of a relatively full picture and the mastery of the fundamental principles and methods. This feature of the book permits its use as handbook by the teachers and students of the various institutions of higher education. Disagreeing with the opinion of the author in the "Preface ", I think that the book can also be well used in the teaching of students of chemical engineering.

The handbook is a modern, concise summary of the laws of physical chemistry, so that it will be used to good advantage by a wide circle of specialists in natural science and engineering, and by teachers and students participating in various forms of education.

In addition to the good points of the book already mentioned it has the great merit of being the first in the Hungarian handbook literature, and one of the first also in international relation, which consequently uses pertinent recommendations of the IUPAC, SI units, and Hungarian Standards (which correspond to ISO standards).

The publication of the book of Professor BERECZ is a great asset not only to the Hungarian but also to the international textbook literature and will contribute to the successful application of deeper and more up-to-date physical-chemical knowledge in various fields of natural and engineering sciences.

L. KISS

Zoltán SZABÓ: *Struktur und Reaktionsfähigkeit*

Akadémiai Kiadó Budapest, 1980, 190 Seiten
(in ungarischer Sprache, betitelt „Szerkezet és Reakcióképesség")

Das Buch ist eine übersichtliche Darstellung der Ergebnisse der sich über nahe fünf Jahrzehnte erstreckenden wissenschaftlichen Tätigkeit von Professor SZABÓ. Es erwuchs aus einem an der Universität Budapest im Studienjahr 1977/78 gehaltenen Spezialkolleg, und die entsprechende Einteilung in 12 Vorlesungen ist im Text auch angedeutet, aber der Stoff ist unabhängig davon inhaltlich in 4 Kapitel gegliedert. Der Titel ist damit begründet, daß fast alle Arbeiten des Verfassers sich in dem Problemkreis der Zusammenhänge zwischen Struktur und Reaktionsfähigkeit einfügen, mit dem Leitgedanken, daß alle diesbezüglichen Erscheinungen letzten Endes auf die elektronische Feinstruktur zurückzuführen sind.

Kapitel 1, mit dem Titel »Feinverteilung der Elektronen und die periodischen Funktionen« führt zunächst die vom Verfasser vorschlagene und bevorzugte tabellarische Darstellung des periodischen Systems vor, in der der sukzessive Ausbau der Elektronenschalen der Atome besonders anschaulich zum Ausdruck kommt und die seinerzeit (1950) noch diskutierte Einreihung der Elemente 90—103 als der Lanthanidenreihe analoge Aktinidenreihe, unterstützt durch Betrachtung ihrer physikalischen Eigenschaften (Schmelzpunkte, Dichten usw.), ganz natürlich erscheint. Im zweiten Teil dieses Kapitels wird über die Aufstellung mathematisch formulierter, seinerzeit prognostisch verwertbarer periodischer Funktionen für die Darstellung der Schmelzpunkte der Elemente berichtet.

Kapitel 2 ist Problemen von Reaktionen in der Gasphase gewidmet. Zunächst wird die Frage der Stärke von Einzelbindungen behandelt und die vom Verfasser und Mitarbeitern in den fünfziger Jahren entwickelte sog. Dekrementenmethode vorgeführt, die darin besteht, daß jeder Bindung ein Grundwert zugeordnet wird, der um die Summe der für die sich an die Pfeileratome anschließenden Atomgruppen charakteristischen Dekremente zu vermindern ist, um die Stärke der fraglichen Bindung in dem jeweils betrachteten Molekül zu erhalten. Die Methode der Berechnung ist dann auf die Bestimmung der Bildungswärmen von Atomgruppen (Radikalen) ausgedehnt worden. Der Einfluß der Dekremente gibt auch gewisse Information über die Elektronendichte und erklärt z. B. das unterschiedliche Reaktionsverhalten von NF_3 bzw. NCl_3 gegenüber Wassermolekülen. Es wurde ferner gezeigt, daß im Fall von kovalenter Bindung ein linearer Zusammenhang zwischen Bindungsstärke und Bindungsabstand besteht. Der Versuch zur Ausdehnung dieses Zusammenhangs auf anorganische Verbindungen zeigte, daß in diesem Fall die Differenz der Elektronegativitäten zu berücksichtigen ist, und es werden entsprechende Formeln vorgeführt und ihre Konsequenzen erörtert.

Das zweite Unterkapitel (Übergangszustände und die Aktivierungsenergie) berichtet über die Aufstellung (1961) einer, von der von POLÁNYI und EVANS verschiedenen Gleichung zur Berechnung von Aktivierungsenergien, wonach diese als die Differenz der Summe der Bindungsstärken der bei der Reaktion aufzulösenden und der sich neubildenden Bindungen dargestellt werden kann, die letztere Summe mit einem Faktor $\alpha < 1$ multipliziert. Für die praktische Anwendung der vorgeschlagenen Gleichung mußte eine Klassifizierung der Reaktionen vorgenommen werden (Zerfall, Isomerisierung, Transfer, Austausch, Addition) und eine weitere Unterteilung nach der Zahl der in dem Übergangszustand betroffenen Zentren (2, 3, 4 bzw. 6). Für jede derartige Gruppe konnten entsprechende Werte von α (im allgemeinen verschiedene) angegeben werden, die ferner auch noch davon abhängen, ob es sich um exo- oder endotherme Reaktionen handelt. Anschließend werden Betrachtungen über die Möglichkeit der Berechnung von Aktivierungsentropien und damit der präexponentiellen Faktoren von Geschwindigkeitskonstanten angestellt.

Im dritten Unterkapitel (Zusammengesetzte Reaktionen: Vierstufenmechanismus) wird zunächst der seinerzeitige Vorschlag der Verfassers, zusammengesetzte Reaktionsmechanismen schematisch durch vier Hauptgeschwindigkeiten (Initiation, Kettenfortsetzung, Verzweigung, Vernichtung der Kettenträger) zu charakterisieren, kurz dargelegt, um dann den zusammen mit P. HUHN und F. MÁRTA aufgeklärten Zerfallmechanismus von Cl_2O eingehender zu erörtern.

Das vierte Unterkapitel handelt von der Beeinflussung des Ablaufs von Gasreaktionen durch Wandeffekte (Initiation und Abbruch) und Zutaten, hauptsächlich paramagnetischen Substanzen wie z. B. NO, die mit den Kettenträgern mehr oder minder lockere, reversible Komplexe bilden (Radikalstabilisierung). Neben einer allgemeinen Erörterung dieser Fragen werden die Ergebnisse der Arbeiten des Verfassers über die Reaktion I + NO (mit PORTER), den thermischen Zerfall von SO_2Cl_2 (mit BÉRCES u. HUHN), Konditionieren der Gefäßwände

in der Oxidation von Kohlenwasserstoffen (mit GÁL), den thermischen Zerfall von Acetaldehyd (mit MÁRTA) und die Bromierung von Äthylen (mit BÉRCES) eingehender dargestellt.

Kapitel 3, das den Titel Lösungschemie trägt, beginnt mit allgemeinen, ziemlich vagen Betrachtungen über Fragen und Problematik der unterschiedlichen Löslichkeit der verschiedenen Verbindungen, wobei darauf hingewiesen wird, daß bei der Behandlung solcher Fragen die kohäsive Struktur und ihre Änderungen bei der Solvatation nicht außer acht gelassen dürfen, und daß z. B. die direkte Messung der Aktivitätsänderungen des Lösungsmittels unter Umständen wertvolle Hinweise auf den Zustand der gelösten Substanz liefern kann. Im weiteren Verlauf wird über einen frühen Versuch (Doktorarbeit des Verfassers) berichtet, aus EMK-Messungen individuelle Ionenaktivitätskoeffizienten abzuleiten, die er dann auch durch Messungen an anisothermen galvanischen Zellen bestätigen konnte. Obwohl es auch heute noch zweifelhaft erscheinen mag, daß individuelle Ionenaktivitätskoeffizienten mit voller thermodynamischer Exaktheit bestimmbar sind, ist z. B. das Ergebnis der Messungen von SZABÓ, wonach in wässrigen HCl-Lösungen der Aktivitätskoeffizient der H^+-Ionen in konzentrierten Lösungen steil ansteigt (bis zu 17,3 in 4,0 *M* Lösung), während der der Cl^--Ionen stetig abnimmt, recht eindrucksvoll, umso mehr als neuere Berechnungen und Messungen von RUFF u.a. diese frühen Ergebnisse im wesentlichen bestätigen konnten.

In einem weiteren Abschnitt dieses Kapitels wird über die Aufklärung der verschiedenen Resonanzstrukturen von Stickstofftetroxid berichtet, durch die das Verhalten dieser Substanz in verschiedenartigen Reaktionen deutbar wird. Der letzte Abschnitt handelt von analytischen Anwendungen komplexchemischer Reaktionen (mit BECK), die seinerzeit, Anfang der 50er Jahre, noch neuartig waren, und schließt mit Betrachtungen über Fragen des Zusammenhangs zwischen heterogener und homogener Katalyse, wobei auf die Rolle von Clusterbildungen in apolaren Medien hingewiesen wird.

Kapitel 4, das ufmangsreichste, ist Fragen der Reaktionen in und an festen Phasen gewidmet. Im ersten Unterkapitel wird über einige Untersuchungen betreffend die Eigenschaften von Festkörperphasen berichtet. Es sind dies: frühe (1944—49) Messungen der Quellung von Aktivkohle bei der Adsorption von Alkoholdampf; Nachweis der Abhängigkeit der Reaktionsfähigkeit von Eisenoxid von der Vorbehandlungstemperatur, wobei in der Gegend von 950 K ein Maximum in der Reaktivität gefunden wurde (Spinellbildung mit CdO, katalytische Aktivität bei der Zersetzung von H_2O_2, Löslichkeit in Salzsäure), entsprechend den Vorstellungen von Hüttig über eine Art »Vorreaktion«, wobei die entsprechenden Änderungen der Leerstellenstruktur durch Leitfähigkeitsmessungen verfolgt werden konnten; Herstellung von reinen und durch ihre katalytische Aktivität eindeutig charakterisierten Al_2O_3-Modifikationen.

Im zweiten Unterkapitel wird über Untersuchungen an Festkörperreaktionen berichtet. Zunächst werden kinetische Studien zur Klärung des Mechanismus der Zersetzung von Silberoxalat und Kaliumpikrat, unterhalb der Explosionstemperatur, erörtert, sodann Austausch- bzw. sog. Switch over-Reaktionen, mit denen sich der Verfasser mit seinen Mitarbeitern zu verschiedenen Zeitpunkten befaßte: die Oxidation von CO durch Ag_2O zur analytischen Bestimmung von CO (1944); Reduzierbarkeit von Sulfaten durch Kohlenstoff und von Nitraten mit Mg—Al-Legierungen, von Phosphaten mit Mg (1978); Bestimmung von SiO_2 in Al_2O_3 mittels der Reaktion $SiO_2 + H_4NF$ (1976). Im weiteren Verlauf werden Untersuchungen über Vereinigungsreaktionen, vornehmlich über Spinellbildung (mit SOLYMOSI u.a.) eingehender besprochen, damit im Zusammenhang Ergebnisse von magnetischen Suszeptibilitäts- und elektrischen Leitfähigkeitsmessungen gezeigt, hauptsächlich aber Fragen der Elektronen- bzw. Defektelektronenstruktur, ihre Beeinflussung durch Zusatzstoffe (Dotierung) und die Auswirkungen auf die katalytische Aktivität erörtert. Als ein wesentliches Ergebnis wird vom Verfasser unter anderem der Nachweis des Auftretens von besonderen Übergangszuständen im Sinn von Hüttig dargestellt.

Das dritte Unterkapitel befaßt sich mit Untersuchungen von einigen heterogenkatalytischen Vorgängen. Es wird zunächst über Nickeloxid, die Änderung der Defektelektronenkonzentration durch Zugaben von Li_2O und Cr_2O_3 und ihre Auswirkung auf katalytische Aktivität und Selektivität beim Zerfall von Ameisensäure berichtet, ferner über das Verhalten von Ni-Katalysatoren auf verschiedenen reinen und gemischten Oxiden als Trägern. Es folgt eine Darstellung umfassender Unteruschungen über den Zerfall von Alkoholen, wobei die Selektivität zwischen Dehydrierung und Dehydratation in Abhängigkeit vom Gittertyp, Koordinationszahl, Bindungsabstand M—O, Ionenradius verfolgt wurde, mit der Feststellung, daß auch in diesem Fall, wie in allen anderen, die durch diese Faktoren bedingte Elektronenverteilung maßgebend ist. Als eine weitere Testreaktion für die katalytische Aktivität wurde der Zerfall von N_2O an CuO untersucht. Während die früheren katalytischen Versuche meist in statischen Reaktoren durchgeführt wurden, wurde in letzter Zeit von Professor SZABÓ (mit JÓVÉR) die Impulstechnik eingesetzt, die die Verfolgung der Änderungen der Katalysator-

oberfläche während der Rekation ermöglicht. Das Buch schließt mit der Schilderung einiger diesbezüglicher Ergebnisse.

Zusammenfassend kann festgestellt werden, daß das Buch ein eindruckvolles Bild der vielseitigen und erfolgreichen wissenschaftlichen Tätigkeit von Professor SZABÓ vermittelt. Der angeführte ausführliche Literaturnachweis sorgt dafür, daß der Leser, der sich in weitere Einzelheiten der behandelten Ergebnisse vertiefen möchte, sich leicht zurechtfinden kann.

G. SCHAY

Endre BERECZ, Márta BALLA-ACHS: *Gas hydrates*

Akadémiai Kiadó, Budapest 1980, 287 pages

Intensive oil and gas production started in the northern regions of the earth and the putting into operation of the connected pipe lines played an important role in the recognition of the technological role of gas hydrates, and promoted research work for the investigation of their properties. The Hungarian chemical literature contains little information on gas hydrates, substances, important from both theoretical and practical aspects, causing many problems. Thus, the work of the authors decidedly fills a gap.

The book is organized into 7 chapters, and is complemented by a bibliography containing 558 references, including publications from 1978, and carefully compiled author and subject indexes, which facilitate for the reader the use of the work as a handbook.

Chapter 1 contains a historical survey of investigations and results in conjunction with gas hydrates. Chapter 2 discusses the structure of gas hydrates. It is divided into several parts, comprising information on clatrate structure, water structure and on the structure, composition and systematization of crystalline gas hydrates, which are needed for the further understanding of the subject.

Chapter 3 discusses the stability conditions of gas hydrates and deals in detail with the problem important from the practical point of view, how hydrate formation can be influenced and prevented.

Chapter 4 presents the theoretical bases and methods of possible calculations according to classical and statistical thermodynamic concepts.

Chapter 5 is very important also for industrial experts. The authors describe the properties of the best known systems containing one and more gas components. The survey of the field of application summarized in Chapter 6 is interesting and giving food for thought, and this is followed in Chapter 7 by a brief description of the fundamental methods of testing.

It can be felt that the authors, who published several papers on this subject, offer far more than the literature summarized by them, and contributed to the Hungarian chemical literature a work of value, useful to all research and industrial chemists.

F. RATKOVICS

INDEX

PHYSICAL AND INORGANIC CHEMISTRY

ORGANIC CHEMISTRY

ANALYTICAL CHEMISTRY

PRINTED IN HUNGARY
Akadémiai Nyomda, Budapest

Les Acta Chimica paraissent en français, allemand, anglais et russe et publient des mémoires du domaine des sciences chimiques.

Les Acta Chimica sont publiés sous forme de fascicules. Quatre fascicules seront réunis en un volume (3 volumes par an).

On est prié d'envoyer les manuscrits destinés à la rédaction à l'adresse suivante:

Acta Chimica
Budapest, P.O. Box 67, H-1450, Hongrie

Toute correspondance doit être envoyée à cette même adresse.

La rédaction ne rend pas de manuscript.

Abonnement en Hongrie à l'Akadémiai Kiadó (1363 Budapest, P.O.B. 24, C. C. B. 215 11488), à l'étranger à l'Entreprise du Commerce Extérieur « Kultura » (H-1389 Budapest 62, P.O.B. 149 Compte-courant No. 218 10990) ou chez représentants à l'étranger.

Die Acta Chimica veröffentlichen Abhandlungen aus dem Bereich der chemischen Wissenschaften in deutscher, englischer, französischer und russischer Sprache.

Die Acta Chimica erscheinen in Heften wechselnden Umfanges. Vier Hefte bilden einen Band. Jährlich erscheinen 3 Bände.

Die zur Veröffentlichung bestimmten Manuskripte sind an folgende Adresse zu senden

Acta Chimica
Budapest, Postfach 67, H-1450, Ungarn

An die gleiche Anschrift ist jede für die Redaktion bestimmte Korrespondenz zu richten.

Manuskripte werden nicht zurückerstattet.

Bestellbar für das Inland bei Akadémiai Kiadó (1363 Budapest, Postfach 24, Bankkonto Nr. 215 11488), für das Ausland bei »Kultura« Außenhandelsunternehmen (H-1389 Budapest 62, P.O.B. 149. Bankkonto Nr. 218 10990) oder seinen Auslandsvertretungen.

«Acta Chimica» издают статьи по химии на русском, английском, французском и немецком языках.

«Acta Chimica» выходит отдельными выпусками разного объема, 4 выпуска составляют один том и за год выходят 3 тома.

Предназначенные для публикации рукописи следует направлять по адресу:

Acta Chimica
Budapest, P.O. Box 67, H-1450, ВНР

Всякую корреспонденцию в редакцию направляйте по этому же адресу.

Редакция рукописей не возвращает.

Отечественные подписчики направляйте свои заявки по адресу Издательства Академии Наук (1363 Budapest, P.O.B. 24, Текущий счет 215 11488), а иностранные подписчики через организацию по внешней торговле «Kultura» (H-1389 Budapest 62, P.O.B. 149. Текущий счет 218 10990) или через ее заграничные представительства и уполномоченных.

Reviews of the Hungarian Academy of Sciences are obtainable at the following addresses:

AUSTRALIA
C.B.D. LIBRARY AND SUBSCRIPTION SERVICE, Box 4886, G.P.O., *Sydney N.S.W. 2001*
COSMOS BOOKSHOP, 145 Ackland Street, *St. Kilda (Melbourne), Victoria 3182*

AUSTRIA
GLOBUS, Höchstädtplatz 3, *1200 Wien XX*

BELGIUM
OFFICE INTERNATIONAL DE LIBRAIRIE, 30 Avenue Marnix, *1050 Bruxelles*
LIBRAIRIE DU MONDE ENTIER, 162 Rue du Midi, *1000 Bruxelles*

BULGARIA
HEMUS, Bulvar Ruski 6, *Sofia*

CANADA
PANNONIA BOOKS, P.O. Box 1017, Postal Station "B", *Toronto, Ontario M5T 2T*

CHINA
CNPICOR, Periodical Department, P.O. Box 50, *Peking*

CZECHOSLOVAKIA
MAD'ARSKÁ KULTURA, Národni třida 22, *115 33 Praha*
PNS DOVOZ TISKU, Vinohradská 46, *Praha 2*
PNS DOVOZ TLAČE, *Bratislava 2*

DENMARK
EJNAR MUNKSGAARD, Norregade 6, *1165 Copenhagen*

FINLAND
AKATEEMINEN KIRJAKAUPPA, P.O. Box 128, *SF-00101 Helsinki 10*

FRANCE
EUROPERIODIQUES S. A., 31 Avenue de Versailles, *78170 La Celle St.-Cloud*
LIBRAIRIE LAVOISIER, 11 rue Lavoisier, *75008 Pari*
OFFICE INTERNATIONAL DE DOCUMENTATION ET LIBRAIRIE, 48 rue Gay-Lussac, *75240 Paris Cedex 05*

GERMAN DEMOCRATIC REPUBLIC
HAUS DER UNGARISCHEN KULTUR, Karl-Liebknecht-Strasse 9, *DDR-102 Berlin*
DEUTSCHE POST ZEITUNGSVERTRIEBSAMT, Strasse der Pariser Kommüne 3—4, *DDR-104 Berlin*

GERMAN FEDERAL REPUBLIC
KUNST UND WISSEN ERICH BIEBER, Postfach 46, *7000 Stuttgart 1*

GREAT BRITAIN
BLACKWELL'S PERIODICALS DIVISION, Hythe Bridge Street, *Oxford OX1 2ET*
BUMPUS, HALDANE AND MAXWELL LTD., Cowper Works, *Olney, Bucks MK46 4BN*
COLLET'S HOLDINGS LTD., Denington Estate. *Wellingborough, Northant NN8 2QT*
WM. DAWSON AND SONS LTD., Cannon House, *Folke tone, Kent CT19 5EE*
H. K. LEWIS AND CO., 136 Gower Street, *London WC1E 3BS*

GREECE
KOSTARAKIS BROTHERS, International Booksellers, 2 Hippokratous Street, *Athens-143*

HOLLAND
MEULENHOFF-BRUNA B.V., Beulingstraat 2, *Amsterdam*
MARTINUS NIJHOFF B.V., Lange Voorhout 9—11, *Den Haag*
SWETS SUBSCRIPTION SERVICE, 347b Heereweg, *Lisse*

INDIA
ALLIED PUBLISHING PRIVATE LTD., 13/14 Asaf Ali Road, *New Delhi 110001*
150 B-6 Mount Road, *Madras 600002*
INTERNATIONAL BOOK HOUSE PVT. LTD., Madame Cama Road, *Bombay 400039*
THE STATE TRADING CORPORATION OF INDIA LTD., Books Import Division, Chandralok, 36 Janpath, *New Delhi 110001*

ITALY
EUGENIO CARLUCCI, P.O. Box 252, *70100 Bari*
INTERSCIENTIA, Via Mazzé 28, *10149 Torino*
LIBRERIA COMMISSIONARIA SANSONI, Via Lamarmora 45, *50121 Firenze*
SANTO VANASIA, Via M. Macchi 58, *20124 Milano*
D. E. A., Via Lima 28, *00198 Roma*

JAPAN
KINOKUNIYA BOOK-STORE CO. LTD., 17-7 Shinjuku-ku 3 chome, Shinjuku-ku, *Tokyo 160-91*
MARUZEN COMPANY LTD., Book Department, P.O. Box 5050 Tokyo International, *Tokyo 100-31*
NAUKA LTD. IMPORT DEPARTMENT, 2-30-19 Minami Ikebukuro, Toshima-ku, *Tokyo 171*

KOREA
CHULPANMUL, *Phenjan*

NORWAY
TANUM-CAMMERMEYER, Karl Johansgatan 41—43, *1000 Oslo*

POLAND
WĘGIERSKI INSTYTUT KULTURY, Marszałkowska 80, *Warszawa*
CKP I W ul. Towarowa 28 *00-95 Warsawa*

ROUMANIA
D. E. P., *Bucureşti*
ROMLIBRI, Str. Biserica Amzei 7, *Bucureşti*

SOVIET UNION
SOJUZPETCHATJ — IMPORT, *Moscow*
and the post offices in each town
MEZHDUNARODNAYA KNIGA, *Moscow G-200*

SPAIN
DIAZ DE SANTOS, Lagasca 95, *Madrid 6*

SWEDEN
ALMQVIST AND WIKSELL, Gamla Brogatan 26, *101-20 Stockholm*
GUMPERTS UNIVERSITETSBOKHANDEL AB, Box 346, *401 25 Göteborg 1*

SWITZERLAND
KARGER LIBRI AG, Petersgraben 31, *4071 Basel*

USA
EBSCO SUBSCRIPTION SERVICES, P.O. Box 1943, *Birmingham, Alabama 35201*
F. W. FAXON COMPANY, INC., 15 Southwest Park, *Westwood, Mass, 02090*
THE MOORE-COTTRELL SUBSCRIPTION AGENCIES, *North Cohocton, N.Y. 14868*
READ-MORE PUBLICATIONS, INC., 140 Cedar Street, *New York, N. Y. 10006*
STECHERT-MACMILLAN, INC., 7250 Westfield Avenue, *Pennsauken N.J. 08110*

VIETNAM
XUNHASABA, 32, Hai Ba Trung, *Hanoi*

YUGOSLAVIA
JUGOSLAVENSKA KNJIGA, Terazije 27, *Beograd*
FORUM, Vojvode Mišića 1, *21000 Novi Sad*

HU ISSN 0001—5407 **Index: 26.007**

ACTA CHIMICA

ACADEMIAE SCIENTIARUM HUNGARICAE

TOMUS 109 FASCICULUS 2

AKADÉMIAI KIADÓ, BUDAPEST

1982

ACTA CHIM. ACAD. SCI. HUNG. ACASA2 109 (2) 111–217 (1982)

ACTA CHIMICA

A MAGYAR TUDOMÁNYOS AKADÉMIA KÉMIAI TUDOMÁNYOK OSZTÁLYÁNAK IDEGEN NYELVŰ KÖZLEMÉNYEI

Acta Chimica is a journal for the publication of papers on all aspects of chemistry in English, German, French and Russian.

Acta Chimica is published in 3 volumes per year. Each volume consists of 4 issues of varying size.

Manuscripts should be sent to

Acta Chimica
Budapest, P.O. Box 67, H-1450, Hungary

Correspondence with the editors should be sent to the same address. Manuscripts are not returned to the authors.

Hungarian subscribers should order from Akadémiai Kiadó, 1363 Budapest, P.O. Box 24. Account No. 215 11488.

Orders from other countries are to be sent to "Kultura" Foreign Trading Company (H-1389 Budapest 62, P.O. Box 149. Account No. 218 10990) or its representatives abroad.

Acta Chimica Academiae Scientiarum Hungaricae, Tomus 109 (2), pp. 111—127 (1982)

CHEMISTRY OF 8-AZASTEROIDS, II*

SYNTHESIS OF 8-AZAGONANE DERIVATIVES

A. VEDRES,[1] P. KOLONITS[2] and CS. SZÁNTAY[2]**

([1]EGYT Pharmacochemical Works, Budapest and
[2]Institute for Organic Chemistry, Technical University Budapest)

Received September 16, 1980

Accepted for publication February 9, 1981

The cycloaddition of 1-acylcycloalkenes to 3,4-dihydroisoquinolines was applied for the synthesis of 8-azagonanes; the effect of acid base catalysis on this reaction was studied.

Introduction

Owing to significant biological effects of 8-azasteroids, the syntheses of these compounds have aroused considerable interest in recent years [1]. One of their representatives, *rac* 3-methoxy-8-aza-19-nor-17a-pregna-1,3,5(10)--trien-20-yn-17-ol-hydrobromide (Estrazinol hydrobromide) [2] is marketed as an estrogen.

Throughout this paper, at variance with Chemical Abstracts naming these compounds as quinolizidine derivatives, we follow the practice of several authors active in this field, using the steroid nomenclature; otherwise the different numbering of centers in compounds with a five- and six-membered D-ring (D-homo derivatives) would make correlation of the two series rather difficult.

In the synthesis of 8-azagonanes we utilized the experiences gained in our work with benzo[*a*]quinolizidine alkaloids [3, 4].

Reaction of 3,4-dihydroisoquinolines with 1-acylcycloalkenes

The 8-azagonanes were prepared by cycloaddition reactions of the 3,4-dihydroisoquinolines **1a—j** and the 1-acetylcycloalkenes **2a—d**.

This procedure is exemplified by the cycloaddition of 1-acetylcyclopentene (**2a**) onto 6,7-dimethoxy-3,4-dihydroisoquinoline (**1b**). When **1b**, as the hydrochloride, was refluxed in ethanol with a twofold excess of **2a**, the reaction went to completion within 36 h. The process was monitored by the

* For Part I, see Ref. [1]
** To whom correspondence should be addressed

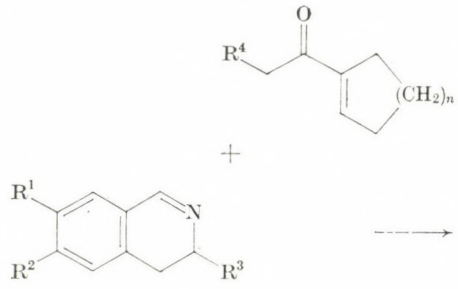

1a—j 2a—d

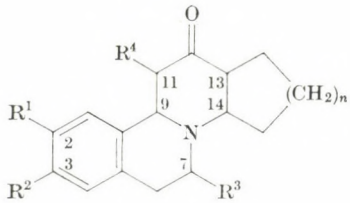

3a*	**15a, b**
4—5a, b	**16c**
6a—c	**17a—c**
7—11a, b	**18b, c**
12a—c	**19—22a**
13a, b	**23**
14a	

change in the UV spectra of samples periodically withdrawn from the reaction mixture. Since the unsaturated ketone components absorb at 230—238 nm, the dihydroisoquinolines at 300—365 nm, and the products at about 280 nm, the disappearance of **1** could be followed conveniently.

In order to establish the optimum molar ratio, the ratio of **2a** to **1b** was varied from one to four and a 2—3-fold excess was found to be the best. Therefore in the following experiments always a 2.5-fold excess of the unsaturated ketone was applied.

The effect of acid catalysis was investigated by allowing **1b** (as the base) to react with **2a** at 70 °C in ethanol in the presence of varying amounts of hydrogen chloride. The progress of the reactions was determined by measuring the disappearance of **1b** by UV spectroscopy. No reaction was detected, however, even after boiling for several days; the UV spectrum remained unchanged and the starting materials could be recovered quantitatively.

When the reaction was repeated after the addition of a few percents of water, both the disappearance of the base (**1b**) and the formation of **5a**+**5b** could be observed in the UV spectrum. Addition of 2.5% water and 2.5% hydrochloric acid substantially accelerated the reaction ($t_{1/2} = 20$ h). On increasing the amount of acid and keeping the water constant, there was a further increase of rate reaching a maximum at 40—50 mol-% hydrochloric acid ($t_{1/2} = 6$ h). An increase beyond 60—70 mol-% showed an unexpected retarding effect: with 80 mol-% and 100 mol-% hydrochloric acid (*i.e.* **1b** hydrochloride) the half-time increased to 28 and 52 h, respectively. With the ketones **2b** and **2c** similar results were obtained (Fig. 1).

	R^1	R^2	R^3	R^4	n	Reference
1a	H	H	H	—	—	[5]
1b	OMe	OMe	H	—	—	[6]
1c	—OCH_2O—		H	—	—	[7]
1d	OEt	OEt	H	—	—	[8]
1e	OH	OH	H	—	—	[8]
1f	O*n*Bu	OMe	H	—	—	[9]
1g	OH	OMe	H	—	—	[8]
1h	H	OMe	H	—	—	[10]
1i	H	H	Me	—	—	[11]
1j	OMe	OMe	Me	—	—	[12]
2a	—	—	—	H	1	[13]
2b	—	—	—	H	2	[14]
2c	—	—	—	H	3	[16]
2d	—	—	—	Me	1	[14]
3a	H	H	H	H	1	
4a, b	H	H	H	H	2	
5a, b	MeO	MeO	H	H	1	
6a—c	MeO	MeO	H	H	2	
7a—b	MeO	MeO	H	H	3	
8a, b	—OCH_2O—		H	H	1	
9a, b	—OCH_2O—		H	H	2	
10a, b	—OCH_2O—		H	H	3	
11a, b	EtO	EtO	H	H	1	
12a—c	EtO	EtO	H	H	2	
13a, b	OH	OH	H	H	1	
14a	*n*BuO	MeO	H	H	2	
15a, b	OH	MeO	H	H	1	
16c	H	MeO	H	H	2	
17a—c	MeO	MeO	H	Me	1	
18c, b	—OCH_2O—		H	Me	1	
19a	H	H	Me	H	1	
20a	H	H	Me	H	2	
21a	MeO	MeO	Me	H	1	
22a	MeO	MeO	Me	H	2	
23	H	H	Me	Me	1	

* The meanings of R^1—R^4 and n for compounds **3**—**23** are given in table below

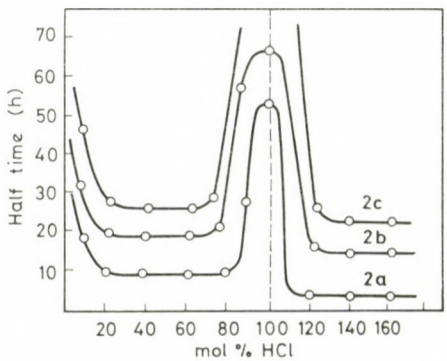

Fig. 1. Reaction rate of **1b** with **2a**—**c** as a function of acid catalysis

Cycloaddition was also accelerated by bases, but to a lesser extent than by hydrochloric acid. On increasing the concentration of the base an optimum was attained, beyond which the catalytic effect decreased.

In the initial phase of our kinetic experiments half-times were found to be erratic and the deviations could be traced back to some impurities in **1b**. When **1b** was carefully purified through its perchlorate, it reacted very slowly as compared with the contaminated samples. One of the impurities, identified as 3,4-dimethoxyphenylethylamine hydrochloride, exhibited a significant catalytic effect on the cycloaddition of **1b**.HCl. This prompted us to examine the catalytic effect of other amines too. Thus **1b** was allowed to react with 1-acetylcyclohexene (**2b**) under standard conditions in the presence of a variety of amine salts [**1b** as the base (10 mmol), ethanol (5 mL), water (0.4 mL), amine salt (1 mmol), **2b** (2.5 mL)]. The corresponding half-times are compiled in Table I.

Table I

Catalytic effect of amine salts

Catalyst	$t_{1/2}$ (h)	Catalyst	$t_{1/2}$ (h)
Methylamine-HCl (MA—HCl)	1.00	Ammonium chloride	13.00
Benzylamine-HCl	1.25	Morpholine-HCl	13.00
3,4-Dimethoxyphenyl-ethylamine-HCl	1.50	Piperidine-HCl	20.00
Ethanolamine-HCl	1.50	Diethylamine-HCl	22.00
Butylamine-HCl	1.50	Triethylamine-HCl	25.00
p-Toluidine-HCl	10.00	Tetraethylammonium iodide	30.00
o-Toluidine-HCl	13.00	Water	52.00

From the data it is apparent that the hydrochlorides of primary amines are the most effective catalysts, their optimum concentrations being 10—20 mol-% in relation to **1b**.

The cycloaddition reactions of **1b** with various ketones (**2a**—**c**), in the presence of different catalysts, were compared under standard conditions. The half-times found are shown in Table II.

From Table II it is apparent that, independently of the catalyst, the reactivity of the ketone decreases with the ring size.

The relative reactivities of some dihydroisoquinolines are shown in Table III.

In order to gain more insight into the course of the acid-catalyzed cycloaddition, a method reported by one of us earlier [17] was applied. At intervals samples were withdrawn from the reaction mixture; the UV spectrum

Table II

Reactivity of 1-acylcycloalkenes towards **1b** *at* 80 °C

Ketone	Catalyst			
	MA–HCl (10 mol-%)	HCl (100 mol-%)	HCl (10 mol-%)	NaOH (10 mol-%)
	$t_{1/2}$ (h)	$t_{1/2}$ (h)	$t_{1/2}$ (h)	$t_{1/2}$ (h)
2a	0.5	11.5	1.5	8.5
2b	1.0	40.0	7.0	40.0
2c	2.8	60.0	8.5	68.0

Table III

Reactivities of some dihydroisoquinolines

Reactants		Products	Relative half-times at 80 °C		
			Ma–HCl 10 mol-%	HCl 10 mol-%	NaOH 1 mol-%
1b	**2a**	**5a, b**	1	1	1
1a	**2a**	**3a, b**	1.1	1.3	1.2
1i	**2a**	**19**	1.1	2.5	1.4
1b	**2b**	**6a, b, c**	1	1	1
1a	**2b**	**4a, b**	2.3	1.2	1.5
1h	**2b**	**16**	1.5	1.1	—
1i	**2b**	**20**	5.0	2.0	—

of half of the sample was recorded directly, the other half was made alkaline, re-acidified after a short time, and its UV spectrum was taken as well. If the intensity of maxima in the second case is less than in the first spectrum, it

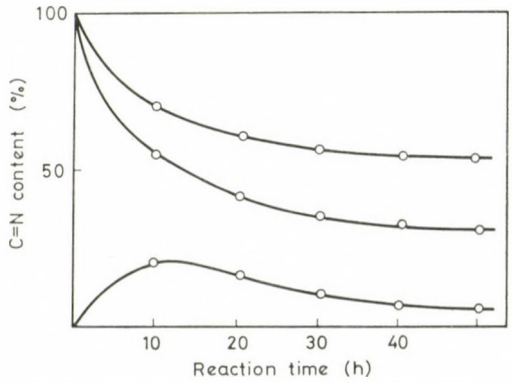

Fig. 2. **Measurement of C=N content in the course of reaction of 1a with 2b. Explanation see in the text**

can be inferred that the reaction involves an intermediate containing a C=N bond. Our results obtained with 1-acetylcyclohexene are shown in Fig. 2.

The upper curve represents the absorbance of the original acidic sample, whereas the middle one that obtained after alkaline treatment, measured at 362 nm, *i.e.* at the wavelength characteristic of the C=N bond. The two curves converge when either less or more than one equivalent of acid is present during cycloaddition. It can be therefore assumed that the reaction proceeds through an intermediate containing a C=N bond, and also that the mechanism of the reaction is analogous to the one established by one of us earlier [17], *i.e.* an immonium salt of type *ii* is first formed which then cyclizes *via* the enol form *iii*.

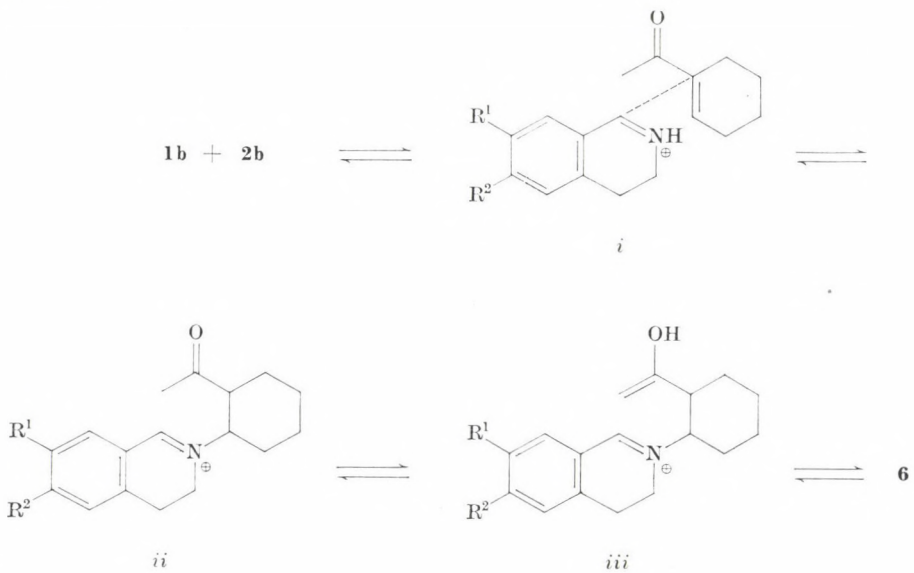

In the case of an acid-catalyzed cycloaddition, the presence of the immonium salt *ii* can only be demonstrated when one equivalent of hydrochloric acid is used (*cf.* Fig. 1). The addition of either more or less acid promotes the formation of the enol from (*iii*), which undergoes cyclization at such a high rate that the immonium salt (*ii*) cannot accumulate.

Using the homologues of **2b**, *i.e.* **2a** and **2c**, no immonium salt could be detected. The mechanism is presumably the same, but the concentration of *ii* remains under the detection limit.

In the cycloadditions mixtures of stereoisomers were obtained, which could be separated in most cases. The stereochemistry of the isomers of **5a, b** and **6a, b, c** was studied in detail, and the results will be presented in subsequent papers.

Experimental

Analyses

M.p.'s were determined on a Boetius M apparatus and are uncorrected. Elementary analyses for nitrogen were performed on a Coleman 29, for carbon and hydrogen on a Coleman 33 analyser. Halogens were determined by the Schöniger method. Rotations were measured on a Perkin-Elmer 242-MC polarimeter.

Solutions were clarified with Acticarbon C-extra; alkaline treatment was effected with saturated sodium carbonate solution.

Spectroscopy

Ultraviolet spectra were recorded on a Pye Unicam SP 8000 spectrophotometer in ethanolic solution. Infrared spectra were taken on Zeiss UR-10 and Perkin-Elmer 157 G type instruments in potassium bromide pellets or chloroform solutions containing 1 and 8% of the substance, respectively. ^{1}H-NMR spectra were recorded on a Perkin-Elmer R 12 60 MHz and a Jeol PD 100 100 MHz instrument using tetramethylsilane as internal standard. Mass spectra were taken on an AEI MS-902 instrument at 70 eV ionization potential with direct inlet at 140 °C.

Cromatography

For chromatography Merck silica gel was used (see later). Diastereomeric ketones could only be separated on layers containing boric acid, while their derivatives were successfully separated also on untreated plates.

Boric acid impregnated plates for preparative layer chromatography were prepared by shaking throughly the adsorbent (Merck, Kieselgel GF_{254} type 60, 16 g) with boric acid (1.6 g) and water (35 mL). This suspension could be spread on a 20×20 cm plate to form a 1 mm layer. After drying in air, the plates were activated at 105 °C for 30 min.

For qualitative studies silica gel layers (0.2 mm) on aluminium foil (DC Alurolle, Kieselgel 60 F 254, Merck) were used, generally of 3×8 cm size. For the separation of the ketones the plates were kept in a 5% methanolic solution of boric acid for 1 h and then activated at 105 °C for 30 min. Impregnation of 2 mm Merck preparative plates with boric acid gave inconsistent results.

For development methanol—chloroform mixtures were used; 9 : 1 mixtures usually afforded medium R_f values. For comparison not the numerical R_f values, but rather co-chromatography with authentic samples was used.

Spots were detected in iodine vapor, by spraying with a 1% solution of potassium permanganate, or in UV light at 254 nm. Detection limits with the individual methods were as follows: iodine vapor 0.01—0.05 ng; $KMnO_4$ solution 0.08—0.1 ng and UV-light 0.1—0.5 ng.

Materials

Dihydroisoquinolines (1) were prepared by the Bischler—Napieralski reaction. For kinetic studies the phenylethylamine impurities were removed from 6,7-dimethoxy-3,4-dihydroisoquinoline (**1b**) as follows: **1b** (57.3 g; 0.3 mol) was dissolved in ethanol (500 mL). To this solution 70% aqueous perchloric acid was added until pH 2 was attained. The precipitated crystals were filtered off and washed with ethanol. After recrystallization from a mixture of ethanol (450 mL) and water (40 mL), 58 g (66%) of pure **1b** perchlorate, m.p. 194—196 °C, was obtained which was free from 2-(3,4-dimethoxyphenyl)ethylamine. The base used for kinetic experiments was liberated from this salt.

1-Acylcycloalkenes (2) were prepared by the acylation of cycloalkenes [13, 14].

Kinetic studies

Determination of the optimal molar ratio

6,7-Dimethoxy-3,4-dihydroisoquinoline hydrochloride (**1b** · HCl, 2.3 g; 0.01 mol), ethanol (5 mL) and 1-acetylcyclopentene [**2a**, 1.1 g (0.01 mol), 2.2 g (0.02 mol), 3.3 g (0.03 mol) or 4.4 g (0.04 mol)] were boiled for 36 h. After evaporation to dryness the residue was taken

up in water (30 mL) and extracted with ether (3×10 mL). The aqueous solutions were made alkaline with saturated sodium carbonate solution and the precipitated oil was extracted with benzene (3×20 mL). After evaporation of the solvent the wight of the crystalline residue (a mixture of the stereoisomeric ketones **5a** + **5b**) was determined: 1.59 g (53%), 2.26 g (75%), 2.43 g (81%), and 2.52 g (84%).

Determination of the half-time of cycloaddition

Half-times were determined from the decrease of the amount of the isoquinoline derivative (**1**) as a function of time. At intervals 25 μL samples were withdrawn from the reaction mixture, acidified with 0.1 *N* hydrochloric acid (1 mL) and made up to 25 mL with ethanol. The UV spectrum of this solution was determined and the isoquinoline content of the sample was calculated from the absorbance characteristic of the isoquinoline in question (363 nm for **1b**). The half-time was assessed from the concentration *vs.* time plot.

Data quoted in Tables I—III and Figure 1 were obtained as follows. A mixture consisting of 10 mmol of the dihydroisoquinoline **1** or its hydrochloride, 2.5 mL of the cycloalkene **2**, the appropriate catalyst (0—14 mmol HCl in 0.4 mL of water, 1 or 10 mmol NaOH in 0.4 mL of water, 1 or 2 mmol of amine salt) was made up to 10 mL with ethanol or some other solvent and kept at the specified temperature in a thermostat. Samples were taken as described above.

Detection of immonium salts

In a 25 mL flask 0.15 g of the ketone **5** or **6** and 10 mL of a 0.1 *N* hydrochloric acid solution were weighed in. The mixture was refluxed and from time to time two samples (50 mL each) were taken. One of them was diluted to 25 mL with ethanol and its UV spectrum recorded. To the other sample some ethanol was added and it was made alkaline. After 30 min the sample was acidified, diluted to 25 mL and its UV spectrum was recorded. The time required for the establishment of an equilibrium was determined from the change of intensity of the band at about 363 nm.

The concentration of the dihydroisoquinoline **1b** was calculated from the absorbance (*H*) by the following formula:

$$\mathbf{1b} = \frac{A \times \mathrm{MW}}{3 \times k} \times 10^4 \,\%$$

where MW is the molecular weight, k the width of the cell in cm and A the molar extinction of **1b**.

The absorbance of the first sample gives the total of **1b** and the corresponding immonium salt, whereas that of the second sample only the concentration of **1b**. The difference between the two corresponds to the concentration of the immonium salt.

8-Azagonane-12-ones

rac-8-Aza-13α-gona-1,3,5(10)-trien-12-one* (3a)

A mixture of **1a** (1.3 g; 0.01 mol, as the base), **2a** (2.5 mL), methylamine-HCl (67 mg) and ethanol (6 mL) was refluxed for 2 h; during this time 95% of **1a** reacted. After adding more ethanol (5 mL) the solution was kept in a refrigerator overnight. The precipitated crystals were filtered off and recrystallized from a tenfold volume of ethanol, to obtain pure **3a** (0.1 g; 20%), m.p. 102—108 °C. The mother liquor contained also the ketone **3b**.

^{1}H-NMR ($CDCl_3$): δ 4.02 (q, 1H, 9-H)**, 7.13 (m, 4H, aromatic H).

IR (KBr): ν 1455, 1500 and 1715 cm^{-1}; ($CHCl_3$): ν 2760, 2810, 2875, 2920, 2945 and 2975 cm^{-1}.

$C_{16}H_{19}NO$ (241.3). Calcd. C 79.63; H 7.94; N 5.80. Found C 79.41; H 8.36; N 5.89%.

rac-8-Aza-D-homo-gona-1,3,5(10)-trien-12-one (4a)

1a (1.3 g; 0.01 mol, as the base), **2b** (2.5 mL), methylamine-HCl (67 mg) and ethanol (6 mL) were refluxed for 6 h, when 90% of **1a** had reacted. After dilution with ethanol (5 mL)

* See: Definitive Rules for Nomenclature of Steroids. Butterworths, London, 1971.
** Coupling constants are listed in Part V.

the mixture was kept in a refrigerator overnight, the product filtered off and recrystallized twice from ethanol to afford pure **4a** (0.25 g; 10%), m.p. 130—132 °C.

^{1}H-NMR ($CDCl_3$): δ 3.90 (q, 1H, 9-H), 7.10 (m, 4H, aromatic H).

IR (KBr): ν 1450, 1500 and 1710 cm^{-1}; ($CHCl_3$): ν 2760, 2815, 2865, 2940 and 2980 cm^{-1}.

$C_{17}H_{21}NO$ (255.4) Calcd. C 79.96; H 8.29; N 5.49. Found C 79.26; H 8.64; N 5.55%.

rac-8-Aza-D-homo-9β,13α-gona-1,3,5(10)-trien-12-one (4b)

The mother liquor of **4a** and that of its recrystallization were combined, evaporated in vacuum and the residue was dissolved in benzene (5 mL). The solution was extracted 10 times with 1% HCl (2 mL) and the combined 5th and 6th extracts were made alkaline with sodium carbonate. The precipitate was filtered off and recrystallized from ethanol (1 mL) to afford pure **4b** (0.02 g), m.p. 145—150 °C.

^{1}H-NMR ($CDCl_3$): δ 4.30 (q, 1H, 9-H), 7.10 (m, 4H, aromatic H).

IR (KBr): ν 1455, 1495 and 1610 cm^{-1}; ($CHCl_3$): ν 2865, 2945 and 2980 cm^{-1}.

Found C 79.68; H 8.68; N 5.37%.

rac-2,3-Dimethoxy-8-aza-13α-gona-1,2,5(10)-trien-12-one (5a)

1b hydrochloride (23 g; 0.10 mol), **2a** (25 mL) and 6 *N* HCl (4.0 mL) were refluxed in ethanol (60 mL) for 8 h. After standing overnight in a refrigerator, the crude product was filtered off, washed with ethanol, dissolved in hot water (800 mL), the solution clarified and while still warm it was made alkaline with sodium carbonate solution. The precipitated crystals were filtered off, washed with ample water and dried. Recrystallization from ethanol (200 mL) afforded pure **5a** (21 g; 70%). m.p. 117—119 °C.

^{1}H-NMR ($CDCl_3$): δ 3.84 (s, 6H, OMe), 3.8 (9-H), 6.61 (s, 2H, aromatic H).

IR (KBr): ν 1520, 1615 and 1715 cm^{-1}; ($CHCl_3$): ν 2760, 2820, 2840, 2880, 2920, 2945 and 2975 cm^{-1}.

UV (EtOH): 283 (3.59) nm (log ε).

MS *m/e* (rel. int.): 301 (70), 300 (100), 258 (20) and 192 (12).

$C_{18}H_{23}NO_3$ (301.4). Calcd. C 71.73; H 7.69; N 4.64. Found C 71.79; H 7.44; N 4.28%.

rac-2,3-Dimethoxy-8-aza-9β,13α-gona-1,3,5-(10)-trien-12-one (5b)

To a solution of **1b** (5.5 g; 28 mmol, as the base) in a mixture of **2a** (9 mL) and ethanol (5 mL) 40% aq. sodium hydroxide (1 mL) and water (4 mL) were added. After refluxing for 8 h and standing overnight in a refrigerator, the crude product was filtered off and washed with ethanol (2×10 mL) to give **5b** contaminated with 10—15% of **5a** (3.1 g; 38%), m.p. 156—158 °C. Recrystallization from ethanol (30 mL) gave pure **5b** (2.1 g; 25%), m.p. 162—164 °C.

^{1}H-NMR ($CDCl_3$): δ 3.83 (s, 6H, OMe), 4.15 (q, 1H, 9-H), 6.60 and 6.65 (singlet each, 2H, aromatic H).

IR (KBr): ν 1520, 1615 and 1715 cm^{-1}; ($CHCl_3$): ν 2840, 2880, 2920, 2945 and 2975 cm^{-1}.

UV (EtOH): 283 (3.59) nm (log ε).

MS *m/e* (rel. int.): 301 (70), 300 (100), 258 (16) and 192 (14).

Found C 71.63; H 7.83; N 4.80%.

rac-2,3-Dimethoxy-8-aza-D-homo-9β,13α-gona-1,3,5(10)-trien-12-one (6b)

A mixture of **1b** (192 g; 1.0 mol, as the base), **2b** (250 mL), ethanol (500 mL) and 0.1% aq. sodium hydroxide solution were refluxed under nitrogen for 55 h. During this period half of **1b** was converted. After standing overnight in a refrigerator the product was filtered off and washed with ethanol (2×100 mL) to yield **6b** (93 g; 30%, m.p. 149—152 °C), contaminated with 5—10% of **6a**. Recrystallization from ethanol (930 mL) gave pure **6b** (73 g; 23%), m.p. 153—154 °C.

^{1}H-NMR ($CDCl_3$): δ 1.2—3.4 (m, 16H), 3.85 and 3.87 (s each, 3H each, OMe) 4.24 (q, 1H, 9-H), 6.47 and 6.56 (s each, 2H, aromatic H).

IR (KBr): ν 1510, 1525 and 1715 cm^{-1} ($CHCl_3$): ν 2845, 2865, 2945 and 2980 cm^{-1}.

UV (EtOH): 283 (3.60) nm (log ε).

MS *m/e* (rel. int.) 315 (84), 314 (100), 272 (50) and 191 (56).

$C_{19}H_{25}NO_3$ (315.4). Calcd. C 72.35; H 7.99; N 4.44. Found C 72.22; H 8.13; N 4.46%.

rac-2,3-Dimethoxy-8-aza-D-homo-gona-1,3,5(10)-trien-12-one (6a)

To the mother liquor of the above described preparation of **6b**, methylamine-HCl (6.7 g; 0.1 mol) was added and the mixture refluxed for 4 h. During this time the remaining half of **1b** underwent cycloaddition. After standing overnight in a refrigerator, the product was filtered off and washed with ethanol (2×100 mL) to yield **6a** contaminated with 10—15% of **6b** (109 g; 35%), m.p. 146—149 °C. Recrystallization from benzene (500 mL) provided pure **6a** (57 g; 19%), m.p. 155—157 °C.

^{1}H-NMR ($CDCl_3$): δ 1.0—3.0 (m, 15H), 3.35 (m, 1H), 3.87 (s, 3H, OMe), 3.90 (s, 3H, OMe), 3.88 (q, 1H, 9-H), 6.51 and 6.58 (s each, 2H, aromatic H): $CDCl_3$ + Eu(dpm)$_3$: δ 4.54 (q, 1H, 9-H), 5.03 and 5.04 (s each, 6H, OMe), 8.00 (s, 2H, aromatic H).

IR (KBr): ν 1520, 1615 and 1705 cm^{-1}; ($CHCl_3$): ν 2765, 2820, 2845, 2945 and 2980 cm^{-1}.

UV (EtOH): 283 (3.60) nm (log ε).

MS *m/e* (rel. int.): 315 (70), 314 (100), 272 (30) and 191 (42).

Found C 72.44; H 8.11; N 4.52%.

From the refrigerated primary mother liquor of **6a** a second crop of product separated, which was filtered off and washed with ethanol (2×50 mL). This (38 g; 12% consisted of 80% of **6a** and 20% of **6b**, m.p. 140—144 °C. The mother liquor was again evaporated and the residue dissolved in benzene (200 mL); the solution was extracted with 2% aq. HCl (5×100 mL). The combined extracts were made alkaline to pH 8 with saturated sodium carbonate solution, washed with water (4×100 mL), dried over sodium sulfate and evaporated to give a mixture of the isomers (55 g; 18%) (50% **6a** and 35% **6b**). The overall yield of cycloaddition was 95%.

rac-2,3-Dimethoxy-8-aza-D-homo-9β-gona-1,3,5(10)-trien-12-one (6c)

A mixture of **1b** hydrochloride (31.4 g; 0.144 mol), **2b** (51 mL), ethanol (46 mL) and water (9 mL) was refluxed under nitrogen for 60 h. After evaporation to half of the original volume, the solution was cooled to room temperature, the precipitated crystals were filtered off and washed with cold ethanol (3×20 mL) to afford a mixture of the hydrochlorides of **6a** and **6b** (16.2 g). The mother liquor was combined with the washings and evaporated. The residue was taken up in water (200 mL) and extracted with benzene (3×50 mL). The aqueous phase was made alkaline with saturated sodium carbonate solution and the base extracted with benzene (200 mL). The benzene solution was extracted with 1% hydrochloric acid (10×10 mL), and the extracts Nos. 3—9 were made alkaline with saturated sodium carbonate solution. The aqueous phase was discarded and the precipitate crystallized from some ethanol and filtered off. Thus a mixture rich in **6c** (6 g) was obtained, which was recrystallized from ethanol (17 mL). Filtration at 25 °C gave crude **6c** (4.5 g) which was contaminated mainly with **6b**. This mixture was dissolved in benzene (100 mL) and extracted with 1% hydrochloric acid (3×10 mL). The first two fractions were combined and made alkaline with saturated sodium carbonate solution; the precipitate which separated was recrystallized from ethanol (80 mL). On filtration at 5 °C impure **6c** (1.4 g) was obtained, which was dissolved in hot methanol (30 mL) and cooled slowly to 10 °C. The precipitated crystals were filtered off and washed with cold methanol to afford pure **6c** (1.25 g; 2.7%), m.p. 154.5—156 °C.

^{1}H-NMR ($CDCl_3$): δ 1.0—3.5 (m, 16H), 3.90 (s, 6H, OMe), 4.75 (t, 1H, 9-H), 6.56 and 6.64 (s each, 2H, aromatic H).

IR (KBr): ν 1515, 1605 and 1705 cm^{-1}; ($CHCl_3$): ν 2840, 2860, 2940 and 2975 cm^{-1}.

UV (EtOH): 283 (3.57) nm (log ε).

MS *m/e* (rel. int.): 315 (75), 314 (100), 272 (35), 191 (45).

Found C 72.56; H 8.10; N 4.50%.

rac-2,3-Dimethoxy-8-aza-D-dihomo-9ξ,13ξ-gona-1,3,5(10)-trien-12-one (7)

A mixture of **1b** (7.65 g; 0.04 mol, as the base), 12 ml **2c**, ethanol (14 mL), 10% NaOH (1.4 mL) and water (5 mL) was refluxed for 65 h. After standing 3 days in a refrigerator, the crystals were separated and washed with ethanol (3×10 mL) to yield crude **7a**, contaminated with 5—10% **7b** (4.6 g; 35%), m.p. 132—136 °C. Repeated recrystallization from ten volumes of ethanol gave pure **7a** (3.0 g; 23%), m.p. 142—144 °C.

^{1}H-NMR ($CDCl_3$): δ 3.83 (s, 6H, OMe), 4.1 (q, 1H, 9-H), 6.53 and 6.61 (s each, 2H, aromatic H).

IR (KBr): ν 1525, 1620 and 1710 cm^{-1}; ($CHCl_3$): ν 2855, 2840, 2940 and 2970 cm^{-1}.

UV (EtOH): 282 (3.63) nm (log ε).

$C_{20}H_{27}NO_3$ (329.4). Calcd. C 72.92; H 8.26; H 4.25. Found C 72.42; H 8.09; N 4.64%.

The combined mother liquor from the above operations containing **7a** and **7b** was evaporated to one-third of its volume and allowed to crystallize in a refrigerator to give a 1 : 1 mixture of **7a** and **7b** (2.4 g). This was dissolved in acetone (80 mL) and acidified with perchloric acid to pH 1. The precipitate was filtered off and washed by suspending it in acetone (20 mL) to afford the perchlorate of **7a** (1.6 g), m.p. 216—226 °C. The mother liquor was evaporated, the residue dissolved in a mixture of hot ethanol (25 mL) and water (4 mL), the solution filtered from undissolved **7a** perchlorate (0.1 g), evaporated to a small volume and the crystals obtained were transferred with some cold ethanol onto a filter. The perchlorate of **7b** (1.5 g, m.p. 165—170 °C) was dissolved in a mixture of warm acetone (25 mL) and water (10 mL) and made alkaline (pH 8—9) to obtain the crude base (1.0 g), m.p. 125—138 °C. Recrystallization from ethanol (5 mL) gave pure **7b** (0.7 g; 5%), m.p. 133—137 °C.

^{1}H-NMR ($CDCl_3$): δ 3.83 (s, 6H, OMe), 4.13 (q, 1H, 9-H), 6.47 and 6.58 (s each, 2H, aromatic H).

IR (KBr): ν 1520, 1615 and 1700 cm^{-1}; ($CHCl_3$): ν 2840, 2955, 2940 and 2975 cm^{-1}.

UV (EtOH): 281 (3.63) nm (log ε).

Found C 73.12; H 8.61; N 4.40%.

rac-2,3-Methylenedioxy-8-aza-13α-gona-1,3,5(10)-trien-12-one (8a)

A mixture of **1c** hydrochloride (2.1 g; 0.01 mol), **2a** (2.5 mL), ethanol (3 mL) and water (0.2 mL) was refluxed for 9 h. After standing overnight at room temperature, the product was filtered off, washed with ethanol, dissolved by heating in a mixture of water (30 mL) and ethanol (10 mL), clarified and made alkaline with saturated sodium carbonate solution to pH 9. The base was filtered off, washed with water and recrystallized from ethanol (20 mL) to yield **8a** (1.0 g; 46%), m.p. 120—122 °C.

^{1}H-NMR ($CDCl_3$): δ 3.92 (q, 1H, 9-H), 5.88 (s, 2H, OCH_2O), 6.51 and 6.54 (s each, 2H, aromatic H).

IR (KBr): ν 1490, 1510 and 1715 cm^{-1}; ($CHCl_3$): ν 2760, 2815, 2880, 2915 and 2980 cm^{-1}.

$C_{17}H_{19}NO_3$ (285.4). Calcd. C 71.56; H 6.71; N 4.91. Found C 70.55; H 6.76; N 4.77%.

rac-2,3-Methylenedioxy-8-aza-9β,13α-gona-1,3,5(10)-trien-12-one (8b)

A mixture of **1c** (1.75 g; 0.01 mol as the base), **2a** (3.5 mL), 10% NaOH, ethanol (1.7 mL) and water (1.0 mL) was refluxed for 8 h. After adding ether (5 mL) and ethanol (1 mL), the solution was allowed to stand overnight. The product was filtered off, washed with cold ethanol (2×5 mL) and recrystallized from ethanol (20 mL) to give pure **8b** (0.5 g; 23%), m.p. 154—156 °C.

^{1}H-NMR ($CDCl_3$): δ 4.12 (q, 1H, 9-H), 5.92 (s, 2H, OCH_2O), 6.57 and 6.60 (s each, 2H, aromatic H).

IR (KBr): ν 1490, 1510 and 1710; ($CHCl_3$): ν 2775, 2830, 2880, 2915 and 2980 cm^{-1}.

Found C 70.34; H 6.89; N 4.99%.

rac-2,3-Methylenedioxy-8-aza-D-homo-9β,13α-gona-1,3,5(10)-trien-12-one (9b)

A mixture of **1c** (52.8 g; 0.3 mol, as the base), **2b** (120 mL), ethanol (250 mL), water (30 mL) and 40% NaOH (10 mL) was refluxed under nitrogen for 74 h, when 74% of **1c** had reacted. After standing in a refrigerator for 2 days, the product was filtered off and washed with ethanol-water (5 : 1, 2×50 mL) to obtain crude **9b** (35 g; 39%) containing about 20—25% of **9a**. This was recrystallized from forty volume of ethanol to give pure **9b** (13 g; 16%), m.p. 202—204 °C.

^{1}H-NMR ($CDCl_3$): δ 4.18 (q, 1H, 9-H), 5.89 (s, 2H, OCH_2O), 6.52 and 6.60 (s each, 2H, aromatic H).

IR (KBr): ν 1490, 1610 and 1715 cm^{-1}; ($CHCl_3$): ν 2775, 2830, 2865, 2940 and 2980 cm^{-1}.

$C_{18}H_{21}NO_3$ (299.4). Calcd. C 72.21; H 7.07; N 4.68. Found C 72.12; H 7.66; N 4.58%.

rac-2,3-Methylenedioxy-8-aza-D-homo-gona-1,3,5(10)-trien-12-one (9a)

The ethanolic mother liquors from the recrystallization of **9b** were evaporated, the residue dissolved in benzene (600 mL) and extracted with 2% hydrochloric acid (300 mL). The crystals which separated from the extract overnight were filtered off, washed with cold ethanol and dissolved in water (200 mL). The aqueous solution was made alkaline (pH 9), the crystalline base filtered off and recrystallized twice from ethanol to give **9a** (5 g; 8%), m.p. 198—201 °C.

^{1}H-NMR ($CDCl_3$): δ 3.90 (q, 1H, 9-H), 5.90 (s, 2H, OCH_2O), 6.55 and 6.60 (s each, 2H, aromatic H).

IR (KBr): ν 2775, 2830, 2855, 2940 and 2980 cm^{-1}.

Found C 71.91; H 7.60; N 4.71%.

rac-2,3-Methylenedioxy-8-aza-D-dihomo-9ξ,13ξ-gona-1,3,5(10)trien-12-one (10)

A mixture of **1c** (17.5 g; 0.1 mol, as the base), **2c** (40 mL), ethanol (50 mL), water (14 mL) and 10% NaOH (4 mL) were refluxed under nitrogen for 77 h. After standing in a refrigerator for 2 days, the product was filtered off and washed with cold ethanol (2×20 mL) to give a mixture of **10a** and **10b** (6.1 g), which was recrystallized three times from 20 volumes of ethanol to yield pure **10b** (1.2 g; 4%), m.p. 165—167 °C.

^{1}H-NMR ($CDCl_3$): δ 4.16 (q, 1H, 9-H), 5.94 (s, 2H, OCH_2O),6.55 and 6.42 (s each, 2H, aromatic H).

IR (KBr): ν 1490, 1510 and 1705 cm^{-1}; ($CHCl_3$): ν 2775, 2835, 2875, 2935 and 2980 cm^{-1}.

$C_{19}H_{23}NO_3$ (313.4). Calcd. C 72.82; H 7.04; N 4.47. Found C 72.67; H 7.67; N 4.32%.

From the mother liquors of the cycloaddition more of the isomeric mixture (7.0 g) could be isolated. The mother liquors from the purification of **10b** were combined and evaporated. The residue (3.4 g) was dissolved in hot ethanol (60 mL) and the crystalline product (2.0 g) filtered off at 30 °C. This was again recrystallized from ethanol and the mother liquor from this operation was cooled to —10 °C to afford **10a** (0.25 g; 0.7%), m.p. 150—152 °C.

^{1}H-NMR ($CDCl_3$): δ 4.00 (s, 1H, 9-H), 5.88 (s, 2H, OCH_2O), 6.48 and 6.55 (s each, 2H, aromatic H).

IR (KBr): ν 1490, 1510 and 1705 cm^{-1}; ($CHCl_3$): ν 2775, 2835, 2875, 2940 and 2985 cm^{-1}.

Found C 72.97, H 7.98, N 4.48%.

rac-2,3-Diethoxy-8-aza-13β-gona-1,3,5(10)-trien-12-one (11a)

A mixture of **1d** hydrochloride (25.0 g; 0.1 mol), **2a** (33 mL), water (6 mL) and ethanol (32 mL) was refluxed for 18 h and kept in a refrigerator overnight. The product (m.p. 185—187 °C) was dissolved in water (300 mL), the solution was clarified and made alkaline (pH 9) with saturated sodium carbonate solution. The crude base was recrystallized from ten volumes of ethanol to give pure **11a** (13.0 g; 40%) m.p. 116—117 °C.

^{1}H-NMR ($CDCl_3$): δ 1.40 (t, 6H, OCH_2CH_3), 4.05 (q, 4H, OCH_2CH_3), 6.56 and 6.60 (s each, 2H, aromatic H).

IR (KBr): ν 1525, 1620 and 1710 cm^{-1}; ($CHCl_3$): ν 2760, 2820, 2880, 2920, 2845 and 2980 cm^{-1}.

$C_{20}H_{27}NO_3$ (329.4). Calcd C 72.92; H 8.25; N 4.25. Found C 72.62; H 8.78; N 4.20%.

rac-2,3-Diethoxy-8-aza-9β,13α-gona-1,3,5(10)-trien-12-one (11b)

The residue from the evaporation of the mother liquor of **11a** hydrochloride was taken up in water (200 mL) and the solution extracted with benzene (3×500 mL). The aqueous phase was made alkaline to pH 9, the precipitate filtered off, washed with water and recrystallized from ten volumes of ethanol to obtain a mixture (5 g) of **11a** and **11b**. To the mother liquor an equal amount of hot water was added. On standing pure **11b** (0.5 g) precipitated m.p. 178—182 °C.

^{1}H-NMR ($CDCl_3$): δ 1.40 (t, 6H, OCH_2CH_3), 4.05 (q, 4H, OCH_2CH_3), 6.60 (s each, 2H, aromatic H).

IR (KBr): ν 1530, 1615 and 1710 cm^{-1}; ($CHCl_3$): ν 2760, 2820, 2880, 2920, 2945 and 2980 cm^{-1}.

$C_{20}H_{27}NO_3$ (329.4). Calcd. C 72.92; H 8.25; N 4.25. Found C 73.46; H 8.69; N 4.45%.

rac-2,3-Diethoxy-8-aza-D-homo-gona-1,3,5(10)-trien-12-one (12a)

A mixture of **1d** hydrochloride (12.0 g; 0.048 mol), **2b** (17 mL), ethanol (16 mL) and water (3 mL) was refluxed for 60 h. After evaporation of the solvents, the residue was taken up in water (400 mL), the solution extracted with benzene (3×50 mL), the aqueous layer made alkaline (pH 9) with saturated aqueous sodium carbonate solution to gave an oil, which could be crystallized by trituration with ethanol. A mixture of isomers (8.0 g; 50%) **12a** and **12b** was obtained, while **12c** remained in the mother liquor. The crystals were dissolved in a tenfold volume of ethanol and the precipitate was filtered off at 30—40 °C. After four successive similar operations, pure **12a** (1.6 g; 10%) was obtained, m.p. 162—163 °C.

^{1}H-NMR ($CDCl_3$): δ 1.40 (t, 6H, OCH_2CH_3), 4.03 (q, 4H, OCH_2CH_3), 6.52 and 6.58 (s each, 2H, aromatic H).

IR (KBr): ν 1520, 1610 and 1705 cm^{-1}; ($CHCl_3$): ν 2760, 2820, 2865, 2940 and 2985 cm^{-1}.

$C_{21}H_{29}NO_3$ (343.5) Calcd. C 73.43; H 8.51; N 4.06. Found C 73.06; H 8.51; N 3.97%.

rac-2,3-Diethoxy-8-aza-D-homo-9β-gona-1,3,5(10)-trien-12-one (12c)

The first mother liquor of **12a** was evaporated, the residue dissolved in benzene (40 mL) and the solution extracted with 2.3% hydrochloric acid (7×15 mL). After standing overnight, the crystals which deposited from Fractions 2 and 3 were separated, dissolved in warm water and the solution was made alkaline. The crude base was filtered off, washed thoroughly with water and recrystallized from a tenfold volume of ethanol to obtain pure **12c** (0.5 g; 3%), m.p. 110—112 °C.

^{1}H-NMR ($CDCl_3$): δ 1.40 (t, 6H, OCH_2CH_3), 4.05 (q, 4H, OCH_2CH_3), 4.59 (t, 1H, 9-H), 6.58 and 6.68 (s each, 2H, aromatic H).

IR (KBr): ν 1520, 1605 and 1715 cm^{-1}; ($CHCl_3$): ν 2870, 2950, 2985 cm^{-1}.

$C_{21}H_{29}NO_3$ (343.5). Calcd. C 73.43; H 8.51; N 4.06. Found C 73.28; H 8.77; N 4.11%.

rac-2,3-Diethoxy-8-aza-D-homo-9β-13α-gona-1,3,5(10)-trien-12-one (12b)

A mixture of **1d** (21.9 g, 0.1 mol, as the base), **2b** (38 mL), ethanol (26 mL), 10% NaOH (4 mL) and water (10 mL) was refluxed under nitrogen for 30 h. After standing overnight in a refrigerator, the product was filtered off and washed with ethanol (2×20 mL). The crude product (15.0 g; 44%), m.p. 145—148 °C, was recrystallized from ethanol (300 mL) to give pure **12b** (12.2 g; 38%), m.p. 149—150 °C.

^{1}H-NMR ($CDCl_3$): δ 1.40 (t, OCH_2CH_3), 4.00 (q, 4H, OCH_2CH_3), 6.50 and 6.58 (s each, 2H, aromatic H).

IR (KBr): ν 1530, 1615 and 1720 cm^{-1}; ($CHCl_3$): ν 2880, 2950 and 2990 cm^{-1}.

$C_{21}H_{29}NO_3$ (343.5). Calcd. C 73.43; H 8.51; N 4.06. Found C 73.45; H 8.93; N 4.06%.

rac-2,3-Dihydroxy-8-aza-13α-gona-1,3,5(10)-trien-12-one (13a)

A mixture of **1e** (10.9 g; 0.05 mol, as the base), **2a** (21 mL), ethanol (24 mL) and water (2 mL) was reluxed for 11 h. The product was precipitated by adding ether, filtered off, and washed with ether to afford a mixture of isomers (1.7 g; 12.5%), m.p. 105—129 °C. The mother liquor was evaporated, the residue triturated with petroleum ether and the undissolved oil was crystallized from a mixture of ether (50 mL) and ethanol (3 mL) at —10 °C. The two crops of crystals were combined and recrystallized three times from fifty volumes of ethanol to yield pure **13a** (2.1 g; 18%), m.p. 146—149 °C.

^{1}H-NMR (d_7-DMF): δ 3.08 (q, 1H, 9-H), 6.20 and 6.22 (s each, 2H, aromatic H).

IR (KBr): ν 1530, 1615, 1705, 3330 and 3495 cm^{-1}.

$C_{17}H_{19}NO_3$ (273.3). Calcd. C 70.31; H 7.00; N 5.13. Found C 70.76; H 7.53; N 4.89%.

rac-2,3-Dihydroxy-8-aza-9β,13α-gona-1,3,5(10)-trien-12-one (13b)

The ethereal mother liquor obtained from the recrystallization of **13a** was evaporated and the residue triturated with some cold acetone. After standing overnight in a refrigerator, the crude product (4.0 g; 29%, m.p. 95—98 °C) was filtered off and recrystallized from a sixfold volume of ethanol—water (2 : 1) to afford pure **13b** (2.6 g; 18%), m.p. 110—113 °C.

^{1}H-NMR (d_7-DMF): δ 3.62 (q, 1H, 9-H), 6.28 (s each, 2H, aromatic H).

IR (KBr): ν 3370, 3605, 1695, 1620 and 1535 cm^{-1}; ($CDCl_3$): ν 2760, 2815, 2880 and 2970 cm^{-1}.

$C_{16}H_{19}NO_3 \cdot H_2O$ (291.3). Calcd. C 65.95; H 7.27; N 4.81. Found C 66.65; H 6.81; N 4.89%.

rac-2-n-Butoxy-3-methoxy-8-aza-D-homo-gona-1,3,5(10)-trien-12-one (14a)

A mixture of **1f** (5.6 g; 0.024 mol, as the base), 1-acetylcyclohexene (**2b**, 8.4 mL), 10% NaOH (1 mL), water (3.5 mL) and ethanol (8.5 mL) was refluxed for 10 h. After standing in a refrigerator for two days, the product was filtered off and washed with cold ethanol to give the crude product (2.1 g; 24.5%), m.p. 108—113 °C. Two recrystallizations from 20 volumes of ethanol yielded pure **14a** (1.0 g; 11.7%), m.p. 117—118.5 °C.

IR (KBr): ν 1520, 1615 and 1710 cm^{-1}; ($CHCl_3$): ν 2870 and 2945 cm^{-1}.

$C_{22}H_{31}NO_3$ (357.5). Calcd. C 73.95; H 8.74; N 3.92. Found C 73.76; H 8.92; N 4.33%.

rac-2-Hydroxy-3-methoxy-8-aza-13α-gona-1,3,5(10)-trien-12-one (15a)

A mixture of **1g** (5.3 g; 0.03 mol), **2a** (10 mL), ethanol (12 mL) and water (2 mL) was refluxed for 8 h. After standing in a refrigerator for 3 days, the product was filtered off and washed with ethanol (3×5 mL) to give the crude product (2.75 g; 32%), m.p. 174—177 °C. This was recrystallized from 13 volumes of ethanol to yield pure **15a** (2.1 g; 25%), m.p. 179—182 °C.

^{1}H-NMR ($CDCl_3$): δ 3.78 (s, 3H, OCH_3), 5.30 (s, 1H, OH), 6.29 and 6.45 (s each, 2H, aromatic H).

IR (KBr): ν 1520, 1600, 1700 and 3370 cm^{-1}; ($CDCl_3$): ν 2760, 2810, 2845, 2880, 2920, 2945, 2975 and 3555 cm^{-1}.

UV (EtOH): 287 (3.63) nm (log ε).

$C_{17}H_{21}NO_3$ (287.4). Calcd. C 71.05; H 7.39; N 4.87. Found C 71.27; H 7.90, N 4.95%.

rac-2-Hydroxy-3-methoxy-8-aza-9β,13α-gona-1,3,5(10)-trien-12-one (15b)

A mixture of **1g** hydrochloride (6.4 g; 0.03 mol), **2a** (10 mL), ethanol (12 mL) and water (3.3 mL) was refluxed for 16 h. After cooling, the product was filtered off and washed with ethanol to give the hydrochloride of a mixture of **15a** and **15b** (7.6 g, m.p. 210—215 °C). This was dissolved in water (200 mL), clarified and made alkaline with saturated sodium carbonate solution. The precipitated oil was separated and triturated with some ethanol. The crystalline product was filtered off and recrystallized from ethanol (30 mL) to yield **15a** containing some **15b** (2.1 g; 24%). The mother liquor was evaporated to one-sixth of its volume, clarified while hot, and cooled to —10 °C. The product was filtered off (0.8 g; m.p. 138—131 °C) and recrystallized first from six volumes of ethanol and then from eight volumes of methanol. The product was filtered off at —20 °C to give pure **15b** (0.3 g; 3.4%), m.p. 139—131 °C.

^{1}H-NMR ($CDCl_3$): δ 3.79 (s, 3H, OCH_3), 3.9 (q, 1H, 9-H), 5.4 (s, 1H, OH), 6.44 and 6.50 (s each, 2H, aromatic H).

IR (KBr): ν 1520, 1605, 1710 and 3370 cm^{-1}; ($CHCl_3$): ν 2760, 2820, 2845, 2880, 2920, 2945, 2975 and 3555 cm^{-1}.

$C_{17}H_{21}NO_3$ (287.4). Calcd. C 71.05; H 7.39; N 4.87. Found C 75.19; H 7.67; N 4.96%.

rac-3-Methoxy-8-aza-D-homo-9β-gona-1,3,5(10)-trien-12-one (16c)

A mixture of **1h** (7.4 g; 0.04 mol, as the base), **2b** (10 mL), water (1.6 mL), methylamine hydrochloride (2.7 g; 0.04 mol) and ethanol (20 mL) was refluxed for 4 h. The reaction mixture was evaporated to dryness, the residue suspended in water (75 mL) and extracted with benzene (2×20 mL). The aqueous phase was clarified and heated slowly to 35 °C. The product was filtered off to afford a mixture of the non-separated isomers (2.3 g; 20%), m.p. 157—168 °C. The mother liquor was cooled to 0 °C, whereupon crude **16c** (0.65 g; 6%, m.p. 179—184 °C) precipitated. The mother liquor of the latter was evaporated and the residue (1.6 g) was recrystallized from 15 volumes of ethanol, to give a mixture of the isomers (m.p. 151—159 °C). The mother liquor of the latter was cooled to 0 °C, whereupon more crude **16c** (0.30 g; 3%, m.p. 177—184 °C) crystallized. The combined crude products were recrystallized twice from ethanol and the products filtered off at —10 °C. This gave pure **16c** (0.70 g; 16%), m.p. 181—184 °C.

^{1}H-NMR ($CDCl_3$): δ 3.75 (s, 3H, OCH_3), 4.65 (t, 1H, 9-H).

IR (KBr): ν 1500, 1580, 1615 and 1710 cm^{-1}; ($CHCl_3$): ν 2840, 2865 and 2945 cm^{-1}.

UV (EtOH): 277 (3.26), 285 (3.24) nm (log ε).

$C_{18}H_{23}NO_2$ (285.3). Calcd. C 75.75; H 8.12; N 4.91. Found C 75.19; H 8.27; N 5.04%.

rac-2,3-Dimethoxy-11ξ-methyl-8-aza-9ξ,13ξ-gona-1,3,5(10)-trien-12-one (17)

A mixture of **1b** hydrochloride (11.4 g; 0.05 mol), **2d** (19 mL), ethanol (20 mL) and water (1 mL) was refluxed for 30 h. After concentration, the mixture was acidified with 1*N* hydrochloric acid, taken up in water (200 mL) and the solution extracted with benzene (3×30 mL). The combined extracts were extracted with 0.6 *N* hydrochloric acid (5×20 mL), the third extract containing mainly **17c**, the fourth and fifth, in turn, **17a**. The former was made alkaline to give an oil which was dissolved in benzene (50 mL) and the solution repeatedly extracted with 0.6 *N* hydrochloric acid (10×10 mL). The third and fourth portions from the latter extraction were combined, made alkaline, the precipitated oil extracted with benzene, the extract evaporated, and the residue triturated with ether to give the crude product (0.5 g). Recrystallization from ether yielded pure **17c** (0.25 g), m.p. 142—146 °C.

^{1}H-NMR ($CDCl_3$): δ 1.12 (d, 3H, 11-CH_3), 3.85 (s, 6H, OCH_3), 3.95 (d, 1H, 9-H), 6.55 and 6.22 (s each, 2H, aromatic H).

IR (KBr): ν 1525, 1615 and 1710 cm^{-1}; ($CHCl_3$): 2760, 2820, 2840, 2880, 2945 and 2970 cm^{-1}.

$C_{19}H_{25}NO_3$ (315.3). Calcd. C 72.35; H 7.89; N 4.44. Found C 72.86; H 8.52; N 4.42%.

The combined fourth and fifth fractions of the first extraction were made alkaline, the product extracted with benzene (50 mL) and this solution extracted with a mixture of water (100 mL) and 6 *N* hydrochloric acid (2 mL) in ten portions. From the first two fractions **17c** was recovered. Fractions 6—9 containing **17a** were combined with Fractions 7—9 of the second extraction of above preparation, made alkaline and extracted with benzene. The extract was dried, evaporated and the residue (2.0 g) dissolved in a mixture of ether and ethanol (2 : 1) and acidified with anhydrous perchloric acid. The crystals (1.8 g) were filtered off and recrystallized from 33% aqueous ethanol (15 mL) to give the perchlorate of **17a** (0.88 g), m.p. 192—200 °C. This was dissolved in aqueous ethanol and made alkaline to give the crude base (0.6 g), which was recrystallized from a mixture of ethanol (6 mL) and water (10 mL) to obtain pure **17a** (0.45 g), m.p. 109—112 °C.

^{1}H-NMR ($CDCl_3$): δ 0.81 (d, 3H, 11-CH_3), 3.85 (s, 6H, OCH_3), 4.26 (d, 1H, 9-H) 6.51 and 6.62 (s, 2H, aromatic H).

IR (KBr): ν1520, 1620 and 1710 cm^{-1}; ($CHCl_3$): ν 2760, 2820, 2840, 2880, 2920, 2945 and 2970 cm^{-1}.

$C_{19}H_{25}NO_3$ (315.4). Calcd. C 72.35; H 7.89; N 4.44. Found C 72.20; H 8.48; N 4.43%.

A mixture of **1b** (9.5 g; 0.05 mol, as the base), **2d** (19 mL), ethanol (20 mL), 10% NaOH (2 mL) and water (3 mL) was refluxed for 16 h. The mixture was evaporated to dryness, the residue taken up in ether (100 mL), washed with water (3×50 mL) and extracted, in 10 portions, with a mixture of 1 *N* hydrochloric acid (10 mL) and water (90 mL). Portions 4—10, containing **17b**, were combined, made alkaline and the product filtered off (6.2 g; 39%, m.p. 109—117 °C). This was recrystallized three times from four volumes of ethanol to afford pure **17b** (0.7 g; 4%), m.p. 126—138 °C.

^{1}H-NMR ($CDCl_3$): δ 0.95 (d, 3H, 11-CH_3), 3.85 (s, 6H, OCH_3), 4.14 (d, 1H, 9-H), 6.58 and 6.62 (s each, 2H, aromatic H).

IR (KBr): ν 1525, 1620 and 1695 cm^{-1}; ($CHCl_3$): ν 2840, 2880, 2920, 2945 and 2970 cm^{-1}.

$C_{19}H_{25}NO_3$ (315.4). Calcd. C 72.35; H 7.89; N 4.44. Found C 72.43; H 8.06; N 4.45%.

rac-2,3-Methylenedioxy-11ξ-methyl-8-aza-9ξ,13ξ-gona-1,3,5(10)-trien-12-one (18)

A mixture of **1c** (9 g; 0.05 mol, as the base), **2d** (19 mL), ethanol (20 mL), 10% NaOH (2 mL) and water (3 mL) was refluxed for 16 h under nitrogen. After evaporation to dryness, the residue was taken up in ether (50 mL), washed with water (3×50 mL) and extracted, in ten portions, with a mixture of 6 *N* hydrochloric acid (10 mL) and water (90 mL). The first two fractions contained unchanged **1c**; the third fraction was made alkaline, and the oily precipitate which separated was triturated with some ethanol to obtain a mixture of **18b** and **18c** (1.35 g; 9%, m.p. 156—173 °C), which was recrystallized twice from 25 volumes of ethanol to give pure **18c** (0.5 g), m.p. 170—173 °C.

^{1}H-NMR ($CDCl_3$): δ 1.12 (d, 3H, 11-CH_3), 3.90 (d, 1H, 9-H), 3.57 (m, 1H, 11-H), 5.88 (s, 2H, OCH_2), 6.50 and 6.55 (s each, 2H, aromatic H).

IR (KBr): ν 1490, 1510 and 1700 cm^{-1}; ($CHCl_3$): ν 2775, 2880, 2920, 2940 and 2980 cm^{-1}.

$C_{18}H_{21}NO_3$ (299.4). Calcd. C 72.21; H 7.07; N 4.68. Found C 72.35; H 7.02; N 4.68%.

Extracts 4—6 of the above preparation were combined, made alkaline and the precipitated oil triturated with some ethanol to give the crude product (3.8 g; 25%), which was recrystallized from ethanol (40 mL) to obtain pure **18b** (2.0 g), m.p. 128—121 °C.

^{1}H-NMR ($CDCl_3$): δ 0.95 (d, 3H, 11-CH_3), 4.10 (d, 1H, 9-H), 3.70 (q, 1H, 11-H), 5.90 (s, 2H, OCH_2O), 6.55 and 6.57 (s each, 2H, aromatic H).

IR (KBr): ν 1490, 1510 and 1705 cm^{-1}; ($CHCl_3$): ν 2740, 2780, 2820, 2880, 2920, 2940 and 2980 cm^{-1}.

$C_{18}H_{21}NO_3$ (299.4). Calcd. C 72.21; H 7.07; N 4.68. Found C 71.83; H 7.20; N 4.73%.

(—)-7ξ-Methyl-8-aza-9ξ,13ξ-gona-1,3,5(10)-trien-12-one (19)

A mixture of (—)-3-methyl-3,4-dihydroisoquinoline (**1i**, 14.5 g; 0.10 mol), **2a** (25 mL), methylamine hydrochloride (0.67 g) and ethanol (75 mL) was kept at 75 °C for 8 h. After standing overnight in a refrigerator, the product was filtered off and washed with ethanol

to give crude **19a** (6.6 g; 26%), m.p. 101—104 °C. Recrystallization from 8 volumes of ethanol gave pure **19a** (4.0 g; 16%), m.p. 102—104 °C; $[\alpha]_D^{20}$ —237° ($c = 1\%$, $CHCl_3$), —243° ($c = 1\%$, ethanol), —233° ($c = 1\%$, dioxane) and —271° ($c = 1\%$, benzene).

^{1}H-NMR ($CDCl_3$): δ 0.91 (d, 3H, 7-CH_3), 4.20 (q, 1H, 9-H), 7.15 (m, 4H, aromatic H).

IR (KBr): ν 1455, 1500 and 1715 cm^{-1}; ($CHCl_3$): ν 2740, 2765, 2840, 2880, 2915, 2940 and 2975 cm^{-1}.

UV (EtOH): 265 (2.79) and 272 (2.77) nm (log ε).

$C_{17}H_{21}NO$ (255.4). Calcd. C 79.96; H 8.29; N 5.49. Found C 79.89; H 8.83; N 5.53%.

(—)-7-ε-Methyl-8-aza-D-homo-9ξ,13ξ-gona-1,3,5(10)-trien-12-one (20)

A mixture of (—)-**1i** (14.5 g; 0.10 mol), **2b** (25 mL), methylamin hydrochloride (0.67 g) and ethanol (75 mL) was kept at 75 °C for 20 h. After standing overnight at room temperature the product was filtered off and washed with cold ethanol to give crude **20a** (10.2 g; 39%, m.p. 134—139 °C), which was recrystallized from five volumes of ethanol to give pure **20a** (8.3 g; 31%), m.p. 136—139 °C.

$[\alpha]_D^{20}$ —132° ($c = 1$, $CHCl_3$), —130° ($c = 1\%$, ethanol), —152° ($c = 1\%$, dioxane), —164° ($c = 1\%$, benzene).

IR (KBr): ν 1450, 1460, 1500 and 1715 cm^{-1}; ($CHCl_3$): ν 2865, 2940 cm^{-1}.

UV (EtOH) 265 (2.71) and 272 (2.70) nm (log ε).

$C_{18}H_{23}NO$ (269.4). Calcd. C 80.25; H 8.61; N 5.20. Found C 79.38; H 8.90; N 5.30%.

***rac*-2,3-Dimethoxy-7ξ-methyl-8-aza-9ξ,13ξ-gona-1,3,5(10)-trien-12-one (21)**

A mixture of **1j** hydrochloride (19.4 g; 0.08 mol), **2a** (26 mL) and ethanol (26 mL) was refluxed for 24 h. After evaporation to dryness the residue was crystallized from acetone (40 mL) to obtain impure **21a** HCl (2.7 g; m.p. 187—193 °C), while the mother liquor contained a mixture of isomers. The crystals were taken up in water, the solution was made alkaline, and the precipitated crude **21a** (0.5 g) was recrystallized from ethanol to give pure **21a** (0.3 g) m.p. 146—147 °C.

^{1}H-NMR ($CDCl_3$): δ 1.35 (d, 3H, 6-CH_3), 3.82 (s, 6H, OCH_3), 4.12 (q, 1H, 9-H), 6.55 (s, 2H, aromatic H).

IR (KBr): ν 1525, 1620 and 1710 cm^{-1}; ($CHCl_3$): ν 2840, 2880, 2920, 2945 and 2980 cm^{-1}.

$C_{19}H_{25}NO_3$ (315.4). Calcd. C 72.35; H 7.99; N 44.44. Found C 72.42; H 8.00; N 4.48%.

***rac*-2,3-Dimethoxy-7ξ-methyl-8-aza-D-homo-9ξ,13ξ-gona-1,3,5(10)-trien-12-one (22)**

A mixture of **1j** (8.85 g; 0.04 mol, as the base), **2b** (15 mL), ethanol and 10% NaOH (2 mL) was refluxed for 32 h. After standing overnight in a refrigerator, the product (1.3 g; m.p. 172—185 °C) was filtered off and recrystallized first from benzene and then from ethanol to give **22a** (0.4 g), m.p. 195—197 °C. The other isomers remained in the mother liquors.

^{1}H-NMR ($CDCl_3$): δ 1.28 (d, 3H, 7-CH_3), 3.82 (s, 6H, OCH_3), 4.22 (q, 1H, 9-H), 6.55 (s, 2H, aromatic H).

IR (KBr): ν 1520, 1620 and 1710 cm^{-1}; ($CHCl_3$): ν 2800, 2850 and 2880 cm^{-1}.

$C_{20}H_{27}NO_3$ (329.4). Calcd. C 72.92; H 8.26; N 4.25. Found C 73.05; H 8.80; N 4.40%.

(—)-7ξ,11ξ-Dimethyl-8-aza-9ξ,13ξ-gona-1,3,5(10)-trien-12-one (23)

A mixture of (—)-**1j** (14.5 g; 0.1 mol), **2d** (25 mL), methylamine hydrochloride (0.67 g) and ethanol (75 mL) was maintained at 75 °C for 20 h. After acidification with anhydrous perchloric acid the perchlorate was filtered off and recrystallized from 50% aqueous ethanol. The product (6.4 g, m.p. 206—209 °C) was converted to the base while stirring it in a mixture of water (100 mL) and chloroform (50 mL). The organic phase was separated and the aqueous phase washed with chloroform (2×20 mL). The combined extracts were evaporated, the residue triturated with some methanol and the crystals obtained (0.8 g) recrystallized from methanol (8 mL) to give **23** (0.5 g), m.p. 123—126 °C.

IR (KBr): ν 1450, 1500 and 1715 cm^{-1}.

$C_{18}H_{23}NO$ (269.4). Calcd. C 80.25; H 8.61; N 5.20. Found C 80.35, H 9.00, N 5.24%.

REFERENCES

[1] SZÁNTAY, Cs., VEDRES, A., TÓTH, G.: Heterocycles, **6,** 1793 (1977)
[2] RASSAERT, C. L., DILASGVALE, G., GIANNINA, T., MANNING, U. P., MELI, A.: Steroids Lipids Res., **4,** 333 (1973)
[3] BEKE, D., SZÁNTAY, Cs.: Chem. Ber., **95,** 2132 (1962)
[4] SZÁNTAY, Cs., TŐKE, L., KOLONITS P.: J. Org. Chem., **31,** 1447 (1966)
[5] SNYDER, H. R., WERBER, T. X.: J. Am. Chem. Soc., **72,** 2962 (1950)
[6] IDE, W. S., BUCK, J. S.: J. Am. Chem. Soc., **60,** 2101 (1938)
[7] DEY, B. B., GOVINDICHARI, T. R.: Proc. Nat. Inst. Sci. India, **6,** 219 (1940); Chem. Abstr., **39,** 2512 (1945)
[8] KALAUS, Gy.: Private communication
[9] BALOGH, Gy.: Private communication
[10] GULLAND, J. M., VIRDEN, C. J.: J. Chem. Soc., **1929,** 1971
[11] POTAPOV V. M., DEMJANOVICH, V. S., SOIFER, A. P., TERENTIEV, A. P.: Zh. Obsh. Khim., **37,** 2679 (1966)
[12] IDE, W. S., BUCK, J. S.: J. Am. Chem. Soc., **62,** 425 (1940)
[13] JONES, N., TAYLOR, H. T.: J. Chem. Soc., **1959,** 4017
[14] DEV, S.: J. Indian Chem. Soc., **33,** 703 (1956)
[15] BAN, Y., YONEMITSU, O., TERASHIMA, M.: Chem. Pharm. Bull., **8,** 194 (1960)
[16] JACQUIER, R., MAURY, G.: Bull. Soc. Chim. France, **1967,** 306
[17] SZÁNTAY, Cs., ROHÁLY, J.: Chem. Ber., **98,** 557 (1965); Magy. Kém. Folyóirat, **70,** 478 (1964)

András VEDRES H-1475 Budapest, 10. P.O. Box 27.

Pál KOLONITS, Csaba SZÁNTAY H-1521 Budapest, Gellért tér 4.

Acta Chimica Academiae Scientiarum Hungaricae, Tomus 109 (2), pp. 129—137 (1982)

CHEMISTRY OF 8-AZASTEROIDS, III*

STEREOCHEMISTRY OF 8-AZAGONAN-12-ONES

A. VEDRES,[1] G. TÓTH[2] and Cs. SZÁNTAY[2]**

([1]EGYT Pharmacochemical Works, Budapest and [2]Institute for Organic Chemistry, Technical University Budapest)

Received September 16, 1980

Accepted for publication February 9, 1981

The stereochemistry of some 8-azagonan-12-ones, obtained by the cycloaddition of 1-acyl-1-cycloalkenes to 3,4-dihydroisoquinolines, was determined and the interconversion of epimers studied. By variation of the reaction conditions stereoselectivity could be improved.

In a previous paper [1] we described a simple, one-step procedure for the convenient preparation of 8-azagonane derivatives by the cycloaddition of 1-acyl-1-cyclohexenes to 3,4-dihydroisoquinolines, giving a mixture of epimers in good yields. Our further studies aimed at the determination of the stereochemistry of the products and the selective preparation of the individual stereoisomers. This paper deals with the products obtained from the reaction of 6,7-dimethoxy-3,4-dihydroisoquinoline with 1-acetyl-1-cyclopentene and 1-acetyl-1-cyclohexene, respectively.

Effect of reaction conditions on the ratio of stereoisomers

Cycloaddition may lead, in principle, to four racemic pairs of diastereoisomers (**1**—**4**) distinguished, following a notation widely used in alkaloid chemistry [2], by the prefixes *normal* (9α, 13β, 14α), *pseudo* (9β, 13β, 14α), *allo* (9α, 13α, 14α) and *epiallo* (9β, 13α, 14α).

The stereoisomers can be separated either on silica gel TLC plates impregnated with boric acid, or sometimes by fractional crystallization [1].

In the reaction mixture obtained from 6,7-dimethoxy-3,4-dihydroisoquinoline and 1-acetyl-1-cyclohexene three stereoisomers (**1b**, **3b** and **4b**), while in that derived from 1-acetyl-1-cyclopentene only two (**2a** and **4a**) could be detected by TLC. Their ratio was determined by UV spectroscopy following the elution of the spots. In order to establish the stereoselectivity, the ratio of the stereoisomers was determined under various reaction conditions at the half-time of the reaction (*cf.* Table I).

* For Part II, see preceding paper.
** To whom correspondence should be addressed.

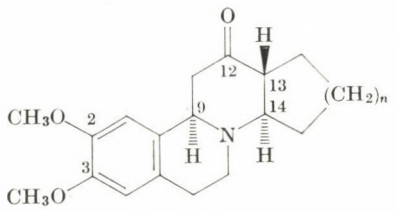

1 *(normal)*

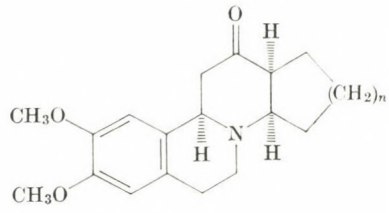

2 *(allo)*

	n
a	1
b	2

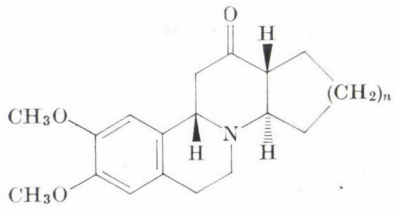

3 *(pseudo)*

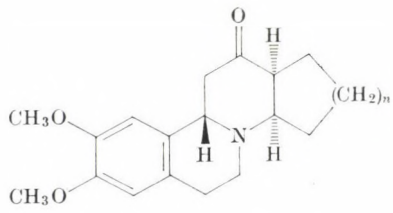

4 *(epiallo)*

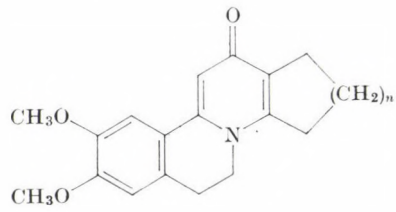

5

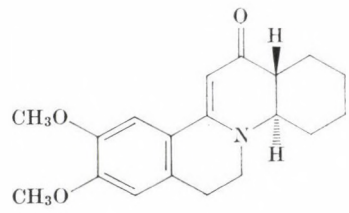

6

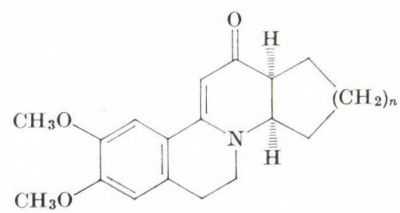

7

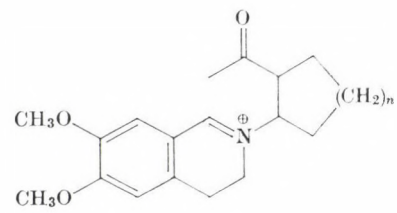

8

From the Table it is apparent that under the conditions of fast and slow conversion the major stereoisomers are different. This finding is independent of the substitution of the aromatic ring. Cycloaddition is thus stereoselective, and the isomeric ratio can be influenced by a proper choice of the catalyst.

Table I

Isomeric ratios at the half-time of the cycloaddition reaction of 6,7-dimethoxy-3,4-dihydroxyisoquinoline and 1-acetyl-cyclopentene or 1-acetyl-cyclohexene

Catalyst	$t_{1/2}$ (h)	**2a** (%)	**4a** (%)	$t_{1/2}$ (h)	**1b** (%)	**4b** (%)	**3b** (%)
Water	11.5	36	64	52	14	69	17
NaOH (1%)	8.5	40	60	40	23	70	7
NaOH (100%)	16.5	30	70	46	22	64	14
HCl (10%)	1.5	65	35	7	70	25	5
HCl (100%)	11.5	46	54	40	36	52	12
Methylamine-HCl (10%)	0.5	70	28	1	75	22	3

While **2a** and **4a**, containing five-membered ring, could be readily separated by crystallization from ethanol, this method was found less efficient in the D-homo series. On the other hand, when the components were allowed to react in the presence of sodium hydroxide, pure **4b** was obtained after refluxing for 24 h, and further refluxing of the mother liquor after the addition of methylamine hydrochloride afforded almost pure **1b**.

Epimerization experiments

Epimerization of the centre of chirality at C-13, adjacent to a carbonyl group, under conditions favouring enolization gave important clues to the stereostructure of our compounds. We have shown earlier [3] that benzo[*a*]-quinolizine-3-ones may epimerize in acids *via* ring cleavage at the bridgehead carbon atom (in our case C-9). Epimerization at C-14 has not been reported.

When refluxed in ethanol for 10 h, **1b** remained unchanged, whereas both **3b** and **4b** gave rise to an equilibrium mixture consisting of 24% **3b** and 75% **4b**. It may be assumed that under such conditions only enolization took place and the substrates are epimers at C-13 Under similar conditions the five membered ring compounds **2b** and **4a** remained unchanged, hence presumably they have the more stable *cis* ring junction at C-13 and C-14.

When refluxed in ethanolic sodium hydroxide for 5 h, **1b** did not change either, while **3b** and **4b**, as well as **2a** and **4a** were converted into equilibrium mixtures of the stereoisomers.

Boiling any of **1b**, **3b**, or **4b** in 0.1 *N* hydrochloric acid gave rise to the same three-component mixture containing 50% of **1b**, 25% of **3b** and 25% of **4b**, while a mixture consisting of 60% of **2a** and 40% of **4a** was obtained under the same conditions either from **2a** or **4a**. This indicated that with the

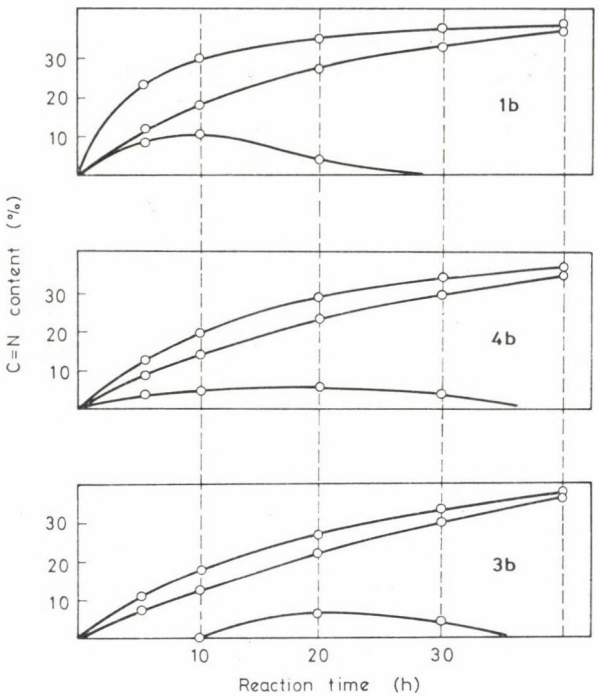

Fig. 1. Conversion of stereoisomers **1b**, **3b** and **4b** on treatment with acid

D-homo compounds both enolization and ring cleavage, while with the five-membered ring compounds only ring cleavage occurred.

Utilizing our method reported earlier [1, 3], ring cleavage was studied in more detail. On heating the ketones in 0.1 *N* hydrochloric acid, the concentration of the C=N chromophore increased due partly to the formation of the immonium salt **8** and partly to the corresponding isoquinoline derivative generated by retro-addition during prolonged heating.

The stereoisomers responded differently to treatment with acid, and these differences could be followed until equilibrium had been attained. With the D-homo ketones this was reached after refluxing in 0.1 *N* hydrochloric acid for 30—40 h. Differences were manifest both in the relative amount of immonium salt (*cf.* Fig. 1) and the primary product of successive epimerization (Fig. 2).

The amounts of both the immonium salt and isoquinoline were determined as a function of time from the acid solution of the D-homo stereoisomers **1b**, **3b** and **4b**. In Figure 1 the upper curve represents the total C=N concentration, the middle one that after making sample alkaline, and the lower curve shows the difference between the first two. With **1b** the amount of immonium salt increases rapidly (20% after 10 h), with **4b** the increase is much slower and,

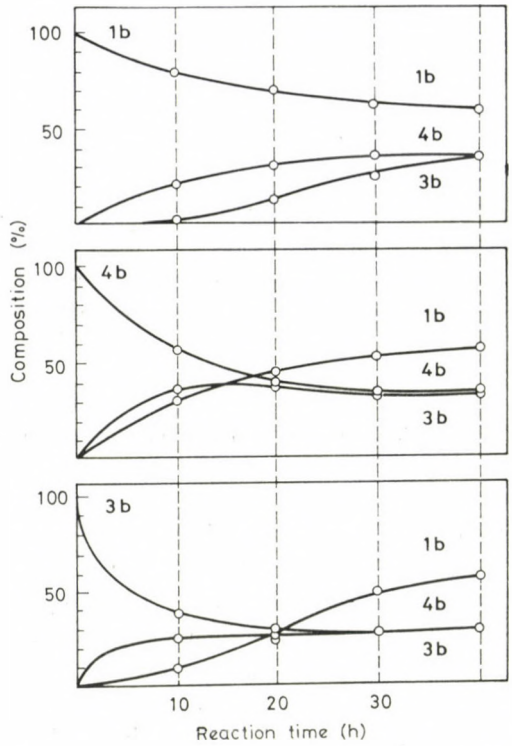

Fig. 2. Primary products of the epimerization of **1b**, **3b** and **4b**

finally, with **3b** the salt can first be detected only after 10 h. The equilibrium concentration of the immonium salt is 10% for all three substrates. The isomeric ratio also has been determined as a function of time (*cf.* Fig. 2).

Dehydrogenation experiments

To make possible correlation of the chiral centers at C-13 and C-14, the centre at C-9 was eliminated by dehydrogenation.

Mercury (II) acetate [4] is a convenient reagent for the oxidation of quinolizidines, and it could be anticipated [5, 6] that oxidation would proceed faster with compounds having a *trans* B/C ring junction as compared with the *cis* isomers. In fact, **1b** and **2a** were dehydrogenated at the highest rate: they are followed by **4a** and **4b**, while **3b** is the slowest to undergo oxidation (*cf.* Fig. 3). This is in accordance with the assignments to be presented later. As products due to over-oxidation, only the achiral 4-pyridone type compounds **5a** and **5b** were isolated.

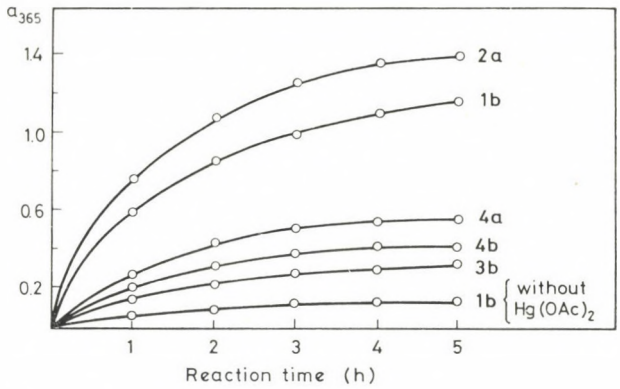

Fig. 3. Reaction rates of the oxidation of stereoisomers

Selective dehydrogenation with DDQ converted both **1b** and **3b** to **6** proving that they are epimeric at C-9, while **4b** gave a different product (**7b**). Also **2a** and **4a** gave rise to the same dehydrogenation product (**7a**) and thus the epimeric relationship has been established.

The enamine structure of **6**, **7a** and **7b** was supported by their ^{1}H-NMR spectra, in which signals for C_9—H and C_{11}—H_2 were replaced by a =CH— signal. Also due to deshielding by the newly introduced double bond, the C_1—H signal had a downfield shift.

In the spectrum of **7b** signals for the C_{13} and C_{14} protons overlap in $CDCl_3$, but can be resolved by the addition of trifluoroacetic acid. Double resonance experiments demonstrated that C_{13}—H had coupling constants of 10, 3, and 3 Hz, respectively, corresponding to one adjacent proton in *anti-periplanar* and two in *synclinal* disposition. C_{14}—H, in turn, exhibited coupling constants (6.3, 6.3 and 2 Hz) indicating three synclinally oriented adjacent protons. From the synclinal relationship of C_{13}—H and C_{14}—H a *cis* C/D ring junction can be deduced for **7b**, and consequently a *trans* one for its epimer (**6**).

Oxidation of the five-membered ring compounds **2a** and **4a** with DDQ yielded the same product (**7a**), they are therefore epimeric at C-9.

Study of the B/C ring junction

The relative rates of oxidation with mercury(II) acetate provided evidence concerning this point, and this could be further corroborated by a study of the solution infrared spectra, which showed pronounced "BOHLMANN bands" in the range of 2700—2800 cm^{-1} for **1b** and **2b**, indicating a *trans-*

quinolizidine structure [8, 9], while compounds **3a**, **4a** and **4b** did not show such bands at all.

The number of stereoisomers formed, *i.e.* three for the six-membered, and two for the five-membered D-ring compounds, needs some comments. As it has been established by FOOT and WOODWARD [11] for the analogous 4-hydrindanones, in contrast to 1-decalones, owing to less ring strain, *cis* ring junction is more stable than *trans*, which well explains that isomers with *trans*-fused rings (**1a** and **3a**) od not appear in the five-membered ring series.

Since *trans* 1-decalones, in turn, are more stable than the *cis* ones [10], tha lack of formation of **2b**, otherwise feasible *via* enolization of **1b**, is not unexpected. Repulsive interactions between the non-bonded electron pair at the nitrogen atom and the C_{16}—H and C_{17}—H bond also contribute to the relative instability of compound **2b**.

The relationship of **3b** and **4b** is, however, different. In **3b** the aromatic ring is *axially* disposed in relation to ring C thus destabilizing the *trans* C/D ring junction to a degree where its energy becomes comparable with that of a *cis* C/D ring junction, such as in **4b**.

A fact still lacking adequate explanation is that **2a** and **4a** can also be interconverted by heating with alkali, though the C_9—H bond, being adjacent to a nitrogen, is expected to be stable under such conditions.

A detailed NMR study of the stereostructures of the compounds and some derivatives will be reported in two subsequent papers.

Experimental

Determination of the ratio of diastereomeric ketones

The mixture (25 mL of a 10% solution) were chromatographed on 1 mm thick, boric acid-impregnated [1] silica gel plates. The spots were scarped off, eluted with ethanol, the eluates made up to 25 mL with ethanol, and their UV absorbance measured at about 283 nm. Finally, the ratio of isomers was calculated from the absorbances.

Epimerization experiments

(*a*) In acid: A solution of the substrate (0.15 g) was refluxed in 0.1 *N* hydrochloric acid (10 mL) and periodically a 25 μL sample was withdrawn; the ratio of stereoisomers was determined by chromatography.

(*b*) In alkali: A solution of the substrate (0.15 g) in ethanol (10 mL) containing 10% NaOH solution (0.1 mL) was refluxed until its composition did not change anymore (5 h); then the ratio of isomers was determined.

(*c*) In ethanol: Experiment (*b*) was repeated without the addition of alkali.

Ring opening of ketones in acid

Stock solutions of the substrates (0.1 mmol in 20 mL 1 *N* hydrochloric acid) were distributed into 5 mL ampoules, each containing 1 mL of sample. After sealing, the ampoules were kept in a thermostat at 75 °C and one of them was periodically removed, opened, its

content transferred to a 25 mL calibrated flask and made up to 25 mL with ethanol. The UV spectrum of the solution was recorded and the absorbance of the band at about 363 nm measured.

Determination of the rates of oxidation of ketones

To a solution of the substrate in acetic acid (0.3 mmol in 10 mL) mercury(II) acetate (0.3 g) was added and the samples were kept in a thermostat at 40 °C. Periodically 50 μL-samples were withdrawn, which were made up to 25 mL with ethanol. The UV absorbance of the samples was determined at 365 nm.

2,3-Dimethoxy-8-aza-gona-1,3,5(10),9,(11),13(14)-pentaen-12-one (5a)

To a solution of mercury(II) acetate (4.0 g; 12.5 mmol) in 5% acetic acid (20 mL) **2a** (1.0 g; 3.3 mmol) was added and the solution heated on a steam bath for 90 min, with stirring. The precipitated mercury (I) acetate was filtered off, then hydrogen sulfide was bubbled through the solution and the precipitate formed was filtered off. The solution was adjusted to pH 9 and extracted with chloroform. The chloroform solution was dried and perchloric acid was added dropwise. The crystals were filtered off and washed with ether to afford **5a** (1.0 g; 75%), m.p. 258—260 °C.

UV (EtOH): 313 (4.24), 257 (4.37) and 237 (4.38) nm (log ε).

2,3-Dimethoxy-8-aza-D-homo-gona-1,3,5(10),9(11),13(14)-pentaen-12-one (5b)

Following the method described for **5a**, **1b** (1.0 g; 3.2 mmol) gave **5b** (1.2 g; 91%), m.p. 286—288 °C.

IR (KBr): ν 1620, 1605, 1575 and 1510 cm^{-1}.

UV (EtOH): 313 (4.24), 257 (4.37), 237 (4.38) nm (log ε).

MS *m/e* (rel. int.): 311 (100), 310 (84), 296 (34) and 294 (17).

rac-2,3-Dimethoxy-8-aza-D-homo-gona-1,3,5(10),9(11)-tetraen-12-one (6)

To a solution of **1b** or **3b** (10 mmol) in benzene (50 mL) a solution of 2,3-dichloro-5,6-dicyanobenzoquinone (5 mmol) in benzene (50 mL) was added in 10 min, with stirring. After refluxing the solution for 2 h, the precipitate containing some starting material and part of the product was filtered off. This was taken up in a mixture of saturated sodium carbonate (20 mL) and water (180 mL), and extracted with benzene. After washing with water the benzene solution was evaporated and the residue recrystallized from benzene. The original mother liquor was washed with dilute sodium carbonate and evaporated. The residue was recrystallized from benzene to afford a second crop. The combined yield, calculated for DDQ was 65—75%, m.p. 230—232 °C.

^{1}H-NMR ($CDCl_3$): δ 3.70 (m, 1H, 14-H), 4.90 (s, 3H, OMe), 3.94 (s, 3H, OMe), 5.71 (s, 1H, 11-H), 6.61 (s, 1H, 4-H), 7.12 (s, 1H, 1-H); ($CDCl_3$ + CF_3COOH): δ 3.80 (t, 2H, 7-CH_3), 3.8 (overlapped, 1H, 14-H), 3.95 (s, 3H, OMe), 4.01 (s, 3H, OMe), 6.23 (s, 1H, 11-H) 6.81 (s, 1H, 4-H) and 7.16 (s, 1H, 1-H).

IR (KBr): ν 1505, 1545, 1585, 1620, 2840, 2860 and 2930 cm^{-1}.

UV (EtOH): 355 (4.34), 282 (4.00) and 236 (4.40) nm (log ε).

MS *m/e* (rel. int.): 313 (100), 285 (22), 258 (37), 230 (17), 205 (32).

$C_{19}H_{23}NO_3$ (313.4). Calcd. C 72.83; H 7.40; N 4.47. Found C 72.80; H 7.10; N 4.48%.

rac-2,3-Dimethoxy-8-aza-13α-gona-1,3,5(10),9(11)-tetraen-12-one (7a)

When oxidized as described above for **6**, both **2a** and **4a** yielded **7a**, (2.0 g; 70%), m.p. 186—188 °C.

^{1}H-NMR ($CDCl_3$): δ 2.95 (m, 1H, 13-H), 3.9 (m, 1H, 14-H), 5.55 (s, 1H, 11-H).

IR (KBr): ν 1510, 1540, 1580 and 1610 cm^{-1}.

UV (EtOH): 364 (3.78), 282 (3.81) and 2.31 (4.00) nm (log ε).

MS *m/e* (rel. int.): 299 (100).

***rac*-2,3-Dimethoxy-8-aza-D-homo-13α-gona-1,3,5(10),9(11)-tetraen-12-one (7b)**

When oxidized as described above for **6**, compound **4b** yielded **7b**, m.p. 186—188 °C.
^{1}H-NMR ($CDCl_3$): δ 2.60 (m, 1H, 17a-H), 2.85—3.0 (m, 3H, 14-H, 6-CH_2), 3.4—3.7 (m, 3H, 14-H, 7-CH_2), 3.98 (s, 3H, OMe), 4.02 (s, 3H, OMe), 5.54 (s. 1H, 11-H), 6.62 (s, 1H, 4-H), 7.11 (s, 1H, 11-H); ($CDCl_3$—CF_3CO_2H): ν 2.60 (m, 1H, 13-H), 3.44 (m, 1H, 14-H), 3.40 (t, 2H, 6-CH_2), 3.95 (t, 2H, 7-CH_2), 3.95 (s, 3H, OMe), 4.01 (s, 3H, OMe), 6.20 (s, 1H, 11-H), 6.85 (s, 1H, 4-H), 7.17 (s, 1H, 1-H).
IR (KBr): ν 1220, 1490, 1510, 1540, 1578, 1608, 2845 and 2940 cm^{-1}.
UV (EtOH): 364 (4.26), 282 (4.00) and 236 (4.30) nm (log ε).
MS *m/e* (rel. int.): 313 (100), 285 (10), 230 (16) and 205 (63).
Found C 72.88; H 7.80; N 4.46%.

REFERENCES

[1] This journal, preceding paper
[2] Janot, M. M., Goutarel, R., Warnhof, E. W., Le Hir, A.: Bull. Soc. Chim. France, **1961,** 637
[3] Szántay, Cs., Rohály J.: Chem. Ber., **98,** 557 (1965); Magy. Kém. Folyóirat, **70,** 478 (1964)
[4] Leonard N. J., Hay, A. S., Fulmer, R. W., Gash V. W.: J. Am. Chem. Soc., **77,** 439 (1955)
[5] Goothes, J., De Roos, A. M., Nauta, W. T.: Rec. Trav. Chim., **85,** 491 (1966)
[6] Brown, R. E., Lustgarten, D. M., Stanback, K., Osborne, M. W., Meltzer, R. F.: J. Med. Chem., **7,** 232 (1964)
[7] Reine, A. H., Meyers, A. F.: J. Org. Chem., **35,** 554 (1970)
[8] Bohlmann, F.: Chem. Ber., **91,** 2157 (1958)
[9] Wenkert, E., Roychendhuri, D.: J. Am. Chem. Soc., **78,** 6417 (1956)
[10] Gulland, J. M., Virden, C. J.: J. Chem. Soc., **1929,** 1791
[11] Potapov, V. M., Demjanovich V. S., Soifert, A. P., Terentiev A. P.: Zh. Obsh. Khim., **37,** 2679 (1966)

András Vedres H-1475 Budapest, 10, P.O. Box 27.

Gábor Tóth
Csaba Szántay } H-1521 Budapest, Gellért tér 4.

Acta Chimica Academiae Scientiarum Hungaricae, Tomus 109 (2), pp. 139—147 (1982)

CHEMISTRY OF 8-AZASTEROIDS, IV*

RELATIONS BETWEEN THE STEREOSTRUCTURE AND REACTIVITY OF SOME 8-AZAGONAN-12-ONES

A. VEDRES,[1] Gy. BALOGH,[1] G. TÓTH[2] and Cs. SZÁNTAY[2]**

([1]EGYT Pharmacochemical Works Budapest, and [2]Institute for Organic Chemistry, Technical University Budapest)

Received September 16, 1980

Accepted for publication February 9, 1981

Stereoisomeric 8-azagonan-12-ones were studied to establish relations between their stereochemistry and basicity, the possibility of quaternization, the stereostructure of their oximes and the elimination of the carbonyl group.

Derivatives of 8-azagonan-12-ones are of interest both as a means of studying the relations between stereostructure and reactivity, and as compounds of pharmacological interest. Actually, some of the oximes showed valuable pharmacological properties; depending on the stereostructure, they have either tranquillizing properties or digitalis-like effects [2, 11].

Basicity and quaternization

Owing to the inductive effect of the carbonyl group, 8-azagonanes, like 4-piperidones [3], are weak bases (*cf.* pK values in Table I).

Table 1

Dissociation constants of ketones

Configuration	Compound	pK_A
pseudo	**3a**	5.10
normal	**1a**	4.83
allo	**2a**	4.66
epiallo	**4b**	4.75
	4a	4.43

The compound with *pseudo* configuration (**3a**) is the most basic, to such an extent that it can be separated from its stereoisomers by extraction with

* For Part III, see Ref. [1].
** To whom correspondence should be addressed.

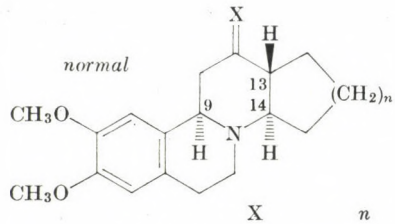

	X	n
1a	O	2
1b	N—OH	2
1c	HO—N	2
1d	H_2	1

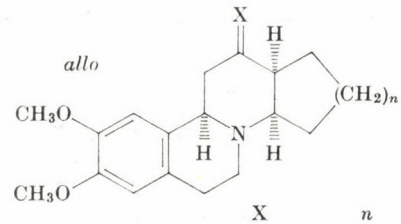

	X	n
2a	O	1
2b	N〰OH	1
2c	N〰OH	1
2d	H_2	1
2e	—NNH—Tos	1

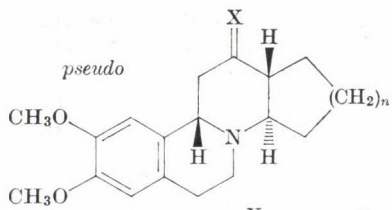

	X	n
3a	O	2
3b	N—OH	2
3c	HO—N	2

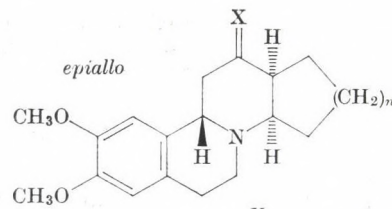

	X	n
4a	O	1
4b	O	2
4c	N〰OH	1
4d	N〰OH	1
4e	N—OH	2
4f	HO—N	2
4g	H_2	1

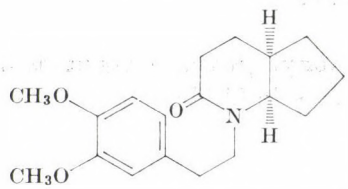

5

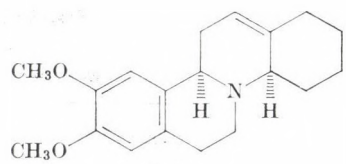

7

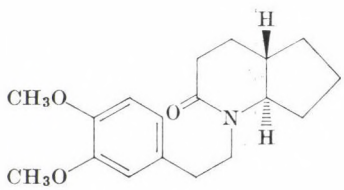

6

acid. This is namely the stereoisomer in which the non-bonding pair of electrons on the nitrogen is the most accessible. Corresponding, the two *epiallo* derivatives **4a** and **4b**, in which the non-bonding pair is most shielded, show the weakest basicity.

The rate of quaternization with methyl iodide follows the grade of basicity. While ketones **1a** and **3a** were completely methylated in dimethyl formamide at room temperature within 5 h, only insignificant conversion was observed under the same conditions with the *epiallo* compounds **4a** and **4b**. It is of interest that **2a** having an *allo* configuration undergoes degradation and gives 6,7-dimethoxy-2-methyl-3,4-dihydroisoquinolinum-iodide as the only isolable product. This can be explained by the proximity of the D-ring and the non-bonding pair, as a consequence of which the entering methyl group is subjected to considerable steric compression.

The oximes

When reacting the ketones **1a**, **2a**, **3a**, **4a** and **4b** with hydroxylamine, eight of the ten different, theoretically possible oximes could be obtained. The reactions were complete within a few minutes at any of the pH values investigated (3.5, 7.0 and 10). Product ratios were determined by TLC, followed by UV spectroscopy, and are shown in Table II.

Table II

Products ratios in the formation of oximes

Ketone	Product (yield, %)		
	acid	neutral medium	alkaline
1a	**1c** (100%)	**1c** (100%)	**1c** (100%)
4b	**4f** (90%) — **4e** (10%)	**4f** (66%) **3c** (34%) —	**4f** (74%) **3c** (26%) —
3a	**3c** (100%)	**3c** (65%) **4f** (35%)	
4a	**4c** (92%) **4d** (8%)	**4c** (92%) **4d** (8%)	

The oxime pairs derived from **2a** and **4a** could not be separated, the other oximes were obtained as pure compounds.

Inspection of models reveals that the (*E*) oximes (**1c** and **3c**) derived from compounds having the *normal* or *pseudo* configuration are sterically much less hindered than their (*Z*) diastereomers. In the *allo* compounds no interference of the D-ring and therefore no preference for one of the oximes can be anticipated. The skeleton of the *epiallo* compounds is flexible, and an *axial* disposition of C_{13}—H favours the formation of an (*E*) oxime, while an *equatorial* one that of a (*Z*) oxime.

In fact, independently of the conditions of the reaction, only one oxime (**1c**) was obtained from the ketone **1a**, having *normal* configuration. In turn, **4b**, with an *epiallo* configuration, afforded the expected pair of oximes, *i.e.* **4e** and **4f**, in acid medium, whereas under neutral or basic conditions **4f** and **3c** formed. As a consequence of epimerization at C_{12}, **3c** has *pseudo* skeleton.

The most direct evidence for skeletal epimerization during oximation is a reversion to the original ketones, provided that the latter process itself does not involve further epimerization. Cleavage of the oximes with bisulfite [4], as well as some other methods resulted in epimerization but, surprisingly, hydrolysis with aqueous ethanolic hydrochloric acid under controlled conditions left the configuration of the skeleton intact. Deoximation experiments are summarized in Table III, suggesting that the skeletal configurations of our oximes are as follows: **1c** *normal*, **4e** and **4f** *epiallo*, the inseparable pairs **2b** + **2c**, and **4c** + **4d** *allo* and *epiallo*, **3c** *pseudo*, respectively.

Table III

Results of deoximation

Oximation		Deoximation
Ketone	Oxime	Ketone
1a	**1c**	**1a**
4b	**4f**	**4b**
	3c	**3a**
	4e	**4b**
3a	**4f**	**4b**
	3c	**3a**
2a	**2b**	**2a**
	2c	
4a	**4c**	**4a**
	4d	

Since the parent ketones **3a** and **4b** undergo interconversion even on heating in aqueous ethanol [1], it is not surprising that the same reaction occurs during oximation. Since the oximes were found to be stable at neutral

pH, epimerization of the oximes themselves can be excluded under such conditions. The interconversion of **3c** and **4f** in alkaline medium associated with an inversion at C_{13}, adjacent to the oxime moiety, was, however, unexpected.

Apart from epimerization alkali also affected the **Z**—**E** isomerization of the oximes. Thus we experienced an equilibration of **2b** and **2c**, as well as of **4e** and **4f**, with **4f** predominating. Oxime **1c** remained unchanged in alkali. These results are in accordance with expectations deduced from a study of molecular models.

The configuration of oximes was assigned by NMR spectroscopy and will be reported in Part V of this series [5].

Elimination of the carbonyl group

The stereostructures of the ketones used in the present work were discussed in Part III of this series [1]. Reduction of the carbonyl group to methylene provides another was to correlate **2a** and **4a**, both containing a five-membered D-ring, since a method elaborated by BROWN *et al.* [6] permitted the synthesis of reference compounds with well defined C/D ring junction. On this analogy, we prepared the epimeric lactams **5** and **6**, followed by ring closure and reduction to yield a mixture of **2d** and **4g** (from **5**), and compound **1d** (from **6**). For comparison of these products with **2a** and **4a**, reduction of the carbonyl group in the latter compounds was necessary.

Under the conditions of Huang—Minlon reduction the substrates suffered decomposition; the hydrazones also failed to undergo reduction in DMSO containing potassium *t*-butoxide [7]. Clemmensen reduction gave a mixture of products. It may be of interest that under such conditions **1a** afforded the dehydro derivative [8] **7**.

Reduction of the tosylhydrazone **2a** with sodium cyanoborohydride [9] was successful. **2a** and **4a** yielded the same hydrazone (**2e**), though **2a** reacted at a higher rate. When the product was reverted to a ketone by treatment with boron trifluoride diethyl etherate in acetone [10], **2a**, containing some **4a**, was obtained; the latter compound probably formed by subsequent isomerization of **2a**.

Reduction of **2e** gave rise to two products, identical with **2d** and **4g**, both prepared independently, whereas the formation of **1d** having a *trans* C/D ring junction could not be detected.

Experimental

Determination of the basicity of ketones: To a solution of the ketone **1**—**4** (0.5 mmol) in ethanol (20 mL), water (20 mL) was added and the solutions were titrated at 20 °C with 0.1 *N* perchloric acid in 50% aqueous ethanol, using a Type PHM 27 pH-meter with glass and saturated calomel electrodes.

Quaternization of ketones: A solution of the ketone **1**—**4** (1 mmol) in dimethyl formamide (5 mL) was allowed to react at room temperature with methyl iodide (0.5 mL). After 5 h insignificant conversion of **4a** and **4b** was observed, while **1b** and **3a** were converted quantitatively to give the corresponding methiodides, m.p. 225—226 °C (from **1b**) and m.p. 205—206 °C (from **3a**).

Compound **2a** gave a quantitative yield of 6,7-dimethoxy-2-methyl-3,4-dihydroisoquinolinium iodide of m.p. 198—200 °C, identical with a sample prepared by reacting 6,7-dimethoxy-3,4-dihydroisoquinoline (1 mmol) with methyl iodide (0.5 mL) in dimethyl formamide (5 mL).

Product ratio in oxime formation:

(*a*) In acid medium: A solution of hydroxylamine hydrochloride (3.0 g) in water (30 mL) was heated to 95 °C, and the appropriate ketone (**1**—**4**) (10 mmol) was added. After allowing the mixture to stand in a refrigerator overnight, the crystals were filtered off, washed with water and dissolved in 50% aqueous ethanol. The solution was made alkaline, the ethanol evaporated, the crystals were filtered off, washed with water and dried to obtain the oxime in the base form in almost quantitative yields.

Fifty-mg samples of the products were chromatographed on silica gel plates (2 mm, Merck), the spots scraped off, eluted with chloroform (10 mL), and the isomeric ratio was determined by measuring the absorbance of the maximum at about 283 nm.

(*b*) In neutral medium: To a solution of the ketone (**1**—**4**) (10 mmol) in hot ethanol (50 mL) there was added a neutralized solution of hydroxylamine hydrochloride (0.8 g) in water (4 mL). After 10 min more water (20 mL) was added and the ethanol evaporated. The product was filtered off, washed with water and dried to give the oxime in the base in quantitative yield. Product ratio was determined as above.

(*c*) In alkaline medium: A hot solution of the ketone (**1**—**4**) (10 mmol) was prepared in ethanol (50 mL), and a solution of hydroxylamine hydrochloride (0.8 g) and sodium hydroxide (0.8 g) in water (5 mL) was added; the experiment was then carried out as described under (*b*).

Deoximation: To a solution of the oxime (1 mmol) in ethanol (10 mL) and water (6 mL), 1 *N* hydrochloric acid (2 mL) was added and the solution refluxed for 2 h. After neutralization the ethanol was evaporated, the product filtered off, washed with water and dried. The products were identified by chromatography and IR spectroscopy.

Skeletal isomerization of oximes: A solution of **3c** or **4f** (0.5 mmol) was prepared in a mixture of ethanol (5 mL) and water (1.5 mL), and 10% NaOH solution (2.4 mL) was added. The mixture was then refluxed for 3 h. One ml of this solution was run on a silica gel plate (2 mm, Merck) and the product ratio was determined as described above. Pure **4f** and **3c** equally gave mixtures consisting of **4f** and **3c** (74% and 26%, respectively).

rac-2,3-Dimethoxy-8-azagona-1,3,5(10)-triene (1d)

rac-2,3-Dimethoxy-8-azagona-1,3,5(10),8(9)-tetraene perchlorate (1.0 g; 2.58 mmol) was hydrogenated at 3.54 bar in 50% aqueous ethanol (500 mL) in the presence of platinum oxide (0.2 g). The solution was filtered while warm, made alkaline and extracted with ether. After evaporation of the solvent, the residue was crystallized from ether—petroleum ether (5 : 2) to give **1d** (0.35 g; 48%), m.p. 120—123 °C, identical with an authentic sample.

IR ($CHCl_3$): ν 2760, 2820, 2840, 2880, 2920, 2945 and 2975 cm^{-1}.

MS *m/e* (rel. int.): 287 (76), 286 (10), 272 (4), 258 (46) and 191 (71).

rac-2,3-Dimethoxy-8-aza-9β,13α-gona-1,3,5(10)-triene (4g)

Reduction of *rac*-2,3-Dimethoxy-8-aza-13α-gona-1,3,5(10),8(9)-tetraene perchlorate (10 g; 2.58 mmol) by the above method gave, after the vaporation of the ethereal solution, a mixture of **2d** and **4g** from which by column chromatography on silica gel with chloroform as the eluant pure **4g** was obtained (0.15 g as HBr salt, m.p. 218—222 °C). The product was identical with an authentic sample.

IR ($CHCl_3$): ν 2840, 2880, 2925, 2945, and 2980 cm^{-1}.

MS m/e (rel. int.): 287 (53), 286 (100), 272 (13), 258 (23), 191 (19).

A mixture of the same isomers (**2d** and **4g**) was obtained on reduction of the tosylhydrazone **2e**. A solution of **2e** (0.94 g; 2 mmol), *p*-toluenesulfonic acid (0.1 g) and sodium cyanoborohydride (0.76 g) in a mixture of dimethylformamide (4 mL) and sulfolane (4 mL)

was heated at 110 °C for 3 h; the same amount of reducing agent was then added and the heating continued for another 5 h. Addition of water, making the mixture alkaline and extraction with benzene and evaporation of the extract gave a mixture of **2d** and **4g** (0.5 g) from which **4g** was isolated as described above.

rac-2,3-Dimethoxy-8-aza-D-homogona-1,3,5(10),12-tetraene (7)

A mixture of zinc powder (5 g), $HgCl_2$ (0.25 g), water (5 mL) and *conc.* HCl (0.25 mL) was shaken for a few minutes and then the liquid phase was decanted. The residue and **1a** (6.3 g, 0.02 mol) were refluxed in a mixture of water (2.5 mL) and *conc.* HCl (12 mL) for 1 h. After adding 40% NaOH solution (40 mL) and water (160 mL), the mixture was extracted with chloroform, the organic layer washed with water and evaporated to give an oil (4.9 g), which was dissolved in ether. Addition of petroleum ether precipitated the product (1.75 g; 29%), m.p. 131—136 °C. Recrystallization from ether gave pure **7** (1.0 g), m.p. 139—142 °C.

^{1}H-NMR ($CDCl_3$): δ 3.84 (s, 6H, OMe), 5.55 (m, 1H, 12-H), 6.67 and 6.53 (s each, 2H, aromatic H).

IR (KBr): ν 1260, 1510, 1520, 1610, 2740, 2860 and 2930 cm^{-1}; ($CHCl_3$): ν 2760, 2805 and 2820 cm^{-1}.

MS *m/e* (rel. int.): 299 (25), 298 (7) and 191 (100).

$C_{19}H_{25}NO_2$ (299.4). Calcd. C 76.22; H 8.42; N 4.68. Found C 76.47; H 8.90; N 4.47%.

rac-2,3-Dimethoxy-8-azagona-1,3,5(10)-trien-12-*p*-toluenesulfonylhydrazone (2e)

A solution of **2a** (4.8 g; 16 mmol) and tosylhydrazone (3.6 g; 19.2 mmol) in ethanol (10 mL) was refluxed for 30 min, crystalline product (6.75 g; 90%) filtered off and recrystallized from five volumes of benzene to yield **2e** (4.2 g), m.p. 150—152 °C. By the same method **4a** afforded **2e** as well.

IR (KBr): ν 1170, 1340, 1520, 1600, 1610, 2880 and 3180 cm^{-1}.

MS *m/e* (rel. int.): 469 (1), 405 (2), 313 (100), 297 (50) and 285 (40).

$C_{25}H_{31}N_3O_4S$ (469.6). Calcd. C 63.95; H 6.65; N 8.95; S 6.83. Found C 63.59; H 7.57; N 8.67; S 6.88%.

To a solution of **2e** (0.47 g) in acetone (10 mL) boron trifluoride etherate (0.19 ml) and water (1 mL) were added and the mixture was left standing at room temperature for 20 h. Evaporation, trituration of the residue with benzene and evaporation of the benzene extract gave **2a** (0.2 g, m.p. 115—119 °C) containing 5—10% **4a**.

rac-(*E*)-2,3-Dimethoxy-8-aza-D-homogona-1,3,5(10)-trien-12-one oxime (1c)

To a warm solution of **1a** (18.4 g; 0.0585 mol) in ethanol (185 mL) there was added hydroxylamine hydrochloride (4.1 g) dissolved in water (30 mL). The solution was made alkaline by the addition of sodium hydroxide solution, and it was refluxed for 5 min. After standing in a refrigerator overnight, the crystals were filtered off, washed with 50% ethanol (3×15 mL) and dried to give a crude product (15.2 g), m.p. 237—242 °C. This was recrystallized from ethanol (1200 mL) to yield **1c** (10.5 g; 55%), m.p. 238—241 °C.

^{1}H-NMR ($CDCl_3$): δ 3.67 (q, 1H, 9-H), 3.84 and 3.86 (s each, 6H, OMe), 6.58 (s, 1H, 4-H), 6.69 (s, 1H, 1-H), 9.75 (s, 1H, =NOH).

IR (KBr): ν 1525, 1620, 1675, 3160 and 3250 cm^{-1}; ($CHCl_3$): ν 2760, 2820, 2845, 2865, 2945 and 2980 cm^{-1}.

UV (EtOH): 285 (3.62) nm (log ε).

MS *m/e* (rel. int.): 330 (62), 329 (25), 313 (100), 272 (33) and 191 (33).

$C_{19}H_{26}N_2O_3$ (330.4). Calcd. C 69.06; H 7.93; N 8.48. Found C 69.05; H 8.13; N 7.60%.

rac-(*E*)-2,3-Dimethoxy-8-aza-D-homo-9β,13α-gona-1,3,5(10)-trien-12-one oxime (4f)

To a solution of hydroxylamine hydrochloride (31.5 g) in water (315 mL), **4b** (31.5 g; 0.1 mol) was added at 95 °C. After boiling for 5 min the solution was cooled to 8 °C, the crystals filtered off and washed with 50% ethanol (3×20 mL) to obtain the hydrochloride (35.7 g; 98%), m.p. 213—217 °C. This was dissolved in hot 50% ethanol (800 mL) and a solution of

NaOH (4.4 g) in water (20 mL) was added. The solution was cooled to room temperature, the precipitate filtered off, washed with 50% ethanol and dried to give **4f** (25.2 g; 77%), m.p. 216—218 °C M.p. after recrystallization from a 100 volumes of ethanol: 217—219 °C.

^{1}H-NMR ($CDCl_3$): δ 3.84 (s, 6H, OMe), 4.05 (q, 1H, 9-H), 6.5 (s, 1H, 4-H), 6.70 (s, 1H, 1-H), 9.70 (s, 1H, =NOH).

IR (KBr): ν 1530, 1620, 1670, 3090 and 3200 cm^{-1}; ($CHCl_3$): ν 2845, 2865, 2945 and 2985 cm^{-1}.

UV (EtOH): 285 (3.59) nm (log ε).

MS *m/e* (rel. int.): 330 (46), 329 (21), 314 (23), 313 (100) and 191 (37).

$C_{19}H_{26}N_2O_3$ (330.4). Calcd. C 69.06; H 7.93; N 8.48. Found C 69.15; H 8.12; N 8.52%.

rac-(*E*)-2,3-Dimethoxy-8-aza-D-homo-9β-gona-1,3,5(10)-trien-12-one oxime (3c)

To a solution of hydroxylamine hydrochloride (1.25 g) in water (13 mL), **3a** (1.25 g, 4 mmol) was added with stirring at 95 °C. Work-up as described for **4f** gave **3c** (1.0 g; 75%); m.p. 220—223 °C.

^{1}H-NMR ($CDCl_3$): δ 3.84 and 3.86 (s each, 6H, OMe), 4.46 (t, 1H, 9-H), 6.52 (s, 1H, 4-H) and 6.90 (s, 1H, 1-H).

IR (KBr): ν 1525, 1615, 1670, 3090 and 3480 cm^{-1}; ($CDCl_3$): ν 2845, 2870, 2950 and 2985 cm^{-1}.

MS *m/e* (rel. int.): 330 (54), 329 (27), 314 (23), 313 (100), 272 (28) and 190 (21).

$C_{19}H_{26}N_2O_3$ (330.4). Calcd. C 69.06; H 7.93; N 8.48. Found C 69.26; H 8.30; N 8.53%.

rac-(*Z*)-2,3-Dimethoxy-8-aza-D-homo-9β-13α-gona-1,3,5(10)-trien-12-one-oxime (4c)

The aqueous mother liquor from the preparation of **4f**, starting from 0.1 mol of **4b**, was evaporated to about half of its original volume. The crystals obtained (6 g) were filtered off and recrystallized from ethyl acetate (100 mL), with treatment with decolorizing carbon. The crystals were filtered off at 25 °C to obtain **4f** (1.7 g) and the mother liquor was cooled further to 10 °C. The precipitate was filtered off, washed with ice-cold ethyl acetate, and dried to give **4c** (0.7 g; 2%), m.p. 131—135 °C.

^{1}H-NMR ($CDCl_3$): δ 3.81 and 3.88 (s each, 6H, OMe), 4.47 (t, 1H, 9-H), 6.52 (s, 1H, 4-H), 6.90 (s, 1H, 1-H) and 9.53 (s, 1H, =NOH).

UV (EtOH): 280 (3.52) nm (log ε).

MS *m/e* (rel. int.): 330 (51), 329 (25), 313 (100), 192 (18), 191 (45), and 190 (30).

$C_{19}H_{26}N_2O_3$ (330.4). Calcd. C 69.06; H 7.93; N 8.48. Found C 68.60; H 8.13; N 8.75%.

rac-(ξ)-2,3-Dimethoxy-8-aza-13α-gona-1,3,5(10)-trien-12-one-oxime (2b and 2c)

To a solution of hydroxylamine hydrochloride (22.0 g) in water (220 mL), **2a** (12.0 g; 0.04 mol) was added at 90 °C. The solution was stirred for 30 min at this temperature and cooled to 20 °C. The crystals which precipitated were filtered off and washed with water to obtain a mixture of **2b** and **2c** (12 g). This was dissolved in warm 50% ethanol (100 mL), made alkaline, and kept in a refrigerator overnight. Compound **2b** (4.4 g) separated and it was recrystallized from acetone (100 mL) to yield pure **2b** (1.9 g; 15%), m.p. 180—182 °C.

^{1}H-NMR ($CDCl_3$): δ 3.80 (s, 6H, OMe), 6.55 and 6.72 (s each, 2H, aromatic H), 9.50 (s, 1H, =NOH).

IR (KBr): ν 1520, 1615, 1670 and 3280 cm^{-1}; ($CDCl_3$): 2760, 2820, 2840, 2880, 2920, 2945 and 2975 cm^{-1}.

$C_{18}H_{21}N_2O_3$ (316.4). Calcd. C 68.33; H 7.64; N 8.85. Found C 68.59; H 8.26; N 8.85%.

The aqueous ethanol from the preparation of **2a** was concentrated, the precipitated product filtered off, and recrystallized from acetone (30 ml). At 5 °C **2b** (0.5 g) was removed by filtration and the remaining solution was slowly cooled to —20 °C to afford, after washing with cold acetone, crude **2c** (2.0 g). Recrystallization from aqueous acetone (1 : 2) gave pure **2c** (1.25 g), m.p. 97—99 °C.

^{1}H-NMR ($CDCl_3$): δ 3.45 (q, 1H, 9-H), 3.89 (s, 6H, OMe), 6.57 and 6.67 (s each, 2H, aromatic H), and 9.3 (s, 1H, =NOH).

IR (KBr): ν 1520, 1615, 1670 and 3480 cm^{-1}, ($CHCl_3$): 2760, 2820, 2840, 2880, 2920, 2950 and 2980 cm^{-1}.

$C_{18}H_{24}N_2O_3$ (316.4). Calcd. C 68.33; H 7.64; N 8.25. Found C 68.51; H 7.48; N 8.81%.

rac-(ξ)-2,3-Dimethoxy-8-aza-9β-13α-gona-1,3,5(10)-trien-12-one oxime (**4c** and **4d**)

To a solution of hydroxylamine hydrochloride (20 g) in water (200 mL), **4a** (10.0 g; 0.033 mol) was added at 80—90 °C, with stirring. Stirring was continued at this temperature for 30 min; the mixture was then cooled to 20 °C, the product filtered off and washed with water to give the hydrochloride (10.2 g; 93%), m.p. 183—185 °C. This was dissolved in warm 50% aqueous ethanol (70 mL), made alkaline, the precipitated product filtered off and washed with water to afford **4c** (7.35 g; 70%), m.p. 208—210 °C. After recrystallization from ten volumes of dioxane: m.p. 211—213 °C. The mother liquors contained the more polar oxime, **4d**.

^{1}H-NMR ($CDCl_3$): δ 3.80 (s, 6H, OMe), 6.55 and 6.70 (s each, 2H, aromatic H).

IR (KBr): ν 1530, 1615, 1670, 3080 and 3190 cm^{-1}.

$C_{18}H_{24}N_2O_3$ (316.4). Calcd. C 68.33; H 7.64; N 8.85. Found C 68.62; H 7.73; N 8.91%.

REFERENCES

[1] This journal, preceding paper
[2] Szántay Cs., Vedres, A., Thuránszky, K., Balogh, Gy., Vedres, M.: Ger. Offen. 2.617.440; Chem. Abstr., **86**, 89640 (1977)
[3] Geneste, P., Hugon, I., Reminiac, C., Lamaty, G., Roque, J. P.: Bull. Soc. Chim. France, **1976**, 845
[4] Pines, S. H., Chemerda, M., Kozlowski, M. A.: J. Org. Chem., **31**, 3446 (1966)
[5] Part V, the next paper
[6] Brown, R. E., Lustgarten, D. M., Stanbach, K., Osborne, M. W., Meltzer, R. F.: J. Med. Chem., **7**, 232 (1964)
[7] Gram, D. J., Sahyon, M. R. V.: J. Am. Chem. Soc., **84**, 1734 (1962)
[8] Org. Reactions, **22**, 404, Wiley, New York, 1975
[9] Hutchins, R. O., Milewski, C. A., Maryamoff, B. E.: J. Am. Chem. Soc., **95**, 3662 (1973)
[10] Sacks, C. E., Fuchs, P. L.: Synthesis, **1976**, 456
[11] Vedres, A., Balogh, Gy., Thuránszky, K., Szántay, Cs.: VIth Internat. Symp. on Med. Chem., Brighton, 1978

András Vedres H-1475 Budapest, 10. P.O. Box 27.
Gyula Balogh H-1780 Budapet, P.O. Box 49.
Gábor Tóth, Csaba Szántay } H-1521 Budapest, Gellért tér 4.

Acta Chimica Academiae Scientiarum Hungaricae, Tomus 109 (2), pp. 149—164 (1982)

CHEMIE DER 8-AZASTEROIDE, V*

^{1}H- UND ^{13}C-NMR-SPEKTROSKOPISCHE UNTERSUCHUNGEN

G. TÓTH,[1]* A. VEDRES,[2] H. DUDDECK[3] and Cs. SZÁNTAY[4]**

([1]NMR-Laboratorium des Instituts für Allgemeine und Analytische Chemie, Technische Universität Budapest, [2]EGYT Pharmazeutische Werke, Budapest, [3]Ruhr-Universität Bochum, Lehrstuhl für Strukturchemie, Bochum, Bundesrepublik Deutschland, [4]Institute für Organische Chemie, Budapest)

Eingegangen am 16. September 1980

Zur Veröffentlichung angenommen am 13. Oktober 1980

Die ^{1}H- und ^{13}C-NMR-Spektren der 8-Azasteroide **1a, 1b, 1c** und **2—8** wurden untersucht. Dabei konnten die Ringverknüpfungen und die Molekülkonfigurationen und -konformationen sowie die Konfigurationen der Oxime eindeutig bestimmt werden.

In unseren früheren Mitteilungen berichteten wir über die Synthesen einiger 8-Azasteroide [1—3]. In dieser Arbeit möchten wir die Stereochemie und die Konformationen der Verbindungen in dieser Klasse auf der Basis ihrer ^{1}H- und ^{13}C-NMR-Spektren diskutieren.

A priori Betrachtung der Konformationen und ihrer Gleichgewichte

Bei Durchführung der früher von uns beschriebenen Cycloaddition von 3,4-Dihydroisochinolinonen und 1-Acetylcycloalkenen sind vier Diastereomerenpaare **1a, 1b, 1c** und **1d** zu erwarten. Es entstehen bei diesen Reaktionen natürlich racemische Gemische; der Übersichtlichkeit halber sind in den Abbildungen aber immer nur Isomere aus einer Enantiomerenreihe dargestellt. Um die Diastereomeren leichter unterscheiden zu können. übernehmen wir die in der Alkaloidchemie gebräuchlichen Bezeichnungen »normal«, »epiallo«, »*pseudo*« und »allo« für die verschiedenen Isomeren [4] (siehe Abb. 1). Im folgenden gehen wir davon aus, daß Ring B in der Halbsessel- und die Ringe C und D nur in der Sesselkonformation vorliegen.

Die einzelnen Konformeren können durch Stickstoff- und/oder Ringinversion ineinander übergeführt werden. Bei einem *trans*-Isomer (*trans*-Verknüpfung der Ringe B und C) führt Stickstoffinversion zu einem *cis*-1- und zusätzliche Ringinversion, die allerdings nur bei *cis*-Verknüpfung der Ringe C und D möglich ist, zu einem *cis*-2-Isomer [4]. Die Konformerengleichgewichte sind durch die unterschiedlichen sterischen Wechselwirkungen in den einzelnen

* S. Lit. [1].

** Korrespondenz bitte an diesen Autor richten.

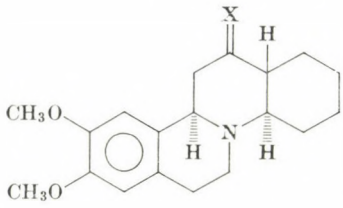

1a: =O

2: =N—OH (*E*)

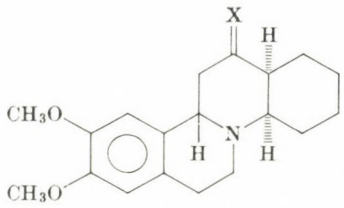

1b: =O

3: =N—OH (*E*)

4: =N—OH (*Z*)

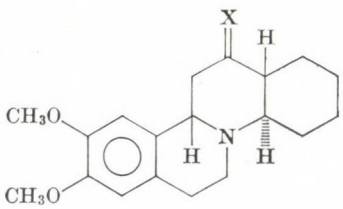

1c: =O

5: =N—OH (*E*)

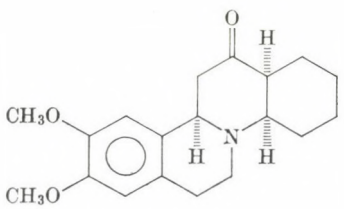

1d

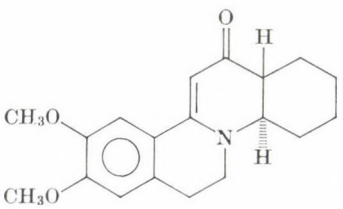

6

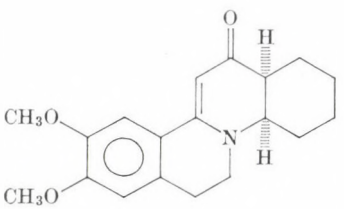

7

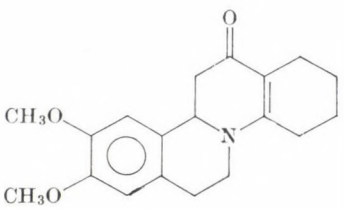

8

Abb. 1

Konformeren bestimmt, wobei die Abstände einzelner Atome anhand von Dreiding-Modellen abgeschätzt werden können. Obwohl die Modelle die wirkliche Geometrie der Moleküle nicht exakt wiedergeben können — die Wechselwirkungen sind durch die Ringedeformationen meist etwas vermindert — war es doch möglich, auf Grund dieser Überlegungen inetwa die relativen Energien der Konformeren mit Hilfe der Bartell-Funktion [5] abzuschätzen. Diese läßt bereits vermuten, daß **1a** überwiegend in der *trans*-Form vorliegt. Für **1b** scheint nach dieser allerdings nur groben Abschätzung die *cis*-1-Form ein wenig gegenüber der *trans*-Form begünstigt zu sein. Die *cis*-2-Form scheidet danach ganz aus. Bei **1d** ist nur das *trans*-Konformer zu erwarten, da bei den *cis*-1- und *cis*-2-Formen ungünstige *syn-diaxiale* Wechselwirkungen auftreten.

Überführung der Epimeren 1a—1d ineinander und ihre thermodynamische Stabilität

Enolisierung der C-12-Ketogruppe führt zu einer Epimerisierung am C-13-Atom, wodurch das normal-(**1a**) und das allo-Isomere (**1d**) ineinander übergeführt werden können. In diesem Gleichgewicht überwiegt auf Grund der günstigeren sterischen Verhältnisse das normal-Epimer **1a**; dementsprechend fanden wir kein allo-Isomer **1d** [2]. Im Epimerisierungsgleichgewicht von **1b** und **1c** ist das Verhältnis 3 : 1, was darauf hinweist, daß in diesem Falle der Energieunterschied geringer ist. Bei der Behandlung mit Säure tritt gleichzeitig Epimerisierung an C-13 und C-9 ein, wodurch man ein Gleichgewichtsverhältnis der Isomeren **1a**, **1b** und **1c** im Verhältnis 2 : 1 : 1 erhält [2]. Dies zeigt, daß erwartungsgemäß das normal-Epimer **1a** das thermodynamisch günstigste ist. Für die Aufklärung der konfigurativen Zusammenhänge der Verbindungen **1a**—**1d** waren selektive Oxidationsreaktionen von großem Nutzen. So führten **1a** und **1c** zum gleichen $\Delta^{9,11}$-Olefin **6**, **1b** jedoch zu **7** (siehe Abb. 2). Dies ist ein weiterer Beweis dafür, daß sich **1a** und **1c** nur durch die Konfiguration an C-9 unterscheiden. Zum Vergleich und für die weiteren spektroskopischen Untersuchungen haben wir auch das $\Delta^{13,14}$-Olefin **8** dargestellt [18].

Stereochemie der C-12-Ketoxime

Umsetzung der Ketone zu den entsprechenden Oximen bringt weitere sterische Wechselwirkungen mit sich. Bei den Verbindungen, in denen die Ringe C und D *trans*-verknüpft sind, d. h. bei **2** und **5**, konnten wir unter Bedingungen, bei denen Epimerisierung an C-13 ausgeschlossen ist, nur die *E*-Isomeren isolieren, da bei *Z*-Konfiguration eine starke Abstoßung zwischen der Hydroxygruppe des Oxims und dem equatorialen Wasserstoffatom an C-17a auftritt.

R
R
X
N
trans
1a: =O
2: =N—OH (E)
cis-1
normal
1c: =O
5: =N—OH (E)
pseudo
1b: =O
3: =N—OH (E)
epiallo
4: =N—OH (Z)
cis-2

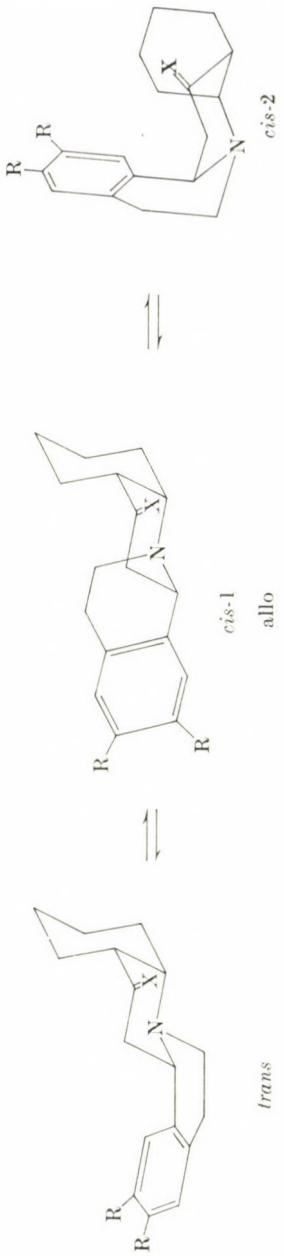

Abb. 2

Betrachten wir die *trans*- und *cis*-1-Konformationen von **1b**, bei denen die Ringe C und D *cis*-verknüpft sind, so können wir erwarten, daß die Bildung der *Z*-Oxime ebenso unwahrscheinlich ist, da auch hier eine entsprechende Wechselwirkung, diesmal jedoch mit dem *axialen* Wasserstoffatom an C-17a, existiert. Wenn trotzdem ein *Z*-Oxim gebildet wird, muß es in der *cis*-2-Konformation vorliegen, da dann diese sterischen Abstoßungen nicht mehr auftreten. Experimentell fanden wir ein Hauptprodukt, daß sich, wie wir im folgenden noch zeigen werden, als *E*-Isomer in der *trans*-Konformation herausstellte, und ein Nebenprodukt, welches das *Z*-Oxim in der *cis*-2-Konformation ist [3].

Spektroskopische Methoden bei der Strukturaufklärung

Die am meisten benutzten spektroskopischen Methoden bei Konformationsbestimmungen von Chinolizidinen, wie es die 8-Azasteroide ja sind, sind die IR-, die ^{1}H-NMR- und seit kurzem auch die ^{13}C-NMR-Spektroskopie.

Die An- bzw. Abwesenheit von Bohlmann—Banden in den IR-Spektren der Lösungen wurden zur Unterscheidung von *trans*- und *cis*-Chinolizidinen herangezogen [6], obwohl einige Autoren gefunden haben, daß diese Absorptionsbanden trotz Vorliegen einer *trans*-Verknüpfung der Ringe manchmal nicht sichtbar sind, wenn Ringverzerrungen auftreten [7]. Andererseits schließt ihr Auftreten einen beträchtlichen Anteil des *cis*-Konformeren im Gleichgewicht nicht unbedingt aus [8].

Bei den ^{1}H-NMR-Untersuchungen wurden folgende Kriterien angewendet:

(*a*) Man kann die Position und die Multiplizität des Signals des angularen Protons benutzen, um die *trans*- von der *cis*-Verknüpfung der Ringe B und C zu unterscheiden. Der Grenzwert von $\delta = 3{,}8$ [9] ist dabei aber nur eine Annäherung, da es auch noch andere Einflüsse auf die Signallagen der Protonen in dieser Position geben kann, und in einigen Fällen fand man, daß dieser Grenzwert ein wenig bei tieferem Feld liegt [10, 13].

(*b*) Steht das freie Elektronenpaar des Stickstoffatoms *antiperiplanar* zu einem Wasserstoffatom, so wird dessen Signal zu hohem Feld verschoben, was bei den Chinolizidinen zu einem Unterschied der chemischen Verschiebungen von *axialen* und *equatorialen* Protonen von *ca.* 0,9 ppm führt; bei Cyclohexanen liegt dieser Wert nur bei 0,5 ppm. Wird das Stickstoffatom protoniert, verschwindet dieser besondere Hochfeldeffekt wieder [11].

(*c*) Die geminale Koppelkonstante von Methylenprotonen neben einem Stickstoffatom zeigt die Stellung des freien Elektronenpaares an. Ist es nämlich *antiperiplanar* zu einem dieser Protonen, vermindert sich der Absolut-

wert der geminalen Koppelkonstante um *ca.* 2 Hz im Vergleich zur *synclinalen* Anordnung [12].

Die Möglichkeiten, die in der Anwendung der ^{13}C-NMR-Spektroskopie bei der Aufklärung der Stereochemie von Chinolizidinen [10, 14] und Steroiden [15] liegen, wurden in einer Reihe von Veröffentlichungen demonstriert. Am deutlichsten kann man dabei eine Unterscheidung von *cis-* und *trans*-Ring-Verknüpfung auf Grund von Hochfeldverschiebungen der Signale von angularen und sich in *γ-gauche*-Position befindlichen Kohlenstoffatomen treffen.

Kürzlich wurde gezeigt, daß das freie Elektronenpaar einen stereospezifischen Einfluß auf die ^{13}C-^{1}H-Koppelkonstante hat [16]. Auf dieser Basis wurden bevorzugte *cis-* und *trans*-Konformationen von Chinolizidinen bestimmt [17].

Diskussion der Ergebnisse

^{1}H-NMR-Untersuchungen

Die ^{1}H-NMR-Untersuchungen lieferten wichtige Hinweise bei der Strukturaufklärung der hier diskutierten Verbindungen, obwohl einige der im vorigen Abschnitt vorgestellten Methoden nicht angewendet werden konnten. So konnten wir z. B. nicht auf die sehr informativen Protonierungs-Shifts [11] zurückgreifen, da Säurezugabe bei diesen Molekülen zu Epimerisierungen führt.

Die Bestimmung der Verknüpfung der Ringe B, C und D ist im Prinzip möglich, wenn man die chemischen Verschiebungen und die Multiplizitäten der Signale der angularen Atome H-9, H-13 und H-14 untersucht. Leider führte in unseren Spektren Überlagerung der Signale von H-13 und H-14 durch die der anderen Gerüstprotonen dazu, daß deren Multiplizität nicht bestimmbar war. Nur das Signal von C-9 konnten wir in einigen Fällen getrennt beobachten. Bei dem Isomeren **1a** war es allerdings von den Signalen der Methoxygruppen bei $\delta = 3{,}87$ und 3,90 überdeckt. Um trotzdem die Multiplizität bestimmen zu können, wurde $Eu(dpm)_3$ nach und nach in kleinen Mengen zugegeben, und bei einem molaren Verhältnis von 0,22 konnte das H-9-Signal getrennt beobachtet werden. Da die induzierten Signalverschiebungen für die Methoxysignale die größten Werte annahmen, schließen wir, daß sich dort der bevorzugte Komplexierungsort befindet. Wir können daher annehmen, daß sich die Konformationsgleichgewichte durch die Zugabe des $Eu(dpm)_3$ nicht wesentlich geändert haben. Dafür spricht auch, daß sich bei verschiedenen Konzentrationen des Shift-Reagenzes die Aufspaltungen des H-9-Signals (11,0 und 3,4 Hz) nicht wesentlich änderten. Die Extrapolation der induzierten Verschiebungen des H-9-Signals auf eine Konzentration des Shift-Reagenzes von 0,0 ergab eine chemische Verschiebung von $\delta = 3{,}88$. Obgleich dieser Wert den von USKOKOVIC angegebenen Grenzwert von 3,8

[9] ein wenig übertrifft, weist er doch eindeutig auf eine *trans*-Verknüpfung der Ringe B und C hin, zumal, wenn man neuere Untersuchungen [10, 13] (siehe oben) berücksichtigt. Außerdem treten bei dem in Chloroform aufgenommenen IR-Spektrum von **1a** die Bohlmann-Banden auf.

Durch Doppelresonanz-Experimente suchten wir unter den Signalen der übrigen Gerüstprotonen zwischen $\delta = 1{,}0-3{,}0$ die der Protonen an C-11. Es stellte sich dabei heraus, daß das Zentrum des AB-Teils dieses ABX-Teilspektrums bei $\delta = 2{,}75$ liegt. Deshalb können die Koppelkonstanten aus den Aufspaltungen des H-9-Signals nicht direkt entnommen werden. Die Summe von 14,4 Hz beweist aber, daß die Ringe B und C *trans*-verknüpft sind. Das Signal des equatorialen H-7 konnte zwar bei $\delta = 3{,}35$ beobachtet werden, doch war auch hier die Koppelkonstante aus der Signalaufspaltung nicht zu entnehmen. Im Oxim **2** jedoch war dies am entsprechenden Signal bei $\delta = 3{,}39$ möglich; die Koppelkonstante $^2J_{7e,7a}$ beträgt 10,5 Hz. Dieser kleine Absolutwert weist darauf hin, daß das freie Elektronenpaar am Stickstoff *antiperiplanar* zum *axialen* Wasserstoff an C-7 steht [12]. Dies ist ein weiteres Argument dafür, daß bei **1a** und **2** das *trans*-Konformer bei weitem überwiegt.

Im Gegensatz zu den sehr ähnlichen chemischen Verschiebungen der beiden H-11-Protonen in **1a** (*ca.* 2,75 ppm), ist in **2** infolge der Anisotropie der Oximgruppe [19] das Signal des *equatorialen* H-11 zu tiefem Feld nach $\delta = 3{,}85$ und das des *axialen* zu hohem Feld nach $\delta = 2{,}09$ verschoben. Außerdem erleidet auch das H-1-Signal eine Tieffeldverschiebung von 0,18 ppm. Dies ist ein eindeutiger Beweis für die *E*-Konfiguration des Oxims.

Beim Isomer **1c** ist die chemische Verschiebung von H-9 mit $\delta = 4{,}75$ recht groß, und sein Signal weist eine Triplettstruktur mit den Koppelkonstanten $J_{9e,11a} = J_{9e,11e} = 5{,}0$ Hz aus, was daraufhin deutet, daß H-9 sich in *equatorialer* Position relativ zu Ring C befindet und das die Ringe B und C *cis*-verknüpft sind. Die Signale der Gerüstprotonen erscheinen als breites Multiplett zwischen $\delta = 1{,}0$ und 3,5; unter ihnen waren nur die Protonen an C-11 identifizierbar. Führten wir das Keton in das Oxim **5** über, beobachteten wir analoge Veränderungen in den Spektren wie bei **2**, d.h. **5** erwies sich ebenso als *E*-Oxim. Entsprechend beobachteten wir in seinem IR-Spektrum keine Bohlmann-Bande, so daß sich für **1c** und **5** die *pseudo*-Konfiguration ergibt, bei der nur ein Konformer möglich ist (siehe Abb. 1).

Im Spektrum von **1b** fanden wir das Signal von H-9 bei $\delta = 4{,}24$ als doppeltes Dublett mit Aufspaltungen von 10,5 und 3,8 Hz. Dies könnte bedeuten, daß wieder eine *cis*-Verknüpfung der Ringe B und C vorliegt, daß diesmal jedoch H-9 in Bezug auf Ring C eine *axiale* Position einnimmt. Wieder wurde keine eindeutige Bohlmann-Bande gefunden. Berücksichtigt man jedoch die Tatsache, daß C-9 und C-15 *gauche*-konfiguriert sind, muß man auch bei BC-*trans*-Verknüpfung mit einem hohen Wert der chemischen Verschiebung für H-9 rechnen [27]. Es ist also aus diesen Daten die Verknüpfung

der Ringe B und C nicht zu entnehmen. Im Spektrum des als Hauptprodukt bei der Oximbildung entstandenen Isomers **3** findet sich das H-9-Signal bei $\delta = 4{,}03$ mit Koppelkonstanten von $J_{9a,11a} = 11{,}0$ und $J_{9a,11e} = 3{,}5$ Hz. Gleichzeitig fanden wir wieder analoge Signalverschiebungen von H-1 und den Protonen an C-11 wie bei **2** und **5**. Dies beweist, daß **3** wieder die *cis*-1-Konformation einnimmt und daß es sich dabei um das *E*-Isomer handelt. Über die B/C-Ringverknüpfung ist jedoch wieder nichts Eindeutiges auszusagen. Bei dem als Nebenprodukt anfallenden Oxim **4** fanden wir das H-9-Signal bei $\delta = 4{,}47$ als Triplett mit einer Aufspaltung von 4,5 Hz, so daß sich ergibt, daß die Ringe B und C *cis*-verknüpft sind, und daß H-9 bezogen auf Ring C *equatorial* steht, d. h. **4** liegt in der *cis*-2-Konformation vor. Das Zentrum der Signale der Protonen an C-11 liegt hier bei $\delta = 2{,}93$. Diesmal jedoch beobachteten wir keine ausgeprägte Tieffeldverschiebung des Signals des *equatorialen* H-11 infolge der Oximbildung wie bei **2**, **3** und **5** und das Signal des *axialen* H-11 ist nicht hoch-, sondern tieffeldverschoben, so daß sich **4** als *Z*-Isomer erweist. Die trotzdem auftretende Tieffeldverschiebung von H-1 läßt sich durch die unterschiedlichen Konformationen von **1b** und **4** erklären. Wir finden praktisch den gleichen Wert wie bei **1c**, in **5** dagegen, wo zusätzlich der Anisotropieeffekt der *E*-Oximgruppe wirkt, ist das H-1-Signal um weitere 0,25 ppm zu tiefem Feld verschoben.

Bei all diesen bisher besprochenen Verbindungen konnten wir die Signale der Protonen an C-13 und C-14 nicht eindeutig bestimmen. Aus diesem Grunde haben wir **1a** und **1c** zu **6** und **1b** zu **7** oxidiert, bei denen es sich um $\Delta^{9,11}$-Dehydroderivate handelt, wie sich einerseits aus dem Vergleich mit dem bekannten Isomeren **8** [18] und andererseits aus dem Verschwinden der Signale der H-9- und H-11-Protonen ergibt. Zu dem konnten wir im Olefinbereich ein Singulett erkennen, das einem Proton entspricht, und infolge der Anisotropie dieser Doppelbindung [20] werden die H-1-Signale in den Spektren von **6** und **7** deutlich tieffeldverschoben.

Obgleich wir im Spektrum von **6** das H-14-Signal bei $\delta = 3.70$ eindeutig auffinden konnten, waren wegen der Tatsache, daß es sich dabei um den X-Teil eines ABMX-Spektrums handelt, die einzelnen Koppelkonstanten nicht bestimmbar. Die Halbwertsbreite ist *ca.* 30 Hz, und aus diesem großen Wert schließen wir, daß H-14 zu H-13 und zu dem *axialen* H-15 *antiperiplanar* steht, was nur bei einer *trans*-Verknüpfung der Ringe C und D möglich ist. Strahlen wir ein H_2-Feld bei $\delta = 2{,}85$ ein, vereinfacht sich das Signal von H-14, so daß wir annehmen daß sich in dieser Gegend das Signal des *axialen* H-13 befindet. Gehen wir von $CDCl_3$ zu einem Gemisch von $CDCl_3/CF_3COOH$ (4 : 1) als Lösungsmittel über, können wir auf Grund der Stickstoffprotonierung eine ausgeprägte Tieffeldverschiebung der Signale der H-11- und H-7-Protonen beobachten. Gleichzeitig stellen wir fest, daß das Enamin-Imin-Tautomeren-Gleichgewicht praktisch vollständig auf die Enamin-Seite ver-

Tabelle I

^1H Chemische Verschiebungen und Signalaufspaltungen

Lösungsmittel	H-1	H-4	H_a-6	H_a-7	H_a-9	H_e-9
1a $CDCl_3$	6,51 s	6,58 s		3,35 m (H_e)	3,88 dd 11,0 Hz; 3,4 Hz	—
2 $CDCl_3$	6,69 s	6,58 s	2,60* (H_a)	3,39 (H_e) J_{gem} = 10,5 Hz; 4,5 Hz, 4,5 Hz	3,67 dd 12,0 Hz; 2,5 Hz	—
1b $CDCl_3$	6,47 s	6,56 s	—	—	4,24 dd 10,5 Hz; 3,8 Hz	—
3 $CDCl_3$	6,70 s	6,59 s	—	—	4,03 dd 11,0 Hz; 3,5 Hz	—
4 $CDCl_3$	6,71 s	6,56 s	—	—	—	4,47 t 4,5 Hz
1c $CDCl_3$	6,64 s	6,56 s	—	—	—	4,75 t 5,0 Hz
5 $CDCl_3$ + CD_3OD 2 : 1	6,90 s	6,52 s	—	—	—	4,46 t 4,5 Hz
6 $CDCl_3$	7,12	6,61 s	—	—	—	—
$CDCl_3$ + TFA 4 : 1	7,16	6,81 s	3,08 t 7 Hz	3,80 t 7 Hz	—	—
7 $CDCl_3$	7,11	6,62 s	2,85—3,00*	3,4—3,7*	—	—
$CDCl_3$ + TFA 4 : 1	7,17	6,85 s	3,44 t 7 Hz	3,85 t 7 Hz	—	—
8 $CDCl_3$	6,60 s	6,58 s	—	3,06 (H_a); 4,07 (H_e)	4,55 dd 15,0 Hz; 4,0 Hz	—

* Diese Werte wurden durch Doppelresonanzexperimente bestimmt.

der 8-Azasteroide **1**—**8**; *in ppm*

H_a-11	H_e-11	H-13	H-14	OH	CH_3O	Gerüstprotonen
	2,75* J_{gem} = 12,0 Hz	—	—	—	3,87 s 3,90 s	1,0—3,0 (15 H)
2,09 t	3,85 J_{gem} = 12,0 Hz	—	—	9,75	3,90 s 3,92 s	1,25—3,05 (14 H)
2,47 dd	2,67 dd J_{gem} = 14,0 Hz	—	—	—	3,85 s 3,87 s	1,2—3,4 (16 H)
2,04 dd	3,76 dd J_{gem} = 14,5 Hz	—	—	9,70	3,89 s 3,91 s	1,25—3,25 (15 H)
	2,93* J_{gem} = 12,0 Hz	—	—	9,58	3,78 s 3,86 s	1,2—3,45 (16 H)
	3,05*	—	—	—	3,90 s 3,90 s	1,0—3,5 m (16 H)
1,45 dd	3,86 dd J_{gem} = 14,5 Hz	—	—	—	3,86 s 3,87 s	1,2—3,6 (15 H)
	5,71 s (1 H)	2,85*	3,70 m $W_{1/2}$ = 30 Hz	—	3,90 s 3,94 s	1,2—3,4 (13 H)
	6,23 s (1 H)		3,80 m	—	3,95 s 4,01 s	1,3—2,85 (9)
	5,54 s (1 H)	2,85—3,00*	3,40—3,70*	—	3,98 s 4,02 s	1,2—2,7 (8)
	6,20 s (1 H)	2,60 ddd 10,5 Hz; 3,0 Hz; 2,5 Hz	3,44 m 6,0 Hz; 3,0 Hz; 2,0 Hz	—	3,95 s 4,01 s	1,3—2,1 (8)
2,47*	2,87*	—	—	—	3,85 s 3,87 s	1,4—3,2 (15 H)

schoben ist.* Leider führte bei 6 auch die Salzbildung nicht zu einer Separierung der H-13- und H-14- Signale. Dies war dagegen im Spektrum von **7** der Fall, wo wir das Signal von H-14 bei $\delta = 3{,}44$ und das des H-13 bei 2,60 fanden. Aus dem H-14-Signal im Spektrum von **7** waren Koppelkonstanten von 6, 3 und 2 Hz ablesbar, was einer Halbwertsbreite von nur 10—12 Hz entspricht. Dies bedeutet, daß H-14 bezogen auf den Ring D in *equatorialer* Stellung steht, woraus sich eindeutig eine *cis*-Verknüpfung der Ringe C und D ergibt. Darauf deutet auch hin, daß im H-13-Signal nur eine große Kopplung von 10,5 Hz identifiziert werden kann; die beiden anderen Kopplungen betragen *ca.* 2 und 3 Hz. Bei der Entkopplung von H-13 vereinfachte sich das H-14-Signal zu einem doppelten Dublett mit den Kopplungen von 6 und 2 Hz, so daß für die $J_{13a,14e}$ ein Wert von 3 Hz resultiert.

Als Schlußfolgerung ergibt sich, daß **1a** und **1c**, welche beide bei der Oxidation in **6** übergeführt werden, die gleiche *trans*-Verknüpfung der Ringe C und D aufweisen. Für **1b** ergibt sich damit die *cis*-Verknüpfung.

Es ist noch erwähnenswert, daß in den Spektren der Salze von **6** und **7** die Signale der H-6- und H-7-Methylenprotonen jeweils Triplettstruktur aufweisen. Offenbar läuft in diesem Fall die Inversion des Ringes B sehr schnell ab, so daß man Equilibrierung der axialen und *equatorialen* Protonen beobachtet.

Im Spektrum von **8** weist das Signal von H-9 bei $\delta = 4{,}55$ eine doppelte Aufspaltung von 15,0 und 4,0 Hz auf, d. h. die Verknüpfung der Ringe B und C ist *cis*, und H-9 steht *axial* in Bezug auf Ring C. Die Koppelkonstante $J_{9a,11a}$ ist damit erheblich größer als die entsprechenden bei den Verbindungen **1**—**5**. Es ist jedoch bekannt, daß ein solcher Wert dann auftritt, wenn die Ringe B und C beide in der Halbsesselkonformation vorliegen [10].

^{13}C-*NMR-Untersuchungen*

Signalzuordnungen

Die Signale der Carbonyl-, Oxim- und Olefinkohlenstoffatome können sehr leicht zugeordnet werden, da sie in den erwarteten charakteristischen Bereichen erscheinen [27]. Die chemischen Verschiebungen der Atome in den Ringen A und B ergeben sich durch Vergleich mit bekannten Spektren von Tetrahydroisochinolin-Derivaten [21, 22] und stimmen gut mit denen überein, die kürzlich für analoge Verbindungen, allerdings ohne Ring D, angegeben wurden [23]. Dies gilt auch für die Kohlenstoffatome in Ring C. Ungewöhnlich kleine chemische Verschiebungen von *ca.* 42 ppm fanden wir für die C-7-Signale von **1a** und **2**, wogegen die der anderen Verbindungen (**1b**, **1c**, **3** und **4**) bei $\delta = 46$—48 lagen. Die hohen Werte erklären sich aus einer *gauche*-

* Unter den Meßbedingungen findet erst frühestens nach einer Woche eine merkliche Epimerisierung von **6** und **7** statt.

Tabelle II

^{13}C Chemische Verschiebungen von 8-Azasteroidderivaten[a]

C	1a	2	1b	3	4	1c	5	8
1	108,9 d	109,4 d	109,1 d	109,5 d	109,9 d	110,2 d	109,8 d	108,7 d
2	147,6 s	147,5 s	147,7 s	147,5 s	147,5 s	147,9 s	147,2 s	148,0 s
3	147,9 s	147,9 s	147,9 s	147,8 s	147,7 s	148,2 s	147,6 s	148,2 s
4	111,5 d	111,4 d	111,9 d	111,7 d	112,1 d	112,4 d	111,6 d	111,4 d
5	126,5 s	126,9 s	126,3 s	126,8 s	127,2 s	127,3 s	126,4 s	126,2 s
6	29,7 t	29,7 t	29,9 t	29,3 t	25,8 t	25,0 t	25,5 t	29,9 t
7	41,4 t	42,2 t	46,9 t	47,7 t	46,3 t	46,0 t	46,1 t	45,1 t
9	62,3 d	61,4 d	54,8 d	53,2 d	49,9 d	58,7 d	58,6 d	57,7 d
10	129,4 s	130,0 s	129,8 s	130,2 s	127,6 s	127,8 s	127,2 s	127,7 s
11	47,0 t	29,7 t	47,2 t	28,9 d	30,5 t	43,5 t	27,3 t	42,5 t
12	1208,7 s	159,5 s	209,3 s	157,4 s	159,7 s	209,7 s	158,3 s	191,3 s
13	52,3 d	44,1 d	48,5 d	40,1 d	36,3 d	52,8 d	45,2 d	108,7 s
14	66,4 d	66,8 d	65,8 d	64,0 d	58,5 d	59,2 d	58,3 d	160,3 s
15	30,9 t	30,7 t	25,7 t	25,9 t	28,2 t	32,4 t	31,0 t	27,7 t
16	24,8 t	25,5 t	24,2 t	23,0 t	20,1 t	24,7 t	65,0 t	22,2 t
17	24,3 t	25,3 t	22,1 t	21,9 t	23,4 t	24,1 t	23,7 t	21,8 t
17a	25,3 t	26,0 t	25,0 t	25,7 t	24,5 t	25,0 t	25,2 t	22,9 t
CH_3O	55,9 q	56,3 q	55,9 q	56,2 q	55,9 q	56,2 q	55,8 q	56,0 q
CH_3O	55,7 q	55,9 q	55,6 q	55,9 q	55,9 q	56,0 q	55,8 q	56,0 q

[a] Chemische Verschiebungen in ppm relativ zu Tetramethylsilan in Deuterochloroform (außer **5**: $CDCl_3/CD_3OD$ (2 : 1)). Die Bezeichnungen s, d, t und q geben die Multiplizität der Signale in den Off-Resonanz-Spektren an.

Wechselwirkung zwischen C-7 und C-15 in **1a** und **2**. Da für alle drei Ketone die entsprechenden Oxime vorlagen, konnten die Signale der Atome in Ring C auf Grund der charakteristischen Verschiebungen zugeordnet werden, die sich bei Vergleich der entsprechenden Keton/Oxim-Paare ergeben [24]. Von den vier Methylenkohlenstoffatomen C-15, C-16, C-17 und C-17*a* in Ring D ist C-15 am stärksten entschirmt, da es sich in β-Position zum Stickstoffatom befindet. Dies ist nur dann nicht der Fall, wenn andere Kohlenstoffatome in *gauche*-Position zu C-15 stehen, z. B. C-9 in **1b** und **3** oder C-7 in **4**. Die übrigen drei Signale liegen meist nahe beieinander, nur in **4** kann das Signal bei höchstem Feld ($\delta = 20{,}1$) C-16 zugeordnet werden, da dieses Atom eine *gauche*-Wechselwirkung mit dem Stickstoffatom N-8 eingeht. Im Spektrum von **8** sind die Signale von C-16, C-17 und C-17*a*, verglichen mit denen der 13,14-Dihydroverbindungen leicht hochfeldverschoben.

Verknüpfung der Ringe B und C

Vergleicht man die *trans*-Verbindungen **1a** und **2** mit **1c**, **4** und **5**, bei denen die Ringe B und C *cis*-verknüpft sind, findet man, daß C-10 seine Position von der *equatorialen* bezüglich Ring C zur *axialen* ändert, während C-7 *equatorial* bleibt. Der Übergang von der *trans*- zur *cis*-Verknüpfung (z. B. **1a** → **1c**) verursacht einen Hochfeldeffekt von 7,2 ppm am C-14-Signal, was sich aus der *gauche*-Stellung der beiden Atome C-10 und C-6 ergibt; in **1a** sind diese *antiperiplanar*. Der entsprechende Wert für Oxime (**2** → **5**) ist 8,5 ppm. Aus dem gleichen Grund erfahren auch die C-6-Signale der zwei B/C-*cis*-Verbindungen diamagnetische Verschiebungen von 4,7 bzw. 4,2 ppm. Die chemischen Verschiebungen der C-12-Atome dagegen bleiben relativ unverändert — die Unterschiede sind nur +1,0 bzw. —1,2 ppm — obwohl C-10 in den B/C-*cis*-Verbindungen zu C-12 *gauche* orientiert ist. Dies erklärt sich leicht aus der Tatsache, daß sich an beiden Kohlenstoffatomen keine Wasserstoffatome befinden [25]. Die C-10-Signale sind in den B/C-*cis*-Isomeren um 1,6 bzw. 2,8 ppm hochfeldverschoben, da sich die C-10-Atome hier in *axialer* Position zu einem Ring, nämlich Ring C, befinden [26].

Mit Hilfe der ^{1}H-gekoppelten ^{13}C-NMR-Spektren läßt sich nun auch die Frage entscheiden, ob **1b** in der *cis*-1- oder der *trans*-Konformation vorliegt. Dies war anhand der ^{1}H-NMR-Spektren ja nicht möglich gewesen (s. o.). Die direkten ^{13}C-^{1}H-Koppelkonstanten der C-9- und C-14-Signale sind in **1a** (all-*trans*-Konformation) mit 131,5 Hz gleich. In **1c** finden wir für C-9 140 und für C-14 132 Hz. Aufgrund der *gauche*-Position von H-9 bezüglich des freien Elektronenpaares des Stickstoffs ergibt sich hier also eine deutliche Vergrößerung der Koppelkonstante bei C-9. Bei dem fraglichen **1b** finden wir 131 Hz für C-9 und 138 Hz für C-14. Dies zeigt eindeutig, daß das freie Elektronenpaar des Stickstoffs bezüglich H-9 *antiperiplanar* und bezüglich H-14 *gauche* angeordnet ist. Damit resultiert für **1b** die *trans*-Konformation,* die auch auf Grund der ^{15}N-NMR Untersuchungen bewiesen wurde [28]. Die verschiedenen Konfigurationen des Ringes C in **3** und **4** können aus der Beobachtung abgeleitet werden, daß im Falle von **3** das C-15-Signal und im Falle von **4** das von C-16 diamagnetische Verschiebung erfährt.

Effekte der Oximbildung

Es gibt einige Untersuchungen über die ^{13}C-NMR-Spektren von Oximen, in denen gezeigt wird, daß ein wesentlicher Unterschied in den chemischen Verschiebungen von Kohlenstoffatomen existiert, die sich in γ_{syn}- bzw. γ_{anti}-

* Zur Bestimmung der konformativen Reinheit der Verbindung **1b** fertigten wir jeweils eine ^{13}C und eine ^{1}H Spektrumaufnahme in einem Gemisch von $CDCl_3$ und CD_3OD 1 : 1 bei 40 °C sowie —60 °C an. Durch die 100 °C Temperaturerniederung änderte sich das Spektrum praktisch nicht. Signale für eine eventuelle Minderheitskonformation traten nicht auf. So können wir mit großer Wahrscheinlichkeit behaupten, daß die Verbindung **1b** konformativ einheitlich ist.

Position bezüglich der Hydroxygruppe des Oxims befinden [24]. Mißt man also die Effekte, die sich aus dem Vergleich der Spektren der Oxime und der entsprechenden Carbonylverbindungen ergeben, erhält man einen deutlichen und zuverlässigen Hinweis auf die Stereochemie der Oximgruppe [24]. In den Spektren von **2**, **3**, **4** und **5** kann die *E*- oder *Z*-Konfiguration leicht durch die Verschiebung der Signale von C-11 und C-13 beim Übergang von den Ketonen zu den Oximen abgeleitet werden. In Adamantanonoxim [24] ist die *syn*-Orientierung mit einer Hochfeldverschiebung von 18 ppm für das Signal des zur Oximgruppe β-ständigen Kohlenstoffatoms und die *anti*-Orientierung mit einer von nur 10 ppm verbunden. In dieser Arbeit sind die β_{syn}-Effekte auf die C-11-Signale bei den *E*-Isomeren —17 bis —19 ppm und die β_{anti}-Effekte auf C-13 *ca.* — 8 ppm. Im *Z*-Isomer **4** dagegen sind die entsprechenden Werte — 16,7 ppm für C-11 (β_{anti}) und —12,2 ppm für C-13 (β_{syn}). Die Abweichungen dieser letzteren Effekte von den üblichen Werten sind auf die Umkehrung der Konformation von Ring C zurückzuführen. So wird die erwartete Effekt von — 18 ppm für das C-13-Signal durch das Fehlen der *gauche*-Wechselwirkung mit der C-7-Methylengruppe die in **1b** existiert, erniedrigt. Für C-11 ist die Situation komplizierter, da durch die Oximbildung die *gauche*-Wechselwirkung mit C-7 durch eine andere mit C-17*a* ersetzt wird. Darum ist in diesem Fall eine quantitative Abschätzung kaum möglich.

Experimenteller Teil

Die ^{1}H-NMR-Spektren wurden mit einem Jeol-PS-100-Spektrometer (100 MHz) aufgenommen. Die ^{13}C-NMR-Spektren erhielten wir mit Hilfe eines Bruker WH-90 (22, 64 MHz) und eines Jeol FX-100 (25,0 MHz). Die Konzentrationen der Lösungen schwankte zwischen 0,5 und 1,0 molar in $CDCl_3$, bei **5** verwendeten wir ein 2 : 1-Gemisch von $CDCl_3$ und CD_3OD. Tetramethylsilan diente als interner Standard. Die Zuordnung der ^{13}C-Signale wurde durch Aufnahme der »Off-Resonance«-Spektren unterstützt.

*

Die Autoren danken Herrn Prof. Dr. G. SNATZKE, Bochum, für hilfreiche Diskussionen. G.T. dankt der Alexander-von-Humboldt-Stiftung für ein Stipendium und H.D. der Deutschen Forschungsgemeinschaft für finanzielle Unterstützung.

LITERATUR

[1] IV. Mitteilung: sehe vorherstehende Mitteilung.
[2] SZÁNTAY, Cs., VEDRES, A., TÓTH, G.: Heterocycles, **6**, 1973 (1977)
[3] SZÁNTAY, Cs., TÓTH, G., VEDRES, A.: 11th IUPAC International Symposium on Chemistry of Natural Products, Bulgaria 1978; Symposium papers Vol. **4**, pp. 357
[4] SZÁNTAY, Cs.: Magyar Kémikusok Lapja, **1971**, 490
[5] BARTELL, L. S.: J. Chem. Phys., **32**, 827 (1960)
[6] BOHLMANN, F.: Chem. Ber., **91**, 2157 (1958)
[7] SIRCAR, J. C., MEYERS, A. I.: J. Org. Chem., **32**, 1248 (1367)
[8] JOHNSON, S. D., JONES, R. A. Y., KATRITZKY, A. R., PALMER, C. R., SCHOFIELD, K., WELLS, R. J.: Chem. Soc., **1965**, 6797; TEMPLE, D. L., SAM, J.: J. Heterocycl. Chem., **7**, 847 (1370)

[9] USKOKOVIC, M., BRUDERER, H., von PLANTA, C., WILLIAMS, T., BROSSI, A.: J. Am. Chem. Soc., **86**, 3364 (1964)
[10] KAMETANI, T., FUKUMOTO, K., IHARA, M., UYIIE, A., KOIZUMI, H.: J. Org. Chem., **40**, 3280 (1975)
[11] HAMLOW, H. P., OKUDA, S., NAKAGAWA, N.: Tetrahedron Lett., **1964**, 2553; CRABB, T. A., NEWTON, R. F., JACKSON, D.: Chem. Rev., **71**, 109 (1971)
[12] CHIVERS, P. J., CRABB, T. A.: Tetrahedron, **26**, 3389 (1970); COOKSON, R. C., CRABB, T. A.: *ibid.* **24**, 2385 (1968); VAN BINST, G., TOURWÉ, D.: Org. Magn. Res., **6**, 590 (1974)
[13] BARFIELD, M., CHAKRABARTI, B.: Chem. Rev., **69**, 757 (1969); TOURWÉ, D., VAN BINST, G., KAMETANI, T.: Org. Magn. Res., **9**, 341 (1977)
[14] ELIEL, E. L., VIERHAPPER, F. W.: J. Org. Chem., **41**, 199 (1976); VIERHAPPER, F. W., ELIEL, E. L.: *ibid.* **42**, 51 (1977); WENKERT, E., BINDRA, J. S., CHANG, C. J., COCHRAN, D. W., SCHELL, F. M.: Acc. chem. Res., **7**, 46 (1974); LEVIN, R. H., LALLEMAND, J. Y., ROBERTS, J. D.: J. Org. Chem., **38**, 1983 (1973); VAN BINST, G., TOURWÉ, D., COCK, E. D.: Org. Magn. Res., **8**, 618 (1976); TOURWÉ, D., VAN BINST, G.: Heterocycles, **9**, 507 (1978)
[15] BLUNT, J. W., STOTHERS, J. B.: Org. Magn. Res., **9**, 439 (1977) and references cited therein
[16] JENNINGS, W. B., BOYD, D. R., WATSON, C. G., BECKER, E. D., BRADLEY, R. B., JERINA, D. M.: J. Amer. Chem. Soc., **94**, 8501 (1972)
[17] VAN BINST, G., TOURWÉ, G.: Heterocycles, **1**, 257 (1973); TOURWÉ, D., VAN BINST, G.: *ibid.* **9**, 507 (1978)
[18] VON STRANDMANN, M., COHEN, M. A., SHEVEL, Jr. J.: J. Org. Chem., **31**, 797 (1966)
[19] MARTIN, G. J., MARTIN, M. L.: The stereochemistry of Double Bonds, in Progress in Nuclear Magnetic Resonance Spectroscopy, Vol. **8.**, Pergamon Press, Oxford, 1972, p. 197 and references therein
[20] ApSIMON, J. W., CRAIG, W. G., DEMARCO, P. V., MATHIESON, D. V., SAUNDERS, L., WHALLEY, W. B.: Tetrahedron, **23**, 2339 (1967)
[21] HUGHES, D. W., HOLLAND, H. L., MACLEAN, B. D.: Can. J. Chem., **54**, 2252 (1976)
[22] ADCOCK, W., GUPTA, B. D., KITCHING, W.: J. Org. Chem., **41**, 1498 (1976)
[23] BUZÁS, A., CAVIER, R., COSSAIS, F., FINET, J., JACQUET, J., LAVIELLE, G., PLATZER, N.: Helvetica, **60**, 2122 (1977)
[24] LEVY, G. C., NELSON, G. L.: J. Amer. Chem. Soc., **94**, 4897 (1972); HAWKES, G. E., HERWIG, K., ROBERT, J. D.: J. Org. Chem., **39**, 1017 (1974); BUNNEL, C. A., FUCHS, P. L.: J. Org. Chem., **42**, 2614 (1977)
[25] BEIERBECK, H., SAUNDERS, J. K.: Can. J. Chem., **54**, 2985 (1976); GRANT, D. M., CHENEY, B. V.: J. Amer. Chem. Soc., **89**, 5315 (1967)
[26] WILSON, N. K., STOTHERS, J. B.: Stereochemical Aspects of ^{13}C NMR Spectroscopy, in Topics in Stereochemistry, Vol. **8**, Wiley-Interscience, New York, 1974, p. 26
[27] PRETSCH, E., CLERC, T., SEIBL, J., SIMON, W.: Strukturaufklärung organischer Verbindungen, Springer-Verlag, Berlin, 1976
[28] TÓTH G., VEDRES, A., SZÁNTAY, Cs.: Mitteilung in Vorbereitung

Gábor TÓTH — H-1521 Budapest, Gellért tér 4.
András VEDRES — H-1475 Budapest, Pf. 27.
Helmut DUDDECK — Lehrstuhl für Strukturchemie, Ruhr-Universität Bochum, D-4630 Bochum-1, Pf. 102148, BRD.
Csaba SZÁNTAY — H-1521 Budapest, Gellért tér 4.

Acta Chimica Academiae Scientiarum Hungaricae, Tomus 109 (2), pp. 165–173 (1982)

STEREOCHEMICAL STUDIES ON COPPER(II) COMPLEXES OF SOME SEMICARBAZONES

S. CHANDRA,* S. P. DUBEY, K. B. PANDEYA and R. P. SINGH

(Department of Chemistry, University of Delhi, Delhi-110007, India)

Received November 17, 1980

In revised form January 30, 1981

Accepted for publiication February 12, 1981

Copper(II) complexes of general composition, $Cu(ligand)_2X_2$, where X = Cl, Br NO_3 or 0.5 SO_4 and ligand = semicarbazones of acetone, ethyl methyl ketone and cyclohexanone have been prepared and characterised by elemental analysis, magnetic moments, electronic infrared and electron spin resonance spectral studies. The chloro, bromo and nitrato complexes are hexa-coordinated and octahedral. The sulphato complex of acetone semicarbazone is square pyramidal and those of ethylmethyl ketone and cyclohexanone are trigonal bipyramidal.

Introduction

CAMPBELL *et al.* have reported electronic spectra [1] and esr spectra [2] of copper(II) complexes of the type $Cu(ligand)_2X_2$, where X = Cl or Br and the ligands are the semicarbazones of cycloheptanone, methyl isopropyl ketone and diacetyl ketone to show that the stereochemistry of the complexes changes from six-coordinate tetragonal to five-coordinate trigonal bipyramidal as the alkyl group on the ketone becomes bulky. In the present studies copper-(II) complexes of the same type with the semicarbazones of acetone (acsc), ethylmethyl ketone (emsc) and cyclohexanone (chsc) and with anions as chloride, bromide, nitrate and sulphate have been prepared and it has been shown that the stereochemistry is also dependent on the coordinated anions. For example, when the coordinating anion is chloride, bromide or nitrate, complexes are hexa-coordinated octahedral, while with the sulphato anion penta-coordinated complexes are obtained. Further among the sulphato complexes, the acetone semicarbazone complex is square pyramidal, whereas those of ethylmethyl ketone and cyclohexanone are trigonal bipyramidal.

Experimental

The semicarbazones were prepared by the literature method [3].

For preparing the complexes, hot aqueous ethanolic solution of the hydrated copper(II) salts and corresponding semicarbazone were mixed in the molar ratio 1 : 2. On cooling crystalline complexes precipitated out in each case. The same were filtered, washed with 5% ethanol and dried in an electric oven at ~60 °C. In all the cases good analytical results were obtained for $Cu(L)_2X_2$ (X = Cl, Br, NO_3 and 0.5 SO_4) (Table I). Chloro, bromo and nitrato complexes

* Present address: Department of Chemistry, Zakir Husain College, Ajmeri Gate, Delhi-110006, India.

Table 1

Colour, composition, magnetic moment and electronic spectra of the complexes

Complex	Colour	Found (Calcd.) %				μ_{eff} (BM)	λ_{max} (cm^{-1})
		Cu	C	H	N		
$Cu(acsc)_2Cl_2$	Green	17.4 (17.42)	26.1 (26.34)	4.8 (4.94)	23.1 (23.04)	1.77	14100 12500
$Cu(acsc)_2Br_2$	Green	14.1 (14.03)	21.2 (21.21)	3.9 (3.97)	18.4 (18.56)	1.81	14100 12500
$Cu(acsc)_2(NO_3)_2$	Green	15.1 (15.21)	22.9 (22.99)	4.2 (4.31)	26.6 (26.83)	2.12	16000 13300
$Cu(acsc)_2SO_4$	Blue	16.2 (16.30)	24.6 (24.65)	4.4 (4.62)	21.5 (21.57)	2.06	13000 11600
$Cu(emsc)_2Cl_2$	Green	16.2 (16.18)	30.6 (30.57)	5.8 (5.60)	21.3 (21.40)	1.96	14800 12900
$Cu(emsc)_2Br_2$	Green	13.2 (13.22)	24.9 (24.97)	4.6 (4.58)	17.5 (17.48)	1.86	14400 12600
$Cu(emsc)_2(NO_3)_2$	Green	14.2 (14.25)	26.7 (26.94)	4.6 (4.94)	25.1 (25.14)	2.03	15500 13200
$Cu(emsc)_2SO_4$	blue	15.2 (15.21)	28.7 (28.74)	5.2 (5.7)	20.1 (20.12)	2.1	11000
$Cu(chsc)_2Cl_2$	Green	14.6 (14.30)	37.7 (37.79)	5.9 (5.84)	18.7 (18.89)	1.88	13800 11500
$Cu(chsc)_2Br_2$	Green	12.1 (11.94)	31.7 (31.61)	4.9 (4.89)	15.9 (15.80)	1.56	12500 11300
$Cu(chsc)_2(NO_3)_2$	Green	13.0 (12.76)	33.9 (33.76)	5.4 (5.33)	22.4 (22.51)	1.94	15400 13000
$Cu(chsc)_2SO_4$	Yellowish	13.7 (13.52)	35.9 (35.78)	5.7 (5.54)	17.8 (17.89)	2.08	11000

are soluble in water, ethanol and methanol. The sulphato complexes are insoluble in water as well as in common organic solvents.

Physical measurements

Magnetic susceptibility measurements were made on finely powdered solid complexes by the GOUY method using mercury tetrathiocyanatocobaltate(II) as a calibrating agent ($\chi_g = 16.44 \times 10^{-6}$ cgs units). Electronic spectra of all the complexes were recorded on nujol mull on an DMR-21 automatic recording spectrophotometer. ESR spectra of the polycrystalline complexes were recorded on a Varian E-4 EPR spectrometer operating at ~9.4 GHz and 100 KHz field modulation.

Results and Discussion

Magnetic moments of all the complexes lie in the range 1.8—2.1 BM (Table I), corresponding to one unpaired spin and suggesting monomeric nature of the complexes.

$Cu(ligand)_2X_2$ (X = Cl or Br)

The electronic spectral bands of all the complexes are presented in Table I. All the chloro and bromo complexes show identical spectra and are, therefore, considered to be isostructural, obviously tetragonal with two (presumbly trans) semicarbazone molecules providing in-plane coordination and the anions interacting along the *Z*-axis [1]. Such a structure for semicarbazide complexes $Cu(sc)_2Cl_2$, has been confirmed by X-ray crystallography [4]. The electronic spectra of these complexes show absorption maxima in the visible region tailing deep into the near i.r. region. The spectra are similar to those reported for octahedral Cu(II) complexes with a very large tetragonal distortion [5—7].

ESR spectra of these complexes are anisotropic characterising tetragonal copper(II) complexes (Fig. 1). The g-tensor values have been evaluated by KNEUBUHL's method [8] and the results are presented in Table II. The g-tensor values obey the criterion [9] of $g_{\|} > g_{\perp}$ for the $d_{x^2-y^2}$ ground state obtaining in the elongated octahedral copper(II) complexes.

Recalling the tetragonal geometry for the complexes stronger interaction along the *Z*-axis is to be accompanied by an increase in the value of $g_{\|}$. Strong axial bonding leads to an increase in the bond length in XY plane, which results in an increase of both in plane covalency and the energy $d_{xy} \rightarrow d_{x^2-y^2}$ transitions [10]. Both these effects are factors, which tend to increase the value of $g_{\|}$. Further in an axial symmetry g-values are related by the expression [11] $G = (g_{\|} - 2)/(g_{\perp} - 2)$, which measures the exchange interaction between copper centers in the polycrystalline solid. According to HATHAWAY [12—15] if the value of G is larger than four, exchange interaction is negligible while G value of less than four indicates considerable exchange interaction in solid complexes. The calculated G-values are given in Table II. For all the ligands the chloro complex exhibits smaller G values and hence larger exchange interaction. For both the anions, the ligands follow the following order of G values, acsc < chsc < emsc.

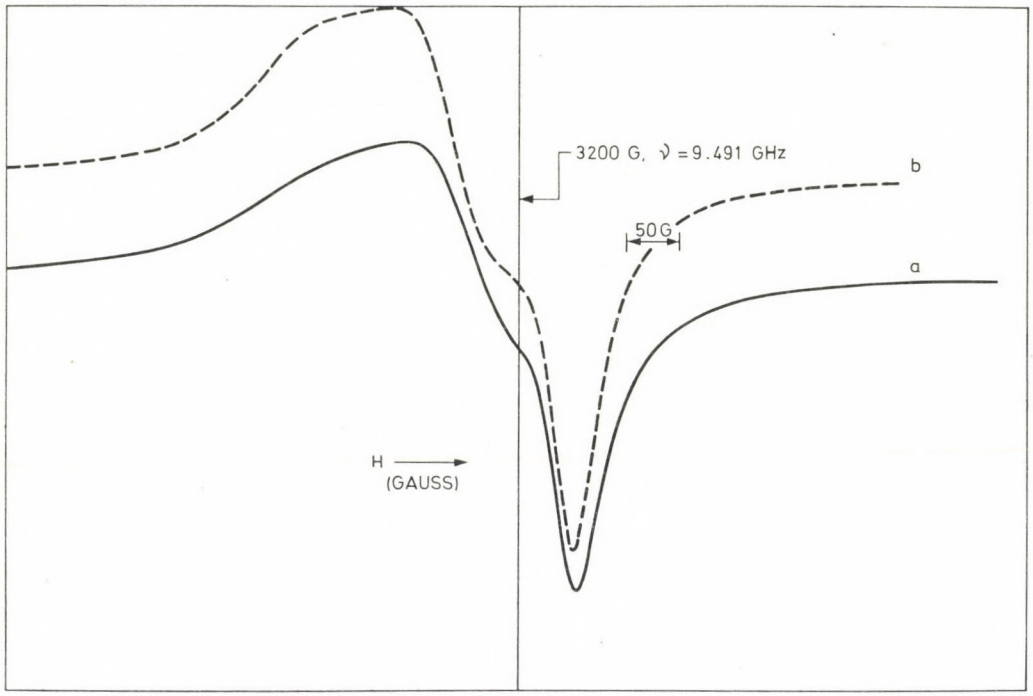

Fig. 1. ERS Spectra of: (a) $Cu(chsc)_2Cl_2$, (b) $Cu(chsc)_2Br_2$

Cu(ligand)$_2$(NO$_3$)$_2$

Nitrate can coordinate as a monodentate as well as bidentate ligand [16—18] so that the possibility of the following two structures arises for the nitrato complexes. Interestingly the complexes under discussion contain both the examples. As will be evident from the discussion on the ESR spectra, the cyclohexanone semicarbazone appears to have structure **I** and the complexes with acetone semicarbazone and ethylmethyl ketone semicarbazone appear to have structure **II**.

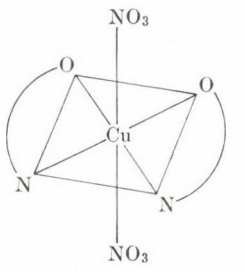

I

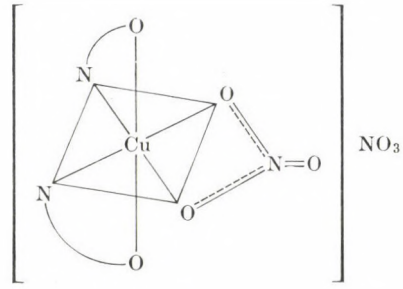

II

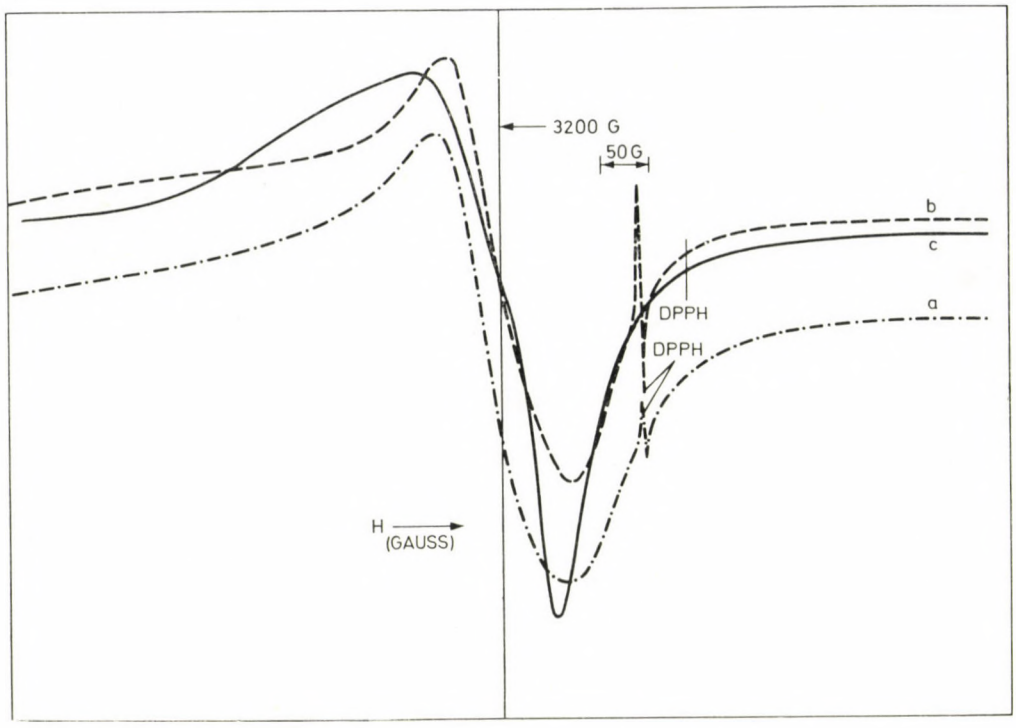

Fig. 2. ESR Spectra of: (a) $Cu(acsc)_2(NO_3)_2(\nu = 9.38\ GH_z)$, (b) $Cu(emsc)_2(NO_3)_2(\nu = 9.381\ GH_z)$, (c) $Cu(chsc)_2(NO_3)_2$ $(\nu = 9.499\ GH_z)$

The infrared spectrum of $Cu(chsc)_2(NO_3)_2$ corresponds to the monodentate behaviour of nitrate groups. It displays i. r. bands at 1425 cm^{-1} (ν_1), 1290 cm^{-1} (ν_5), 1010 cm^{-1} (ν_2) and 820 cm^{-1} (ν_6). In the infrared spectrum there is no band at 1390 cm^{-1} which is assignable to the ionic nitrate, suggesting that both nitrate groups are coordinated to copper. Further this complex is a non-electrolyte in nitro-methane, indicating that both nitrates are in the coordination sphere. The electronic spectrum of this complex is also similar to the halide complexes. $Cu(acsc)_2(NO_3)_2$ and $Cu(emsc)_2(NO_3)_2$ show molar conductance 80 $ohm^{-1}\ cm^2\ mole^{-1}$, indicating that these are uni-univalent electrolytes. Thus a penta-coordinated structure is also possible for these complexes. But i.r. electronic and esr spectra to be discussed below, indicate that these complexes are hexa-coordinated octahedral. Infrared spectra of these complexes display bands at 1505 cm^{-1} (ν_1) 1390 cm^{-1} (ν_3), 1290 cm^{-1} (ν_5), 1030 cm^{-1} (ν_2) and 825 cm^{-1} (ν_6). The separation of >200 cm^{-1} between ν_1 and ν_5 indicates the bidentate nature of nitrate group. Broad adsorption band at 1390 cm^{-1} is assignable to ν_3 of uncoordinated nitrate. It indicates that one nitrate is ionic and other coordinates to copper. Further electronic

and esr spectra of these complexes are similar to the octahedral copper(II) complexes.

ESR spectrum of $Cu(chsc)_2(NO_3)_2$ (Fig. 2) is characteristic of the elongated tetragonal geometry and is similar to those of the chloro and the bromo complexes discussed above. The complex may, therefore, be assigned to

Table II

ESR parameters of the chloro, bromo and nitrato complexes

Complex	$g_{\|\|}$	$g_\perp$	g_0	G
$Cu(acsc)_2Cl_2$	2.260	2.139	2.179	1.87
$Cu(acsc)_2Br_2$	2.260	2.124	2.169	2.09
$Cu(acsc)_2(NO_3)_2$	2.208	2.077	2.121	2.70
$Cu(emsc)_2Cl_2$	2.244	2.089	2.141	2.74
$Cu(emsc)_2Br_2$	2.245	2.082	2.136	2.98
$Cu(emsc)_2(NO_3)_2$	2.219	2.072	2.121	3.04
$Cu(chsc)_2Cl_2$	2.260	2.124	2.169	2.10
$Cu(chsc)_2Br_2$	2.260	2.118	2.165	2.20
$Cu(chsc)_2(NO_3)_2$	2.261	2.109	2.159	2.39

structure(**I**). ESR spectra of $Cu(acsc)_2(NO_3)_2$ and $Cu(emsc)_2(NO_3)_2$ (Fig. 2) are similar to each other but are entirely different from that of $Cu(chsc)_2(NO_3)_2$. In these latter complexes the $g_{||}$ absorption is very weak and $g_\perp$ signal is broader as compared to that of the $Cu(chsc)_2(NO_3)_2$ spectra and appears to be a composite absorption of two components. It is not possible to analyse the two spectra because of their complicated nature. But it is apparent that the ground state in the two complexes has contributions from both $d_{x^2-y^2}$ and d_{z^2}.

Cu(ligand)$_2$SO$_4$

Infrared spectra of these complexes show monodentate behaviour of the sulphato group (Fig. 3). A penta-coordinated structure is, thus, readily suggested for these complexes. There are two basic configurations [19] that can be adopted by complex compounds of coordination number five, the trigonal bipyramidal (TBP) and the square pyramidal (SP). In practice there appears to be very little difference in energy [20] between the two configurations and the large distortions form the ideal geometries obtaining in the complexes of the type being discussed makes this difference still smaller. It is not surprising, therefore, that while $Cu(acsc)_2SO_4$ is square pyramidal $Cu(emsc)_2SO_4$ and $Cu(chsc)_2SO_4$ are trigonal bipyramidal.

The two configurations SP and TBP are characterized by the ground states $d_{x^2-y^2}$ and d_{z^2}, respectively [21, 22]. ESR spectra of copper(II) (Fig. 4)

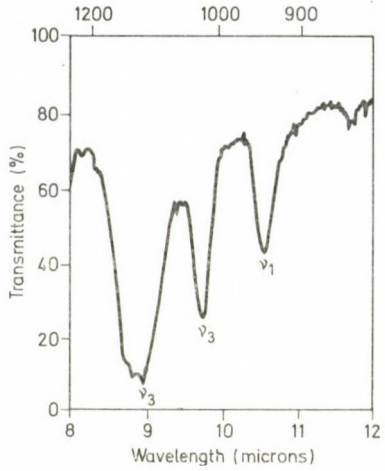

Fig. 3. Infrared spectrum of $Cu(chsc)_2SO_4$

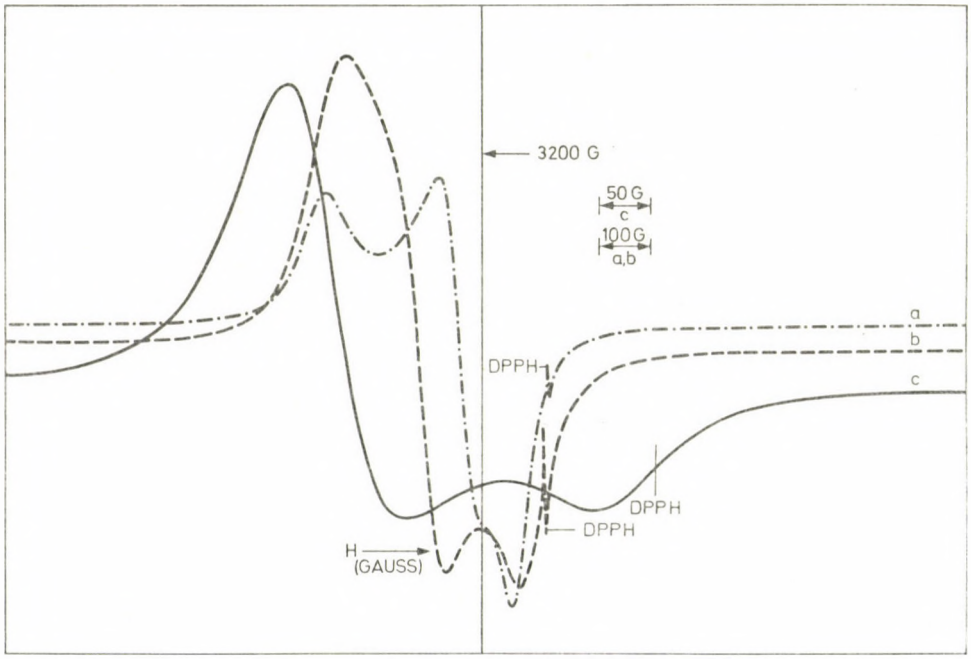

Fig. 4. ESR Spectra of: (*RT*) (a) $Cu(acsc)_2SO_4$ ($\nu = 9.38$ GH_z), (b) $Cu(emsc)_2SO_4$ ($\nu = 9.383$ GH_z), (c) $Cu(chsc)_2SO_4$ ($\nu = 9.44$ GH_z)

complexes provide a very good basis for distinguishing between these two ground states. For systems with $g_3 > g_2 > g_1$ the ratio [22] of $(g_2 - g_1)/(g_3 - g_2)$ (hereafter called as parameter R) is a very useful parameter for this purpose. If the ground state is predominantly d_{z^2} the value of R is greater

than one. On the other hand, for the ground state being predominantly $d_{x^2-y^2}$ the value [23] of R is less than one. All the three sulphato complexes give ESR spectra showing three g-values. The values of g_1, g_2, g_3, and R are presented in Table III. The calculated value of R (Table III) for $Cu(acsc)_2SO_4$

Table III

ESR parameters of the sulphato complexes

Complex	g_1	g_2	g_3	g_0	R
$Cu(acsc)_2SO_4$	2.049	2.117	2.327	2.164	0.324
$Cu(emsc)_2SO_4$	2.043	2.190	2.29	2.174	1.47
$Cu(chsc)_2SO_4$	2.040	2.158	2.223	2.160	1.81
$Cu(cpsc)_2SO_4$*	2.037	2.161	2.282	2.160	1.025

* Ref. [27].

indicates a $d_{x^2-y^2}$ ground state which is consistent with a distorted square pyramidal structure which is in agreement with the electronic absorption spectra. The nujol mull electronic spectrum for this complex exhibits a band around 13000 cm^{-1} with a shoulder around 11600 cm^{-1}. These data are comparable with a square pyramidal structure [11—13]. However, since the crystal structure of this complex is not known, we can not conclude to what extent the g-values reflect the actual molecular structure.

The values of R calculated for $Cu(emsc)_2SO_4$ and $Cu(chsc)_2SO_4$ reveal d_{z^2} ground state, *i.e.* trigonal bipyramidal geometry for these complexes. However, the g_1 value is 2.00 for an ideal trigonal bipyramidal copper(II) complex. Such high values suggest considerable distortion from the trigonal bipyramidal geometry as also expected. Higher g-values of this order have earlier been observed [24, 25] in trigonal [Cu(tren)NCS] SCN in which the trigonal axes are aligned parallel to one another and in [Cu(bipy)I] I in which the trigonal axes are also lined up but the trigonal bipyramidal structure is rather distorted [26].

The electronic spectra of $Cu(emsc)_2SO_4$ and $Cu(chsc)_2SO_4$ complexes show one intense absorption each at 11000 cm^{-1}, assignable to the $^2A_1' \rightarrow {}^2E'$ transition. These are similar to earlier reported trigonal bipyramidal Cu(II) complexes [24—26]. In such complexes the transition $^2A_1 \rightarrow {}^2E''$ is normally forbidden. However, the crystal structure of these complexes are not able to conclude to what extent the g-values reflect the molecular structure.

*

Our grateful thanks are due to C.S.I.R. (New Delhi) for awarding a S.R.F. to one of the author (S. CHANDRA).

REFERENCES

[1] CAMPBELL, M. J. M., GRZESKOWIAK, R.: Inorg. Nucl. Chem. Lett., **5**, 27 (1969)
[2] CAMPBELL, M. J. M., GRZESKOWIAK, R.: Inorg. Nucl. Chem. Lett., **10**, 473 (1974)
[3] VOGEL, A. I.: "A Text Book of Practical Organic Chemistry" Longmen, 344 (1973)
[4] NARDELLI, M., GASSPARI, G. F., BOLDARINI, P., BATTISTINI, G. G.: Acta Crystallogr., **19**, 491 (1965)
[5] EARNSHAW, A., LARKWORTHY, L. F., PATEL, K. C.: J. Chem. Soc. *A*, **1969**, 1339; LEVER, A. B. P., MANTOVANI, E.: Inorg. Chem., **10**, 817 (1971); HATHAWAY, B. J.: Struct. Bonding, **14**, 49 (1973)
[6] TOMILNSON, A. A. G., HATHAWAY, B. J., BILLING, D. E., NICHOLLS, P.: J. Chem. Soc. *A*, **1969**, 65
[7] LEVER, A. B. P.: "Inorganic Electronic Spectroscopy", (Elsevier Pub. Company, Amsterdam), p. 275 (1968)
[8] KNEUBUHL, F. K.: J. Chem. Phys., **33**, 1074 (1960)
[9] BALLHAUSEN, C. J.: Introduction to Ligand Field Theory, McGraw-Hill, New York, p. 134 (1962)
[10] SMITH, D. W.: J. Chem. Soc. *A*, **1970**, 3108
[11] PROCTER, I. M., HATHAWAY, B. J., NICHOLLS, P.: J. Chem. Soc. *A*, **1968**, 1678
[12] HATHAWAY, B. J., BILLING, D. E.: Coord. Chem. Rev., **5**, 143 (1970)
[13] HATHAWAY, B. J., in "Essay in Chemistry", Ed. J. N. BRADLEY and R. D. GILLARD, Academic Press, p. 61 (1971)
[14] HATHAWAY, B. J., DUDLEY, R. J., NICHOLLS, P.: J. Chem. Soc. *A*, **1968**, 1845
[15] DUDLEY, R. J., HATHAWAY, B. J.: J. Chem. Soc. *A*, **1970**, 1725
[16] CURTIS, N. F., CURTIS, Y. M.: Inorg. Chem., **4**, 804 (1965)
[17] KOMIYAMA, Y., LINGAFELTER, E. C.: Acta, Cryst., **17**, 1145 (1954)
[18] BURMEISTER, J. L.: Coord. Chem. Rev., **1**, 205 (1966); **3**, 225 (1968)
[19] SACCONI, L.: "Transition Metal Chemistry", Vol., **4**, Ed. R. L. CARLIN (Marcel Dekker), N. Y. 221 (1968)
[20] BALLHAUSEN, C. J., JORGENSEN, C. J.:Kgl. Danska Videnskab. Selskab. Mat. Eys. Medd., **29**, 14 (1955)
[21] BARBUCCI, R., BEUCINI, A., GATTESCHI, D.: Inorg. Chem., **16**, 2117 (1977)
[22] BENCINI, A., CATTESCHI, D.: Inorg. Chem., **16**, 1994 (1977)
[23] EL-SHAZLY, M. F., EL-DISSOWKY, A., SALEM, T., OSMAN, M.: Inorg. Chim. Acta, **40**, 1 (1980)
[24] JAIN P. C., LINGAFELTER, E. C.: J. Am. Chem. Soc., **89**, 724 (1967)
[25] SLADE, R. C., TOMILNSON, A. A. G., HATHAWAY, B. J., BILLING, E. E.: J. Chem. Soc. *A*, **1968**, 61
[26] BARCLAY, G. A., HOSKINS, B. F., KENNARD, C. H. L.: J. Chem. Soc., **1963**, 5691
[27] NIGAM, I., NIGAM, H. L., PANDEYA, K. B.: J. Inorg. Nucl. Chem., **42**, 1558 (1980)

Sulekh CHANDRA
Satendra Prakash DUBEY
Krishna Bihari PANDEYA
Rajendra Pal SINGH

Department of Chemistry, University of Delhi, Delhi-110007 (INDIA)

Acta Chimica Academiae Scientiarum Hungaricae, Tomus 109 (2), pp. 175—187 (1982)

AMINOPYRAZOLES, II*

SYNTHESIS OF PYRAZOLO[3,4,-*b*]PYRIDINES *VIA* VILSMEIER—HAACK REACTION OF 5-ACETAMINOPYRAZOLES**

A. SIMAY, K. TAKÁCS and L. TÓTH

(Research Department of CHINOIN Pharmaceutical and Chemical Works, Budapest)

Received December 14, 1980

Accepted for publication February 12, 1981

The title compounds **4** and **5** were isolated as by-product in the Vilsmeier—Haack reaction of 5-acetylaminopyrazoles **1**. The structures were supported spectroscopically and proved by a preparative route. On the basis of preliminary investigation of the mechanism, the conditions of the Vilsmeier—Haack reaction were modified to obtain **4** and **5** as major products. Some chemical transformations of **5b**, including the synthesis of the dipyrazolo[3,4-*b*; 4',3'-*e*]pyridine derivative **20** are also reported.

Earlier we reported [1] that 5-acetylaminopyrazoles **1**, as well as their 5-formyl- and 5-benzoylamino analogues, under the conditions of the Vilsmeier–Haack reaction with dimethylformamide–phosphoryl chloride reagent undergo acyl-splitting to form products **2** and **3**.

In the case of compounds **1**, however, unlike the related formyl- and benzoylamino derivatives, minor amounts of acid-insoluble by-products were also isolated. These proved to be mixtures of two compounds which were separated by column chomatography. Spectroscopic and analytical data of the products supported structures **4** and **5** (Scheme 1).

Analogous cyclization of acetanilide and acetaminothiophene derivatives was recently reported [2] to give quinolines and thieno[3,4-*c*]pyridines, without any structure proof for the products beeing indicated. The unequivocal structure elucidation of compounds **4b** and **5b** was performed by a preparative route, shown in Scheme 2.

Compound **6** was synthesized by a literature method [3], condensing the corresponding 5-aminopyrazole-4-carbaldehyde with malononitrile. In an analogues process, using ethyl cyanoacetate instead of malononitrile, the ester derivative **7** was obtained, which was alternatively synthesized also by acid-catalyzed alcoholysis of **6**. Basic hydrolysis of either **6** or **7** gave the carboxylic acid **8**.

Compound **8** was decarboxylated to give **9** which, in turn, reacted with phosphorous pentachloride resulting in a product, identical with **4b** obtained *via* Vilsmeier—Haack reaction of **1b**.

* For Part I, see Ref. [1].

** Presented at the Annual Session of the Hungarian Academy of Sciences, Section Heterocyclic Chemistry, Balatonfüred, Hungary, 1977.

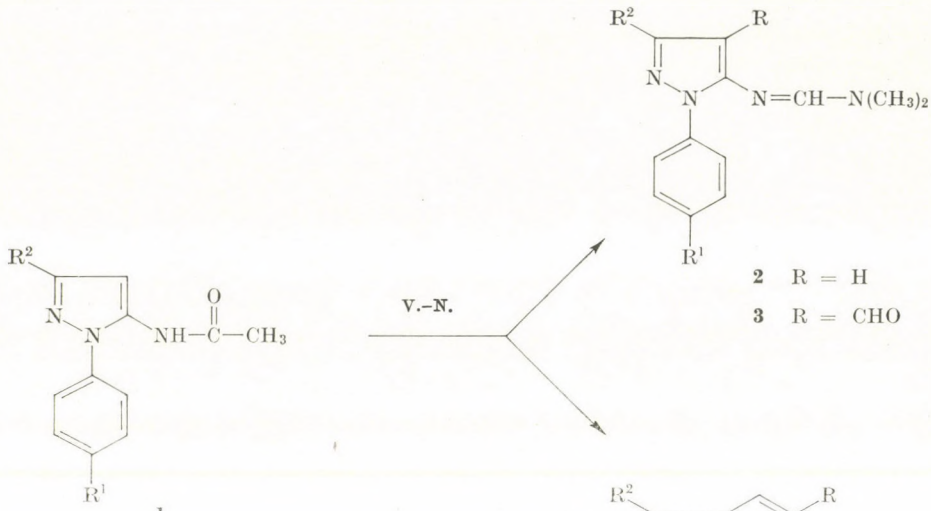

1—5	R^1	R^2
a	H	H
b	H	Me
c	H	Ph
d	Cl	H
e	NO_2	H

Scheme 1

The structure elucidation of **5b** was also based on compound **8**. Namely, hydrolysis of **5b** afforded **10**, which was oxidized to **8**, identical with the sample prepared from **6** or **7** as described previously.

Preliminary investigations concerning the route of the cyclization process **1** → **4**+**5** were also carried out. Neither the transformation of **9** to **4**, nor that of **10** to **5** could be observed under the Vilsmeier—Haack conditions. Formylation of **4** to give **5** also failed. Consequently, both the formation of the imidoyl chloride moiety and the C-formylation steps must precede the cyclization to **4** or **5**. Furthermore, the cyclization reaction to give **4** and **5** took place only at higher temperatures (above 60 °C), while at room temperature exclusively deacylated products **2** and **3** were obtained.

On the basis of the above observations, the Vilsmeier—Haack reaction of compounds **1** was carried out under modified and carefully controlled conditions (*cf.* [1] and Experimental). In this way only minor amounts of compounds **3** were formed and mixtures of **4** and **5** were obtained as the major products

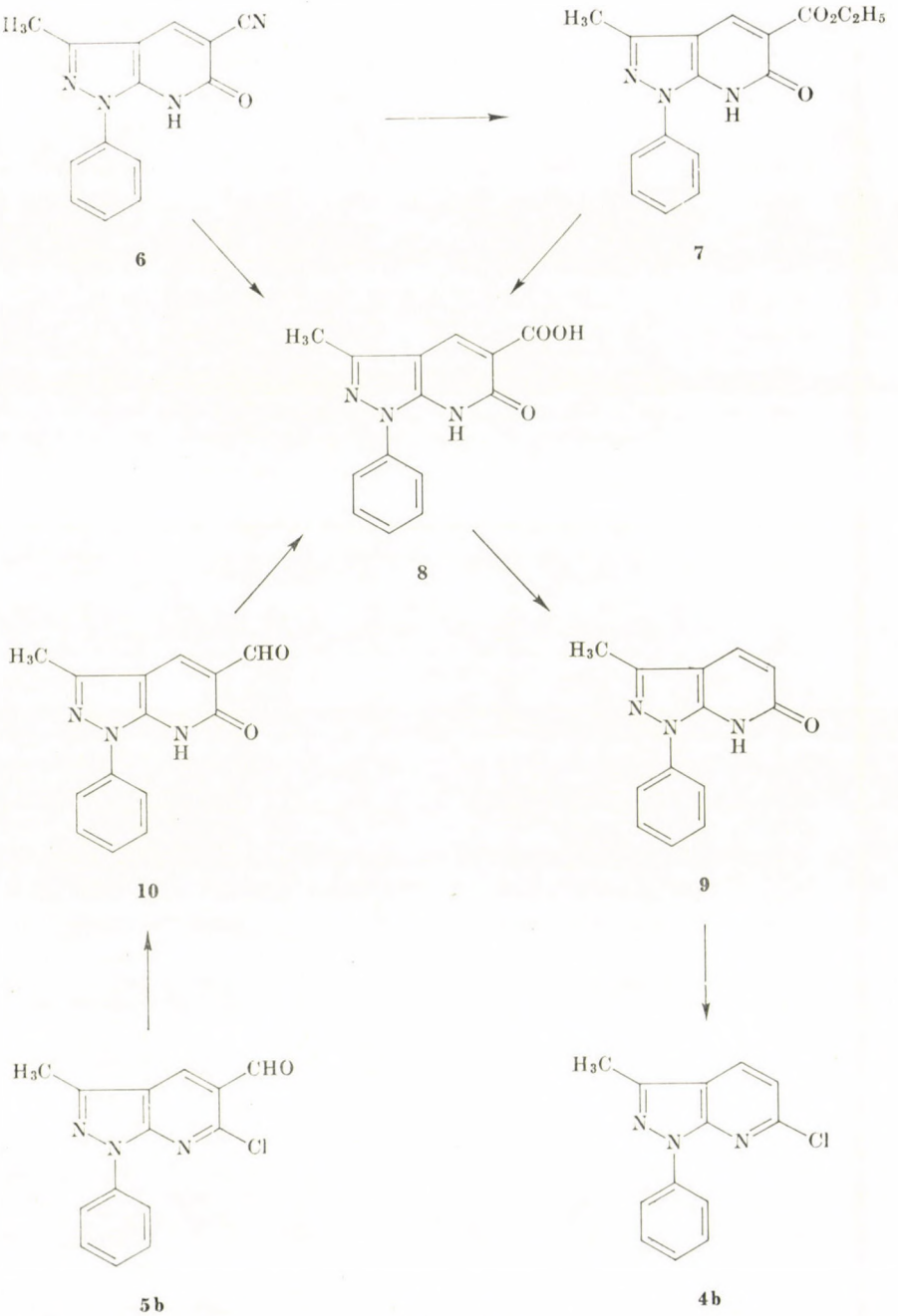
H3C
CN
N
N
N
H
O
6
H3C
CO2C2H5
N
N
N
H
O
7
H3C
COOH
N
N
N
H
O
8
H3C
CHO
N
N
N
H
O
10
H3C
N
N
N
H
O
9
H3C
CHO
N
N
N
Cl
5b
H3C
N
N
N
Cl
4b

Scheme 2

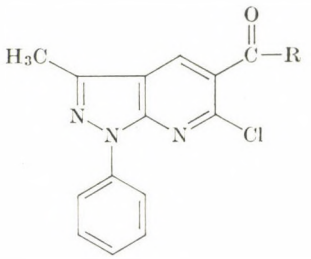

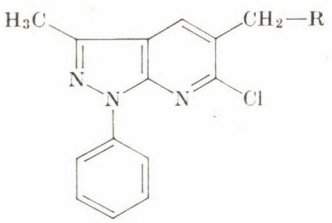

11 R = OH
12 R = OEt
13 R = Cl
14 R = NH—R^1
a R^1 = Ph
b R^1 = CH_2—CH_2—(3,4-dimethoxyphenyl)

15 R = OH
16 R = O—C(=O)—Ar
a Ar = Ph
b Ar = Py-3
17 R = Cl
18 R = NH—R^1
a R^1 = Ph
b R^1 = CH_2—CH_2—(3,4-dimethoxyphenyl)
c R^1 = *n*-Bu

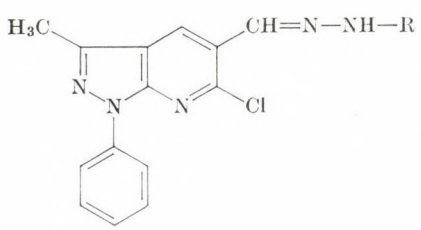

19a R = H
b R = Ph
c R = $CONH_2$

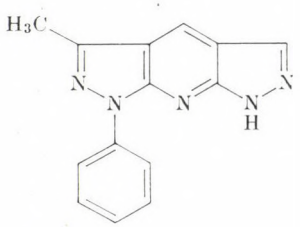

20

Scheme 3

in reasonable yields. Separation of the products was performed by column chromatography on silica.

Chemical transformations of compound **5b** allowed the preparation of a number of pyrazolo[3,4-*b*]pyridine derivatives shown in Scheme 3.

$KMnO_4$ oxidation of **5b** gave the carboxylic acid **11** which was esterified to **12** or chlorinated to **13**. Aminolysis of the latter gave rise to carboxamide derivatives **14a** and **b**.

On $NaBH_4$ reduction of **5b**, the hydroxymethyl derivative **15** was obtained. It was esterified with acid chlorides to give **16a, b** or chlorinated to **17**. Aminolysis of **17** with primary amines resulted in the secondary amines **18**.

The aldehyde grouping of **5b** reacted with hydrazine and its derivatives to form hydrazone compounds **19a—c**. Prolonged heating of **5b** (or **19a**) with hydrazine hydrate gave, however, the tricyclic dipyrazolo[3,4-*b*; 4',3'-*e*]-pyridine derivative **20**. Similar cyclization could not be effected by phenylhydrazine; even after 60 hours of heating exclusively **19b** was isolated. On treatment with hydrazine hydrate, however, **19b** was also converted into **20** in good yield.

Experimental

M.p.'s are uncorrected. All new compounds had satisfactory C, H, N, Cl and/or S microanalyses, accurate within 0.40%. IR spectra were obtained on a Zeiss UR 20 type spectrometer in KBr pellets and UV spectra on a Unicam SP 800 A spectrometer in 96% ethanol solution. The IR data are given as ν_{max} in cm^{-1}, the UV data as $\lambda_{max}(\log \varepsilon)$ in nm. ^{1}H-NMR spectra were recorded on a Bruker WP-80 (80 MHz) instrument, unless otherwise indicated. The chemical shifts are given in ppm (δ) downfield from TMS as internal standard.

Vilsmeier—Haack reaction of compounds 1

Compound **1** [1] (10 mmol) was warmed on a water-bath at 90—95 °C for 3 h with 6.3 mL (70 mmol) of $POCl_3$. DMF (3.2 mL, 40 mmol) was added gradually and warming was continued for an additional 2 h. After pouring into ice-water the separated solid was filtered off, washed with 2 *N* HCl and dried. The crude product was chromatographed on 50-fold weight of silica with dichloromethane–petroleum ether (b.p. 40—70 °C) 1 : 1 vol/vol mixture as eluent. Compounds **4** and **5** synthesized in this way are listed in Table I.

1-Phenyl-3-methylpyrazolo[3,4-*b*]pyridin-6(7*H*)-one-5-carbonitrile (6)

This compound was synthesized by the literature method [3].

Ethyl 1-phenyl-3-methylpyrazolo[3,4-*b*]pyridin-6(7*H*)-one-5-carboxylate (7)

Method A

1-Phenyl-3-methyl-5-aminopyrazole-4-carbaldehyde [1, 3] (4.0 g; 20 mmol) and ethyl malonate (5.0 mL; 33 mmol) were boiled in AcOH (50 mL) for 30 h. After evaporation to one-third volume and standing overnight, crystalline **7** separated from the reaction mixture.

Method B

Compound **6** (1.0 g; 4 mmol) was dissolved in 15 mL of *conc* H_2SO_4. To the solution 15 mL of EtOH was added gradually, and the mixture was warmed on a water-bath for 10 h. On pouring into ice-water, compound **7** separated which was filtered off, dried and recrystallized.

1-Phenyl-3-methylpyrazolo[3,4-*b*]pyridin-6(7*H*)-one-5-carboxylic acid (8)

Method A

Compound **6** (1.0 g; 4 mmol) was refluxed in 40 mL of 5% NaOH for 5 h. After cooling the solution was acidified, the separated solid was filtered off, washed, dried and recrystallized.

Table I

Some physical and spectral data of compounds **4** *and* **5**

Compd.	Yield, %	M.p., °C (solvent)	UV λ_{max} (log ε)	IR		^{1}H-NMR[c], δ ppm			
				νC=O	νaromatic	aromatic	R[a]	4-CH	R
4a	14	65—6 (a)	254 (4.11) 310 (3.38)	—	1603 s 762 s 1510 m 696 m	7.2—7.65 m 8.1—8.3 m	8.16 s[d]	8.03 d[d] (J = 8.5 Hz)	7.19 d[d]
5a	53	155—8 (EtOH)	260 (4.38) 270 sh (4.32) 310 (3.79)	1694 s	1598 s 775 s 1510 m 702 m	7.25—8.0 m 8.2—8.6 m	8.46 s[d]	8.82 s (1H)	10.64 s (1H)
4b	23	87—8 (a)	257 (4.37) 316 (3.61)	—	1596 s 769 s 1515 s 701 m	7.3—7.65 m 8.1—8.3 m	2.61 s (3H)	7.94 d[d] (J = 8.5 Hz)	7.16 d[e]
5b	47	184—6 (MeCN)	264 (4.35) 270 sh (4.26) 317 (3.76)	1693 ms	1600 s 761 s 1520 m 700 w	7.3—7.65 m 8.1—8.3 m (5H)	2.65 s (3H)	8.62 s (1H)	10.50 s (1H)
4c	25	128—30 (a)	252 (4.17) 263sh (4.15) 335 (3.68)	—	1600 s 771 s 1515 s 700 m	7.3—7.7 m 8.2—8.4 m	7.3—7.7 m[d] 7.8—8.1 m	8.33 d[d] (J = 8 Hz)	7.25 d[de]
5c	49	208—10 (EtOAc)	255[b] 268 sh 337	1694 m	1598 s 765 s 1516 m 700 m	7.3—7.7 m 8.1—8.4 m	7.3—7.7 m[d] 7.8—8.1 m	8.94 s (1H)	10.52 s (1H)
4d	13	142—3 (a)	260 (4.21) 310 (3.46)	—	1603 m 834 ms 1508 m	7.48 d 8.23 d (J = 9 Hz)	8.16 s[d]	8.04 d[d] (J = 8 Hz)	7.20 d[de]
5d	53	189—91 (EtOAc)	264 (4.44) 307 (3.83)	1685 ms	1619 s 839 s 1510 s	7.50d—2H 8.22 d (J = 9 Hz)	8.32 s[d]	8.69 s (1H)	10.50 s (1H)
4e	8	251—4 (EtOH)	230[b] 283 sh 325	not measured		8.39d—2H 8.66d—2H (J = 9.5 Hz)	8.25 s (1H)	8.10 d (1H) (J = 8.5 Hz)	7.32 d[e]
5e	35	216—9 (EtOAc)	231[b] 284 sh 326	1685 m	1605 s 1532 s 1510 s 1350 s 865 s	8.37 d 8.59 d (J = 9.5 Hz)	8.37 s[d]	8.70 s[d]	10.37 s (1H)

[a] Petroleum ether (b.p. 40—70 °C); [b] Owing to insufficient solubility, log ε cannot be given; [c] All spectra recorded in $CDCl_3$ solution; [d] Overlapping with the 1-PhH signal; [e] Overlapping with the solvent signal.

Method B

Compound **7** (0.3 g; 1 mmol) was refluxed in 12 mL of 5% NaOH for 2 h. The mixture was worked up as given in *Method A*.

Method C

Compound **10** (0.5 g; 2 mmol) was dissolved, with boiling, in 100 mL of 2% NaOH containing 15 drops of pyridine. After cooling to room temperature 0.35 g (2.2 mmol) of $KMnO_4$ was added to the solution and the mixture was stirred for 8 h. The precipitated MnO_2 was filtered off and the filtrate acidified. The separated solid was filtered off, washed, dried and recrystallized.

1-Phenyl-3-methylpyrazolo[3,4-*b*]pyridin-6(7*H*)-one (9)

Compound **8** (1.0 g; 3.7 mmol) was heated at 260 °C for 3 h in a sublimation apparatus. The sublimed product was collected and recrystallized.

1-Phenyl-3-methylpyrazolo[3,4-*b*]pyridin-6(7*H*)-one-5-carbaldehyde (10)

Method A

Compound **5b** (2.7 g; 10 mmol) and 0.4 g (10 mmol) of powdered NaOH were suspended in 20 mL of DMF and the suspension was warmed on a water-bath for 6 h, then poured into water. The precipitated solid was filtered off, washed, dried and recrystallized.

Method B

Compound **5b** (2.0 g; 7.5 mmol) was dissolved in 10 mL of *conc* H_2SO_4. The solution was warmed on a water-bath for 3 h, then poured into ice-water and the precipitated solid isolated as given in *Method A*.

1-Phenyl-3-methyl-6-chloropyrazolo[3,4-*b*]pyridine-5-carboxylic acid (11)

Compound **5b** (10.0 g; 37 mmol) and 10.0 g (63 mmol) of powdered $KMnO_4$ were suspended in 100 mL of pyridine. While stirring and cooling, 6 mL of water was added dropwise at room temperature and the mixture was stirred for additional 6 h. After the addition of 150 mL of water, the insoluble material was filtered off. The filtrate was neutralized with 5 *N* HCl, treated with activated carbon, filtered and the filtrate acidified. The precipitated creamy solid was filtered off to give 6.7 g of **11**.

Ethyl 1-phenyl-3-methyl-6-chloropyrazolo[3,4-*b*]pyridine-5-carboxylate (12)

Compound **11** (1.5 g; 5.2 mmol) was refluxed for 7 h in 15 mL of EtOH containing 1 mL of *conc* H_2SO_4 to give a clear solution. On cooling 1.4 g of **12** crystallized.

1-Phenyl-3-methyl-6-chloropyrazolo[3,4-*b*]pyridine-5-carboxylic acid chloride (13)

To 4.9 g (17 mmol) of compound **11** 30 mL of $SOCl_2$ was added and the mixture was warmed on a water-bath for 4 h. The resulting yellow solution was evaporated, the residue suspended in petroleum ether (b.p. 40—70 °C) and filtered to give 4.9 g of **13**.

1-Phenyl-3-methyl-6-chloropyrazolo[3,4-*b*]pyridine-5-carboxamides (14)

(*a*) Compound **13** (0.9 g; 3mmol) dissolved in 15 mL of $CHCl_3$ was added at room temperature, with cooling, to a solution of 0.28 mL (3 mmol) of aniline and 0.42 mL (3 mmol) of Et_3N in 10 mL of $CHCl_3$. The reaction mixture was allowed to stand at room temperature for 60 h, then extracted successively with 2 *N* HCl, water, 5% NaOH and water. The $CHCl_3$ phase was dried, evaporated and the residue recrystallized to give 0.42 g of **14a**.

Table II

Some physical and spectral data of compounds **6—10**

Compd.	Yield, % (Method)	M.p., °C (Solvent)	UV λ_{max}(log ε)	IR		^{1}H-NMR[e], δ ppm			
				νHN—C=O / νR[c]		Solvent	3-C<u>H</u>$_3$	4-C<u>H</u>	R[e]
6	59	306—8[a] (AcOH)	264 (4.38) 315 (3.93)	3600—3300 w, br 3300—2600 w, br 1663 s	2239 m	TFA[f]	2.80 s (3H)	8.82 s (1H)	—
7	28 (*A*) 42 (*B*)	193—4 (PhH)	266 (4.43) 316 (3.99)	3600—3300 w, br 3200—2500 w, br 1663 s	1625 m[d]	$CDCl_3$	2.59 s (3H)	8.55 s (1H)	1.47 t—3H 4.48q—2H (J = 7 Hz)
8	66 (*A*) 82 (*B*) 52 (*C*)	257—60 (MeCN)	263 (4.33) 315 (3.92)	3200 sh, 3160 m 3050 m 1648 s	1710 s	DMSO-d_6	g	8.75 s (1H)	—
9	84	175—8 (PhH)	258 (4.10) 296 (3.68)	3200—2600 m, br 3069 m 1668 vs	—	$CDCl_3$	2.48 s (3H)	7.75 d[h] (J = 9 Hz)	6.41 d (1H) (J = 9 Hz)
10	22 (*A*) 62 (*B*)	247—50 (BuOH)	270[b] 331	3600—3300 w, br 3300—2600 m, br 1660 s	1687 ms	TFA-d_1	2.75 s (3H)	8.86 s (1H)	10.06 s (1H)

[a] *Lit.* [3] m.p. 316 °C; [b] Owing to insufficient solubility, log ε cannot be given; [c] R: substituent in position 5; [d] Hydrogen bonded C=O (*cf.* [4]); [e] 1-Ph protons: multiplet at 7.1—8.5 in $CDCl_3$ or DMSO-d_6, singulet at 7.75—7.80 in TFA (integral: 5H); [f] Spectrum recorded on a Perkin-Elmer R 12 (60 MHz) instrument; [g] Obscured by the solvent signal; [h] Overlapping with the 1-Ph<u>H</u> signal.

(*b*) Compound **13** (1.5 g; 5 mmol) dissolved in 15 mL of $CHCl_3$ was added at room temperature, with cooling, to a solution of 1.8 g (10 mmol) of 2-(3,4-dimethoxyphenyl)ethylamine in 10 mL of $CHCl_3$. The solution was allowed to stand at room temperature for 60 h, then extracted with water. The $CHCl_3$ phase was dried and evaporated to about one-third volume. On cooling 1.8 g of **14b** crystallized.

1-Phenyl-3-methyl-5-hydroxymethyl-6-chloropyrazolo[3,4-*b*]pyridine (15)

Compound **5b** (13.6 g; 50 mmol) was suspended in 300 mL of MeOH. $NaBH_4$ (2.0 g; 50 mmol) was added in small portions while stirring and cooling. The resulting solution was allowed to stand overnight at room temperature, then evaporated to about one-third volume. After the addition of water the precipitated solid was filtered off, washed, dried and recrystallized to obtain 10.8 g of **15**.

1-Phenyl-3-methyl-5-acyloxymethyl-6-chloropyrazolo[3,4-*b*]pyridine (16)

To 5.5 g (20 mmol) of compound **15** dissolved in 45 mL of acetone there was added 25 mmol of Et_3N in 10 mL of acetone, with stirring; this was followed by the addition of a solution of 25 mmol of benzoyl chloride or nicotinoyl chloride in 25 mL of acetone. The reaction mixture was stirred for 10 h at room temperature and then evaporated to dryness. The residue was taken up in water, filtered, washed successively with 2 *N* HCl, water, 5% NaOH and water, dried and recrystallized.

1-Phenyl-3-methyl-5-chloromethyl-6-chloropyrazolo[3,4-*b*]pyridine (17)

Compound **15** (10 g; 36.5 mmol) was dissolved in 60 mL of benzene. To the solution 15 mL (0.2 mol) of $SOCl_2$ was added gradually, and the mixture was warmed on a water-bath for 8 h, then poured into ice-water. The phases were separated, the benzene layer washed with water, dried and evaporated. The residue was taken up in cyclohexane and filtered to obtain 8.0 g of **17**.

1-Phenyl-3-methyl-5-(substituted amino)methyl-6-chloropyrazolo[3,4-*b*]pyridines (18)

To 1.45 g (5 mmol) of compound **17**, suspended in 15 mL of EtOH, 15 mmol of aniline, 2-(3,4-dimethoxyphenyl)ethylamine or *n*-butylamine was added, and the reaction mixture was refluxed for 5 h. After cooling overnight, the separated solid was filtered off and recrystallized to give **18a**, **b** and **c**, respectively.

1-Phenyl-3-methyl-6-chloropyrazolo[3,4-*b*]pyridine-5-carbaldehyde hydrazone derivatives (19)

To 5 mmol of compound **5b**, suspended in 60 mL of EtOH, 5.5 mmol of hydrazine hydrate, phenylhydrazine or semicarbazide was added and the mixture refluxed for 4 h. After cooling overnight the crystallized product was filtered off to obtain the corresponding hydrazone (**19a**) phenylhydrazone (**19b**) or semicarbazone (**19c**), respectively.

1-Phenyl-3-methyl-1,7-dihydrodipyrazolo[3,4-*b*; 4',3'-*e*]pyridine (20)

To 2 mmol of compound **5b**, **19a** or **19b**, suspended in 10 mL of EtOH, 2 mL of hydrazine hydrate was added and the mixture was refluxed for 18 h. After cooling, the crystalline product **20** (yields: 81%, 92% and 73%, respectively) was filtered off and recrystallized.

M.p. 236—238 °C (*i*-PrOH).

UV: 265 (4.47), 310 (4.03), 315 (4.05), 342 (3.87).

IR: 3220 ms, br (NH), 1625 s (C=N), 1602 ms, 1508 ms (aromatic), 756 ms, 695 m (monosubst.).

^{1}H-NMR (DMSO-d_6): 2.69 s (3-C$\underline{H}_3$); 8.42 s and 8.82 s (4-C$\underline{H}$ and 5-C$\underline{H}$); 7.3—7.85 m and 8.35—8.6 m (1-Ph$\underline{H}$); 13.75 bs (N$\underline{H}$).

Table III

Some physical and spectral data of compounds **11**—**14**

Compd.	Yield, %	M.p., °C (Solvent)	UV λ_{max} (log ε)	IR		^{1}H-NMR[a], δ ppm			
				νC=O	νR	Solvent	3-C<u>H</u>$_3$	4-C<u>H</u>	R
11	63	214—5 (EtOH)	263 (4.45)	1705 s	3200—2400 w, br (OH)	DMSO-d_6[b]	2.63 s (3H)	8.84 s (1H)	5.5 bs (changeable)
12	86	120—1 (EtOH)	264 (4.46)	1735 s	1246 vs, 1145 m (COC)	DMSO-d_6[b] + $CDCl_3$	2.66 s (3H)	8.68 s (1H)	1.46 t—3H 4.81 q—2H (J = 7 Hz)
13	94	144	not measured	1777 s	—	TFA[b]	3.02 s (3H)	8.37 s (1H)	—
14a	40	178 (EtOH)	264 (4.35) 322 (3.38)	1665 ms 1558 ms	3280 m, br (NH)	$CDCl_3$	2.66 s (3H)	8.56 s (1H)	7.1—7.3 m[c]
14b	80	162—4 (EtOH)	262 (4.25) 320 (3.32)	1670 s	3265 ms (NH) 1265 m, 1035 m (OCH_3) 895 w, 813 m (trisubst.)	TFA[b]	2.95 s (3H)	8.72 s (1H)	6.9—7.3 m (3H; Ar<u>H</u>) 3.97 s (6H; CH_3O) 3.1 bs; 4.0 bs (2×2H, —(C<u>H</u>$_2$)$_2$—)

[a] 1-Ph protons: multiplet at 7.3—8.4 in DMSO-d_6 or $CDCl_3$, singulet at 7.75 in TFA (integral: 5H); [b] Spectrum recorded on a Perkin-Elmer R 12 (60 MHz) instrument; [c] Overlapping with the 1-Ph<u>H</u> signal.

Table IV

Some physical and spectral data of compounds **15—18**

Compd.	Yield, %	M.p., °C (Solvent)	UV λ_{max} (log ε)	IR νR	^{1}H-NMR[b], δ ppm				
					Solvent	3-C<u>H</u>$_3$	4-C<u>H</u>	5-C<u>H</u>$_2$	R
15	79	118– 9 (PhH)	not measured	3600—3000 m, br (OH)	$CDCl_3$[c]	2.60 s (3H)	8.16 s[d]	4.84 s (2H)	—
16a	58	140—1 (EtOH)	259 (4.28) 320 (3.26)	1735 s (C=O) 1280 vs, 1140 m (COC)	$CDCl_3$[c]	2.63 s (3H)	8.15 s[d]	5.61 s (2H)	7.2—8.5 m[d]
16b	61	160 (BuOH)	260 (4.27) 320 (3.34)	1735 s (C=O) 1290 s, 1130 m (COC)	$CDCl_3$	2.62 s (3H)	8.14 s[d]	5.58 s (2H)	9.25 b; 8.75b (1H) (1H) 8.3 b[d]; 7.6 b[d]
17	75	140—2 (PhH)	261 (4.23) 321 (3.35)	—	$CDCl_3$	2.62 s (3H)	8.13 s[d]	4.78 s (2H)	—
18a	48	170—5 (PhMe)	260[a] 325	3280 m, br (NH)	$CDCl_3$	2.56 s (3H)	8.03 s[d]	4.52 s (2H)	4.22 bs — 1H (changeable) 6.5—7.7 m[d]
18b	62	120 (MeCN)	261 (4.24) 323 (3.40)	3295 w (NH) 1262 s, 1040 m (OCH_3) 860 w, 817 m (trisubst.)	C_6D_6	2.34 s (3H)	7.78 s[d]	3.83 s (2H)	1.55 bs — 1H (changeable) 2.83 t—4H[e] 3.53 s; 3.56 s—6H 6.77 s—3H
18c	88	90—3 (EtOH)	260 (4.23) 322 (3.40)	3300 w (NH)	TFA[e]	2.92 s (3H)	8.82 s (1H)	4.85 s (2H)	1.02 t—3H 1.7—2.2 m—4H 3.5 bs—2H

[a] Owing to insufficient solubility, log ε cannot be given; [b] 1-Ph protons: multiplet at 7.2—8.5 in $CDCl_3$, at 7.0—8.8 in C_6D_6; singulet at 7.70 in TFA (integral: 5H); [c] Spectrum recorded on a Perkin-Elmer R 12 (60 MHz) instrument; [d] Overlapping with the 1-PhH signal; [e] After addition of TFA: 2.37 t (J = 6 Hz), 2H, C—C<u>H</u>$_2$—C; 3.09 t (J = 6 Hz), 2H, C—C<u>H</u>$_2$—N.

Table V

Some physical and spectral data of compounds **19**

Compd.	Yield, %	M.p., °C (Solvent)	UV λ_{max} (log ε)	IR		^{1}H-NMR[a], δ ppm				
				νC=N	νNH–R	Solvent	3-C<u>H</u>$_3$	4-C<u>H</u>[b]	C<u>H</u>=N[b]	R
19a	81	155—8 (MeOH)	292 (4.46) 345 (3.76)	1620 sh	3370 mw 3290 w 3200 w	DMSO-d_6[c]	2.64 s[d]	8.32 s (1H)	8.64 s (1H)	5.42 s—2H (changeable)
19b	86	229—31 (BuOH)	265 (4.08) 343 (4.18) 395 (3.79)	1647 sh	3310 m	DMSO-d_6	2.68 s[d]	8.25 s (1H)	8.78 s (1H)	7.1—7.8 m[e] 10.75 bs—1H (changeable)
19c	76	280—3 (DMF)	258 (3.94) 294 (4.21) 342 (3.50)	1615 sh	3485 ms 3400— —2800 m 1712 s	TFA-d_1	2.86 s (3H)	8.45 s (1H)	9.03 s (1H)	—

[a] 1-Ph protons: multiplet at 7.1—8.3 in DMSO-d_6, singulet at 7.56 in TFA-d_1; [b] Assignment is arbitrary; [c] Spectrum recorded on a Perkin-Elmer R 12 (60 MHz) instrument; [d] Overlapping with the solvent signal; [e] Overlapping with the 1-PhH signal.

*

The authors are indebted to Dr. I. REMPORT and his group for the microanalyses, to Dr. K. HORVÁTH and Miss I. SZILÁGYI for the spectra and to Miss K. HÓDI and Mrs. M. DOUBLINSZKY for technical assistance.

REFERENCES

[1] SIMAY, A., TAKÁCS, K., HORVÁTH, K., DVORTSÁK, P.: Acta Chim. Acad. Sci. Hung., **105,** 127 (1980)
[2] (*a*) METH-COHN, O., NARINE, B.: Tetrahedron Letters, **1978,** 2045; (*b*) *Idem.*: PCT Int. Appl. 79 00,540; Chem. Abstr., **92,** 111035 (1980)
[3] HÄUFEL, J., BREITMAIER, E.: Angew. Chem., **86,** 671 (1974)
[4] SCHNELLER, S. W., MOORE, D. R.: J. Heterocycl. Chem., **1978,** 319

Antal SIMAY
Kálmán TAKÁCS
László TÓTH
H-1325 Budapest, P.O.B. 110

Acta Chimica Academiae Scientiarum Hungaricae, Tomus 109 (2), pp. 189–198 (1982)

PREPARATION AND STUDY OF CHELATING RESINS, III

PROTONATION STUDIES OF A NEW CHELATING ION-EXCHANGE RESIN WITH DIETHYLENE TRIAMINE TETRAACETIC ACID FUNCTIONAL GROUPS

Ö. SZABADKA[1], K. W. BURTON[2] and J. INCZÉDY[1]*

([1] Department of Analytical Chemistry, University of Veszprém, Veszprém, [2] Department of Science, The Polytechnic of Wales, Pontypridd, CF37 1DL, U.K.)

Received January 12, 1981

Accepted for publication February 17, 1981

The protonation constants of the DTTA chelating ion exchange resin, containing diethylene triamine tetraacetic acid functional groups, were determined at 25 °C by batch titration of the resin with standard alkali at ionic strengths of 0.01, 0.1 and 1.0 mol dm^{-3}.

The constants were calculated using a modified BJERRUM $\bar{n}$ method and a general resin protonation equation to give the following values:

$$\log \beta_1 = 10.38 \pm 0.05$$

$$\log \beta_2 = 18.74 \pm 0.10$$

$$\log \beta_3 = 23.04 \pm 0.11$$

$$\log \beta_4 = 25.87 \pm 0.11$$

The theoretical titration curve generated from these values agreed well with the experimental data obtained at all three ionic strengths.

Further refinement of the protonation constants was carried out using a modified MINIQUAD computer programme, which yielded protonation constants with an even better fit to the experimental data, although the values of the protonation constants appeared to shift slightly with ionic strength.

Introduction

Previous work has shown that chelating ion-exchange resins of well defined and reproducible chemical composition containing either polyamino- or polyamino-polycarboxylic acid functional groups can be synthetized by careful amination or amination and subsequent carboxymethylation of chloromethylated polystyrene-divinylbenzene copolymer [1]. The resin described in this paper (the DTTA resin) is one containing diethylene triamine tetraacetic acid functional groups (Fig. 1).

As part of the programme aiming to study the properties of these resins and the development of analytical methods based upon the use of these it is

* To whom correspondence should be addressed.

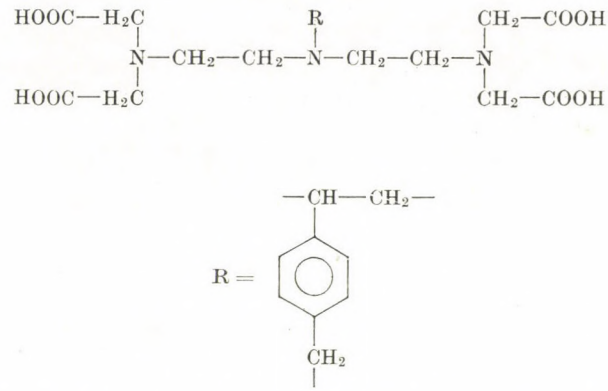

Fig. 1. The immobilised active group of the DTTA-resin. R: the matrix of the resin

necessary to establish values for the protonation and cation-resin stability constants. The determination of the protonation constants of Ligandex-E, containing ethylene diamine triacetic acid functional groups, has been described earlier [2], and the techniques developed in that work have now been applied to a study of the protonation equilibria of the DTTA resin. It was shown there that stepwise protonation equilibria of the type

$$\overline{R}^- + \overline{G}^+ + H^+_{aq} \rightleftharpoons \overline{RH} + G^+_{aq} \tag{1}$$

may be described by equations of the form

$$\log K = pH + \log \frac{1 - \bar{\alpha}}{\bar{\alpha}} + \log \frac{a_G}{(G)} \tag{2}$$

where the bar refers to parameters in the resin phase, $\bar{\alpha}$ being the degree of dissociation of the resin:

$$\bar{\alpha} = \frac{\overline{R}}{\overline{RH} + \overline{R}},$$

(G) is the total molality of the counter ion in the resin phase,
a_G is the activity of the counter ion in the aqueous solution, and pH refers to the pH of the aqueous solution. These equations enabled the calculation of the stepwise protonation constants of the Ligandex-E resin.

By defining $p\overline{H}$, the pH of the resin phase as

$$p\overline{H} = pH + \log \frac{a_G}{(G)}$$

and correcting for the autodissociation of water by introducing

$$\bar{\alpha}^* = \bar{\alpha} + \frac{(H^+) + (OH^-)}{C_{\bar{L}}}$$

[3], where $C_{\bar{L}}$ is the analytical concentration of the active groups in the resin phase, mmol · g^{-1} water, equation (2) reduces to the form

$$\log K = p\bar{H} + \log \frac{1 - \bar{\alpha}^*}{\bar{\alpha}^*} \tag{3}$$

being completely analogous to those equations describing homogeneous systems. It therefore follows that any of the conventional homogeneous protonation equations, such as that of BJERRUM's $\bar{n}$ method, may be applied to the resin equilibria. This has been discussed more fully in recent papers [4, 5].

Experimental

To study the protonation of the DTTA resin, a batch method was used to ensure that full equilibration was reached. The hydrogen form of the resin converted by treatment with dilute hydrochloric acid was washed with distilled water until free from chloride ions, and then dried in air. The water content of the air-dried resin was determined by drying small samples of the resin at 110 °C for 24 hours. The titration curves were obtained over a range of ionic strengths $I = 0.01$, 0.1, 1.0 by weighing exactly known quantities (0.5 + 0.01 g) of the air dried hydrogen form resin into 100 cm^3 Quickfit Erlenmeyer flasks, adding various known amounts of 0.1 *M* carbonate-free potassium hydroxide solution, followed by the requisite quantity of potassium chloride solution, to give the desired ionic strength upon dilution to a final volume of 100 cm^3 with CO_2-free distilled water. The flasks were sealed under argon atmosphere and then left at a constant temperature for 2—3 weeks until equilibration had been reached. Measurements of the solution pH were then made under argon atmosphere using a calibrated glass electrode. Several series of measurements were necessary in order to establish that equilibrium had been reached.

After measurement of the pH, the resin samples were separated from the solution phase by centrifugation, the resin weighed, and then dried in a vacuum oven at 80 °C to constant weight. This weight difference, when referred to the dry hydrogen form resin, gave the water content, $\overline{H_2O}$, in g g^{-1}.

Uptake of potassium ions by the resin occurs by neutralization of the hydrogen form resin (carboxylic acid functional groups — chemically bound potassium ions) and by ion invasion, as potassium chloride penetrates the resin lattice because of osmotic pressure differences between the aqueous and resin phases (invaded potassium ions). The quantities of potassium ions in the resin arising from these two processes were obtained by eluting the resin with a known amount of standard 0.1 *M* nitric acid, washing well with distilled water and then determining the chemically bound potassium ions from an acid-base titration, and the 'invaded' potassium ions from a Mohr's titration of the associated chloride ions. The washed resin was then dried to constant weight at 105 °C to give the weight for the dry resin in the hydrogen form.

Results and Discussion

The experimental data obtained are summarized in Tables I, II and III.

The plots of $\bar{G}_K$, the amount of chemically bound potassium ions, against pH for the three ionic strengths all show a major inflection point at $\bar{G}_K =$

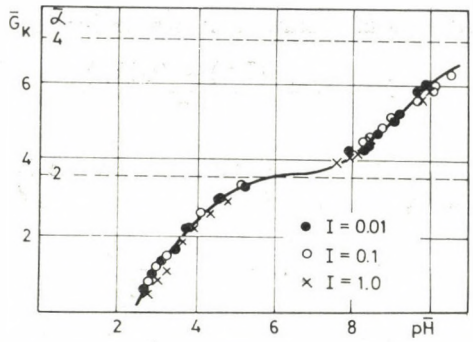

Fig. 2. The quantity of chemically bound ions as a function of the calculated $p\bar{H}$ of the resin phase. This curve is used for the determination of the capacity of the resin, Q and for the degree of titration in the resin phase, $\bar{\alpha}$

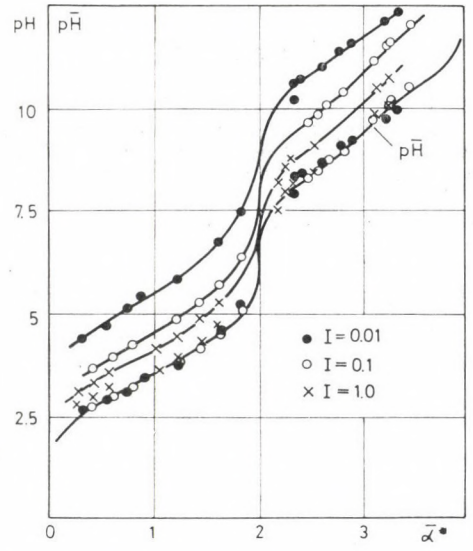

Fig. 3. pH of the equilibrium solution as a function of the real degree of titration in the resin phase, $\bar{\alpha}^*$, in solutions of ionic strength 0.01, 0.1 and 1.0

$= 3.60$ mmole g^{-1} resin, and a further not so well defined reflection at $\bar{G}_K = 5.40$ mmole g^{-1} resin (Fig. 2). This gives a value for Q, the capacity of the resin, of 1.80 mmole g^{-1} resin, from which the $\bar{\alpha}^*$-values may be calculated, and then plotted as a function of pH and of $p\bar{H}$ (Fig. 3). It may be seen that with the $p\bar{H} - \bar{\alpha}^*$ plot the points all appear to lie on the same titration curve, from which it may be inferred that the protonation constants are apparently independent of the ionic strength of the aqueous solution. This was also observed in the earlier work with the Ligandex-E resin.

Table I

Titration data at an ionic strength of 0.01

pH	$p\overline{H}$	$\overline{G}_K$	$\overline{G}_I$	$\overline{H_2O}$	(G)	$\overline{\alpha}^*$
4.370	2.624	0.596	0.033	1.256	0.501	0.335
4.720	2.838	1.013	0.033	1.528	0.685	0.567
5.070	3.041	1.374	0.033	1.467	0.959	0.768
5.430	3.420	1.642	0.033	1.821	0.920	0.918
5.800	3.690	2.179	0.033	1.911	1.158	1.218
6.770	4.568	2.921	0.033	2.066	1.430	1.632
7.440	5.203	3.242	0.033	2.112	1.551	1.811
10.190	7.874	4.186	0.033	2.270	1.859	2.339
10.590	8.281	4.208	0.033	2.320	1.828	2.351
10.680	8.360	4.317	0.033	2.320	1.875	2.412
10.970	8.623	4.680	0.033	2.360	1.997	2.615
11.410	9.048	5.006	0.033	2.440	2.065	2.797
11.540	9.170	5.170	0.033	2.470	2.107	2.888
12.100	9.710	5.818	0.033	2.652	2.206	3.250
12.270	9.871	6.012	0.033	2.687	2.250	3.359

Tables I, II, III: pH = solution pH; $p\overline{H}$ = resin pH; $\overline{G}_K$ = mmoles chemically bound K^+g^{-1} dry H—form resin; $\overline{G}_I$ = mmoles invaded K^+g^{-1} dry H—form resin; $\overline{H_2O}$ = water content, $g \cdot g^{-1}$ dry H—form resin; (G) = molality of total K^+, moles K^+ kg^{-1} water in the resin phase, $\overline{\alpha}^*$ = real degree of dissociation of the resin.

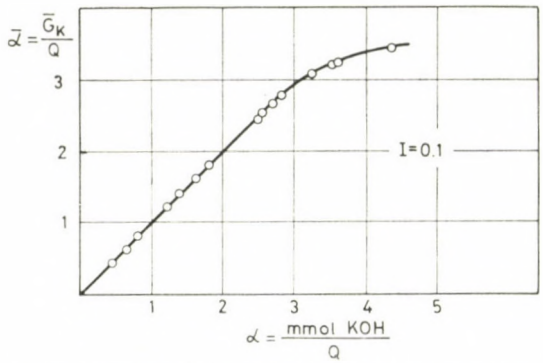

Fig. 4. The degree of the titration of the active groups in the resin, $\overline{\alpha}$, as a function of the degree of titration calculated from the added quantity of potassium hydroxide, α

It is also found, as with the Ligandex-E resin, that the uptake of potassium hydroxide by the DTTA resin is at first quantitative, but that this uptake falls off at higher α-values. This is shown in Fig. 4 for $I = 0.1$. On the other hand, the amount of invaded potassium chloride is apparently independent

Table II

Titration data at an ionic strength of 0.1

pH	$p\overline{H}$	$\overline{G}_K$	$\overline{G}_I$	$\overline{H_2O}$	(G)	$\overline{z}^*$
3.670	2.760	0.788	0.146	1.357	0.688	0.442
3.920	2.934	1.129	0.168	1.582	0.820	0.632
4.200	3.173	1.467	0.123	1.763	0.902	0.820
4.870	3.729	2.212	0.130	2.000	1.171	1.236
5.250	4.061	2.581	0.133	2.075	1.308	1.442
5.710	4.484	2.899	0.144	2.135	1.425	1.620
6.340	5.079	3.275	0.107	2.187	1.546	1.830
9.620	8.253	4.452	0.132	2.322	1.974	2.487
9.820	8.442	4.616	0.110	2.335	2.024	2.579
10.070	8.680	4.788	0.120	2.361	2.079	2.675
10.371	8.966	5.044	0.103	2.393	2.151	2.818
11.160	9.714	5.589	0.097	2.405	2.364	3.122
11.540	10.076	5.832	0.116	2.411	2.467	3.258
11.580	10.115	5.890	0.100	2.426	2.469	3.290
12.040	10.549	6.228	0.114	2.419	2.622	3.479

Table III

Titration data at an ionic strength of 1.00

pH	$p\overline{H}$	$\overline{G}_K$	$\overline{G}_I$	$\overline{H_2O}$	(G)	$\overline{z}^*$
3.110	2.756	0.523	1.013	1.116	1.377	0.294
3.320	2.948	0.801	1.025	1.275	1.433	0.448
3.590	3.203	1.043	1.071	1.424	1.485	0.583
4.110	3.634	1.839	1.053	1.587	1.822	1.028
4.400	3.891	2.184	1.039	1.638	1.968	1.220
4.820	4.288	2.560	1.018	1.725	2.074	1.430
5.260	4.708	2.862	1.009	1.782	2.172	1.599
8.130	7.519	3.916	0.949	1.955	2.489	2.187
8.560	7.940	4.036	0.946	1.964	2.537	2.255
8.730	8.106	4.151	0.971	1.999	2.563	2.319
9.060	8.426	4.523	0.967	2.094	2.622	2.527
10.490	9.820	5.605	1.002	2.318	2.851	3.131
10.700	10.017	5.822	1.006	2.327	2.934	3.252

of the degree of titration, but it is a function of the ionic strength of the aqueous phase, as would be expected (Table IV). Thus the water uptake should be defined by the degree of titration, that is to say, by the quantity of chemically bound potassium ions in the resin, as was found in the case of the Ligandex-E resin.

Table IV

The amount of potassium chloride in the resin phase, G_I, at various values of the ionic strength

Ionic Strength	G_I
0.01	0.03
0.1	0.12 ± 0.02
1.0	1.02 ± 0.04

It should be noted that when calculating the pH of the resin phase, $p\overline{H}$, the key parameters are the activity of the counter ion in the aqueous solution, a_G, and the molality of the counter ion in the resin phase, (G). As this latter

$$(G) = \frac{\bar{G}_K + \bar{G}_I}{\overline{H_2O}}$$

term is given by and both $\bar{G}_K$ and $\overline{H_2O}$ are functions of $\bar{\alpha}^*$, whereas $\bar{G}_I$ is essentially independent, it might be expected that (G) is also a function of $\bar{\alpha}^*$. In fact, plots of (G) against $\bar{\alpha}^*$ exhibit a linear behaviour for both the DTTA and Ligandex-E resins, and this relationship may be used to model protonation equilibria for any given solution pH, yielding the protonation constants [5].

It may be seen from the titration curves (Figs. 2, 3) that not all the inflection points are clearly defined, so that there must be some overlap of the protonation equilibria. Thus it is not possible to use the equations describing simple one step equilibria to calculate the protonation constants of the DTTA resin and it is necessary to employ more general equations to obtain values for two or more protonation constants simultaneously. As has been mentioned earlier, any of the conventional equations describing homogeneous protonation equilibria may be used to describe resin protonation equilibria after modification of the solution terms pH, $[H^+]$ and $[OH^-]$ to the resin terms $p\overline{H}$, (H^+) and (OH^-).

Thus using the modified BJERRUM $\bar{n}$ method, the following equations must be solved:

$$\bar{n} = \frac{(4 - \alpha) C_{\bar{L}} + (OH^-) - (H^+)}{C_{\bar{L}}} \tag{4}$$

$$\bar{n} = \frac{(H^+) K_1 + 2(H^+)^2 K_1 K_2 + 3(H^+)^3 K_1 K_2 K_3 + 4(H^+)^4 K_1 K_2 K_3 K_4}{1 + (H^+) K_1 + (H^+)^2 K_1 K_2 + (H^+)^3 K_1 K_2 K_3 + (H^+)^4 K_1 K_2 K_3 K_4}. \tag{5}$$

In fact, since there is a well defined inflection point in the titration curve at $\bar{\alpha}^* = 2$, the equations may be simplified into ones describing the pairs K_1 and K_2, and K_3 and K_4.

Alternatively, the general equation for resin protonation equilibria described by SZABADKA may be used [4]:

$$\sum_{j=0}^{4} (\bar{\alpha}^* - 4 + j)\beta'_j(H^+)^j = 0. \qquad (6)$$

Values of the four protonation constants obtained by using both of these methods, applying simple linear regression analysis, are summarized in Table V. These are the average values obtained by consideration of the data at all three ionic strengths. Results of analysis of variance to compare calculated and experimental $\bar{\alpha}^*$-values derived from these protonation constants are summarized in Table VI, and it may be seen from this that the constants

Table V

Protonation constants calculated by the BJERRUM $\bar{n}$ *method and the general equation for resin equilibria*

$\log \beta_1$	$\log \beta_2$	$\log \beta_3$	$\log \beta_4$
10.38 ± 0.05	18.74 ± 0.10	23.04 ± 0.11	25.87 ± 0.11

Table VI

Analysis of variance — comparison of calculated and experimental $\bar{\alpha}^*$ *values*

I	σ^2 due regression	σ^2 about regression	% Fit	N
0.01	13.84	0.12	99.2	15
0.10	16.16	0.04	99.7	15
1.00	10.54	0.04	99.6	13

N = number of observations

describe quite adequately the protonation equilibria of the DTTA resin, the fit of the calculated and experimental $\bar{\alpha}^*$-values is reasonably good. This is further confirmed by the theoretical titration curve shown in Figure 3 which upon visual examination appears to fit the experimental points well.

These protonation constant values were then used as input for a modified form* of the computer programme MINIQUAD [6], and runs carried out

* Details of modification available from K. W. BURTON.

with data for all three ionic strengths to obtain improved values for the protonation constants. This programme also carries out a statistical analysis of the residuals of the mass balance equations, by means of which it is possible to pick up any systematic errors in the chemical model or the experimental data. The protonation constants so obtained, and the statistical analysis of residuals, are summarized in Table VII. From these results it would appear that the agreement of data for any specific ionic strength is quite good, the standard deviations of the protonation constants being reasonably low.

Considering the somewhat limited number of observations, the approach of the residuals distribution to a Gaussian distribution is in fact quite close, the goodness of fit statistic χ^2 being substantially less than 12.60 (95% confidence level) in all three cases. However, the data at an ionic strength of 0.01 exhibit some abnormalities, there being negative skew (greater residuals for the lower $\bar{\alpha}^*$ values than expected for a normal distribution), and also a moment coefficient of kurtosis of 5.7 (leptokurtic behaviour). This is also borne out by the higher standard deviations in the protonation constant values obtained at $I = 0.01$. However, comparison of calculated and experi-

Table VII

Calculation of the logarithms of the overall protonation constants by means of the MINIQUAD *programme*

	Log of the overall protonation constants		
Ionic Strength	0.01	0.1	1.0
$\log \beta_1$	10.11 ± 0.05	10.59 ± 0.03	10.52 ± 0.05
$\log \beta_2$	18.67 ± 0.06	18.95 ± 0.04	18.94 ± 0.06
$\log \beta_3$	23.00 ± 0.13	23.14 ± 0.07	23.33 ± 0.09
$\log \beta_4$	25.62 ± 0.15	25.82 ± 0.09	26.30 ± 0.10

Statistical analysis of residuals

Parameter	0.01	0.1	1.0
Arithmetic Mean	—0.11 — 04	—0.11 — 0.6	—0.62 — 05
Mean Deviation	0.23 — 03	0.19 — 03	0.16 — 03
Standard Deviation	0.34 — 03	0.22 — 03	0.22 — 03
Variance	0.12 — 06	0.49 — 07	0.48 — 07
Moment Coefficient of Skewness	—0.11 + 01	—0.76 — 03	—0.23 + 00
Moment Coefficient of Kurtosis	0.57 + 01	0.21 + 01	0.33 + 01
Chi Square	8.93	5.73	2.31
Crystallographic Factor	0.011	0.007	0.006

mental $\bar{\alpha}^*$-values by analysis of variance shows that the fit is good (although only marginally better than that of Table VI), which further validates the values obtained for the protonation constants (Table VIII). It is nevertheless

Table VIII

Comparison of calculated MINIQUAD *and experimental* $\bar{\alpha}^*$*-values*

I	σ^2 (due regression)	σ^2 (about regression)	% Fit	N
0.01	12.81	0.08	99.4	15
0.1	14.03	0.03	99.8	15
1.0	10.92	0.04	99.7	13

found that there are greater deviations of the calculated values from the experimental ones at low $\bar{\alpha}^*$ (low pH), which might be brought about by the presence of a further overlapping protonation reaction involving a $-COO^-$ or $\geqslant N$ group. Computation of an additional (fifth) protonation constant on the basis of the present data, using MINIQUAD, is not possible, the standard deviations of the $\log \beta_4$ and $\log \beta_5$ values being too great. Further experimental work involving titration of the DTTA resin with acid must be carried out before such calculations may be attempted.

There would appear to be some shift in the protonation constant values at different ionic strengths, revealing somewhat lower values at an ionic strength of 0.01 mol dm^{-3} in most cases.

*

The authors wish to express their appreciation for the technical assistance provided by E. VARGA. K. W. BURTON visited Veszprém under the Anglo-Hungarian Cultural Exchange Agreement, and would like to thank the Institute of Cultural Relations. Budapest, and the British Council for the organization and financial assistance which made this possible.

REFERENCES

[1] SZABADKA, Ö., INCZÉDY, J.: Acta Chim. Acad. Sci. Hung., **99**, 11 (1979)
[2] SZABADKA, Ö., INCZÉDY J.: Acta Chim. Acad. Sci. Hung., **104**, 13 (1980)
[3] SCHWARZENBACH G.: Helv. Chim. Acta **33**, 947 (1950)
[4] SZABADKA, Ö., INCZÉDY J.: Fourth Int. Symp. Ion Exchange, Siófok, Hungary, May 1980; J. Chromatogr., **201**, 59 (1980)
[5] BURTON, K. W., SZABADKA, Ö., INCZÉDY J.: Fourth Int. Symp. Ion Exchange, Siófok, Hungary, May 1980; J. Chromatogr., **201**, 67 (1980)
[6] SABATINI, A., VANCE, A., GANS, P.: Talanta, **21**, 53 (1974)

Ödön SZABADKA
János INCZÉDY } H-8201 Veszprém
Kenneth Williams BURTON Pontypridd, CF37 1DL, U.K.

Acta Chimica Academiae Scientiarum Hungaricae, Tomus 109 (2), pp. 199—217 (1982)

BEITRÄGE ZUR KENNTNIS DER KRACKREAKTIONEN, IV

MECHANISMEN DER AN MORDENITEN VERLAUFENDEN KATALYTISCHEN REAKTIONEN VON PARAFFINISCHEN KOHLENWASSERSTOFFEN

H. K. BEYER,[1] F. RÉTI[1] und J. HORVÁTH[2]

([1] Zentralforschungsinstitut für Chemie der Ungarischen Akademie der Wissenschaften, Budapest, [2] Donau-Erdölverarbeitungskombinat, Százhalombatta)

Eingegangen am 30. Januar 1981

Zur Veröffentlichung angenommen am 17. Februar 1981

Es werden die bei der Umsetzung von Propan, *n*-Butan, *i*-Butan und *neo*-Pentan and Ca- und Sr-Mordenit sowie von *n*- und *i*-Butan an H-Mordenit verlaufenden Reaktionen untersucht. Die Methan (im Falle des *n*-Butans auch Äthan) als paraffinisches Reaktionsprodukt liefernde Krackung des Typs I und die Dehydrierung des Reaktanten sind unabhängig vom Olefinpartialdruck und erfordern keine sauren Zentren des Brönsted-Typs, sondern nur solche des Lewis-Typs. Die mit abnehmender Oberflächenkonzentration der sauren Brönstedzentren zugunsten der Dehydrierung eintretende Selektivitätsverschiebung wird mit der Annahme erklärt, daß für die Dehydrierung des paraffinischen Reaktanten eine Hydridabstraktion an einem sauren Lewiszentrum und gleichzeitig eine Protonenabstraktion an einem benachbarten basischen Brönstedzentrum erfolgen muß.

Die insbesondere am H-Mordenit verlaufende, bei der Umsetzung der Butane ausschließlich Propan liefernde Krackung des Typs II sowie die Isomerisierung und die Bildung längerkettiger Paraffine sind stark abhängig vom Olefinpartialdruck und verlaufen nur an saure Zentren des Brönsted-Typs aufweisenden Katalysatoren. Die experimentellen Ergebnisse sind nicht mit dem klassischen Karbeniumionenmechanismus der katalytischen Krackung zu vereinbaren. Für die Umsetzungen von Paraffinen mit Kettenlängen bis zu 5 C-Atomen wird ein Mechanismus angegeben, der auf intermolekularem Hydridtransfer und Hydrid-Methanion-Transfer zwischen dem (wahrscheinlich an basischen Brönstedzentren oder sauren Lewiszentren chemisorbierten) Reaktantmolekül und einem Karbeniumion beruht.

Saure Zentren aufweisende Zeolithe zeichnen sich als Katalysatoren für die katalytische Krackung von Kohlenwasserstoffen gegenüber amorphen SiO_2/Al_2O_3 nicht nur durch eine um bis zu 4 Größenordnungen höhere Aktivität, sondern auch durch eine vom wirtschaftlichen Standpunkt aus günstigere Selektivität aus [1—4]. Bei der Umsetzung von C_4- bis C_6-Paraffinen an »superaktiven« Zeolithen werden praktisch keine kleineren Spaltprodukte als Propan und keine olefinischen Reaktionsprodukte erhalten [1, 2]. An den weniger aktiven amorphen Katalysatoren, aber z. B. auch an H-Klinoptilolit [5] werden dagegen — natürlich bei entsprechend höheren Reaktionstemperaturen — auch größere Mengen an Methan, Äthan, Wasserstoff und Olefinen gebildet. Es ist offensichtlich, daß es sich hierbei um verschiedenen Reaktionstypen handeln muß.

In der vorangegangenen Mitteilung dieser Reihe [6] wurde gezeigt, daß bei der Umsetzung von Propan an H-Mordenit das nach dem allgemein akzeptierten Karbeniumion-Mechanismus* [7] zu erwartende Reaktionsprodukt (Methan), aber auch ein atypisches primäres paraffinisches Reaktionsprodukt (Äthan) auftritt. Die beiden Krackreaktionen verlaufen nach grundsätzlich verschiedenen Mechanismen und wurden als »Typ I« (mit für den klassischen Karbeniumionen-Mechanismus typischen Reaktionsprodukten) und »Typ II« (atypische Krackprodukte) bezeichnet.

H-Mordenit hat sich als Katalysator mit sehr hoher Selektivität für die Krackung des Typs II erwiesen. Diesen Umstand nutzend werden in der vorliegenden Mitteilung die Krackung des Typs II und Reaktionen mit ähnlichem Mechanismus an Hand der Umsetzung der Butane näher untersucht.

Material und Versuchsausführung

Herstellung und Aktivierung des als Katalysator eingesetzten NH_4-Mordenits mit der Elementarzellen-Zusammensetzung

$$(NH_4)_{4,82}Na_{2,93}[Al_{7,76}Si_{40,24}O_{96}] \cdot 24{,}1\ H_2O$$

wurden bereits in der vorangegangenen Mitteilung dieser Reihe [6] angegeben. Ca- und Sr-Mordenit wurden wie der NH_4-Mordenit aus dem synthetischen Zeolith »Na-Zeolon 100« der NORTON Co. durch Ionenaustausch mit 1 *N* $CaCl_2$- bzw. $Sr(NO_3)_2$-Lösung hergestellt. Beim Ca-Mordenit betrug der Austauschgrad 62%, beim Sr-Mordenit 65%. Die Erdalkalimetall-Mordenite wurden auf gleiche Weise wie der NH_4-Mordenit aktiviert.

Für die katalytischen Versuche wurde ein in Einzelheiten schon beschriebener [5] geschlossener, quasistationär arbeitender Zirkulationsreaktor mit einem Gesamtvolumen von etwa 0,2 dm^3 verwendet, die Entfernung der Olefine aus dem zirkulierenden Gasstrom durch selektive Absorption wurde allerdings nur beim Einsatz von Ca- oder Sr-Mordenit vorgenommen. Bei Verwendung von NH_4-Mordenit als Katalysator traten praktisch keine olefinischen Reaktionsprodukte in der Gasphase auf, so daß kein Olefin-Absorber in den Zirkulationskreis einbezogen werden mußte.

Die als Katalysatoren eingesetzten Zeolithe wurden im allgemeinen nach jedem Versuch mit O_2 bei 720—730 K regeneriert.

Experimentelle Ergebnisse

Bei der katalytischen Krackung der in Tab. I angeführten Reaktanten an Ca- und Sr-Mordenit tritt bei kontinuierlicher Entfernung der olefinischen Reaktionsprodukte aus der Gasphase des Rezirkulationsreaktors praktisch nur Methan — im Falle des *n*-Butans auch Äthan — als paraffinisches-Reaktionsprodukt auf (s. Tab. I). Neben der Krackung verläuft auch die Dehydrierung des Reaktanten. Im Vergleich zur Umsetzung an H-Klinoptilolit [5],

* In der Literatur wird oft die Bezeichnung »Karboniumion« gebraucht. Wir folgen dem Nomenklaturvorschlag von OLAH [8], nach dem das durch Protonaddition an ein Olefinmolekül entstehende Ion als »Karbeniumion«, das Produkt der Protonenanlagerung an ein Paraffinmolekül dagegen als »Karboniumion« bezeichnet wird.

Tabelle I

Sorption der paraffinischen Reaktanten und Geschwindigkeitskonstanten der Dehydrier- und Krackreaktionen an Ca- *und* Sr-*Mordenit*

Vers. Nr.	Gitterkation	Reaktant	Vorb.-Temp. K	Reak.-Temp. K	Anfangsdruck kPa	Sorb. Menge $Mol \cdot g^{-1} \cdot 10^6$	Reaktionsgeschw.—Konstante $Mol \cdot s^{-1} \cdot Pa^{-1} \cdot g^{-1} \cdot 10^{12}$			
							H_2	CH_4	C_2H_6	C_3H_8*
1	Ca	Propan	844	765	18,3	18	0,71	0,77	—	—
2		*i*-Butan	770	765	18,0	26	18,75	4,74	—	0,09
3		*i*-Butan	844	765	15,9	26	15,90	4,91	—	0,11
4		*n*-Butan	844	765	16,7	32	2,20	2,08	1,14	0,09
5		*n*-Butan	967	765	16,8	32	2,75	1,27	0,36	0,02
6		*neo*-Pentan	967	763	17,6	23	—	12,8	—	0,04**
7	Sr	Propan	873	764	16,9	18	0,38	0,41	—	—
8		*i*-Butan	873	765	15,7	27	5,27	1,31	—	0,02
9		*n*-Butan	873	741	15,1	41	0,38	0,49	0,28	0,01
10		*neo*-Pentan	873	732	14,7	38	—	24,10	—	0,08**

* Die Reaktion ist nicht 1. Ordnung. Die auf die Zeit Null extrapolierte Reaktionsgeschwindigkeit ist lediglich zum besseren Vergleich mit den Geschwindigkeitskonstanten der anderen Reaktionen durch den Anfangspartialdruck des Reaktanten geteilt.

** *i*-Butan.

H-Mordenit [6], H—Y [9] und H-Chabasit [10] werden die paraffinischen Reaktionsprodukte, die der Krackung des Typs II zuzuordnen sind (z. B. Äthan aus Propan und Propan aus *n*- oder *i*-Butan), in wesentlich geringerer Menge gebildet, und zugleich wird eine viel schnellere Desaktivierung des Katalysators beobachtet. Kinetisch verwertbare Daten stellen damit nur die durch Extrapolation auf die Zeit Null erhaltenen Anfangsgeschwindigkeiten der Reaktionen an frisch regeneriertem Ca- bzw. Sr-Mordenit dar. Sowohl die Methan (im Falle des n-Butans auch Äthan) als primäres paraffinisches Reaktionsprodukt liefernde Krackung als auch die Dehydrierung sind — wie auch bei der Umsetzung an H-Zeolithen [5, 6, 9, 10] — erster Ordnung in Bezug auf den Reaktantpartialdruck und unabhängig vom Olefinpartialdruck. Die Geschwindigkeit der Krackung des Typs II ist dagegen, wie an H-Zeolithen bereits festgestellt wurde [5, 6], stark vom Olefinpartialdruck abhängig. Die Bestimmung der Reaktionsordnung ist deswegen äußerst problematisch, da der Olefinpartialdruck im Katalysatorbett wegen des simultanen Verlaufs der Olefine liefernden Krackung des Typs I und der Dehydrierung nicht konstant und nicht zu kontrollieren ist.

Ein nicht unbeträchtlicher Teil des in den Reaktor eingespeisten Reaktanten wird bei den relativ hohen Reaktionstemperaturen um 750 K reversibel sorbiert. In Abb. 1 ist als Beispiel die Druck- und Temperaturabhängigkeit

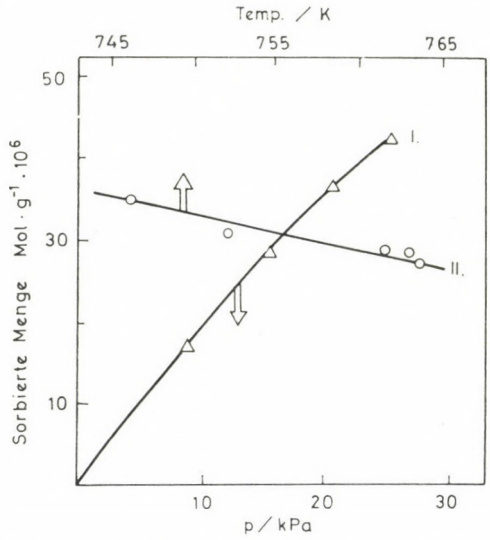

Abb. 1. Isotherme der Chemisorption von *i*-Butan an Sr-Mordenit bei 762 K (I) und Temperaturabhängigkeit der Chemisorption bei 15,5 kPa (II)

der Sorption von *i*-Butan am Sr-Mordenit dargestellt. Die adsorbierte Menge nimmt in der Reihenfolge Propan — *i*-Butan — *n*-Butan zu und ist sowohl von der Vorbehandlungstemperatur des Katalysators als auch von der Art des Gitterkations unabhängig (vgl. Vers. Nr. 2 und 3 sowie 4 und 5 bzw. 1 und 4 sowie 3 und 8 in Tab. I). Es scheint sich somit um eine aspezifische Sorption an Sauerstoffatomen des Kristallgitters zu handeln, wobei allerdings auch die Struktur des Mordenitgitters eine entscheidende Rolle spielen muß, da ein solcher Sorptionseffekt bei Klinoptilolit, Zeolith Y und Chabasit [5, 9, 10] nicht oder viel weniger ausgeprägt zu beobachten ist.

Aus Abb. 2 ist zu ersehen, daß Krack- und Dehydrieraktivität mit steigender Vorbehandlungstemperatur durch ein Maximum gehen. Das gleiche gilt für Sr-Mordernit. Diese Zeolithe verhalten sich damit im Prinzip wie einige H-Zeolithe [5, 9, 10], unterscheiden sich aber von diesen durch eine sich mit der Vorbehandlungstemperatur wesentlich stärker zugunsten der Dehydrierreaktion verschiebende, aber selbst auch wesentlich höhere Selektivität.

An durch thermische Zersetzung der NH_4-Form erhaltenem H-Mordenit werden dagegen die Butane bei den für die Umsetzung dieser Reaktanten an Ca- und Sr-Mordenit und einigen H-Zeolithen [5,9, 10] erforderlichen Reaktiontemperaturen von über 700 K in einer sehr schnellen (mit der gegebenen Apparatur nicht mehr zu verfolgenden) Reaktion, d.h. in wenigen Sekunden in Propan überführt, das in praktisch äquimolarer Menge gebildet wird. In der Gasphase des Zirkulationssystems treten dabei auch dann nur sehr geringe Olefinmengen auf, wenn keine selektive Absorption erfolgt. Aus der Massen-

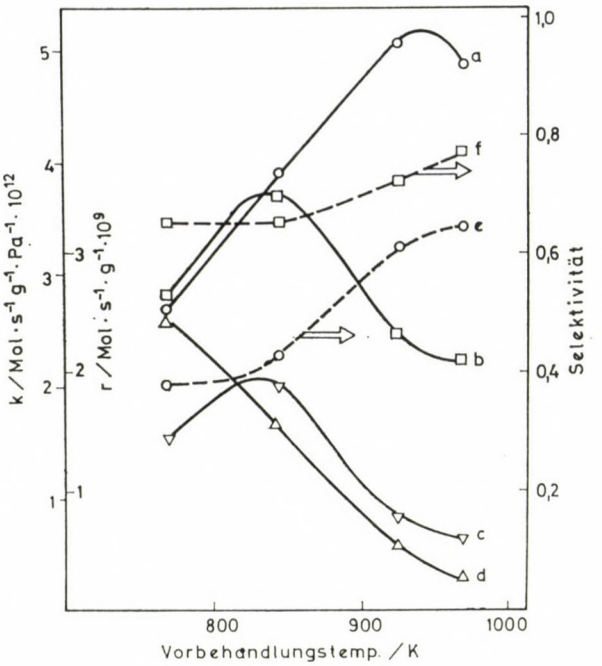

Abb. 2. Änderung der Krack- und Dehydrieraktivität und der Selektivität (gestrichelte Kurven) von Ca-Mordenit in Abhängigkeit von der Vorbehandlungstemperatur. Reaktant: *n*-Butan; Reak.-Temp.: 765 K. a, b, c: Geschwindigkeitskonstanten der Dehydrierung und der Methan bzw. Äthan liefernden Krackung des Typs I; d: Geschwindigkeit der Propan ergebenden Krackung des Typs II bei einem Reaktantpartialdruck von 16,8 kPa; e, f: Dehydrierselektivität ($k_a(\Sigma k)^{-1}$) und Selektivität der Krackung des Typs I [$k_b \cdot (k_b + k_c)^{-1}$]

bilanz ergibt sich damit, daß bei der Umsetzung der Butane zu Propan ein sicher mehr oder weniger polymerisiertes olefinisches Produkt am Katalysator chemisorbiert bleibt, das natürlich bei Temperaturen über 670 K in völlig unübersichtlicher Weise weiterreagiert, womit schnell eine ganze Reihe von sekundären Reaktionsprodukten in der Gasphase auftreten.

H-Mordenit ist so aktiv, daß diese Reaktion selbst noch bei Temperaturen um 470 K mit gut meßbarer Geschwindigkeit verläuft. Bei diesen relativ niedrigen Temperaturen machen sich sekundäre Reaktionen des sich am Katalysator abscheidenden polymeren olefinischen Produktes noch nicht störend bemerkbar. Zusammen mit Propan treten jedoch auch stets das isomere Butan und Pentane als primäre Reaktionsprodukte auf, letztere jedoch immer in geringerer Menge als Propan. Bemerkenswert ist, daß Veränderungen des Katalysators bzw. der Reaktionsbedingungen sich stets in gleicher Weise auf den Verlauf der drei Reaktionen, der Propan ergebenden »Krackung«, der Isomerisierung und der zur Bildung von Pentanen führenden Reaktion auswirken, die im weiteren unter den Sammelbegriff »Reaktionen des Typs II« zusammengefaßt werden.

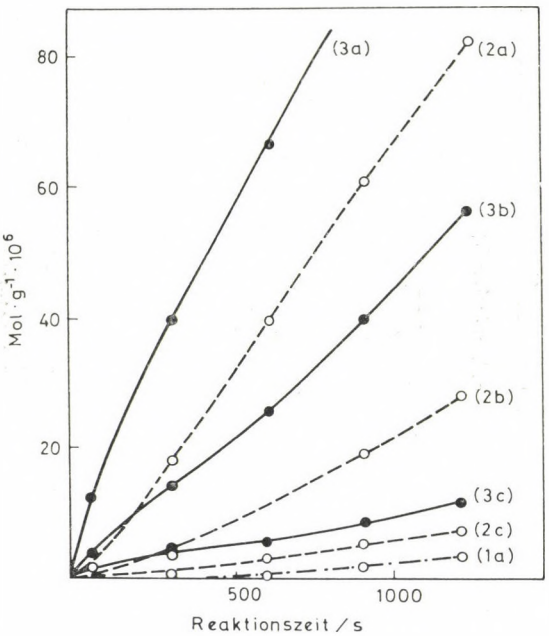

Abb. 3. Bildung von *i*-Butan (a), Propan (b) und *i*-Pentan (c) bei der Umsetzung von *n*-Butan (Ausgangsmenge 1,42 mmol · g^{-1} gleich 22,7 kPa) an verschieden vorbehandeltem H-Mordenit. *n*- und *neo*-Pentan werden ebenfalls, jedoch in wesentlich geringerer Menge als *i*-Pentan gebildet. Reakt.-Temp.: 486 K. Vorbehandlung: O_2-Einwirkung, 3-stündiges Evakuieren und H_2-Einwirkung bei 763 K, danach (1) keine weitere Vorbehandlung, (2) Sauerstoffbehandlung bei 486 K, (3) Chemisorption von Äthylen (34 μMol · g^{-1}) bei 486 K

Die Reaktionen des Typs II setzen am H-Mordenit bei Temperaturen von 450—530 K erst nach einer relativ langen Induktionsperiode ein, sofern der Katalysator vor dem Einsatz bei Temperaturen um 670 K mit Wasserstoff behandelt wurde (s. Abb. 3). Unterbleibt die Wasserstoffbehandlung oder folgt ihr eine Behandlung mit Sauerstoff bei etwa 470 K, so setzen die Reaktionen des Typs II praktisch sofort ein, der von der Abszisse her gesehen konvexe Verlauf der Umsatzkurven deutet jedoch ebenfalls auf eine autokatalytische Reaktion hin. Dieser Effekt ist noch ausgeprägter, wenn die Behandlung mit Sauerstoff bei Temperaturen um 670 K erfolgt. Setzt man schließlich *n*- oder *i*-Butan an dem thermisch vorbehandelten NH_4-Mordenit um, an dem vorher bei der Reaktionstemperatur Äthylen (oder ein anderes Olefin) chemisorbiert wurde, so setzen die Reaktionen des Typs II — wie aus Abb. 3 zu ersehen ist — sofort ein und die Umsatzkurven zeigen zumindest im Anfangsabschnitt den normalen Verlauf. Erst nach längeren Reaktionszeiten bzw. größeren Umsätzen weisen die Kurven einen von der Abszisse her gesehen konvexen Abschnitt auf.

Diese Beobachtungen lassen eindeutig den Schluß zu, daß die Reaktionen des Typs II nur in Gegenwart von sorbierten (und polymerisierten) Olefinen

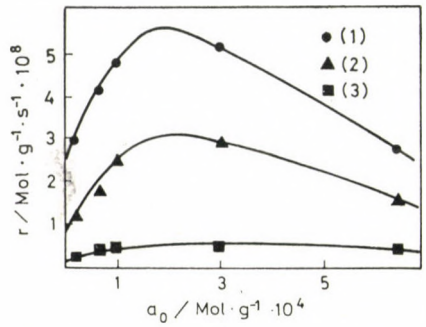

Abb. 4. Bildungsgeschwindigkeit r der bei den Reaktionen des Typs II and *n*-Butan entstehenden Reaktionsprodukte in Abhängigkeit von der präsorbierten Propylenmenge a_0. Reakt.-Temp.: 479 K. Reaktantpartialdruck: 14,5 kPa. (1) = *i*-Butan; (2) = Propan; (3) = *i*-Pentan

ablaufen und der autokatalytische Charakter dieser Reaktionen auf die Bildung solcher Olefinspecies bei der Krackung des Typs II zurückzuführen ist. Weiterhin folgt, daß in Sauerstoffatmosphäre thermisch vorbehandelter NH_4-Mordenit Zentren (oder Verunreinigungen) mit Oxydationswirkung aufweist, die Paraffine durch partielle oxydative Dehydrierung in Olefine zu überführen vermögen [7].

Um festzustellen, ob die Art des präsorbierten Olefins den Verlauf der Umsetzung von Paraffinen (als Reaktant wurde *n*-Butan gewählt) beeinflußt, wurden in getrennten Versuchen gleiche Gewichtsmengen von Äthylen, Propylen und 2-Butylen bei der Reaktionstemperatur am H-Mordenit chemisorbiert. Die aus den Anfangsgeschwindigkeiten der Bildung der einzelnen Reaktionsprodukte berechneten Selektivitätswerte sind in Tab. II zusammengefaßt und lassen den Schluß zu, daß die Umsetzung der Paraffine unabhängig von der Art des an der Reaktion beteiligten Olefins ist. Ein Zusammenhang besteht jedoch zwischen der Menge des präsorbierten Olefins und der Reaktionsgeschwindigkeit, wie aus Abb. 4 zu ersehen ist.

Tabelle II

Selektivität von H-Mordenit nach Präsorption von Olefinen bei der Umsetzung von n-Butan
T_{act}: 796 K; *RT*: 479 K

Reaktionsprodukt	Produktverteilung nach Präsorption von		
	Äthylen 20,4 Mol · g^{-1} · 10^{-6}	Propylen 16,2 Mol · g^{-1} · 10^{-6}	*tr*-2-Butylen 9,4 Mol · g^{-1} · 10^{-6}
Propan	0,39	0,35	0,37
i-Butan	0,54	0,57	0,57
i-Pentan	0,05	0,05	0,04
n-Pentan	0,02	0,03	0,02
neo-Pentan	0,001	0,005	0,004

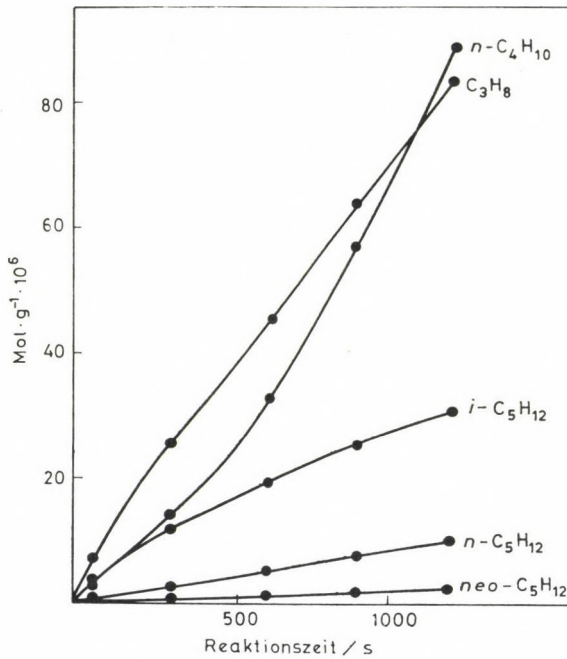

Abb. 5. Reaktionsprodukte bei der Umsetzung von *i*-Butan (22,4 kPa) an H-Mordenit. Reakt.-Temp.: 486 K. Vorbehandlung wie (3) in Abb. 3

i-Butan verhält sich hinsichtlich der hier behandelten Reaktionen prinzipiell wie *n*-Butan, Unterschiede sind jedoch — wie ein Vergleich der Umsatzkurven der Abb. 5 mit den entsprechenden Umsatzkurven des *n*-Butans (3a, 3b und 3c in Abb. 3) zeigt — hinsichtlich der Selektivität zu beobachten. Beim *i*-Butan verläuft — im Gegensatz zum *n*-Butan — die Krackung schneller als die Isomerisierung, außerdem werden auch die Pentane in größerer Menge gebildet.

Mit steigender Vorbehandlungstemperatur nimmt die Aktivität des H-Mordenits für die Reaktionen des Typs II ab und erreicht bei Temperaturen über 950 K, bei denen lieser Zeolith erfahrungsgemäß praktisch vollständig dehydroxyliert ist [9], einen sehr geringen Wert (s. Abb. 6). An einem thermisch in so einem Maße desaktivierten, weitgehend dehydroxylierten Mordenit verlaufen die Reaktionen des Typs II auch bei Temperaturen über 700 K noch so langsam, daß sie mit der gegebenen Apparatur verfolgt werden können. Unter diesen Reaktionsbedingungen verlaufen allerdings auch die Reaktionen des Typs I mit kommensurabler Geschwindigkeit.

Die Konzentration der Reaktionsprodukte geht mit steigender Reaktionszeit durch ein Maximum, wobei sich die Kurve des Propans im Verlauf von den der anderen Produkte unterscheidet (vgl. Abb. 7). Das erklärt sich

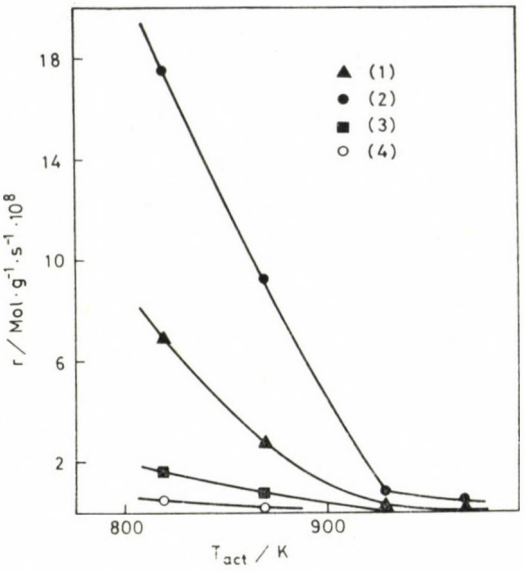

Abb. 6. Bildungsgeschwindigkeit r der bei den Reaktionen des Typs II aus *n*-Butan entstehenden Reaktionsprodukte in Abhängigkeit von der Vorbehandlungstemperatur T_{act} des als Katalysator eingesetzten H-Mordenits. Reakt.-Temp.: 486 K. p: ~18 kPa. (1) = Propan; (2) = *i*-Butan; (3) = *i*-Pentan; (4) = *n*-Pentan

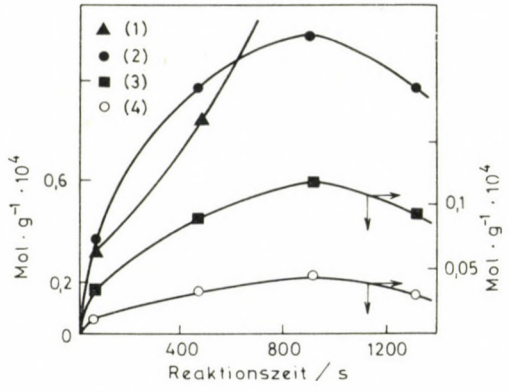

Abb. 7. Auf die Gewichtseinheit des als Katalysator eingesetzten H-Mordenits bezogene, in der Gasphase vorliegende Mengen der bei der Umsetzung von *n*-Butan entstehenden Reaktionsprodukte in Abhängigkeit von der Reaktionszeit. Reakt.-Temp.: 479 K. Reaktantpartialdruck: 16,4 kPa. Präsorbierte Äthylenmenge: $2 \cdot 10^{-5}$ Mol · g^{-1}. T_{act}: 796 K. (1) = Propan; (2) = *i*-Butan; (3) = *i*-Pentan; (4) = *n*-Pentan

dadurch, daß Propan unter den gegebenen Reaktionsbedingungen ein stabiles Endprodukt ist, während das isomere Butan und die Pentane die gleichen Reaktionen wie der Reaktant (im gegebenen Falle *n*-Butan) eingehen und somit auch Propan liefern.

H-Mordenit unterscheidet sich von anderen H-Zeolithen jedoch nicht nur durch die ausgesprochen hohe Aktivität für Reaktionen des Typs II, sondern auch darin, daß er eine überraschend große Menge des paraffinischen Reaktanten bei den Reaktionstemperaturen um 470 K reversibel zu chemisorbieren vermag. Mit steigender Vorbehandlungstemperatur wird — wie aus Tab. III zu ersehen ist — die chemisorbierte Butanmenge im Temperaturbereich von 820—920 K kleiner. Im gleichen Temperaturbereich nimmt auch die Geschwindigkeit der Anfangskonversion, die in Tab. III ebenfalls angegeben ist, ab. Bemerkenswert ist jedoch, daß die chemisorbierte Butanmenge nur auf etwa 50% des ursprünglichen Wertes abfällt, während die Aktivität praktisch den Wert Null erreicht. Die katalytische Aktivität kann also nicht oder nicht allein auf den Chemisorptionseffekt zurückgeführt werden. Ein anderer Befund macht jedoch sehr wahrscheinlich, das die Chemisorption des

Tabelle III

Chemisorption und Geschwindigkeit der Konversion von n-Butan an bei verschiedenen Temperaturen vorbehandeltem H-Mordenit bei 486 K

Vorbehandl.—Temperatur K	Chemisorbierte *n*-Butanmenge mMol · g^{-1}	Geschw. der Konversion Mol · s^{-1} · g^{-1}
791	0,29	$3{,}4 \cdot 10^{-7}$
819	0,28	$3{,}3 \cdot 10^{-7}$
871	0,25	$1{,}6 \cdot 10^{-7}$
928	0,15	$0{,}09 \cdot 10^{-7}$
967	0,14	$0{,}03 \cdot 10^{-7}$

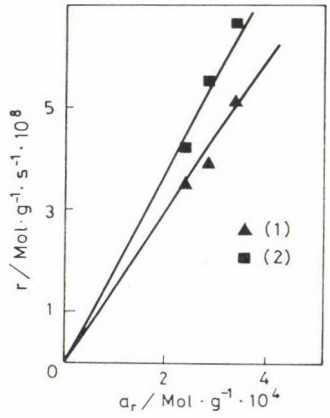

Abb. 8. Bildungsgeschwindigkeit r der bei der Krackung des Typs II und der Isomerisierung aus *i*-Butan entstehenden Reaktionsprodukte in Abhängigkeit von der Menge des an dem als Katalysator verwendeten H-Mordenit chemisorbierten Reaktanden a_r. Reakt.-Temp.: 479 K. (1) = Propan; (2) = *n*-Butan

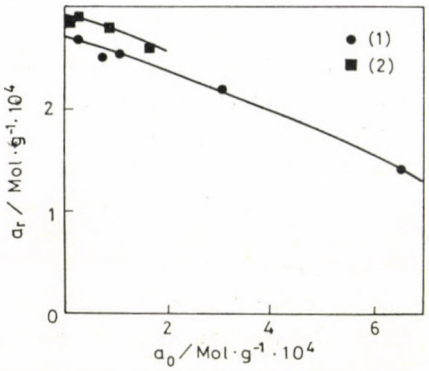

Abb. 9. Chemisorption von *n*-Butan an bei 760 K vorbehandeltem H-Mordenit in Abhängigkeit von der Menge des präsorbierten Olefins. T_{act}: 791 K. (1) = Äthylen; 486 K; Partialdruck des Butans: 18,6 kPa; (2) = Propylen; 479 K; Partialdruck des Butans: 14,7 kPa

Reaktanten eine Rolle im Reaktionsmechanismus der Reaktionen des Typs II spielt. Diese Reaktionen verlaufen nämlich in Bezug auf die vom Katalysator chemisorbierte Menge des Reaktanten nach erster Ordnung. Diese in Abb. 8 dargestellte Abhängigkeit deutet darauf hin, daß das chemisorbierte Paraffinmolekül reagiert.

Mit steigender Olefinvorbeladung des H-Mordenits nimmt die Menge des chemisorbierten Reaktanten etwas, aber nicht sehr ausgeprägt ab. Dieser Effekt wird an Hand experimenteller Daten in Abb. 9 veranschaulicht.

Diskussion

Nach dem Karbeniumionen-Mechanismus der katalytischen Krackung von paraffinischen Kohlenwasserstoffen erfolgt zunächst intermolekularer Hydridtransfer zwischen einem zur Initiierung der Reaktion notwendigen, beliebigen Karbeniumion und einem Reaktantmolekül:

$$R^+ + R_1—CH_2—CH_2—CH_2—R_2 \rightleftharpoons RH + R_1—\overset{+}{C}H—CH_2—CH_2—R_2 \quad (1)$$

Das gebildete Karbeniumion wird in β-Stellung zu dem die Ladung tragenden C-Atom gespalten (β-Regel), wobei ein Olefinmolekül und ein primäres-Karbeniumion mit kürzerer Kette entstehen. Letzteres reagiert — eventuell nach Umlagerung in ein stabileres sekundäres oder tertiäres Ion — mit einem Reaktantmolekül unter Transfer eines Hydridions, so daß also ein Reaktionszyklus vorliegt:

$$R_1—\overset{+}{C}H—CH_2—CH_2—R_2 \rightarrow R_1—CH=CH_2 + \overset{+}{C}H_2—R_2 \quad (2a)$$

$$R_1—CH_2—CH_2—CH_2—R_2 + \overset{+}{C}H_2—R_2 \rightleftharpoons R_1—\overset{+}{C}H—CH_2—CH_2—R_2 + CH_3—R_2 \quad (2b)$$

Bei der katalytischen Krackung von Propan bzw. *i*-Butan sind nach diesem Mechanismus Methan und Äthylen bzw. Propylen als primäre Reaktionsprodukte zu erwarten. Hält man an der β-Regel fest, so muß man annehmen, daß dabei die energetisch nicht begünstigten primären Karbeniumionen reagieren. Das gleiche trifft für die unter Bildung von Äthan und Äthylen verlaufende Spaltung der 2-Bindung von *n*-Butan zu. An der Methan und Propylen ergebenden Krackung der 1-Bindung sollten dagegen nur sekundäre Butylkarbeniumionen beteiligt sein.

Die angeführten Reaktionsprodukte treten bei der Krackung von Propan und Butanen an zeolithischen Katalysatoren im allgemeinen auch auf. Allerdings ist der klassische Mechanismus — zumindest bei der Krackung kurzkettiger Kohlenwasserstoffe— mit einer Reihe experimenteller Befunde nicht zu vereinbaren. Die Reaktivität von Propan und *i*-Butan z. B. unterscheiden sich um Größenordnungen, obwohl in beiden Fällen die Bildung primärer Karbeniumionen vorauszusetzen ist. Andererseits ist für die Spaltung der 1- und 2-Bindung des *n*-Butans die gleiche scheinbare Aktivierungsenergie aufzubringen, und beide Reaktionen verlaufen mit vergleichbarer Geschwindigkeit, obzwar die Spaltung der 1-Bindung ein sekundäres, die der 2-Bindung dagegen ein primäres Butylkarbeniumion voraussetzt (s. [5] und Tab. I). Um diese Befunde auf der Basis der klassischen Mechanismusvorstellungen erklären zu können, müßte eine Spaltung der zu dem die Ladung tragenden C-Atom in α-Stellung stehenden Bindung ebenfalls angenommen werden, was aber zugleich die nicht wahrscheinliche Voraussetzung in sich einschließt, daß energiereiche primäre Karbeniumionen aus viel stabileren sekundären oder sogar tertiären Ionen entstehen. Schwerwiegendere Argumente gegen den klassischen Karbeniumionen-Mechanismus liefern jedoch die Beobachtungen, daß die zu den erwähnten primären Reaktionsprodukten führenden Krackreaktionen unabhängig vom Olefinpartialdruck sind [5, 6] und nicht an sauren Zentren des Brönsted-Typs, sondern an solchen des Lewis-Typs verlaufen [9, 11]. Diese — im weiteren als Krackreaktionen des Typs I bezeichneten — Reaktionen werden also ausgelöst, wenn das kurzkettige Paraffinmolekül eine Hydridabstraktion oder zumindest eine in diese Richtung gehende Polarisation erfährt [9, 11].

Bereits bei der Aufstellung des klassischen Karbeniumionen-Mechanismus wurde als Möglichkeit in Erwägung gezogen, daß die für die Initiierung der Krackreaktionszyklen notwendigen Ionen durch Hydridabstraktion aus Molekülen des paraffinischen Reaktanten gebildet werden [7]. Später wurde dann auch ein Mechanismus vorgeschlagen, der als wesentlichen Schritt die Spaltung der durch Hydridabstraktion gebildeten Ionen in sich einschließt [4].

Mit den Krackreaktionen des Typs I geht stets die Dehydrierung des Reaktanten einher, die ebenfalls unabhängig vom Olefinpartialdruck ist und deshalb dem Reaktionstyp I zugeordnet wird. Es wird angenommen, daß eine

Zweizentren-Chemisorption des Reaktantmoleküls Voraussetzung für die Dehydrierung ist [11]. Als aktives Zentrenpaar fungieren ein saures Lewiszentrum (Hydridabstraktion) und ein in geeigneter Entfernung sich befindendes basisches Brönstedzentrum (Protonabstraktion).

Die Ausbildung saurer Zentren bei der thermischen Aktivierung von mehrwertige Gitterkationen (Me) enthaltenden Zeolithen kann durch die Gleichungen

$$Me_x^{2+}(H_2O)_x \cdot OZ_{2x}^- \rightleftharpoons Me(OH)_x^+, OZ_x^- + HOZ_x \qquad (3a)$$

$$Me(OH)_x^+ \cdot OZ_x^- + HOZ_x \rightleftharpoons Me_x^{2+} \cdot OZ_{2x}^- + x\, H_2O \qquad (3b)$$

beschrieben werden [12, 13]. OZ^- bezeichnet den auf eine negative Ladung entfallenden Teil des Gitters. Als saure Lewiszentren kommen für die Reaktantmoleküle zugängliche Gitterpositionen einnehmende Gitterkationen Me^{2+} in Frage. Die bei der Absättigung der negativen Gitterladungen durch Protonen zustande kommenden Hydroxylgruppen sind saure Brönstedzentren. Schließlich sind die Gittersauerstoffatome, die die negativen Gitterladungen tragen, als basische Brönstedzentren anzusehen. Da die negativen Ladungen an verschiedenen Stellen des Gitters fixiert sind, können sie von mehrwertigen Gitterkationen nicht vollständig abgeschirmt werden.

Generell sind für die praktisch vollständige Entfernung von molekularem Wasser aus Zeolithen wesentlich tiefere Temperaturen als die in dieser Arbeit angewandten Vorbehandlungstemperaturen ausreichend. Damit ist zur Deutung der Versuchsergebnisse nur die Reaktion (3b) von Interesse. KARGE [14] hat durch IR-spektrophotometrische Untersuchungen gezeigt, daß die Dehydroxylierung von zwei- und dreiwertigen Gitterkationen enthaltenden Mordeniten tatsächlich nach (3b) verläuft und die von H-Zeolithen her bekannte Dehydroxylierung

$$2\, HOZ \rightarrow OZ^- + Z^+ + H_2O \qquad (4)$$

keine Rolle dabei spielt.

Mit steigendem T_{act} nimmt nach (3b) die Konzentration der sauren Brönstedzentren ab, die der basischen Brönsted- und sauren Lewiszentren dagegen zu. Es liegt damit nahe, den anfänglichen Anstieg der Krack- und Dehydrieraktivität mit der Vermehrung eines oder beider dieser Zentrentypen in Zusammenhang zu bringen. Bei Temperaturen über 900 K ist die Dehydroxylierung — wie thermoanalytische Untersuchungen ergeben haben — praktisch abgeschlossen, und damit sollte die Aktivität bei weiterer Erhöhung von T_{act} konstant bleiben. Jedoch ist nicht prinzipiell auszuschließen, daß mit steigender Temperatur eine Migration der als saure Lewiszentren fungierenden zweiwertigen Gitterkationen auf für Reaktantmoleküle unzugängliche Gitter-

positionen erfolgt. (Bei La-Y und Ca-Y wurde ein solcher Effekt beobachtet [15]). Der in Abb. 2 dargestellte Verlauf der Dehydrieraktivität ist damit durch die Überlagerung der beiden — entgegengesetzt gerichtete Wirkungen ausübenden — Vorgänge zu erklären.

Die Annahme einer Zweizentren-Chemisorption im Mechanismus der Dehydrierung scheint recht plausibel zu sein. Da die zum Protonenentzug aus einer Alkylgruppe notwendige Energie (gerade umgekehrt wie die für die Hydridabstraktion) in der Reihenfolge primär-sekundär-tertiär zunimmt, ist z. B. im Falle von *n*-Butan die chemisorbierte Spezies wie folgt zu formulieren:

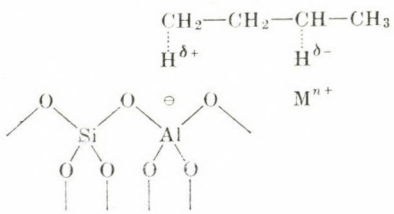

M^{n+} ist ein als saures Lewiszentrum fungierendes mehrwertiges Gitterkation oder eine bei der Dehydroxylierung aus dem anionischen Gitter austretende und kationische Positionen einnehmende Al-Spezies (z. B. AlO^+). Die Hydrierung erfolgt, indem zwischen dem Hydridion und dem Proton (bzw. den partiell negativ und positiv geladenen H-Atomen) eine neue Bindung zustande kommt.

Bei der Krackung erfolgt dagegen nur eine Hydridabstraktion am sauren Lewiszentrum, wobei durch die einseitig gerichtete Polarisation eine der C—C-Bindungen geschwächt und aufgespalten wird:

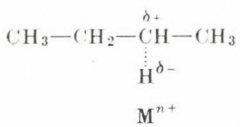

Wie aus Tab. I zu ersehen ist, wird jedoch auch *neo*- Pentan sehr gut gekrackt, obwohl dieser Kohlenwasserstoff nur an tertiärem Kohlenstoff gebundenen Wasserstoff enthält, eine Hydridabstraktion energetisch also nicht begünstigt ist. Es muß somit angenommen werden, daß auch eine durch Protonenabstraktion an basischen Brönstedzentren bedingte Chemisorption zu solchen Elektronenverschiebungen Anlaß geben kann, die zur Aufspaltung einer C—C-Bindung führen.

Die bei der Umsetzung von Paraffinen an Ca- und Sr-Mordenit mit steigendem T_{act} erfolgende Selektivitätsverschiebung zugunsten der Dehydrierung, wobei im Temperaturbereich von etwa 830—930 K Dehydrier- und Krackaktivität sogar einen entgegengesetzten Verlauf zeigen, legt auf den ersten Blick die Annahme nahe, daß im Mechanismus der Krackung auch

saure Brönstedzentren als ein zweiter aktiver Zentrentyp direkt eine Rolle spielen. Dem steht aber entgegen, daß Zeolithe, die nur saure Lewiszentren enthalten, auch eine größenordnungsmäßig mit der Dehydrieraktivität zu vergleichende Krackaktivität aufweisen [11]. Auch aus dem Verlauf der Kurven b und c in Abb. 2 ist zu ersehen, daß bei hohem T_{act}, also praktisch bei Abwesenheit von sauren Brönstedzentren, eine Restaktivität verbleibt.

Es kann jedoch leicht eine Erklärung für die Selektivitätsverschiebung gegeben werden, wenn man den sauren Brönstedzentren nur eine indirekte, desaktivierende Rolle im Dehydrierprozeß zuschreibt. Das Wasserstoffatom eines sauren Brönstedzentrums ist nicht an ein bestimmtes Gittersauerstoffatom gebunden, sondern springt — wie NMR-spektrophotometrische Untersuchungen gezeigt haben [16] — mit einer bestimmten Frequenz von O-Atom zu O-Atom. Es liegt somit auf der Hand, daß mit steigender Konzentration der sauren Oberflächen-Hydroxylgruppen die Wahrscheinlichkeit abnimmt, daß das sich zu einem sauren Lewiszentrum in einem für die Zweizentren-Chemisorption optimalen Abstand befindende basische Brönstedzentrum frei ist, d.h. nicht gerade durch ein Proton blockiert wird. Danach ist also die Selektivitätsverschiebung mit steigendem T_{act} darauf zurückzuführen, daß die Dehydrierung bei hohen Konzentrationen an Oberflächen-Hydroxylgruppen durch teilweise Blockierung der aktiven basischen Brönstedzentren inhibiert wird. Damit reagiert ein grösserer Teil der durch Hydridabstraktion chemisorbierten paraffinischen Spezies auf dem Wege der Krackung weiter als am vollständig dehydroxylierten Katalysator, der eine maximale Konzentration der für die Dehydrierung notwendigen Doppelzentren aufweist.

Die Selektivität des Ca- und Sr-Mordenits ist im Vergleich zu der einiger H-Zeolithe (5, 9, 10] beträchtlich zugunsten der Dehydrierung verschoben, was ebenfalls mit den dargelegten Mechanismusvorstellungen vereinbar ist. Bei den Erdalkalimetall-Mordeniten liegen nämlich von vornherein mehr saure Lewiszentren (zweiwertige Kationen) und weniger saure Brönstedzentren vor als in H-Zeolithen.

Für die bei der Umsetzung von *n*-Butan mit steigendem T_{act} beobachtete Veränderung der Krackselektivität zugunsten der Spaltung der 1-Bindung (s. Kurve f in Abb. 2) können wir keine Erklärung geben.

Bei der Umsetzung von Butanen an Ca- und Sr-Mordenit tritt auch Propan als primäres Reaktionsprodukt auf. Bei kontinuierlicher Entfernung der Olefine aus der Gasphase des Rezirkulationsreaktors verläuft diese — als Krackung des Typs II bezeichnete — Reaktion wesentlich langsamer als die Reaktionen des Typs I. Das gleiche gilt für die Wasserstoff-Form von Klinoptilolit [5], Y [9], Chabasit [10] sowie Erionit und ZSM-5 [17]. H-Mordenit nimmt dagegen insofern eine Sonderstellung ein, als daran die Krackung des Typs II um Größenordnungen schneller als an anderen Zeolithen verläuft. Diese »Superaktivität« des H-Mordenits ist zwar schon lange bekannt

[1, 2], jedoch scheinen die Aktivitätsunterschiede im Vergleich zu beispielsweise H—Y order H-Chabasit doch größer zu sein, als aus den Literaturangaben hervorgeht.

Die Abnahme der Aktivität mit steigendem T_{act} (s. Abb. 6), also mit zunehmender Degradation der sauren Brönstedzentren, und die Notwendigkeit von Olefinen für die Initiierung der Reaktionen des Types II (s. Abb. 3) lassen eindeutig den Schluß zu, daß im Reaktionsmechanismus Karbeniumionen involviert sind. Schon länger ist übrigens bekannt, daß Olefine die Krackung von *n*-Butan an H—Y beschleunigen [18]. Weiterhin ist es sehr wahrscheinlich, daß chemisorbierte Paraffinspezies an der Reaktion teilnehmen. Dafür spricht einmal die Tatsache, daß gerade H-Mordenit, der Paraffine bei den verhältnismäßig hohen Reaktionstemperaturen um 480 K als einziger H-Zeolith in überraschend großer Menge chemisorbiert, auch eine außerordentlich hohe Aktivität für die Reaktionen des Typs II aufweist. Ein noch deutlicherer Hinweis darauf ist jedoch darin zu sehen, daß die Reaktionen in bezug auf die Oberflächenkonzentration des chemisorbierten Reaktanten nach erster Ordnung verlaufen (s. Abb. 8) und nicht in bezug auf dessen Partialdruck in der Gasphase.

Die Präsorption von Olefinen am H-Mordenit beeinflußt die nachfolgende reversible Chemisorption von Butanen etwas, steht jedoch nicht im stöchiometrischen Verhältnis mit der Abnahme der Sorptionskapazität für das Paraffin (s. Abb. 9). Aus diesen Versuchsergebnissen lassen sich somit keine eindeutigen Schlußfolgerungen hinsichtlich der Frage ziehen, ob die Chemisorption der Olefine und Paraffine am gleichen oder an verschiedenen Zentren erfolgt. Dafür kann aber aus der Beobachtung, daß die Menge des chemisorbierten Butans mit steigendem T_{act} zwar etwas abnimmt, aber selbst bei praktisch vollständiger Dehydroxylierung (T_{act} über 900 K) nur auf etwa 50% des ursprünglichen Wertes absinkt (s. Tab. III), gefolgert werden, daß saure Zentren des Brönstedtyps nicht als Chemisorptionszentren für Paraffine in Frage kommen.

Die Anfangsgeschwindigkeit der Reaktionen des Typs II geht mit steigender Olefinvorbeladung des H-Mordenits durch ein Maximum (Abb. 4), und zwar bei einem Wert (0,2 mMol $\cdot$ g^{-1}), der bei weitem noch nicht der Oberflächenkonzentration der sauren Brönstedzentren (1,64 mVal $\cdot$ g^{-1}) entspricht. Demnach muß also — wenn die Reaktionen zwischen einem reversibel chemisorbierten Paraffinmolekül und einem durch Chemisorption eines Olefinmoleküls an einem sauren Brönstedzentrum gebildeten Karbeniumion verlaufen — ein Teil des Olefins auch an den für die Paraffinchemisorption verantwortlichen Zentren gebunden werden, bei denen es sich wahrscheinlich um saure Zentren des Lewistyps und/oder basische Brönstedzentren handelt.

Die experimentellen Ergebnisse lassen sich erklären, wenn man einen intermolekularen Hydrid- und Methaniontransfer zwischen den chemisorbier-

ten Paraffinmolekülen und den Karbeniumionen annimmt. In diesem Mechanismus spielen zwei Prozesse eine wesentliche Rolle, nämlich der zwischen einem Karbeniumion und

1. einem (möglicherweise an einem basischen Brönstedzentrum) chemisorbierten Paraffinmolekül verlaufende Methanion-Hydrid-Transfer (MH—T), der — für *n*-Butan — folgendermaßen zu formulieren ist:

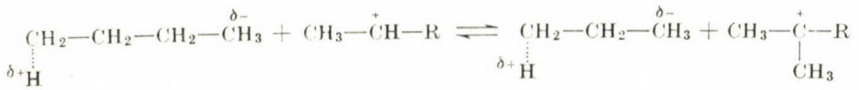

(5)

2. einem (möglicherweise an einem sauren Lewiszentrum) chemisorbierten Paraffinmolekül verlaufende Hydrid-Transfer (H—T):

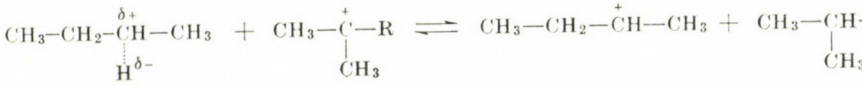

(6)

Ein derartiger Hydridtransfer wird übrigens auch im klassischen Krackmechanismus — s. Gleichungen (1) und (2)b — und im Mechanismus der Alkanisomerisierung von Paraffinen [19] als ein wesentlicher Reaktionsschritt angenommen.

Die folgenden (mit Formeln ohne H-Atome angegebenen) Reaktionsfolgen spiegeln die Vorstellungen über den Mechanismus der Reaktionen des Typs II von *n*- und *i*-Butan wider:

n-Butan	a) $n\text{-}C_4 + C_3^+ \rightleftharpoons C_3 + n\text{-}C_4^+$	H—T	
	b) $n\text{-}C_4 + n\text{-}C_4^+ \rightleftharpoons C_3 + i\text{-}C_5^+$	MH—T	
	c) $n\text{-}C_4 + i\text{-}C_5^+ \rightleftharpoons i\text{-}C_5 + n\text{-}C_4^+$	H—T	(7)
	d) $i\text{-}C_5 + n\text{-}C_4^+ \rightleftharpoons i\text{-}C_4 + i\text{-}C_5^+$	MH—T	
	e) $n\text{-}C_4 + i\text{-}C_5^+ \rightleftharpoons C_3 + i\text{-}C_6^+$	MH—T	
	f) $H^+ + i\text{-}C_6^+ \rightleftharpoons 2\ C_3^+$		
i-Butan	a) $i\text{-}C_4 + C_3^+ \rightleftharpoons C_3 + i\text{-}C_4^+$	H—T	
	b) $i\text{-}C_4 + i\text{-}C_4^+ \rightleftharpoons C_3 + i\text{-}C_5^+$	MH—T	
	c) $i\text{-}C_4 + i\text{-}C_5^+ \rightleftharpoons i\text{-}C_5 + i\text{-}C_4^+$	H—T	(8)
	d) $i\text{-}C_5 + i\text{-}C_4^+ \rightleftharpoons n\text{-}C_4 + i\text{-}C_5^+$	MH—T	
	e) $i\text{-}C_4 + i\text{-}C_5^+ \rightleftharpoons C_3 + i\text{-}C_6^+$	MH—T	
	f) $H^+ + i\text{-}C_6^+ \rightleftharpoons 2\ C_3^+$		

Der a-Schritt kann auch als Methanion-Hydrid-Transfer aufgefaßt werden. In diesem Falle ergibt sich für die Reaktionsschritte a) und b) des *n*-Butans:

$$\text{a)}\quad n\text{-}C_4 + C_3^+ \rightleftharpoons C_3 + i\text{-}C_4^+ \qquad \text{MH—T}$$

$$\text{b)}\quad n\text{-}C_4 + i\text{-}C_4^+ \rightleftharpoons C_3 + i\text{-}C_5^+ \qquad \text{MH—T}$$

Es soll bemerkt werden, daß der reaktionsinitiierende Schritt a) nur als Beispiel mit einem Propylkarbeniumion formuliert wurde. Selbstverständlich kann auch jedes andere Karbeniumion die Reaktion auslösen.

Die Krackung des Typs II wird durch die Reaktionsschritte a—b—e—f der Reaktionsfolgen (7) und (8) beschrieben. Die im b-Schritt gebildeten *i*-Pentylkarbeniumionen reagieren aber auch nach c) weiter. Die Produkte dieses Reaktionsschrittes reagieren entweder dem b- oder dem d-Schritt entsprechend. In beiden Fällen handelt es sich um einen Reaktionszyklus. Die Bruttogleichung des Zyklus c—b lautet: $2\ n\text{-}C_4$ (bzw. $2\ i\text{-}C_4$) $\rightarrow C_3 + i\text{-}C_5$, die des Zyklus c—d: $n\text{-}C_4 \rightarrow i\text{-}C_4$ bzw. $i\text{-}C_4 \rightarrow n\text{-}C_4$. Der erste Zyklus beschreibt also die zu Paraffinen mit größerem Molekulargewicht führende Disproportionierung des Reaktanten, die zweite dagegen die Isomerisierung. Letztere kann natürlich auch nach dem bereits beschriebenen Mechanismus [19] durch intramolekularen Methanion-Hydrid-Transfer erfolgen:

$$\text{a)}\quad n\text{-}C_4^+ \rightleftharpoons i\text{-}C_4^+ \qquad \text{intramol. MH—T}$$

$$\text{b)}\quad n\text{-}C_4 + i\text{-}C_4^+ \rightleftharpoons i\text{-}C_4 + n\text{-}C_4^+ \qquad \text{intermol. H—T} \qquad (9)$$

Die Reaktionsfolgen (7) und (8) vermitteln natürlich nur ein sehr vereinfachtes Bild von dem sehr komplexen Reaktionsgeschehen, da nicht nur der Reaktant, sondern auch die gesättigten Produkte der Reaktionsschritte c) und d) mit jedem der Karbeniumionen reagieren können. Gleichzeitig können sich auch die Karbeniumionen durch Di- bzw. Oligomerisation und Krackung ineinander umlagern. Da bei Präsorption von verschiedenen Olefinen keine Unterschiede in der Produktverteilung auftreten (vgl. Tab. II), ist anzunehmen, daß diese Umlagerungen viel schneller als die Transfer-Reaktionen verlaufen und somit stets eine Gleichgewichtsverteilung der Karbeniumionen vorliegt.

Bei den Transfer-Reaktionen muß in erster Linie mit der Ausbildung der energetisch begünstigteren tertiären Karbeniumionen gerechnet werden. Daneben treten natürlich auch — im geringeren Maße — sekundäre Ionen auf. Deshalb ist unter den Reaktionsprodukten stets auch *n*-Pentan zu finden, allerdings in viel geringeren Konzentrationen als *i*-Pentan. *Neo*-Pentan wird praktisch nicht gebildet, was mit dem erörterten Mechanismus im Einklang steht, denn dieser Prozeß setzt im b-Schritt der Reaktionsfolgen (7) bzw. (8) die Bildung von primären Karbeniumionen voraus.

Das Gleichgewicht des Reaktionsschrittes (9a) muß aus energetischen Gründen nach der rechten Seite der Reaktionsgleichung verschoben sein. Daraus folgt — wie experimentell auch bestätigt wurde (vgl. Abb. 3 und 5) —, daß die Isomerisierung beim *n*-Butan wesentlich stärker als beim *i*-Butan ausgeprägt sein muß.

Wenn man die Möglichkeit der Bildung primärer Karbeniumionen praktisch ausschließt, was aus energetischen Gründen berechtigt erscheint, so ist nach dem dargelegten Mechanismus in Übereinstimmung mit den experimentellen Befunden als kleinstes paraffinisches Reaktionsprodukt der Krakkung des Typs II Propan zu erwarten. Propan wird zwar auch nach diesem Reaktionstyp unter Bildung von Äthan weiter umgesetzt, aber erst bei um mehr als 200 K höheren Temperaturen [6]. Es liegt also kein Widerspruch vor, denn unter diesen Reaktionsbedingungen kann die Aktivierungsenergie für die Bildung primärer Ionen aufgebracht werden.

Wenn die Existenz primärer Karbeniumionen ausgeschlossen werden kann, so ist nach dem klassischen Mechanismus nur die Krackung von *n*-Hexan bzw. Alkylhexanen und Paraffinen mit längerer Kohlenstoffkette möglich. Nach dem derzeitigen Stand unserer Kenntnisse besteht kein Anlaß, den klassischen Mechanismus auch in diesen Fällen in Zweifel zu ziehen. Der in der vorliegenden Arbeit dargelegte Mechanismus bezieht sich also nur auf Paraffine mit Kettenlängen von weniger als 6 C-Atomen.

LITERATUR

[1] Miale, J. N., Chen, N. Y., Weisz, P. B.: J. Catalysis, **6,** 278 (1966)
[2] Frilette, V. J., Rubin, M.: J. Catalysis, **4,** 310 (1965)
[3] Benesi, H. A.: J. Catalysis, **8,** 368 (1967)
[4] Tung, S. E., McIninch, E.: J. Catalysis, **10,** 175 (1968)
[5] Beyer, H.: Acta Chim. (Budapest), **84,** 25 (1975)
[6] Beyer, H. K.: Acta Chim. (Budapest), **95,** 41 (1977)
[7] Greensfelder, B. S., Voge, H. H., Good, G. M.: Ind. Eng. Chem., **41,** 2573 (1949)
[8] Olah, G. A.: Angew. Chem., **85,** 183 (1973)
[9] Réti, F., Beyer, H. K.: React. Kin. Cat. Lett. (im Druck)
[10] Beyer, H. K., Horváth J., Jacobs, P. A.: Acta Chim. Acad. Sci. Hung. (im Druck)
[11] Beyer, H. K., Horváth, J., Réti, F.: React. Kin. Cat. Lett, **14,** 395 (1980)
[12] Hirschler, A. E.: J. Catalysis, **43,** 428 (1963)
[13] Planck, C. S.: Proc. 3rd Intern. Congr. Catalysis, Amsterdam 1964, North-Holland Publ. Comp., Amsterdam, 1965, Band I, S. 727
[14] Karge, H. G.: ACS Symp. Ser., **40,** 584 (1977)
[15] Costenoble, M. L., Mortier, W. J., Uytterhoeven, J. B.: JCS Faraday Trans. I, **73,** 466 (1977)
[16] Freude, D., Oehme, W., Schmiedel, H., Staudte, B.: J. Catalysis, **49,** 123 (1977)
[17] Eigene unveröffentlichte Ergebnisse
[18] Miale, J. N., Trenton, N. J., Weisz, P. B.: US-Patent 3,280,212 (1960)
[19] Pines, H.: Adv. Catalysis, **1,** 201 (1948)

Hermann K. Beyer
Ferenc Réti
H-1025 Budapest, Pusztaszeri u. 57—69.

József Horváth
H-2440 Százhalombatta

INDEX

PHYSICAL AND INORGANIC CHEMISTRY

ORGANIC CHEMISTRY

PRINTED IN HUNGARY
Akadémiai Nyomda, Budapest

Les Acta Chimica paraissent en français, allemand, anglais et russe et publient de mémoires du domaine des sciences chimiques.

Les Acta Chimica sont publiés sous forme de fascicules. Quatre fascicules seront réunis en un volume (3 volumes par an).

On est prié d'envoyer les manuscrits destinés à la rédaction à l'adresse suivante:

Acta Chimica
Budapest, P.O. Box 67, H-1450, Hongrie

Toute correspondance doit être envoyée à cette même adresse.

La rédaction ne rend pas de manuscript.

Abonnement en Hongrie à l'Akadémiai Kiadó (1363 Budapest, P.O.B. 24, C. C. B. 215 11488), à l'étranger à l'Entreprise du Commerce Extérieur «Kultura» (H-1389 Budapest 62, P.O.B. 149 Compte-courant No. 218 10990) ou chez représentants à l'étranger.

Die Acta Chimica veröffentlichen Abhandlungen aus dem Bereich der chemischen Wissenschaften in deutscher, englischer, französischer und russischer Sprache.

Die Acta Chimica erscheinen in Heften wechselnden Umfanges. Vier Hefte bilden einen Band. Jährlich erscheinen 3 Bände.

Die zur Veröffentlichung bestimmten Manuskripte sind an folgende Adresse zu senden

Acta Chimica
Budapest, Postfach 67, H-1450, Ungarn

An die gleiche Anschrift ist jede für die Redaktion bestimmte Korrespondenz zu richten.

Manuskripte werden nicht zurückerstattet.

Bestellbar für das Inland bei Akadémiai Kiadó (1363 Budapest, Postfach 24, Bankkonto Nr. 215 11488), für das Ausland bei »Kultura« Außenhandelsunternehmen (H-1389 Budapest 62, P.O.B. 149. Bankkonto Nr. 218 10990) oder seinen Auslandsvertretungen.

«Acta Chimica» издают стильи по химии на русском, английском, французском и немецком языках.

«Acta Chimica» выходит отдельными выпусками разного объекта, 4 выпуска составхяют одинтом и за год выходят 3 тома.

Предназначенные для публикации рукописи следует направлять по адресу:

Acta Chimica
Budapest, P.O. Box 67, H-1450, BHP

Всякую корреспонданцию в редакцию направляйте по этому же адресу.

Редакция рукописе не возвращает.

Отечественные подписчики направляйте свои заявки по адресу Издательств. Академии Наук (1363 Budapest, P.O.B. 24. Текущий счет 215 11 488), а иностранные одписчики через организацию по внешней торговле «Kultura» (H-1389 Budapest 62, P.O.B. 149. Текущий счет 218 10990) или через ее заграничные представительства и уполномеченных.

Reviews of the Hungarian Academy of Sciences are obtainable at the following addresses:

AUSTRALIA
C.B.D. LIBRARY AND SUBSCRIPTION SERVICE, Box 4886, G.P.O., *Sydney N.S.W. 2001*
COSMOS BOOKSHOP, 145 Ackland Street, *St. Kilda (Melbourne), Victoria 3182*

AUSTRIA
GLOBUS, Höchstädtplatz 3, *1200 Wien XX*

BELGIUM
OFFICE INTERNATIONAL DE LIBRAIRIE, 30 Avenue Marnix, *1050 Bruxelles*
LIBRAIRIE DU MONDE ENTIER, 162 Rue du Midi, *1000 Bruxelles*

BULGARIA
HEMUS, Bulvar Ruski 6, *Sofia*

CANADA
PANNONIA BOOKS, P.O. Box 1017, Postal Station "B", *Toronto, Ontario M5T 2T*

CHINA
CNPICOR, Periodical Department, P.O. Box 50, *Peking*

CZECHOSLOVAKIA
MAD'ARSKÁ KULTURA, Národni třida 22, *115 33 Praha*
PNS DOVOZ TISKU, Vinohradská 46, *Praha 2*
PNS DOVOZ TLAČE, *Bratislava 2*

DENMARK
EJNAR MUNKSGAARD, Norregade 6, *1165 Copenhagen*

FINLAND
AKATEEMINEN KIRJAKAUPPA, P.O. Box 128, *SF-00101 Helsinki 10*

FRANCE
EUROPERIODIQUES S. A., 31 Avenue de Versailles, *78170 La Celle St.-Cloud*
LIBRAIRIE LAVOISIER, 11 rue Lavoisier, *75008 Pari*
OFFICE INTERNATIONAL DE DOCUMENTATION ET LIBRAIRIE, 48 rue Gay-Lussac, *75240 Paris Cedex 05*

GERMAN DEMOCRATIC REPUBLIC
HAUS DER UNGARISCHEN KULTUR, Karl-Liebknecht-Strasse 9, *DDR-102 Berlin*
DEUTSCHE POST ZEITUNGSVERTRIEBSAMT, Strasse der Pariser Kommüne 3—4, *DDR-104 Berlin*

GERMAN FEDERAL REPUBLIC
KUNST UND WISSEN ERICH BIEBER, Postfach 46, *7000 Stuttgart 1*

GREAT BRITAIN
BLACKWELL'S PERIODICALS DIVISION, Hythe Bridge Street, *Oxford OX1 2ET*
BUMPUS, HALDANE AND MAXWELL LTD., Cowper Works, *Olney, Bucks MK46 4BN*
COLLET'S HOLDINGS LTD., Denington Estate. *Wellingborough, Northant NN8 2QT*
WM. DAWSON AND SONS LTD., Cannon House, *Folke tone, Kent CT19 5EE*
H. K. LEWIS AND CO., 136 Gower Street, *London WC1E 3BS*

GREECE
KOSTARAKIS BROTHERS, International Booksellers, 2 Hippokratous Street, *Athens-143*

HOLLAND
MEULENHOFF-BRUNA B.V., Beulingstraat 2, *Amsterdam*
MARTINUS NIJHOFF B.V., Lange Voorhout 9—11, *Den Haag*
SWETS SUBSCRIPTION SERVICE, 347b Heereweg, *Lisse*

INDIA
ALLIED PUBLISHING PRIVATE LTD., 13/14 Asaf Ali Road, *New Delhi 110001*
150 B-6 Mount Road, *Madras 600002*
INTERNATIONAL BOOK HOUSE PVT. LTD., Madame Cama Road, *Bombay 400039*
THE STATE TRADING CORPORATION OF INDIA LTD., Books Import Division, Chandralok, 36 Janpath, *New Delhi 110001*

ITALY
EUGENIO CARLUCCI, P.O. Box 252, *70100 Bari*
INTERSCIENTIA, Via Mazzé 28, *10149 Torino*
LIBRERIA COMMISSIONARIA SANSONI, Via Lamarmora 45, *50121 Firenze*
SANTO VANASIA, Via M. Macchi 58, *20124 Milano*
D. E. A., Via Lima 28, *00198 Roma*

JAPAN
KINOKUNIYA BOOK-STORE CO. LTD., 17-7 Shinjuku-ku 3 chome, Shinjuku-ku, *Tokyo 160-91*
MARUZEN COMPANY LTD., Book Department, P.O. Box 5050 Tokyo International, *Tokyo 100-31*
NAUKA LTD. IMPORT DEPARTMENT, 2-30-19 Minami Ikebukuro, Toshima-ku, *Tokyo 171*

KOREA
CHULPANMUL, *Phenjan*

NORWAY
TANUM-CAMMERMEYER, Karl Johansgatan 41—43, *1000 Oslo*

POLAND
WĘGIERSKI INSTYTUT KULTURY, Marszałkowska 80, *Warszawa*
CKP I W ul. Towarowa 28 *00-95 Warsawa*

ROUMANIA
D. E. P., *Bucureşti*
ROMLIBRI, Str. Biserica Amzei 7, *Bucureşti*

SOVIET UNION
SOJUZPETCHATJ — IMPORT, *Moscow*
and the post offices in each town
MEZHDUNARODNAYA KNIGA, *Moscow G-200*

SPAIN
DIAZ DE SANTOS, Lagasca 95, *Madrid 6*

SWEDEN
ALMQVIST AND WIKSELL, Gamla Brogatan 26, *101-20 Stockholm*
GUMPERTS UNIVERSITETSBOKHANDEL AB, Box 346, *401 25 Göteborg 1*

SWITZERLAND
KARGER LIBRI AG, Petersgraben 31, *4071 Basel*

USA
EBSCO SUBSCRIPTION SERVICES, P.O. Box 1943, *Birmingham, Alabama 35201*
F. W. FAXON COMPANY, INC., 15 Southwest Park, *Westwood, Mass, 02090*
THE MOORE-COTTRELL SUBSCRIPTION AGENCIES, *North Cohocton, N.Y. 14868*
READ-MORE PUBLICATIONS, INC., 140 Cedar Street, *New York, N. Y. 10006*
STECHERT-MACMILLAN, INC., 7250 Westfield Avenue, *Pennsauken N.J. 08110*

VIETNAM
XUNHASABA, 32, Hai Ba Trung, *Hanoi*

YUGOSLAVIA
JUGOSLAVENSKA KNJIGA, Terazije 27, *Beograd*
FORUM, Vojvode Mišića 1, *21000 Novi Sad*

HU ISSN 0001—5407 **Index: 26.007**

ACTA CHIMICA

ACADEMIAE SCIENTIARUM HUNGARICAE

TOMUS 109 FASCICULUS 3

AKADÉMIAI KIADÓ, BUDAPEST

1982

ACTA CHIM. ACAD. SCI. HUNG. ACASA2 109 (3) 219–329 (1982)

ACTA CHIMICA

A MAGYAR TUDOMÁNYOS AKADÉMIA
KÉMIAI TUDOMÁNYOK OSZTÁLYÁNAK
IDEGEN NYELVŰ KÖZLEMÉNYEI

Acta Chimica is a journal for the publication of papers on all aspects of chemistry in English, German, French and Russian.

Acta Chimica is published in 3 volumes per year. Each volume consists of 4 issues of varying size.

Manuscripts should be sent to

Acta Chimica
Budapest, P.O. Box 67, H-1450, Hungary

Correspondence with the editors should be sent to the same address. Manuscripts are not returned to the authors.

Hungarian subscribers should order from Akadémiai Kiadó, 1363 Budapest, P.O.B. 24. Account No. 215 11488.

Orders from other countries are to be sent to "Kultura" Foreign Trading Company (H-1389 Budapest 62, P.O.B. 149. Account No. 218 10990) or its representatives abroad.

Acta Chimica Academiae Scientiarum Hungaricae, Tomus 109 (3), pp. 219—222 (1982)

STRONG TENDENCY TO IMIDE FORMATION OF AN ISOASPARAGINE DERIVATIVE

(PRELIMINARY COMMUNICATION)

I. SCHŐN

(Chemical Works of Gedeon Richter Ltd., Budapest)

Received September 18, 1981
Accepted for publication November 10, 1981

Boc-Asp(OBzl)-$NHCH_2CH_2NH$—Z* (**I**) is not a useful intermediate for peptide synthesis, because its saponification and catalytic hydrogenolysis result in heterogeneous mixtures owing to its strong tendency to base-catalyzed ring closure, followed by hydrolytic decomposition. These observations are inconsistent with previous reports [1, 2].

Recently the synthesis of the so-called 8-β-D-homolysine (N^{CO}-aminoethylisoasparagine) analog of vasopressin, possessing a selective antidiuretic effect has been reported [1, 2]. Key compound **I**, synthesized by the mixed anhydride method, was saponified and the resulting product transformed to an active ester for incorporation into the peptide chain.

Knowing the strong tendency to base catalyzed ring closure followed by hydrolysis of asparagine derivatives [3] and β-benzylaspartyl peptides [4, 5], and on the basis of our keen interest in this field [6, 7], we have doubted that **I** could have been unequivocally saponified.

Therefore **I**, synthesized by us with the pentafluorophenyl ester technique, was saponified with 1.1 equivalent of sodium hydroxide in aqueous ethanol, as reported [8]. Compound **I** disappeared within 15 min, and two products, **III** and **IV**, could be detected by TLC (Fig. 1). **III** and **IV** were separated by column chromatography and isolated in a ratio of 5 to 1. Their structures were confirmed by IR and ^{1}H-NMR spectra and potentiometric titration. It must be mentioned that all fractions collected during the column chromatography contained a trace of the succinimide derivative **II**. It is obvious to suppose that **III** and **IV** formed through the succinimide derivative **II**, which cannot be isolated in aqueous base. However, conversion of **I** to **II** has been observed in dimethylformamide and chloroform in the presence of one equivalent of triethylamine, and even in ethanol without base.

* Abbreviations: Boc = *t*-butyloxycarbonyl, Bzl = benzyl, Z = benzyloxycarbonyl, Pfp = pentafluorophenyl.

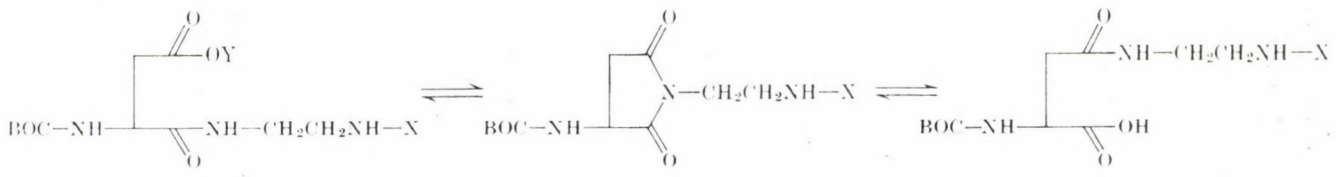

	X	Y
I	Z	Bzl
IV	Z	H
V	H	H

	X
II	Z
VI	H

	X
III	Z
VII	H

Fig. 1. Reaction scheme showing the instability of **I** and its derivatives under the usual conditions of peptide synthesis

Catalytic hydrogenolysis of **I** resulted in **V**, which is very unstable in organic solvents, especially on heating, so during the usual work-up of the reaction mixture and attempted purification by crystallization from ethanol, **V** partially transformed to the succinimide derivative **VI** and to the β-amide **VII**. The same conversion of **V** to **VI** and **VII** was observed in the presence of one equivalent of hydrochloric acid, too. Catalytic hydrogenolysis of **II, III** and **IV** gave a mixture of **V, VI** and **VII** after the usual work-up.

These results suggest that the selected key compound **I** cannot be applied for the synthesis of peptides containing the isoasparagine derivative because of its strong tendency to ring closure followed by hydrolytic decomposition to an unfavorable isomeric mixture. Derivatives of asparagine (**III, VII**) and isoasparagine (**IV, V**) bearing a free carboxyl group also tend to form cyclic derivatives (**II, VI**), especially when the carboxyl is ionized in consequence of the presence of a free amino group (**V, VII**).

Experimental

M.p.'s were taken on a Tottoli (Büchi) apparatus and are uncorrected. Optical rotations were determined on a Perkin–Elmer 141 photoelectric polarimeter. TLC tests were run on precoated silica gel plates (Merck), using the following solvent systems: (1) EtOAc : (pyridine : : AcOH : water = 20 : 6 : 11) = 9 : 1; (2) EtOAc : (pyridine : AcOH : water = 20 : 6 : 11) = = 3 : 2; (3) EtOAc : (pyridine : AcOH : water = 20 : 6 : 11) = 1 : 1; (4) chloroform : methanol = 9 : 1. The chromatograms were visualized by spraying the plates with ninhydrin then with tolidine/KI after chlorination. IR spectra were recorded on a Perkin–Elmer 257 IR spectrophotometer. The ^{1}H-NMR spectra were obtained with a Varian EM 360 spectrometer with TMS as internal standard. Potentiometric titrations were made in 30% aqueous methanol with a Radiometer RTS 822 apparatus, using a saturated calomel/glass electrode pair.

Boc-Asp(OBzl)-NHCH$_2$CH$_2$NH–Z (I)

To a suspension of 2.07 g (9.0 mmol) Z–NHCH$_2$CH$_2$NH$_2$ · HCl [9] and 1.26 mL (9.0 mmol) triethylamine in 10 mL dimethylformamide, 4.41 g (9.0 mmol) Boc-Asp(OBzl)-OPfp (prepared in the usual manner [10] m.p. 81—82 °C) was added. After one hour the reaction mixture was evaporated and a solution of the residue in chloroform was washed with 1 mol/L HCl and 5% $NaHCO_3$ solutions, then the solvent was evaporated. Trituration of the residue with dry ether resulted in 4.35 g **I** which was recrystallized from ethyl acetate/*n*-hexane, to obtain 4.0 g (89.0%) of **I**, m.p. 124—125 °C, $[\alpha]_D^{26}$ —10.2° (c = 1.0; DMF), R_f^1 = 0.7.

IR (KBr): 3310 cm^{-1} (NH), 1730—1630 cm^{-1} (broad, CO), 1240 cm^{-1} (C—O—C), 753, 734 and 697 cm^{-1} (aromatic).

^{1}H-NMR (DMSO): δ 1.55 ppm (s, 9H, ^{t}Bu), about 2.7 ppm (m, 2H, β-CH$_2$), 3.11 ppm (broad, 4H, 2 N—CH$_2$), 4.3 ppm (m, 1H, α-CH), 5.05 ppm (s, 2H, Z—CH$_2$), 5.1 ppm (s, 2H, β-benzyl ester CH$_2$), 6.8—7.5 ppm (broad, 2H, 2 NH, exchangeable with D$_2$O), 7.35 ppm (s, 10H, aromatic), 7.85 ppm (broad, 1H, NH, exchangeable with D$_2$O).

Saponification of I

To a solution of 1.0 g (2.0 mmol) **I** in 20 mL 50% aqueous dioxane, 2.4 ml of a 1 mol/L NaOH solution was added. After 20 min the pH of the reaction mixture was adjusted to 7 with 2.4 mL of a 1 mol/L HCl solution, the dioxane was evaporated, the aqueous solution acidified to pH 3 and extracted five times with a mixture of chloroform/*n*-butanol. The organic phase was evaporated, the crystalline residue dissolved in solvent mixture No. 1 and chromatographied on a silica gel column, using the same solvent mixture. Evaporation of fractions

No. 16 to 25 resulted in 70 mg of the α-amide **IV**, m.p. 108—114 °C, $[\alpha]_D^{28}$ —2.5° (c = 1.0; EtOH), R_f^1 = 0.3, pK = 4.55 (30% methanol).

IR (KBr): 3325 cm^{-1} (NH), 1685 and 1655 cm^{-1} (CO), 1260 cm^{-1} (C—O—C), 750 and 695 cm^{-1} (aromatic).

The β-amide **III** 350 mg was isolated from fractions No. 31 to 52, m. p. 145—146 °C, $[\alpha]_D^{28}$ —0.6° (c = 1.06; EtOH), R_f^1 = 0.1, R_f^2 = 0.6, pK 4.10 (30% methanol).

IR (KBr): 3315 cm^{-1} (NH), 1684 and 1645 cm^{-1} (CO), 1265 cm^{-1} (C—O—C), 750 and 695 cm^{-1} (aromatic).

^{1}H-NMR (DMSO): δ 1.4 ppm (s, 9H, ^{t}Bu), 2.5 ppm (m, 2H, β-CH_2), 3.2 ppm (broad, 4H, 2 N—CH_2), 4.3 ppm (m, 1H, α-CH), 5.6 ppm (s, 2H, Z—CH_2), 6.6 ppm (m, 1H, NH, exchangeable with D_2O), 7.0 ppm (broad, 1H, NH, exchangeable with D_2O), 7.35 ppm (s, 5H, aromatic), 7.8 ppm (m, 1H, NH, exchangeable with D_2O), 5.5—8.0 ppm (very broad, CO_2H + + HDO, exchangeable with D_2O).

All fractions contained a trace of the succinimide derivative **II** which could be removed by trituration with ether during the isolation of **III** and **IV**.

Decomposition of I

To a solution of 0.50 g (1.0 mmol) of **I** in 10 mL dimethylformamide, 0.14 mL (1.0 mmol) triethylamine was added. On TLC 90% conversion was observed after 24 h and transformation of **I** to **II** was complete in 48 h. The reaction mixture was evaporated and the residue triturated with water, resulting in 0.37 g (94.8%) of **II**, m.p. 44—50 °C, R_f^1 = 0.6, R_f^4 = 0.5, $[\alpha]_D^{22}$ +3.2° (c = 1.0; EtOH).

IR (KBr): 3330 cm^{-1} (NH), 1780 cm^{-1} (CO_{imide}), 1730—1640 cm^{-1} (broad, CO), 1240 cm^{-1} (C—O—C), 735 and 697 cm^{-1} (aromatic).

^{1}H-NMR ($CDCl_3$): δ 1.35 ppm (s, 9H, ^{t}Bu), 2.70 ppm (m, 2H, β-CH_2), 3.0—3.85 ppm (broad, 4H, 2 N—CH_2), 4.11 ppm (q, 1H, α-CH), 5.02 ppm (s, 2H, Z—CH_2), 5.7—6.2 ppm (broad, 2H, 2 NH, exchangeable with D_2O), 7.28 ppm (s, 5H, aromatic).

50% conversion of **I** to **II** was observed in chloroform in the presence of one equivalent of triethylamine within 72 h, or in ethanol without triethylamine within 48 h.

Catalytic hydrogenolysis of I, II, III and IV was carried out in the usual way in ethanol, dimethylformamide and in their mixture, resulting in heterogeneous mixtures of **V** (R_f^3 = 0.3), **VI** (R_f^3 = 0.5) and **VII** (R_f^3 = 0.25).

*

The author is grateful to B. Hegedűs for interpretation of the IR spectra, to A. Csehi for interpretation of the ^{1}H-NMR spectra, to F. Trischler for determination of pK values and to Zs. Muck for her skilful technical assistance.

REFERENCES

[1] Tóth, G., Varga, J., Penke, B., Kovács, K.: Abstracts of the Conference of the Hungarian Chemical Society, 1981, Szeged, p. 185.
[2] Kovács, K.: Proc. 21st Hung. Annual Meeting for Biochem., Veszprém, 1981, p. 9.
[3] König, W., Volk, A.: Chem. Ber., **110,** 1 (1977)
[4] Bodanszky, M., Kwei, J. Z.: Int. J. Peptide Protein Res., **12,** 69 (1978)
[5] Bodanszky, M., Tolle, J. C., Deshame, S. S., Bodanszky, A.: Int. J. Peptide Protein Res., **12,** 57 (1978)
[6] Schön, I., Kisfaludy, L.: in Peptides, Structure and Biological Function: Gross, E., Meienhofer, J., eds., Pierce Chemical Co., Rockford, 1979, p. 277.
[7] Schön, I., Kisfaludy, L.: Int. J. Peptide Protein Res., **14,** 485 (1979)
[8] Tóth, G.: personal communication
[9] Lawson, W. B., Leafer, M. D., Tewes, A.: Z. Physiol. Chem., **349,** 251 (1968)
[10] Kisfaludy, L., Lőw, M., Nyéki, O., Szirtes, T., Schön, I.: Ann., **1973,** 1421

István Schön H-1475 Budapest, P.O. Box 27

Acta Chimica Academiae Scientiarum Hungaricae, Tomus 109 (3), pp. 223—228 (1982)

MOLECULAR REARRANGEMENTS, XVII*

PHOTOLYSIS OF ACID AMIDES AND PHENYLACETANILIDE[a]

M. Z. A. BADR,** M. M. ALY, A. M. FAHMY and F. F. ABDEL-LATIF

(Chemistry Department, Faculty of Science, Assiut University, Assiut, Egypt, A. R. E.)

Received October 1, 1980
Accepted for publication November 11, 1980***

The acetone-initiated photolysis of phenylacetamide in air gives benzaldehyde, toluene, bibenzyl, stilbene and phenanthrene. Similar products, in addition to benzylamine, are obtained from the photolysis of *N*-benzylphenylacetamide. α-phenylacetanilide on photolysis gives the same compounds together with aniline, *N*-benzylaniline and a mixture of *o*- and *p*-aminodiphenylmethanes.

The photosensitized mechanism is suggested to proceed through phenylcarbene and aminyl radicals, whereas the nonsensitized mechanism in proposed to start with the homolysis of the amide C—N linkage to give phenylacetyl and aminyl radicals which subsequently contribute to the formation of the identified products.

Formamide has been reported to undergo photolytic decomposition [1] into hydrogen and amidyl radicals that can affect the amidation of olefinic and acetylenic compounds. The initial attack of the carbamoyl radicals on terminal olefins occurs mainly at the terminal carbon atom, *i.e.* in an anti-Markownikoff reaction. The amidation of aromatic hydrocarbons also readily takes place on photolysis with formamide in acetone solution, the solvent acting as a sensitizer [2]. The photolysis of acetamide [3] in aqueous medium leads to the formation of ammonium acetate through homolysis into amino and acetyl radicals, the latter subsequently undergoing, decarbonylation to CO and $\cdot CH_3$. Ascending in the series of alkyl acid amides [4], the presence of hydrogen among the photolysates becomes apparent, indicating preferential homolysis of the nitrogen-hydrogen of the amide.

N-Aryl acid amides were reported to undergo photo-induced Fries rearrangement [5] to the corresponding *o*- and *p*-aminophenyl alkyl ketones through a free radical intermolecular mechanism involving homolysis of the acyl-N bond.

The present paper deals with the partial photolysis of acid amides (about 50% conversion) avoiding complications due to secondary photolysis of the initially formed products.

* Part XVI, See M. Z. A. BADR, M. M. ALY and A. M. FAHMY: Canad. J. Chem., **58**, 1229 (1980).

** To whom correspondence should be addressed.

*** In final form accepted July 7, 1981.

[a] Presented in part at the 8th IUPAC Symposium on Photochemistry, Seefeld, Austria, July 13—19, 1980.

Phenylacetamide and *N*-benzylphenylacetamide were found to be photochemically stable in both carbon tetrachloride and isopropanol solutions, even after prolonged irradiation periods. However, phenylacetamide did undergo acetone-initiated photolysis to give benzaldehyde, toluene, bibenzyl, *trans*-stilbene and phenanthrene as neutral products, besides ammonia. The same products and benzylamine are also obtained in the photolysis of *N*-benzylphenylacetamide in acetone.

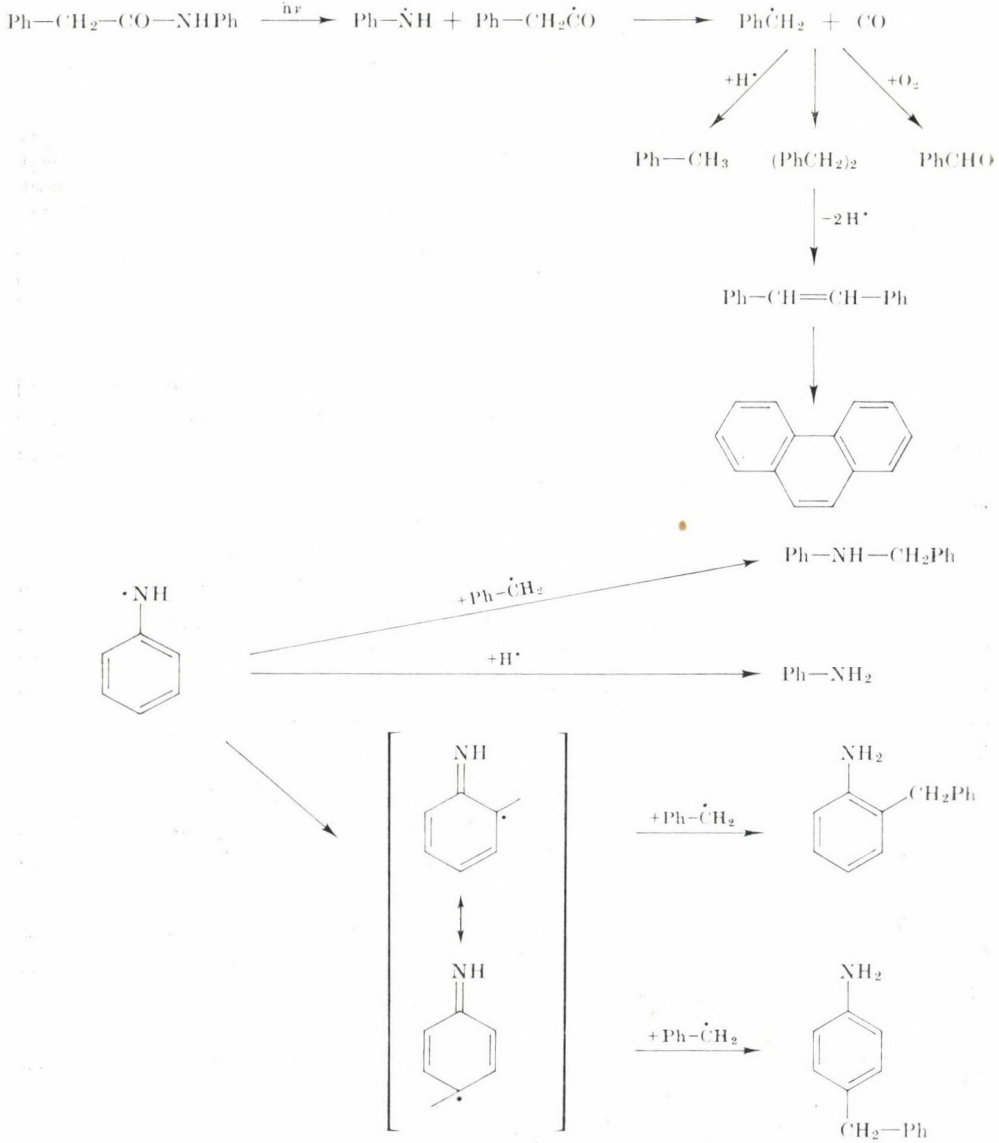

Scheme 1

On the other hand, α-phenylacetanilide undergoes facile non-sensitized photodecomposition on irradiation in carbon tetrachloride solution to give the same products as *N*-benzylphenylacetamide does, in addition to aniline, *N*-benzylaniline and a mixture of *o*- and *p*-aminodiphenylmethanes. Such a non-sensitized process must involve the preliminary homolysis of the amide C—N linkage into phenylacetyl and aminyl radicals. Phenylacetyl radicals undergo then decarbonylation [6] rather than dimerization giving rise to carbon monoxide and benzyl radicals, which subsequently undergo atmospheric oxidation to benzaldehyde [7], abstract hydrogen to given toluene, or dimerize to bibenzyl, the latter, in turn, undergoes dehydrogenation in part to yield *trans*-stilbene and phenanthrene, as shown in Scheme 1. The aminyl radicals (PhNH) are converted partially to the corresponding primary amine through hydrogen abstraction (Scheme 1), or they are attacked by the benzyl radicals in the *o*- and *p*-positions to afford the isomeric *o*- and *p*-aminodiphenylmethanes.

In the photosensitized reaction it seems unlikely that the process involves direct energy transfer from acetone in its excited state to the anilide, since acetone has a lower *Eo* value than the anilides under investigation. The more likely role of acetone as a sensitizer is its tendency to form ketyl radicals [8], especially in the presence of amides, which are known to possess potential reactive C—H bonds [9].

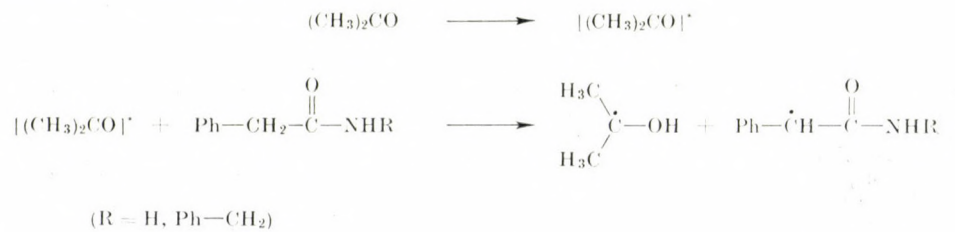

(R = H, Ph—CH_2)

The anilide radicals so obtained from phenylketone and aminyl radicals in an analogous manner to that proposed for the thermolysis [10] and photolysis [11] of phenolic esters.

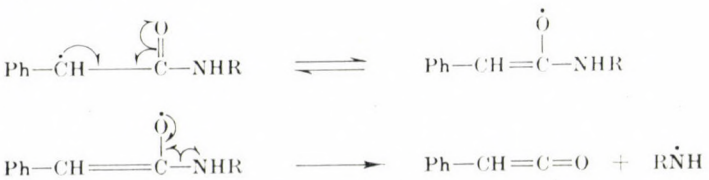

Phenylketene decomposes readily to give phenylcarbene and CO [12].

The phenylcarbene is then converted by H abstraction to benzyl radicals, which subsequently participate in the formation of the identified products as mentioned before.

Stilbene is rationally assumed to be formed from bibenzyl through hydrogen abstraction as described in a previous work [13] and not through dimerization of phenylcarbene that would ultimately form 1,2,3-triphenylcyclopropane. The absence of this compound among the products strongly suggests the preferential conversion of phenylcarbene to benzyl radicals.

Although bibenzyl is formed through dimerization of the benzyl radicals, the corresponding amino dimers, *viz.*, hydrazine, *sym*-diphenylhydrazine and *sym*-dibenzylhydrazine are not detected among the products. These hydrazine derivatives are quite stable under such irradiation conditions [14], hence it can be concluded that the aminyl radicals preferably react by hydrogen abstraction.

Stilbene can be assumed to be the precursor of phenanthrene, undergoing first cyclization to dihydrophenanthrene, followed by hydrogen abstraction by free radicals present in the reaction medium, and probably by atmospheric oxygen [15].

Experimental

Melting and boiling points are uncorrected. The purity of the starting materials was checked by gas-liquid chromatographic analysis (GLC) using a Pye-Unicam gas chromatograph, "Series 104", equipped with a dual flame ionization detector, Model 24, using nitrogen as the carrier gas. The products were characterized by comparison of the GLC retention times with those of authentic samples on two columns with different separation characteristics, or on one column at two different flow rate of the carrier gas. The columns used were 5 m × 5 mm and packed with 20% SE 30 on Chromsorb W (35—80 mesh) or 10% SE 30 on Celite (60—80 mesh). Quantitative GLC was accomplished by determination of the peak areas of the products. Ultraviolet irradiation was carried out using a Mallinkrodt 150 W mercury discherge lamp and the solutions were contained in open-topped pyrex beakers. The solvents used were of "AnalaR" grade and used without further purification.

Photolysis of amides

The amide (0.01 mole) in the solvent used (100 mL) was directly irradiated on the top surface of solution at room temperature (~25 °C) for 15 h. The photolysate was separated as indicated in previous work [15] into amine and neutral products and analyzed by GLC. Phenanthrene was further identified by preparative TLC (Merck Silica Gel F_{254}, 70% ethanol) and picrate formation; m.p. and mixed m.p. 142—143 °C. The results are summarized in Table I.

Preparation of the reference compounds

Bibenzyl [17]: crystals from ethanol, m.p. 52 °C; 4,4'-dinitro derivative, m.p. 180 °C.
trans-Stilbene [18]: crystals from ethanol, m.p. 123—4 °C.
N-Benzylaniline [19]: b.p. 148—9 °C 4 mbar, m.p. 36 °C; picrate, m.p. 48 °C
Phenylacetamide [20]: crystals from dilute ethanol, m.p. 155—6 °C.
α-Phenylacetanilide [21]: crystals from dilute ethanol, m.p. 116—7 °C.

Table I

Composition of amide photolysates

Products, in g (%)	Phenylacetamide in acetone		α-Phenylacetanilide* in carbon tetrachloride		*N*-Benzylphenylacetamide in acetone	
Unchanged amide	0.547	(40.50)	0.981	(45.50)	1.039	(46.20)
Benzaldehyde	0.029	(2.15)	0.035	(1.66)	0.024	(1.07)
Toluene	0.070	(5.18)	0.080	(3.80)	0.200	(0.88)
Stilbene	0.220	(16.30)	0.170	(8.05)	0.140	(6.22)
Bibenzyl	0.150	(11.11)	0.100	(4.74)	0.080	(3.55)
Phenanthrene	0.340	(25.18)	0.250	(11.85)	0.520	(23.11)
R-NH_2	(a)		0.300	(14.21)[b]	0.420	(18.68)[c]
N-Benzylaniline	—		0.140	(6.63)	—	
o-Aminodiphenylmethane	—		0.083	(3.98)	—	
p-Aminodiphenylmethane	—		0.062	(2.94)		

[a] Ammonia evolved, [b] aniline, [c] benzylamine. * In the absence of photosensitizer.

N-Benzylphenylacetamide [22]: crystals from dilute ethanol, m.p. 116—7 °C.
o-Aminodiphenylmethane [23]: crystals from petrol. ether (40—60 °C), m.p. 52 °C; *N*-acetyl derivative, m.p. 135 °C.
p-Aminodiphenylmethane [24]: b.p. 165—7 °C/2.66 mbar, crystals from petroleum ether (40—60 °C), m.p. 34—36 °C; picrate, m.p. 179 °C.
1,2,3-Triphenylcyclopropane [25]: crystals from ethanol, m.p. 61—63 °C.

REFERENCES

[1] Elad, D., Rokach, J.: J. Chem. Soc., **1965,** 800
[2] Elad, D.: Tetrahedron Letters, **2,** 77 (1963)
[3] Volman, D. V.: J. Am. Chem. Soc., **63,** 2000 (1941)
[4] Farkas, L., Jones, W.: Z. Physik. Chem., **18,** 124 (1932)
[5] Kobsa, C. F. H.: J. Org. Chem., **27,** 2293 (1962)
[6] Winstein, S., Seubold, F. H., Jr.: J. Am. Chem. Soc., **69,** 2916 (1947)
[7] Woodward, A. E., Mesrobian, R. B.: J. Am. Chem. Soc., **75,** 6189 (1953)
[8] Chapman, O. L.: Organic Photochemistry, Vol. II, p. 8, M. Dekker, New York 1969
[9] Nikishin, Q. I., Mustafaev, R. I.: Dokl. Akad. Nauk SSSR, **158,** 1127 (1964)
[10] Hurd, C. D., Blunk, F. H.: J. Am. Chem. Soc., **60,** 2419 (1938)
[11] Meyer, J. W., Hammond, G. S.: J. Am. Chem. Soc., **94,** 2219 (1972)
[12] Norrish, R. G. W., Corne, H. G., Saltmarsh, O.: Chem. Soc., **1933,** 1533
[13] Badr, M. Z. A., Aly, M. M., El-Sherief, H. A. H., Abdel-Rahman, A. E.: J. Appl. Chem., Biotechnol, **27,** 291 (1977)
[14] Ratcliff, M. A., Kochi, J. K.: J. Org. Chem., **37,** 3268 (1972)
[15] Hugelshofer, P., Kalvoda, J., Schaffnes, K.: Helv. Chim. Acta, **43,** 1322 (1960)
[16] Badr, M. Z. A., Aly, M. M.: Can. J. Chem., **52,** 293 (1974)
[17] Cannizaro, L., Rossi, G.: Ann., **251,** 121 (1862)
[18] Ballard, D. A., Dehn, W. M.: J. Am. Chem. Soc., **54,** 3969 (1932)
[19] Vogel, A. I.: Practical Organic Chemistry, p. 572. Longmans, London 1956

[20] MEYER, H.: Monatsh., **27**, 34 (1906)
[21] STAUDINGER, H.: Ber., **44**, 537 (1011)
[22] RAMART, P., HALLER, A.: Compt. rend., **178**, 1585 (1924)
[23] HEWETT, C. L., LERMIT, L. J., OPENSHAW, H. T., TODD, A. R., WILLIAMS, A. H., WOODWARD, F. N.: J. Chem. Soc., **1948**, 292
[24] HICKINBOTTOM, W. J.: J. Chem. Soc., **1937**, 119
[25] BRIDSON, J. F. S., BUCKLEY, F. D., CROSS, L. H., DRIVER, A. P.: J. Chem. Soc., **1951**, 2999

M. Z. A. BADR
M. M. ALY
A. M. FAHMY
F. F. ABDEL-LATIF

Chemistry Department, Faculty of Science, Assiut Univ. Assiut, Egypt

Acta Chimica Academiae Scientiarum Hungaricae, Tomus 109 (3), pp. 229—236 (1982)

C-NUCLEOSIDES, IV*

PREPARATION OF 2-(POLYHYDROXYALKYL)-5-CHLORO- AND 2-β-D-GLYCOSYL-5-CHLOROBENZOTHIAZOLE DERIVATIVES

I. F. SZABÓ, L. SOMSÁK, GY. BATTA and I. FARKAS**

(Institute of Organic Chemistry, Kossuth Lajos University, Debrecen, and Antibiotics Chemical Research Group, Hungarian Academy of Sciences, Debrecen)

Received October 16, 1980
Accepted for publication February 24, 1981

2-(Polyacetoxyalkyl)- and 2-(per-*O*-acyl-β-D-glycosyl)-5-chlorobenzothiazoles were prepared by the condensation of appropriate acetylated aldonic nitriles or peracylated β-D-glycosyl cyanides with 2-amino-4-chlorothiophenol. The compounds can be deacetylated to obtain crystalline hydroxy derivatives. On the basis of NMR investigations, the β configuration can be assigned to the compounds of the *C*-nucleoside type.

In the course of our earlier research it was established that per-*O*-acylated aldonic nitriles can be converted with 2-aminothiophenol into the corresponding 2-(polyacetoxyalkyl)-benzothiazoles in satisfactory yields [1]. In two cases the reaction was also employed for the synthesis of 2-(polyhydroxyalkyl)-5-chlorobenzothiazoles [1]. Peracylated β-glycosyl cyanides yielded 2-glycosylbenzothiazoles in this manner [2, 3, 4].

Recently, ZHDANOV *et al.* [5] synthesized 2-(polyhydroxyalkyl)-benzothiazoles from *al*-sugar derivatives through carbanion addition (the carbanion is formed in the reaction mixture by interaction of phenyllithium and benzothiazole).

TRONCHET and GENTILE [6] prepared so-called "inverse" 2-glycosylbenzothiazoles from *aldehydo*-sugar derivatives and 2-aminothiophenol by oxidative condensation reactions.

The method developed by us is significantly simpler than the syntheses used heretofore.

In continuation of our research, the formation in good yields of 2-(polyacetoxyalkyl)- (**11**—**16**) and 2-(per-*O*-acyl-β-glycosyl)-5-chlorobenzothiazoles (**17**—**20**) was observed from 2-amino-4-chlorothiophenol and the appropriate acylated aldonic nitrile or glycosyl cyanide (Fig. 1). The most important data of the compounds are given in Tables I and II.

The acyl derivatives, which are homogeneous crystalline substances except for **13**—**15** and **19**, can be deacylated with methanolic sodium methoxide solution to give the crystalline hydroxy derivatives **21**—**30**.

* For Part III, see Ref. [4].
** To whom correspondence should be addressed.

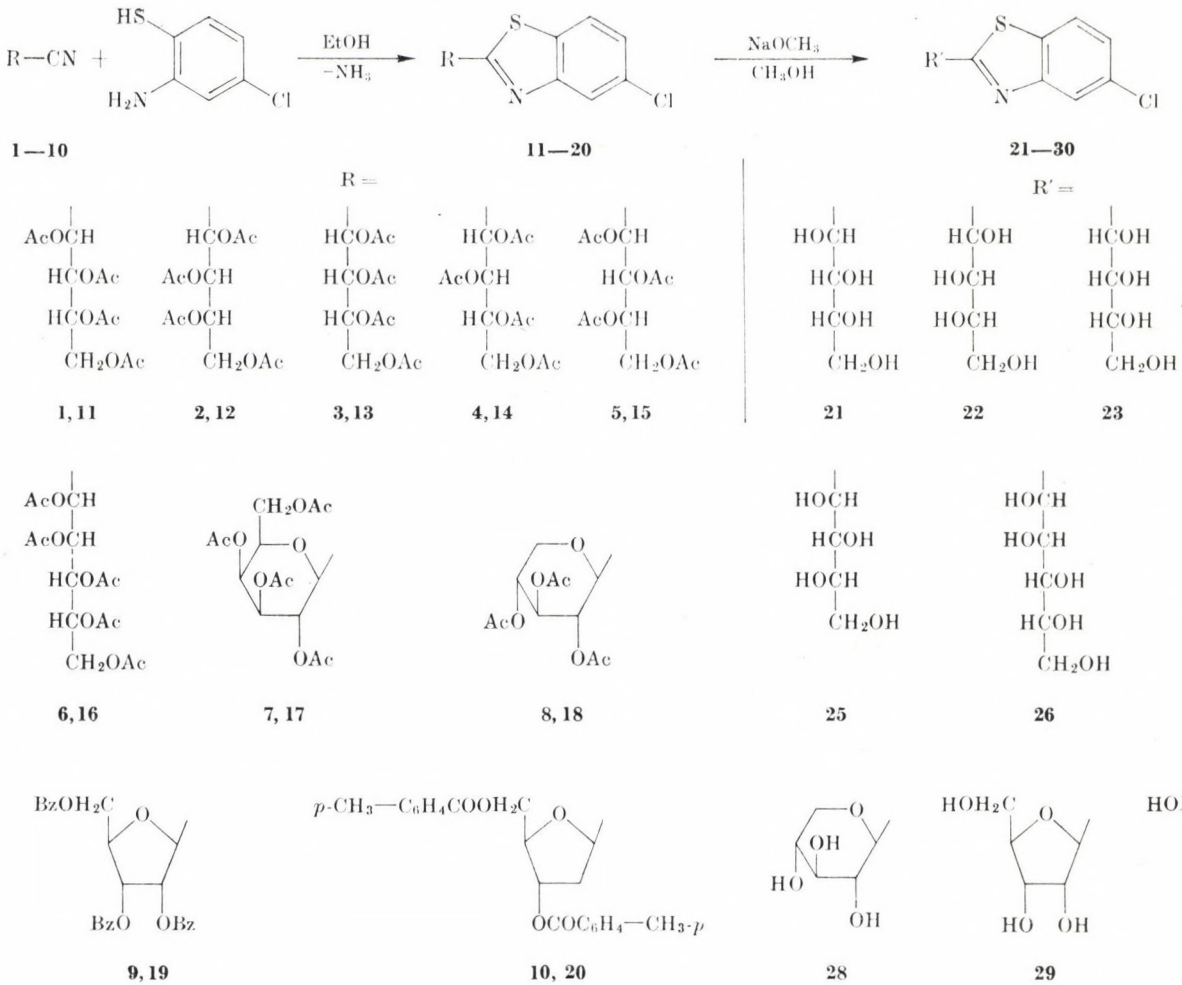
R—CN +
HS
H2N
Cl
EtOH
−NH3
S
N
NaOCH3
CH3OH
1—10
11—20
21—30
R =
R′ =
AcOCH
HCOAc
CH2OAc
HCOAc
AcOCH
HCOH
HOCH
CH2OH
1, 11
2, 12
3, 13
4, 14
5, 15
21
22
23
24
AcO
OAc
6, 16
7, 17
8, 18
25
26
27
BzOH2C
BzO
OBz
9, 19
p-CH3—C6H4COOH2C
OCOC6H4—CH3-p
10, 20
28
29
30

Fig. 1

Table I

Preparation of 2-(polyacetoxyalkyl)- and 2-(polyhydroxy-alky)-5-chlorobenzothiazoles

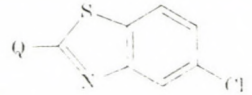	Yield, %	M.p., °C	$[\alpha]_D$	Molecular formula (M. w.)	Analysis					
					Calculated			Found		
					N	S	Cl	N	S	Cl
D-*arabo*-tetraacetoxy-butyl (**11**)	65	147—148	−5.9*	$C_{19}H_{20}NO_8SCl$ (457.9)	3.06	7.00	7.74	2.99	6.94	7.84
L-*arabo*-tetraacetoxy-butyl (**12**)	70	147—148	+5.8*					3.00	6.83	7.81
D-*manno*-pentaacetoxy-pentyl (**16**)	86***	119	+16.7*	$C_{22}H_{30}NO_{10}SCl$ (536.0)	2.61	5.98	6.61	2.73	5.98	6.75
D-*arabo*-tetrahydroxy-butyl (**21**)	83	217—218	−140.7**	$C_{11}H_{12}NO_4SCl$ (289.7)	4.83	11.07	12.24	4.71	11.17	12.42
L-*arabo*-tetrahydroxy-butyl (**22**)	86	217—218	+149.1**					4.76	11.21	12.22
D-*ribo*-tetrahydroxy-butyl (**23**)	69	209—210	+92.3*					4.63	11.03	12.33
D-*xylo*-tetrahydroxy-butyl (**24**)	67	176—177	−111.0**					4.65	11.19	12.49
L-*xylo*-tetrahydroxy-butyl (**25**)	70	176—177	−115.7**					4.67	10.97	12.46
D-*manno*-pentahydroxy-pentyl (**26**)	75	215	−68.1**	$C_{12}H_{15}NO_5SCl$ (320.8)	4.37	10.00	11.05	4.35	9.95	11.10

* In chloroform; ** in pyridine; *** by acetylation of the hydroxy derivative **26**.

Table II

Preparation of 2-(β-D-glycosyl)-

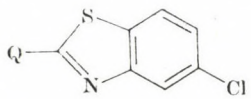	Yield, %	M.p., °C	$[\alpha]_D$	Molecular formula (M. w.)
tetra-*O*-acetyl-β-D-galacto-pyranosyl (**17**)	85	160—161	+11.3*	$C_{21}H_{22}NO_9SCl$ (499.9)
β-D-galactopyranosyl (**27**)	93	191—192	+36.5**	$C_{13}H_{14}NO_5SCl$ (331.8)
tri-*O*-acetyl-β-D-xylopyranosyl (**18**)	77	178—179	−44.5*	$C_{18}H_{18}NO_7SCl$ (427.9)
β-D-xylopyranosyl (**28**)	78	191	−28.6**	$C_{12}H_{12}NO_4SCl$ (301.7)
β-D-ribofuranosyl (**29**)	63	207—208	−46.7**	$C_{12}H_{12}NO_4SCl$ (301.7)
di-*O*-*p*-toluoyl-2-desoxy-β-D-ribofuranosyl (**20**)	70	98—100	−32.0**	$C_{28}H_{24}NO_5SCl$ (522.0)
2-desoxy-β-D-ribofuranosyl (**30**)	94	148	+43.9**	$C_{12}H_{12}NO_3SCl$ (285.7)

* In chloroform; ** in pyridine.

Table III

First order analysis of the ^{1}H-NMR *spectra* (100 MHz) *of 2-(polyacetoxy-alkyl)-*

Compd. Conf.	Chemical shift (δ, ppm)									
	H-1	H-2	H-3	H-4	H-4′	H-5	H-5′	OH-1	OH-2	OH-3
11 D-arabino	6.46	5.81	5.33	4.36	4.18	—	—	—	—	—
16 D-manno	6.15	5.75	5.67	5.18	—	4.28	4.10	—	—	—
21 D-arabino						—	—	6.5		
23 D-ribo	5.40	4.15				—	—	6.6	4.8	4.6
24 D-xylo	5.35	4.21				—	—	6.5		
26 D-manno	5.14	4.83			—			6.6		

5-chlorobenzothiazoles

Analysis					
Calculated			Found		
N	S	Cl	N	S	Cl
2.80	6.41	7.09	2.87	6.67	7.15
4.22	9.66	10.69	4.09	9.63	10.66
3.27	7.49	8.29	3.23	7.58	8.12
4.64	10.63	11.75	4.44	10.45	11.64
4.64	10.63	11.75	4.38	10.58	11.70
2.68	6.14	6.79	2.60	6.13	6.78
4.90	11.22	12.41	4.74	11.37	12.45

and 2-(polyhydroxyalkyl)-5-chlorobenzothiazoles

Coupling constant, Hz											Solvent, temp.
$J_{1,2}$	$J_{2,3}$	$J_{3,4}$	$J_{3,4'}$	$J_{4,4'}$	$J_{4,5}$	$J_{4,5'}$	$J_{5,5'}$	$J_{OH1\,H1}$	$J_{OH2\,H2}$	$J_{OH3\,H3}$	
2.8	8.9	3.0	4.6	12.6	—	—	—	—	—	—	$CDCl_3$, room temp.
8.6	~2	8.8	—	—	3.0	5.0	12.4	—	—	—	$CDCl_3$, room temp.
					—	—	—				DMSO-d_6 room temp.
~4.6	6				—	—	—	~6	~6	~5	DMSO-d_6 $t = +80$°C
3.8	3.6				—	—	—	~5			DMSO-d_6 $t = 80$ °C
8			—	—				~6			DMSO-d_6 room temp.

Table IV

First order analysis of the ^{1}H-NMR *spectra* (100 MHz)

Compd.	Chemical shift (δ, ppm)								
	$H_{1'}$	$H_{2'}$ a	$H_{2'}$ b	$H_{3'}$	$H_{4'}$	$H_{5'}$ a	$H_{5'}$ b	$H_{6'}$ a	$H_{6'}$ b
17	4.92	5.47	—	5.29	5.58	4.25	—	4.25	4.25
18*	4.84	5.46	—	5.23	5.14	4.36	3.57	—	—
20	5.6	2.7	2.7			4.6	4.6	—	—
27	5.00	4.61	—	4.17	4.51	4.15	—	4.25	4.25
28	4.96	4.3	—	4.3	3.7	4.1		—	—
29	5.65	4.62	—	4.70	4.84	4.2	4.2	—	—
30	5.96	2.86	2.58	4.92	4.67	4.16	4.06	—	—

* The assignment of H-2′ and H-3′ is interchangeable.

Similarly to the case of the compounds prepared earlier [1], the polyhydroxyalkyl derivatives **21**—**26** obey the "general heterocyclic rule" [7] regarding the direction of optical rotation and the configuration of the carbon atom of the polyhydroxyalkyl chain attached to the hetero ring. In connection with this, the conformational conditions of the compounds were investigated by NMR spectroscopic methods. It was found that the side-chain in the polyacetoxyalkyl derivatives **11** and **16** had practically the same conformation (Table III) as in the benzothiazole derivatives examined earlier [8]. The present NMR data did not provide sufficient information regarding the conformations of the polyhydroxyalkyl derivatives **21**—**26**.

In the compounds of the *C*-nucleoside type, the coupling constants of the anomeric protons (*cf.* Table IV) unambiguously indicate the β-configuration of glycopyranosides **17**, **18**, **27** and **28** ($J_{1',2'} = 9$ Hz). The sum of the coupling constants of the anomeric protons ($J_{1'2'a} + J_{1,2'b} = 16$ Hz) in the 2-desoxy-D-ribofuranoside derivatives (**20** and **30**) allows assuming their β-configuration [9]. All these are in agreement with our earlier observations [3, 4] that the conversions do not alter the anomeric configuration. Although no information is provided by the spectral data regading the anomeric configuration of the ribofuranoside derivative **29**, β-configuration can be assigned also to this compound on the basis of the stereoselectivity of analogous reactions.

of 2-(β-D-glycosyl)-5-chlorobenzothiazoles

Coupling constant, Hz									Solvent, temp.
$J_{1'2'a}$	$J_{1'2'b}$	$J_{2'a,3'}$	$J_{2'a,2'b}$	$J_{2'b3'}$	$J_{3'4'}$	$J_{4'5'a}$	$J_{4'5'b}$	$J_{5'a5'b}$	
8.8	—	10.0	—	—	3.2		—	—	$CDCl_3$, room temp.
9.6	—	9.4	—	—	9.4	5.6	10.4	10.8	$CDCl_3$, room temp.
6	10								$CDCl_3$, room temp.
9.5	—	9.0	—	—	3.6	1.2	—	—	Py-d_5 $t = +75$ °C
8.8									Py-d_5 $t = +80$ °C
4.8	—	7.8	—	—	4.0	4.8	1.2	—	Py-d_5 $t = +75$ °C
6.8	9.0	2.8	12.8	5.6	2.5	4.5	5	12	Py-d_5 room temp.

Experimental

Optical rotation of the substances was measured with a Perkin–Elmer 241 polarimeter. The NMR spectra (100 MHz) were recorded with a JEOL Minimar MH-100 spectrometer. The internal standard was TMS or, in the case of compounds **21**, **23**, **24**, **26**, HMDS.

The spectra were analysed in the first order. The spectrum of the entirely assigned compound **30** was simulated in the first order [10].

M. p.'s are uncorrected. The solutions were dried over anhydrous $MgSO_4$ and evaporated to dryness on a water bath at 40—50 °C under reduced pressure.

Preparation of 2-(per-*O*-acetyl-polyhydroxyalkyl)- and 2-(per-*O*-acyl-β-D-glycosyl)-5-chlorobenzothiazoles (11—20)

The per-*O*-acetylated aldonic nitrile (**1**—**6**) (10 mmole) or per-*O*-acyl-β-D-glycosyl cyanide (**7**—**10**) was dissolved in hot anhydrous ethanol (about 40 mL), 2-amino-4-chlorothiophenol (15 mmole, 2.4 g) was added to the solution and it was refluxed on a water bath while nitrogen gas was passed through it, for 4 h.

After cooling, the crystalline product was filtered off with suction and recrystallized from anhydrous ethanol (**11**, **12**, **17**, **18**, **20**).

Since the peracetates **13**—**15** could not be crystallized, the solutions were evaporated to dryness and deacetylated to give the polyhydroxyalkyl derivatives **23**—**25** (see later).

Compounds **16** and **19** could not be isolated as homogeneous substances either. Therefore, they were deacetylated to obtain **26** and **29**. Acetylation of the former yielded crystalline **16**-acetate (see later).

Deacylation of the peracylated derivatives (11—20)

The isolated crystalline ester (**11**, **12**, **17**, **18**, **20**) or the syrup obtained on evaporation of the ethanolic solution (**13**—**16**, **19**) was dissolved in about 6—10 parts of hot anhydrous methanol, then methanolic 1*N* sodium methoxide solution was added to it to adjust a stable alkaline reaction (pH = 8). The solution was cooled and maintained at 0 °C for 16 h. The reaction mixture was then acidified with glacial acetic acid and processes as follows.

(*a*) The crystalline product which separated was filtered off by suction and recrystallized from 50% aqueous ethanol (**21**, **22**, **26**), a mixture of ethanol and water (2.5:1) (**23**), ethanol (**24**, **25**, **28**), from methanol (**29**), or from methanol or water (**27**).

(*b*) In the deacylation of **20**, the methanolic solution obtained according to the foregoing procedure was evaporated to dryness. The residual syrup was rubbed with ether whereupon it solidified, this product was recrystallized from ethanol (**30**).

2-(D-Manno-pentaacetoxypentyl)-5-chlorobenzothiazole (16)

The hydroxy derivative **26** (0.5 g) was allowed to stand in a mixture of anhydrous pyridine (5 mL) and acetic anhydride (5 mL) at 20 °C for 18 h. The solution was evaporated to dryness in vacuum, then ethanol was distilled from it repeatedly. The residue was crystallized from a mixture of ether and petroleum ether.

*

The authors' thanks are due to Dr. J. HARANGI for his assistance in the computerized simulation of spectra.

REFERENCES

[1] BOGNÁR, R., FARKAS, I., SZILÁGYI, L., MENYHÁRT, M., N.-NEMES, É., F.-SZABÓ, I.: Acta Chim. Acad. Sci. Hung., **62**, 179 (1969)
[2] FARKAS, I., F.-SZABÓ, I., BOGNÁR, R.: Carbohydr. Res., **56**, 404 (1977)
[3] FARKAS, I., F.-SZABÓ, I., BOGNÁR, R., SZILÁGYI, L.: Khim. Geterotsikl. Soedin., **1978** (7), 893
[4] F.-SZABÓ, I., FARKAS, I., SOMSÁK, L., BOGNÁR, R.: Acta Chim. Acad. Sci. Hung., **106**, 61, (1981).
[5] ZHDANOV, J. A., ALEKSEIEVA, V. G., FOMINA, V. N., MIRNÜJ, V. N.: Dokladi Akad. Nauk. SSR, **221**, 100 (1975)
[6] TRONCHET, J. M. J., GENTILE, B.: Helv. Chim. Acta, **62**, 1298 (1979)
[7] EL-KHADEM, H., EL-SHAFEI, Z. M.: Tetrahedron Letters, **1963**, 1887; HORTON, D., LIAV, A.: Carbohydr. Res., **47**, 81 (1976)
[8] SZILÁGYI, L., BOGNÁR, R., FARKAS, I.: Carbohydr. Res., **26**, 305 (1973)
[9] KOLB, A., GOUYETTE, C., HUYNH-DINH, T., IGOLEN, J.: Tetrahedron, **31**, 2914 (1975); HUYNH-DINH, T., IGOLEN, J., BISANI, E., MARQUET, J. P., CIVIER, A.: J. Chem. Soc. Perkin I, **1977**, 761
[10] WRIGHT, J. R., ROBINSON, J. L.: J. Chem. Ed., **56**, 643 (1979)

Ilona FARKAS-SZABÓ
László SOMSÁK
Gyula BATTA
István FARKAS

H-4010 Debrecen, P.O. Box 20.

Acta Chimica Academiae Scientiarum Hungaricae, Tomus 109 (3), pp. 237—240 (1982)

STUDIES ON PYRIDAZINE DERIVATIVES, IX*

NOTE ON THE ETHOXYCARBONYLATION OF PYRIDAZINYLHYDRAZONES

P. MÁTYUS[1]**, G. SZILÁGYI[1], E. KASZTREINER[1], M. SÓTI[1] and P. SOHÁR[2]

([1] Institute for Drug Research, Budapest and [2] EGYT Pharmacochemical Works, Budapest)

Received January 26, 1981
Accepted for publication February 24, 1981

The reaction with diethyl pyrocarbonate of the pyridazinylhydrazone **1** led either to the *s*-triazolo[4,3-*b*]pyridazine-3-one derivative **3**, or to the *endo*-*N*-ethoxycarbonyl compound **6**, depending on the reaction conditions. The structures of the compounds were established both by chemical and spectroscopic studies.

We have previously reported that the reaction with diethyl pyrocarbonate of antihypertensive pyridazinylhydrazones **I** [1, 2] could lead to the *endo*- (**II**) and/or *exo*-*N*-ethoxycarbonyl derivatives (**III**) [3, 4].

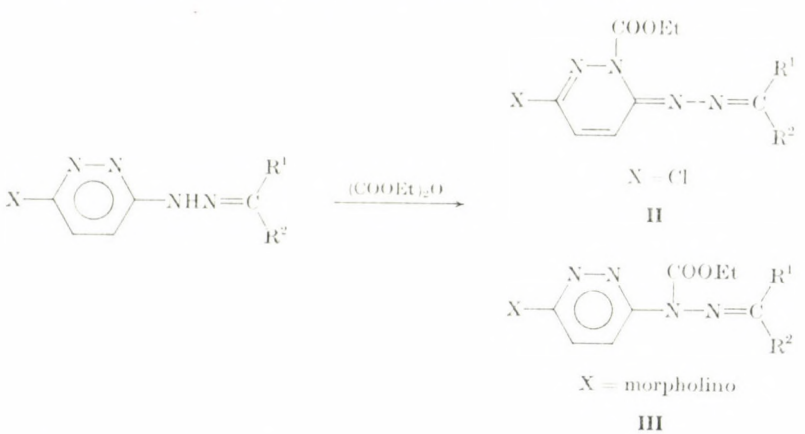

In the course of our further studies on structure–activity relationships synthesis of the *N*-ethoxycarbonyl derivative of the most effective compound of this series (**1**) [1, 2] appeared desirable. On the basis of our previous results the reaction with diethyl pyrocarbonate of **1** was expected to give an *exo*-acyl derivarive of type **III**.

However, treatment of **1** with diethyl pyrocarbonate in dichloromethane at room temperature gave the unexpected 2,3-dihydro-*s*-triazolo[4,3-*b*]pyr-

* For Part VIII, see Ref. [1].
** To whom correspondence should be addressed.

idazine derivative **3**, presumably *via* the intramolecular ring closure of the intermediate **2**.

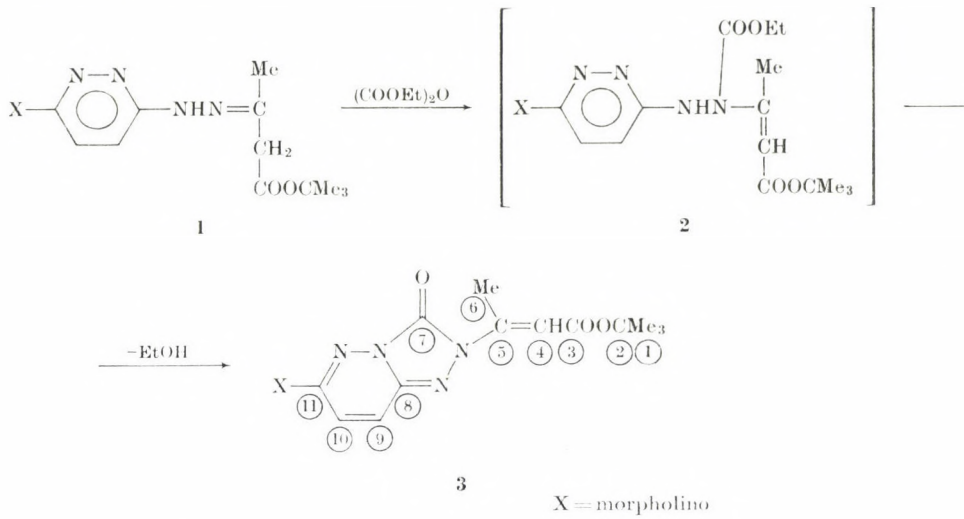

1 2 3

In the ^{1}H-NMR spectrum of compound **3*** the olefinic proton in the side chain appeared as a quartet, due to allylic coupling with the methyl hydrogens at 6.90 ppm.**

The assumed structure of **3** was also confirmed by synthesis. Treatment with hydrogen chloride of **3** led by N—C bond fission to 6-morpholino-2,3-dihydro-*s*-triazolo[4,3-*b*]pyridazine-3-one (**4**) which was also prepared from the known 6-chloro-2,3-dihydro-*s*-triazolo[4,3-*b*]pyridazine-3-one (**5**) [5].

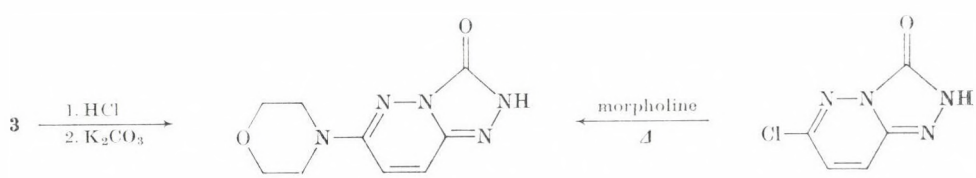

4 5

When the ethoxycarbonylation reaction was repeated at higher temperatures (*e.g.* at 40 °C), or at room temperature for a longer time, the *endo*-acyl compound (**6**) was formed as red needles.

* Numbering in the formula relates to the ^{13}C-NMR data only.

** The 1-(6-morpholino-3-pyridazinyl)-3-methyl-4-(*t*-butoxycarbonyl)-5-hydroxypyrazole and its tautomers with the same elementary composition, which might have been formed from the *exo*-acyl derivative, could be ruled out by the presence of an olefinic proton with the chemical shift of 6.90 ppm.

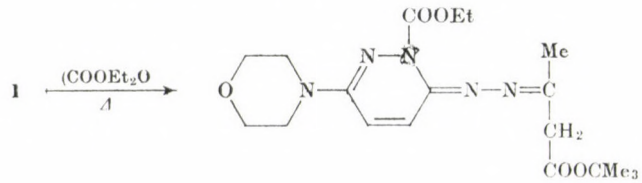

6

In the ^{1}H-NMR spectrum of **6** the difference in the chemical shifts of the H-5 and H-4 atoms ($\Delta\delta$H-4,5) was 0.25 ppm, while the urethane carbonyl frequency appeared at 1670 cm^{-1} in the IR spectrum. Consequently, the *exo*-acyl structure could be ruled out [3, 4].

Compound **6** was found to be thermally stable, since only unchanged starting material could be detected after heating for two hours at 180 °C in Dowtherm. Thus, the assumption that **6** might be an intermediate of the **1** → **3** transformation could be excluded.

Of the new compounds only **6** showed a moderate antihypertensive activity, the others were ineffective. These results have also confirmed that substitution on the N_1-atom is disadvantageous [1].

Experimental

M.p.'s were determined on a Boetius apparatus and are uncorrected.

The IR spectra were taken in KBr pellets on a Perkin–Elmer 577 spectrometer, the ^{1}H-NMR spectra on instruments JEOL 60 HL at 60 MHz and Varian EM-390 at 90 MHz, using TMS as internal standard in $CDCl_3$ and in DMSO-d_6 at room temperature. The ^{13}C-NMR spectrum was recorded on a Varian XL-100 spectrometer at 25.2 MHz in $CDCl_3$.

6-Morpholino-2-(1-(*t*-butoxycarbonyl)-1-propen-2-yl)-2,3-dihydro-*s*-triazolo-[4, 3-*b*]pyridazine-3-one (3)

A mixture of 2.10 g (0.0063 mole) of **1** [2], 2.10 g (0.013 mole) of diethyl pyrocarbonate and 70 cm^3 of dichloromethane was stirred at room temperature for 90 min, then concentrated under reduced pressure and the oily residue was allowed to stand at −10 °C for 5 days. After purification by chromatography on Brockmann-I Al_2O_3 with dichloromethane as eluant and recrystallization from isopropanol, 1.14 g (50.4%) of **3** was obtained, m.p. 185—186 °C. (Repetition of the reaction of 5 °C for 2 h, then at room temperature for 48 g yielded 0.69 h (30.4%) of **3**.)

$C_{17}H_{23}N_5O_4$ (361.39). Calcd. C 56.50; H 6.41; N 19.39. Found C 56.71; H 6.37; N 19.09%.

IR (KBr): νC=O: 1720 (ester + carbonyl group of triazole ring); νC=N: 1630 cm^{-1} (νC=N type group vibration of the fused ring system).

^{1}H-NMR ($CDCl_3$) (δ, ppm): CH_3: 1.5 s (9H) and 2.72 d (3H); NCH_2: 3.48 m (4H); OCH_2: ~3.80 m (4H); H-1': 6.90 q (overlapped with H-7, J = 1.2 Hz); H_B-7: 6.90 d, H_A-8: 7.40 d (J_{AB} = 9 Hz).

^{13}C-NMR ($CDCl_3$) (δ, ppm): C-6: 14.7 q (^1J = 130, ^3J = 6.7 Hz); C-1: 28.0 q (126.5); C-12: 46.0 t (141); C-13: 65.8 t (138); C-2: 79.5 s; C-4: 109.0 d (^1J = 165, ^3J = 4 Hz); C-10: 118.5 d (170); C-9: 124.5 d (180); C-8: 136.0 s (^2J = 3, ^2J = 10 Hz); C-7: 147.0 s; C-11: 148.0 s; C-5: 153.5 s (^2J = 8.6 Hz); C-3: 166 s.

6-Morpholino-2,3-dihydro-*s*-triazolo[4,3-*b*] pyridazine-3-one (4)

Method A

A mixture of 1.71 g (0.01 mole) of **5** [5] and 1.74 g (0.02 mole) of morpholine was heated at 130 °C for 1 h. The residue was mixed with cold water, then filtered. The crude product was suspended in hot 96% ethanol and filtered to obtain 1.25 g (56.6%) of **4**, m.p. 270—271 °C.

$C_9H_{11}N_5O_2$ (221.22). Calcd. C 48.86; H 5.01; N 31.66. Found C 48.72; H 5.15; N 31.51%.

IR (KBr): νNH: 3200—2700; νC=O: 1690 cm^{-1}.

^{1}H-NMR (DMSO-d_6) (δ, ppm): NCH_2: 3.42 t (4H, J = 6 Hz); OCH_2: 3.75 t (4H); H_B-7: 7.1 d (1H, J_{AB} = 9 Hz); H_B-8: 7.5 d (1H, J_{AB} = 9 Hz).

Method B

A mixture of 1 g (0.0028 mole) of **3** with 35 cm^3 of ethanol containing 8% hydrogen chloride was stirred at room temperature for 4.5 h, then filtered. The filtrate was evaporated under reduced pressure and the residue suspended in a 1 : 1 mixture of ethanol and ethyl ether and filtered to give 0.55 g (76.3%) of **4** as the hydrochloride, m.p. 255—256 °C.

The base liberated with 10% K_2CO_3 solution from the above HCl salt was in all respects identical with the product described under *A*.

1-Ethoxycarbonyl-3- morpholino-6(1*H*)-(2-(1-*t*-butoxycarbonyl-2-propylidene)-hydrazono)-pyridazine (6)

A mixture of 4 g (0.012 mole) of **1**, 4.49 g (0.028 mole) of diethyl pyrocarbonate and 80 cm^3 of dichloromethane was refluxed for 5.5 h, set aside overnight, then the solvent was evaporated in vacuum and the solid residue triturated with 3×20 cm^3 of diethyl ether to yield 2.35 g (48.4%) of **6** m.p. 108—109 °C. (After a 30-hour reaction time at room temperature and purification by chromatography on Brockmann-I Al_2O_3 with dichloromethane as the eluant, compound **6** was obtained in a yield of 36.2%.)

$C_{19}H_{29}N_5O_5$ 407.75. Calcd. C 56.00; H 7.17; N 17.19. Found C 56.30; H 7.21; N 16.89%.

IR (KBr): νC=O: 1725 (ester), 1670 cm^{-1} (urethane).

^{1}H-NMR ($CDCl_3$) (δ, ppm): CH_3: 1.36 t (3H, J = 7 Hz) and 1.47 s (9H); NCH_2: 3.15 m (6H, overlapped with CH_2); OCH_2: 4.30 q (2H) and 3.76 m (4H); H_B-4: 6.55 d, H_A-5: 6.80 d (J_{AB} = 9 Hz).

*

The authors are indebted to Mrs. G. BODROGAI for the microanalyses, to Miss Zs. DARUKA, Mrs. É. BIRÓ and Miss V. WINDBRECHTINGER for valuable technical assistance, and to Mrs. É. VIDA for the careful preparation of the manuscript.

REFERENCES

[1] SZILÁGYI, G., KASZTREINER, E., MÁTYUS, P., KOSÁRY, J., CZAKÓ, K., CSEH, GY., HUSZTI, ZS., TARDOS, L., KÓSA, E., JASZLITS, L.: J. Med. Chem. (To be published)

[2] SZILÁGYI, G., KASZTREINER, E., KOSÁRY, J., MÁTYUS, P., HUSZTI, ZS., CSEH, GY., KENESSEY, Á., TARDOS, L., KÓSA, E., JASZLITS, L., ELEK, S., ELEKES, I., POLGÁR, I.: Ger. Offen. 2 825 861 (1979); Chem. Abstr., **90,** 186985 m (1979)

[3] SOHÁR, P., MÁTYUS, P., SZILÁGYI, F.: J. Molecular Struct., **60,** 43 (1980)

[4] MÁTYUS, P., SZILÁGYI, G., KASZTREINER, E., SOHÁR, P.: Acta Chim. Acad. Sci. Hung. **106,** 205 (1981)

[5] FRANCAVILLA, P., LAURIA, F.: J. Heterocyclic Chem., **8,** 415 (1971)

Péter MÁTYUS
Géza SZILÁGYI
Endre KASZTREINER
Márta SÓTI

H-1325 Budapest, P.O. Box 82

Pál SOHÁR

H-1475 Budapest, P.O. Box 100

Acta Chimica Academiae Scientiarum Hungaricae, Tomus 109 (3), pp. 241—244 (1982)

STUDY OF THE RATE OF CORROSION OF METALS BY A FARADAIC DISTORTION METHOD, IV

APPLICATION OF THE METHOD FOR THE CASE OF REVERSIBLE CHARGE TRANSFER REACTION

L. MÉSZÁROS* and J. DÉVAY

(Research Laboratory for Inorganic Chemistry of the Hungarian Academy of Sciences, Budapest)

Received April 10, 1981
Accepted for publication May 25, 1981

In our previous communication [1, 2, 3] an a.c. method based on faradaic distortion has been presented for the determination of the rate of corrosion of metals if both the anodic and the cathodic processes of the electrode reaction have a Tafel-type current-potential characteristics. In the present communication we demonstrate the applicability of the method for the determination of the kinetic parameters of reversible redox reactions.

In our previous communications [1, 2, 3] a method based on faradaic distortion has been described for the determination of the kinetic parameters of corrosion processes. In these studies both the anodic and cathodic reactions have been assumed to exhibit a Tafel-type current-voltage characteristics. We have examined the harmonic and intermodulation components of the a.c. flowing through the electrode polarized by the sum of two sinusoidal voltages of frequencies ω_1 and ω_2 respectively, superimposed on the direct voltage as a function of the latter and the amplitudes of the alternating voltages. The charecteristic parameters of the corrosion process (such as corrosion current and Tafel slopes) have been found to be related to the amplitudes of the harmonic and intermodulation components of the current, respectively, as measured at the corrosion potential or at one potential either in the anodic or in the cathodic Tafel range of the polarization curve.

In the present communication the application of the above method to a reversible charge transfer will be presented.

We assume that the rate determining step of the electrode process is a reversible charge-transfer reaction according to equation (1)

$$O + ne \rightleftarrows R \tag{1}$$

and the polarization curve of the electrode process can be represented by equation (2)

$$\mathbf{j} = \mathbf{j}_0\left(e^{\frac{\alpha nF}{Rt}\eta} - e^{-\frac{(1-\alpha)nF}{RT}\eta}\right), \tag{2}$$

* To whom correspondence should be addressed.

where $\mathbf{j}$ is the current density, $\mathbf{j}_0$ is the exchange-current density, α is the charge-transfer coefficient of the anodic reaction, n is the number of electrons exchanged in the reaction and η is the overvoltage.

Comparing equation (2) with the polarization curve of the corrosion process represented by equation (4) in our previous communication [3] we note that the two equations are formally identical, merely corrosion current density $\mathbf{j}_k$ of the latter is substituted by exchange-current density $\mathbf{j}_0$ in equation (2) while polarization ΔE is substituted by overvoltage η and, in the present case, β_b and β_c are given by

$$\beta_a = \frac{RT}{\alpha n F} \quad \text{and} \quad \beta_c = \frac{RT}{(1-\alpha) n F}, \tag{3}$$

respectively.

Consequently the relationships obtained in our previous communication [3] for the determination of the corrosion-current density and parameters β_a and β_c can be applied for the evaluation of the kinetic characteristics (exchange current density and transfer coefficient) of a charge transfer reaction of the form of equation (1) by substituting $\mathbf{j}_0$ for $\mathbf{j}_k$ and η for ΔE.

The calculation is simplified in this case since it is sufficient to determine either β_a od β_c. The second parameter can only be used for the control of the result.

Thus the kinetic parameters of the charge-transfer reaction can be determined if the harmonic or the intermodulation components of the faradaic current are known at one potantial; either at the reversible potential ($\eta = 0$) or at one potential in the anodic or in the cathodic Tafel range.

Another possibility for the determination of the kinetic parameters is offered by relationships (66) through (71) of our previous communication [3] which give the first, second and third harmonic components respectively, of the faradaic current at the reversible potential ($\eta = 0$) when the electrode is polarized by the sum of two sinusoidal voltages of small amplitudes U_1 and U_2 and frequencies ω_1 and ω_2, respectively. The following formulas are obtained for a reversible electrode reaction:

$$\hat{\mathbf{j}}_0(\omega_1) = \mathbf{j}_0 \left\{ \frac{nF}{RT} + \left(\frac{nF}{RT}\right)^3 (1 - 3\alpha + 3\alpha^2) \frac{U_2^2}{4} \right\} U_1, \tag{4}$$

$$\hat{\mathbf{j}}_0(\omega_2) = \mathbf{j}_0 \left\{ \frac{nF}{RT} + \left(\frac{nF}{RT}\right)^3 (1 - 3\alpha + 3\alpha^2) \frac{U_1^2}{4} \right\} U_2, \tag{5}$$

$$\hat{\mathbf{j}}(2\omega_1) = \mathbf{j}_0 \left| \left(\frac{nF}{RT}\right)^2 (2\alpha - 1) + \left(\frac{nF}{RT}\right)^4 (2\alpha - 1)(2\alpha^2 - 2\alpha + 1) \frac{U_2^2}{4} \right| \frac{U_1^2}{4}, \tag{6}$$

$$\hat{\mathbf{j}}_0(2\omega_2) = \mathbf{j}_0 \left| \left(\frac{nF}{RT}\right)^2 (2\alpha - 1) + \left(\frac{nF}{RT}\right)^4 (2\alpha - 1)(2\alpha^2 - 2\alpha + 1) \frac{U_1^2}{4} \right| \frac{U_2^2}{4}, \tag{7}$$

$$\hat{\mathbf{j}}_0(3\omega_1) = \mathbf{j}_0 \left\{ \left(\frac{nF}{RT}\right)^3 [\alpha^3 + (1-\alpha)^3] + \left(\frac{nF}{RT}\right)^5 [\alpha^5 + (1-\alpha)^5] \frac{U_2^2}{4} \right\} \frac{U_1^3}{24}, \tag{8}$$

$$\hat{\mathbf{j}}_0(3\omega_2) = \mathbf{j}_0 \left\{ \left(\frac{nF}{RT}\right)^3 [\alpha^3 + (1-\alpha)^3] + \left(\frac{nF}{RT}\right)^5 [\alpha^5 + (1-\alpha)^5] \frac{U_1^2}{4} \right\} \frac{U_2^3}{24}, \tag{9}$$

(where $\hat{\mathbf{j}}_0$-s are the amplitude of the respective harmonic components at the reversible potential and ω_1, ω_2, $2\omega_1$, $2\omega_2$, $3\omega_1$, and $3\omega_2$ refer to the frequency of the given harmonic component).

The kinetic parameters can be determined by varying amplitudes U_1 and U_2. The exchange-current density can be evaluated from equation (4) if $U_2 = 0$ or from equation (5) if $U_1 = 0$ according to

$$[\hat{\mathbf{j}}_0(\omega_1)]_{U_2=0} = \mathbf{j}_0 \frac{nF}{RT} U_1, \tag{10}$$

or

$$[\hat{\mathbf{j}}_0(\omega_2)]_{U_1=0} = \mathbf{j}_0 \frac{nF}{RT} U_2, \tag{11}$$

respectively.

The transfer coefficient can be calculated from the following formulas

$$\frac{\hat{\mathbf{j}}_0(\omega_1) - [\hat{\mathbf{j}}_0(\omega_1)]_{U_2=0}}{[\hat{\mathbf{j}}_0(\omega_1)]_{U_2=0}} = \left(\frac{nF}{RT}\right)^2 (1 - 3\alpha + 3\alpha^2) \frac{U_2^2}{4}, \tag{12}$$

or

$$\frac{\hat{\mathbf{j}}_0(\omega_2) - [\hat{\mathbf{j}}_0(\omega_2)]_{U_1=0}}{[\hat{\mathbf{j}}_0(\omega_2)]_{U_1=0}} = \left(\frac{nF}{RT}\right)^2 (1 - 3\alpha + 3\alpha^2) \frac{U_1^2}{4}. \tag{13}$$

Similar formulas are obtained for the second and third harmonic components [equation (6) through (9), respectively].

The transfer coefficient (α) can be obtained from anyone of the following equations

$$\frac{\hat{\mathbf{j}}_0(2\omega_1) - [\hat{\mathbf{j}}_0(2\omega_1]_{U_2=0}}{[\hat{\mathbf{j}}_0(2\omega_1)]_{U_2=0}} = \left(\frac{nF}{RT}\right)^2 (1 - 2\alpha + 2\alpha^2) \frac{U_2^2}{4}, \tag{14}$$

$$\frac{\hat{\mathbf{j}}_0(2\omega_2) - [\hat{\mathbf{j}}_0(2\omega_2)]_{U_1=0}}{[\hat{\mathbf{j}}_0(2\omega_2)]_{U_1=0}} = \left(\frac{nF}{RT}\right)^2 (1 - 2\alpha + 2\alpha^2) \frac{U_1^2}{4}, \tag{15}$$

$$\frac{\hat{\mathbf{j}}_0(3\omega_1) - [\hat{\mathbf{j}}_0(3\omega_1)]_{U_2=0}}{[\hat{\mathbf{j}}_0(3\omega_1)]_{U_2=0}} = \left(\frac{nF}{RT}\right)^2 \frac{\alpha^5 + (1-\alpha)^5}{\alpha^3 + (1-\alpha)^3} \frac{U_2^2}{4}, \tag{16}$$

$$\frac{\hat{\mathbf{j}}_0(3\omega_2) - [\hat{\mathbf{j}}_0(3\omega_2)]_{U_1=0}}{[\hat{\mathbf{j}}_0(3\omega_2)]_{U_1=0}} = \left(\frac{nF}{RT}\right)^2 \frac{\alpha^5 + (1-\alpha)^5}{\alpha^3 + (1-\alpha)^3} \frac{U_1^2}{4}, \tag{17}$$

while exchange current density $\mathbf{j}_0$ can be calculated according to equation (6) through (9) if α is known. It is advisable to evaluate $\mathbf{j}_0$ from equation (6)

and (8) when $U_2 = 0$ and from equation (7) and (9) when $U_1 = 0$:

$$\mathbf{j}_0 = [\hat{\mathbf{j}}_0(2\omega_1)]_{U_2=0} \left(\frac{RT}{nF}\right)^2 \frac{4}{(2\alpha - 1)\, U_1^2} = [\hat{\mathbf{j}}_0(2\omega_2)]_{U_1=0} \left(\frac{RT}{nF}\right) \frac{4}{(2\alpha - 1)\, U_2^2} =$$

$$= [\mathbf{j}_0(3\omega_1)]_{U_2=0} \left(\frac{RT}{nF}\right)^2 \frac{24}{[\alpha^3 - (1-\alpha)^3\, U_1^3} = \tag{18}$$

$$= [\hat{\mathbf{j}}_0(3\omega_2)]_{U_1=0} \left(\frac{RT}{nF}\right)^2 \frac{24}{[\alpha^3 - (1-\alpha)^3]\, U_2^3}.$$

It is noteworthy that the above formulas relate to the faradaic current exempt of capacitive components. The capacity of the double layer was assumed to be linear *i.e.* independent of the potential. If this assumption is valid higher harmonic or intermodulation components are not generated by the double layer capacity and the measured values of the higher harmonic and intermodulation current components do not contain capacitive current and can directly be substituted in the above formulas. However, the measured values of the fundamental harmonic components also contain capacitive current. The latter can be eliminated by the method outlined in our previous communication [2].

The experimental verification of the above relationships will be presented in the near future.

REFERENCES

[1] DÉVAY, J., MÉSZÁROS, L.: Acta Chim. Acad. Sci. Hung., **100**, 183 (1979)
[2] DÉVAY, J., MÉSZÁROS, L.: Acta Chim. Acad. Sci. Hung., **104**, 311 (1980)
[3] MÉSZÁROS, L., DÉVAY, J.: Acta Chim. Acad. Sci. Hung., **105**, 1 (1980)

Lajos MÉSZÁROS
József DÉVAY
H-1112 Budapest, Budaörsi út 45.

Acta Chimica Academiae Scientiarum Hungaricae, Tomus 109 (3), pp. 245—248 (1982)

STUDY OF THE RATE OF CORROSION OF METALS BY A FARADAIC DISTORTION METHOD, V

EFFECT OF THE NON-LINEARITY OF THE DOUBLE LAYER CAPACITY

L. MÉSZÁROS* and B. LENGYEL

(Research Laboratory for Inorganic Chemistry, Electrochemical and Corrosion Group, Hungarian Academy of Sciences)

Received April 17, 1980
In revised form January 13, 1981
Accepted for publication March 11, 1981

The effect of the non-linearity of the double layer capacity on the measurement of faradaic distortion has been studied. The non-linear double layer capacity also generates harmonic components which are added to those of the faradaic current. A method was developed which permits the separation of the components of the capacitive current from those of the faradaic current.

In our earlier communications [1, 2, 3, 4] a method based on faradaic distortion was presented for the study of the kinetics of electrode processes. The double layer capacity connected parallelly with the charge transfer resistance was assumed to be a linear circuit element *i.e.* independent of potential. Thus the higher harmonic components and intermodulation components of the current passing through the electrode are generated as a consequence of the non-linearity of the faradaic process only. The elimination of the capacitive current from the fundamental harmonic component was reported earlier [2].

The assumption of a constant double layer capacity, however, is only valid in certain potential ranges. A particularly strong dependence of the double layer capacity on potential is observed in dilute electrolytes and in the presence of readily adsorbed ions. The potential dependence of the double layer capacity has been treated in many theoretical and experimental studies, *e.g.* in the excellent monographs of DELAHAY [5] and of PAYNE [6]. An effect analogous to faradaic distortion and faradaic rectification also appears on non-linear double layer capacities [7, 8]. Thus if the electrode–electrolyte interface is polarized with a non-distorted sinusoidal alternating voltage at a constant time average potential higher harmonic components are generated in addition to the fundamental one and the charge of the double layer is also varied.

The effect of the non-linearity of the double layer capacity on the measurement of faradaic distortion is presented in this communication.

* To whom correspondence should be addressed.

Let us assume that the charge of the electrode in a relatively narrow potential range can be expressed by the following third-order polynomial:

$$Q_{\mathrm{Me}} = A_0 + A_1 \Delta E + A_2 \Delta E^2 + A_3 \Delta E^3 \tag{1}$$

where Q_{Me} is the charge of the metal electrode per unit surface area, and ΔE is the potential difference referred to an arbitrary reference electrode. ($A_0 = 0$ if the potential is related to the potential of zero charge.) The current density charging the double layer capacity is

$$\mathrm{j}_c = \frac{\mathrm{d}Q_{\mathrm{Me}}}{\mathrm{d}t} \tag{2}$$

where t is time. If the electrode is polarized with alternating voltage ΔE superimposed on direct voltage $\overline{\Delta E}$,

$$\Delta E = \overline{\Delta E} + U_0 \sin \omega t \tag{3}$$

where U_0 is the amplitude and ω is the angular frequency of the alternating voltage, the capacitive current density can be expressed, on the basis of Eqs (1), (2) and (3) by the following formula

$$\mathrm{j}_c = \frac{\mathrm{d}}{\mathrm{d}t}\left[\sum_{k=1}^{3} k A_k (\overline{\Delta E} + U_0 \sin \omega t)^k\right] = \\ = \left[\sum_{k=1}^{3} k A_k (\overline{\Delta E} + U_0 \sin \omega t)^{k-1}\right] \omega U_0 \cos \omega t. \tag{4}$$

After performing the above operations and the trigonometric transformations, the capacitive current density is obtained in the form of a third-order Fourier polynomial:

$$\mathrm{j}_c = \hat{\mathrm{j}}_{c1} \cos \omega t + \hat{\mathrm{j}}_{c2} \sin 2\omega t - \hat{\mathrm{j}}_{c3} \cos 3\omega t \tag{5}$$

where $\hat{\mathrm{j}}_{c1}$, $\hat{\mathrm{j}}_{c2}$ and $\hat{\mathrm{j}}_{c3}$ denote the amplitudes of the harmonic components of the capacitive current:

$$\hat{\mathrm{j}}_{c1} = \left(A_1 + 2A_2 \overline{\Delta E} + 3A_3 \overline{\Delta E^2} + \frac{3}{4} A_3 U_0^2\right) \omega U_0 \tag{6}$$

$$\hat{\mathrm{j}}_{c2} = (A_2 + 3A_3 \overline{\Delta E}) \omega U_0^2 \tag{7}$$

$$\hat{\mathrm{j}}_{c3} = \frac{3}{4} A_3 \omega U_0^3. \tag{8}$$

The first three terms in the expression in parenthesis of Eq. (6) denoting the amplitude of the fundamental harmonic yield the differential capacity C_{d}

corresponding to the potential $\overline{\Delta E}$. From Eq. (1)

$$C_d = \frac{dQ_{Me}}{d\Delta E} = A_1 + 2A_2\overline{\Delta E} + 3A_3\overline{\Delta E^2} \tag{9}$$

and hence

$$\hat{\mathbf{j}}_{c1} = \left(C_d + \frac{3}{4}A_3 U_0^2\right)\omega U_0. \tag{6a}$$

It is noteworthy that amplitude U_0 of the alternating voltage affects the measured vapacity calue C_{dm}, since

$$C_{dm} = \frac{\hat{\mathbf{j}}_{c1}}{\omega U_0} = C_d + \frac{3}{4}A_3 U_0^2. \tag{10}$$

The actual differential capacity is obtained by extrapolation of the measuring voltage to zero:

$$\lim_{U_0 \to 0} C_{dm} = C_d \tag{11}$$

Eq. (11) is correct in the case of any measuring equipment. Thus in the measurement of non-linear capacities particular attention must be paid to employ a constant and frequency — independent measuring voltage having an amplitude as low as possible or else the capacity values obtained will be erroneous and a capacity dispersion will be observed in the capacity values measured as a function of frequency. This fact is already known from literature [6].

In the case of non-linear (potential dependent) double layer capacities, the capacitive current also contains harmonic components. Thus the former will not only affect the fundamental harmonic of the faradaic current as pointed out in our earlier communication [2]. The harmonic components of the faradaic current are the following [1]:

$$\hat{\mathbf{j}}_F = \hat{\mathbf{j}}_1 \sin\omega t - \hat{\mathbf{j}}_2 \cos 2\omega t - \hat{\mathbf{j}}_3 \sin 3\omega t. \tag{12}$$

A comparison of Eqs (5) and (12) indicate that a phase angle difference of $\pi/2$ and $-\pi/2$ exists between the harmonic components of the capacitive current and those of the faradaic current. This phase shift permits the distinction between the harmonic components of the faradaic current and those of the capacitive current by using a phase-sensitive measuring receiver. The capacitive current can be eliminated from the actually measured current in the manner reported in our earlier paper [2]: the sum of the amplitudes of the harmonic components of the actually measured alternating current is given by the following equations taking into account the phase angle difference of $\pm\pi/2$

$$\hat{\mathbf{j}}_{1m}^2 = \hat{\mathbf{j}}_1^2 + \hat{\mathbf{j}}_{c1}^2 \tag{13}$$

$$\hat{\mathbf{j}}_{2m}^2 = \hat{\mathbf{j}}_2^2 = \hat{\mathbf{j}}_{c2}^2 \tag{14}$$

$$\hat{\mathbf{j}}_{3m}^2 = \hat{\mathbf{j}}_3^2 + \hat{\mathbf{j}}_{c3}^2 \tag{15}$$

where index m referes to the measured current. According to Eqs (5), (7) and (8), all three capacitive current components are proportional to ω, while the faradaic current components are independent of frequency (*Cf.* Eqs (21), (22) and (23) in ref. [2]), consequently straight lines are obtained if the amplitudes on the left-hand sides of Eqs (13), (14) and (15) measured at several frequencies are plotted as a function of ω^2. The values of the components $\hat{\mathbf{j}}_1$, $\hat{\mathbf{j}}_2$ and $\hat{\mathbf{j}}_3$ can be obtained by extrapolation of those plots to $\omega = 0$.

In concentrated electrolytes (*e.g.* $c \geq 1$ mol/dm^3) the double layer capacity is dependent on potential to a less degree, and hence in many cases the harmonic components of the capacitive current are small and negligible as ompared to the components of the faradaic current. This fact can easily be shown, since according to Eqs (14) and (15), the ratios of the measured current components and the faradaic current components are

$$\frac{\hat{\mathbf{j}}_{2m}}{\hat{\mathbf{j}}_2} = \sqrt{1 + \left(\frac{\hat{\mathbf{j}}_{c2}}{\hat{\mathbf{j}}_2}\right)^2} \tag{16}$$

$$\frac{\hat{\mathbf{j}}_{3m}}{\hat{\mathbf{j}}_3} = \sqrt{1 + \left(\frac{\hat{\mathbf{j}}_{c3}}{\hat{\mathbf{j}}_3}\right)^2} \tag{17}$$

and if

$$\frac{\hat{\mathbf{j}}_{c2}}{\hat{\mathbf{j}}_2} \leqslant 10^{-1} \quad \text{and} \quad \frac{\hat{\mathbf{j}}_{c3}}{\hat{\mathbf{j}}_3} \leqslant 10^{-1},$$

then

$$\frac{\hat{\mathbf{j}}_{2m}}{\hat{\mathbf{j}}_2} \leqslant 1.005 \quad \text{and} \quad \frac{\hat{\mathbf{j}}_{3m}}{\hat{\mathbf{j}}_3} \leqslant 1.005$$

respectively, that is, the error caused by the capacitive component is 0.5%. This value is comparable to or smaller than the usual error of measurements with selective measuring receivers.

REFERENCES

[1] DÉVAY, J., MÉSZÁROS, L.: Magy. Kém. Foly., **85**, 209 (1979); Acta Chim. Acad. Sci. Hung., **100**, 183 (1979)
[2] DÉVAY, J., MÉSZÁROS, L.: Magy. Kém. Foly., **85**, 218 (1979)
[3] MÉSZÁROS, L., DÉVAY, J.: Magy. Kém. Foly., **85**, 305 (1979)
[4] MÉSZÁROS, L., DÉVAY, J.: Magy. Kém. Foly., **85**, 313 (1979)
[5] DELAHAY, P.: Double Layer and Electrode Kinetics. Interscience Publishers, New York 1965
[6] PAYNE, R.: The study of the ionic double layer and adsorption phenomena. In: E. YEAGER, A. J. SALKIND: Techniques of Electrochemistry. Wiley-Interscience, New York 1972
[7] BARKER, G. C.: Faradaic Rectification In: E. YEAGER, Transaction of the Symposium on Electrode Processes. Wiley, New York 1961
[8] SENDA, M., IMAI, H., DELAHAY, P.: J. Phys. Chem., **65**, 1253 (1961)

Lajos MÉSZÁROS
Béla LENGYEL
H-1112 Budapest, Budaörsi út 45.

Acta Chimica Academiae Scientiarum Hungaricae, Tomus 109 (3), pp. 249—259 (1982)

EFFECT OF MOLECULAR STRUCTURE ON THE RADIOLYSIS OF DIMETHYLCYCLOHEXANE ISOMERS

L. KOZÁRI, L. WOJNÁROVITS* and G. FÖLDIÁK

(Institute of Isotopes of the Hungarian Academy of Sciences, Budapest)

Received December 8, 1980
Accepted for publication March 11, 1981

Liquid phase γ radiolysis of structural and geometrical dimethylcyclohexan isomers was studied, and a correlation was searched for between molecular structure and product distribution using end-product analysis. The differences found in product yields were attributed, in case of structural isomers, to differences in the carbon skeleton and, consequently, to the selectivity of C—C bond ruptures, whereas in the case of geometric isomers, to the intramolecular repulsion between the methyl group in *axial* position in less stable isomers and the cyclohexane ring. It has been demonstrated that the conformation of the irradiated molecule is reflected by the yields of fragment and open-chain C_n products. Consequently, if biradical intermediates are involved in their formation, these biradicals react further very rapidly (within 10^{-13}—10^{-12} s) before attaining equilibrium conformation.

Introduction

The search for a correlation between molecular structure of the compound irradiated and radiolytical product distribution is one of the important activities of radiation chemists. The diversities found between product yields of radiolysis of aliphatic and cyclic alkanes, as well as the reason why these differences occur, are reasonably well known [1], and the influence of monoalkyl substitution of cycloalkanes on the yields, has also been well demonstrated in numerous works [2—4]. However, relatively little attention has been paid to the radiolysis of cycloalkanes containing more alkyl groups and to the effect of structural and geometrical isomerism frequently encountered with these compounds [5—8].

Structure of dimethylcyclohexanes (DMCH)

In this work we have investigated the radiolysis of both geometrical isomers *(cis* and *trans)* of the structural isomer 1,2-, 1,3- and 1,4-dimethylcyclohexanes. The methyl groups in these compounds take up *equatorial*

* To whom correspondence should be addressed.

positions falling in the plane of the cyclohexane ring or *axial* positions perpendicular to the ring. In the case of *equatorial* position, the molecule attains a stability 6.7 kJ mol^{-1} higher than that of the molecule with the methyl group in *axial* position; thus, in the most favourable conformation of *trans*-1,2-, *cis*-1,3- and *trans*-1,4-DMCH, which exist in both *diequatorial* and *diaxial*

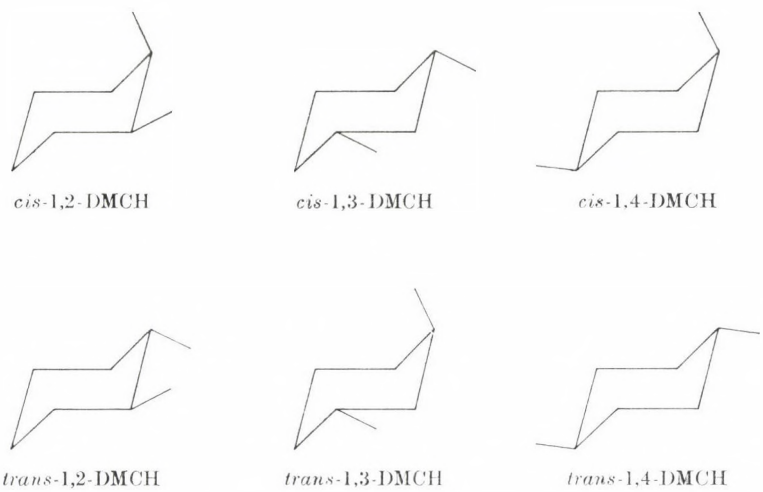

Fig. 1. Most stable conformations of dimethylcyclohexanes

form, both methyl groups (at least in 99% of the molecules) take up *equatorial* positions. In the case of *cis*-1,2-, *trans*-1,2- and *cis*-1,4-DMCH one of the methyl groups is always in *axial* position, therefore, these compounds are less stable than *trans*-1,2-, *cis*-1,3- and *trans*-1,4-DMCH, respectively.

Experimental

Purum grade DMCH compounds produced by Fluka were further purified by preparative gas chromatography. The ampoules (0.5—1.0 cm^3) were sealed by the usual vacuum technique. The samples were irradiated using the 3 PBq nominal activity ^{60}Co γ source of this Institute [9]. The dose rate was 5 Gy s^{-1}; the hydrocarbons were exposed to irradiation for 2 or 4 hrs, at room temperature, in liquid phase, though some experiments were carried out with solid phase samples, at 77 K. The dose was measured using alcoholic chlorobenzene dosimetry [10]. The amount of hydrogen produced was determined by TOEPLER'S method (accuracy $\pm 2.5\%$), while the qualitative and quantitative analysis of hydrocarbon products was done by gas chromatography; the systematic error in case of compounds of higher G values was about $\pm 4\%$, with products of lower G values ($G \leq 0.3$) $\pm 4-10\%$.

Results and Discussion

The most important products formed in the room temperature radiolysis of DMCH isomers are shown in Tables I, II and III.

As is seen in the Tables, the yields of the corresponding products in the different DMCH isomers are strongly different. Differences —observed in the yields of products formed *via* C—C bond rupture processes can be attributed to the different carbon skeletons of the structural isomers, in accord with the generally accepted view that C—C bond rupture is a selective process governed by the properties of the bond to be broken (*i.e.* the order of the corresponding carbon atoms). The probability of bond rupture was shown to vary in the order

$$C_{tert} - C_{tert} > C_{tert} - C_{sec} > C_{sec} - C_{sec} \qquad (1)$$

in agreement with the reverse order of bond dissociation energies. Correspondingly, *e.g.* the yield of octenes formed *via* the rupture of the bond between the two tertiary carbon atoms of 1,2-DMCH isomers is considerably higher than that of the ring-opening products produced by the cleavage of a bond between two secondary carbon atoms (Table II). Similarly, if we reconstruct the G values of the individual bond ruptures in the ring considering the yields of smaller molecular mass fragments (Table III), the same conclusion can be drawn as suggested earlier [2, 6], namely, that fragmentation proceeding through the cleavage of C—C bonds connecting two tertiary carbon atoms is highly preferred and is, therefore, accompanied by particularly high yields.

The DMCH isomers display considerably different yields of hydrogen. This fact cannot be attributed to a selectivity in C—H bond rupture processes,

Table I

Product yields of dimethylcyclohexane radiolysis (*molecule*/100 eV)
(Dose = 37 kGy)

Hydrocarbons / Products	1,2-DMCH		1,3-DMCH		1,4-DMCH	
	cis	*trans*	*cis*	*trans*	*cis*	*trans*
Hydrogen	3.09	2.88	3.58	3.87	3.71	3.36
Dimers	0.42	0.57	0.71	0.65	0.78	0.83
Cyclomonoalkenes	2.42	2.11	2.57	2.89	2.60	2.30
Ring-opening products	1.568	1.687	0.744	0.643	0.765	0.850
Fragmentation products	0.603	0.616	0.296	0.244	0.261	0.331
Ring fragmentation	0.261	0.260	0.130	0.103	0.106	0.134
Methane	0.114	0.109	0.121	0.132	0.126	0.122
Cyclic isomer	1.63	0.67	0.48	2.19	2.04	0.55

because not only the total number but also the character of C—H bonds in the compounds studied in the present work do not differ at all. Nevertheless, it is apparent that the DMCH isomers displaying lower yields of fragmentation and ring-opening show higher yields of hydrogen; this implies that differences occurring in the carbon skeleton of structural DMCH isomers affect even the yields of hydrogen, probably by competitive C—C bond rupture processes. This latter relationship is likely to be due to the fact that in radiolytic systems both end-products and intermediates are formed by numerous processes, and the latter ones can usually be stabilized by several routes. Based on our own experience as well as on those found in the literature, the following reactions can contribute to the radiolysis of DMCH isomers [2, 11—14]:

$$cyclo\text{-}C_8H_{16} \rightsquigarrow cyclo\text{-}C_8H_{16}^{*} \quad (2)$$

$$cyclo\text{-}C_8H_{16} \rightsquigarrow cyclo\text{-}C_8H_{16}^{+} + e^{-} \quad (3)$$

$$cyclo\text{-}C_8H_{16}^{+} + e^{-} \longrightarrow cyclo\text{-}C_8H_{15}^{*} \quad (4)$$

$$cyclo\text{-}C_8H_{16}^{*} \rightarrow cyclo\text{-}C_8H_{14} + H_2 \quad (5)$$

$$cyclo\text{-}C_8H_{16}^{*} \rightarrow cyclo\text{-}C_8H_{15}^{\cdot} + H \quad (6)$$

$$H + cyclo\text{-}C_8H_{16} \longrightarrow cyclo\text{-}C_8H_{15}^{*} + H_2 \quad (7)$$

$$2\ cyclo\text{-}C_8H_{15}^{\cdot} \rightarrow cyclo\text{-}C_8H_{14} + cyclo\text{-}C_8H_{16} \quad (8)$$

$$2\ cyclo\text{-}C_8H_{15}^{\cdot} \rightarrow cyclo\text{-}C_8H_{15}\text{-}cyclo\text{-}C_8H_{15} \quad (9)$$

$$cyclo\text{-}C_8H_{16}^{*} \longrightarrow \cdot C_8H_{16} \cdot \quad (10)$$

$$\cdot C_8H_{16} \cdot \rightarrow cyclo\text{-}C_8H_{16} \quad (11)$$

$$\cdot C_8H_{16} \cdot \rightarrow C_8H_{16} \quad (12)$$

$$\cdot C_8H_{16} \cdot \rightarrow \text{ring fragmentation} \quad (13)$$

$$cyclo\text{-}C_8H_{16}^{*} \rightarrow \text{ring fragmentation} \quad (14)$$

$$cyclo\text{-}C_8H_{16}^{*} \rightarrow CH_3^{\cdot} + C_7H_{13}^{\cdot} \quad (15)$$

As a rather complicated sequence of competitive and consecutive reactions takes place during radiolysis, the yields display a strong interdependence. The yields of products shown in Fig. 2 as a function of the hydrogen yields serve as a demonstration of this fact.

As is seen in Table I and Fig. 2 not only the yields of products formed in radiolysis of structural isomers show considerable differences, but also those of the geometrical isomers; the G values of fragment and ring-opening products

Table II

Yields of ring-opening products (*molecule*/100 eV)
(Dose = 37 kGy)

Hydrocarbons	Prdoucts	Alkane	1-Alkene	*cis*-2-Alkene	*trans*-2-Alkene	Σ
1,2-DMCH	*cis*	0.049	0.152	0.275	0.679	1.155
	trans	0.055	0.343	0.162	0.698	1.258
	cis	0.028	0.177	0.071	0.078	0.354
	trans	0.031	0.154	0.119	0.057	0.361
1,3-DMCH	*cis*	0.019	0.135	0.011	0.108	0.273
	trans	0.016	0.100	0.046	0.083	0.245
	cis	0.038	0 .143	0.032	0.231	0.444
	trans	0.047	0.109	0.059	0.158	0.373
1,4-DMCH	*cis*	0.078	0.289	0.129	0.223	0.728
	trans	0.110	0.321	0.091	0.284	0.806

Hydrocarbons	Products	Alkane	1-Alkene	Σ
1,2-DMCH	*cis*	0.002	0.023	0.025
	trans	0.004	0.025	0.029
	cis	0,003	0.031	0.034
	trans	0.002	0.037	0.039
1,3-DMCH	*cis*	0.003	0.024	0.027
	trans	0.002	0.023	0.025
1,4-DMCH	*cis*	0.009	0.028	0.037
	trans	0.011	0.033	0.044

Table III

Yields of lower molecular mass products (*molecule*/100 eV)
(Dose = 70 kGy)

Scission products \ Hydrocarbons	1,2-DMCH		1,3-DMCH		1,4-DMCH	
	cis	*trans*	*cis*	*trans*	*cis*	*trans*
Methane	0.114	0.109	0.121	0.132	0.126	0.122
Ethane + ethene	0.125	0.133	0.063	0.050	0.073	0.105
Acetylene	0.003	0.002	0.001	0.002	0.002	0.002
Propane	0.017	0.020	0.012	0.009	0.010	0.013
Propene + cyclopropane	0.131	0.128	0.105	0.095	0.080	0.093
Allene	0	0	0.001	0	0.001	0.002
n-Butane	0.033	0.040	0	0	0.007	0.010
1-Butene	0.062	0.071	0.001	0.001	0.016	0.018
cis-2-Butene	0.095	0.066	0.001	0.001	0.021	0.011
trans-2-Butene	0.039	0.097	0	0.001	0.006	0.016
Isobutane	0	0	0.001	0	0.001	0.001
Isobutene	0.002	0.002	0.003	0.001	0.010	0.012
n-Pentane	0.009	0.012	0.014	0.011	0	0
1-Pentene	0.019	0.023	0.030	0.021	0.001	0
cis-2-Pentene	0.022	0.019	0.022	0.029	0	0.001
trans-2-Pentene	0.008	0.027	0.031	0.012	0	0
Isopentane + isopentene	0.003	0.003	0.003	0.002	0.002	0.004
2-Methylpentane + 2-methylpentene	0.001	0	0.007	0.008	0	0
3-Methylpentane + 3-methylpentene	0.002	0.003	0	0.001	0	0.001
2,3-Dimethylbutane + 2,3-dimethylbutene	0.001	0.001	0	0	0.002	0.001
n-Hexane + hexene	0	0	0.001	0	0.029	0.041
Methylcyclohexane	0.033	0.039	0.035	0.041	0.037	0.032
1-Methylcyclohexene	0.046	0.019	0.002	0.001	0.005	0.007
3- and 4-Methylcyclohexene	0.037	0.032	0.080	0.078	0.075	0.077

formed from the less stable isomers are lower, while those of hydrogen and methane higher than the corresponding yields from the more stable isomers. This relationship can presumably be associated with the position of methyl groups that are different in *cis* and *trans* isomers. In less stable isomers, a higher intramolecular repulsive interaction arises between hydrogen atoms, owing to the presence of an *axial* methyl group in the molecule which is in a so-called butane *gauche* interaction with the cyclohexane ring: the result is an increased rate of detachment of hydrogen atoms or molecules and methyl groups. This implies that in the group of DMCH's the yields of hydrogen and methane display similar behaviour, *i.e.* both yields increase with the lowering

of C—C bond ruptures in the ring, the detachment of hydrogen and methane exerting a "protecting" effect of ring decomposition (Fig. 2).

Similarly to the overall yields of C—C bond ruptures, the *G* values of individual ring-opening products from the more stable isomers are also higher than the *G* values from the less stable ones (Table II), the notable exceptions

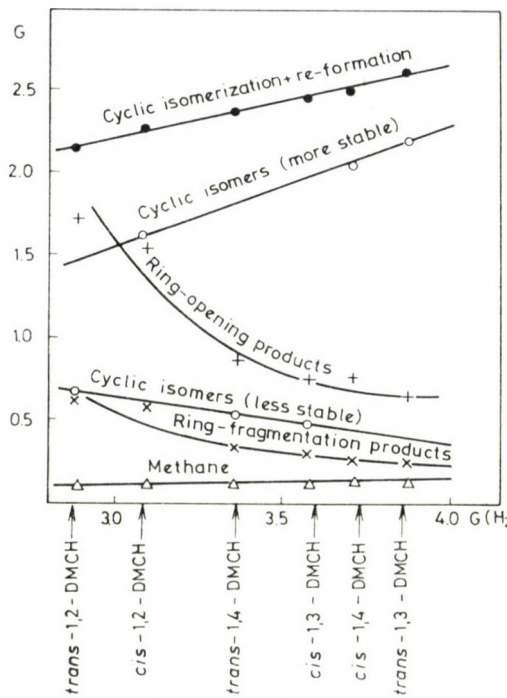

Fig. 2. G value of dimethylcyclohexane transformations as a function of hydrogen yield

to this rule being those products which exist in *cis* and *trans* isomer forms themselves, too. Let us consider as an example the yields of *cis*- and *trans*-4-methyl-2-heptenes which are produced in the radiolysis of 1,3-DMCH isomers. In the radiolysis of the *trans* isomer, the *G* value of these products amounts to 0.06+ + 0.16 = 0.22, whereas in the case of the more stable *cis* form this is 0.03 + 0.23 = 0.26, *i.e.* a value higher by about 20%, however, this relationship is by far not true for the individual *cis* and *trans* ismers. Considering the data in Table II it is to be noted that in the radiolysis of those DMCH isomers which have one methyl group in *axial* position in the most favourable conformation, higher yields of *cis* isomer products are found among ring-opening products displaying geometrical isomerism; this means that the yields

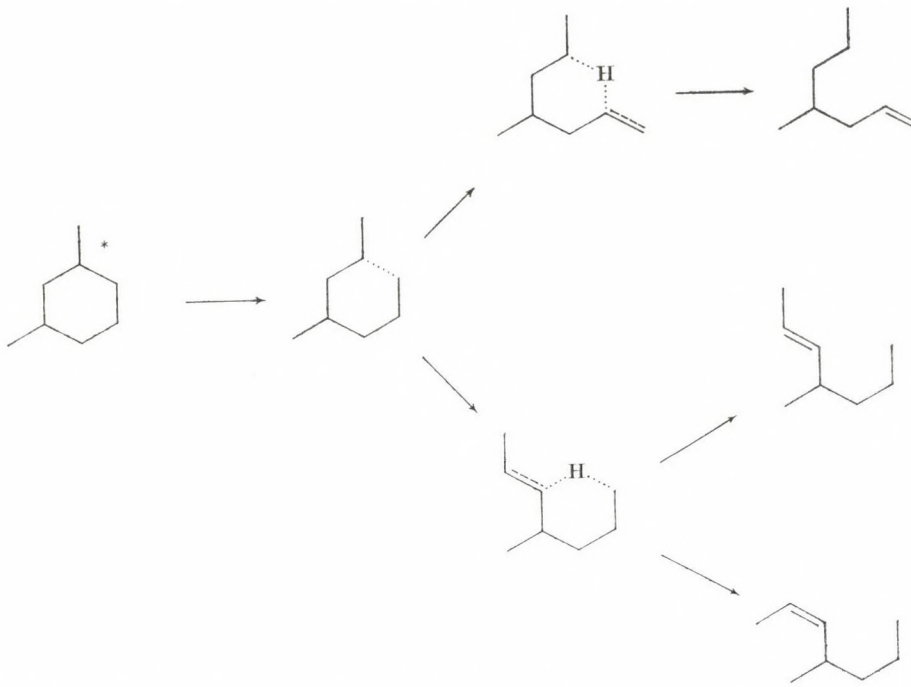

Fig. 3. Biradical mechanism of 1,3-dimethylcyclohexane isomerization to isooctenes

Table IV

Temperature dependence of ring-opening products from 1,4-*dimethylcyclohexanes*
(*molecule*/100 eV)
(Dose = 37 kGy)

	cis-1,4-DMCH		*trans*-1,4-DMCH	
	298 K	77 K	298 K	77 K
3-Methylheptane	0.087	0.026	0.110	0.037
3-Methyl-1-heptene	0.216	0.104	0.233	0.051
5-Methyl-1-heptene	0.073	0.114	0.088	0.173
cis-5-Methyl-2-heptene	0.129	0.127	0.091	0.094
trans-5-Methyl-2-heptene	0.223	0.061	0.284	0.102
Sub-total	0.728	0.432	0.806	0.457
2,5-Dimethylhexane	0.009	0.005	0.011	0.007
2,5-Dimethyl-1-hexene	0.028	0.013	0.033	0.019
Sub-total	0.037	0.018	0.044	0.026
Total	0.765	0.450	0.850	0.483

of ring-opening products reflect the structure of the decomposing hydrocarbon.

On the basis of the biradical mechanism of the ring-opening assumed in the literature [2, 13] which is illustrated for the rupture of the bond between the third and fourth carbon atoms of the 1,3-DMCH compounds in Fig. 3, we may suppose a longer lifetime for the intermediates. Therefore, it is expected that the biradicals formed from the two isomer hydrocarbons have slightly different conformation at the instant of their formation and attain the same steric structure in the course of a rotation requiring only little activation energy, and thus the ratio of yields of the *cis* and *trans* products is independent of the fact that the starting DMCH was of the *cis* or the *trans* structure. As this was not observed, it has to be assumed that the formation of ring-opening products occurs in rather fast processes, and the lifetime of the intermediate biradical is in the order of internal rotation around a C—C bond *i.e.* 10^{-13}—10^{-12} s (in accordance with our experience [2] that the yields of ring-opening products formed from cycloalkanes and alkylcycloalkanes show only a minor reduction in the presence of radical acceptors).

In order to study the influence of the matrix of neighbouring molecules on the further reactions of biradicals, we investigated the low temperature, solid phase radiolysis of DMCH isomers. Experimental data on the radiolysis of 1,4-DMCH are displayed in Table IV. The data show that the yields corresponding to the individual ring-opening reaction types are usually lower in the solid than in the liquid phase. Whereas 37% 5-methyl-2-heptenes formed in the room temperature radiolysis of *cis*-1,4-DMCH, which has an *axial* methyl group, is of the *cis* form, in the low temperature solid phase radiolysis of the same compound the contribution of the *cis* form increased to 68%, *i.e.* the structure of the starting molecule is more effectively reflected by the product in solid phase radiolysis than in the liquid state. Both observations can be traced back to the phenomenon that as the ring-opening requires a positive activation volume and a greater activation energy is necessary for the formation of a hole in the solid state, the transient biradicals have a much smaller free space to use when carrying out the relaxation motion required in the production of ring-opening products.

The *cis*-to-*trans* ratio of unsaturated fragment products is also strongly dependent on which one of the geometrical isomers was the starting hydrocarbon: in the case of DMCH isomers containing also an *axial* methyl group the *cis* form is produced with a higher yield, *i.e.* the conformation of the original carbon skeleton is reflected also in the yields of ring fragments. Consequently, we may assume that the rupture of the two C—C bonds occurs simultaneously, or more exactly, within the time required for the intermediate to change its conformation, although the latter process is known to take place within about 10^{-12} s.

Table V

Estimated yields for the reformation of the rings (molecule/100 eV)

Hydrocarbons / Products	1,2-DMCH		1,3-DMCH		1,4-DMCH	
	cis	*trans*	*cis*	*trans*	*cis*	*trans*
Re-formation	0.62	1.48	1.97	0.41	0.45	1.82
Cyclic isomer	1.63	0.67	0.48	2.19	2.04	0.55
Total	2.25	2.15	2.45	2.60	2.49	2.37

Ring isomerization processes are most effectively influenced by differences in the stability of geometrical isomers. This can easily be understood if we take into account that in the radiolysis of one of the pairs of isomers a structure with higher stability is formed whereas in the radiolysis of the other one a less stable structure is created. Thus, the data points corresponding to the yields of cyclic isomeric products shown in Fig. 2 fall on two curves, instead of one. The intermediates of Eqs (8) and (11) can move on not only to form the geometrical isomer of the starting compound, but they can also undergo re-formation of the original structure (7, 15). Although there is no direct experimental method available for the determination of this latter reaction, the G value can be estimated by supposing that the yields fall also on the corresponding curves in Fig. 2. G values for re-establishing the original structure can thus be determined and, in addition, the overall yield of re-formation and ring isomerization can be evaluated, too (Table V). The curves in Fig. 2 show that the total yields of cyclic isomerization + re-formation increase linearly with the G value of H_2; consequently, one may assume that these processes are associated mainly with the C—H bond rupture reactions, *i.e.* the total yield of Reaction (8) has to be much greater than the yield of Reaction (11).

As a summary we confirmed again [8] that the products observed in the radiolysis of alkanes are formed in competitive reactions, the rates of which can be correlated with the molecular structure. Even such minor differences in the molecular structure that can be found between the two geometrical isomers of the dimethylcyclohexanes exhibit well-defined and strong effects on the product yields.

REFERENCES

[1] FÖLDIÁK, G., WOJNÁROVITS, L.: Acta Chim. Acad. Sci. Hung., **82,** 269 (1974)
[2] WOJNÁROVITS, L., FÖLDIÁK, G.: Acta Chim. Acad. Sci. Hung., **82,** 285 (1974)
[3] WOJNÁROVITS, L.: Radiochem. Radioanal. Lett., **38,** 83 (1979)
[4] FREEMAN, G. R., STOVER, D.: Can. J. Chem., **46,** 3235 (1968)

[5] WOJNÁROVITS, L., FÖLDIÁK, G.: Radiochem. Radioanal. Lett., **23,** 257 (1975)
[6] MAKAROV, V. I., CHERNYAK, N. Ya.: Khim. Vys. Energ., **2,** 408 (1968)
[7] EBERHARDT, M. K.: J. Phys. Chem., **72,** 4509 (1968)
[8] WOJNÁROVITS, L., FÖLDIÁK, G.: Acta Chim. Acad. Sci. Hung., **93,** 1 (1977)
[9] HIRLING, J., STENGER, V.: Energia és Atomtechnika, **22,** 466 (1969)
[10] HORVÁTH, Zs., BÁNYAI, É., FÖLDIÁK, G.: Radiochim. Acta, **13,** 150 (1970)
[11] FREEMAN, G. R.: J. Chem. Phys., **36,** 1534 (1962)
[12] AVDONINA, E. N.: Radiat. Eff., **10,** 157 (1971)
[13] FREEMAN, G. R.: J. Chem. Phys., **36,** 1542 (1962)
[14] KOZÁRI, L.: Thesis, Budapest, 1980
[15] WOJNÁROVITS, L., FÖLDIÁK, G.: Radiochem. Radioanal. Lett., **23,** 343 (1975)

László KOZÁRI
László WOJNÁROVITS
Gábor FÖLDIÁK
H-1525 Budapest, P.O.B. 77

Acta Chimica Academiae Scientiarum Hungaricae, Tomus 109 (3), pp. 261—266 (1982)

ACTIVE PHASE-CARRIER INTERACTIONS IN COBALT OXIDE ON γ-ALUMINA, DOPED WITH THE HEAVIEST ALKALI CATIONS

A. LYCOURGHIOTIS,* D. VATTIS, PH. ARONI,** and N. KATSANOS

(Physical Chemistry Laboratory, University of Patras, Patras, Greece)

Received February 10, 1981
Accepted for publication March 11, 1981

The effects of rubidium and cesium content on the active phase-carrier interactions in cobalt oxide on γ-alumina catalysts were studied using diffuse reflectance spectroscopy (D.R.S.).

A number of specimens with various amounts of Rb or Cs cations, all containing 2.8% g Co_3O_4, were prepared by pore filling impregnation of the γ-alumina with aqueous alkali nitrate solutions, followed by pore volume impregnation of the alkali doped solids with aqueous cobalt(II) nitrate solutions.

An increase of the active phase-support interactions due to the presence of Rb^+ or Cs^+ was generally observed by D.R.S. The opposite effect was observed when the method of dry coimpregnation is employed, whereas no effect was detected when the inverse dry impregnation was used. The above findings allows us to shed more light on the mechanism whereby the alkali cations control the kind of cobalt species formed on γ-alumina surface. The main points of this mechanism are illustrated.

Introduction

The problem of control of active phase species formed during the preparation of supported metal oxide catalysts (S.M.O.C.) is of great importance for their tailor-made fabrication.

Concerning cobalt oxide supported on γ-alumina catalysts, recent investigations [1—5] demonstrated that such a control could be obtained by incorporating suitable additives into the carrier. To be specific, it was found that a deposition of Li^+ on the support surface causes a decrease of interactions of the active phase with the carrier which in turn results in quite high values of the $Co_3O_4/CoAl_2O_4$ ratio at a given temperature [3]. In contrast to that, an addition of Na^+ or K^+ to γ-Al_2O_3 causes an increase of the active phase-carrier interactions, thus facilitating the formation of sufficient amounts of $CoAl_2O_4$ [1, 2, 4, 5]. Moreover, the sodium cations bring about a drastic increase of the dispersity of the active phase species [1, 2, 5]. In a tentative explanation of the above mentioned effects given previously [2], it was assumed that the size of the alkali cations was not a decisive factor with respect to their controlling capabilities.

* To whom correspondence should be addressed.
** Present address: Physical Chemistry Laboratory, University of Athens, Athens, Greece.

In the present paper, using D.R.S., we attempt to investigate the validity of the above assumption, by studying the influences of Cs^+ and Rb^+ on the kind of cobalt species formed on γ-Al_2O_3 surface. Moreover, a comparison of the effects caused by *all* alkali cations helps a refinement to be made on the mechanism by which they regulate the kind of the active species.

Experimental

Preparation of the specimens

Rubidium and cesium doped γ-Al_2O_3 specimens, containing various amounts of the alkali ions have been prepared by the standard pore filling impregnation technique [1—5]. $RbNO_3$ (Fluka *p.a.*), $CsNO_3$ (Fluka *p.a.*) and alumina powder, obtained by grinding Houdry Ho 415 alumina of specific area (S_{BET}) 160 m^2/g and pore volume 0.45 $cm^3\,g^{-1}$, have been used. The calcination temperature, for most of the samples was 600 °C. A number of doped aluminas was also calcined at 100, 200, 400 and 500 °C.

The doped γ-Al_2O_3 samples were used as supports for the preparation of the cobalt containing samples. The deposition of cobalt species on the doped supports was performed by pore volume impregnation of the γ-Al_2O_3 with aqueous solutions of $Co(NO_3)_2 \cdot 6H_2O$ (Merck *p.a.*), followed by drying at 100 °C for 2 h and air calcination at various temperatures. In all cases the quantity of active phase corresponded to 2.8 g Co_3O_4 per 100 g of the impregnated support. Certain specimens were prepared by co-impregnation with aqueous $Co(NO_3)_2$/alkali nitrate solutions of γ-Al_2O_3, as well as by inverse impregnation (first cobalt and then alkali). The preparation method for a few samples synthesized with γ-Al_2O_3 doped with Li^+, Na^+ and K^+, has been reported elsewhere [1—4].

Notation

The specimens prepared by "normal impregnation", *i.e.* first alkali and then cobalt, will be designated by the formula M-*X*-*Y*-Co-*Z*, where *M* = alkali action, *X* = nominal composition as mmol of the alkali ion per g of γ-Al_2O_3, *Y* = calcination temperature before cobalt impregnation, and *Z* = calcination temperature after cobalt impregnation.

To symbolize the samples prepared by inverse impregnation, we use the formula Co-*Z*-M-*X*-*Y*, where the symbols have the same meaning as before. Finally, to denote samples prepared by co-impregnation, we employ the formula M-(Co)-*X*-*Y*.

Diffuse reflectance spectroscopy

Electronic reflectance spectra were recorded on a Cary 219 spectrophotometer equipped with a D.R.S. accessory in the range 800—400 nm, at room temperature. In all cases the corresponding support of a given sample was used as reference. Two quartz cells with thicknesses higher than 0.1 cm, to guarantee the determination of R_∞, were used as holders.

The KUBELKA—MUNK function at infinite thickness, $F(R_\infty)$, was determined using the well known equation

$$F(R_\infty) = \frac{(1 - R_\infty)^2}{2R_\infty}.$$

Results

It is well established that the spectra recorded in the region 800—400 nm for the cobalt containing specimens exhibit generally, three characteristic reflections [2]: a triplet band at about 600 nm attributed to the formation of the $CoAl_2O_4$ phase, a shoulder at about 750 nm and a broad band at 425 nm, which reflect the presence of the Co_3O_4 phase.

The colour of all samples of the M-*X*-*Y*-Co-100, Co-100-M-*X*-*Y* and M(Co)-*X*-100 series with M=Rb or Cs, was similar to the yellow-red colour of aqueous solutions of $Co(NO_3)_2 \cdot 6H_2O$. Moreover, the spectra obtained with the above specimens suggest the absence of any detectable amount of Co_3O_4 and $CoAl_2O_4$.

The Co_3O_4 phase was predominant in all samples of the M-*X*-*Y*-Co-500, Co-500-M-*X*-*Y* and M(Co)-*X*-500 series (M=Rb or Cs). The colour of these samples was black. The above is also valid for the corresponding specimens calcined at 600 °C. An additional increase of the calcination temperature promotes the transformation of Co_3O_4 to $CoAl_2O_4$ inferred, by the appearance of the characteristic triplet at 600 nm, together with the change of the colour of the specimens from black to blue, and the decrease of the magnitude of the bands at 750 and 425 nm.

Table I summarizes the values of $F(R_\infty)$ determined at 750 nm. According to the literature [3], and assuming similar texture for the samples, these values are analogous to the concentration of the Co_3O_4 phase; they thus can be used to estimate the extent of the $Co_3O_4 \rightleftharpoons CoAl_2O_4$ solid state reaction. An inspection of the values compiled in the Table indicates that

Table I

Values of KUBELKA—MUNK *function obtained at 750 nm for the specimens prepared*

Sample	$F(R_\infty)$	Sample	$F(R_\infty)$	Sample	$F(R_\infty)$
M-0.000-600-Co-500	1.75	M-0.000-600-Co-600	1.20	M-0.000-600-Co-650	0.40
Rb-0.392-600-Co-500	1.49	Rb-0.392-600-Co-600	0.93	Rb-0.392-600-Co-650	0.05
Rb-0.984-600-Co-500	0.87	Rb-0.984-600-Co-600	0.60	Rb-0.984-600-Co-650	0.01
Rb-2.470-600-Co-500	0.60	Rb-2.470-600-Co-500	0.45	Rb-2.470-600-Co-650	0.06
Cs-0.392-600-Co-500	1.49	Cs-0.392-600-Co-600	1.13	Cs-0.392-600-Co-650	0.10
Cs-0.984-600-Co-500	1.20	Cs-0.984-600-Co-600	0.82	Cs-0.984-600-Co-650	0.03
Cs-2.470-600-Co-500	1.38	Cs-2.470-600-Co-600	1.13	Cs-2.470-600-Co-650	0.20
Co-500-Rb-0.984-500	1.75	Co-600-Rb-0.984-600	1.20	Co-650-Rb-0.984-600	0.39
Co-500-Cs-0.984-500	1.74	Co-600-Cs-0.984-600	1.21	Co-650-Cs-0.984-600	0.39
Rb(Co)-0.984-500	1.80	Rb(Co)-0.984-600	1.26	Rb(Co)-0.984-600	0.48
Cs(Co)-0.984-500	1.82	Cs-(Co)-0.984-600	1.30	Cs(Co) -0.984-600	0.49
Rb-0.984-100-Co-600	1.79	Rb-0.984-300-Co-600	1.22	Rb-0.984-400-Co-600	0.41
Cs-0.984-100-Co-600	1.81	Cs-0.984-300-Co-600	1.23	Cs-0.984-400-Co-600	0.41
Rb-0.984-500-Co-600	0.61				
Cs-0.984-500-Co-600	0.82				

the extent of the above solid state transformation is a function of the X, Y, Z values, as well as of the preparation method. Thus, the concentration of the Co_3O_4, in all samples prepared by normal impregnation with Rb or Cs doped supports, is lower than that obtained in the samples prepared with undoped γ-Al_2O_3, provided that the comparison concerns samples with the same Z

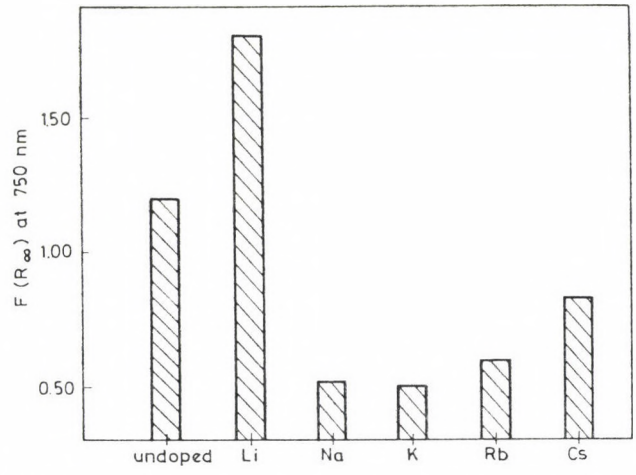

Fig. 1. Values of KUBELKA—MUNK function determined at 750 nm for the M-0.984-600-Co-600 specimens

value; in these samples, and for most of the cases, the minimum concentration is obtained in the specimens with $X = 0.984$. Practically, no effect is apparent when the inverse impregnation is adopted as a preparation method. In fact, the $F(R_\infty)$ values obtained for the samples prepared by this method are almost identical with those obtained for the specimens prepared on undoped γ-Al_2O_3 having the same Z values. An increase of the Co_3O_4 concentrations, compared to those obtained on undoped samples with the same Z values, is observed in cases where the co-impregnation method is used or where the normal impregnation is employed, but the Y values are <400. Concerning the samples prepared by the normal impregnation, we can observe that the extent of transformation of Co_3O_4 to $CoAl_2O_4$ is higher in the samples containing Rb than those containing Cs.

Figure 1 illustrates the $F(R_\infty)$ values at 750 nm obtained for the M-0.984--600-Co-600 specimens. These values indicate that among alkali cations, only Li^+ decreases the interactions between the active phase and carrier; all others promote the formation of $CoAl_2O_4$. Such a promotion is more pronounced in the samples doped with sodium or potassium.

Discussion

From the results obtained we can conclude that the assumption made concerning the influence of the size of alkali cations on the control of active phase-carrier interactions must be correct. In fact, the behaviour of Rb^+ and Cs^+ was found to be closer to that of Na^+ rather than to that exhibited by K^+.

Moreover, the experimental observations obtained here, together with those obtained in previous works [1—5], allows general considerations to be made concerning the mechanism whereby the alkali cations regulate the kind of the active species. We think now that we are in a position to approach the principal points of this mechanism.

(i) The alkali cations regulate the local surface pH of γ-Al_2O_3. Thus, they increase the extent of the $Co(NO_3)_2$ hydrolysis during the second impregnation [2, 6, 7].

(ii) During the first and/or second impregnation the alkali cations hydrolyze to a small extent the γ-Al_2O_3 surface, and thus they promote the formation of surface $Al_2O_4^{2-}$ species [2].

(iii) Species of the alkali cations serve as centers of nucleation of Co^{2+} agglomerates during the second impregnation. These agglomerates are transformed to Co_3O_4 aggregates at higher temperatures.

The function of mechanisms (i) and (ii) causes an increase of the interactions between cobalt species and γ-Al_2O_3 which results in the formation of $CoAl_2O_3$. On the contrary, the function of mechanism (iii) favours the formation of Co_3O_4 aggregates.

The experimental results obtained for all the alkali cations demonstrate that mechanisms (i) and (ii) prevail in the case of samples doped with sodium, potassium, rubidium and cesium, while mechanism (iii) is predominant in the samples containing lithium cations. Furthermore, the experimental results demonstrate that mechanisms (i) and (ii) are generally predominant in the samples containing medium amounts of alkali cations. At extremely high alkali contents, mechanism (iii) becomes quite important.

Further, we must point out that the fraction of participation of mechanisms (i), (ii) and (iii) in the whole control process is strongly dependent on the details of the preparation method. Thus, the co-impregnation of γ-Al_2O_3 with aqueous alkali nitrate and cobalt nitrate solutions favours mechanism (iii) [8]. The same is true when normal impregnation is followed, but the calcination temperature before cobalt deposition is lower than 400 °C. This suggests that effects (i) and (ii) commence to appear after a particular temperature, at which a suitable alkali species starts to form [4, 8].

Finally, it must be noted that in specimens prepared by inverse impregnation no alkali effect was detected. This suggests a quite high stability for the cobalt species formed during the first calcination.

*

The authors acknowledge the help of Mrs. Margaret BARKOULA.

REFERENCES

[1] LYCOURGHIOTIS, A., DEFOSSÉ, C , DELMON, B.: Rev. Chim. Miner., **16,** 473 (1979)
[2] LYCOURGHIOTIS, A., DEFOSSÉ, C., DELANNAY, F., LEMAITRE, J., DELMON, B.: J. Chem. Soc. Faraday I, **76,** 1677 (1980)
[3] LYCOURGHIOTIS, A., VATTIS, D., ARONI, Ph.: Z. Phys. Chem. (N. F.), **120,** 211 (1980)
[4] LYCOURGHIOTIS, A., VATTIS, D., ARONI, Ph.: Z. Phys. Chem. (N. F.), **121,** 257 (1980)
[5] DEFOSSÉ, C., HOUALLA, M., LYCOURGHIOTIS, A., DELANNAY, F.: 7th International Congress on Catalysis, July 1980, Tokyo, Paper A4
[6] TEWARI, P. H., LEE, W.: J. Colloid. Interface Sci., **52,** 77 (1975)
[7] TEWARI, P. H., CAMPBELL, A. B., LEE, W.: Canad. J. Chem., **50**, 1642 (1972)
[8] LYCOURGHIOTIS, A., DEFOSSÉ, C., DELMON, B.: Bull. Soc. Chim., Belge, **89,** 929 (1980)

A. LYCOURGHIOTIS
D. VATTIS
N. KATSANOS
Physical Chemistry Laboratory, University of Patras, Patras, Greece

PH. ARONI
Physical Chemistry Laboratory, University of Athens, Athens, Greece

Acta Chimica Academiae Scientiarum Hungaricae, Tomus 109 (3), pp. 267—274 (1982)

ALKALOIDS CONTAINING THE INDOLO[2,3-*c*] QUINAZOLINO[3,2-*a*]PYRIDINE SKELETON, X*

REDUCTION OF *trans*- AND *cis*-HEXAHYDRORUTECARPINE

K. HORVÁTH-DÓRA[1]**, G. TÓTH[1], F. HETÉNYI[1], J. TAMÁS[3] and O. CLAUDER[1]

([1] Institute of Organic Chemistry, Pharmaceutical Faculty, Semmelweis University, Medical Budapest, [2] Institute of General and Analytical Chemistry, Technical University, Budapest, and [3] Central Research Institute of Chemistry, Hungarian Academy of Sciences, Budapest)

Received January 21, 1981
Accepted for publication March 25, 1981

The regioselective reduction of *trans*- (**1**) and *cis*-hexahydrorutecarpine (**2**) give various reduced products: *trans*- (**3**) and *cis*-octahydrorutecarpine (**4**), *trans*- (**7**) and *cis*-hexahydrorutecarpene (**8**), *trans*- (**9**) and *cis*-hexahydrorutecarpene-21-ol (**10**), further, *trans*- (**5**) and *cis*-hexahydrorutecarpane (**6**). Dehydration of the ene-ols **9** and **10** yielded the dienederivative **11**. The structures of the compounds have been verified by UV, IR ^{1}H-NMR, ^{13}C-NMR, and MS investigations.

In continuation of our earlier work [1, 2], we studied the reduction of *trans*- (**1**) and *cis*-hexahydrorutecarpine (**2**) hydrogenated in ring E. In these rutecarpine derivatives diminished conjugation makes possible the regioselective reduction of the functional groups.

trans-Hexahydrorutecarpine (**1**) and *cis*-hexahydrorutecarpine (**2**) were reduced with sodium borohydride in methanol, or in the presence of Adams catalyst in ethanol. Reduction of the C=N double bond occurred to give *trans*- (**3**) and *cis*-octahydrorutecarpine (**4**). In the course of the work-up of the reaction mixture, unchanged starting material was removed by preparative thin-layer chromatography Kieselgel 60 $HF_{254+366}$ layer; developing solvent mixture: benzene—acetone 4 : 1. The reduced product was crystallized from alcohol. The UV spectra of **3** an **4** afforded direct evidence to show that the reduction had occurred. Owing to the C=N double bond, the maximum characteristic of indole 280, 288, 296 nm is observed. In the IR spectra the C=O stretching vibration of the lactam is found at 1630 cm^{-1}. The considerable chemical shift δ ppm 5.63 and 5.55 of H—C(3) in the ^{1}H-NMR is evidence for the so-called dihydrolactam structure. The extraordinarily intensive signals of the *M*-1 fragments in the mass spectra also confirm the presence of H-C(3) hydrogen (Fig. 1).

When *trans*- (**1**) and *cis*-hexahydrorutecarpine (**2**) were reduced with lithium aluminium hydride in ether, simultaneous reduction of the C=O

* Part IX: PÁL, Z., HORVÁTH-DÓRA, K., TÓTH G., CLAUDER, O., TAMÁS, J.: Acta Chim. Acad. Sci. Hung., **102**, 127 (1979).

** To whom correspondence should be addressed.

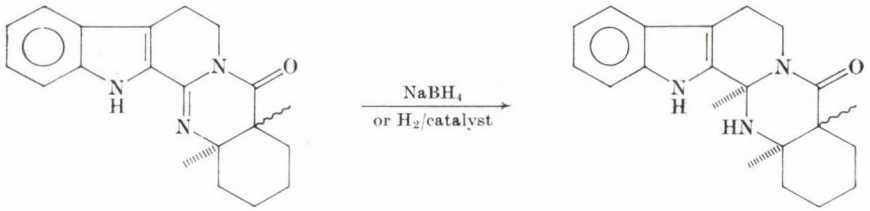

H—C(20) = β **1** **3**

= α **2** **4**

Fig. 1

H—C(20) = β **1** **5**

= α **2** **6**

Fig. 2

H—C(20) = β **1** **7**

= α **2** **8**

Fig. 3

and C=N double bonds occurred to give the hexahydrorutecarpanes **5** and **6**. These compounds differ from the yohimbane skeleton [3] in that they contain an NH group instead of the methylene group at C(14). These so called azayohimbanes will be discussed in a forthcoming communication (Fig. 2).

When in the reduction process just mentioned a smaller amount of lithium aluminium hydride was used two- or threefold excess *trans*- (**7**) and *cis*-hexahydrorutecarpene (**8**) formed as by-products as a result of the reduction of the C=O group. Adequately pure samples of these compounds were prepared by means of fractional crystallization or preparative chromatography.

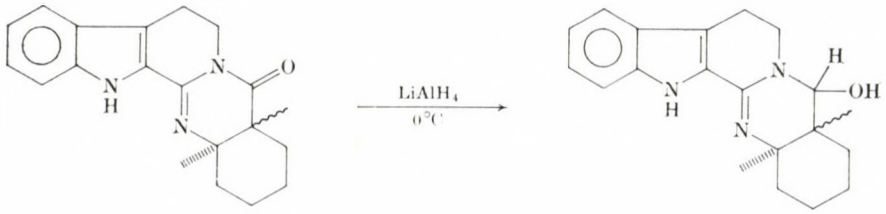

H—C(20) = β **1** **9**

= α **2** **10**

Fig. 4

The UV spectra of **7** and **8** have maxima at 315 mn, due to the presence of the C=N double bond. The stretching vibration of the C=N double bond appears in the IR spectrum at 1630 cm^{-1} (Fig. 3).

Next we investigated the lithium aluminium hydride reduction of *trans*- (**1**) and *cis*-hexahydrorutecarpine (**2**), in dry ether and in dry tetrahydrofuran, at various temperatures. Work-up of the reaction mixtures and subsequent study of the products revealed that reductions effected at 0 °C caused conversion of the lactam C=O group into an alcohol; the products thus obtained were *trans*- (**9**) and *cis*-hexahydrorutecarpene-21-ol (**10**) (Fig. 4).

Compounds **9** and **10** have characteristic "ene" UV spectra, with a maximum at 315 nm. No lactam C=O is found in their IR spectra; the νC=N vibration of **9** appears at 1615 cm^{-1}, that of **10** at 1630 cm^{-1}. Molecular weights are, according to mass spectrometry, 295, as expected. The principal fragment of each of these two compounds can be derived from the molecular ion by loss of OH. The loss of water, at least in part, is due to thermal effects. The fragment of *m/e* 238 (*M*-57) is a consequence of cleavage of ring E; the deviation in intensity is in agreement with the *cis-trans* isomerism [1].

The chemical shift of H—C (21) in the ^{1}H-NMR spectra is 4.63 and 4.54 respectively. The small coupling 1.5 and 2 Hz with the H—C(20) proton is evidence for the *gauche* position of the H-21 and H-20 protons and for the nearly 90° dihedral angle made by them. Since H—C(20) has *axial* position in *trans*-hexahydrorutecarpine (**1**), this coupling is possible only when H—C(20) is in equatorial position. It follows thereform that HO-C(21) in **9** must be *axial*. Either an *axial* or an *equatorial* H—C(21) in the *cis* compound **10** may appear as a slightly split doublet in the ^{1}H-NMR spectrum, because H—C(20) is here *equatorial*. Therefore, the steric position of HO—C(21) in **10** cannot be determined on the basis of ^{1}H-NMR spectra.

In the ^{13}C-NMR spectra, the signal of C(21) is found at 80.5 and 82.2 respectively; this is in agreement with the structure where nitrogen and an oxygen are connected to this carbon atom. The doublet multiplicity found in

the off-resonance spectrum suggests the presence of one hydrogen directly attached. The *axial* position of the HO—C(21) group also in *cis*-hexahydrorutecarpenol (**10**) follows then from the interpretation of the ^{13}C-NMR spectra of these ene-ols, based on the following arguments. Introduction of the *axial* OH group into *trans*-hexahydrorutecarpen-21α-ol (**9**), whose structure is doubtless, brings about a decrease of some 6 ppm in the chemical shift of C(15) as compared with the case of *trans*-hexahydrorutecarpene (**7**), this being a consequence of the well known *γ-gauche* steric interaction [4]. The diminution, by 5 ppm, of the chemical shift of the corresponding C(15) signal in the *cis*-ene-ol (**10**) is also considerable; this proves that also here the OH group is in *axial* position. A further argument is that the decrease of the chemical shift of C(19) is 2 ppm as compared with the case of the corresponding hexahydrorutecarpene (**8**), which can be explained here by the *γ-anti* effect. For an

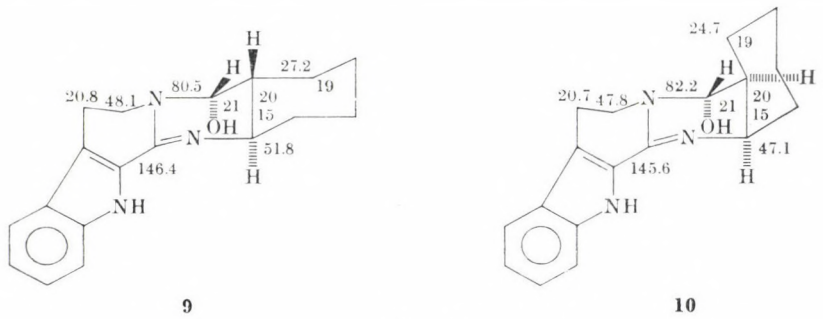

9 **10**

Fig. 5

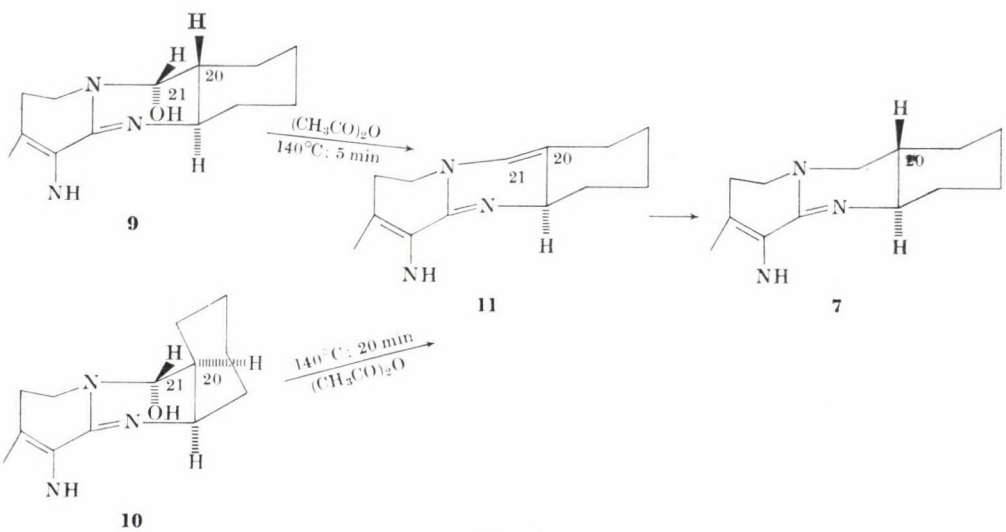

9 **11** **7** **10**

Fig. 6

equatorial OH group a decrease by to 6 ppm should here been observed because of the *γ-gauche* interaction of OH and C(19) (Fig. 5).

^{1}H-NMR studies of the reduction mixture have also shown that the reduction of the lactam C=O bond occurs with a very high degree of stereoselectivity: compound **1** and **2** are reduced exclusively to **9** and **10**, respectively. Thus hydrogen attacks from the upper side of the molecule in both cases. The other two possible C(21) epimers could not be detected within the range of the NMR spectroscope.

The structures of the ene-ols have also been substantiated by chemical reactions. The reaction of **9** and **10** with acetic acid anhydride resulted in dehydratation HO—C(21) from and H—C(20); the chirality of the centre C(20) has thus been destroyed to give the same *bis*-dehydroderivative (**11**) from both compounds. By antiperiplanar E_2 elimination the *trans*-ene-ol **9** is converted into **11** in 5 minutes at 140 °C; the *cis*-ene-ol **10** is converted into **11** in 20 minutes at 140 °C, supposedly by the thermal elimination of the acetic acid ester formed primarily.

The new C=C bond appeared as a new maximum at 303 nm in the UV spectrum of **11**. In the IR spectra νC=N and νC=C are found at 1705 and 1620 cm^{-1}, =CH is at 3050 cm^{-1}, and the NH vibration of the indole at 3280 cm^{-1}. The C(21) olefinic proton can be identified as a singulet at 5.65 in the ^{1}H-NMR spectrum. The mass spectral data give the expected molecular weight; also the fragments can be deduced from the suggested structure, mainly by losses of H or H_2.

Reduction experiments with the diene **11** have shown that hydrogenation in the presence of Adams catalyst or palladium-on-carbon, first results in the saturation of the C=C double bond. Hydrogen approaches the C(20) carbon atom from the sterically more accessible side and *trans*-hexahydrorutecarpene (**7**) is formed (Fig. 6).

Experimental

M.p.'s were determind with a Boetius M. micro melting point apparatus. UV spectra were recorded with a UNICAM SP 8—100 instrument; for IR spectra a UNICAM SP 1200 spectophotometer was used. ^{1}H-NMR spectra were recorded with a JEOL JNM PS-100 (100 MHz), the ^{13}C-NMR spectra with a JEOL JNM FX-100 (100 MHz) instrument. TMS was used as an internal standard; chemical shifts are given in δ ppm. An AEI-902 type instrument was used for recording the mass spectra (70 eV).

trans-3,14,15,16,17,18,19,20-Octahydrorutecarpine (3)

(*a*) *trans*-Hexahydrorutecarpine (**1**) (0.10 g) dissolved in a mixture of methanol (10 mL) and chloroform (5 mL) and cooled to 0 °C was mixed, with stirring, with $NaBH_4$ (0.10 g) added in small portions. Stirring was continued at room temperature for 1 h, then the solvent was evaporated under reduced pressure on a water bath. The residue was diluted with water (10 mL) and extracted with one 30 mL, and two 20 mL portions of chloroform. After drying,

and evaporation a white solid residue was obtained. According to chromatography and UV spectra this product contained about 50% of compound **1**. Purification by means of preparative layer chromatography on Kieselgel $PF_{254+366}$ with a 4 : 1 mixture of benzene and acetone afforded a fraction of R_f 0.73, which was eluted with anhydrous ethanol. Filtration, evaporation and crystallization from ethanol gave 42 mg (41%) of the product, m.p. 265—267 °C.

$C_{18}H_{21}ON_3$ (295). Calcd. C 73.23; H 7.12; N 14.24. Found C 73.17; H 7.09; N 14.22%.
UV (EtOH) [λ max (log ε)]: 225 (4.56), 280 (3.93), 288 (3.94), 292 (3.88).
IR (KBr): 3330 (νNH), 1630 (νC=O), 775, 740 cm^{-1} (γCH).
^{1}H-NMR ($CDCl_3$):* H-C(3) 5.62 (s, 1H); H_e-C(5) 5.08 (m, 1H), H-N (indole) 8.30 (s, 1H).
MS (*m/e*): 295 (M^+, 60) 294 (100), 293 (30), 264 (9), 250 (22), 238 (8), 191 (10), 185 (10), 170 (10), 169 (35).

(*b*) Adams catalyst (2 mg) was pre-hydrogenated in alcohol (5 mL), then compound **1** (20 mg; 0.66 mmole) dissolved in alcoho [illegible]) was added. Hydrogenation was continued for 2 h at room temperature, then the catalyst was removed by filtration and the filtrate evaporated. The white, crystalline residue was purified by chromatography as described above under (*a*), to obtain 9 mg (45%) of the product.

cis-3,14,15,16,17,18,19,20-Octahydrorutecarpine (4)

(*a*) Compound **2** (0.10 g; 0.34 mmole) was reduced with $NaBH_4$ in a mixture of methanol 10 mL) and chloroform (5 mL), as described for compound **3**. Chromatography and UV spectroscopy showed that the crude product contained about 25% of the unchanged starting material **2**. Purification was effected by chromatography on a preparative layer of Kieselgel 60 $HF_{254+366}$ with a 1 : 1 mixture of benzene and acetone as the eluant. The fraction at R_f = 0.50 was recovered and crystallized from methanol (70 mg; 70%), m.p. 277—229 °C.
$C_{18}H_{21}ON_3$ (295). Calcd. C 73.23; H 7.12; N 14.24. Found C 73.21; H 7.14; N 14.20%.
UV (EtOH) [λ max (log ε)]: 225 (4.50), 272 (3.87), 280 (3.88), 292 (3.76).
IR (KBr): 3395, 3320 (νNH), 1635 (νC=O), 760, 740 cm^{-1} (γCH); $CHCl_3$: 3465, 3320 (νNH), 1635 cm^{-1} (νC=O).
^{1}H-NMR ($CDCl_3$): H-C(3) 5.55 (s, 1H); H_e-C(5) 5.06 (m, 1H); H_a-C(5) 2.97 (1H); H_e-C(15) 3.39 (q, 1H), H_a-C(20) 2.50 (1H).
MS: M^* = 295.

(*b*) Compound **2** (20 mg; 0.66 mmole) was reduced in the presence of Adams catalyst (2 mg) as described for compound **3**. The yield was 11 mg (55%).

trans-15,16,17,18,19,20-Hexahydrorutecarpene (7)

trans-Hexahydrorutecarpine (**1**) (1.16 g; 4 mmoles) was dissolved in *abs.* ether (50 mL) which had been distilled off from $LiAlH_4$. To this solution, with stirring and cooling in cold water, $LiAlH_4$ (0.45 mg; 12 mmoles) was added. The reaction mixture was refluxed for 10 h. After cooling and with further cooling, the mixture was decomposed by the addition of water (5 mL). The ether was decanted from the precipitate which was then washed several times with ether. The combined ether solutions were dried. Evaporation to dryness under reduced pressure gave 1.10 g of an off-white crystalline residue which contained about 30% of **7**.

(*a*) Purification was effected on a preparative layer of Kieselgel $PF_{254+366}$ with a 3.5 : 1.5 mixture of benzene and methanol. Compound was found **7** in the fraction of R_f 0.47. Yield 0.25 g (22%); m.p. after crystallization from methanol was 224—226 °C.

(*b*) The residue was dissolved in warm methanol (10 mL) and the solution was allowed to cool. The crystals which separated were removed from time to time, by filtration to obtain the following fractions: I: 0.50 g of compound **5**; II: 0.20 g, a mixture of compounds **5** and **7**; III: 0.15 g (12%) of **7**.
$C_{18}H_{21}N_3$ (279). Calcd. C 77.43; H 7.53; N 15.05. Found C 77.35; H 7.40; N 15.02%.
UV (EtOH)[λ max (log ε)]: 239 (4.24), 311 (4.26).
IR (KBr): 3250—2400 (νNH, cyclic dimer), 1615 (νC=N), 775, 740 (γCH); $CHCl_3$: 3460, 3280 (νNH), 1615 cm^{-1} (νC=N).
^{1}H-NMR ($CDCl_3$): H-C(20) 2.25 (m, 1H); H_2-C(5), H_2-C(6), H_a-C(21) 2.92—3.24 (m, 5H); H-C(15), H_e-C(21) 3.24—3.74 (2H).

* A detailed analysis of the ^{1}H-NMR and ^{13}C-NMR spectra will be published in a forthcoming paper.

MS (*m/e*): 279 (M^+ 100), 278 (50), 264 (8), 237 (12), 236 (50), 222 (36), 210 (12), 169 (10), 155 (10).

7. HCl, m.p. 240—242 °C.

cis-15,16,17,18,19,20-Hexahydrorutecarpene (8)

Compound **2** (1.16 g; 4 mmoles) was reduced with $LiAlH_4$ in the same way as described for compound **7**. The crude product was purified by means of preparative chromatography on Kieselgel $PF_{254+366}$ with a 100 : 14 mixture of chloroform and methanol. The fraction of R_f 0.60 was eluted, evaporated and crystallized from methanol to obtain 0.23 g (20%) of **8** as white crystals m.p. 234—236 °C.

$C_{18}H_{21}N_3$ (279). Calcd. C 77.43; H 7.53; N 15.05. Found C 77.30; H 7.38; N 15.10%

UV (EtOH) [λ max (log ε)]: 239 (4.33), 311 (4.36).

IR (KBr): 3250—2400 (νNH, cyclic dimer), 1615 (νC=N), 745, 735 (γCH); $CHCl_3$; 3450, 3280 (νNH), 1615 cm^{-1} (νC=N).

^{1}H-NMR ($CDCl_3$): H-C(20) 2.16 (m, 1H); H_2-C(6), H_α-C(21) 3.04 (m, 3H).

MS (*m/e*): 279 (M^+ 100), 278 (50), 264 (10), 250 (10), 237 (15), 236 (55), 222 (44), 210 (15), 169 (20), 168 (11), 155 (14).

8. HCl m.p. 285—287 °C.

trans-15,16,17,18,19,20-Hexahydrorutecarpen-21α-ol (9)

trans-Hexahydrorutecarpine (**1**) (0.60 g; 2 mmoles) dissolved in *abs.* THF (100 mL) was cooled to 0 °C and $LiAlH_4$ (0.20 g; 10 mmoles) was added to the stirred solution. Stirring at 0 °C was continued for 1 h, then decomposition with water (2 mL) followed. To the resulting mixture a 4 *M* solution of NaOH (10 mL) and chloroform (50 mL) were added. After separation of the phases, the aqueous part was shaken with two 30 ml portions of chloroform. The organic phases were combined and evaporated. The residue was dissolved in dichloromethane (20 mL), this solution was dried and evaporated to dryness. A white solid was obtained which was crystallized from methanol to yield 0.52 g (86%) of snow-white crystals, m.p. 264—265 °C.

$C_{18}H_{21}ON_3$ (295). Calcd. C 73.23; H 7.12; N 14.23. Found C 73.18; H 7.05; N 14.20%.

UV (EtOH)[λ max (log ε)]: 234 (4.17), 240 (4.22), 310 (4.25).

IR (KBr): 3300 (νOH, NH), 1615 (νC=N), 745, 735 (γCH); ($CHCl_3$): 3580, 3290 (νOH), 3470 (νNH), 1630 cm^{-1} (νC=N).

^{1}H-NMR ($CDCl_3$ + CD_3OD): H—C(20) 2.34 (m, 1H); H_2-C(6) 3.05 (m, 2H); H-C(21) 4.64 (d, 1H), W_1 = 3.6 Hz, H-Ar 6.98—7.58 (m, 4H).

MS (*m/e*): 295 (M^+ 100), 294 (11), 279 (10), 278 (38), 277 (14), 276 (13), 248 (19), 185 (13), 169 (9).

cis-15,16,17,18,19,20-Hexahydrorutecarpen-21α-ol (10)

Compound **2** (0.60 g; 2 mmoles) in *abs.* THF (100 mL) was reduced with $LiAlH_4$ (0.20 g; 10 mmoles) in the same was as described for the preparation of **9**. The product was crystallized from a 1 : 1.5 mixture of methanol and chloroform to obtain 0.54 g (90%) of snow-white crystals, m.p. 208—209 °C.

$C_{18}H_{21}ON_3$ (295). Calcd. C 73.23; H 7.12; N 14.23. Found C 73.20; H 7.08; N 14.21%

UV (EtOH) [λ max (log ε)]: 230 (4.27), 240 (4.31), 315 (4.30).

IR (KBr): 3420 (νOH mon.), 3300—3100 (νOH, NH asym.), 1630 (νC=N), 726—735 (γCH); ($CHCl_3$) 3570 (νOH mon.), 3450 (νNH), 3300 (νOH asym.), 1630 cm^{-1} (νC=N).

^{1}H-NMR ($CDCl_3$ + CD_3OD): H-C(20) 2.12 (m, 1H); H_2-C(6) 3.04 (2H); H-C(15) 3.48 (m, 1H); H_2-C(5) 3.86 (m, 2H); H-C(21) 4.52 (d, 1H); ^3J = 2.0 Hz, H-Ar 6.98—7.60 (m, 4H)...

MS (*m/e*): 295 (M^+ 100), 294 (18), 278 (35), 277 (16), 276 (15), 248 (19) , 238 (9), 185 (9) 169 (11).

15α,16,17,18,19,20-Hexahydrorutecarpadiene-3(14),20 (11)

(*a*) *trans*-Hexahydrorutecarpenol (**9**) (300 mg; 1 mmole) was mixed with freshly distilled acetic acid anhydride (15 mL) and the mixture was stirred in a paraffin bath at 140 °C for 5 min. *Abs.* ethanol (30 mL) was added, then evaporation under reduced pressure followed. The residue was mixed with water (10 mL) and chloroform (30 mL), cooled in ice-water and made alkaline with *conc.* NH_4OH. Extraction with two 20 mL portions of chloroform gave a

combined solution which, after drying, was evaporated. The residue was crystallized from methanol to obtain 250 mg (90%) of **11**, m.p. 237—239 °C (d.).

$C_{18}H_{19}N_3$ (277). Calcd. C 77.99; H 6.86; N 15.16. Found C 77.88 H 6.80 N 15.14%.
UV (EtOH) [λ max (log ε)]: 225 (4.24), 235 (4.24), 243 (4.23), 302 (4.30), 312 (4.30).
IR (KBr): 3280 (νNH indole), 1705 (νC=C), 1625 (νC=N), 742, 730 cm^{-1} (γCH).
^{1}H-NMR ($CDCl_3$): H-C(15) 4.36 (m, 1H); H-C(21) 5.65 (s, 1H); H_2-C(5) 3.57 (t, 1H): H_2-C(6) 3.05 (t, 2H).
MS (*m/e*): 277 (M^+ 78), 276 (96), 275 (27), 274 (33), 273 (12), 272 (15), 249 (35), 248 (100), 234 (14).

(*b*) The *cis*-ene-ol (**10**) (300 mg; 1 mmole) was treated in the same way as the trans compound **9** (*a*). Dehydratation was effected at 140 °C for 20 min to obtain 220 mg (80%) of **11**, m.p. 237—239 °C (d.).

Reduction of the diene 11

Adams catalyst (5 mg) was prehydrogenated in 96% alcohol (3 mL), and a solution of the diene **11** (54 mg; 0.2 mmole) in 96% alcohol was added. Hydrogenation was carried out at room temperature for 3 h, then the catalyst was removed by filtration. The filtrate crystallized to yield 40 mg (71%) of a product, m.p. 234—236 °C, which was identified by chromatography and spectroscopy as *trans*-hexahydrorutecarpene (**7**).

REFERENCES

[1] HORVÁTH-DÓRA, K., TÓTH, G., TAMÁS, J., CLAUDER, O.: Acta Chim. Acad. Sci. Hung., **94**, 345 (1977)
[2] TÓTH, G., HORVÁTH-DÓRA, K., CLAUDER, O., DUDECK, H.: Ann., **1977**, 529
[3] JANOT, M. M., GOUTAREL, R., WARNHOFF, K., LE HIR, A.: Bull, Soc. Chim. (France), **1961**, 637
[4] WEHRLI, F. W., WIRTHLIN, T.: Interpretation of ^{13}C-NMR Spectra; p. 27. Heyden and Son, London 1976

Klára HORVÁTH-DÓRA
Ferenc HETÉNYI
Ottó CLAUDER
H-1092 Budapest, Hőgyes E. u. 7.

Gábor TÓTH
H-1521 Budapest, Gellért tér 4.

József TAMÁS
H-1025 Budapest, Pusztaszeri út 59/67.

Acta Chimica Academiae Scientiarum Hungaricae, Tomus 109 (3), pp. 275–285 (1982)

FLUORINATED STEROIDS, III*

TRIFLUORO DERIVATIVES

Á. NÉDER, I. PELCZER, ZS. MÉHESFALVI and J. KUSZMANN**

(Institute for Drug Research, Budapest)

Received January 31, 1981
Accepted for publication March 25, 1981

Addition of fluorine — generated *in situ* from $Pb(OAc)_4$ and HF — to 5,6-unsaturated steroids afforded in the case of the 3β-acetoxy derivative **6** the 5α,6α-difluoro derivative (**7**) and 5,5-difluoro-A-*homo*-B-*nor*-steroid (**8**) in a ratio of 1 : 3, whereas when starting from 3β-fluoro derivatives (**17**, **19**) only the latter type rearranged products were obtained. In the case of 3β-fluoropregna-5,6-dien-20-one (**21**) besides 3β,5,5-trifluoro-A-*homo*-B-*nor*-steroid (**22**) 3β-fluoro-5β-methyl-19-*nor*-pregna-8,14,16-trien-20-one (**28**) could be isolated as a by-product. A mechanism for this reaction is proposed. The structures of all fluorinated steroids were proved by their ^1H- and ^{13}C-NMR spectra.

The interesting biological properties of fluorinated steroids [1] prompted us to continue our research in this field [2, 3], aiming at the synthesis of the hitherto unknown 3,5,6-trifluoro derivatives. Starting from 3-acetoxy- or 3-hydroxy-5,6-unsaturated steroids **1**, theoretically two routes are possible: first the double bond can be saturated with fluorine to obtain **2**, followed by introduction of the fluorine to C-3, which, according to the mechanism of this process, leads to inversion of configuration at this centre (**3**) [4]; or a reverse order of the reactions (**1** → **4** → **5**) can be applied, which in the case of the

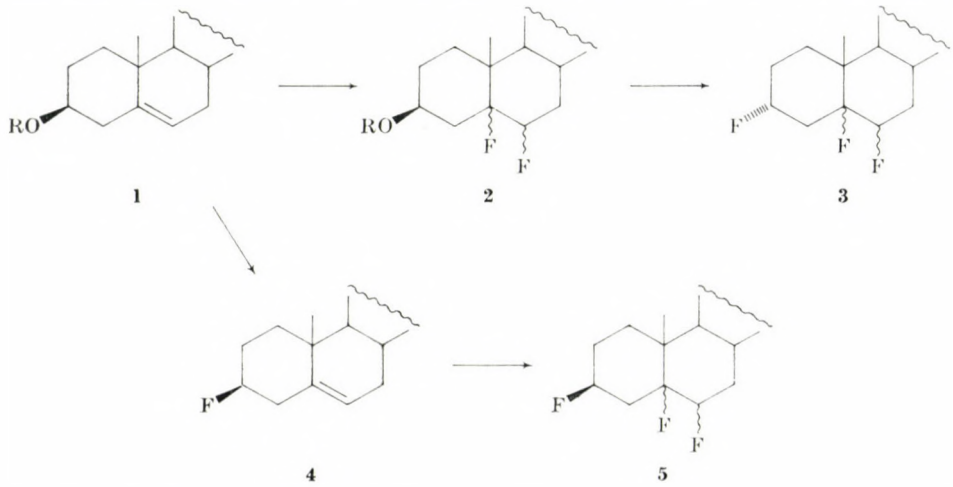

1 **2** **3**

4 **5**

* For Part II, see Ref. [3].
** To whom correspondence should be addressed.

same starting material should lead to a diastereomeric trifluoride (**5**) [2] having the fluorine at C-3 in the opposite configuration compared to **3**.

The addition of fluorine to the double bond of unsaturated steroids by using lead(IV) diacetate difluoride as a source of fluorine was studied first by BOWERS *et al.* [5, 6] in the early sixties. The fluorinating reagent was generated *in situ* from lead tetraacetate and hydrogen fluoride as described by DIMROTH and BOCKEMÜLLER [7] in 1931, who at that time presumed that lead tetrafluoride was the agent responsible for saturating the double bond of olefins. The real nature of this reagent was proved only in 1968 by BORNSTEIN and SKARLOS [8] — after whom it was named "BORNSTEIN's reagent" — and the mechanism of the reaction with olefins was established by TANNER and BOSTELEN [9] in 1972.

The application of BORNSTEIN's reagent to pregnenolone acetate (**6**) yielded — depending on the reaction temperature — either the expected 5,6-difluoride **7** in a low yield besides unchanged starting material, or, under more forcing conditions, an isomeric difluoride was obtained, the structure of which was not elucidated [5, 6]. Several years later this reaction was reinvestigated by LEVISALLES *et al.*, who published their results in a series of papers [10—12]. Based solely on ^{19}F-NMR data they suggested for the isomeric difluoride a rearranged *A-homo*-B-*nor* skeleton **8** containing two geminal fluorine atoms at C-5*. They also proposed a reaction mechanism, which seems to be generally valid for the reaction of unsaturated steroids with lead(IV) diacetate difluoride.

As for our further studies both isomers, **7** and **8**, were potential starting materials, we repeated the experiment of BOWERS [6] using pregnenolone acetate (**6**) as the starting compound. When the recation was carried out at —75 °C, the vicinal (**7**) and geminal difluoride (**8**) were formed simultaneously in a ratio of 1 : 3, in agreement with the published data [12]. As the structures of all compounds had been suggested only on the basis of their ^{19}F-NMR spectra, it seemed to be worthwhile to record their ^{1}H- and ^{13}C-NMR spectra, to obtain additional information about the structure. For this reason both isomers, **7** and **8**, were deacetylated to yield **9** and **10**, respectively, and subsequently oxidized by CrO_3 [14] to the 3-oxo derivatives **11** and **12**. It is interesting to note that the 3-oxo-5,6-difluoride **11** is unstable in chloroform solution and is completely converted after two days at 40 °C, *via* elimination

* According to the IUPAC nomenclature [13] the numbering of A-*homo*-B-*nor*-steroids should be as depicted below, but for a better comparability of the NMR data we retained the original numbering of the carbon atoms for the rearranged skeleton.

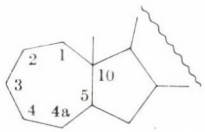

of hydrogen fluoride, into the more stable 4,5-unsaturated derivative **13**, as proved by NMR (see Tables I and II).

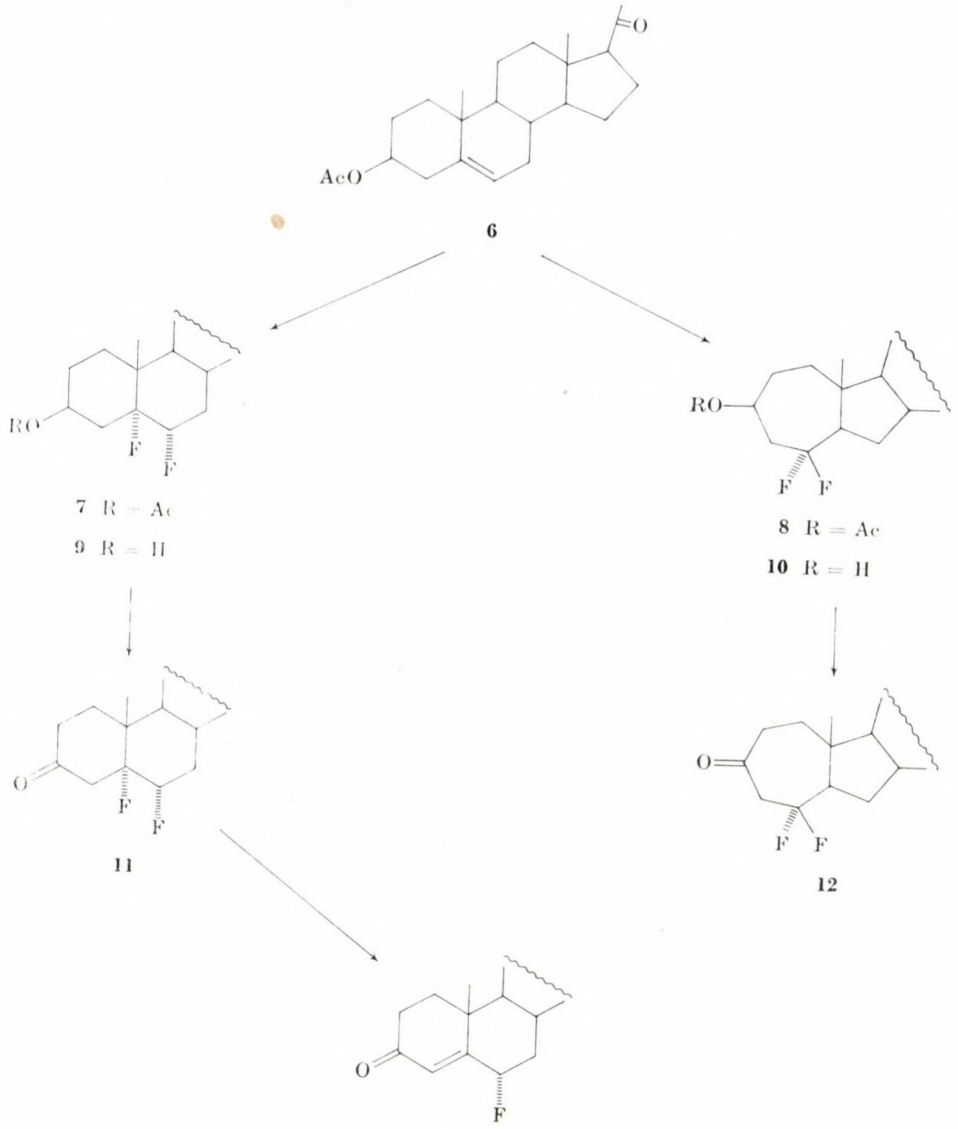

According to our original aim, the 3-hydroxy-5,5-difluoride **10** was treated with 2-chloro-1,1,2-trifluorotriethylamine (FAR [2]) for converting it into the trifluoride **14**. This compound was formed, however, only as a minor component, as mainly elimination of water took place, leading to an unsaturated compound, the structure of which could be either **15** or **16**. According to ^{13}C-NMR, structure **16** could be ruled out, as from among the two olefinic

Table I

^{1}H-NMR data[a] of fluorinated steroids **7**—**13**, **15**, **18**, **20**, **22** *and* **28**

Compound	Me-18	Me-19	Me-21	H-3	$J_{2,3}+J_{3,4}+J_{H3-F5}$	Other signals
7	0.61	0.98	2.12	4.98*m*	35	2.02 AcO; 4.43 H-6 (*dddd*; $J_{6,7}=10$; $J_{6,7'}=7$; $J_{H6-F6}=49$; $J_{H6-F5}=26$)
8	0.62	0.98	2.12	4.93*m*	30	2.01 AcO
9[b]	0.60	0.97	2.13	3.80*m*	30	4.47 H-6 (*dddd*; $J_{6,7}=9$; $J_{6,7'}=6$; $J_{H6-F6}=52$; $J_{H6-F5}=26$)
10	0.61	0.96	2.12	3.86*m*	30	—
11	0.63	1.18	2.12	—	—	4.60 H-6 (*dddd*; $J_{H6,7}=10$; $J_{H6,7'}=6$; $J_{H6-F6}=47$; $J_{H6-F5}=26$)
12	0.64	1.05	2.12	—	—	—
13	0.68	1.19	2.12	—	—	6.08 H-4 (*d*; $J_{4,6}=2$) 5.10 H-6 (*dddd*; $J_{6,7}=12$; $J_{6,7'}=6$; $J_{H6-F6}=48$)
15	0.62	0.95	2.12	4.50*m*[c]	—[c]	5.4 H-2 m[c]
18	0.61	0.98	2.10	4.62*m*	30	$J_{H3-F3}=46$
20	0.88	1.00	—	4.59*m*	25	$J_{H3-F3}=45$
22	0.88	1.00	2.24	4.62*m*	30	6.67 H-16 (*t*; $J_{15,16}=J_{15',16}=3$) $J_{H3-F3}=45$
28	1.11	1.01*d*[e]	2.31	4.83*dp*	15	6.05 H-15 7.21 H-16 (*d*; $J_{15,16}=2.9$)

[a] δ-scale, $CDCl_3$ solution; coupling constants are given in Hz; [b] $CDCl_3$ + DMSO-d_6 solution; [c] overlapping multiplets $\Delta \approx 70$ Hz; [e] β-Me at C-5, $J_{Me-F}=1$.

carbon atoms (127.7 and 122.3 ppm) only the latter one showed two long-range couplings (*dd*) with the fluorine atoms at C-5, while the other, being at a four-atom distance, gave no measurable coupling. This is in good agreement with our previous results [3] according to which the treatment of 3-hydroxy-5,6-dihalogen compounds with FAR results in 2,3-unsaturated derivatives, containing the double bond separated by a methylene group from the halogen-containing carbon atom.

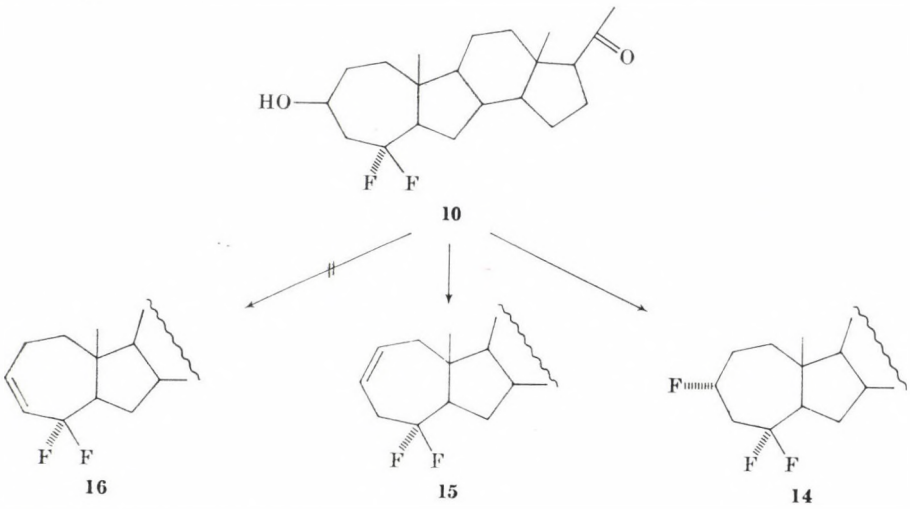

Table II

^{13}C-NMR data[a] of fluorinated steroids **7**—**13**, **15**, **18**, **20**, **22** *and* **28**

Carbon atom \ Compound	7	8	9[b]	10	11	12	13	15	18	20	22	28
1	31.2	32.6*d*	30.1[c]	32.6[c]	33.7[c]	(39.6)[c,e]	33.8	31.3*d*[d]	31.4*d*[c]	30.8*d*[c]	32.6*dd*	30.3
2	26.3	28.8	31.5	32.6	38.5	(31.6)[e]	32.5	127.7	29.6*d*	29.5*d*	31.1*d*	32.3*d*
3	69.6*d*	70.0*d*[c]	65.45*d*	67.9*d*[c]	206.8	203.7*dd*	198.5	122.3*dd*	88.95*ddd*	88.9*ddd*	89.0*ddd*	89.5*d*
4	31.5*dd*	42.9*dd*	35.0*dd*	46.3*dd*	43.0*dd*	52.9*t*	119.7*d*	38.6*t*	43.8*td*	43.6*td*	43.8*td*	44.4*d*
5	98.7*dd*	123.6*dd*	99.2*dd*	123.9[i]	100.1*dd*	122.6*dd*	165.8*d*	125.3*dd*	123.4*ddd*	123.1*ddd*	123.2*ddd*	47.9
6	90.0*dd*	56.4*t*	90.2*dd*	56.3*t*	89.8*dd*	55.75*dd*	88.1*d*	56.0*dd*	56.3*t*	56.1*t*	56.3*dd*	21.8
7	39.9*dd*	30.2*t*	39.7*dd*	30.4*dd*	40.3*dd*	30.75*dd*	38.5*d*	36.0*t*	30.3*dd*	29.4*dd*	29.7*t*	26.2
8	33.7*d*	(38.6)[e]	33.2*d*	(38.5)[e]	33.5*d*	(38.6)[e]	33.4*d*	39.2	(38.5)[e]	38.3	34.2	123.9
9	45.3[e]	58.6	45.2[e]	58.6	45.7[e]	57.1	53.5	56.1	58.6	58.7	59.2	138.8
10	31.8*dd*	41.6*d*[c]	32.3*dd*	41.8*d*	32.0*dd*	41.9*d*[c]	39.2*d*	44.2*dd*	41.8*d*	41.7*d*	41.8*d*[c]	32.7
11	21.2	21.1	20.8	21.1	21.1	20.9	21.0	21.3	21.0	20.2	20.9	19.4
12	38.7	(38.7)[e]	38.6	(38.8)[e]	37.0	(38.7)[e]	36.4	38.9	(38.75)[e]	31.3	37.0	37.5
13	44.2	45.2	44.0	45.4	44.1	45.3	43.9	45.4	45.3	48.8	47.6	50.7
14	55.7	56.4	55.7	56.5	55.7	56.2	55.6	56.4	56.5	51.3	56.3	151.8
15	24.3	23.3	24.1	23.4	24.4	23.3	24.4	23.4	23.4	22.4	29.9	117.5
16	22.9	24.6	22.7	24.7	23.0	24.6	23.0	24.7	24.6	35.7	144.0	142.5
17	63.5	62.95	63.3	63.1	63.4	62.9	63.5	63.2	63.0	219.4	155.2	166.8
18	13.4	13.6	13.3	13.7	13.4	13.7	13.3	13.6	13.6	14.1	16.2	20.0
19	16.1*d*	25.1	16.0*d*	25.3	15.9	25.1	18.1	25.8	25.2	25.2	25.2	—
20	209.0	208.8	208.6	209.5	208.8	209.2	208.8	209.3	208.9	—	196.2	192.2
21	31.4	31.3	31.2	31.4	31.4	31.4	31.4	31.4	31.3	—	27.1	26.5
other	170.2[f]	169.6[f]										17.3*d*[h]
	20.9[g]	21.1[g]										

[a] δ scale, $CDCl_3$ solution; [b] $CDCl_3$ + DMSO-d_6 solution; [c] line broadening; [d] arbitrary assignment [f] $CH_3\underline{C}O^-$; [g] $\underline{C}H_3CO^-$; [h] 5β-Me; [i] not clearly assignable because of poor relaxation.

As the synthesis of the required trifluorides could not be effected according to the first approach, the second possibility, starting from 3-fluoro-5-ene-derivatives was tried.

Treatment of 3β-fluoropregn-5-en-20-one (**17**) with BORNSTEIN's reagent [9] afforded the A-*homo*-B-*nor* geminal difluoride **18** and no isomer containing vicinal fluorine atoms could be detected in the mother liquor by NMR. 3β-Fluoroandrost-5-en-17-one (**19**) gave in a similar reaction the analogous geminal difluoride **20** as the sole product, whereas the corresponding 3β-fluoropregna-

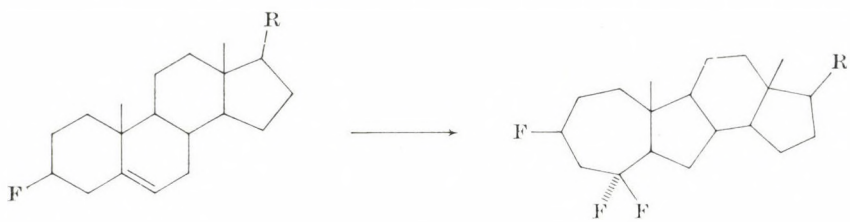

17 R = $COCH_3$ **18** R = $COCH_3$

19 R = O **20** R = O

5,16-dien-20-one (**21**) yielded, besides the trifluoride **22**, a partially rearranged, unsaturated mono-fluoro derivative **28**. The structure of this compound was proved unambigously by NMR. In the ^{1}H-NMR spectrum the signal of two olefinic protons appeared at 6.05 and 7.21 ppm, respectively, with a coupling of 2.9 Hz, proving their *cis* arrangement [23]. The signal of the 18-methyl group was shifted downfield to 1.11 ppm, whereas the 19-methyl group appeared at 1.01 ppm and showed a long range ^{1}H- ^{19}F coupling of 1 Hz, suggesting their 1,3-*diaxial* arrangement [15]. The signal of H-3 showed identical couplings with vicinal protons — which results in a clear pentet splitting — ($J_{2,3} \cong J_{2',3} \cong J_{3,4} \cong J_{3,4'} \cong 3$ Hz) proving its symmetrical *equatorial* arrangement, consequently βF-3 must be in *axial* position. In the ^{1}H-coupled ^{13}C-NMR spectrum two strongly shifted tertiary (142.5 and 166.8 ppm) as well as four quaternary carbon atoms (123.9; 138.8; 150.8 and 166.8 ppm) could be detected besides the carbonyl carbon (192.2 ppm), suggesting the presence of three double bonds. According to the ^{13}C-^{19}F couplings only one fluorine atom is present in the molecule, but the 19-methyl group showed a longe range coupling of $J_{CF} = 6.3$ Hz, being consistent with a 1,3-*diaxial* arrangement, suggested by the ^{1}H-NMR data too. As the fluorine at C-3 was originally in *equatorial* position [2] and no inversion could occur at this centre, its *axial* arrangement can only be the consequence of the *cis* junction of the originally *trans*-fused A/B rings, and the F-3 — Me-19 1,3-*diaxial* arrangement suggests that simultaneously the migration of Me-19 from C-10 to C-5 must have taken place. A similar rearrangement was observed when 3β-fluoroandrost-5-en-17-one was treated with hydrogen fluoride [3]. According to these facts structure

27 or **28** had to be taken into consideration for the new compound, differing only in the place of one double bond (C-9,10 or C-8,9). As both olefinic C-15 and C-16 atoms show besides the $^1J_{CH}$ coupling only one $^2J_{CH}$ coupling of 4.5 and 6.4 Hz, respectively, and no further $^3J_{CH}$ coupling can be detected, structure **27** can be ruled out, where H-8 should cause a further splitting of the C-15 signal.

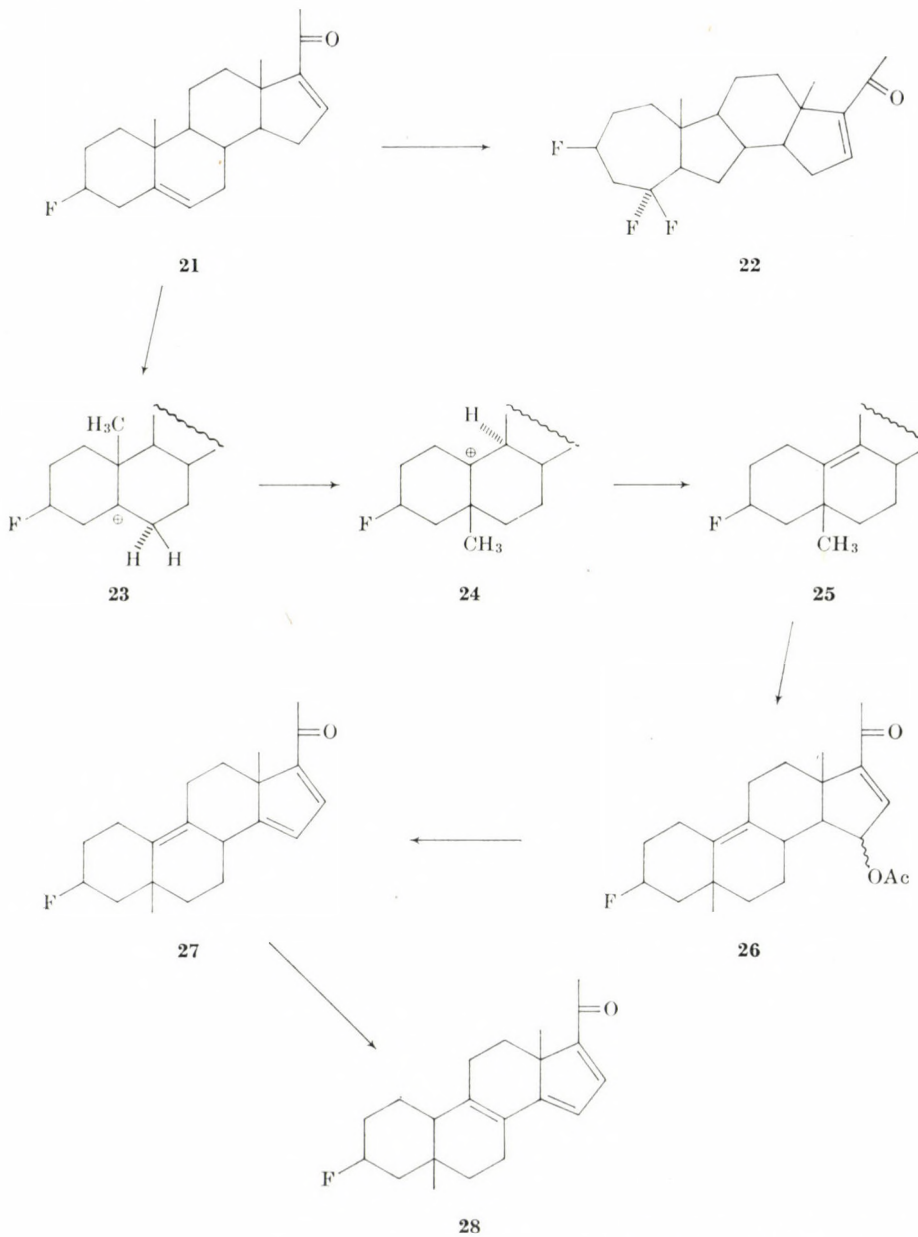

The formation of **28** from **21** can be explained *via* the following reactions. First the 5,6-double bond is protonated by hydrogen fluoride, yielding a carbonium ion at C-5 **23** which suffers a Westphalen rearrangement [16] to give **24**. In the androstane series the so formed ion was attacked by fluorine to give a 10-βF derivative [3], but in the present case the system is stabilized by elimination of H-9 to yield the 9,16-diene **25**. The allylic methylene group (C-15) of the latter is oxidized by lead tetraacetate [17], being present in the reaction mixture, affording the 15-acetoxy derivative **26**, which is converted into the 9,14,16-triene **27** by elimination of acetic acid. The 9,10 double bond of the latter is then shifted into 8,9 position yielding **28** with a more stable conjugated triene system.

The chemical shifts, as well as the ^{1}H-^{1}H, ^{1}H-^{19}F and ^{13}C-^{19}F coupling constants,obtained from the ^{1}H- and ^{13}C-NMR spectra (see Tables I and II)made possible the unambiguous structure determination of all fluorinated steroids. The assignment of the signals was made by comparison with analogous systems [18, 19, 20]; the analysis of configuration and conformation was based on the structure dependence of the ^{13}C-^{19}F couplings [21,22]. From these data the A-*homo*-B-*nor* structure of compounds **8**, **10**, **12**, **15**, **18**, **20** and **22**, as well as the conformation of the seven-membered ring could be established. The C-5 atom containing two fluorine atoms is readily distinguished at about 120 ppm in the ^{13}C-spectra, due to the ^{13}C-^{19}F couplings of about 240 Hz. Because of the differences in the one-bond carbon-fluorine coupling constants and chemical shifts of the *axial* and *equatorial* fluorine atoms, the fluorine-bearing carbon signal (X part of an ABX system) appears as a quadruplet in the ^{13}C-NMR spectrum. The same holds for carbons involved in two-bond and three-bond couplings, $^2J_{CF}$ (20—30 Hz) and $^3J_{CF}$ ($\sim$10 Hz), with the fluorine atoms. From among the two carbon atoms, being adjacent to the CF_2 group, one belongs to a methylene and the other to a methine group (proved by off-resonance). On the other hand, the long-range coupling of C-3 — which can be easily assigned because of its substitution with the fluorine atoms of the CF_2 group — is $\sim$10 Hz, being in agreement with a $^3J_{CF}$ coupling; consequently the CF_2 group is incorporated in the A-ring (C-5). All these data prove the *A-homo* structure. The absence of any long-range coupling of the 19-methyl group with the F-5 atoms exludes the presence of an *axial* βF-5 atom which, according to the "converging vector rule" [15], should cause a significant splitting. Accordingly, βF-5 is *equatorially* and βF-5 is *axially* oriented.

Experimental

M.p.'s were determined with a Beotius apparatus and are uncorrected. TLC was effected on Kieselgel HF_{254} with benzene-tetrahydrofuran 40 : 3 (*A*) and 4 : 1 (*B*); for detection a 20% solution of $SbCl_5$ in chloroform was used with subsequent heating at 110 °C. Column

chromatography was carried out on Woelm Silica Gel (63—200 μm) using benzene-tetrahydrofuran 25 : 1 (*C*) for elution. The ^{1}H-NMR spectra were recorded at 90 MHz with a VARIAN EM-390 spectrometer and the ^{13}C-NMR spectra at 25.16 MHz with a VARIAN XL-100 spectrometer in $CDCl_3$ solution, using tetramethylsilane as internal standard. The coupling constants were read by the assumption of first order splitting.

All evaporation were effected in a rotary evaporator under diminished pressure, after having dried the organic solutions over sodium sulfate. Reactions with hydrogen fluoride were carried out in polyethylene bottles. Optical rotations were determined in chloroform ($c = 1$).

Reaction of 3β-acetoxypregn-5-en-20-one (6) with BORNSTEIN's reagent

To a stirred slurry of lead tetraacetate (16 g) in a mixture of methylene dichloride (40 mL) and dry hydrogen fluoride (11 g), a solution of **6** (5 g) in methylene dichloride was added at −75 °C. The reaction was monitored by TLC (*A*). After the disappearance of the starting material (4 h), the temperature was raised to 0 °C and the mixture was poured into ice-water. After neutralization with sodium carbonate the organic solution was separated, washed with water, dried and evaporated. The residue gave on separation by column chromatography and subsequent recrystallization from ethanol the following components:

3β-Acetoxy-5,5-difluoro-A-*homo*-B-*nor*-6β-pregnan-20-one (**8**, 2.42 g; 43.7%), m.p. 129—130 °C, $[\alpha]_D^{20}$ +79°, R_F 0.72 (*A*); *lit.* [6] m.p. 126—127 °C, $[\alpha]_D^{20}$ +83°.

3β-Acetoxy-5α,6α-difluoropregnan-20-one (**7**, 0.93 g; 16.8%), m.p. 177—179 °C, $[\alpha]_D^{20}$ +98°, R_F 0.57 (*A*); *lit.* [5] m.p. 178—180 °C, $[\alpha]_D^{20}$ +100 °C.

3β-Hydroxy-5α,6α-difluoropregnan-20-one (9)

A solution of the acetate **7** (0.6 g) in methanol (50 mL) was hydrolyzed with a solution of K_2CO_3 (0.5 g) in water (2.7 mL), as described for compound **10**, to give pure **9** (0.51 g; 94.7%), m.p. 221—224 °C, R_F 0.45 (*B*); *lit.* [6] m.p. 221—223 °C.

3β-Hydroxy-5,5-difluoro-A-*homo*-B-*nor*-6β-pregnan-20-one (10)

To a solution of **8** (4.2 g) in methanol (350 mL) a solution of K_2CO_3 (3.5 g) in water (18.5 mL) was added and the reaction mixture was boiled for 5 min. The cooled solution was filtered, the filtrate diluted with water (250 mL) and the methanol was evaporated. The precipitated material was filtered and washed with water to give pure **10** (3.6 g; 96.2%), m.p. 193—195 °C, R_F 0.55 (*B*); *lit.* [6] m.p. 194—196 °C.

5α,6α-Difluoropregna-3,20-dione (11)

To a stirred solution of **9** (0.45 g) in acetone (65 mL) JONES reagent [14] (0.7 mL) was added at 0 °C. Stirring was continued for 10 min, and the reaction mixture was then poured into ice-water. The precipitate was filtered off, washed with water, dried and recrystallized from benzene to yield **11** (0.32 g; 71.5%), m.p. 227—230 °C, R_F 0.50 (*A*); *lit.* [12] m.p. 224—227 °C.

5,5-Difluoro-A-*homo*-B-*nor*-6β-pregna-3,20-dione (12)

A solution of **10** (0.25 g) in acetone (32 mL) was oxidized with JONES reagent (0.4 mL) as described for compound **11** to yield **12** (0.19 g; 76.5%), m.p. 176—178 °C, R_F 0.65 (*A*); *lit.* [12] m.p. 178 °C.

Reaction of compound 10 with FAR

To a stirred solution of **10** (3.5 g) in dry chloroform (40 mL) FAR reagent [2] (3.8 mL) was added dropwise at 0 °C. Stirring was continued for 3 h, then NaF (2 g) and, after 1 h, methanol (2 mL) were added. The reaction mixture was allowed to stand at room temperature overnight and was then filtered and evaporated. The residue was separated by column chromatography (*C*) to give, after recrystallization from ethanol, the following compounds:

3α,5,5-Trifluoro-A-*homo*-B-*nor*-6β-pregnan-20-one (**14**, 0.1 g; 2.8%), m.p. 184—190 °C, R_F 0.65 (*A*).

$C_{21}H_{31}OF_3$ (356.46). Calcd. F 16.0. Found F 15.72%.

5,5-Difluoro-A-*homo*-B-*nor*-6β-pregn-2-en-20-one (**15**, 1.78 g; 53.2%), m.p. 141—145 °C, R_F 0.73 (*A*).

$C_{21}H_{30}OF_2$ (336.45). Calcd. F 11.25. Found F 11.15%.

3β-5,5-Trifluoro-A-*homo*-B-nor-6β-pregnan-20-one (18)

A solution of compound **17** [2] (4.0 g) in dry methylene dichloride (70 mL) was added dropwise at —75 °C to a stirred slurry of lead tetraacetate (12.8 g) in dry methylene dichloride (35 mL) containing dry hydrogen fluoride (8 g). The reacation mixture wasworked up as described for compound **6** to give after column chromatography and recrystallization from ethanol, pure **18** (2.15 g; 47.8%), m.p. 154—157 °C, $[\alpha]_D^{20}$ +84.9°, R_F 0.75 (*A*).

$C_{21}H_{31}OF_3$ (356.46). Calcd. F 16.00. Found F 15.97%.

3β,5,5-Trifluoro-A-*homo*-B-*nor*-6β-androstan-17-one (20)

A solution of compound **19** [2] (3.6 g) in dry methylene dichloride (80 mL) was added dropwise at —75 °C to a stirred slurry of lead tetraacetate (12 g) in methylene dichloride (30 mL) containing dry hydrogen fluoride (10.8 g). According to TLC the reaction was complete in 3 h and was then processed as decribed for compound **6** to give pure **20** (1.76 g; 42.8%), m.p. 158—162 °C, $[\alpha]_D^{20}$ +59°, R_F 0.73 (*A*).

$C_{19}H_{27}OF_3$ (329.12). Calcd. F 17.35. Found F 17.18%.

Reaction of compound 21 with BORNSTEIN's reagent

A solution of **21** [2] (2.5 g) was treated with lead tetraacetate-hydrogen fluoride as described for compound **6**. The reaction mixture was processed after 3.5 h to give a crude mixture (2.62 g) which was separated by column chromatography. Rec[illegible]lization from ethanol yielded the following two compounds:

3β,5,5-Trifluoro-A-*homo*-B-*nor*-6β-pregn-16-en-20-one (**22**, 0.91 g; 31.64%), m.p. 129—131 °C, $[\alpha]_D^{20}$ +43 °, R_F 0.80 (*A*).

$C_{21}H_{29}OF_3$ (354.45). Calcd. F 16.15. Found F 16.08%.

3β-Fluoro-5β-methyl-19-*nor*-pregna-8,14,16-triene-20-one (**28**, 0.68 g; 27.4%), yellow needles, m.p. 206—208 °C, R_F 0.55 (*A*).

$C_{21}H_{27}OF$ (314.43). Calcd. F 6.05. Found F 6.28%.

*

The authors are indebted to Dr. L. RADICS and Dr. E. BAITZ-GÁCS (NMR Laboratory of the Central Research Institute of Chemistry, Hungarian Academy of Sciences, Budapest) for recording some of the ^{13}C-NMR spectra.

REFERENCES

[1]Ciba Foundation Symposium: Carbon-Fluorine Compounds. Ass. Sci. Publ., Amsterdam—London—New York 1972
[2] NÉDER, Á., USKERT, A., NAGY, É., MÉHESFALVI, Zs., KUSZMANN, J.: Acta Chim. Acad. Sci. Hung., **103**, 231 (1980)
[3] NÉDER, Á., USKERT, A., MÉHESFALVI, Zs., KUSZMANN, J.: Acta Chim. Acad. Sci. Hung., **104** ,123 (1980)
[4] AYER, D. E.: Tetrahedron Lett., **1962**, 1065
[5] BOWERS, A., DENOT, E., URQUIZA, R.: Tetrahedron Lett., **1960**, 34
[6] BOWERS, A., HOLTON, P. G., DENOT, E., LOZA, M. C., URQUIZA, R.: J. Am. Chem. Soc., **84**, 1050 (1962)
[7] DIMROTH, O., BOCKEMÜLLER, W.: Ber., **64**, 516 (1931)
[8] BORNSTEIN, J., SKARLOS, L.: J. Am. Chem. Soc., **90**, 5044 (1968)
[9] TANNER, D. D., VAN BOSTELEN, P.: J. Am. Chem. Soc., **94**, 3187 (1972)
[10] LEVISALLES, J., MOLIMARD, J.: Bull. Soc. Chim. France, **1971**, 2037
[11] EPHRITIKHINE, M., LEVISALLES, J.: Chem. Commun., **1974**, 429
[12] EPHRITIKHINE, M., LEVISALLES, J.: Bull Soc. Chim. France, **1975**, 339

[13] IUPAC-IUB Revised Tentative Rules for Nomenclature of Steroids (IUPAC Commission on the Nomenclature of Organic Chemistry), Biochem., **8**, 2227 (1969)
[14] BOWERS, A., HALSALL, T. G., JONES, E. R. H., LEMIN, A. J.: J. Chem. Soc., **1953**, 2548
[15] CROSS, D., LANDIS, P. W.: J. Am. Chem. Soc., **86**, 4005 (1964)
[16] COXON, J. M., FISCHER, A., HARTSHORN, M. P., LEWIS, A. J., RICHARDS, K. E.: Steroids, **13**, 51 (1969)
[17] FIESER, L. F., STEVENSON, R.: J. Am. Chem. Soc., **76**, 1728 (1954)
[18] BLUNT, J. W., STOTHERS, J. B.: Org. Magn. Reson., **9**, 439 (1977)
[19] Atlas of Carbon-13 NMR Data (Eds: BREITMAIER, E., HAAS, G., VOELTER, W.) Heyden, London 1979
[20] DAVE, V., STOTHERS, J. B.: Can. J. Chem. **57**, 1550 (1979)
[21] SCHNEIDER, H. J., GSCHWENDTNER, W., HEISKE, D., HOPPEN, V., THOMAS, F.: Tetrahedron, **33**, 1769 (1977)
[22] WRAY, V.: J. Chem. Soc. Perkin II, **1976**, 1598
[23] SOHÁR, P.: Nuclear Magnetic Resonance Spectroscopy (in Hungarian), Vol. **1**, p. 71. Akadémiai Kiadó, Budapest 1976

Ágnes NÉDER
István PELCZER
Zsuzsa MÉHESFALVI
János KUSZMANN

H-1045 Budapest, Szabadságharcosok útja 47—49.

Acta Chimica Academiae Scientiarum Hungaricae, Tomus 109 (3), pp. 287—293 (1982)

THE TRANSIENT RESPONSE OF STAGEWISE EXTRACTION COLUMNS WITH BACKMIXING TO CONCENTRATION DISTURBANCES

J. SAWINSKY* and J. HUNEK

(Department of Chemical Engineering, Technical University of Budapest)

Received September 16, 1980
In revised form March 16, 1981
Accepted for publication April 7, 1981

An analytical solution is given for the concentration response of a countercurrent extractor following a step change in the concentration of the feed stream. The dynamic model of the extractor includes the effects of backmixing in both phases.

It was assumed that equilibrium is reached in the stages, and the distribution coefficient, the hold-up and phase ratio are constant.

Introduction

The knowledge of the dynamic behaviour of mass transfer equipments is important for calculating the start-up time and designing control systems. A number of papers have been published so far mainly on the unsteady-state behaviour of distillation columns, but there is little in the literature on that of extraction columns.

In the case of these latter the exact mathematical description even of the steady state operation involves some difficulties because the backmixing in the continuous and dispersed phase must be considered.

POLLOCK and JOHNSON [1] have given a critical review of works published before 1969 on extraction column dynamics. JONES and WILKINSON [2] have studied a mechanically agitated multistage column and presented experimental results and a theoretical treatment of concentration transients for disturbances in the input streams. A non-equilibrium stage model with backmixing was used in their work.

Similar work has been reported by SOUHRADA *et al.* [3] for a reciprocating plate column. Frequency-response comparisons of the backmixing model with experimental data have been made by MCSWAIN and DURBIN [4] for a packed countercurrent absorber. Some of the recently spreading digital simulation routines specially developed for the numerical solution of sets of first order differential equations have been successfully used by DUNN and INGHAM [5, 6] in modelling non-equilibrium multistage extraction column dynamics with backmixing in both phases.

* To whom correspondence should be addressed.

Mathematical model

Considering a countercurrent stagewise extractor which consists of perfectly mixed stages with backmixing between them (Fig. 1). Our model is based upon the following assumptions:

1. The phases in each stage are in equilibrium.
2. Backmixing occurs in both phases. The coefficients of backmixing do not vary from stage to stage.
3. The holdups of the phases are constant along the entire column length.
4. The flow rates of the inlet phases do not vary in time.
5. Variations in holdup and backmixing over the transient period are negligible.

   The above conditions imply a constant mean residence time in every stage.
6. The equilibrium relationship is linear

$$Y^* = m \cdot X$$

where X is the concentration of solute in the raffinate phase and Y^* is that of the extract phase which is in equilibrium with X.

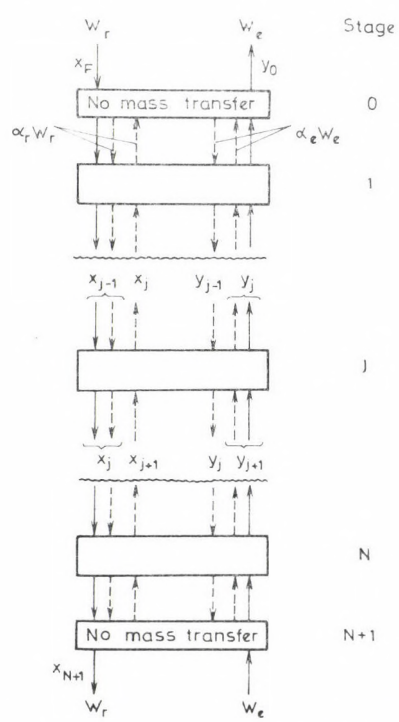

Fig. 1. The stage model with backmixing of the countercurrent extractor

7. The change in the mutual solubility of the solvents in the examined concentration interval is negligibly small.
8. The column is initially in the steady state.

In the present study we consider a step disturbance in the inlet raffinate phase composition. The deviation of concentrations from the initial steady state values X_i and Y_i are

$$x = X(t) - X_i$$

$$y = Y(t) - Y_i$$

where $X(t)$ and $Y(t)$ are the concentrations of the solute in the raffinate and extract phases respectively at time t. In view of the above considerations the following solute balance can be written for the stages $1 \leq j \leq N$ in Fig. 1.

$$a \cdot x_{j-1} - b \cdot x_j + c \cdot x_{j+1} = T \frac{\mathrm{d}x_j}{\mathrm{d}t}. \tag{1}$$

The end zones of the column are negligibly small in volume and no mass transfer takes place there. The solute balance for the zeroth stage:

$$\frac{1}{\alpha_0} \cdot x_F - g \cdot x_0 + x_1 = 0 \tag{2}$$

and for the $(N + 1)$th stage:

$$x_{N+1} - h \cdot x = 0 \tag{3}$$

After taking the Laplace transforms and rearranging :

$$1 \leq j \leq N; \; q \cdot \bar{x}_{-1} - p \cdot \bar{x}_j + \bar{x} = 0 \tag{4}$$

$$j = 0; \qquad \frac{1}{\alpha_0} \cdot \bar{x}_F - g \cdot \bar{x}_0 + \bar{x}_1 = 0 \tag{5}$$

$$j = N + 1; \qquad \bar{x}_{N+1} - h \cdot \bar{x}_N = 0 \tag{6}$$

Solution procedure

The solution of the above set of linear second order difference equations (4) with constant coefficients can be written as

$$_j = B_1 \cdot r_1 + B_2 \cdot r_2^j \tag{7}$$

with characteristic roots

$$r_{1,2} = \frac{1}{2}(p \pm i\sqrt{4q - p^2}). \tag{8}$$

These may be written in the following form in terms of periodical functions:

$$r_{1,2} = \sqrt{q}\,(\cos\psi \pm i \sin\psi) \tag{9}$$

The transformed response function for the jth stage is

$$x_j = q^{\frac{j}{2}}(C_1 \cos j\psi + iC_2 \sin j\psi). \tag{10}$$

The arbitrary constants C_1 and C_2 have to be determined satisfying the boundary conditions given in Eqs (5) and (6).

The general solution for $\bar{x}_j$ is given by

$$\frac{\bar{x}_j}{\bar{x}_F} = \frac{D(\psi)}{E(\psi)} \tag{11}$$

$$D(\psi) = \frac{q^{\frac{-1}{2}}}{\alpha_0}\,[\sqrt{q} \cdot \sin(N+1-j)\psi - h \cdot \sin(N-j)\psi] \tag{12}$$

$$E(\psi) = h \cdot \sin(N-1)\psi - 2\sqrt{q} \cdot \sin N\psi + g \cdot \sin(N+1)\psi \tag{13}$$

The inversion of $\bar{x}_j$ into the time domain was made by the method of residues [7, 8] to give the step response of the system:

$$\frac{x_j(\vartheta)}{x_F(\infty)} = \frac{x_j(\infty)}{x_F(\infty)} + \sum_{k=1}^{N} \frac{D(\psi_k)}{s_k \cdot E'(\psi_k)} \frac{\mathrm{d}s_k}{\mathrm{d}\psi_k} \cdot \mathrm{e}^{-s_k\vartheta} \tag{14}$$

where the poles are:

$$s_k = c(1 + q - 2\sqrt{q}\cos\psi_k) \tag{15}$$

and

$$D(\psi_k) = D(\psi)\big|_{\psi=\psi_k} \tag{16}$$

$$E'(\psi_k) = \left.\frac{\mathrm{d}E(\psi)}{\mathrm{d}\psi}\right|_{\psi=\psi_k} = h(N-1)\cos(N-1)\psi_k - 2N\sqrt{q} \cdot \cos N\psi_k + g(N+1)\cos(N+1)\psi_k \tag{17}$$

$$\left.\frac{\mathrm{d}s}{\mathrm{d}\psi}\right|_{\psi=\psi_k,\ s=s_k} = 2c\sqrt{q} \cdot \sin\psi_k\,. \tag{18}$$

The N values of ψ_k are the roots of Eq. (13) in the interval $0 \leq \psi_k \leq \pi$.

The steady-state solution of the solute balance [*i. e.* Eqs (1)...(3)] is [9]

$$\frac{x_j(\infty)}{x_F(\infty)} = \frac{K \cdot q^{j-1} - q^{N-1}}{K^2 - q^{N-1}} \tag{19}$$

and for the special case of $K = 1$

$$\frac{x_j(\infty)}{x_F(\infty)} = \frac{1 + \alpha_0 + N - j}{1 + 2\alpha_0 + N}\,. \tag{20}$$

In the literature there are special solutions available for limiting conditions such as $\alpha = 0$ and $K = 0$ respectively. In the case of zero backmixing the step-response function. $x_j(\vartheta)$, reduces to the same expression published by MARSHALL and PIGFORD [10], JENSON and JEFFREYS [8]. If there is no mass transfer between the phases ($K = 0$) Eq. (14) for the outlet ($j = N$) agrees with the cumulative residence time distribution function given by ROEMER and DURBIN [11]. A special solution was obtained by DECKWER and POPOVIC [12] for a continuous reactor with first order reaction. Comparison of Eq. (14) and the solution of DECKWER and POPOVIC reveals that these analytical expressions become identical for a system without mass transfer and reaction.

Numerical results and conclusions

Based on the above equations the concentration response in the extract and raffinate phases has been calculated to a step perturbance in the feed concentration. Figure 2 shows the normalized transition curves of the raffinate phase leaving the countercurrent extractor containing 5 and 30 stages, respectively. In the presented cases the extraction coefficient and the steady

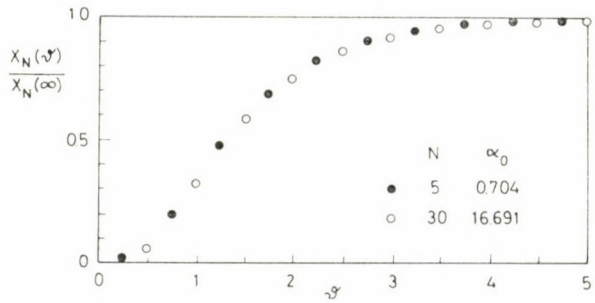

Fig. 2. Normalized raffinate phase concentration response for step change in the feed concentration

state concentration value were identical $K = 3$ and $x_N(\infty)/x_F(\infty) = 0.01$. Numerical calculations have been made in the following parameter range: $K = 1 \ldots 5$, $N = 3 \ldots 30$ and $\alpha_0 = 0 \ldots \infty$. It has been found that the transition functions are in good agreement with each other if the extraction coefficient and the steady-state concentration values are identical. Simulation by a MEDA 40 TA analog computer gave similar results [13].

Notation

$a = \dfrac{1+\alpha_0}{1+K}$

$A = \dfrac{1+m\cdot f}{1+m\cdot\varphi}\cdot\dfrac{1+\varphi}{1+f}$

$b = 1+\dfrac{2\alpha_0}{1+K}$

$c = \dfrac{K+\alpha_0}{1+K}$

$f = \dfrac{W_e}{W_r}$ feed phase ratio

$g = \dfrac{1+\alpha_0}{\alpha_0}$

$h = \dfrac{\alpha_0}{K+\alpha_0}$

$i = \sqrt{-1}$

j stage number
$K = m\cdot f$ extraction coefficient
$m = Y^*/X$ distribution ratio
N total number of stages

$p = 1+q+\dfrac{s\cdot T}{c}$

$q = \dfrac{1+\alpha_0}{K+\alpha_0}$

s [s^{-1}] Laplace transform variable
t [s] time

$\bar{t} = \dfrac{V}{W_e+W_r}$ [s] mean residence time

$T = \dfrac{\bar{t}}{N\cdot A}$

V [m^3] volume of the extractor
W [$m^3\cdot s^{-1}$] volumetric flow rate
x [$g\cdot m^{-3}$] deviation of the raffinate phase concentration from the initial steady-state value
$\bar{x}$ Laplace transform of x
X [$g\cdot m^{-3}$] concentration of solute in the raffinate phase
Y [$g\cdot m^{-3}$] concentration of solute in the extract phase
Y^*[$g\cdot m^{-3}$] Y concentration in equilibrium with X

Greek symbols

α backmixing coefficient
$\alpha_0 = \alpha_r + K\cdot\alpha_e$ overall backmixing coefficient
$\varphi = \Phi_e/\Phi_r$ holdup ratio
Φ holdup
$\vartheta = t/T$ dimensionless time

$\psi = \arccos\dfrac{p}{2\sqrt{q}}$

Subscript

0, 1, 2, . . ., j stage number
N last stage
e extract phase
F feed
i initial steady-state value
r raffinate phase

REFERENCES

[1] POLLOCK, G. G., JOHNSON, A. I.: Canad. J. Chem. Eng., **47**, 469 (1969)
[2] JONES, D. A., WILKINSON, W. L.: Chem. Eng. Sci., **28**, 539 (1973)
[3] SOUHRADA, F., LANDAU, J., PROCHAZKA, J.: Canad. J. Chem. Eng., **48**, 322 (1970)
[4] MCSWAIN, C. V., DURBIN, L. D.: Separation Sci., **4**, 25 (1969)
[5] DUNN, I. J., INGHAM, J.: Chem. Eng. Sci., **27**, 1751 (1972)
[6] DUNN, I. J., INGHAM, J.: Verfahrenstech., **6**, 1 (1972)
[7] CHURCHILL, R. V.: Operationa ematics. McGraw Hill, New York 1958
[8] JENSON, V. G., JEFFREYS, G. V.: Mathematical Methods in Chemical Engineering, Academic Press, New York 1963
[9] SLEICHER, C. A.: A. I. Ch. E. J., **6**, 529 (1960)
[10] MARSHALL, W. R., PIGFORD, R. L.: The Application of Differential Equations to Chemical Engineering Problems, University of Delaware, 1947
[11] ROEMER, M. H., DURBIN, L. D.: Ind. Eng. Chem. Fund., **6**, 120 (1967)
[12] DECKWER, W., POPOVIC, M.: Chemie-Ing. Techn., **45**, 984 (1973)
[13] SAWINSKY, J., PEKOVITS, L., HUNEK, J.: Int. Chem. Eng., **18**, 325 (1978)

János SAWINSKY
József HUNEK
} H-1521 Budapest, Műegyetem rkp. 3.

Acta Chimica Academiae Scientiarum Hungaricae, Tomus 109 (3), pp. 295—301 (1982)

DETERMINATION OF WEAR METALS IN USED LUBRICATING OILS BY ATOMIC ABSORPTION SPECTROMETRY

Zs. WITTMANN

(Hungarian Oil and Gas Research Institute, Veszprém)

Received December 28, 1980
Accepted for publication April 16, 1981

Analysis of used lubricating oils for traces of wear metals has been recognized long before as essential for the prevention of major breakdown in engines.

In this paper an organic-based mixed solvent system and inorganic compounds dissolved in an organic solvent as mixed standard were used for the determination of wear metals as iron, chromium, nickel, copper and lead in used lubricating oils of diesel and gasoline engines in air–acetylene flame by atomic absorption spectroscopy.

An increase in the wear metal content of crank-case and circulated lubricating oils signifies a source of potential trouble in an engine. The actual metal may indicate the location of the trouble.

Presence of lead and copper might mean wear in a bearing; iron, chromium and nickel would be present because of piston wear. Copper may be present as a contaminant introduced during refining or storage and treating processes.

Periodical analyses of the lubricating oils enables such troubles to be located and corrected before they cause a major breakdown.

For rapid analysis of many samples methods have been developed for for the determination of metals using organic solvents as medium for spraying the samples directly into the flame. These techniques are almost free of interference effects, but there are problems, for example the question of viscosity, particle size, applied standards, *etc.*

Several investigators have examined the relationship for metal particle size and recovery efficiency [1, 2, 3, 4]. But this effect must be shared by every method that uses unashed oil. Some work try to reduce this error in different ways [1, 5]. So the experts at the engine have to be satisfied usually with an approximate result of the metal concentration of the used oil as the extreme high metal concentration values mean the trouble in the engine.

IBRAHIM and SABBAH [6] studied the effect of the differences in viscosity between samples and standard solutions on element concentration measurements in crude oil diluted with xylene and established that the viscosities of the unknown sample and the calibrating solution should be approximately the same.

In most methods solution containing about 10—35% *w/v* of oil with constant dilution ratio of the sample oil and the metal free oil in standard solution, respectively, are used. These solutions are not too viscous to be sprayed through the atomizer.

Diluting the used oil with mehtyl *iso*-butyl ketone (MIBK) (oil/MIBK 1 : 2 *v/v*) was used by JACKSON, SALAMA and DUNN [2]. By SPARGUS and SLAVIN [7], S. SLAVIN and W. SLAVIN [8] 10% *v/v* of oil in MIBK was used for preparing sample and standard solutions. 20% *w/v* of oil in MIBK was applied by BURROWS, HEERDT and WILLIS [9]; 10% *v/v* of oil in xylene by KAHN, PETERSON and MANNING [10], MEANS and RATCLIFF [4]; 10% *v/v* of oil in *iso*-octane by ROBINSON [11].

On the one hand the great oil content is advantageous to rise the measured absorbance, but at the same time the increasing viscosity can ruin the increased sensitivity, makes spraying difficult and sometimes the choice of dilution is closely linked with the "memory" effect obtained in different solutions. A slow rise to a maximum reading sometimes requires about 30—40 sec.

The present work investigates a simple measuring condition to determine the wear metals (copper, chromium, nickel, iron and lead) in used lubricating oil of diesel and gasoline engine without prior ashing of the sample. On the one hand the viscosity should not be considered as far as possible. On the other hand instead of using metallo-organic compounds in mixed standards (mixed standards have been used also by other authors [7, 8, 9]) the more available and cheeper inorganic compounds in mixed standard were tried to use like in our carlier measurements for the determination of calcium, magnesium and zink in lubricating oils and additives [12].

Experimental

The effect of viscosity on the determination of wear metals in used lubricating oils is the question of applied solvent. Therefore the two more often used solvent MIBK and xylene further an organic solvent mixture (toluene—glacial aceticacid) according to GUTTENBERGER [13] and our earlier experiments were tried in the present ecperiments. A 3 : 2 *v/v* mixture of the two solvents dissolves the oil sample readily and there is no flame extinction yet.

First, several solutions of different viscosities were prepared by mixing base oil (metal-free 0 — about 150—200 cS at 37.8 °C) with metal-free solvents. These samples were prepared to establish a connection between viscosity and the added base oil in different solvents (Fig. 1). The viscosity measurements were performed according to [14] in the mixed solvent and MIBK; the viscosity values of xylene were taken from the literature [6]. Further on the basis of the results of viscosity measurements and because the "memory" effect often has appeared in xylene during previous metal content determinations, only the two solutions: MIBK and the organic solvent mixture were examined.

In the next step from alcohol soluble inroganic metal salts [nickel(II) chloride, copper (II) chloride, lead(II) nitrate, chromium(III) chloride, iron(III) chloride] standard solutions were prepared in ethanol. From these alcoholic solutions two kinds of standard solution were prepared, the first type contained one of the metals the second one contained all the examined metals in MIBK and in the organic solvent mixture. The absorbance values of these solutions have not shown interelement effect in the chosen organic solvent during the wear metals determination according to Table I.

Figures 2 and 3 show curves for the absorbances of metals in organic solvent mixture and MIBK containing different quantities of oil. In MIBK a decrease of the absorption of the metal at increasing oil concentration was found but in organic solvent mixture increasing the viscosity of solvents does not seem to effect the absorption values as far as the oil content is 10 *w/v* %. So it is not necessary to add oil to the solutions used for calibration.

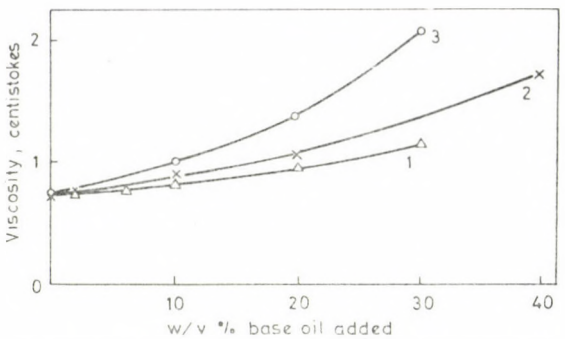

Fig. 1. Viscosity at 25 °C versus volume of added base oil. 1: solvent mixture, 2: MIBK, 3: xylene

Solution (without oil) prepared from the five alcohol soluble inorganic metal salts in an organic solvent mixture (toluene : glacial acetic acid = 3 : 2) is available for standard solutions during determination of wear metals in lubricating oil by AAS. These standard solutions are normally stable for months. Figure 4 shows typical calibration curves for the five metals in organic solvent mixture containing no oil. The conditions of the determinations are given in Table II.

In the case of samples (the measured solution never contained more than 10 *w/v* % used lubricating oil) the absorption reading levels off after 10—20 s and returns rapidly to zero

Table I

Interelement interference in the determination of wear metals in organic solvents

Metal	Concentration (μg/ml)	Other metals present (μg/ml)	Absorbance	
			in MIBK	in an organic solvent mixture
Cu	6.0	—	0.545	0.492
Cu	6.0	Ni 6.0; Cr 10.0; Fe 10.0; Pb 10.0	0.540	0.487
Ni	6.0	—	0.382	0.353
Ni	6.0	Cu 6.0; Cr 10.0; Fe 10.0; Pb 10.0	0.379	0.355
Cr	10.0	—	0.275	0.225
Cr	10.0	Cu 6.0; Ni 6.0; Fe 10.0; Pb 10.0	0.272	0.244
Fe	10.0	—	0.510	0.845
Fe	10.0	Cu 6.0; Ni 6.0; Fe 10.0; Pb 10.0	0.507	0.845
Pb	10.0	—	0.254	0.351
Pb	10.0	Cu 6.0; Ni 6.0; Cr 10.0; Fe 10.0	0.252	0.350

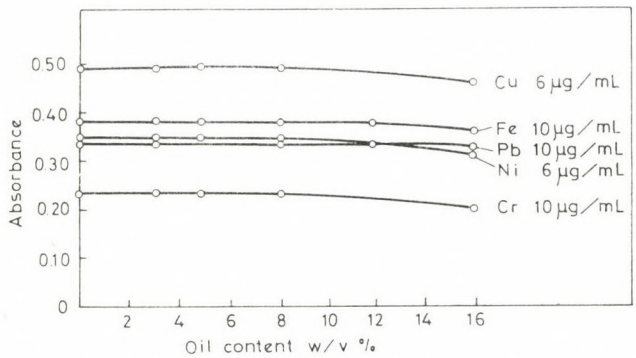

Fig. 2. Absorbance of metals in an organic solvent mixture containing different amounts of oil

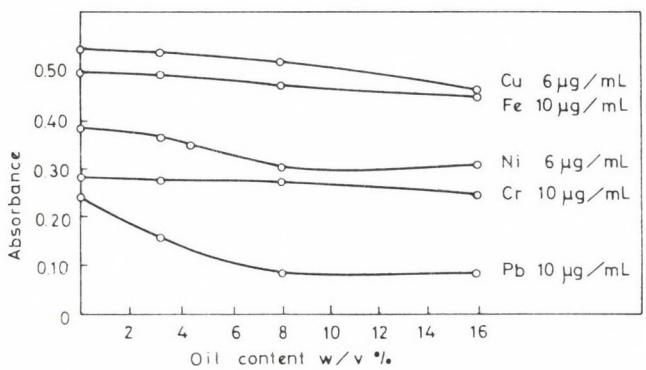

Fig. 3. Absorbance of metals in MIBK containing different amounts of oil

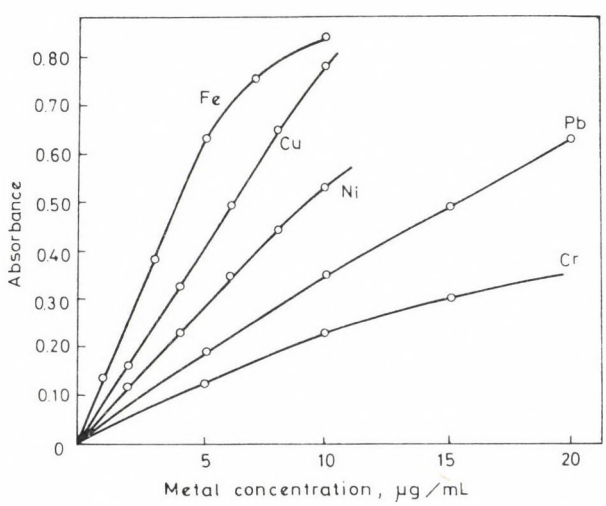

Fig. 4. Calibration curves for metals in an organic solvent mixture

Table II

Operating conditions for the AAS determination of near metals in oil

Metals	Cu	Ni	Cr	Fe	Pb
Wave length (nm)	324.7	232.0	357.9	248.3	283.3
Lamp current (mA)	4	4	7	7	4
Slit width (mm)	0.04	0.04	0.06	0.05	0.04
Seale expansion	3×	1×	8×	5×	5×
Burner height (mm)	5	5	5	6	5
Flame	air — acetylene				

Apparatus: Spektromom 190 A

Table III

Comparison of different methods to determine wear metals in oil

Sample	Cu, μg/mL		Ni, μg/mL		Fe, μg/mL			Pb, μg/mL		Cr, μg/mL	
	Direct	Ashed	Direct	Ashed	Direct	Ashed	Titration	Direct	Ashed	Direct	Ashed
1	13.1	14.7	3.2	3.1	68.1	74.0	73.1	41.6	40.5	27.7	29.1
2	44.1	43.2	11.8	13.8	128.7	153.4	152.0	37.0	37.8	42.2	43.7
3	26.3	28.3	7.7	7.7	96.4	124.0	121.0	15.4	13.9	32.2	34.5
4	23.4	24.5	9.7	10.6	110.0	113.0	110.5	26.9	25.4	23.6	22.7
5	18.9	19.9	13.3	13.9	182.0	220.5	202.1	10.1	43.3	121.7	132.3
6	18.8	17.9	6.1	7.0	112.2	115.4	111.3	27.7	25.4	59.9	57.4
7	21.3	20.9	5.1	5.3	64.0	65.1	67.0	52.5	50.6	51.5	49.6
8	10.8	11.5	9.0	9.8	90.3	114.9	111.7	29.2	32.5	67.9	71.3
9	11.6	10.6	4.3	4.6	41.8	41.2	42.5	13.4	14.1	3.5	3.4
10	9.3	9.0	3.7	3.5	26.3	25.6	27.1	41.0	12.2	4.5	5.0
11	14.3	15.5	3.6	5.0	75.4	73.1	74.6	22.0	21.6	65.2	67.0
12	19.7	20.9	3.5	4.4	54.0	52.8	52.7	60.4	57.1	12.0	11.1

when spraying is discontinued. Only a very short period is needed to wash out the spray or with pure solvent between the samples.

Some results of the determination by the developed method can be seen in Table III. The different metals (iron, chromium, nickel, copper, lead) in used lubricating oils were determined by the direct method (in inorganic solvent mixture) and after ashing by AAS, and after ashing by complexometric titration (in the case of iron).

The results of the metal concentration determined by the three different methods agree well in most of the cases. There are some samples where especially iron concentration measured after ashing is higher than the result of the direct AAS method, because in these samples particles larger than a few microns are present and they do not contribute to the absorption. For this reason several oils were filtered (samples 2, 3, 5 and 8) consecutively through filters of size 16.6 and 9.8 micron, respectively, and the filtrates were analyzed (Table IV).

It can be seen that the majority of iron is present as particle smaller than about 10 microns in diameter or dissolved, and so particles larger than about 10 microns do not contrib-

Table IV

Filtration study

Sample	Without filtration		Filtration			
			on 16.6 μ filter		on 9.8 μ filter	
	Direct	Ashed	Direct	Ashed	Direct	Ashed
2	128.7	153.4	127.5	149.7	122.3	126.1
3	96.4	124.0	94.2	123.5	95.9	100.6
5	182.0	200.5	179.3	182.0	175.3	—
8	90.3	114.9	88.9	113.1	88.1	90.7

ute to the absorption signal (similar to the results of TAYLOR, BARTELS and CRUMP [3]). By means of nitrous oxide/acetylene flame the value of the absorption signal may be improved [15].

Recommended procedure

Apparatus: Atomic absorption spectrophotometer with iron, chromium, nickel, copper and lead hollow-cathode lamps. The determination can be carried out in air–acetylene flame under the conditions given in Table II.

Preparation of standards: 500 μg/mL stock solutions are prepared by dissolving iron(III) chloride ($FeCl_3$), chromium(III) chloride ($CrCl_3 \cdot 6\ H_2O$), nickel(II) chloride ($NiCl_2 \cdot 6\ H_2O$), copper(II) chloride ($CuCl_2 \cdot 2\ H_2O$), lead(II) nitrate [$Pb(NO_3)_2$] in ethanol and standardized by complexometric titration.

From these stock solutions five calibrating solutions are prepared according to Table V.

0.0, 0.25, 0.5, 0.75 and 1.0 mL of copper, nickel, and iron and 0.0, 0.5, 1.0, 1.5 and 2.0 mL of chromium, and lead alcoholic stock solution are transferred into 50 mL calibrated flasks, to each flask 30.0 mL toluene is added and diluted up to the calibration mark with glacial acetic acid.

Table V

Metal concentration of the calibrating solutions

	1	2	3	4	5
	μg/mL				
Cu	0.0	2.5	5.0	7.5	10.0
Ni	0.0	2.5	5.0	7.5	10.0
Cr	0.0	5.0	10.0	15.0	20.0
Fe	0.0	2.5	5.0	7.5	10.0
Pb	0.0	5.0	10.0	15.0	20.0

Table VI

Reproducibility of direct method on replicate samples measured at the same time

Metal	Conc. in oil, μg/mL	Relative std. dev., %
Cu	13.1	0.8
Cr	27.7	1.5
Ni	11.8	1.0
Pb	13.4	3.3
Fe	26.3	2.2

Preparation of samples: weigh into a 50 mL beaker maximum 5.000 grams of lubricating oil. Add 30.0 mL toluene and shake the solution. Transfer the solution into a 50 mL calibrated flask by glacial acetic acid and dilute up to the calibration mark with glacial acetic acid.

The relative standard deviations calculated for ten replicate measurements are given in Table VI.

REFERENCES

[1] Bartels, T. T., Slater, M. P.: Atomic Absorption Newsletter, **9**, 75 (1970)
[2] Jackson, D. R., Salama, C., Dunn, R.: Canadian Spectroscopy, **1970**, 17
[3] Taylor, J. H., Bartels, T. T., Crump, N. L.: The Behavior of Metal Particles Compared to Organo-Metallic Compounds in Flames Measured by Atomic Absorption Spectrophotometry. Paper presented at the 11th Rocky Mountain Spectroscopy Conference, Denver, Colorado, August, 1969
[4] Means, E. A., Ratcliff, D.: Atomic Absorption Newsletter, **4**, 1/4 (1965)
[5] Kriss, R. H., Bartels, T. T.: Atomic Absorption Newsletter, **9**, 78 (1970)
[6] Ibrahim, R. J., Sabbah, S.: Atomic Absorption Newsletter, **14**, 131 (1975)
[7] Sprague, S., Slavin, W.: Atomic Absorption Newsletter, **4**, 367 (1965)
[8] Slavin, S., Slavin, W.: Atomic Absorption Newsletter, **5**, 106 (1966)
[9] Burrows, J. A., Heerdt, J. C., Willis, J. B.: Anal. Chem. **37**, 579 (1965)
[10] Kahn, H. L., Peterson, G. E., Manning, D. E.: Atomic Absorption Newsletter, **9**, 79 (1970)
[11] Robinson, J. W.: Anal. Chim. Acta, **24**, 451 (1961)
[12] Wittmann, Zs.: Analyst, **104**, 156 (1979)
[13] Guttenberger, J., Harold, M.: Z. Anal. Chem., **262**, 102 (1972)
[14] MSZ 3256—57
[15] Golden, G. S.: Applied Spectroscopy, **25**, 668 (1971)

Zsuzsa Wittmann H-8021 Veszprém, József A. u. 34.

Acta Chimica Academiae Scientiarum Hungaricae, Tomus 109 (3), pp. 303—311 (1982)

POSITRON LIFE TIME AND ANNIHILATION DOPPLER BROADENING MEASUREMENTS ON TRANSITION METAL COMPLEXES

B. LÉVAY,[1] Cs. VÁRHELYI[2] and K. BURGER[3]*

([1] Department of Physical Chemistry and Radiology, Eötvös University of Budapest,
[2] Chemistry Department, Babes Bólyai University, Cluj Roumania,
[3] Institute of Inorganic and Analytical Chemistry, Eötvös University of Budapest)

Received February 18, 1981
Accepted for publication April 16, 1981

Positron life time and annihilation Doppler broadening measurements have been carried out on 44 solid coordination compounds. Several correlations have been found between the annihilation life time (τ_1) and line shape parameters (L) and the chemical structure of the compounds. Halide ligands were the most active towards positrons. This fact supports the assumption on the possible formation of $[e^+X^-]$ positron–halide bound state. The life time was decreasing and the annihilation energy spectra were broadening with the increasing negative character of the halides. The aromatic base ligands affected the positron-halide interaction according to their basicity and space requirement and thus indirectly the annihilation parameters, too. In the planar and tetrahedral complexes the electron density on the central metal ion affected directly the annihilation parameters, while in the octahedral mixed complexes only indirectly through the polarization of the halide ligands.

As a result of complex interactions, positrions (e^+) entering the medium and slowed down by it will finally annihilate into gamma photons with the electrons of the medium. The probability and other parameters of the positron annihilation strongly depend on the electron density at the site of the positron and generally on the physical and chemical properties of the medium [1]. This is why the methods based on the measurement of the characteristic parameters of the positron annihilation keep spreading in studies of the physical and chemical properties of the matter.

The main aim of our first systematic investigations on complex compounds by the positron annihilation method [2] was to find out what kind of information can be gained about the chemical structure in solid phase. The results of measurements in mixed complexes of *bis*(dimethylglyoximato)-Co(III) with unidentate ligands have proved convincingly that the changes observed in the annihilation parameters (*e.g.*, the lifetime of the positrons, the angular correlations of the annihilation gamma photons) correlate with the coordination chemical changes and the effect of structural irregularities in the solid state is negligible.

* To whom correspondence should be addressed.

It was shown [1], that the sample preparation has practically no effect on the positron annihilation parameters. Comparing the data for polycrystalline powders and samples pelleted under high pressure practically no difference was found. This result indicated the fact that, in the course of high pressure pressing, no new defects and positron traps were formed in the substances investigated, consequently they had probably been saturated with them. It is known [1b] that at high concentration of the defects the annihilation parameters are not sensitive for further changes and are mainly determined by the average size of the traps *i.e.*, by the size of missing molecules. The average size of the traps for series of samples with very similar structure can be estimated to be similar as well. Hence it was reasonable to assume that the changes in the annihilation parameters could be attributed to chemical changes in the surroundings of the positrons.

The aim of the present work was to extend the above investigations over a wider range of solid complex compounds with emphasis on the role of the central metal ion not investigated earlier. Results of annihilation measurements on 44 complex compounds are presented. The complexes investigated belong to the following three groups:

$$[Co(III)en_2AX]C_2,\ MeA_xX_y \text{ and } MeB_2$$

where Me = Fe^{2+}, Fe^{3+}, Co^{2+}, Co^{3+}, Ni^{2+}, Cu^{2+}, Zn^{2+} or Cd^{2+}; A = NH_3, pyridine, picolines, aniline, benzylamine or *m*-toluidine; X = Cl^-, Br^-, I^- or NCS^-; C = NO_3^- or ClO_4^- and B = SA, Cl-SA or NO_2-SA (en = ethylenediamine, SA = salicylaldoxime). Positron life time data are presented for all the three groups while Doppler broadening of the annihilation energy spectra was investigated only in the compounds of the first two groups.

Experimental

The complexes investigated were prepared by methods described in the literature [3], their composition was checked by elemental analysis. The $Ni(NH_3)_2X_2$ (X = Cl^-, Br^-, I^-) compounds were made from the corresponding $[Ni(NH_3)_6]X_2$ compounds by thermal decomposition. The chloride, bromide and iodide, were dried for 30 minutes at 150—160 °C, 130—140 °C and 125—235 °C respectively. The weight loss in all cases agreed within ±5% with the calculated one.

The positron life time spectra were recorded as published earlier [2]. The spectra were analysed for two life time components by the RESOLUTION [4] computer program, which automatically calculates also the parameters of the resolution curve of the measuring apparatus.

The Doppler broadened energy spectra of the annihilation gamma-photons were recorded by a Princeton Gamma Tech. Mod. LGC 9HT Type Ge(Li) detector. The energy resolution of the detector for the 514 keV line of a ^{85}Sr source was FWHW = 1.3 keV. The detector signals were fed through a preamplifier and an amplifier into a multichannel analyser with digital spectrum stabilizer. One channel of the MCA corresponded to 0.125 keV energy. A brass tube with a diameter and depth of 10 mm contained the sample in the form of polycrystalline powder. The positron source (about 10 μCi $^{22}NaCl$ sandwiched between 1 mg/cm^2 Kapton polyimid foils) was placed into the centre of the sample holder. About 2.7×10^6 pulses were

recorded for the total spectrum in the 512 channels of the MCA. About 2.3×10^6 pulses were recorded under the annihilation peak (in about 100 channels). One spectrum was recorded in about 1 hour.

Results and Discussion

I.1. The relative intensity ($I_2\%$) of the so-called long life time component ($\tau_2 \sim 1-2$ ns) of the positron life time spectra was less then 3% in all the cases but one. These results indicate that the probability of positronium (Ps) formation [1] in these complexes in negligible. In the $Znpy_2Cl_2$ (py = pyridine) complex, however, $I_2 = 39.0 \pm 1.5\%$ was measured with a life time of $\tau_2 = 887 \pm 12$ ps. It is very probable that the central Zn^{2+} ion is responsible for the high intensity of the positronium formation, since similarly high Ps intensities were found in two other Zn compounds measured for comparison. Zn-acetate: $I_2 = 49.1 \pm 1.5\%$, $\tau_2 = 947 \pm 8$ ps and Zn-dibenzyldithiocarbamate: $I_2 = 32.0 \pm 1.0\%$, $\tau_2 = 1200 \pm 10$ ps. Presently we are not able to interpret this extraordinary behaviour of the Zn ion.

The short-lived component of the life time spectra (τ_1) has varied in the 300—380 ps interval similarly to our earlier measurements [2].

2. The Doppler broadening of the energy spectra of the annihilation gamma photons can be characterized by different line shape parameters [5]. We have used the so-called L parameter:

$$L = \frac{n_1}{n_2 + n_3}$$

where

$$n_1 = \sum_{i=299}^{308} n_i; \quad n_2 = \sum_{i=285}^{295} n_i; \quad n_3 = \sum_{i=312}^{322} n_i$$

and n_i is the content of the ith channel of the spectrum. In our case the maximum of the annihilation line was in the 303—304 channels.

The L parameter for the non-broadened spectrum of ^{85}Sr (taking into account the shift of the peak) was $L = 13.32 \pm 0.04$, while for the samples investigated it varied in the $(1.0-1.5) \pm 0.002$ range. The accuracy of the L parameter is characterized by the statistical error. The L parameter was well reproducible within the statistical error if the source strength and measuring geometry were constant. Changes in these parameters, however, resulted in greater changes than the statistical error. This was why all the samples were measured by the same source and in a well-defined geometry.

Both the Doppler broadening of the annihilation energy spectra and the angular distribution of the annihilation gamma photons are determined by the momentum distribution of the annihilating positron-electron pairs. The momentum of the annihilating pair comes practically from the momentum

of the electron bound in a chemical compound. Therefore investigating either the angular correlation or the Doppler broadening essentially the same information is gained. The stronger the bond of the positron to the atoms of the medium at the moment of annihilation, the wider the annihilation energy spectrum (the smaller the L parameter), and the wider the angular correlation spectrum. In the case of positronium formation the annihilation of the *o*- and *p*-Ps components result in a wide and a very narrow components in the spectra, respectively [1].

The results (the values of τ_1 and L) are presented in Tables I—III.

II.1. In Table I the results obtained for the Co(III)-ethylenediamine mixed complexes are shown in the order of increasing L parameters. The sequence of compounds clearly shows that they fall into groups according to their chemical structure. The Doppler broadening is the greatest (*i.e.*, the L parameter [2] is the smallest) in compounds not containing aromatic base ligand in their inner coordination sphere. The positron lifetime is also the shortest in these compounds. Complexes with one aromatic and one Cl^- ligand belong to the next group, while the third group consists of similar compounds but with Br^- instead of Cl^-.

As seen the Doppler broadening is first of all affected by the type and number of the halide ligands and the role of the aromatic base ligands is less pronounced. Similarly to what was found earlier in the *bis*(dimethylglyoximato)Co(III) mixed complexes [2], greater broadening is observed in the presence of the more negative Cl^- ligands. On the other hand, in complexes investigated earlier, shorter life times corresponded to the broader angular

Table I

Positron annihilation parameters (τ_1, L) for Co(III)-ethylenediamine mixed complexes

No.	Compound	Life time τ_1, ps	L parameter (± 0.002)
1.	$[Co(en)_2Cl_2]ClO_4$	310±3	0.982
2.	$[Co(en)_2Br_2]NO_3$	335±3	1.095
3.	$[Co(en)_2Cl$ aniline$](NO_3)_2$	362±2	1.097
4.	$[Co(en)_2Cl$ *β*-pic$](ClO_4)_2$	364±3	1.106
5.	$[Co(en)_2Cl$ benz$](No_3)_2$	352±2	1.117
6.	$[Co(en)_2Br$ *m*-tol$](NO_3)_2$	351±3	1.141
7.	$[Co(en)_2Br$ *β*-pic$](NO_3)_2$	349±3	1.152
8.	$[Co(en)_2Br$ benz$](NO_3)_2$	343±3	1.158
9.	$[Co(en)_2Br$ *γ*-pic$](NO_3)_2$	347±3	1.178

en = ethylenediamine; -pic = -picoline; benz = benzylamine; -tol = -toluidine

correlation curves. In this seris of compounds this correlation is not universally valid. In complexes with one Br^- ligand the positron life time is constant within the experimental accuracy irrespective of the value of the L parameter and, whereas unexpected, it is somewhat shorter than that for the Cl^- complexes.

2. Within the groups of Cl^-- and Br^--containing complexes the change of the L parameter is obviously related to the character of the aromatic base ligands. It seems that in both groups the value of the L parameter increases parallel with the basicity of the ligands. (Compounds 8 and 9 are the only exceptions.)

The decreasing localization of the positrons manifests itself in the narrowing of the energy spectra. Therefore this effect may be reasonably well explained as follows. The ligands with greater protonation constant have probably greater affinity towards the positrons, consequently they decrease the positron–halide interaction. The decreasing positron–halide interaction, as it has been seen, results in the narrowing of the energy spectra.

The same effect, however, can be interpreted also in another way based on the change of complex stability. In the complexes with stronger donor bases, the increasing strength of the metal-basic-N bond results in the decrease of the strength of metal–halide bond and, consequently, in decreasing polarization of the halide ligand. The decreased polarization may result in decreasing positron–halide interaction. This assumption is supported by the data obtained for complexes 31—33. In these analogous systems the differences in the metal–halide bond strength caused by the different central ions may explain the differences in positron lifetimes.

III. With the series of complexes shown in Table II one can study the effect of halide ligands, their inner or outer sphere position and the role of the central metal ion.

1. In all series of complexes with similar structure a close correlation exists between the annihilation parameters and the negative character of the halide ligands, as it was already observed in the bis(dimethylglyoximato)-Co(III) complexes [2] and partly also in the Co(III)-ethylenediamine mixed complexes (Table I). The positron–halide interaction increases with increasing negative character of the ligands which results in decreasing positron life time and L parameter in the order of I^-, Br^- and Cl^-. (See *e.g.*, the 10, 11, 12; 13, 14, 15; 16, 17, 18; 25, 26 and 29, 30 compounds.) As it was pointed out in our earlier paper such kind of changes in the annihilation parameters correspond to the theoretical calculations on the $[e^+X^-]$ positron–halide bound state.

2. In addition to the character of the halide ligands also their position in the complex (inner or outer sphere) can play an important role. For a clear-cut investigation of this effect we have only a single pair of cobalt complexes

Table II

Positron annihilation parameter (τ_1, L) for MeA_xX_y complexes

No.	Compound	Life time τ_1, ps	L-parameter (±0.002)
10.	$[Ni(NH_3)_6]Cl_2$	329±3	1.237
11.	$[Ni(NH_3)_6]Br_2$	331±3	1.330
12.	$[Ni(NH_3)_6]I_2$	363±3	1.447
13.	$[Ni(NH_3)_2Cl_2]$	335±1	1.167
14.	$[Ni(NH_3)_2Br_2]$	350±2	1.233
15.	$[Ni(NH_3)_2I_2]$	358±1	1.327
16.	$[Ni(py)_4Cl_2]$	332±3	1.178
17.	$[Ni(py)_4Br_2]$	337±3	1.221
18.	$[Ni(py)_6]I_2$	349±3	1.282
19.	$[Ni(\beta\text{-pic})_4Br_2]$	326±3	1.211
20.	$[Ni(\alpha\text{-pic})_2(NCS)_2]$	349±3	1.186
21.	$[Ni(NH_3)_4(NCS)_2]$	353±2	1.185
22.	$[Ni(py)_4(NCS)_2]$	363±2	1.187
23.	$[Ni(\gamma\text{-pic})_4(NCS)_2]$	376±3	1.344
24.	$[Ni(\beta\text{-pic})_4(NCS)_2]$	381±3	1.377
25.	$[Co(NH_3)_6]Cl_3$	305±3	1.133
26.	$[Co(NH_3)_6]Br_3$	308±3	1.202
27.	$[Co(NH_3)_5Cl]Cl_2$	339±3	1.139
28.	$[Co(py)_4Cl_2]Cl$	367±2	1.176
29.	$[Co(py)_4Cl_2]$	320±2	1.140
30.	$[Co(py)_4Br_2]$	325±3	1.171
31.	$Cu(py)_2Cl_2$	316±2	1.140
32.	$Zn(py)_2Cl_2$	334±8	1.328
33.	$Cd(py)_2Cl_2$	335±3	1.178
34.	$Cd(py)_2Br_2$	344±3	1.207

py = pyridine

(25, 27). These data suggest that the positron life time is longer and the energy spectrum is narrower, *i.e.*, the positron–halide interaction is stronger, if the Cl^- ligand sits in the inner coordination sphere. A similar trend of the life times can be observed in the corresponding $[Ni(NH_3)_6]X_2$ and $[Ni(NH_3)_2X_2]$ outer and inner sphere complexes, respectively. On the other hand, in this

case the L parameter is not greater but smaller in the complexes with inner sphere halide ligands. The evaluation of the effect in these systems, however, is distributed by the fact, that the structure and symmetry of the coordination sphere change appreciably when the halide enters into the inner sphere.

In the dimethylgyloxime mixed complexes an opposite trend of the life times was observed [2] when the halide ligand entered into the inner coordination sphere. Therefore, to clarify this effect further investigations have to be carried out on inner and outer sphere complexes of analogous structure.

3. In the series of Ni-thiocyanate mixed complexes one can observe again the parallel change of positron life time and L parameter. On the other hand, the effect of aromatic base ligands does not show the correlation with their basicity observed in the case of Co(III)-ethylenediamine mixed complexes. In the complex containing the very small NH_3 ligand (21) or in the complex with only two α-picoline molecules instead of four (20), in spite of the greater basicity as compared to the pyridine, the life times are shorter and the energy spectra are wider, *i.e.*, the interaction between the positron and the thiocyanate ligand is stronger than expected. In the ammine complex (21) probably the smaller space requirement of these ligands compensates the effect of the stronger basicity, as the thiocyanate ligand becomes less screened and consequently its interaction with the positrons increases. Because of the smaller coordination number in the α-picoline complex (20) the thiocyanate ligand is bound stronger to the central Ni ion and becomes more polarized, which may explain its stronger interaction with the positrons.

4. Comparing the corresponding pairs of complexes with analogous structure in Table II one can study the effect of the central metal ion on the annihilation parameters. In all pairs of Ni- and Co-complexes (10, 25; 11, 26; 16, 29, and 17, 30) shorter positron life time and smaller L parameter were observed in the cobalt ones irrespective of whether the central atom was a high spin Co(II) or a low spin Co(III). In the series of $Me(py)_2Cl_2$ complexes (31—34) the life time and L parameter increase in the sequence of Cu—Zn—Cd. (The extremely high L value of the Zn complex can be well explained by the high intensity of positronium formation. The *para*-Ps component may cause the extreme narrowness of the spectrum.)

As it is to be seen, the life times and L parameters decrease with decreasing electron density on the central metal ion, consequently in these complexes the central metal ion may be responsible for the changes of the annihilation parameters only indirectly. The positron interacts with electrons of the ligands and feels the effect of changes on the central metal ion only indirectly through the changes caused on the ligands. Similar conclusion was drawn when the annihilation and ESCA parameters of the *bis*(dimethylglyoximato)Co(III) complexes were compared [2]. In the $Me(py)_2Cl_2$ complexes the positron life time increases with decreasing stability, *i.e.*, with decreasing polarization

Table III

Positron life time data for salicyl aldoxime complexes

No.	Compound	Life time τ_1, ps
35.	$Ni(SA)_2$	318±3
36.	$Cu(SA)_2$	324±2
37.	$Co(SA)_2$	357±3
38.	$Fe(SA)_2$	359±3
39.	$Fe(OH)(SA)_2$	370±2
40.	$Ni(Cl—SA)_2$	324±2
41.	$Cu(Cl—SA)_2$	324±2
42.	$Ni(NO_2—SA)_2$	332±3
43.	$Cu(NO_2—SA)_2$	347±2
44.	$Fe(NO_2—SA)_2$	360±2

SA = salicyl aldoxime

of the Cl^- ligand. It seems that the decreasing polarization of the Cl^- ligand decreases also its interaction with the positron, as it was seen above and in our earlier investigations [2].

IV. In Table III the positron life times measured in the planar and tetrahedral salicylaldoxime complexes are shown. Because of the planar and tetrahedral structures of the coordination sphere the central metal ion may more easily interact with the positron than in the octahedral complexes. Hence it is expected that the electron density on it may affect the positron life time directly.

The symmetry of the coordination sphere of the Ni and Cu complexes is the closest to the regular square planar configuration, while that of the Fe(III) complex is closest to the regular tetrahedron [6]. Because of steric reasons the structural change from planar to tetrahedral may hinder the metal–positron interaction and increase the positron life time. In other respect, on the basis of magnetic susceptibility measurements [7] the number of unpaired electrons on the central metal ion of these complexes increases in the following order: Ni (0), Cu (1), Co (3), Fe(II) (4) and Fe(III) (5). The increase of the number of unpaired electrons in these systems goes together with the decrease of the number of the 3d4s electrons. This fact may also be the reason for the increasing positron life time in the same order. This latter conclusion is supported also by the effect of the substituents of the salicylaldoxime ligands.

The electron withdrawing substituents decrease the electron density also on the central metal ion [8] deforming the symmetry of the coordination sphere only slightly, consequently increasing the positron life time.

Conclusions

Positron annihilation measurements carried out on 44 solid compounds have confirmed our earlier conclusion, that the positron annihilation parameters reflect well the changes in the chemical structures of the compounds. Thus the method can be used for the study of the chemical structure also in solid phase.

Because of the complicated composition of the complexes, the effect of their constituents (central metal ion, inner and outer sphere ligands) on the annihilaton parameters can be interpreted only by studying systematically chosen series. Several questions still remained to be answered and we are going to continue our systematic investigations.

*

One of the authors (B. L.) acknowledges the hospitality of the Chemistry Department of the Risö National Laboratory where he had the opportunity to carry out the positron annihilation measurements.

REFERENCES

[1a] LÉVAY, B.: Atomic Energy Rev., **17**, 413 (1979)
[1b] WEST, R. N.: Adv. Phys., **22**, 263 (1973)
[2] BURGER, K., LÉVAY, B., VÉRTES, A., VÁRHELYI, Cs.: J. Phys. Chem., **81**, 1424 (1977)
[3] Inorganic Synthesis. Vol. I, p. 186; Vol. II, pp. 217, 219; Vol. III, pp. 178, 194; Vol. V, p. 185; Vol. VI, pp. 182, 192—198; Vol. VIII, p. 198; Vol. IX, pp. 160, 163. McGraw Hill, New York
[4] KIRKEGAARD, P., ELDRUP, M.: RESOLUTION computer program, unpublished
[5] CAMPBELL, J. L.: Appl. Phys., **13**, 356 (1977)
[6] BURGER, K., RUFF, F., RUFF, I., EGYED, I.: Acta Chim. Acad. Sci. Hung., **46**, 1 (1965)
[7] BURGER, K.: Coordination Chemistry: Experimental Methods. p. 221 Butterworths, London 1973
[8] BURGER, K., BUVÁRI, Á.: Inorg. Chim. Acta, **11**, 25 (1974)

Béla LÉVAY H-1088 Budapest, Puskin u. 7.
Csaba VÁRHELYI Roumania, Cluj-Napoca, Arany J. u. 1.
Kálmán BURGER H-1088 Budapest, Múzeum krt. 4/B.

Acta Chimica Academiae Scientiarum Hungaricae, Tomus 109 (3), pp. 313—325 (1982)

DIRECT DETERMINATION OF TRACE ELEMENTS IN POLYACRYLAMIDE SOLUTIONS BY FLAME ATOMIC ABSORPTION SPECTROPHOTOMETRY, I

THE MATRIX EFFECT OF POLYMERS

I. LAKATOS

(Petroleum Engineering Research Laboratory, Hungarian Academy of Sciences, Miskolc-Egyetemváros)

Received October 24, 1980
Accepted for publication April 20, 1981

The study deals with the determination of the trace elements of polyacrylamide solutions by direct flame atomic absorption spectrometry, and within this, with the disadvantageous matrix effect of polymers. Rank correlation was used for the evaluation of experimental data. It was stated that the absorption signal substantially decreases in the presence of polymers, depending on the type and concentration of the polymer. The reason of the matrix effect of polymers is to be sought in the nebulization process, primarily in the decrease of take-up rate. Sodium chloride reduces the matrix effect of polymers through its influence on solution viscosity and consequently on take-up rate. The author attributes the diminishing of the take-up rate to an increase in viscosity of the polymer solutions and, in general, to changes in solution structure. Ultimately, it is advantageous in the direct flame atomic absorption analysis of polymer solutions if the test solution contains only one polymer of known type, and sodium chloride in a concentration of 1.5—2.5 g dm^{-3}. According to experimental data, the take-up rate can be used for the correction of the analytical curves.

Introduction

The sweep efficiency of polymer solutions used in enhanced oil recovery is controlled in the laboratory test and in the field operation by the determination of tracer compounds and often of trace elements. In view of the fact that this task means series of analyses for one or two elements in a great number of liquid samples from the laboratory or the reservoir, the application of atomic absorption method seems obvious. So far only a few publications [1—6] deal with the determination of the metal content of polymers or polymer solutions by atomic absorption methods, and of these only HENN [4] reported data on the detection of trace elements in polyacrylamides. A common feature of these publications is however, that mostly flameless methods, particularly graphite furnace atomization was used, or the solution technique was preceded by ashing, and possibly by acid extraction. For lack of an electrothermic atomization technique, a direct flame atomic absorption process has been developed by us for the trace analysis of polymer solutions. The first part of publication summarizes the results of investigations connected with the matrix effect. Within the frame of this work, the effect of the polymer concentration

and structure, the viscosity of the solution and the structural characteristics of the solution (gel concentration, size and density of the random coils) on the magnitude of the signal and on the rate of nebulization have been studied. A non-parametric rank correlation matrix is used for the determination of the closeness of relationship between the single characteristics and for the selection of the factor or factors determining the matrix effect, most suitable for the correction of the analytical curves.

Experimental

Water soluble polymers of various structure (average relative molecular mass, degree of hydrolysis) were used for the laboratory tests. However, the intensive study of the matrix effect involved only polyacrylamides, because at present other polymers used in the petroleum industry amount only to 10—15%. The average molecular mass of the polymers varied between $(0.5-14)\times10^6$, their degree of hydrolysis between 0 and 40%. Generally, manganese was used as model element, though studies were extended also to other elements of practical importance (*e.g.* Al^{3+}, Ca^{2+}, Mg^{2+}, *etc.*). In addition, aqueous solutions contained also sodium chloride in various concentrations for the simulation of the ionic strength of brines.

A Pye-Unicam Model SP 190 single beam atomic absorption spectrophotometer was used for the laboratory tests together with a manganese hollow cathode lamp. Other experimental conditions were as follows:

Wave length	279.5 nm
Slit width	0.15 mm
Burner head slot	10 cm (acetylene–air flame)
Air flow rate	5 dm^3/min
Acetylene flow rate	1.8 dm^3/min
Flame height of detection	8 mm.

Absorbance values were recorded by an integration time of 4 s with a Philips digital printer. Sets of 20 data were processed by elementary tests (outliers or r_m test, normality test, trend analysis, F test), the probability level of which was 95%.

In view of the fact that non-normal distribution was characteristic for some sets of data without trend, SPEARMAN's and KENDALL's rank correlation and KENDALL's concordance analysis were used for statistical evaluation [7]. Since the latter two did not yield new information, the results of SPEARMAN's rank correlation will only be given in this paper. Both the elementary tests and rank correlation calculations were run on a CDC 3300 computer.

Results and Discussion

In Fig. 1 the effect of water soluble polymers of various types on the absorbance of manganese is plotted as a function of polymer concentration. The figure shows the matrix effect of a hydroxyethylcellulose (Hercules Co., USA), a polysaccharide (CX-12, CECA A.S., France) and of three polyacrylamides, of which two are American (Separan NP-10 and AP-30, Dow Chemical) and one a GFR (AN-34, Industria Chemical) products.

It can be seen from the figure that water soluble polymers of different types decrease to a rather different extent the absorbance measured at the manganese line. This has from the analytical aspect the consequence that

errors of different magnitude can be committed, if the type and concentration of the polymer changes in the sample solution. This circumstance made necessary an intensive investigation of the matrix effect, and the selection of a factor for the correction of this unfavourable effect. It would be favourable

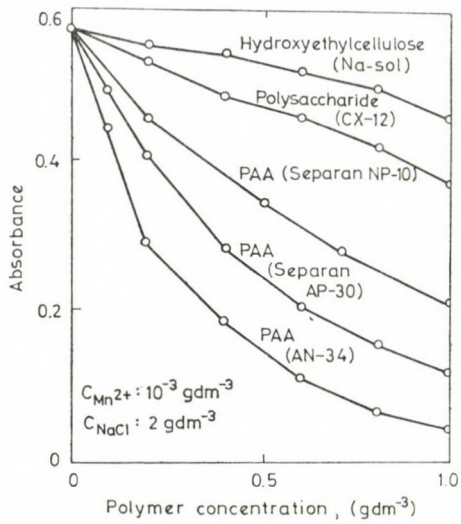

Fig. 1. Effect of water soluble polymers of different type on the absorbance of the manganese line in the presence of 2 g dm^{-3} sodium chloride

if the correction factor were a general characteristic of the solution or the solution structure, and not an individual property of the single polymer types. Therefore, the investigation of the matrix effects was extended to the qualitative analysis of the following functional relationship:

$$A_{\dot{x}} = f(c_{\text{pol}}, \overline{M}_{\text{r}}, H_{\text{degr}}, v, \mu, c_{\text{gel}}, \varrho_{\text{eq}}, d_{\text{eq}}, c_{\text{NaCl}}) \quad (1)$$

where A_x is the absorbance, c_{pol} the polymer concentration, M_r the average relative molecular mass of the polymer, H_{degr} the degree of hydrolysis of the polymer, v the rate of nebulization, μ the dynamic viscosity of the polymer solution, c_{gel} the gel concentration of the polymer solution, ϱ_{eq} the density of the random coil, d_{eq} the equivalent diameter of the random coil and c_{NaCl} the concentration of sodium chloride present.

Considering that these factors are partly interdependent variables, the matrix effect was analyzed by the calculation of the total correlation matrix. Of these the study of the dependence of nebulization or take-up rate on the properties of the test solution is emphasized. By analogy to the above relationship, this is characterized by the following correlation:

$$v = f(c_{\text{pol}}, \mu, c_{\text{gel}}\ \varrho_{\text{eq}}, d_{\text{eq}}, c_{\text{NaCl}}) \quad (2)$$

It simplified laboratory work that the extensive study of phenomena was restricted to polyacrylamides. Two acrylamide — acrylic acid copolymers of the following characteristics were selected as model substances:

	$\overline{M}_r$	Degree of hydrolysis (%)
Separan NP-10	10^6	5—7
Separan AP-30	3.5×10^6	30

In Fig. 2, besides the change in absorbance of manganese, changes measurable at the magnesium and calcium lines are plotted as a function of the two polymer concentrations. It should be mentioned as a general experience that the trend of the signal reducing effect of the polymers is similar for all elements, however, as concerns the extent of change, lesser or greater differences can be found in the individual cases. To limit independent variables, in most of the cases detailed studies were carried out only on manganese solutions of 1 mg dm^{-3} concentration.

As the first step of the investigation of the matrix effect, a relationship was sought between the absorbance and the molecular mass and the degree of hydrolysis, characteristic of the polymer structure. In connection with polyacrylamide AN-34 shown in Fig. 2, we add as complementary information that its average relative molecular mass and degree of hydrolysis is about $(12—14)\times10^6$ and 40%, respectively. Comparing the effect of the three acrylamides and their chemical structure, the conclusion can be drawn that the larger the average molecular mass and the degree of hydrolysis of the polymer, the greater is the matrix effect. Figure 3 presents a basis for the evaluation of the role of the two factors. It shows the matrix effect of polymers of nearly identical molecular mass $(2.0—2.2)\times10^6$ but hydrolyzed to 0—10—20—30% in solutions without NaCl addition and with 2 g dm^{-3} NaCl.

The course of the curves belonging to various polymer concentrations demonstrates that in the deterioration of absorbance basically the increase of the degree of hydrolysis plays a decisive role, while the effect of the molecular mass is relatively negligible. Presumably, this is connected with the fact that in the shaping of the rheological and structural properties of polymer solutions, too, the extent of hydrolysis is decisive.

The salt content of connate waters (brines) and the well-known effect of inorganic salts on the properties of polymer solutions justified a study of the effect of salt content. Figure 4 shows that the matrix effect of a 1 g dm^{-3} polymer solution decreases somewhat up to a NaCl concentration of 1 g dm^{-3}, to attain then essentially an equilibrium (above this value absorbance changes

but slightly). Eventually, the presence of sodium chloride reduces the signal reducing effect of the polymer matrix, that is to say, it increases the sensitivity of atomic absorption to the metallic components of polymer solutions.

When elucidating the cause of the matrix effect, comparison of the efficiency of the nebulization process with the change in absorbance is a logical step. Thus, Fig. 4 shows besides the data mentioned already the dependence of

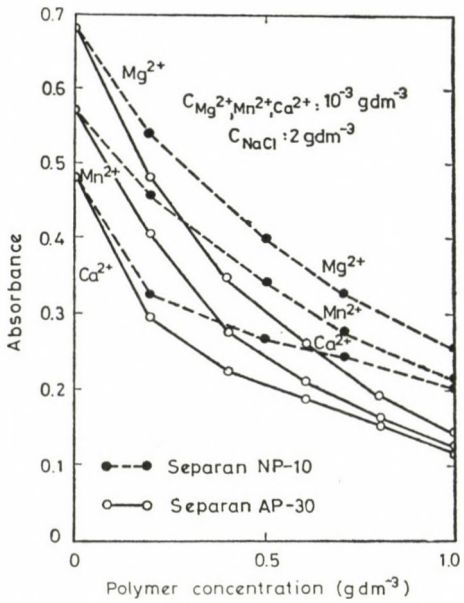

Fig. 2. Effect of the concentration of two polymers with different structure on the absorbance of manganese, magnesium and calcium lines

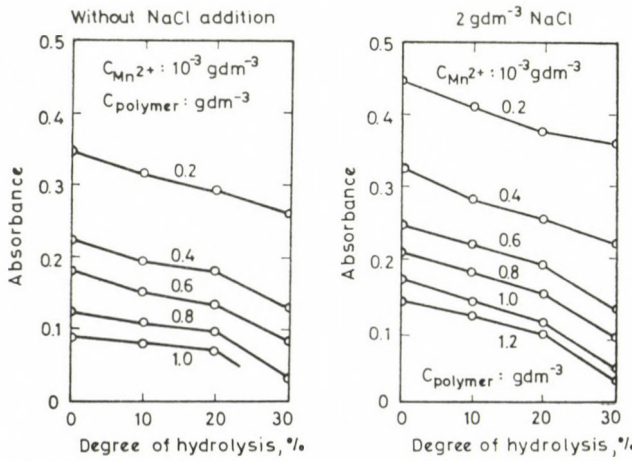

Fig. 3. Effect of the degree of hydrolysis of polymers on the absorbance of manganese line in solutions without NaCl addition and in the presence of 2 g dm^{-3} sodium chloride

the take-up rate on sodium chloride concentration. It can be seen that the character of both curves follows the change in absorbance, *i.e.* the matrix effect of polymers can be partly traces back to a decrease in nebulization rate. The similarity is still more conspicuous when Fig. 5, showing the relationship take-up rate *vs.* polymer concentration, is compared with the two curves of polymers NP-10 and AP-30 in Fig. 1.

In accordance with Fig. 5 the matrix effect of polymers is clearly illustrated by Fig. 6, in which the change in absorbance is plotted as a function of take-up rate for solutions of various sodium chloride concentration. The characteristic curves of the figure are also numerically in good agreement with respective data in the literature [8].

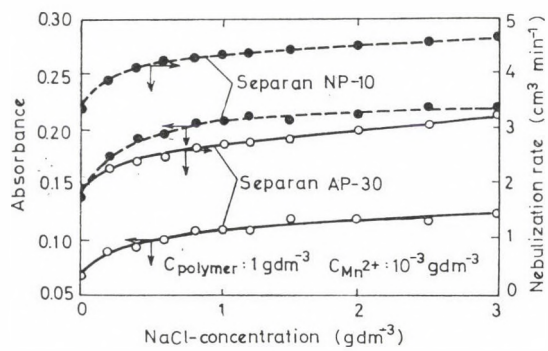

Fig. 4. Effect of sodium chloride concentration on the absorbance of manganese line and on the take-up rate of the polymer solution

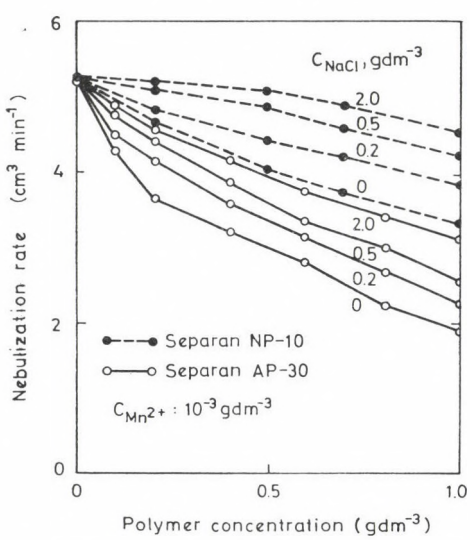

Fig. 5. Take-up rate as a function of the polymer and sodium chloride concentrations

The effect of the changes in polymer and sodium chloride concentrations can be interpreted, if the extreme viscosity increasing action of chain like polymers having large molecular mass is taken into consideration. As it is shown in Fig. 7, these substances increase the viscosity of the test solution several times at relatively low concentrations. The increase in viscosity is influenced to a small extent by the molecular mass, and to a large extent by the degree

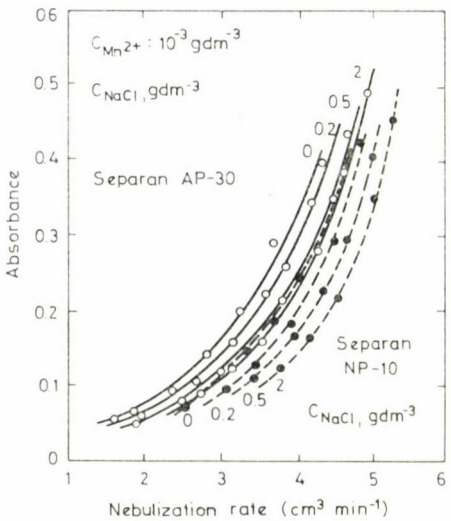

Fig. 6. Absorbance of manganese line as a function of take-up rate

of hydrolysis. The difference between polymers with respect to increasing the viscosity arises from this fact. On the other hand, the sensitivity of the polymers to salts also increases with increasing degree of hydrolysis and consequently, the changes in viscosity, nebulization rate and absorbance produced by NaCl are greater in the case of the polymer of type AP-30, than in that of polymer NP-10, as it is shown partly by Fig. 8.

However, the decreasing take-up rate is only one consequence of the presence of polymers. It has been assumed that besides the take-up rate the efficiency of nebulization and the dimension and dispersity of the aerosol are also substantially changing. First of all the nebulization efficiency was determined for polymer-free solutions and solutions of high polymer concentration, forming limiting cases from the aspect of viscosity. Taking into consideration also standard deviations, it was found that an important increase in the viscosity of the solution essentially does not affect the nebulization efficiency. Within the 1—20 mPas viscosity interval investigated, the nebulization efficiency of the solutions varied between 10 and 12%, which is also close to the

values given for pneumatic nebulizers [8]. Moreover, it should be mentioned that the surface tension of polymer solutions does not differ from that of polymer-free solutions, so that also in principle no change in nebulization efficiency is to be expected. Mention must be made, however, that the nebulization efficiency was not corrected with the volume of the solvent (water) evaporated during the nebulization in the spray chamber. On the other hand, results of qualitative investigations permit to conclude that in aerosols obtained by the nebulization of polymer solutions the droplet dimensions are larger

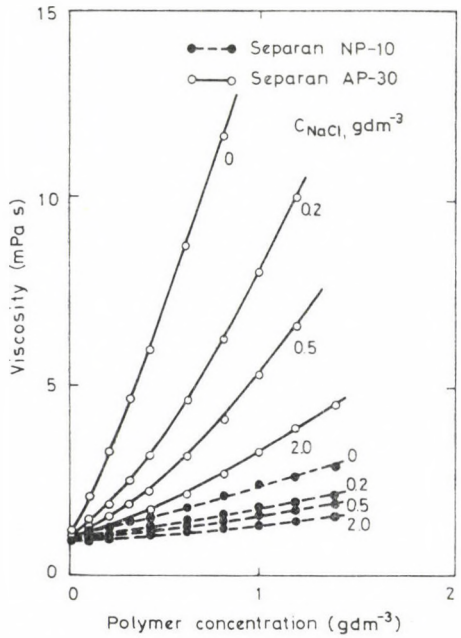

Fig. 7. Dynamic viscosity of the polymer solution as a function of polymer and sodium chloride concentrations

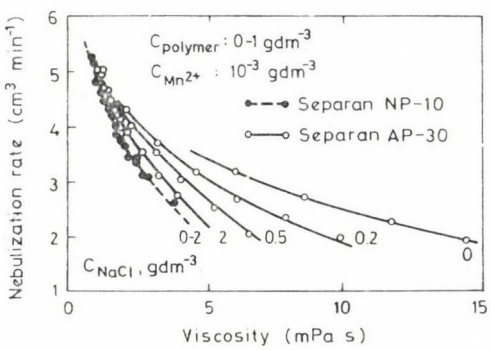

Fig. 8. Take-up rate as a function of dynamic viscosity of polymer solution

than *e.g.* in the nebulization of distilled water. This conclusion was reached on the basis of the results of the following very simple and by far not exact experiment. The apparatus was zeroed in flameless state, and polymer solution and water were nebulized into the burner head at identical rates. (In the latter case this was attained by an adequate reduction of air flow rate.) Absorbance produced by the aerosol formed from the polymer solution was by about 30—40% lower than that produced by the aerosol formed from polymer-free water. In view of the fact that the decrease in intensity caused by light scattering is proportional to the number of particles in the light path, the decrease in absorbance is probably indicative of an increase in droplet volume. (It should be emphasized that the take-up rate and the nebulization efficiency were identical during the experiment, and the transmittance of the dissolved substance was 100% at the given wave length.) It was assumed on the basis of theoretical considerations that the dispersity of the aerosol obtained by pneumatic nebulization changed also as a function of polymer concentration [9—12]. According to DAVIES [12], in the case of colloid dispersions the dimension of the aerosol particles is determined by the dimension (the equivalent diameter, d_{eq}) of the random molecular coils. Thus, in principle the efficiency of nebulization should increase up to a gel concentration of 100%. Above this, the degree of dispersity of the aerosol increases anyhow, because such solution is already solvent-deficient, and due to the partial overlap of random coils can be actually considered as a gel. Thus, it was expected on the basis of the change in dispersity of the aerosol that up to a gel concentration of 100% the decrease in absorbance will be less steep than after this concentration, because of the decrease in take-up rate. However, the four curves in Fig. 9 do not exhibit a break in the vicinity of 100% gel concentration, from which the conclusion can be drawn that the possible effect of the differences in the degree of dispersity can be neglected beside the decrease in take-up rate.

With the aim to elucidate indirectly the role of the degree of dispersity of the aerosol, the change in absorbance was also compared with other struc-

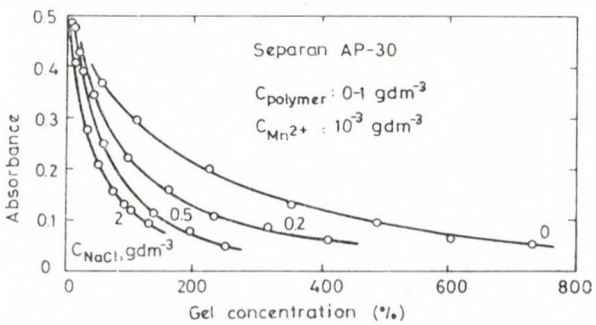

Fig. 9. Absorbance of manganese line as a function of gel concentration of polymer solution

tural properties of the solution, thus *e.g.* with the density and the equivalent diameter of the random molecular coils. These investigations indicate that the particle size of the aerosol decreases with increasing NaCl concentration, while the density of the random coil increases, which is indicative of the increase in free solvent (bulk phase) in the solutions. Both findings can be used for the interpretation of the dependence (increase) of absorbance on salt concentration, but nevertheless, the effect of sodium chloride on the viscosity of the polymer solution and the increase in take-up rate ensuing from it is considered as the determining factor.

Contrary to the usual case, in the atomic absorption spectrometry of polymer solutions, macromolecules and even molecular coils consisting of chain substances and absorbed water participate in the atomization processes besides the low molecular inorganic substances. The circumstance that polymers containing acrylic acid segments (hydrolyzed polyacrylamides) form poorly dissociating salts with multivalent cations further complicates the evaporation and thermal decomposition processes. The effect of these processes cannot be completely excluded. However, experimental findings unequivocally prove that basically the effect of the polymers on nebulization process is responsible for the deterioration of absorption measured at the analytical lines.

Since the effect of polymers in nebulization processes and atomization phenomena could not be sharply distinguished, the two effects of identical direction have been treated together by rank correlation analysis. The rank correlation matrix calculated made also possible the mutual correlation of every factor of the qualitative relationships (1) and (2). Thus, the matrix effect could be reduced through intermediate steps to characteristics of solvent structure (*e.g.* absorbance → take-up rate → viscosity → polymer concentration → gel concentration, *etc.*). Of the results of statistical calculations the most important are given in Tables I and II, in which the SPEARMAN's rank correlation coefficients of absorbance and of take-up rate are summarized. The first column of the tables is pertinent to solutions without NaCl additive, the second column to solutions containing 2 g dm^{-3} sodium chloride. In the third column c_{NaCl} and in the fourth the polymer type was also treated as independent variable. Thereby we intended to clarify the question of sensibility of the matrix effect of polymer solutions to the quantity of foreign ions present in the solution and to the type of the polymer.

The SPEARMAN's correlation coefficients fall into the $[-1, +1]$ interval. The sign indicates only the direction of the two rank vectors, *i.e.* whether the two factors compared change in an identical or opposite direction. It can be stated after these preliminaries that the absorbance is well correlated with take-up rate, polymer and gel concentrations and the dynamic viscosity of the solution, if both the type of the polymer and the salt content are constant in the sample solution. However, the matrix effect cannot be brought even

Table I

SPEARMAN's *rank correlation coefficients of absorbance at various sodium chloride concentrations*
Polyacrylamide: Separan AP-30

	$c_{NaCl} = 0$ g/L	$c_{NaCl} = 2$ g/L	$c_{NaCl} = 0$—2 g/L	$n_{PAA} = 2$*
$c_{polymer}$	—0.9726	—1.000	—0.9430	—0.762
v	0.9726	1.000	0.9759	0.8035
μ	—0.9726	—1.000	—0.8719	—0.7114
c_{gel}	—0.9726	—1.000	—0.8719	—0.7227
ϱ_{eq}	0.8433	0.1515	0.5020	0.1645
d_{eq}	—0.9087	—0.1581	—0.5053	—0.4413
c_{NaCl}	—	—	0.2953	0.1252

* Polymers Separan AP-30 and Separan NP-10 together

Table II

SPEARMAN's *rank correlation coefficients of the take-up rate at various sodium chloride concentrations*
Polyacrylamide: Separan AP-30

	$c_{NaCl} = 0$ g/L	$c_{NaCl} = 2$ g/L	$c_{NaCl} = 0$—2 g/L	$n_{PAA} = 2$*
$c_{polymer}$	—1.000	—1.000	—0.8762	—0.4788
μ	—1.000	—1.000	—0.9452	—0.8815
c_{gel}	—1.000	—1.000	—0.9452	—0.8842
ϱ_{eq}	0.8941	0.1515	0.6523	0.3591
d_{eq}	—0.9452	—0.1581	—0.6542	—0.6269
c_{NaCl}	—	—	0.4605	0.2472

* Polymers Separan AP-30 and Separan NP-10 together

in this case in direct correlation (at best under analysis of NaCl-free solutions) with the characteristics of solutions structure (size and density of the random molecular coil), which presumably exert an important effect on nebulization processes. The correlation coefficients are poorer somewhat, if the test solutions contain also foreign electrolytes at different ratios. The poorest correlation is obtained when the type of the polymer is also an independent variable. Correlation coefficients decrease from a value of about $+1$ to $\pm$ 0.7—0.8, though only two chemically very similar polymers were included in the studies.

The correction of the matrix effect will be suitably carried out with that or those factors, which are in closest correlation with absorbance. It can be seen from Table I that the correlation coefficient is highest between absorbance

Table III

Confidence levels of the rank correlation of take-up rate at various sodium chloride concentration
Polyacrylamide: Separan AP-30

	$c_{NaCl} = 0$ g/L	$c_{NaCl} = 2$ g/L	$c_{NaCl} = 0$—2 g/L	$n_{PAA} = 2$*
N	12	11	27	51
f	11	10	26	50
$c_{polymer}$	99.9	99.9	99.9	99.9
μ	99.9	99.9	99.9	99.9
c_{gel}	99.9	99.9	99.9	99.9
ϱ_{eq}	98—99	90	90	90—95
d_{eq}	90	95—98	99.9	99.9
c_{NaCl}	—	—	90	90—95

* Polymers Separan AP-30 and Separan NP-10 together

and take-up rate. This has to be considered as a favourable circumstance from the practical aspect, because during the analysis of polymer solutions of unknown composition the determination of the take-up rate is sufficient for the correction of the matrix effect. However, the comparison of the correlation coefficients also shows that the most accurate results are given by a correlation of this type if the solutions to be analyzed contain only one polymer of possibly known type and if they contain sodium chloride in a concentration (about 1.5—2.5 g dm^{-3}) which provides for the equilibrium of the solution structure properties.

The SPEARMAN's rank correlation has the advantage that if the data (N) and the degree of freedom (f) are known, the confidence level can be calculated. On the basis of data in Table III it can be stated with a reliability of of 99.9% that there is a correlation *e.g.* between absorbance and take-up rate if the type and the concentration of the polymer and the salt concentration are changing in the test solution. However, it remains an open question whether for correlation coefficients of 0.7—0.8 the correction of the matrix effects through the take-up rate yields acceptable results from the analytical point of view. An answer to this question will be the aim of our next paper.

Conclusions

In the study of the unfavourable matrix effect met in the analysis of the trace elements of polyacrylamide solutions by direct flame atomic absorption spectrometry, the following has been concluded:

a) The absorption signal decreases with the increase of relative molecular mass, degree of hydrolysis and concentration of the polymer.

b) The trend character of the matrix effect is identical for all the elements, however, depending on the elements, there may be larger or smaller differences in the decrease of absolute absorbance.

c) The cause of the matrix effect is to be sought primarily in the nebulization processes, and within these, in the decrease of take-up rate.

d) The decrease in take-up rate can be traced back to increasing polymer concentration and solution viscosity, in general, to changes in solution structure.

e) Through its effect on the structure and viscosity of the polymer solution and consequently on the take-up rate, sodium chloride decreases the disadvantageous matrix effect of polyacrylamides.

f) According to rank correlation analysis, the absorbance is in close correlation with take-up rate, solution viscosity and polymer and gel concentrations alike.

g) The closeness of correlation worsens if the analysis is extended simultaneously to several types of polymers.

In summary, the direct trace analysis of polyacrylamide solutions by flame atomic absorption spectrometry will be suitably carried out on a polymer of known type, and at a sodium chloride concentration of 1.5—2.5 g dm^{-3}. From the point of view of practical work, it is advantageous to use the take-up rate as the correction factor.

REFERENCES

[1] Morgan, R. S., Morgan, N. H., Guinavan, R. A.: Analyt. Biochem., **45**, 668 (1972)
[2] Price, J. D.: 168th A.C.S. Nat. Meeting, Atlantic City, 1974
[3] Ramirez-Munoz, J.: Flame Notes, **6**, 8 (1974)
[4] Henn, E. L.: Anal. Chim. Acta, **73**, 273 (1974)
[5] Oguro, H.: Bunseki Kagaku, **24**, 797 (1975)
[6] Ruddle, L. H.: Pye Unicam 3rd Anal. Conf., Birmingham, 1976
[7] Siegel, S.: Nonparametric Statistics for the Behavioral Sciences, McGraw Hill, New York 1956
[8] Price, W. J.: Analytical Atomic Absorption Spectrometry, Heyden and Sons, London 1972
[9] O'Konski, C., Doyle, C.: Anal. Chem., **27**, 694 (1955)
[10] Langer, G., Lieberman, A.: J. Colloid Sci., **15**, 357 (1960)
[11] Robinson, M.: Anal. Chem., **33**, 109 (1961)
[12] Davies, C. N.: Aerosol Sciences, Acad. Press, New York 1966

István Lakatos H-3515 Miskolc-Egyetemváros, P.O. Box 2.

RECENSIONES

M. NÓGRÁDI: *Stereochemistry. Basic Concepts and Applications*

Akadémiai Kiadó, Budapest and Pergamon Press, Oxford, New York, Toronto, Sydney, Paris, Frankfurt, 1981. XV+283 pages

The present book is a significantly revised and completed English version of the book "Bevezetés a sztereokémiába" (Introduction into Stereochemistry) published in Hungarian (Műszaki Könyvkiadó, Budapest, 1975, 245 pages) by the same author. The title of the Hungarian version "Introduction into Stereochemistry" was extremely modest; in the same way, the main title of the present edition, "Stereochemistry" can be, without the subtitle printed in much smaller letters, "Basic Concepts and Applications", rather misleading, particularly in view of the only 283 pages volume.

For these reasons, it must be stated at the beginning here that the present book is of much higher level than suspected on the basis of the title and the relatively small volume. It is not concerned with the fundamental concepts in this branch of science as an introductory work of for deeped studies, but presents very concise, high level, and really original material.

The book is not simply a description of the basic phenomena in stereochemistry, but the theoretical principles and the correlations between them are surveyed, which have increasing importance in today's preparative and theoretical organic chemistry, pharmaceutical and biochemistry, polymer chemistry and also in inorganic chemistry; this is followed by illustrative examples of applications, treated sometimes in great detail. In view of these facts, the emphasizing of the expression "Basic Concepts and Applications", instead of using it as merely a subtitle, would have been justified to indicate the real content and originality of the book. "Basic Concepts and Applications of Stereochemistry" or "Basic Principles of Stereochemistry" could have been a better title for the book written by M. NÓGRÁDI.

Professor W. D. OLLIS presents the book to the reader in a Foreword, then the author describes his concepts in the Preface. Already this sparkling introduction may suggest that the book will contain more than a conventional stereochemical work.

The history of stereochemistry can be divided into three main periods. The first, lasting for almost eight decades, starting with the verification of the tetrahedron theory by van't HOFF and LE BEL (1874), exploiting then the various possibilities in stereochemistry and synthesizing the appropriate basic compounds, was followed, after 1950, by the introduction and widespread application of the conformation theory. Further rapid development was supported by the increasing use of new, powerful instrumental methods of examination. In the present, third, period, stereochemistry is no longer just an independent branch of science, but an indispensable part of the majority of chemical and biochemical sciences. The author has written a book corresponding to this third period, introducing the stereochemical principles, theoretical correlations and their practical applications, emphasizing the general concepts. This approach made possible that, in spite of the small volume, all important stereochemical problems could be included in this very up-to-date work.

There are three main chapters in the book. The first chapter, Static stereochemistry (111 pages) treats the geometric conditions in molecules, molecular symmetry. Grouping of the molecules is based on the SCHÖNFLIESS point group notation (pages 9—16), and this is consistently used then throughout the book. Further main sections in Chapter 1 deal with the chirality of molecules, with molecules having several centres of asymmetry, determination of absolute and relative configurations and the separation of enantiomers (pages 22—92); then the conformational analysis of carbon compounds is discussed (pages 93—111).

The part dealing with molecular chirality (pages 19—40), points 1.1.6—1.1.6.6. (Molecular chirality; The chiral centre: The sequence rules relating to the chirality centres: The conventions of CAHN, INGOLD and PRELOG; The chiral axis; The chiral plane; Helices; Stereoisomerism in penta- and hexa-coordinate compounds) is more detailed than point 1.1.7 (pages

41—53) dealing with molecules containing more than one centre of asymmetry. Point 1.1.8 (The experimental determination of configuration; Absolute and relative configuration) (pages 54—86) and the subsequent Point 1.1.9 (Principles relating to the separation of enantiomers) (pages 87—92) are very informatory.

Section 1.2. Conformation of carbon compounds (pages 93—111), dealing with the fundamental principles of conformational analysis and the conformation of basic molecules, appears at first sight to be very short and concise. The subsections are: 1.2.1. The conformation of ethane; Torsional strain (pages 94—95); 1.2.2. The conformation of *n*-butane; Non-bonding interactions (pages 96—99); 1.2.3. The conformation of cyclohexane (page 100—111). A discussion on the conformation of other cyclic systems, particularly of saturated heterocycles would have been welcome.

This short chapter on conformational analysis given in the first part of the book should be considered, however, in correlation with the second and third main chapters. In Chapter 2, Dynamic stereochemistry (pages 112—179) and Chapter 3, Applied stereochemistry (pages 180—268), several subchapters deal again with the conformations of cyclic systems, of example, 2.2.4. Conformational equilibria in ring systems; Ring inversion (pages 163—179) and 3.1.2.2, Conformation and reactivity (pages 203—20). This is an example to show the way of approaching and discussing a given problem in the book.

In the same way, the second main chapter (Dynamic stereochemistry 2.2.1 Intramolecular symmetry relations between groups of the same structure and position; Topicity (pages 112—119) gives a discussion of the fundamental phenomena treated already in the chapter on static stereochemistry, at a higher level.

In 2.2, the kinetics of configurational and conformational change (pages 133—151), isomerisation, epimerisation and configurational inversion are discussed very exactly, on the basis of energetical considerations; the subject of section 2.2.3 (pages 152—163) is hindered rotation.

On the basis of the title, Applied stereochemistry, one may expect that Chapter 3 describes the practical applications of the knowledge presented in the previous chapters. This is true, however, only partly. Even the titles show that new topics are also discussed in this section. These largely belong to the recent results of organic chemistry or biochemistry. The very high-level theoretical discussion assumes, of course, the knowledge of the previous parts of the present work and familiarity of the reader with the elements of molecular orbital theory, as indicated in the Note in page 212.

Particularly noteworthy sections in subchapter 3. (Reactivity and molecular symmetry) (pages 180—235) are: 3.1.12, Transformations involving molecular faces (pages 185—195); 3.1.2.1. Configuration and reactivity (pages 196—202); 3.1.2.2, Conformation and reactivity (pages 203—209).

Special attention should be paid to the subsequent section 3.1.3, The stereochemistry of concerted reactions. The conservation of orbital symmetry (210—241) is discussed in the following points: 3.1.3.1. The symmetry of molecular orbitals; 3.1.3.2, Electrocyclic reactions; Conrotation and disrotation; 3.1.3.3, Cycloaddition and cycloreversion; Suprafacial and intrafacial processes; 3.1.3.4, Cheletropic reactions; 3.1.3.5, Sigmatropic rearrangements; Retention and inversion.

The very profound discussion of the WOODWARD—HOFFMANN rules is also a characteristic example of the general virtues of the treatment applied in the book: it is modern and of high level. It is particularly evident in this chapter, but characteristic of the whole book, that a rich amount of figures helps the understanding. In paragraph 3.1.3, covering 32 pages, the contents consist of figures in about 50%, and there is also a table. On these 15 pages, the figures are very carefully and economically constructed, like the total figure content of the book. The formulas are clear and have the optimum size. This is also in accordance with the concise style, and contributed to the small volume of the book despite its rich material.

In the following part of Chapter 3, the author treated three topics of general interest: the stereochemistry of enzymatic processes (pages 242—248), stereoselectivity in the biosynthesis of steroids (pages 249—259) and the stereoisomerism of monotonous polymers (pages 260—264). The final section (3.4) entitled: Stereoisomerism in some inorganic complexes (pages 265—278). Except these four pages — and apart from a few examples — the book deals only with the stereochemistry of organic molecules.

The number of references is 169, including all modern stereochemical books and review papers. Some particularly important original papers are also cited. The literature contains almost exclusively the product of the last 12 years, and also refers to works being in the press in 1980. Orientation of the reader is facilitated by listing the full titles not only for the books, but also for the reviews and original papers. In view of the careful editing, it seems to be strange that the close reference 64 and 69 are the same.

The stereochemical language and manner of treatment are strictly exact throughout the book. This manifests itself in the use of exact terminology and in endeavouring to consequent conciseness, not abandoning these principles even for the sake of better readability.

In summary, it can be stated that a very valuable book of original views has been added to the stereochemical literature, which treats the earlier and most recent knowledge in stereochemistry at a high level.

G. BERNÁTH

J. FALBE (editor): *New Syntheses with Carbon Monoxide*

Springer Verlag, Berlin, Heidelberg, New York

The book "New Syntheses with Carbon Monoxide" was published in 1980 as the 11th volume in the series "Reactivity and Structure Concepts in Organic Chemistry".

The publication of this work — as stated by the Editor in the Preface — was justified, since the last edition of the book "Carbon Monoxide in Organic Synthesis" was published more than a decade ago, and in this period the importance of the chemistry of carbon monoxide has become, more and more evident; the oil crisis, the constant fear of depleting the oil reserves and the "rediscovery" of coal as raw material have greatly increased the research activity in this field. Processes almost forgotten, such as the Fischer—Tropsch synthesis, have got into the centre of research interest. Thus it was high time to revise thoroughly the previous book. New chapters, like "Homologation" or "Hydrogenation of carbon monoxide" have been included, while others, for example, "The conversion of synthesis gas into methanol and higher alcohols" are omitted.

The modern work consisting of 465 pages and divided into six chapters does not cover the entire content, however, since as it will be seen below, not the "new syntheses" are emphasized (the book does not even aim at completeness in this respect), but the scope and limitations, mechanisms, and the know-how of preparative reactions and industrial processes used for a long time are presented in an excellent way.

Chapter 1, "Hydroformylation, oxo synthesis, Roelen's reaction" (B. CORNILS), which can be regarded as typical in respect of structure is a good illustration for the above statements:

1.1 Introduction
1.2 Mechanism
1.3 Effect of reaction conditions on the conversion: selectivity, the course of the oxo synthesis
1.4 Examples of the reaction for different types of compounds
1.5 Side reactions
1.6 Industrial oxo syntheses. Economy.

The scope of the following five chapters are presented by listing the titles.

Chapter 2: Homologation of alcohols (H. BAHRMANN, B. CORNILS)
Chapter 3: Carbonylation catalyzed by metal carbonyls; the Reppe reaction (A. MULLEN)
Chapter 4: Hydrogenation of carbon monoxide (C. D. FROHNING)
Chapter 5: The Koch reaction (H. BAHRMANN)
Chapter 6: Cyclization reactions with carbon monoxide (A. MULLEN)

The volume is excellently edited; the authors of the chapters strictly considered the rules of lucid presentation, consequently, the book makes enjoyable reading.

References are complete, including the patent literature, up to 1978 but citations of 1979 and 1980 can also been found. The value of the information content of the book is greatly increased by 119 figures and 127 tables.

In all chapters, the industrial practice of "carbonylation" is emphasized, and related problems, such as the composition of catalysts, contaminant, perspective of application, economy, are also discussed in detail.

The book can be regarded as an excellent comprehensive reference material for all readers interested in catalytic carbonylation, carbon monoxide-based industrial syntheses, or in teaching chemical technology, but it can be interesting for preparative organic chemists, too. It may be mentioned that Hungarian authors are often cited in the book, particularly in Chapter 6.

L. TŐKE

INDEX

PHYSICAL AND INORGANIC CHEMISTRY

ORGANIC CHEMISTRY

ANALYTICAL CHEMISTRY

CHEMICAL TECHNOLOGY

PRINTED IN HUNGARY
Akadémiai Nyomda, Budapest

Les Acta Chimica paraissent en français, allemand, anglais et russe et publient des mémoires du domaine des sciences chimiques.

Les Acta Chimica sont publiés sous forme de fascicules. Quatre fascicules seront réunis en un volume (3 volumes par an).

On est prié d'envoyer les manuscrits destinés à la rédaction à l'adresse suivante:

Acta Chimica
Budapest, P.O.B. 67, H-1450, Hongrie

Toute correspondance doit être envoyée à cette même adresse.

La rédaction ne rend pas de manuscript.

Abonnement en Hongrie à l'Akadémiai Kiadó (1363 Budapest, P.O.B. 24, C. C. B. 215 11488), à l'étranger à l'Entreprise du Commerce Extérieur «Kultura» (H-1389 Budapest 62, P.O.B. 149. Compte-courant No. 218 10990) ou chez représentants à l'étranger.

Die Acta Chimica veröffentlichen Abhandlungen aus dem Bereich der chemischen Wissenschaften in deutscher, englischer, französischer und russischer Sprache.

Die Acta Chimica erscheinen in Heften wechselnden Umfanges. Vier Hefte bilden einen Band. Jährlich erscheinen 3 Bände.

Die zur Veröffentlichung bestimmten Manuskripte sind an folgende Adresse zu senden:

Acta Chimica
Budapest, Postfach 67, H-1450, Ungarn

An die gleiche Anschrift ist jede für die Redaktion bestimmte Korrespondenz zu richten:

Manuskripte werden nicht zurückerstattet.

Bestellbar für das Inland bei Akadémiai Kiadó (1363 Budapest, Postfach 24, Bankkonto Nr. 215 11488), für das Ausland bei »Kultura« Aussenhandelsunternehmen (H-1389 Budapest 62, P.O.B. 149. Bankkonto Nr. 218 10990) oder seinen Auslandsvertretungen.

«Acta Chimica» издают статики по химии на русском, английском, французском и немецком языках.

«Acta Chimica» выходит отдельными выпусками разного объекта, 4 выпуска составхяют один том и за год выходят 3 тома.

Предназначенные для публикации рукописи следует направлять по адресу:

Acta Chimica
Budapest, P.O.B. 67, H-1450, ВНР

Всякую корреспонденцию в редакцию направляйте по этому же адресу.

Редакция рукописей не возвращает.

Отечественные подписчики направляйте свои заявки по адресу Издательства Академии Наук (1363 Budapest, P.O.B. 24, Текущей счет 215 11488), а иностранные подписчики через организацию по внешней торговые «Kultura» (H-1389 Budapest 62, P.O.B. 149. Текущий счет 218 10990) или через ее заграничные представительства и уполномеченных.

Reviews of the Hungarian Academy of Sciences are obtainable at the following addresses:

AUSTRALIA
C B.D. LIBRARY AND SUBSCRIPTION SERVICE. Box 4886, G.P.O., *Sydney N.S.W. 2001*
COSMOS BOOKSHOP, 145 Ackland Street, *St. Kilda (Melbourne), Victoria 3182*

AUSTRIA
GLOBUS, Höchstädtplatz 3, *1200 Wien XX*

BELGIUM
OFFICE INTERNATIONAL DE LIBRAIRIE, 30 Avenue Marnix, *1050 Bruxelles*
LIBRARIE DU MONDE ENTIER, 162 Rue du Midi, *1000 Bruxelles*

BULGARIA
HEMUS, Bulvar Ruski 6, *Sofia*

CANADA
PANNONIA BOOKS, P.O. Box 1017, Postal Station "B", *Toronto, Ontario M5T 2T8*

CHINA
CNPICOR, Periodical Department, P.O. Box 50, *Peking*

CZECHOSLOVAKIA
MAD'ARSKÁ KULTURA, Národni tr'da 22, *115 33 Praha*
PNS DOVOZ TISKU, Vinohradská 46, *Praha 2*
PNS DOVOZ TLACE, *Bratislava 2*

DENMARK
EJNAR MUNKSGAARD, Norregade 6, *1165 Copenhagen*

FINLAND
AKATEEMINEN KIRJAKAUPPA, P.O. Box 128, *SF-00101 Helsinki 10*

FRANCE
EUROPERIODIQUES S.A., 31 Avenue de Versailles, *78170 La Celle St. Cloud*
LIBRAIRIE LAVOISIER, 11 rue Lavoisier *75008 Paris*
OFFICE INTERNATIONAL DE DOCUMENTATION ET LIBRAIRIE, 48 rue Gay-Lussac, *75240 Paris Cedex 05*

GERMAN DEMOCRATIC REPUBLIC
HAUS DER UNGARISCHEN KULTUR, Karl-Liebknecht-Strasse 9, DDR-*102 Berlin*
DEUTSCHE POST ZEITUNGSVERTRIEBSAMT, Strasse der Pariser Kommüne 3—4, *DDR-104 Berlin*

GERMAN FEDERAL REPUBLIC
KUNST UND WISSEN ERICH BIEBER, Postfach 46, *7000 Stuttgart 1*

GREAT BRITAIN
BLACKWELL'S PERIODICALS DIVISION, Hythe Bridge Street, *Oxford OX1 2ET*
BUMPUS, HALDANE AND MAXWELL LTD., Cower Works, *Olney Bucks MK46 4BN*
COLLET'S HOLDINGS LTD., Denington Estate, *Wellingborough, Northants NN8 2QT*
WM. DAWSON AND SONS LTD., Cannon House, *Folkestone, Kent CT19 5EE*
H. K. LEWIS AND CO., 136 Gower Street, *London WC1E 3BS*

GREECE
KOSTARAKIS BROTHERS, International Booksellers, 2 Hippokratous Street, *Athens-143*

HOLLAND
MEULENHOFF-BRUNA B.V., Beulingstraat 2, *Amsterdam*
9—11, *Den Haag*
SWETS SUBSCRIPTION SERVICE 347b Heereewg, *Lisse*

INDIA
ALLIED PUBLISHING PRIVATE LTD., 13/14 Asaf Ali Road, *New Delhi 110001*
150 B-6 Mount Road, *Madras 600002*
INTERNATIONAL BOOK HOUSE PVT. LTD., Madame Cama Road, *Bombay 400069*
THE STATE TRADING CORPORATION OF INDIA LTD., Books Import Division, Chandralok, 36 Janpath, *New Delhi 110001*

ITALY
EUGENIO CARLUCCI, P.O. Box 252, *70100 Bari*
INTERSCIENTIA, Via Mazzé 28, *10149 Torino*
LIBERIA COMMISSIONARIA SANSONI, Via Lamarmora 45, *50121 Firenze*
SANTO VANASIA, Via M. Macchi 58, *20124 Milano*
D. E. A., Via Lima 28, *00198 Roma*

JAPAN
KINOKUNIYA BOOK-STORE CO. LTD., 17-7 Shinjuku-ku 3 chome. Shinjuku-ku, *Tokyo 160-91*
MARUZEN COMPANY LTD., Book Department, P.O. Box 5050 Tokyo International, *Tokyo 100-61*
NAUKA LTD. IMPORT DEPARTMENT, 2-40-19 Minami Ikebukuro, Toshima-ku, *Tokyo 171*

KOREA
CHULPANMUL, *Phenjan*

NORWAY
TANUM-CAMMERMEYER, Karl Johansgatan 41—43, *1000 Oslo*

POLAND
WEGIERSKI INSTYTUT KULTURY, Marszalkowska 80, *Warszawa*
CKP I W ul. Towarowa 28 *00-958 Warszawa*

ROUMANIA
D. E. P., *Bucureşti*
ROMLIBRI, Str. Biserica Amzei 7, *Bucureşti*

SOVIET UNION
SOJUZPETCHATJ — IMPORT, *Moscow*
and the post offices in each town
MEZHDUNARODNAYA KNIGA, Moscow G-*200*

SPAIN
DIAZ DE SANTOS, Lagasca 95, *Madrid 6*

SWEDEN
ALMQVIST AND WIÓSELL, Gamla Brogatan 26, *101 20 Stockholm*
GUMPERTS UNIVERSITETSBOKHANDEL AB. Box 346, *401 25 Göteborg 1*

SWITZERLAND
KARGER LIBRI AG, Petersgraben 31, *4011 Base*

USA
EBSCO SUBSCRIPTION SERVICES, P.O. Box 1943, *Birmingham, Alabama 35201*
F. W. FAXON COMPANY, INC., 15 Southwest Park, *Westwood, Mass. 02090*
THE MOORE-COTTRELL SUBSCRIPTION AGENCIES, *North Cohocton, N. Y. 14868*
READ-MORE PUBLICATIONS, INC., 140 Cedar Street, *New York, N. Y. 10006*
STECHERT-MACMILLAN, INC., 7250 Westfield Avenue, *Pennsauken N. J. 08110*

VIETNAM
XUNHASABA, 42, Hai Ba Trung, *Hanoi*

YUGOSLAVIA
JUGOSLAVENSKA KNJIGA, Terazije 27, *Beograd*
FORUM, Vojvode Mišića 1, *21000 Novi Sad*

HU ISSN 0001-5407 Index: 26.007

ACTA CHIMICA

ACADEMIAE SCIENTIARUM HUNGARICAE

TOMUS 109 FASCICULUS 4

AKADÉMIAI KIADÓ, BUDAPEST

1982

ACTA CHIM. ACAD. SCI. HUNG. ACASA2 109 (4) 331–448 (1982)

ACTA CHIMICA

A MAGYAR TUDOMÁNYOS AKADÉMIA KÉMIAI TUDOMÁNYOK OSZTÁLYÁNAK IDEGEN NYELVŰ KÖZLEMÉNYEI

Acta Chimica is a journal for the publication of papers on all aspects of chemistry in English, German, French and Russian.

Acta Chimica is published in 3 volumes per year. Each volume consists of 4 issues of varying size.

Manuscripts should be sent to

Acta Chimica
Budapest, P.O. Box 67, H-1450, Hungary

Correspondence with the editors should be sent to the same address. Manuscripts are not returned to the authors.

Hungarian subscribers should order from Akadémiai Kiadó, 1363 Budapest, P.O.B. 24. Account No. 215 11488.

Orders from other countries are to be sent to "Kultura" Foreign Trading Company (H-1389 Budapest 62, P.O.B. 149. Account No. 218 10990) or its representatives abroad.

Acta Chimica Academiae Scientiarum Hungaricae, Tomus 109 (4), pp. 331–340 (1982)

POTENTIOSTATIC DOUBLE PULSE METHOD FOR THE STUDY OF THE KINETICS OF RAPID ELECTRODE PROCESS

J. DÉVAY[1]*, I. SZVITACS[2] and L. MÉSZÁROS[1]

([1]Research Laboratory for Inorganic Chemistry, Hungarian Academy of Sciences, Budapest, [2]Technical College Mihály Pollack, Pécs)

Received April 28, 1980
In revised form January 12, 1981
Accepted for publication February 17, 1981

A new pulse technique, termed potentiostatic double pulse technique, has been developed for the study of fast electrode reactions. The first large amplitude pulse rapidly charges the double layer capacitor to the level corresponding to the second potential step and consequently very fast chargetransfer processes can be investigated, as the current can be extrapolated to $t = 0$ from the initial period of the current-time transient. Thus it is possible to evaluate the faradaic current more precisely.

The technique permits the determination of the heterogeneous rate constant up to $k = 10$ cm s^{-1} with an acceptable accuracy. This is a considerable improvement as compared to single potential pulse technique which can be employed for the calculation of the heterogeneous rate constant with reasonable accuracy when $k < 10^{-2}$ cm s^{-1}.

Introduction

Charge transfer between the metal and the respective component of the solution is an essential step of the kinetics of electrode processes.

Several methods have been developed for the determination of the kinetic parameters of electrode reactions [1, 2]. Relaxation techniques form an important class of these methods. In these techniques the electrode in equilibrium is perturbed either by a controlled current signal or by a controlled potential function, and the response which is determined by the kinetic characteristics of the electrode process is measured and analyzed.

The well-known faradaic impedance method consists in perturbing the electrode with a sinusoidal current or potential function. The kinetic parameters of the electrode reaction are determined from the measured electrod impedance data. The faradaic rectification method utilizing the non-linearity

* To whom correspondence should be addressed.

of the faradaic impedance is also generally accepted. However, these methods can only be used in the case of steady state (or quasi-stationary) systems.

When using dynamic methods, the study of the transient signals permits to draw conclusions on the kinetic parameters of the charge transfer process.

Dynamic measurement can be carried out according to two different principles depending on whether the potential or the current of the electrode is changed according to a given signal.

Perturbation is produced with a current pulse in the galvanostatic current step method. The coulostatic charge pulse method is similar to the latter. In these methods the change in time of the overvoltage produced by the current pulse or charge pulse respectively is measured.

The potential or voltage step methods belong to another important group of dynamic techniques. In the voltage step method the voltage of the measuring cell is changed by a voltage step of given magnitude, and the change in time of the current produced is analyzed. The overvoltage of the electrode also changes as a function of time because the overvoltage is the difference of the voltage step (ΔV) and of the voltage drop at resistance R of the circuit:

$$\eta = \Delta V - JR$$

The measuring conditions become better defined, if instead of the cell voltage the electrode potential is controlled by a step function. The intensity of the current is determined by the transfer resistance and diffusion resistance. In this case, however, the current can only be measured after the decay of the capacitive current. Since the overvoltage produced by a potential step E_2 varies exponentially with time (because of the finite time of the charging of the capacity of the double-layer), the method is only suitable for the study of relatively slow processes having a heterogeneous rate constant of 10^{-2} cm s^{-1} or lower.

Similarly to most of the transient methods the potential step method can also be interpreted with functions interrelating current, potential, time and concentration.

Let us consider the most simple electrode process:

$$R \rightleftarrows O + ze \qquad (1)$$

where R and O are the reduced and oxidized forms, respectively, of the reacting species and z is the number of electrons taking part in the charge transfer reaction.

The theoretical bases of the analysis of the results obtained by the potential step method have been developed in detail by SMUTEK [3] and independently from him by KAMBARA and TACHI [4] as well as by DELAHAY [5], and by GERISCHER and VIELSTICH [6].

The following are the essential points of their results:

1) The charge transfer current density (faradaic current) is given by the following formula

$$\mathbf{j} = \mathbf{j}_0 \exp(\lambda^2 t)\, erfc(\lambda \sqrt{t}) \tag{2}$$

where $\mathbf{j}(0)$ is the current density at $t = 0$, and factor λ is defined by the following formula

$$\lambda = \frac{\mathbf{j}_0}{zF}\left[\frac{1}{C_R^0 \sqrt{D_R}} \exp\left(\frac{\alpha z F}{RT}\eta\right) + \frac{1}{C_O^0 \sqrt{D_0}} \exp\left(-\frac{(1-\alpha) z F}{RT}\eta\right)\right] \tag{3}$$

where $\mathbf{j}_0$ is the exchange current density, α the symmetry factor, η the overvoltage, C_O^0 and C_R^0 are the bulk concentrations of the oxidized and the reduced form, respectively while D_O and D_R are the diffusion coefficients of the oxidized and reduced form respectively, z is the number of electrons exchanged in the electrode reactions while F, R and T have their usual significance.

2) Current density at time $t = 0$: is given by

$$\mathbf{j}(0) = \mathbf{j}_0\left\{\exp\left(\frac{\alpha z F}{RT}\eta\right) - \exp\left(-\frac{(1-\alpha) z F}{RT}\eta\right)\right\} \tag{4}$$

It can be seen from the aforegoing that charge-transfer overvoltage is only observed at $t = 0$.

The above relationships refer to systems, in which both the reduced and the oxidized forms are present in the solution. If, however, the solution contains only the oxidized form, or only the reduced one other relationships must be used. In the study of rather rapid processes as the reduction of some cations (*e.g.* Cd^{2+}, Pb^{2+}) the following assumptions are made:

1) The reduced form produced in the cathodic process is deposited on or dissolved in the electrode with amalgam formation,

2) material transport only takes place by diffusion,

3) the ohmic resistance of the cell is zero, and thus, the capacity of the double layer is charged at $t = 0$.

The following relationships are valid under these conditions

1) The charge transfer current density is expressed by relationship (2), where factor (3) has the following modified form:

$$\lambda = \frac{k_0 \exp\left(-\dfrac{(1-\alpha) z F}{RT}\eta\right)}{\sqrt{D_0}} = \frac{k}{\sqrt{D_0}} \tag{5}$$

where k_0 is the formal rate constant of the electrode reaction at the formal potential of the electrode reaction, and k is the potential dependent rate constant the value of which is conveniently referred to the half-wave potential.

2) Current density at $t = 0$ is:

$$\mathbf{j}(0) = zFkC_0^0 \tag{6}$$

GERISCHER and VIELSTICH [6] also analyzed the above expressions in detail and found that the current density can be approximated with the following formula if $\lambda\sqrt{t} \ll 1$, *i.e.* time is sufficiently short,

$$\mathbf{j} = \mathbf{j}(0)\left(1 - \frac{2}{\sqrt{\pi}}\lambda\sqrt{t}\right) \tag{7}$$

Thus the faradaic current is obtained by extrapolation of the function **j** *vs.* $\sqrt{t}$ to $t = 0$. The exchange current density is given by the relationship

$$\mathbf{j}_0 = zFk_0C_0^{\alpha}C_R^{(1-\alpha)} \tag{8}$$

well known in literature.

Since the instantaneous setting of the electrode potential to the desired overvoltage is impeded by the delayed charging of the double layer capacity an attempt has been made to develop a method which permitted to charge the double layer capacity in a very short period of time (within a few μs). Thus a potentiostatic double pulse method was developed. The first potential pulse of a large amplitude (E_1) charges the double layer capacity to the level corresponding to the second potential step (E_2). Consequently the capacitive current is not observed after the first pulse. The kinetic parameters are calculated according to the principles of the potentiostatic potential-step method.

The potentiostatic double pulse method

Actually, in the case of the simple potential step method the overvoltage does not change according to a true step function because the double layer capacity is charged to the desired overvoltage according to the following equation (neglecting the faradaic current):

$$E(t) = E_2\left[1 - \exp\left(-\frac{t}{R_C C_K}\right)\right] \tag{9}$$

where C_k is the double layer capacity, R_C the cell resistance and t the time.

It is apparent from Eq. (9) that if the ohmic resistance of the cell is reduced to a value approaching zero (*e.g.* with ohmic compensation), then the exponential term also tends to zero, thus in the limiting case $E(t)$ will be equal to E_2 at $t = 0$.

A dummy cell was assembled for the study of the aforesaid case. The measuring equipment is shown in Fig. 1. The potential between points A and B was measured with an oscilloscope. The effect of ohmic compensation

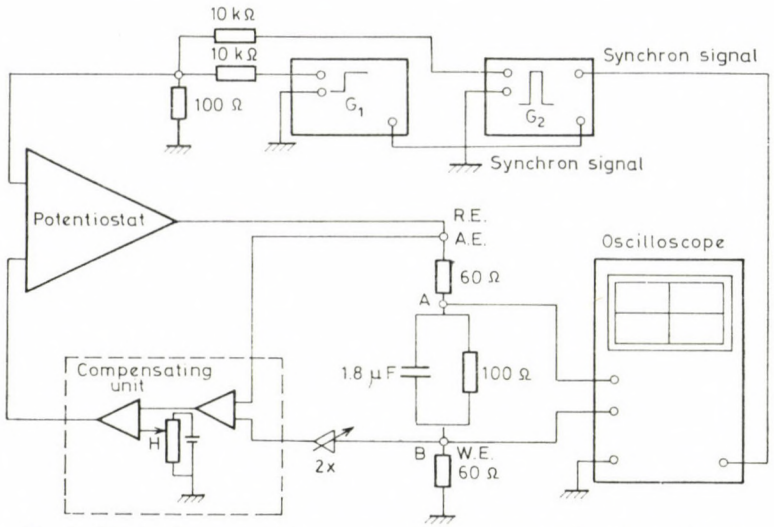

Fig. 1. **Block diagram of the measuring system with a dummy cell**

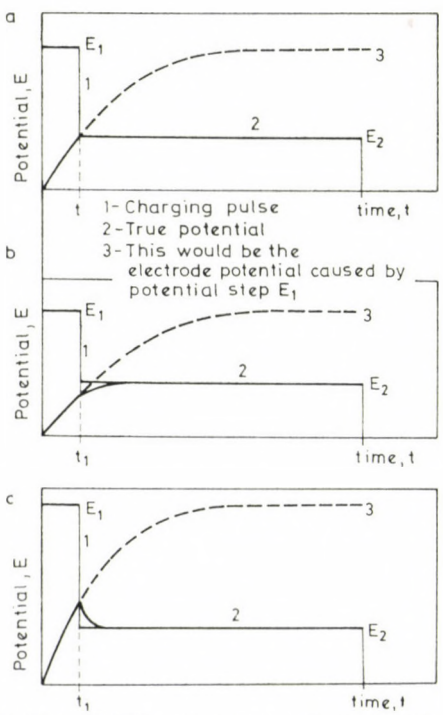

Fig. 2. **Potential function imposed on the electrode**

on the transient was found to be unsatisfactory because $E(t)$ attains E_2 exponentially in the same way as without ohmic compensation. This can be attributed to the following fact: though the response time of pulse potentiostats is about 10^{-7} s in the case of ohmic load, this value, however, is reduced to 10^{-4} s when the load also contains a capacitive component because of the phase-shift caused by the capacitive component.

The frequency transfer of the Tacussel Model PIT 20—2x potentiostate equipped with an ohmic compensating unit CDCO 1, was measured using a load containing a capacitive component. Ohmic compensation was found to become abruptly ineffective at frequencies higher than 10 kHz. Consequently another way had to be found to impose the desired potential step on the electrode in the shortest possible time.

The principle of the method is the following: The signal shown in Fig. 2a is imposed on the electrode. The amplitude of the first relatively short pulse (E_1), must be chosen so that the double layer is charged to the level corresponding to potential E_2. The following potential step, E_2, permits the observation of the current time transient from which the kinetic parameters can be calculated. Figures 2b and 2c illustrate the cases, when the amplitude of E_1 is smaller or larger, resp., than the required one.

It is apparent from the figure that when a charging pulse is smaller than the required one the double layer is not charged to a level corresponding to E_2 during time t_1, which is the duration of the potential pulse E_1. On the other hand, a larger pulse than needed produces overcharging. The respective current-time transients of these cases are shown in Figs 3a, 3b and 3c.

Theoretically, the proper ratio of the two potentials is selected in the following way: it can be assumed that the current flowing through the cell during the first short pulse completely charges the double layer capacity. Thus, the overvoltage due to the capacity can be calculated when C_{dl} and R_C are known. At time $t = t_1$, $E(t)$ must be equal to the second step, E_2, $[E(t) = E_2]$.

However, an appropriate adjustment can be also made experimentally. Figure 3c illustrates the cases in which the first pulse E_1 overcharges the capacity of the doble layer at $t = t_1$, and consequently a discharge current and the faradaic current drops below the level of the faradaic current. The correct value (E_1) of the pulse can adjusted by changing its amplitude until the overcharge transient observed after $t = t_1$ disappears. From the current-time transient obtained by the extrapolation of the plot of **j** *vs.* $\sqrt{t}$ to $t = 0$.

The redox system 10^{-3} mol dm^{-3} $K_4Fe(CN)_6$ — 10^{-3} mol dm^{-3} $K_3Fe(CN)_6$ was studied in order to prove the applicability of the above measuring method to rapid electrode process ($k > 10^{-2}$ cm s^{-1}). Y mol dm^{-3} KCl was used as the supporting electrolyte, a Pt needle as the working electrode, and normal calomel electrode as the reference electrode. Measurements were

carried out at 25 °C. The circuit diagram of the potentiostatic double pulse measuring set is shown in Fig. 4.

The signal of generators G_1 and G_2 (generator G_1 was a pulse generator Model EMG—1157, generator G_2 a function generator AILTECH Series Model

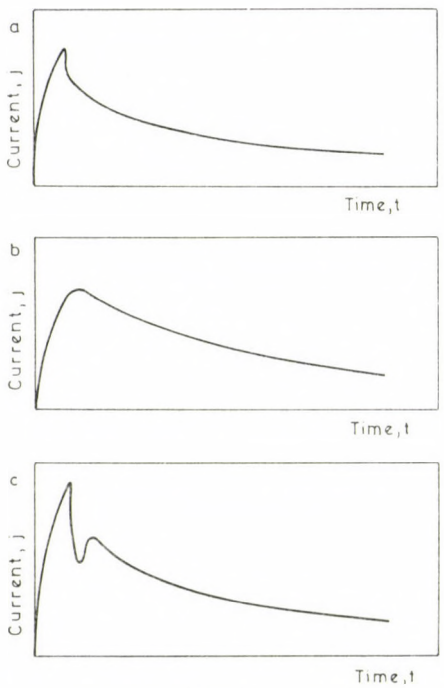

Fig. 3. Current — time transient generated by the potential step in the case of a charging pulse (E_1) of various amplitude

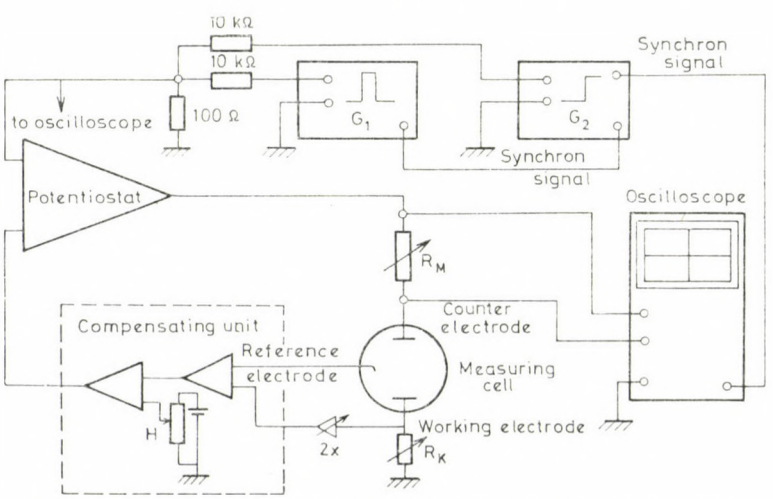

Fig. 4. Block diagram of the potentiostatic double pulse measuring system

505) are connected to a voltage adding circuit. Measurement is started by the synchron signal of generator G_1, which at the same time ensures the synchronous operation of generator G_2 and of memory oscilloscope Model Tetronix 7633/R7633. The double pulse was set to an adequate level with helicoidal potentiometer H.

The current flowing through measuring resistance R_M was measured with an oscilloscope. The potential step controlling the potentiostat was similarly adjusted with an oscilloscope.

The equilibrium potential of the system was measured with a millivoltmeter (this was found to be $E = 198$ mV at 25 °C). The latter potential was adjusted with potentiometer H. Then potential steps of ± 10, ± 20, ± 30, ± 40 and ± 50 mV were applied and the **j** *vs.* t transient were recorded; **j** *vs.* $\sqrt{t}$ diagrams were plotted from these transient data. The faradaic current values were calculated by extrapolation of these plots to $t = 0$.

An example of such an extrapolation is shown in Fig. 5, where **j** *vs.* $\sqrt{t}$ diagram was plotted from a current time transient produced by an anodic potential step of 40 mV.

Exchange current density $\mathbf{j}_0$ relating to the equilibrium potential was determined by Tafel extrapolation, from the faradaic current values obtained from the **j** *vs.* $\sqrt{t}$ plots and the rate constant of the charge-transfer reaction was calculated using this data. The anodic transfer coefficient (α) is determined from the slope of the Tafel line. The faradaic currents relating to given potentials are listed in Table I. The Tafel lines obtained with these data are shown in Fig. 6. The exchange current density $\mathbf{j}_0$ was found to be $\mathbf{j}_0 = 10.5 \times 10^{-3}$ A cm^{-2}. The rate constant of the charge-transfer reaction can be calculated using Eq. (8). If $C_O = C_O^0$ and $C_R = C_R^0$, and $C = C_R^0 = C_O^0$ are the initial concentrations at $t = 0$, then Eq. (8) is reduced to the following expression:

$$\mathbf{j}_0 = zFCk \tag{10}$$

Table I

Faradaic current in the case of anodic polarization

E_2 (mV)	10	20	30	40	50
j (mA cm^{-2})	6.54	10.2	14.1	18.8	22.2

Faradaic current in the case of cathodic polarization

E_2 (mV)	−10	−20	−30	−40	−50
j (mA cm^{-2})	7.9	16.2	21.5	27.2	34.4

In the case of the present system $z = 1$ and $C = 10^{-6}$ mol cm^{-3}.

Thus

$$k_0 = \frac{10.5 \cdot 10^{-3}}{96\,500 \cdot 1 \cdot 10^{-6}} = 1.09 \cdot 10^{-1} \text{ cm s}^{-1}.$$

The transfer coefficient was calculated from the Tafel lines in the usual way.

The slope of the anodic branch were found to be $m_a = 6.45$ V^{-1}, while that of the cathodic one $m_k = 10.48$ V^{-1}.

The transfer coefficient calculated from the anodic branch was $\alpha = 0.381$ which is in good agreement with that calculated from the cathodic branch $\alpha = 0.380$.

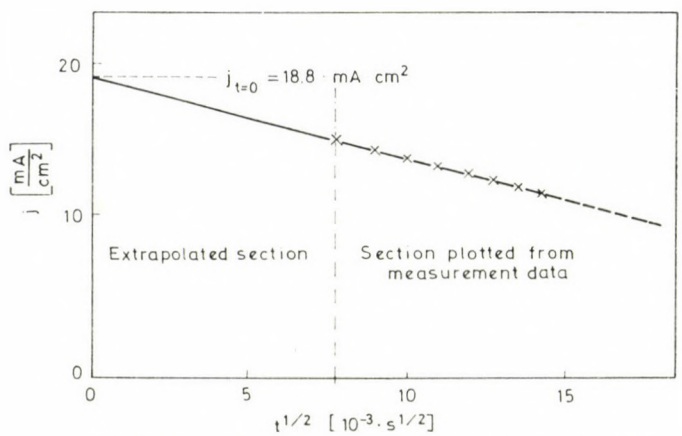

Fig. 5. Current generated by potential step E_2 as a function of the square root of time

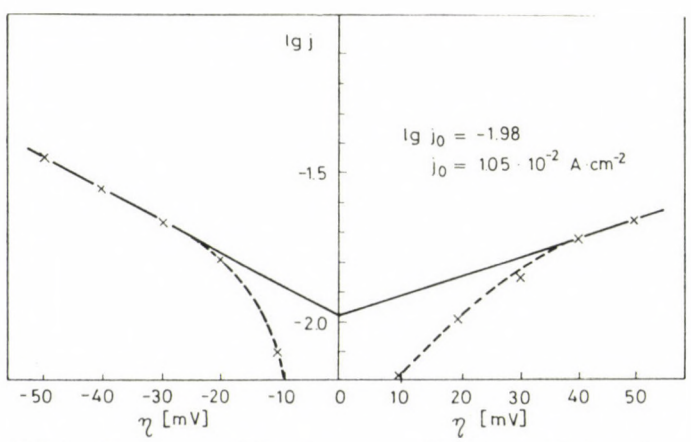

Fig. 6. Polarization curves of the charge transfer process of the redox system $[Fe(CN)_6]^{4-}/[Fe(CN)_6]^{3-}$; lg $i_0 = -1.98$; $i_0 = 1.05 \times 10^{-2}$ A cm^{-2}

Table II

	Temperature (°C)	$E_{1/2}$* (mV)	k (cm s^{-1})	α	$k_{lit.}$ (cm s^{-1})	$\alpha_{lit.}$
10^{-3} mol dm^{-3} $CdCl_2$ 1 mol dm^{-3} KCl 10^{-2} mol dm^{-3} HCl	22	−685	0.95	0.20	2.9	0.22
10^{-3} mol dm^{-3} $Pb(NO_3)_2$ 1 mol dm^{-3} $NaClO_4$	22	−425	1.70	0.39	3.3	0.40

* Referred to normal calomel electrode.

The kinetic parameters of the above system reported in the review of TANAKA and TAMAMUSHI are the following: $\alpha = 0.39$ and $k = 0.52 \cdot 10^{-1}$ cm $\cdot$ s^{-1}.

It is apparent that the above experimental results are in good agreement with literature data.

The reduction of Cd(II) and of Pb(II) ions was also studied. In the former case a 10^{-3} mol dm^{-3} Cd(II) solution was prepared and a 1 mol dm^{-3} KCl solution was used as the supporting electrolyte, while in the letter case a 10^{-3} mol dm^{-3} Pb(II) solution was used, and the supporting electrolyte was 1 mol dm^{-3} $NaClL_4$. The pH of the solutions was adjusted to pH = 2 in both cases.

Dropping mercury electrode was used as the working electrode while mercury pool as the auxiliary electrode, and normal calomel electrode as the reference electrode. Measurements were carried out at 22 °C.

Our results and data published in the work of TANAKA and TAMAMUSHI [2] are summarized in Table II. It is apparent that a good agreement exists between our results and literature data.

REFERENCES

[1] THIRSK, H. R. HARRISON, J. A.: A Guide to the Study of Electrode Kinetics. Academic Press, London 1972
[2] TANAKA, N., TAMAMUSHI, R.: Electrochim. Acta, **9**, 963 (1964)
[3] SMUTEK, M.: Proc. 1st Polarogr. Congr., **1**, 677 (1952)
[4] KAMBRA, T., TACHI, I.: Bull. Chem. Soc. (Japan), **25**, 135 (1952)
[5] DELAHAY, P.: J. Am. Chem. Soc., **75**, 1430 (1953)
[6] GERISCHER, H., VIELSTICH, W.: Z. Physik. Chem. (Neue Folge), **3**, 16 (1905)

József DÉVAY
Lajos MÉSZÁROS } H-1112 Budapest, Budaörsi u. 45.
István SZVITACS H-7624 Pécs, Boszorkány u. 2.

Acta Chimica Academiae Scientiarum Hungaricae, Tomus 109 (4), pp. 341—343 (1982)

A DEVIATION FROM THE WITTIG REACTION, III

S. VERMA*, N. M. KANSAL and M. M. BOKADIA

(School of Studies in Chemistry, Vikram University, Ujjain, M.P., India)

Received December 16, 1980
Accepted for publication February 25, 1981

A new diphosphirane (**III**) has been isolated from the reaction of bromoform with triphenylphosphine and potassium *t*-butoxide, using both of the latter reagents in excess. The reactions of **III** with carbonyl compounds gave new oxadiphospholanes (**IV** and **V**) which have also been characterized by elemental analysis and spectral data.

Continuation of our studies on ylides has led to the isolation of a diphosphirane formed by a modified Wittig reaction. Formation of a dibutoxy-ylide when using potassium *t*-butoxide in excess and the formation of a phosphirane in the presence of excess triphenylphosphine have been reported by us [1, 2]. Now we report the formation of 1,1,1,2,2,2-hexaphenyl-3,3-di-(*t*-butoxy)diphosphirane (**III**). The reaction can be represented as shown by Eq. (1).

i) $Ph_3P + (CH_3)_3COK + CHBr_3 \longrightarrow Ph_3P{=}CBr_2 + KBr + (CH_3)_3COH$

I

ii) $Ph_3P{=}CBr_2 + 2(CH_3)_3COK \longrightarrow Ph_3P{=}C[OC(CH_3)_3]_2 + 2KBr$

II

iii) **II** + $Ph_3P \longrightarrow$ $Ph_3P{-}\overline{C}[OC(CH_3)_3]_2$ (1)

$|$

Ph_3P^+

$\downarrow$

$Ph_3P{-}C[OC(CH_3)_3]_2$

$\diagdown\ \diagup$

Ph_3P

III

* To whom correspondence should be addressed.

The formation of the non-isolated dibromo-ylide (**I**) was first reported by SPEZIALE *et al.* [3] in the reaction of triphenylphosphine, potassium *t*-butoxide and bromoform, all taken in equimolar amounts. In our experiments, potassium *t*-butoxide was present in excess which being a strong base, replaced both halogen atoms of the ylide **I**, to give rise to the ylide **II**. The fact that phosphorus can undergo bonding both by using its empty 3d orbitals, as well as by using its lone pair of electrons, suggests that triphenylphosphine, which also is present in excess in the reaction mixture, can attack the double bond between the phosphorus and carbon atoms to give the diphosphirane **III**.

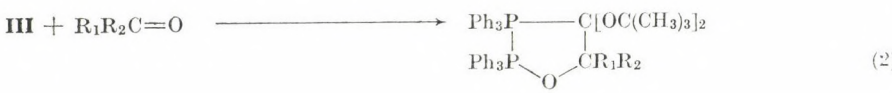

(2)

IV, V

IV $R_1 = R_2 = C_6H_5$; **V** $R_1 = H$, $R_2 = C_6H_4OCH_3$

The structures of compounds **III**, **IV** and **V** have been confirmed by elemental analysis and spectral data.

The diphosphirane **III** was allowed to react with various carbonyl compounds and the products were identified as the oxadiphospholanes **IV** and **V**. The reaction can be represented by Eq. (2).

Experimental

Preparation of the diphosphirane III

Triphenylphosphine (0.02 mole) and potassium *t*-butoxide (0.02 mole) [prepared by dissolving potassium (1 g) in *t*-butanol (100 mL) and evaporating the solvent under reduced pressure], was taken up in dry, distilled petroleum ether (100 mL). The mixture was cooled in ice. To this ice-cold mixture a solution of bromoform (0.01 mole) in petroleum ether (20 mL) was added, with constant stirring. The addition of the bromoform produced a dark orange colour indicating the formation of the bromo-ylide (**I**), but soon the solution became colourless. The reaction mixture was allowed to warm to room temperature and let to stand for one day. The mixture was then filtered and the filtrate concentrated to obtain a yellow oil which gave two spots in TLC corresponding to unchanged triphenylphosphine and the product. Column chromatography of the reaction mixture afforded unreacted triphenylphosphine (with petroleum ether) and the product (with ether as the eluting solvent). Recrystalization from benzene-ether gave the product with m.p. 160—161 °C in 40% yield.

$C_{45}H_{48}O_2P_2$. Calcd. C 79.1; H 7.0; P 9.09. Found C 78.8; H 7.5; P 9.6%.

The IR spectrum had main bands due to P—Ph (1440), $-C(CH_3)_3$ (1930), C—O—C—O—C (1110 and 1000) [4] and P—P (450) [5].

The H-NMR spectrum of the product showed complex aromatic signals in the range 2.0—3.0 (τ) and aliphatic signals in the range 8.0—9.0 (τ).

Reaction of III with benzophenone

The diphosphirane **III** was prepared in the same manner as described above. After the addition of bromoform, benzophenone (0.01 mole) in petroleum ether (25 mL) was added, with constant stirring. After one day, the reaction mixture was filtered and the filtrate concentrated and then subjected to column chromatography. Elution with petroleum ether gave unchanged triphenylphosphine; benzene eluted then the unreacted benzophenone, and finally elution with ether gave a solid which was recrystallized from ether-benzene; m.p. 168—169 °C; yield: 30%.

$C_{58}H_{58}O_3P_2$. Calcd. C 80.5; H 6.7; P 7.2%. Found C 80.2; H 6.4; P 7.7%.

The IR spectrum had main absorption bands due to P—Ph (1435), P—O—C (1190), C—O—C—O—C (1110 and 1000) [4] and P—P (460) [5].

The ^{1}H-NMR spectrum showed complex aromatic signals in the range 2.0—3.0 (τ) and complex aliphatic signals in the range 8.0—9.0 (τ).

Reaction of III with anisaldehyde

The reaction was performed in the same manner as described above. The product was obtained from the ether elution of the column chromatography and was recrystallized from benzene-ether; m.p. 165—166 °C; yield: 35%.

$C_{53}H_{56}O_4P_2$. Calcd. C 77.7; H 6.8; P 7.5. Found C 77.5; H 6.4; P 7.9%.

The IR spectrum had main absorption bands due to P—Ph (1450), C—O—C—O—C (1160 and 1030), P—O—C (1190), 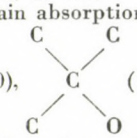 (1920) [4] and P—P (460) [5].

The ^{1}H-NMR spectrum showed complex aromatic and aliphatic signals in the range of 2.0—3.0 (τ) and 8.0—9.0 (τ), respectively.

*

Two of the authors (S. V. and N. M. K.) are thankful to the University Grants Commission, New Delhi, for the award of J. R. F. and T. R. F., respectively.

REFERENCES

[1] Verma, S., Kansal, N. M., Bokadia, M. M.: Indian J. Chem., **19B**, 318 (1980)
[2] Kansal, N. M., Verma, S., Bokadia, M. M.: Indian J. Chem., **19B**, 611 (1980)
[3] Speziale, A. J., Marco, G. J., Ratts, K. W.: J. Am. Chem. Soc., **82**, 1260 (1960); **84**, 854 (1962)
[4] Bellamy, L. J.: "The Infrared Spectra of Complex Molecules". Methuen, London, 1958
[5] Thomas, L. C.: "The Interpretation of Infrared Spectra of Phosphorus Compounds". Heyden, London, 1974

S. Verma
N. M. Kansal
M. M. Bokadia
Vikram University, Ujjain 456—010 M. P. India

Acta Chimica Academiae Scientiarum Hungaricae, Tomus 109 (4), pp. 345—353 (1982)

KINETICS AND MECHANISM OF THE REACTION OF Cr(III) WITH METAL CYANIDES, II

COMPLEX FORMATION WITH OCTACYANOMOLYBDATE(IV)

W. U. MALIK, S. P. SRIVASTAVA*, K. K. THALLAM and V. K. GUPTA

(Department of Chemistry, University of Roorkee, Roorkee, India)

Received September 8, 1980
Accepted for publication March 12, 1981

The complex formation between Cr(III) and $Mo(CN)_8^{4-}$ follows a second order kinetics, being first order in each reactant. The rate is linearly related to pH in the low pH range. The salt effect is negative and exponential in character. The rate decreases with an increase in dielectric constant. Thermodynamic parameters have been evaluated. Chemical analysis corresponds to the formula $CrMo(CN)_6(H_2O)(OH)$. The formation of $Cr(CN)_2^+$ as an intermediate has been identified polarographically. A possible reaction mechanism has been proposed and the corresponding rate law derived.

Introduction

Metal ions like silver, thallium, copper and cobalt react with potassium octacyanomolybdate(IV) to give insoluble complexes, the composition of which were investigated by WARDLAW and co-workers [1] using various physico-chemical methods. However, Fe(III) and Cr(III) form soluble complexes with potassium octacyanomolybdate. Studies on the nature and composition of these and other complexes formed with potassium octacyanomolybdate(IV) were carried out by MALIK and co-workers [2, 3] by spectrophotometric method. However, a review of the literature shows that the kinetics of these complexation reactions has not been studied. Hence a systematic kinetic study of the interaction of Cr(III) with metal cyanides was undertaken with a view to elucidate the mechanism of these interactions, and the present paper describes our results on the study of the interaction of Cr(III) with octacyanomolybdate.

Experimental

Methods and Materials

Potassium octacyanomolybdate(IV) was prepared by the method of ROSENHEIM [4] as modified by FIESER [5]. Its solution was standardized by the procedure recommended by KOLTHOFF [6] and stored in a coloured bottle. Chromic chloride, Analar, grade, was dissolved in double distilled water and its strength was determined iodometrically after oxidizing the solution to chromate with Na_2O_2. Sodium acetate-hydrochloric acid buffer was used to maintain the pH of the solutions. All other salts used were of Anala^R grade.

* To whom correspondence should be addressed.

Chemical analysis

A red coloured complex separated after about 3 hours of mixing of equimolar aqueous solutions of octacyanomolybdate(IV) and chromic chloride. It was recrystallized from absolute ethanol, dried over quick lime for about 24 hrs and heated at 110 °C for about an hour to remove water of hydration.

0.1 g of the dehydrated complex was decomposed by heating with *conc.* sulphuric acid for nearly one hour, cooled and diluted with water. A clear solution was obtained and its Mo content was determined by precipitating with benzoinoxime and weighed as MoO_3 [7], Cr was determined iodometrically. The results of chemical analysis are listed below:

	Mo	Cr	H	C	N
Found	28.11	15.26	0.91	21.31	24.82
Calc. for $CrMo(CN)_6(H_2O)(OH)$	28.31	15.34	0.89	21.24	24.78

Kinetic measurements

The spectrophotometric measurements were made on a Unicam SP – 500 spectrophotometer. The λ_{max} for the reddish brown coloured solution obtained on mixing aqueous solutions of octacyanomolybdate(IV) and chromic chloride, and for the aqueous solution of the complex obtained by isolation of the complex from absolute alcohol was found to be 360 nm. Further the λ_{max} of the reaction mixture did not change with time. It is worth-while to point out here that the two reactants do not have any appreciable absorbance at this wavelength. Further the solution of potassium octacyanomolybdate(IV) was taken as the blank. The reaction mixture was kept in a thermostated cell, the temperature of which was maintained constant within ± 0.1 °C. The course of the reaction was followed by measuring the absorbance at 360 nm at different intervals of time and the concentration of the complex was evaluated from the calibration curve (Fig. 1).

The polarographic measurements were made on a Toshniwal manual polarograph, with a scalamp galvanometer in the external circuit and using a d.m.e. against a saturated calomel electrode. The capillary characteristics in the open circuit were: drop time 3.86 sec Hg pressure 40 cm. pH measurements were carried out on a Cambridge bench type pH meter.

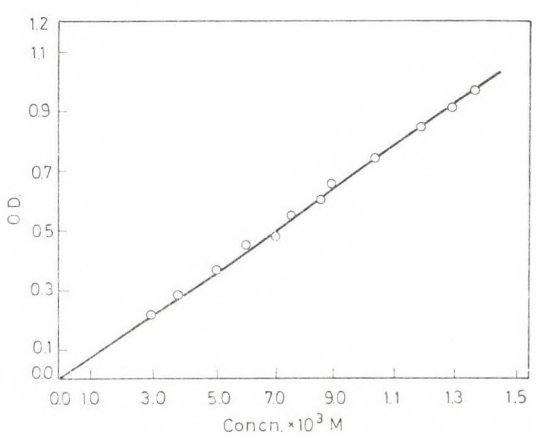

Fig. 1. Calibration curve for the complex

Results and Discussion

Effect of pH

For determining the most suitable pH for complex formation, the kinetic runs were made between pH 1.0 and 4.6. At pH 4.6 precipitation occurred and hence the effect of pH greater than this could not be investigated. Further it was observed that the rate constant increased with an increase of $[OH^-]$ and reached a maximum at $[OH^-]$ 2.0×10^{-10} mol dm^{-3} corresponding to pH 4.3. Hence subsequent kinetic runs were made at pH 4.3. Further a plot of log k_2 *vs* log $[OH^-]$ was found to be linear (Fig. 2).

Order of reaction

A plot of $\frac{a}{a-x}$ (a is the initial concentration of reactants and x is the conc. of complex formed after time t) *vs* time at equimolar concentration of the reactants was found to be linear suggesting that the reaction follows second order kinetics. The order with respect to each reactant was determined by carrying out the reaction at varying concentrations in each case but at nearly constant ionic strength. From these runs the value of $\left(\frac{dx}{dt}\right)$ was evaluated by plane mirror method [8]. A plot of log $\left(\frac{dx}{dt}\right)$ *vs* log c (where c is the

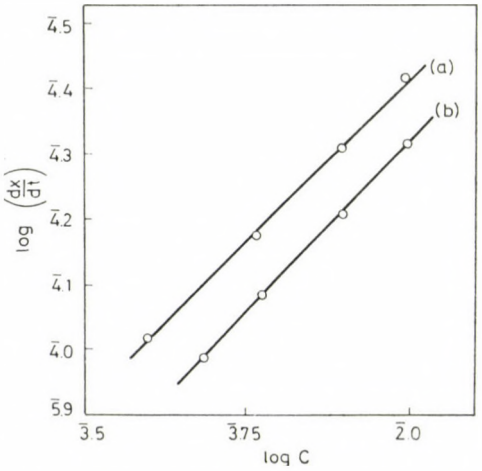

Fig. 2. Plots for order in Cr(III) and $Mo(CN)_8^{4-}$. Curve(a) — Variation of $[Mo(CN)_8^{4-}]$ at 50 °C, $[Cr(III)] = 2.0\times10^{-2}$ mol dm^{-3} Curve(b) — Variation of [Cr(III)] at 50 °C, $[Mo(CN)_8^{4-}] = 2.0\times10^{-2}$ mol dm^{-3}

corresponding concentration of the reactant taken) was found to be linear (Fig. 3) with slopes of 1.01 and 1.1, indicating first order behaviour in $Mo(CN)_8^{4-}$ as well as in Cr(III).

Effect of reactant concentration

From the kinetic results at varying concentration of the reactants but at nearly constant ionic strength the second order rate constants (k_2) were evaluated (Table I). It was seen that the reactant concentration has very little

Table I

Effect of reactants concentration on second order rate constant

(A)	$[Mo(CN)_8^{4-}] = 2\times10^{-2}$ mol dm^{-3}	[KCl] = 0.2 mol dm^{-3}				Temp. = 50 °C	
(B)	$[Cr(III)] = 2\times10^{-2}$ mol dm^{-3}	[KCl] = 0.2 mol dm^{-3}				Temp. = 50 °C	
(A)	$[Cr(III)]\times10^{-2}$ mol dm^{-3}	2.0	1.0	0.8	0.6	0.5	0.4
	$k_2\times10^3$ dm^{3}mol$^{-1}M^{-1}$	9.86	9.64	9.38	9.01	8.89	8.50
(B)	$[Mo(CN)_8^{4-}]\times10^{-2}$ mol dm^{-3}	2.0	1.0	0.8	0.6	0.5	0.4
	$k_2\times10^3$ dm^{3}mol$^{-1}M^{-1}$	9.86	9.60	9.40	9.13	8.81	8.76

effect on the second order rate constant. This consistency in second order rate constants with the varying concentration of reactants further confirms the second order kinetic behaviour for this reaction.

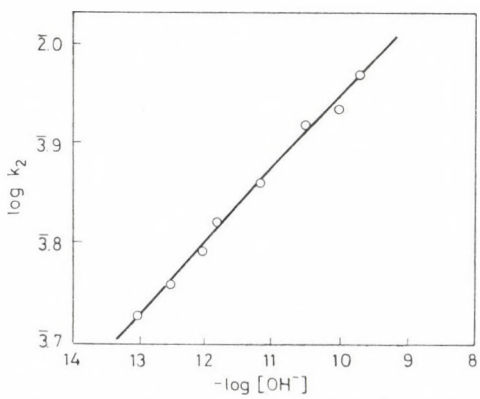

Fig. 3. Effect of $[OH^-]$ on the second order rate constant. $[Mo(CN)_8^{4-}] = [Cr(III)] = 1\times10^{-2}$ mol dm^{-3}, temp. = 50 °C, CH_3COONa = HCl buffer

Thermodynamic parameters

By studying the kinetics at 318, 323, 328, 333 and 338 K, the activation energy, entropy of activation and frequency factors were evaluated. Activation energy: 89.45 $kJmol^{-1}$; entropy of activation: 166.0 $JK^{-1}mol^{-1}$, and frequency factor: 6.1×10^7 $dm^3\,mol^{-1}\,s^{-1}$.

Salt effect

The nature of salt effect was investigated by using KCl as a neutral salt. The plot of $\log k_2$ *vs.* $\mu^{1/2}$ was found to be linear with a slope of 3.95 (Fig. 4), indicating that the negative salt effect was exponential in character. This suggested that the rate-determining process was the reaction between ions of opposite charge. The specific effect of different ions investigated *viz.*, K^+, Na^+, Mg^{++}, Cl^-, Br^-, I^-, Ac^-, NO_3^-, ClO_4^-, SO_4^{--} was rather negligible. The effect of Cu^{2+}, Ag^+, Mn^{2+} Zn^{2+}, Ca^{2+} and Ba^{2+} could not be investigated because of precipitate formation.

Solvent effect

The reaction was studied in the following solvent systems of varying composition: methanol-water, ethanol-water and dioxane-water. The corresponding dielectric constants for these solvent systems were obtained from literature [9, 10], the interpolated values being used when required. In all the three solvent mixtures (methanol-water, ethanol-water and dioxane-water) the rate decreases with an increase in dielectric constant. The plot of $\log k_2$ *vs.* $\frac{1}{D}$ (Fig. 5) was linear only in the rate of higher dielectric constants, suggesting that the rate determining process should be between oppositely charged ions [11].

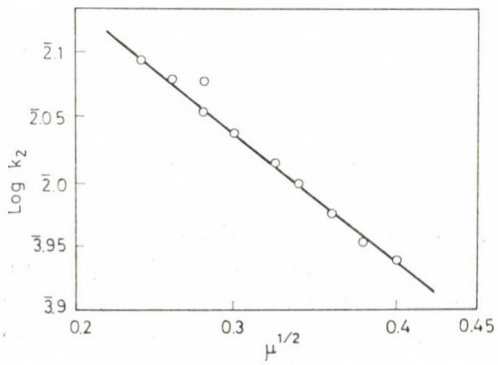

Fig. 4. Effect of ionic strength. $[K_4Mo(CN)_8] = [CrCl_3] = 5.0 \times 10^{-3}$ mol dm^{-3}, temp. 50 °C

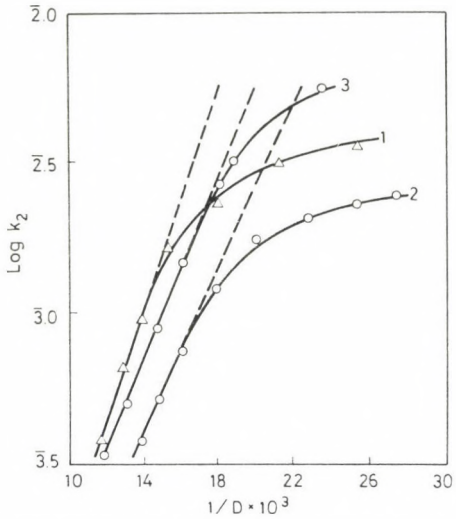

Fig. 5. Effect of dielectric constant. 1-C_2H_5OH + H_2O mixture, 2-CH_3OH + H_2O mixture, 3-Dioxane + H_2O mixture, $[K_4Mo(CN)_8] = [CrCl_3] = 5.0 \times 10^{-3}$ mol dm^{-3}, temp. 30 °C

PH *change with time*

It was seen that in an unbuffered medium, there was a slight increase in pH early during the reaction after which it attained a constant value (Table II).

Table II

Change of pH *with time*

$[Mo(CN)_8^{4-}] = [Cr(III)] = 1.0 \times 10^{-2}$ mol dm^{-3}; Temp. = 50 °C

Time (min)	2	10	20	30	40	50	60	80
pH	4.01	4.16	4.22	4.25	4.32	4.34	4.34	4.34

Polarographic evidence for the intermediate $Cr(CN)_2^+$

The evidence for the presence of $Cr(CN)_2^+$ was obtained polarographically using LINGANE's method. The polarogram of $CrCl_3$ in 0.1 moldm^{-3} KCl as a supporting electrolyte was first of all recorded and $E_{1/2}$ measured. Thereafter the $E_{1/2}$ was recorded in the presence of various CN^- concentrations. From the plot of $E_{1/2}$ *vs.* log CN^- (Fig. 6), the formula of the complex was found to be $Cr(CN)_2^+$ (slope = −0.113).

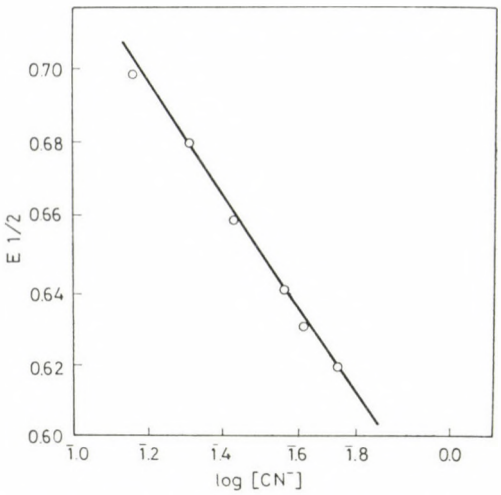

Fig. 6. Shift of $E_{1/2}$ with change in $[CN^-]$

Mechanism

On the basis of kinetic and other evidences the following reaction mechanism is proposed:

$$Mo(CN)_8^{4-} + 2H_2O \overset{K^1}{\rightleftharpoons} Mo(CN)_8(H_2O)_2^{4-} \quad (1)$$

$$Mo(CN)_8(H_2O)_2^{4-} \overset{K^2}{\rightleftharpoons} Mo(CN)_6(H_2O)_2^{2-} + 2CN^- \quad (2)$$

$$CN^- + H_2O \overset{K^3}{\rightleftharpoons} HCN + OH^- \quad (3)$$

$$Mo(CN)_6(H_2O)_2^{2-} + OH^- \overset{K^4}{\rightleftharpoons} Mo(CN)_6(H_2O)(OH)^{3-} \quad (4)$$

$$Cr(III) + 2CN^- \overset{K^5}{\rightleftharpoons} Cr(CN)_2^+ \quad (5)$$

$$Mo(CN)_6(H_2O)(OH)^{3-} + Cr(CN)_2^+ \overset{K^6}{\rightleftharpoons} Cr[Mo(CN)_6(H_2O)(OH)] + 2CN^- \quad (6)$$

According to the above mechanism the rate of formation of the complex (denoted by P) is given by,

$$\frac{d[P]}{dt} = k^6[Mo(CN)_6(H_2O)(OH)^{3-}][Cr(CN)_2^+] \quad (i)$$

From equilibrium processes (1), (2) and (4),

$$[Mo(CN)_6(H_2O)(OH)^{3-}] = \frac{K^1K^2K^4[Mo(CN)_8^{4-}][OH^-]}{[CN^-]^2} \quad (ii)$$

whereas from equilibrium process (5)

$$[Cr(CN)_2^+] = K^5[Cr(III)][CN^-]^2 \qquad \text{(iii)}$$

Substituting these values,

$$\frac{d[P]}{dt} = K^1K^2K^4K^5K^6[Mo(CN)_8^{4-}][Cr(III)][OH^-]$$
$$= k_2[Mo(CN)_8^{4-}][Cr(III)][OH^-] \qquad \text{(iv)}$$

where k_2 is the experimental second order rate constant.

In the above mechanism equilibria (1—5) are rapidly established and as such process-6 is the rate controlling one.

It may be pointed out that octacyanomolybdates have been shown by JAKOB and JAKOB [12] to form the anion $Mo(CN)_8R_2^{4-}$ where R is H_2O or NH_3. Further it is worth-while to mention that a change in the spectra of the system $Mo(CN)_8^{4-} + H_2O$ with time had been reported by COLLENBERG [13]. The spectra of the system $Cr(III) + CN^-$ also changes with time indicating the formation of $Cr(CN)_2^+$, which has also been confirmed polarographically.

The rate equation derived above shows the first order dependence of rate on $[Cr(III)]$, $[Mo(CN)_8^{4-}]$ and $[OH^-]$ as observed experimentally. The rate rapidly increases with an increase in $[OH^-]$, the limitation above pH 4.5 is the precipitation of Cr(III). Chemical analysis data also support the above mechanism so far as the final product is concerned. Process (6) a reaction between a negative and a positive ion is supported by the nature of salt effect and solvent effect observed. Besides this, the positive value of the entropy of activation is in agreement with that theoretically expected.

*

One of us (VKG) is thankful to C. S. I. R., New Delhi, India for awarding a post-doctoral fellowship.

REFERENCES

[1] WARDLAW, W. *et al.*: J. Chem. Soc., **1927,** 512
[2] MALIK, W. U., ALI, S. I.: Bull. Chem. Soc. Japan, **34,** 1306, 1310 (1961), Talanta **1961,** 737; J. Inorg. Nucl. Chem., **20,** 155 (1961)
[3] MALIK, W. U., JAIN, J. P.: J. Indian Chem. Soc., **5,** 1071 (1968)
[4] ROSENHEIM, A.: Z. anorg. Chem., **49,** 148 (1906); **54,** 97 (1907)
[5] FIESER, L. F.: J. Am. Chem. Soc., **52,** 5226 (1930)
[6] KOLTHOFF, I. M.: J. Phys. Chem., **46,** 247 (1936)
[7] VOGEL, A. I.: A Text book of Quantitative inorganic Analysis, Longman's London, 4th Ed. 1978, p. 471—472
[8] LATASHAW, M.: J. Am. Chem. Soc., **47,** 793 (1925)
[9] AKERLOF, G.: J. Am. Chem. Soc., **54,** 4125 (1932)
[10] AKERLOG, G., SHORT, O. A.: J. Am. Chem. Soc., **58,** 1241 (1936)

[11] AMIS, E. S.: Solvent Effect on Reaction Rates and Mechanism, Academic Press, N. Y. 1966
[12] JAKOB, W., JAKOB, Z.: Chem. Abstr., **48**, 8690 (1954); **57**, 13326 (1962)
[13] COLLENBERG, O.: Z. Physik Chem., **109**, 359 (1924)

Wahid U. MALIK
S. P. SRIVASTAVA
K. K. THALLAM
V. K. GUPTA

Department of Chemistry University of Roorkee, Roorkee-247672, India

Acta Chimica Academiae Scientiarum Hungaricae, Tomus 109 (4), pp. 355—362 (1982)

SOLVOLYSIS RATES IN AQUEOUS-ORGANIC MIXED SOLVENTS, X

SOLVOLYSIS OF DICHLOROACETATE ION IN *i*-PROPYL ALCOHOL-WATER SOLVENT MIXTURES

E. M. DIEFALLAH[1]*, H. A. GHALY[1], M. A. ASHY[2], A. O. BAGHLAF[2] and A. A. EL-BELLIHI[1]

([1]Department of Chemistry, Assiut University, Assiut, Egypt, [2]Department of Chemistry, King Abdul-Aziz University, Jeddah, Saudi Arabia)

Received February 10, 1981
Accepted for publication April 20, 1981

The kinetics of the alkaline solvolysis of dichloroacetate ion in *i*-propyl alcohol-water solvent mixtures have been studied over the temperature range 50.0 to 65.0 °C. The reaction follows a second-order rate law and the reaction is first order with respect to both dichloroacetate and hydroxide ions. The enthalpy and entropy of activation for the reaction shows a minimum at about 0.9 water mole fraction. The significance of these results from the viewpoint of the electrostatic theory and the changing of solvent structure in such mixtures is discussed.

Introduction

The alkaline solvolysis of monochloroacetate ion in binary alcohol-water systems [1—3] proceeds by a direct displacement, a one-step S_N2 mechanism, first order with respect to both monochloroacetate and hydroxide ion. On the other hand, in the alkaline solvolysis of trichloroacetate ion [4—6], the rate-determining step is the breaking of the carbon-carbon bond with concomitant release of CO_2 and the formation of a trichloromethyl carbanion intermediate. Trichloromethanide reacts further with base and ultimately yields salts of hydrochloric and formic acids [4, 5]. A detailed study of the alkaline solvolysis of dichloroacetate ion has not been reported and a comparison of the results obtained in this case with those reported previously for mono- and tri-chloroacetates would be desirable. The results have shown that there are large differences in solvolysis reaction order, specific rate constants and mechanisms between mono-, di- and tri-chloroacetate ions.

The extensive investigation of FAINBERG and WINSTEIN [7] on the change in $\Delta H^{\ddagger}$ and $\Delta S^{\ddagger}$ with solvent composition for the solvolysis of *t*-butyl chloride showed a dramatic change in these parameters with solvent composition and the need for a detailed study of solvent effects in solvolysis reactions was clearly indicated. The variation in the activation parameters has been

* For correspondence: Faculty of Science, Zagazig University of Benha, Benha, Egypt.

discussed in terms of the change in the polarity of the substrate in the activation process and more recently in terms of the effect of added co-solvent on the structure of water [8, 9]. The unusual properties resulting from the structural nature of water are reflected in the properties of aqueous solutions of ions and weakly polar molecules and in solvolytic reactions, these unusual properties are expected to be evident in the experimental results [10].

Experimental

For all rate determinations, C. P. grade dichloroacetic acid (obtained from Riedel-de Haen Ab Seelze-Hannover) was used without further purification; *i*-propyl alcohol, reagent grade (obtained from BDH Chemicals, Ltd., England) was distilled (b.p. 82.5 °C) and the middle fraction used. Doubly distilled water and purified alcohol were used to prepare all the solutions. All solvent mixtures used throughout the investigation were mixed by weight, and mole fractions were then calculated. Enough of each solvent mixture was made to complete the series of studies and for each kinetic run solutions of the acid or base of the appropriate concentration in the appropriate solvent were prepared immediately before doing each experiment.

The rate of reaction was followed in the temperature range 50.0 to 65.0, by following the release of chloride ions using a titrimetric method [11]. The initial concentrations of dichloroacetic acid were in the range 0.2 to 0.4 mol/L, while the initial concentrations of base were in the range 0.05 to 0.4 mol/L. In each reaction mixture, the concentration of the base was always less than twice that of the dichloroacetate ion in the reaction solution. In solvent mixtures rich in *i*-propyl alcohol (with less than 50 wt. % water) and especially at the higher temperatures, there appears a dark brown oily layer in the reaction solution due to a slow side reaction, which is probably an esterification going in parallel to the solvolysis reaction. This causes a scatter in the data and, therefore, experiments at temperatures higher than 60 °C and in solvent mixtures with more than about 50 wt. % *i*-propyl alcohol have been discontinued.

Calculations

In dilute alkaline solution, dichloroacetate ion is hydrolyzed according to the equation:

$$CHCl_2{-}\overset{\displaystyle O}{\overset{\|}{C}}{-}O^- + 2\,OH^- \rightarrow CH{-}\overset{\displaystyle O}{\overset{\|}{C}}{-}O^- + 2\,Cl^- + H_2 \qquad (1)$$

It is found experimentally that the rate of reaction is first order with respect to both dichloroacetate and hydroxide ion concentration. The rate of solvolysis follows the second order rate expression:

$$(dx/dt) = k(a - x)(b - 2x) \qquad (2)$$

which yields the integrated form:

$$kt = \frac{1}{2a - b} \ln \frac{b(a - x)}{a(b - 2x)} \qquad (3)$$

where x = amount of dichloroacetate ion (mol/L) reacting in time t, a = initial concentration of dichloroacetate ion, b = initial concentration of base, and k = specific reaction rate constant. The rate constants were evaluated from the slopes of the straight lines obtained when $\ln\left((b(a - x)/a(b - 2x)\right)$ is

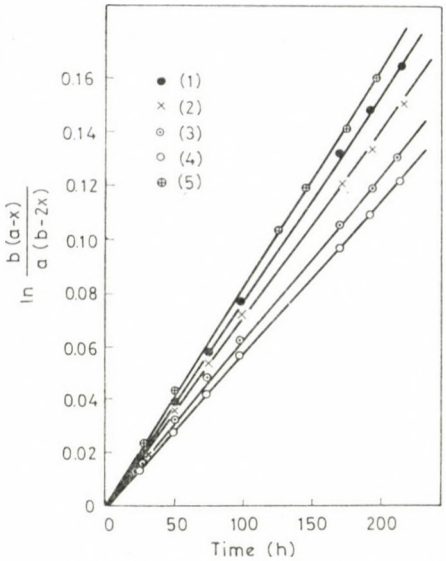

Fig. 1. Second-order plots at 60.0 °C in *i*-propyl alcohol-water solvent mixtures. Water mole fraction: (1) 1.00; (2) 0.968; (3) 0.930; (4) 0.769; (5) 0.690

plotted against t. Figure 1 shows typical plots in *i*-propyl alcohol—water solutions at 60 °C.

Energies of activation in the various solvent mixtures were calculated from the temperature coefficient of the reaction rates. Activation entropies and enthalpies were calculated from the rate constants using the absolute rate theory equations [12]:

$$k = \frac{RT}{Nh} e^{-\Delta H^{\ddagger}/RT} e^{\Delta S^{\ddagger}/R} \tag{4}$$

and

$$\Delta S^{\ddagger} = R\left(\ln A - \ln\left(eRT/Nh\right)\right) \tag{5}$$

where A is the frequency factor, (R/N) is the Boltzmann gas constant and h is Planck's constant.

Results and Discussion

The solvolysis of dichloroacetate ion in *i*-propyl alcohol—water mixtures was investigated over the temperature range 50.0—65.0 °C. The rate of reaction was first order with respect to both dichloroacetate and hydroxide ions. The base-induced hydrolysis of dichloroacetate ion would thus involve an initial slow attack of hydroxide ion and formation of the unstable chlorohydroxyacetate intermediate:

$$\begin{array}{l} \mathrm{Cl} \\ | \\ \mathrm{H{-}C{-}COO^-} \\ | \\ \mathrm{Cl} \end{array} + \mathrm{OH^-} \xrightarrow[-\mathrm{Cl^-}]{\text{slow}} \begin{array}{l} \mathrm{OH} \\ | \\ \mathrm{H{-}C{-}COO^-} \\ | \\ \mathrm{Cl} \end{array} \tag{6}$$

This, in turn, is followed by a fast step in which the reaction intermediate eliminates hydrochloric acid to yield glyoxylate:

$$\begin{array}{l} \mathrm{OH} \\ | \\ \mathrm{H{-}C{-}COO^-} \\ | \\ \mathrm{Cl} \end{array} \xrightarrow[-\mathrm{HCl}]{\text{fast}} \begin{array}{l} \mathrm{O} \\ \| \\ \mathrm{H{-}C{-}COO^-} \end{array} \qquad (7)$$

Table I shows the results of the rate constants obtained at different temperatures and in different solvent mixtures. The rate constants represent the average of at least three determinations. In each solvent mixture, the dielectric constant (D) was taken from the experimental data of AKERLÖF [13] or calculated from these values by interpolation between different temperatures or between different solvent composition. It can be seen that the rate of reaction first decreases, as the *i*-propyl alcohol content of the solution increases to a broad minimum between 0.8 and 0.95 water mole fraction depending on temperature, and then increases. These results are different from those of the solvolysis of mono- and tri-chloroacetates in aqueous alcohol solvent systems, which would probably be due to differences in reaction mechanisms [1—6]. In the alkaline solvolysis of dichloroacetate ion, since the highly polar transition state is more strongly solvated relative to the less polar ground state, it is expected that as the solvent polarity increases the reaction rate increases [14]. However, data in Table I show that this is only satisfied in the water-rich solvent mixtures and the plot of $\log k$ *vs.* $1/D$, shown in Figure 2 is nonlinear, giving a broad minimum at about 0.88 water mole fraction.

A change in solvent usually affects both the enthalpy and entropy of activation [15]. Energies of activation were found from the temperature dependence of the rate constants according to the Arrhenius equation, making

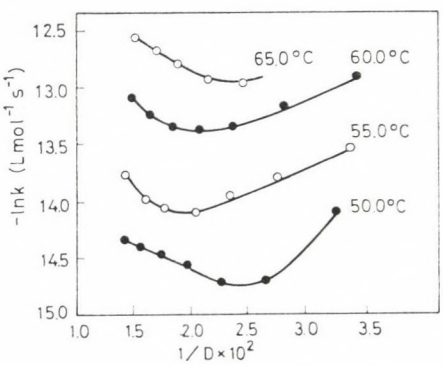

Fig. 2. Dependence of the second-order rate constant on the dielectric constant of the medium

use of the method of least squares. Activation entropies and enthalpies were then calculated according to the absolute rate theory equations [12]. Table II shows the activation parameters calculated at 50.0 °C. The free energies of activation $\Delta G^{\ddagger}$, listed in Table II do not change much with solvent composition. This must be due to the linear compensation between $\Delta H^{\ddagger}$ and $\Delta S^{\ddagger}$. The plot of $\Delta H^{\ddagger}$ *vs.* $\Delta S^{\ddagger}$ gave rise to a straight line as shown in Figure 3. This behaviour is expected if the solvents in a series play closely similar roles in the reaction [15] and has been observed in many systems as well as for the solvolysis of mono- and trichloroacetate ions in aqueous organic solvent binary mixtures [1—4].

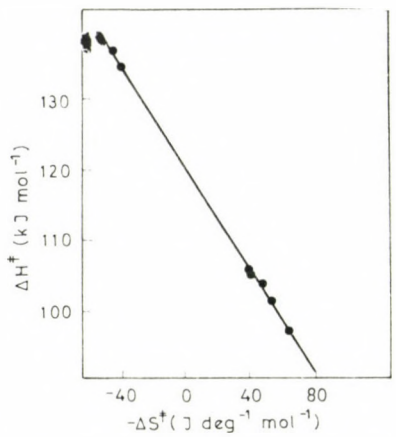

Fig. 3. A plot of $\Delta H^{\ddagger}$ *vs.* $\Delta S^{\ddagger}$ for the alkaline solvolysis of dichloroacetate ion in a series of *i*-propyl alcohol-water solvent mixtures

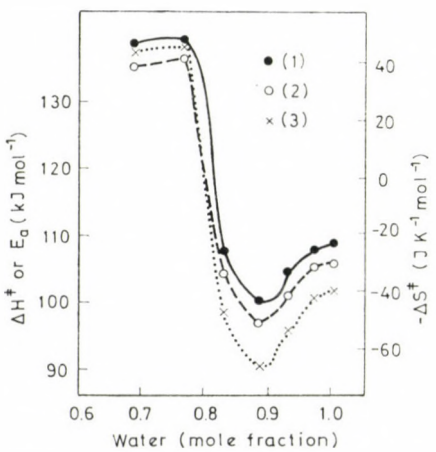

Fig. 4. Dependence of E_a, $\Delta H^{\ddagger}$ and $\Delta S^{\ddagger}$ on solvent composition: (1) E_a; (2) $\Delta H^{\ddagger}$; (3) $\Delta S^{\ddagger}$

The variation of $\Delta H^{\ddagger}$ and $\Delta S^{\ddagger}$ with solvent composition is shown in Figure 4. It is seen that when the concentration of *i*-propyl alcohol in the solvent mixture is increased, the enthalpy and entropy of activation first decrease to a minimum at about 0.88 water mole fraction, and then increase. The depth of $\Delta H^{\ddagger}$ minimum relative to pure water is about 8.4 kJ/mol and

Table I

Effect of temperature and solvent composition on the rate constants of the alkaline solvolysis of dichloroacetate ion in i-propyl alcohol-water solvent mixtures

i-propyl alcohol (wt. %)	Temp. (°C)	Dielectric Constant	$k \times 10^7$ (M^{-1} s^{-1})
0	50.0	69.85	5.89±0.3
	55.0	68.13	10.42±0.06
	60.0	66.62	20.25±0.6
	65.0	64.99	34.36±0.3
10	50.0	63.12	5.56±0.2
	55.0	61.83	8.33±0.08
	60.0	60.24	17.61±0.03
	65.0	58.94	31.39±0.08
20	50.0	56.61	5.14±0.1
	55.0	55.35	7.92±0.1
	60.0	53.87	15.75±0.6
	65.0	52.71	27.78±0.08
30	50.0	50.18	4.81±0.1
	55.0	48.91	7.36±0.1
	60.0	47.58	15.47±0.3
	65.0	46.49	23.75±0.7
40	50.0	43.54	4.03±0.1
	55.0	42.50	8.75±0.6
	60.0	41.35	15.94±0.3
	65.0	40.33	23.33±1.3
50	50.0	37.03	4.11±0.08
	55.0	36.06	10.00±0.5
	60.0	35.05	18.72±0.6
60	50.0	30.67	5.44±0.3
	55.0	29.69	12.89±0.6
	60.0	28.90	24.39±0.3

Table II

Activation parameters (at 50.0 °C) for the alkaline solvolysis of dichloroacetate ion in i-propyl alcohol-water solvent mixtures

i-Propyl alcohol (wt. %)	Water mole fraction	E_a (kJ/mol)	$\Delta H^{\ddagger}$ (kJ/mol)	$-\Delta S^{\ddagger}$ (J/K mol)	$\Delta G^{\ddagger}$ (kJ/mol)
0	1.00	108.3	105.6	38.34	118.0
10	0.968	107.9	105.2	40.52	118.3
20	0.930	104.4	101.7	51.94	118.5
30	0.866	100.6	97.95	64.00	118.6
40	0.833	107.0	104.3	44.95	118.8
50	0.769	135.9	133.2	−44.41	118.8
60	0.690	134.4	131.7	−42.11	118.1

that for $\Delta S^{\ddagger}$ is about 25 J/K mol. These values are about one-half of that found in the solvolysis of monochloroacetate ion [1] and trichloroacetate ion [4] in water–methanol solutions and indicate that the nature of the alcohol co-solvent is important in determining the magnitude of the depth of the extrema in the activation parameters observed for many solvolysis reactions in binary alcohol–water solvent systems [2]. It can also be seen that for solvent mixtures with less than about 30 wt. % *i*-propyl alcohol (0.88 water mole fraction) the principal contribution toward decreasing rate is from the decrease in $\Delta S^{\ddagger}$ which outweighs the increase in rate caused by the decrease in $\Delta H^{\ddagger}$. On the other hand, for solvent mixtures with more than about 30 wt. % *i*-propyl alcohol, the increase in $\Delta S^{\ddagger}$ (by about 100 J/K mol between 0.88 and 0.7 water mole fraction) causes an increase in reaction rate which outweighs the decrease in rate caused by an increase in $\Delta H^{\ddagger}$.

It is believed that hydrolytic reactions in water reflect and indeed are to some considerable extent determined by the properties of liquid water [16]. The extremum behaviour of the activation parameters reflects a common solvent behaviour [8—10], which has been related to the accompanying solvent re-organization accompanying the activation process in binary alcohol–water systems [10]. Water is a very highly structured liquid, made of a mixture of fluctuating regions of three-dimensional hydrogen-bonded polymers in equilibrium with randomly arranged H_2O monomer molecules. On the other hand, aliphatic alcohols have a considerable fraction of their molecules joined in rings and chains, but they do not seem to participate in the formation of three-dimensional clusters that are characteristic of water [8]. The changes in structural features surrounding the reacting species and the transition state as well as the breaking of the solvent structure during the attainment of the transition state are specifically influential in controlling the rate of reaction

and hence the magnitude of the enthalpies and entropies of activation for the reaction [9].

It can be deduced that the reduction in $\Delta H^{\ddagger}$ on the addition of small increments of alcohol to water is the consequence of compensating changes in the solvation of the initial state [9]. Each added increment of alcohol appears to move the initial state solvation shell closer to that of the transition state. ARNETT and co-workers [8] claimed that the addition of small increments of alcohol to water produce a greater degree of hydrogen bonding. This extended quasi-aqueous structure is sensitive to changes in temperature [9] and pressure [17]. The capacity of water to maintain a quasi-aqueous structure presumably through an extension of co-operative hydrogen bonding in the presence of increasing concentrations of weakly polar alkyl groups is distinctly limited, the limit depending in an obvious way on the size of the alkyl group [2, 9]. Any addition of co-solvent beyond that limit (about 0.1 mole fraction for *i*-propyl alcohol), leads to a rapid change in the properties of the solvent consistent with a break down of solvent structure. In such cases it is concluded that hydrogen bonding maintaining extended co-operative structure is weaker than the thermal agitation tending to disorganize structure and the quasi-aqueous structure is replaced by a solvent with quite different characteristics [9, 18].

REFERENCES

[1] AZZAM, A. M., DIEFALLAH, E. M.: Z. Phys. Chem. Neue Folge, **91,** 44 (1974)
[2] DIEFALLAH, E. M.: Can. J. Chem., **54,** 1687 (1976)
[3] DIEFALLAH, E. M., KHAIL, A. M.: Ind. J. Chem., **14A,** 1012 (1976)
[4] DIEFALLAH, E. M., GHONAIM, S. A.: J. Chem. Soc. Perkin II, **1977,** 1237
[5] DIEFALLAH, E. M., EL-NADI, A. M.: Can. J. Chem., **56,** 2053 (1978)
[6] DIEFALLAH, E. M.: Z. Naturforsch., **34**b, 744 (1979)
[7] WINSTEIN, S., FAINBERG, A. H.: J. Am. Chem. Soc., **79,** 5937 (1957)
[8] ARNETT, E. M., BENTRUDE, W. G., BURKE, J. J., DUGGLEBY, P. M.: J. Am. Chem. Soc., **87,** 1541 (1965)
[9] ROBERTSON, R. S., SUGAMORI, S. E.: J. Am. Chem. Soc., **91,** 7254 (1969)
[10] ROBERTSON, R. E.: Prog. Phys. Org. Chem., **4,** 213 (1967)
[11] VOGEL, A. I.: A Text-book of Quantitative Inorganic Analysis, 2nd. ed. Longmans Green and Co. 1957
[12] FROST, A. A., PEARSON, R. G.: Kinetics and Mechanism, 2nd. ed., Chapter **7,** John Wiley & Sons, Inc., New York 1961
[13] AKERLÖF, G.: J. Amer. Chem. Soc., **54,** 4125 (1932)
[14] INGOLD, C. K.: Structure and Mechanism in Organic Chemistry, Chapter **7,** Cornell University Press, Ithaca, New York 1953
[15] LEFFLER, J. E.: J. Org. Chem., **20,** 1202 (1955)
[16] ROBERTSON, R. E., SUGAMORI, S. E.: Can. J. Chem., **50,** 1353 (1972)
[17] DICKSON, S. J., HYNE, J. B.: Can. J. Chem., **49,** 2394 (1971)
[18] FRANKS, F., IVES, D. J. G.: Quart. Rev., **20,** 1 (1966)

E. M. DIEFALLAH
H. A. GHALY
A. A. EL-BELLINI
} Assiut Univ., Assiut, Egypt

M. A. ASHI
A. O. BAGHLAF
} King Abdul-Aziz Univ., Jeddah, Saudi Arabia

Acta Chimica Academiae Scientiarum Hungaricae, Tomus 109 (4), pp. 363—377 (1982)

LOCATION OF THE SADDLE POINT AND HEIGHT OF THE ACTIVATION BARRIER IN ATOM TRANSFER REACTIONS

T. BÉRCES*, B. LÁSZLÓ and F. MÁRTA

(Central Research Institute for Chemistry, Hungarian Academy of Sciences, Budapest)

Received March 10, 1981
Accepted for publication April 20, 1981

The location and height of the activation barrier in homologous series of A + + BC → AB + C atom transfer reactions has been investigated using the BSBL (bond-strength-bond-length) method. For all reaction series invetisgated, the barrier is shifted to an earlier position along the reaction coordinate as the ratio V^0_{BC}/V^0_{AB} decreases (where V^0_{BC} and V^0_{AB} designate the energies of the splitting and forming bonds, respectively). Correlations between barrier height and V^0_{BC}/V^0_{AB}, as well as between barrier height and location are valid for series of hydrogen atom transfer reactions where A or C is varied, however, these correlations fail for groups of halogen atom transfer reactions differing from one another in the transferred atom B.

Introduction

The activation energy of a chemical reaction generally decreases with increasing exothermicity in a homologous series. Several empirical schemes were suggested to predict correlations between the activation energies and the reaction heats of related hydrogen atom transfer reactions. The first and best known correlation, the OGG—POLANYI (OP) relationship [1], predicts a linear dependence of the Arrhenius activation energy on the reaction energy:

$$E_A = E_0 - \alpha q \tag{1}$$

where E_0 and α are empirical parameters and q, the reaction energy, is positive for exothermic reactions. Although the OP relationship is obeyed in many series of reactions, a number of exceptions are also known. MOK and POLANYI [2] examined related families of reactions in the LONDON—EYRING—POLANYI—SATO (LEPS) [3] and the bond-energy-bond-order (BEBO) [4] approximation, and found that the OP relationship fails to apply even qualitatively for series H + XX, X + HBr and X + HI (X = F, Cl, Br and I). Some halogen atom abstraction reactions also show the reverse trend [5].

* To whom correspondence should be addressed.

On the other hand, the reaction energy appears to influence the location of the saddle point, too, in series of related reactions. This type of correlation, which was first recognized by HAMMOND [6] and set forth in detail by POLANYI [2], predicts early saddle points and transition states resembling the reactants for highly exothermic reactions, while late saddle points and transition states resembling the products are predicted for endothermic reactions.

Furthermore, MOK and POLANYI [2] pointed out that, within a series of related reactions, an increase in the barrier height is accompanied by a shift of the barrier to later locations along the reaction coordinate.

The study of the barrier location and barrier height in

$$A + BC \rightarrow AB + C \tag{2}$$

type atom transfer reactions, carried out by MOK and POLANYI (MP) on the basis of the LEPS and BEBO approximation, allowed the authors to suggest the following relationships:

$$\Delta \log V^{\ddagger} = \alpha \Delta (V^0_{BC} - V^0_{AB}) \tag{3}$$

$$\Delta \log V^{\ddagger} = -\beta \Delta X^{\ddagger}_{AB} \tag{4}$$

$$\Delta (V^0_{BC} - V^0_{AB}) = -(\beta/\alpha)\, \Delta X^{\ddagger}_{AB} \tag{5}$$

In these equations a and β are constants within a reaction series, $(V^0_{BC} - V^0_{AB})$ is the energy of the products minus the energy of the reactants (without inclusion of zero-point energies), $V^{\ddagger}$ is the classical barrier height (without inclusion of zero-point energies), and $X^{\ddagger}_{AB} = R^{\ddagger}_{AB} - R^0_{AB}$ designates the extension of the A—B bond at the saddle point.

A method, called bond-strength-bond-length (BSBL) treatment, has been recently developed for the calculation of rate coefficients and Arrhenius parameters of atom transfer reactions [7]. Activated complex properties predicted by the BSBL method were shown to agree very well with potential energy surface properties obtained from "*ab initio*" quantum mechanical calculations [9]. The success achieved in predicting kinetic parameters and activated complex properties for atom transfer reactions on the basis of the BSBL approximation prompted us to re-examine the location and height of the activation barrier in real series of related reactions of the type A + BC → → AB + C.

Method of calculation and data

In the BSBL treatment [7], the energy of ABC in atom transfer reactions

$$\dot{A} + B : C \rightarrow [ABC] \rightarrow A : B + \dot{C}$$

is obtained along a single collinear minimum energy path leading from reagent to product, without introducing adjustable parameters. As a first approximation, it is supposed that the energy of the triatomic complex ABC can be decomposed into

(i) contribution of the bonding energies in structure $\cdot$A B : C and A : B C$\cdot$;

(ii) stabilization energy contribution due to the delocalization of the odd electron over the three atoms of the complex;

(iii) triplet repulsion energy contribution due to the antibonding between end atoms A and C.

On the basis of these assumptions, the potential energy along the minimum energy path (as compared with the energy of the reagent state) is given by

$$V = \{V_{BC}^0 - g_{BC} V_{BC} - g_{AB} V_{AB}\} + A_{AC} g_{AC} V_{AC} \tag{6}$$

where V_{BC}^0 and V_{AB}^0 denote the potential energy of dissociation (classical dissociation energy) of bonds B—C and A—B, respectively, in isolated BC and AB molecules, $-V_{BC}$ and $-V_{AB}$ stand for the bonding energies in structures $\cdot$ A B : C and A : B C $\cdot$, respectively, g_{AB}, g_{BC} and g_{AC} areweighting functions, and A_{AC} is an end group parameter.

In Eq. (6), $(V_{BC}^0 - g_{BC}V_{BC})$ is associated with the energy required for the partial splitting of the bond B—C, while $-g_{AB}V_{AB}$ corresponds to the energy released in the formation of the partial bond between A and B. Thus, the terms in the { } brackets in Eq. (6) give an estimate of the bonding contributions without the inclusion of the stabilization energy. These contributions will be referred to as the "intrinsic bond rearrangement energy", which we shall designate further on by $V_{b.r.}$. The stabilization energy (*i.e.* that part of the bonding energy which is due to the delocalization of the odd electron) together with the triplet repulsion energy contribution is taken into account in the last term of Eq. (6). This term will be referred to as the end group contribution, which we shall designate by $V_{e.g.}$. It follows from the above discussion that in the BSBL approximation, at any point along the reaction coordinate (including the saddle point as well), the energy of the system ABC (relative to the energy of the reactant configuration) is obtained as the algebraic sum of the intrinsic bond rearrangement energy and the end group contribution:

$$V = V_{b.r.} + V_{e.g.} \tag{7}$$

The procedure of obtaining V from $V_{b.r.}$ and $V_{e.g.}$, adapted in the BSBL treatment, has considerable practical advantages. Namely, it allows us to avoid the separate calculation of the delocalization energy and the triplet repulsion energy, which are quantities hard to estimate [8].

It would be desirable to know the share of the total bonding contribution V_b [contribution (i) plus contribution (ii)] and that of the triplet repulsion energy V_{rep} to the energy V of the system ABC:

$$V = V_{b.} + V_{rep.} \tag{8}$$

The contributions indicated on the right hand side of Eq. (8) cannot be obtained one by one from the BSBL treatment, however, we shall obtain a rough estimate of the triplet energy from the equation [9]

$$V_{rep} = \frac{1}{\alpha_{AC}} V^0_{AC} \exp(-2\beta_{AC} X_{AC})[1 + (\beta_{AC} X_{AC})^{2\alpha_{AC}}] \tag{9}$$

(where $X_{AC} = R_{AC} - R^0_{AC}$ and R^0_{AC}, V^0_{AC} and β_{AC} designate the length, the energy and the Morse constant, respectively, of the A—C bond in isolated molecule AC). With this estimate we may obtain $V_{b.}$ as the difference $(V - V_{rep.})$ from V calculated by the BSBL method.

In the BSBL treatment, the function describing the reaction path (or minimum energy path) in the $X_{AB} - X_{BC}$ plane[1] is given by

$$\exp(-2\beta_{AB} X_{AB}) + \exp(-2\beta_{BC} X_{AC}) = 1 \tag{10}$$

where β_{AB} and β_{BC} designate the Morse constants for A—B and B—C, respectively. The location of any point $p(X_{AB}, X_{BC})$ on this collinear reaction path may be characterized either by the slope of the reaction path,

$$S_p = \left(\frac{dX_{BC}}{dX_{AB}}\right)_p = \frac{\beta_{AB}}{\beta_{BC}} [1 - \exp(2\beta_{AB} X_{AB})]^{-1} \tag{11}$$

or by the reaction coordinate, which is given as an arc length measured along the reaction path from an arbitrary point [7].

Simply for practical reasons, we use in this paper a modified definition for the slope of the reaction path and for the reaction coordinate. Be the new slope at point $p(R_{AB}, R_{BC})$ of the reaction path

$$s_p = \frac{\beta_{BC}}{\beta_{AB}} S_p \tag{12}$$

and the new reaction coordinate (rc)

$$(rc)_p = \frac{s_p}{s_p - 1}. \tag{13}$$

This reaction coordinate[2] increases from $rc = 0$ (reactant state) to $rc = 1$ (product state).

[1] Note that $X_{ij} = R_{ij} - R^0_{ij}$, where R designates the bond length, and the superscript refers to the equilibrium value.

[2] Note that $\frac{s}{s-1} = \exp(-2\beta_{AB} X_{AB})$ and $\left(1 - \frac{s}{s-1}\right) = \exp(-2\beta_{BC} X_{BC})$.

Using the new designations s and $\frac{s}{s-1}$, one may rewrite the BSBL expressions (7) for bond rearrangement energy and end group contribution as follows:[3]

$$V_{\text{b.r.}} = V^0_{\text{BC}} + V^0_{\text{AB}} \frac{s}{s-1}\left[\frac{s}{s-1} - 2\left(\frac{s}{s-1}\right)^{1/2}\right] + \\ + V^0_{\text{BC}}\left(1 - \frac{s}{s-1}\right)\left[\left(1 - \frac{s}{s-1}\right) - 2\left(1 - \frac{s}{s-1}\right)^{1/2}\right] \tag{14}$$

$$V_{\text{e.g.}} = A_{\text{AC}} V^0_{\text{AC}} \exp\left(-2\beta_{\text{AC}} \Delta R^0\right)\left[\left(\frac{s}{s-1}\right)^{\beta_{\text{AC}}/\beta_{\text{AB}}}\left(\frac{s}{s-1}\right)^{\beta_{\text{AC}}/\beta_{\text{BC}}}\right] \tag{15}$$

where $\Delta R^0 = R^0_{\text{AB}} + R^0_{\text{BC}} - R^0_{\text{AC}}$.

In the following section we shall use the BSBL approximation [*i.e.* Eq. (7) with (14) and (15)] as a means to examine the location of the saddle point, the height of the activation barrier and their correlation in series of related atom transfer reactions. Application of the BSBL method requires certain properties of the AB, BC and AC molecules as input parameters. The sources of these data are given in ref. [9].

Results and Discussion

Three types of series of related atom transfer reactions A + BC → → AB + C shall be dealt with. Those homologous series in which A is varied from member to member will be referred to as "type A". The group of reactions differing from one another in the nature of C will be called "type C". Finally homologous series where reactions differ from one another in the transferred atom B will be referred to as "type B".

Reaction profiles for two homologous series which belong to types A and C are shown in Figs 1 and 2, respectively. Certain correlations are immediatelly apparent from the reaction profiles of reactions X + H—I (X = F, Cl, Br, I) and H + H—R [R = CH_3, C_2H_5,$(CH_3)_2$ CH, $(CH_3)_3$C] shown in the Figures and from similar plots of other A and C type reaction groups. The generalizations valid for all A and C type homologous series investigated may be summarized as follows:

(i) Exothermic reactions have "early" saddle points $\left(\frac{s^\ddagger}{s^\ddagger - 1} < \frac{1}{2}\right)$, while endothermic reactions are characterized by "late" saddle points $\left(\frac{s^\ddagger}{s^\ddagger - 1} > \frac{1}{2}\right)$. As the exothermicity increases in a series of related reactions,

[3] R^0_{ij} and V^0_{ij} designate the bond length and potential energy of dissociation, respectively, of bond $i - j$ in the isolated molecule ij.

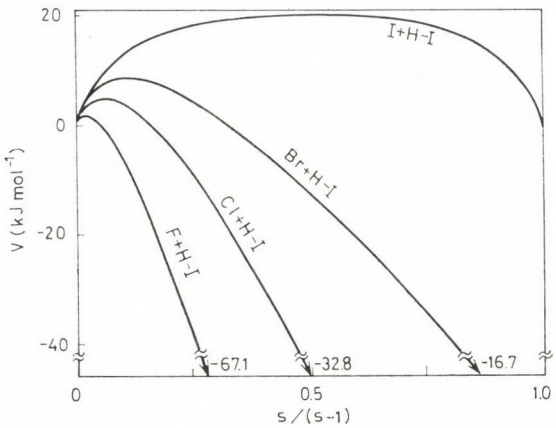

Fig. 1. Reaction profiles for homologous series X + H—I belonging to type A

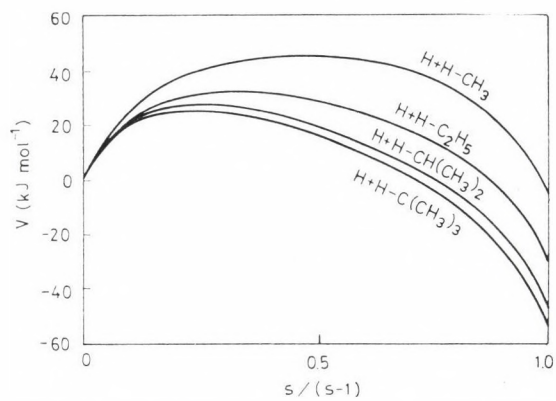

Fig. 2. Reaction profiles for homologous series H + H—R belonging to type C

the saddle point is shifted towards smaller values of the reaction coordinate (*i.e.* towards the reactant state);

(ii) The height of the potential barrier decreases with increasing exothermicity within a series of homologous reactions;

(iii) There is a correlation between barrier location and barrier height: a shift in the barrier location to smaller reaction coordinates is accompanied by a decrease in the barrier height within a series of related reactions.

The validity of these generalizations is also demonstrated by the data[4] given in Tables I and II, where the location of the saddle point $\left(\frac{s^{\ddagger}}{s^{\ddagger}-1}\right.$,

[4] Note that $(V^0_{BC} - V^0_{AB})$ is the reaction energy which is negative for exoergic and positive for endoergic reactions.

Table I

Saddle point location $\left(\frac{s^{\ddagger}}{s^{\ddagger}-1}\right)$ *and barrier height* ($V^{\ddagger}$) *in homologous series belonging to type* A

Series	Reaction	$(V^{0}_{BC}-V^{0}_{AB})$ (kJ/mol)	$\frac{V^{0}_{BC}}{V^{0}_{AB}}$	$\frac{s^{\ddagger}}{s^{\ddagger}-1}$	$V^{\ddagger}$ (kJ/mol)	$V^{\ddagger}_{b}$ (kJ/mol)	$V^{\ddagger}_{rep}$ (kJ/mol)
X + H−Br	I + H−Br	69.9	1.224	0.883	78.7	66.2	12.5
	Br + H−Br	0.0	1.000	0.500	24.3	−1.1	25.4
	Cl + H−Br	−67.4	0.850	0.134	11.9	−4.8	16.7
	F + H−Br	−211.1	0.644	0.060	6.1	−1.7	7.9
X + H−I	I + H−I	0.0	1.000	0.500	19.6	−2.5	22.1
	Br + H−I	−69.9	0.817	0.117	8.8	−3.8	12.5
	Cl + H−I	−137.4	0.695	0.064	5.0	−5.3	10.3
	F + H−I	−281.0	0.527	0.025	1.6	−6.9	8.5
RO + H−H	HOO + H−H	64.5	1.163	0.807	83.4	65.7	17.7
	CH_3O + H−H	2.5	1.005	0.528	35.1	13.1	22.0
	HO + H−H	−61.6	0.882	0.203	22.1	−1.9	24.0

Table II

Saddle point location $\left(\frac{s^{\ddagger}}{s^{\ddagger}-1}\right)$ *and barrier height* ($V^{\ddagger}$) *in homologous series belonging to type* C

Series	Reaction	$(V^{0}_{BC}-V^{0}_{AB})$ (kJ/mol)	$\frac{V^{0}_{BC}}{V^{0}_{AB}}$	$\frac{s^{\ddagger}}{s^{\ddagger}-1}$	$V^{\ddagger}$ (kJ/mol)	$V^{\ddagger}_{b}$ (kJ/mol)	$V^{\ddagger}_{re}$ (kJ/mol)
H + H−X	H + H−F	134.9	1.294	0.888	148.2	131.3	16.9
	H + H−Cl	−8.7	0.981	0.356	26.6	−10.6	37.2
	H + H−Br	−76.1	0.834	0.137	12.2	−9.9	22.1
	H + H−I	−146.1	0.681	0.070	5.5	−8.0	13.5
H + H−R	H + H−CH_3	−5.4	0.988	0.460	45.9	2.9	43.1
	H + H−C_2H_5	−30.5	0.934	0.322	32.5	−3.0	35.5
	H + H−$C(CH_3)_2$	−47.2	0.897	0.262	27.0	−3.7	30.7
	H + H−$C(CH_3)_3$	−53.1	0.884	0.245	25.3	−3.8	29.1
HO + H−R	HO + H−CH_3	−67.0	0.871	0.205	23.0	−17.3	40.3
	HO + H−C_2H_5	−92.1	0.823	0.157	17.2	−11.9	29.1
	HO + H−$CH(CH_3)_2$	−108.9	0.791	0.135	14.6	−14.9	29.5
	HO + H−$C(CH_3)_3$	−114.7	0.779	0.129	13.8	−14.7	28.5

reaction coordinate) and the height of the barrier ($V^{\ddagger}$, potential energy of activation) are indicated in columns 5 and 6, respectively.

Among the six series presented in Tables I and II there are three which were dealt with by MOK and POLANYI (MP), too. These are series X + H—Br, X + H—I and H + H—X. Regarding the trend in the location of the saddle point and barrier height, our results agree with those of MP for series H + + H—X, while they are at variance for series X + H—Br and X + H—I. Namely, for the first three members of series X + H—Br and X + H—I, OP obtained with the BEBO method an increase in the barrier height and a shift in the barrier location to later positions along the reaction coordinate with increasing exothermicity. This disagreement is obviously caused by the failure of the BEBO method used by OP.

According to our results, it appears to be *generally valid for all* A and C type series that in order of increasing exothermicity the potential barrier is shifted to an earlier position along the reaction coordinate (in accordance with previous suggestions of J. C. POLANYI [2] and in conformity with the HAMMOND postulate [6]), barrier height is decreased with increasing exothermicity (as required by the OGG—POLANYI (OP) type relationships [1]), and for decreasing barrier height the barrier moves to successively smaller reaction coordinates (as predicted by MP [2]).

A detailed examination of the data given in Tables I and II shows that dependence of the barrier location and height on V^0_{BC}/V^0_{AB} can be given by the relationships

$$\ln \frac{s^{\ddagger}}{s^{\ddagger} - 1} = a_1 \frac{V^0_{BC}}{V^0_{AB}} - b_1 \tag{16}$$

and

$$\ln V^{\ddagger} = a_2 \frac{V^0_{BC}}{V^0_{AB}} - b_2 \tag{17}$$

where a_1, b_1, a_2 and b_2 are constants within a reaction series.

The $\frac{s^{\ddagger}}{s^{\ddagger} - 1}$ and $V^{\ddagger}$ values taken from the Tables are plotted against V^0_{BC}/V^0_{AB} in Figs 3—5 for series A and in Figs 6—8 for series C. Curves were calculated according to relationships (16) and (17) using the parameters given in Table III. Both relationships are seen to describe the data reasonably well.

The saddle point for symmetric reactions (like Br + H—Br and I + + H—I) is at $\frac{s^{\ddagger}}{(s^{\ddagger} - 1)} = \frac{1}{2}$. One also expects that non-symmetric thermoneutral reactions have saddle points which are not far removed from the location $\frac{s^{\ddagger}}{(s^{\ddagger} - 1)} = \frac{1}{2}$. Substitution of $V^0_{BC}/V^0_{AB} = 1$ in Eq. (16) yields

Table III

Parameters for relationships (16)—(18); *homologous series* A *and* C

	Series A			Series C		
	X + H–Br	X + H–I	RO + H–H	H + H–X	H + H–R	HO + H–R
a_1	5.2	5.6	4.8	4.8	6.2	4.8
b_1	6.3	6.7	5.6	5.9	6.9	5.8
a_2	4.4	4.5	4.7	5.4	5.5	4.0
b_2	1.2	1.6	1.1	2.0	1.6	0.4
a_3	82	73	92	81	101	109

$\frac{s^\ddagger}{(s^\ddagger - 1)} = \exp(a_1 - b_1)$. With the a_1 and b_1 parameters given in Table III, one obtains from this equation $\frac{s^\ddagger}{(s^\ddagger - 1)}$ values which are somewhat smaller than $\frac{1}{2}$. The discrepancy may originate either from the errors of the a_1 and b_1 parameters (which are mainly due to the errors in the input data used in the BSBL calculations of the saddle point locations) or from the approximate nature of Eq. (16). The study of further reactions seems to confirm the first suggestion (consider for instance the parameters indicated in Table V).

It follows from Eqs (16) and (17) that the correlation between barrier location and barrier height should be approximated by

$$V^\ddagger = \exp\left\{(a_2 - a_1)\frac{V^0_{BC}}{V_{AB}} - (b_2 - b_1)\right\}\frac{s^\ddagger}{s^\ddagger - 1} \qquad (18')$$

However, since parameters a_1 and a_2 are similar (if not identical), the terms in braces $\{\}$ can be considered constant in a series, and Eq. (18′) may be replaced[5] by the linear relationship

$$V^\ddagger = a_3\frac{s^\ddagger}{s^\ddagger - 1}. \qquad (18)$$

The similar dependences of $\frac{s^\ddagger}{s^\ddagger - 1}$ and $V^\ddagger$ on V^0_{BC}/V^0_{AB} apparent from Figs 3—8, as well as plots of $V^\ddagger$ against $\frac{s^\ddagger}{s^\ddagger - 1}$ indicate that an approxima-

[5] Considering the probable errors of the input data (bond strengths, bond lengths and vibrational frequencies) used in the calculation of the barrier height and location, one realizes that the difference between the values of a_1 and a_2 is around the error limits. Thus, there is no good reason for preferring the more complicated Eq. (18′) to the simpler relationship (18).

tely linear relationship does exist between barrier height ($V^{\ddagger}$) and barrier location $\left(\frac{s^{\ddagger}}{s^{\ddagger}-1}\right)$ for A and C type series. Parameters a_3 obtained from the slope of such plots are given in Table III.

Barrier locations and barrier heights for three series belonging to type B are given in Table IV. All the reactions presented in the Table are halogen

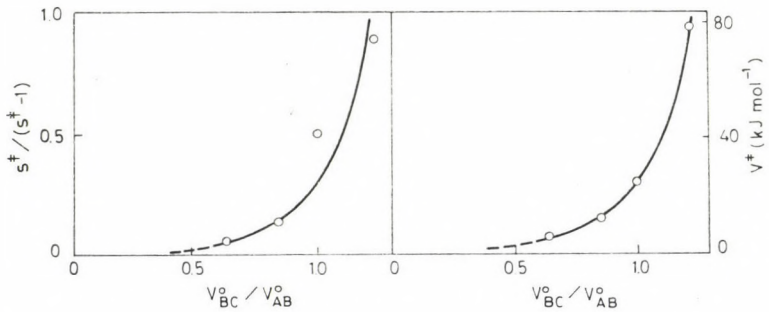

Fig. 3. Dependence of the location and height of barrier on V^0_{BC}/V^0_{AB} in series X + H—Br

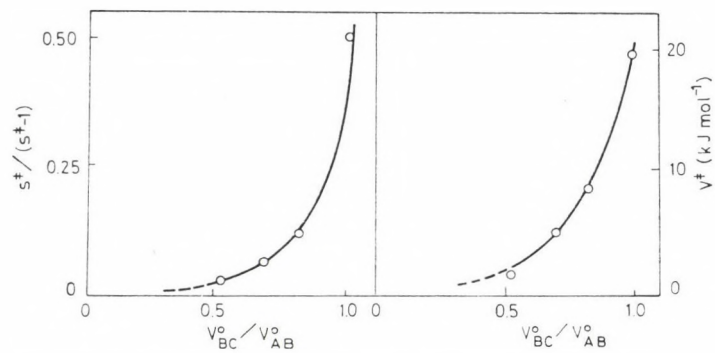

Fig. 4. Dependence of the location and height of barrier on V^0_{BC}/V^0_{AB} in series X + H—I

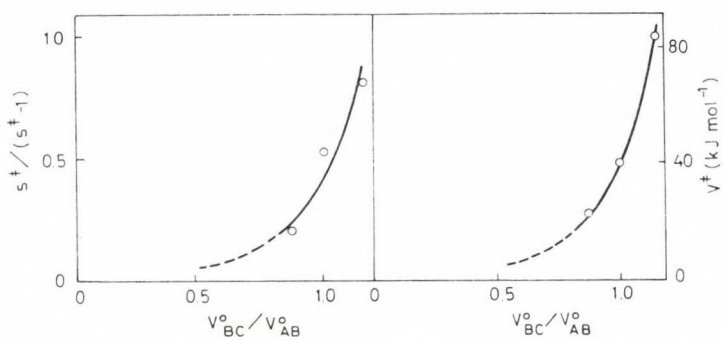

Fig. 5. Dependence of the location and height of barrier on V^0_{BC}/V^0_{AB} in series RO + H—H

atom transfer processes. Series H + X—H and H + X—CH_3 consist of symmetrical and unsymmetrical B type reactions, respectively, while both B and C atoms are varied in series H + X—X.

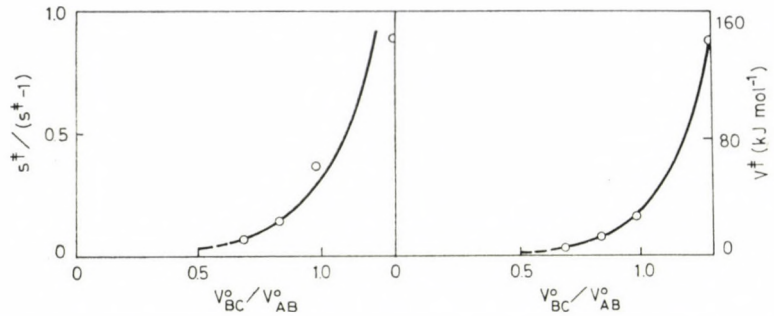

Fig. 6. Dependence of the location and height of barrier on V^0_{BC}/V^0_{AB} in series H + H—X

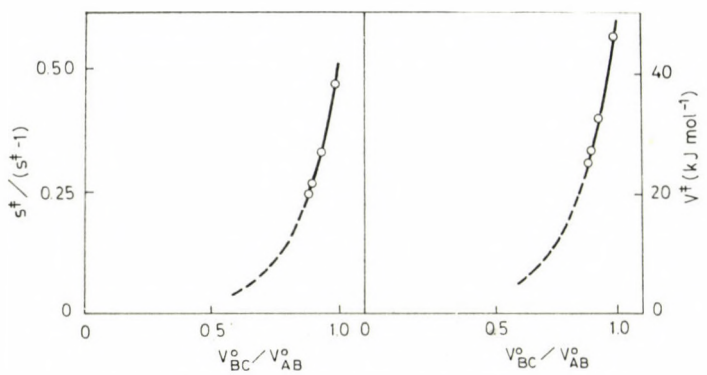

Fig. 7. Dependence of the location and height of barrier on V^0_{BC}/V^0_{AB} in series H + H—R

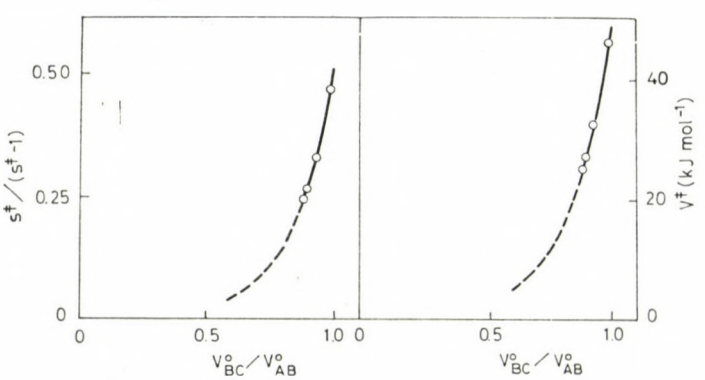

Fig. 8. Dependence of the location and height of barrier on V^0_{BC}/V^0_{AB} in series HO + H—R

Table IV

Saddle point location $\left(\frac{s^{\ddagger}}{s^{\ddagger}-1}\right)$ *and barrier height* ($V^{\ddagger}$) *in series belonging to type* B

Series	Reaction	$(V^0_{BC}-V^0_{AB})$ (kJ/mol)	$\frac{V^0_{BC}}{V^0_{AB}}$	$\frac{s^{\ddagger}}{s^{\ddagger}-1}$	$V^{\ddagger}$ (kJ/mol)	$V^{\ddagger}_0$ (kJ/mol)	$V^{\ddagger}_{re\nu}$ (kJ/mol)
H + X—H	H + F—H	0.0	1.000	0.500	51.7	36.9	14.8
	H + Cl—H	0.0	1.000	0.500	38.6	37.3	1.4
	H + Br—H	0.0	1.000	0.500	32.8	32.3	0.5
	H + I—H	0.0	1.000	0.500	26.8	26.7	0.1
H + X—CH_3	H + I—CH_3	−74.1	0.763	0.123	7.9	7.8	0.1
	H + Br—CH_3	−86.3	0.774	0.129	10.3	10.0	0.3
	H + Cl—CH_3	−95.9	0.787	0.136	12.9	12.1	0.7
	H + F—CH_3	−131.5	0.778	0.136	17.4	8.7	8.7
H + X—X	H + I—I	−160.0	0.488	0.036	1.67	1.65	0.02
	H + Br—Br	−187.6	0.509	0.040	2.36	2.28	0.07
	H + Cl—Cl	−204.4	0.546	0.047	3.48	3.26	0.22
	H + F—F	−429.6	0.276	0.010	0.50	0.29	0.21

While the sequence of reaction energy ($V^0_{BC} - V^0_{AB}$) and the order of ratio V^0_{BC}/V^0_{AB} agree in type A and C series, this is not the case for groups of reactions belonging to type B. Relationships (16) and (17) suggest that one should regard the barrier location and the barrier height as a function of V^0_{BC}/V^0_{AB} rather than ($V^0_{BC} - V^0_{AB}$).

It may be seen from the data presented in Table IV that the saddle point for thermoneutral reactions $\left(\frac{V^0_{BC}}{V^0_{AB}}=1\right)$ is at $\frac{s^{\ddagger}}{s^{\ddagger}-1}=\frac{1}{2}$ and for exothermic reactions $\left(\frac{V^0_{BC}}{V^0_{AB}}<1\right)$ it is in the reactant valley $\left(\text{at } \frac{s^{\ddagger}}{s^{\ddagger}-1}<\frac{1}{2}\right)$. As the ratio V^0_{BC}/V^0_{AB} decreases, the saddle point is shifted to an earlier position $\left(\text{smaller} \frac{s^{\ddagger}}{s^{\ddagger}-1}\right)$ along the reaction coordinate, just as in the case of type A and C series. Relationship (16), which described the location of the barrier in series belonging to type A and C, is valid also for series B. One obtains $a_1 = 4.8$ and $b_1 = 5.7$ for series H + X—CH_3, while $a_1 = 6.0$ and $b_1 = 6.3$ for series H + X—X. These parameters are in accordance with the ones reported for A and C type reaction groups.

The Ogg—Polanyi relationship fails to apply even qualitatively for series belonging to type B. Regarding the dependence of the barrier height on V^0_{BC}/V^0_{AB} and the correlation between barrier height and barrier location,

these correlations appear to apply qualitatively for series H + X—CH_3 and H + X—X, however, relationships (17) and (18) are not valid. Turning to series H + X—H, one may notice immediately that no correlation exists either between $V^{\ddagger}$ and V^0_{BC}/V^0_{AB} or between $V^{\ddagger}$ and $\frac{s^{\ddagger}}{s^{\ddagger}-1}$

Our results presented in this paper indicate that correlation between barrier location and V^0_{BC}/V^0_{AB} applies both for A and C type series and for B type reaction groups. On the other hand, correlations between barrier height and barrier location or between barrier height and V^0_{BC}/V^0_{AB} apply only for A and C type series (hydrogen atom transfer reactions), but fail[6] for B type reaction groups (halogen atom transfer reactions).

In order to inquire into the causes which bring about the break-drown of correlations involving the barrier height for series of type B, we shall attempt to get some idea of the factors which play a predominant role in the determination of the activation barrier. According to Eq. (8), one can decompose the potential energy of activation ($V^{\ddagger}$), obtained by the BSBL method, into total bonding contribution ($V^{\ddagger}_b$) and triplet repulsion energy ($V^{\ddagger}_{rep}$), provided that one of the last two terms can be estimated. Equation (9) was shown to give a good estimate of the triplet energy for the simplest systems [8]. Although this function is definitely less successful in predicting repulsion energies for more complicated cases, nonetheless, the qualitative picture based on $V^{\ddagger}_{rep}$ obtained from Eq. (9) is expected to be correct. With these limitations, we can decompose $V^{\ddagger}$ into $V^{\ddagger}_b$ and $V^{\ddagger}_{rep}$ contributions. The results appear in the last two columns in Tables I, II and IV.

It may be seen from the data given in Tables I and II that the total bonding contributions are typically small negative values[7] for the hydrogen atom transfer reactions which form the A and C type series. In the formation of the activated state, the energy release associated with the partial development of the new bond does somewhat exceed the energy required to split partially the B—C bond. More important, the repulsion energy proves to be larger than the bonding contribution for A and C type series. Thus, the triplet repulsion energy seems to be the predominant factor that determines the barrier height (activation energy) and its variations in the hydrogen atom transfer reactions belonging to the A and C type homologous series.

In the B type series of halogen atom transfer reactions, on the other hand, the bonding contributions are almost without exception comparatively large positive values which definitely exceed the repulsion energies. Thus, the total bonding contribution seems to be the predominant factor that determines

[6] Note that the use of Eqs (17) and (18) would require extreme values for a_2, b_2 and a_3 in case of series H + X—CH_3 and H + X—X.

[7] For endothermic reactions, the bonding energy minus the reaction energy (*i.e.* $V^{\ddagger}_b - (V^0_{BC} - V^0_{AB})$) should be taken into account.

the barrier height (activation energy) and its variation in the halogen atom transfer reactions belonging to the B type series.

It follows from the discussion presented above that the existence of the correlations of the activation barrier for hydrogen atom transfer reactions in series A and C on one hand and the invalidity of these correlations for halogen atom transfer reactions in series B on the other hand may be associated with the difference in the nature of the potential barrier (activation energy) in these two families of atom transfer reactions.

However, the different nature of the potential barrier in hydrogen atom transfer reactions and in halogen atom abstractions cannot be the only reason for the breakdown of the correlations involving the barrier height in case of the B type homologous series presented in Table V. This may be realized if

Table V

Parameters for relationships (16)—(18); C type reaction groups of halogen atom transfer reactions (see text)

	H + F–Y	H + Cl–Y	H + Br–Y	H + I–Y
a_1	5.4	5.2	5.2	5.1
b_1	6.1	6.0	6.0	5.9
a_2	6.5	5.3	5.3	5.4
b_2	2.4	1.6	1.8	2.1
a_3	96	82	67	55

the halogen atom transfer reactions appearing in Table IV are considered as C type reaction groups. Thus one reaction group will consist of reactions H + F—H, H + F—CH_3 and H + F—F, *etc.* It can be shown that relationships (16), (17) and (18) with the parameters given in Table V describe the data of halogen transfer reactions reasonably well. Hence, one may suggest that the breakdown of relationships (17) and (18) is expected in any B type group of reactions where the members differ from one another in the transferred atom, irrespective of the nature of atom B. The study of metathetical reactions other than hydrogen and halogen atom transfers is required in order to confirm this suggestion.

REFERENCES

[1] Ogg, R. A., Polanyi, M.: Trans. Faraday Soc., **31,** 604 (1935); Evans, M. G., Polanyi, M.: Trans. Faraday Soc., **32,** 1333 (1936); Evans, M. G., Polanyi, M.: Trans. Faraday Soc., **34,** 11 (1938); Semenov, N. N.: "Some Problems of Chemical Kinetics and Reactivity", Vol. I, p. 29. Princeton University Press, Princeton, N. J., 1958

[2] Mok, M. H., Polanyi, J. C.: J. Chem. Phys., **51,** 1451 (1969)

[3] SATO, S.: Bull. Chem. Soc. Japan, **28,** 450 (1955); SATO, S.: J. Chem. Phys., **23,** 592, 2465 (1955)
[4] JOHNSTON, H. S., PARR, C.: Amer. Chem. Soc., **85,** 2544 (1963); JOHNSTON, H. S.: "Gas Phase Reaction Rate Theory", Ronald Press Co., New York, 1966
[5] KRECH, R. H., MCFADDEN, D. L.: J. Amer. Chem. Soc., **99,** 8402 (1977)
[6] HAMMOND, G. S.: J. Amer. Chem. Soc., **77,** 334 (1955)
[7] BÉRCES, T., DOMBI, J.: Int. J. Chem. Kinet., **12,** 123 (1980)
[8] BÉRCES, T.: React. Kinet. Catal. Lett., **7,** 379 (1977)
[9] BÉRCES, T., DOMBI, J.: Int. Chem. Kinet., **12,** 183 (1980)

Tibor BÉRCES
Barna LÁSZLÓ
Ferenc MÁRTA
H-1025 Budapest, Pusztaszeri út 59/67.

Acta Chimica Academiae Scientiarum Hungaricae, Tomus 109 (4), pp. 379—388 (1982)

CATALYTIC CONVERSION OF ALCOHOLS, XVII*

COMPARISON OF THE SELECTIVITY OF *ALPHA* AND TRANSITIONAL ALUMINAS

B. H. DAVIS

(Institute for Mining & Minerals Research, University of Kentucky, P.O. Box 13015, Lexington, Ky. 40583 U.S.A.)

Received March 9, 1981
Accepted for publication April 26, 1981

α-Alumina, unlike transitional aluminas, is not a selective dehydration catalyst. For acyclic alcohols the dehydration/dehydrogenation ratio varies from about 0.1 to 0.4; it is a more selective dehydration catalyst for cyclic alcohols (0.4 to 1.3) but still does not approach the selectivity of transitional aluminas. A much larger amount of the *trans*-2- alkene isomer is obtained from 2-ols with α-alumina than with the transitional alumina. *Cis-trans* isomerization of pure *cis-* or pure *trans*-2-methylcyclohexanol is about as rapid as the combined dehydration and dehydrogenation reactions; *cis-trans* isomerization does not occur with transitional alumina.

Introduction

Alumina has been widely studied as an alcohol dehydration catalyst [1, 2, 3]. Attempts have been made to relate catalytic activity to some property of the catalytic solid such as ionic radius [4] or heat of formation of the oxide [5]. Much work has been directed toward relating alcohol conversion rates to the transitional alumina crystal type [for example, 6, 7, 8, 9].

Recently it was reported that transitional aluminas pretreated at 550—600 °C with oxygen may be as active for dehydrogenation as they are for dehydration [10]. DALLA LANA and co-workers [11] observed a similar pretreatment dependency in their i.r. studies. Furthermore, studies with α-alumina have shown that it has some, or only, dehydrogenation activity for isopropyl alcohol [for example, 6, 8].

In this study we have examined the dehydration-dehydrogenation selectivity and the alkene selectivity of α-alumina with several alcohols to compare the selectivity to that of the transitional aluminas.

Experimental

Catalysts. Nordstrandite alumina (Al—N) was prepared according to Example 1 in Reference [12]. With this method an aluminum chloride solution is added, with stirring, to a solution of ammonium hydroxide and ammonium carbonate. The resulting gel is aged overnight, washed, dried at 120 °C, and then calcined in air at 550 °C. The BET surface area of the alumina was 220 m^2/g.

* Part XVI.: J. Chem. Soc., Faraday I, **76**, 1971 (1980).

α-Alumina was prepared by heating a portion of the above alumina in air at 1200 °C for three days. The BET surface area of the material was 4.5 m^2/g. The x-ray diffraction pattern was consistent with that expected for α-alumina [13]. The surface area loss and preparation procedures are expected to lead to α-alumina [13].

Alon-C was obtained from Cabot Corp. and had a surface area of 106 m^2/g.

Al—W was provided by Professor W. H. WADE and is designated Sample B in Reference [14]. It is γ-alumina with a surface area of 104 m^2/g.

Catalyst Regeneration. After each run the reactant flow was stopped, and the catalyst was cooled to room temperature and then flushed with air at room temperature prior to heating 250 °C in air. After about 3 h at 250 °C, the temperature was increased to 500 °C in air: after 1 h the air was replaced by an oxygen flow; and after 3 h the oxygen was replaced by hydrogen and the catalyst was held at 500 °C in hydrogen for 4 to 7 h. The catalyst was cooled to the reaction temperature in flowing hydrogen. When results are given for an oxygen pretreated catalyst, the above procedure was followed except the hydrogen pretreatment was omitted.

Alcohols. Alcohols were purchased from commercial sources. Most alcohols contained less than 1% ketone, and in many cases it was much less than this. However, 2-octanol contained approximately 1.5% 2-octanone. The pure *cis-* or *trans*-2-methylcyclohexanol contained less than 0.5% of the other isomer.

Procedure and analyses. The reactor system was of conventional design with a motor-driven syringe liquid feed, an electrically heated plug flow reactor, and a liquid sample collector. The alcohol was pumped over the catalyst at atmospheric pressure without added carrier gas. The LHSV was varied from 0.4 to 12 h^{-1} in order to obtain a conversion, in most cases, of less than 30%. The liquid products were collected at intervals and analyzed for conversion by temperature-programmed gas chromatography (gc) using a Carbowax 20M column. The alkene fraction was analyzed by operating the gc column appropriate for the alkenes (Carbowax 20M, β,β′-oxydipropinonitrile, or UC—W) isothermally at a temperature where the alkenes were separated but the retention time for the ketone and alcohol was very long so that several samples could be analyzed before the ketone or alcohol eluted. The *cis-* and *trans-*2-methylcyclohexanols were analyzed using a diglycerol gc column at 100 °C.

Results

The dehydration-dehydrogenation selectivity, S, for the conversion of several alcohols over α-alumina are presented in Table I. The values of S represent the range of values obtained for several (4—9) samples taken at increasing time-on-stream. α-Alumina is active for both dehydrogenation and dehydration and, except for the higher temperatures, is considerably more active for dehydrogenation than for dehydration. With increasing time-on-stream S may change slightly so that alumina becomes a more selective dehydration catalyst. The selectivity depends more on temperature and α-alumina becomes a more selective dehydration catalyst with increasing temperature (Figure 1). All of the transitional aluminas listed in the experimental section, as well as the hydrogen pretreated transitional aluminas in Reference [4], were essentially 100% selective for dehydration.

The temperature coefficients for dehydration and dehydrogenation of four alcohols with α-alumina are presented in Table II. For dehydrogenation all four alcohols gave the same temperature coefficient ($E = 92$ kJ/mol). The coefficient for dehydration was higher than for dehydrogenation; for the acyclic alcohols the coefficient is slightly higher than the values reported in the literature for the transitional aluminas. For 2-methylcyclohexanol the

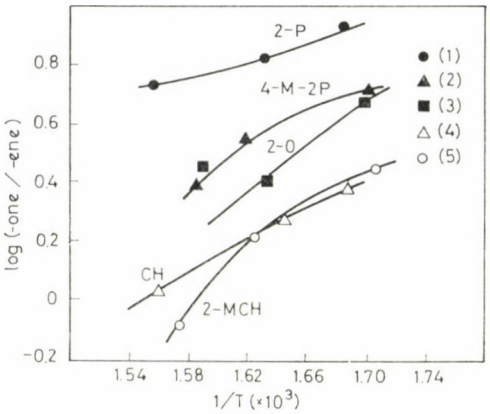

Fig. 1. Dependence of the selectivity ratio (ketone/alkene) on the reaction temperature for the conversion of alcohols (1: 2-pentanol; 2: 4-methyl-2-pentanol; 3: 2-octanol; 4: cyclohexanol; 5: 2-methyl-cyclohexanol) with an α-alumina catalyst

Table I

Dehydration-dehydrogenation selectivity, S, *for the conversion of alcohols over an alpha-alumina catalyst that had been pretreated with hydrogen at* 550 C°

Alcohol	Reaction Temp., °C	Conversion Range %	Selectivity *S* -ene/-one
2-Pentanol	320	38—30	0.11—0.12
	340	33—28	0.15—0.16
	360	35—34	0.18—0.20
3-Pentanol	335	45—22	0.18—0.22
2-Octanol	315	31—32	0.19—0.25
	340	34—29	0.40—0.48
	350	31—38	0.33—0.45
4-Methyl-2-pentanol	315	31—25	0.18—0.19
	342	42—36	0.24—0.29
	360	24—17	0.36—0.38
Cyclohexanol	320	26—20	0.23—0.40
	335	19—13	0.40—0.50
	370	22—12	0.90—1.10
(cis + trans)-2-methylcyclo-	315	23—23	0.35—0.37
hexanol	340	45—40	0.51—0.63
	360	45—38	1.10—1.30

Table II

Temperature coefficients for the conversion of alcohols over transitional and α-alumina

Alcohol	Temperature coefficient, kJ/mol		
	Transitional Alumina	α-Alumina	
	Dehydration	Dehydration	Dehydrogenation
2-pentanol	92—120[a]	125	92
4-methyl-2-pentanol		125	92
2-octanol		140	92
(cis + trans)-2-Methyl-cyclohexanol[b]	120	160	92

[a] Reference [14].

[b] The mixture contained 53.1 mole % of the *cis*- and 46.9 mole % of the *trans* isomer.

coefficient with α-alumina of 160 kJ/mol is higher than the 120 kJ/mol we obtained with a transitional alumina. This value for transitional alumina is similar to those obtained by other workers [15, 16]. For the other cyclic alcohol we tested, cyclohexanol, the Arrhenius plot was not linear for either dehydration or dehydrogenation over the α-alumina catalyst and the catalytic activity was considerably lower than with methylcyclohexanol.

With the transitional alumina catalyst Al—N, *cis-trans* isomerization of 2-methylcyclohexanol does not occur at a rate that is significant in comparison to the alcohol dehydration reaction. The 1-methylcyclohexene : 3-methylcyclohexene isomer ratio from dehydration of the *trans*- alcohol over Al—N was 17 : 83; for the *cis*- alcohol it was 76 : 24. In the conversion of a *cis*- plus *trans*-2-methylcyclohexanol mixture, we assume that: (a) the *cis-trans* alcohol isomerization does not occur and (b) each alcohol isomer will give the same methylcyclohexene ratio as was obtained from the pure alcohol isomers. These two assumptions enable us to calculate the amount of conversion of each alcohol isomer required to yield the experimentally observed methylcyclohexene composition; from this we can calculate the amount of *cis*- and *trans*- alcohol isomer unconverted. The alcohol composition of the liquid reaction products calculated using these assumptions is in good agreement with the experimental value (Table III) and indicates that the *cis*- alcohol reacts more rapidly than the *trans*- isomer in the competitive conversion over transitional aluminas. This agrees with the results of prior workers and with results obtained with the pure alcohols in this study.

Table III

Comparison of experimental and calculated trans-2-methylcyclohexanol from the conversion of a mixture of cis- + trans-2-*methylcyclohexanol over transitional alumina* (Al-N)

Temperature °C	Time on Stream, min	% *cis* isomer converted / % *trans* isomer converted	% *trans*-2-methyl-cyclohexanol	
			Exp.	Calc.[a]
232	45	3.7	72	69
	57	4.9	71	68
188	290	26	60	59

[a] See text for assumptions in making the calculation; alcohol charge was 53.1 mole % of the *cis*-alcohol isomer.

α-Alumina does not resemble the transitional aluminas for the conversion of 2-methylcyclohexanol. The product composition from *trans*-2-methylcyclohexanol at 345 °C shows that *cis-trans* isomerization of the alcohol charge occurs; this isomerization is approximately half as great as the total dehydration-dehydrogenation reactions (Table IV). The alkene isomers obtained from

Table IV

Products from the conversion of trans-2-*methylcyclohexanol over α-alumina at* 345 °C

Time, min	Total Conv., Mole %	*cis*- isomer, % of unconverted alcohol	Methylcyclohexene, Mole %	
			3—	1—
53	39	26	45	55
67	37	25	43	57

the *trans*- alcohol over the α-alumina differs from the transitional alumina. A mixture of 1-octene and *trans*-2-methylcyclohexanol (10 wt.% of alcohol) was passed over the catalyst under the same conditions used obtain the data in Table IV (the total flow was adjusted to give the same alcohol flow rate in both cases). The alcohol conversion, including the *cis-trans* alcohol isomerization, was similar to that obtained with the pure alcohol. In addition, the 1-octene isomerization was lower than we could accurately determine (certainly much less than 1% of the amount charged). This suggests that a secondary reaction involving a gas phase alkene does not alter the primary alkene product composition obtained for the dehydration of *trans*-2-methylcyclohexanol with α-alumina.

A comparison of the alkene distribution (Table V) for α-alumina and Alon-C catalyzed dehydration of acyclic alcohols emphasizes another difference

between the two catalysts. Alon-C gives an alkene distribution with a small amount of the *trans*-2- isomer and nearly equal amounts of the 1- and *cis*-2- isomer from 2-ols (Figure 2); this is identical to other hydrogen pretreated transitional aluminas [1, 2, 3, 17]. In addition, neither the alkene isomer distribution nor the dehydrogenation/dehydration selectivity of Alon-C and Al—W depended on the pretreatment. In contrast, α-alumina produces a large amount of the *trans*-2- isomer from 2-ols and, in some instances, more of the 1-isomer than the *cis*-2- isomer (Figure 3).

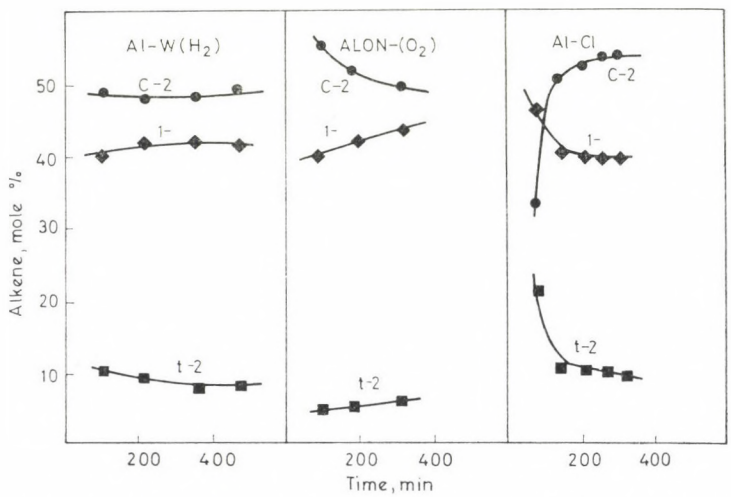

Fig. 2. Octene isomer distribution from the conversion of 2-octanol over nonporous Alon and Al—W alumina and porous alumina

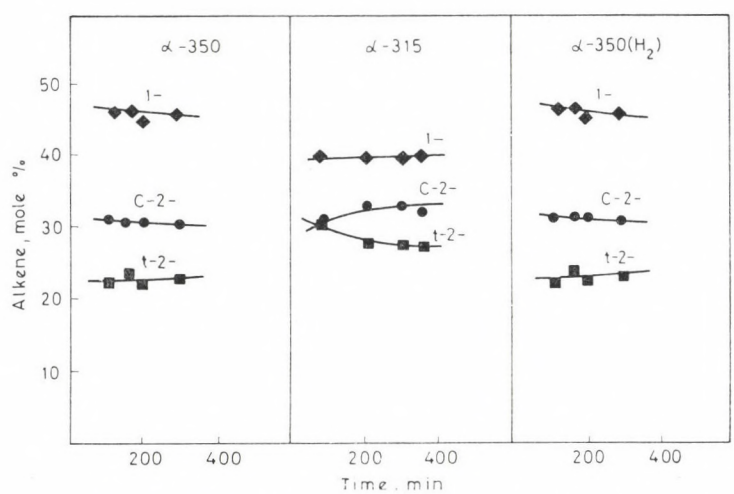

Fig. 3. Octene distribution obtained with α-alumina

Table V

Alkene distribution from the conversion of acyclic alcohols over alpha and transitional aluminas

Alcohol	Temperature °C	Alkene, Mole %			Temperature	Alkene, Mole %		
		1—	*trans*-2-	*cis*-2-		1—	*trans*-2-	*cis*-2-
			α-alumina			transitional alumina		
2-Pentanol	320	38	27	36	175	(41	10	49)[a]
	340	39	25	37				
	365	38	26	36				
3-Pentanol	335	2.4	45	52	175	(trace	25	75)[a]
4-Methyl-2-Pentanol	315[b]	43	51		175	(47	53	)[a]
	345	44	48					
	360	40	52					
2-Octanol	316	40	28	32	200	(46	5.8	49)[c]
	350	46	22	32	210	(43	8.4	49)[d]
					215	(41	7.6	52)[e]

[a] Alon with hydrogen pretreatment.

[b] At 315 °C there was 4.4% of other isomers, at 340 °C this was 7.2% and at 360 °C this was 6.8%.

[c] Alon with oxygen pretreatment.

[d] Al-W with hydrogen pretreatment.

[e] Al-W with oxygen pretreatment.

The alkene distribution from 3-pentanol differs widely for the transitional and α-alumina. With both catalysts insignificant amounts of positional isomerization to the 1-alkene occurred. With transitional aluminas there is a high selectivity for the *cis*-2- isomer and this isomer comprises about 75—80% of the alkenes. With α-alumina nearly equal amounts of the *cis*- and *trans*-2- isomers are formed.

There does not appear to be a significant difference in the alkene distribution from the various 2-ols converted over α-alumina : 2-butanol, 2-pentanol, 2-hexanol and 2-octanol.

Discussion

The dehydrogenation-dehydration selectivity of many transitional aluminas depends on pretreatment [4]. Hydrogen pretreated samples, in addition to being more selective for dehydration, also produced less of the *trans*-2-

alkene from 2-ols than oxygen pretreated samples. Both Alon-C and Al—W are reported to be γ-alumina and based on Reference 4, the selectivity is expected to depend on pretreatment. However, both of these γ-aluminas were selective for dehydration even when pretreated with oxygen; both samples produced very little of the *trans*-2- isomer from 2-ols whether the pretreatment was with hydrogen or oxygen. Alon-C and Al—W differ from most transitional aluminas since they are nonporous materials and have been used as standard nonporous materials [18]. These results are consistent with the view that the oxygen pretreatment creates dehydrogenation sites only in pores and/or at highly unsaturated sites (in the sense of TAYLOR's active points [19]) but not on the uniform crystallographic surface planes of the transitional aluminas.

Alon-C and Al—W produced essentially the same alkene distribution as we previously reported for several porous transitional aluminas [17]. However, α-alumina produces much different alkene distribution. With the latter alumina *trans*-2- isomer forms in nearly as large an amount as the other two isomers. The *cis*-2-/1- isomer ratio is also much lower for the α-alumina than for the transitional aluminas. Thus, in going from transitional aluminas to α-alumina there is a shift in the alkene distribution to: (a) favor the 1-isomer relative to the *cis*-2- isomer and (b) a pronounced increase in the relative amount of the *trans*-2- isomer.

This study concentrates on selectivities rather than a comparison of reaction rates. Literature data for the conversion of ethanol over a series of aluminas [14] suggest that the absolute rate is not a linear function of the surface area; rather, the rate per unit surface area reaches a maximum and then declines as the surface area is increased further. Our hydrogen pretreated transitional aluminas, with surface areas in the 100—250 m^2/g range, show no change in alkene selectivity that follows the change of surface area. A high surface area oxygen pretreated transitional alumina sample, relative to the same alumina pretreated with hydrogen, show: (a) an absolute decrease in dehydration activity, (b) an absolute increase in dehydrogenation activity, and (c) an increase in the amount of *trans*-2- alkene. Thus, oxygen pretreatment of porous transitional aluminas changes the dehydration selectivity in the direction to resemble α-alumina.

The classical E2 elimination theory predicts the formation, by an *anti* elimination of water, of predominately 3-methylcyclohexene from *trans*-2-methylcyclohexanol and the more stable 1-methylcyclohexene from *cis*-2-methylcyclohexanol. For alumina, PINES and co-workers [1] obtained an alkene distribution that strongly supported this E2 mechanism. However, the results from the deuterium labeled alcohol, as well as the results of HALL and co-workers [16] with a hydroxyapatite catalyst, suggest that the mechanism for the *trans* alcohol may be more complicated than a simple E2 mechanism. Our results with *cis*- or *trans*-2-methylcyclohexanol and transitional

alumina catalysts are in excellent agreement with those of PINES [1] and show that transitional alumina does not catalyze a *cis-trans* alcohol isomerization at an appreciable rate in comparison to the dehydration rate. With the α-alumina, *cis-trans* isomerization of the reactant alcohol is approximately as rapid as the conversion of the alcohol to other products; furthermore, dehydrogenation to methylcyclohexanone is as, or more, important than the dehydration to methylcyclohexenes. The alcohol isomerization makes a comparison of the alkene selectivity to that of the transitional alumina difficult. The 3-methylcyclohexene formed from the *trans*-2-methylcyclohexanol is present in a much larger amount than was obtained from the *cis* isomer and is larger than the equilibrium composition. This suggests that the *trans* alcohol gave a high selectivity for the 3-methylcyclohexene isomer; however, we would need to make a much more detailed study to verify this.

Two properties of catalysts that have been used in correlations are the heat of formation and the ionic radius. FAHRENFORT, VAN REYEN and SACHTLER [20] found a spread of 250—290 kJ/mol related to one equivalent of the heat of formation of the formates in going from the low activity metals at the left base of a volcano shaped curve to the low activity metals on the right side of the volcano. VIJH [21] also reported a volcano relationship for the decomposition of N_2O on metal oxides and the spread of the heat of formation from base to base was about 250 kJ/mol per equivalent. The difference in the heat of formation of α-Al_2O_3 and γ-Al_2O_3 is only 24 kJ/mol (4 kJ/mol per equivalent [22]); consequently, both aluminas will not fit on a volcano type selectivity curve for the dehydrogenation-dehydration selectivity. EUCKEN [23] found a linear correlation of the function $\eta = [(\text{cation radius})^3/\text{molecular volume/cation}) (\text{valence})]$ with the dehydration-dehydrogenation selectivity for isopropyl alcohol conversion. However the selectivity differences of γ- and α-Al_2O_3 would appear to eliminate functions based only on charge and/or radius for correlations with alcohol conversion selectivity.

DOWDEN related the relative dehydrogenation and dehydration activity to the number of cation vacanciens on the surface [24]. Our results [4] for hydrogen and oxygen pretreatment effects on selectivity are in agreement with this view. However, uncertainty about the crystal faces exposed, the degree of surface hydration, and the alcohol surface coverage, make a detailed mechanistic description of this view difficult.

*

Acknowledgement is made to the Donors of the Petroleum Research Fund, administered by the American Chemical Society, for support of this research.

REFERENCES

[1] PINES, H., MANASSEN, J.: Adv. Catal., **16**, 49 (1966)
[2] KNOZINGER, H.: in The Chemistry of the Hydroxyl Group, (S. PATAI, Ed.) Interscience Pub., New York, 1971

[3] NATARI, B.: Chim. Ind., **51.** 1200 (1969)
[4] KRYLOV, O. V.: Catalysis by Nonmentals, Academic Press, New York, 1970
[5] MARS, P.: in The Mechanism of Heterogeneous Catalysis, (J. H. de BOER, Ed.) Elsevier, Amsterdam, 1960, pp. 49—63
[6] SEDZIMIR, A.: Rocz. chem. Ann. Soc. Chim. Polonorum, **41,** 655 (1967)
[7] SZABÓ, Z. G., JOVER, B.: Proc. 5th Intern. Cong. Catal., Miami Beach, 1972, North-Holland, Amsterdam, Vol. **1,** 1973, p. 833
[8] BREMER, H., GLIETSCH, J.: Z. anorg. Chem., **395**, 82, 91 (1972)
[9] PEPE, F., STONE, F. S.: Proc. 5th Intern. Congr. Catal., Miami Beach, 1972, North-Holland, Amsterdam Vol. **1,** 1973, p. 137
[10] DAVIS, B. H.: J. Catal., **26,** 348 (1973); Colloid and Interface Sci., (M. KERKER, ed.), Vol. **III,** Academic Press, New York, 1976, p. 115
[11] LIU, C. L., CHUANG, T. T., DALLA LANA, I. G.: J. Catal., **26,** 474 (1972); CHUANG, T. T., DALLA LANA, I. G.: J. Chem. Soc., Faraday Trans. I, **68,** 773 (1972)
[12] U. S. Patent 3, 328, 122, June 27, 1967
[13] NEWSOME, J. W., HEISER, H. W., RUSSELL, A. S., STUMPF, H. C.: Alumina Properties, Tech. Paper No. 10, 2nd Revision, Aluminum Co. of America, Pittsburgh, Pa., 1960
[14] WADE, W. H., TERANISKI, S., DURHAM, J. L.: J. Phys. Chem., **69,** 590 (1965)
[15] KNOZINGER, H., BUHL, H., KOCHLOEFL, K.: J. Catal., **24,** 57 (1972)
[16] KIBBY, C. L., LANDE, S. S., HALL, W. K.: J. Am. Chem. Soc., **94,** 214 (1972)
[17] DAVIS, B. H.: J. Org. Chem., **37,** 1240 (1972)
[18] PAYNE, D. A., SING, K. S. W.: Chem. & Ind., **1969,** 918
[19] TAYLOR, H. S.: Proc. Roy. Soc., **A 108,** 105 (1925)
[20] FAHRENFORT, J., van RAYEN, L. L., SACHTLER, W. M. H.: in The Mechanism of Heterogeneous Catalysis, (J. H. BEBOER, Ed.) Elsivier, Amsterdam, 1960, p. 23
[21] VIJH, A. K.: J. Catal., **31,** 51 (1973); **33,** 385 (1974)
[22] LANGE's Handbook of Chemistry, 11th Ed., McGraw-Hill Book Co., New York, 1973
[23] EUCKEN, A.: Naturwissenschaften, **36,** 48 (1949)
[24] DOWDEN, D. A.: J. Chem. Soc., **1950,** 242

B. H. DAVIS University of Kentucky, Lexington, Kentucky, USA.

Acta Chimica Academiae Scientiarum Hungaricae, Tomus 109 (4), pp. 389—398 (1982)

MO-LCAO CALCULATIONS ON POLYMETHINES, XV*

NATURE OF THE CRYPTOCYANINE CHROMOPHORE AND FLUOROPHORE

J. FABIAN**[1], F. DIETZ[2] and N. TYUTYULKOV[3]

([1]Sektion Chemie der Technischen Universität Dresden, DDR,
[2]Sektion Chemie der Karl-Marx-Universität Leipzig, DDR,
[3]Institut für Organische Chemie der Bulgarischen Akademie der Wissenschaften, Sofia, Bulgarien)

Received June 27, 1980
In revised form March 24, 1981
Accepted for publication April 27, 1981

Singlet-singlet transitions of Cryptocyanine (DCI) have been calculated by the PARISER—PARR—POPLE method including the lowest-energy doubly and triply excited configurations into the configuration interaction treatment. The red and blue fluorescence has been attributed to the $S_1 \rightarrow S_0$ and $S_2 \rightarrow S_0$ transition, respectively. According to analyses of the wavefunctions, both the electronic transitions $S_0 \rightarrow S_1$ and $S_0 \rightarrow S_2$ and the electronic states S_1 and S_2 are fully delocalized. The lowest-energy doubly excited configuration contributes markedly to the S_2 state. Molecular relaxation of the FRANCK—CONDON excited state is stronger for the planar S_2 than for the planar S_1 state. The formation of a non-planar molecule in the S_2 excited state cannot be excluded with certainty. It should, however, affect the non-radiative rather than the radiative deactivation of the S_2 state.

Various polymethine dyes have unusual photophysical properties in that they display dual fluorescence [2—10]. Besides the well-known long wave fluorescence, short wavelength fluorescence is elicited both by high intensity, pulse-shaped laser light [2] and steady-state excitation by standard light sources [6, 10]. The short wave fluorescence is weaker than the long wavelength fluorescence [10] and the fluorescence life-time of the higher energy fluorescence state is longer than that of the lower energy fluorescence [8]. To date, the interpretation of the short wave fluorescence of polymethine dyes is controversial. Whereas in other series of compounds (nonalternant hydrocarbons, thiocarbonyl compounds) short wave fluorescence results unequivocally from higher excited states, the corresponding upper state fluorescence has been questioned in the case of polymethine dyes. It has been argued, in particular, that a $S_2 \rightarrow S_0$ type transition would be too low in energy to be compared with the $S_0 \rightarrow S_2$ absorptive transition [4, 7].

In the main, three interpretations have been put forward to explain the short-wave fluorescence.

(i) Emission of certain impurities or photo-degradation products [11,12].

* For part XIV, see Ref. [1].
** To whom correspondence should be addressed.

(ii) Emission from molecular excited states that are merely localized at the heterocyclic end groups [5, 6, 13, 14].

(iii) Emission from an electronic state generated through a two electron excited state [15, 16]. Conjugation in that electronic state is removed either by changing the molecular geometry [4] or by adding solvent molecules to certain sites of the polymethine molecule [15].

The identity of the fluorescence excitation spectra of the long and short wave fluorescence [6, 10] contradicts the first interpretation. The second interpretation appears doubtful in the light of the following experimental results. Shorter wavelength fluorescence also occurs in the absence of heterocyclic end groups and the fluorescence wavelengths differ between vinylogues having the same heterocyclic residues [4]. The third interpretation is rather hypothetical, although doubly excited states have been proved to be of the greatest importance in understanding the photophysics of various alternant [17] and non-alternant hydrocarbons [18].

The purpose of the present paper is to shed light on the nature of the lowest-energy polymethine singlet excited states and the role of the two-electron excitation. Cryptocyanine (1,1′-diethyl-4,4′-carbocyanine iodide, DCI), which belongs to the best studied polymethine dyes [19—25], will serve as an example. DCI displays a red fluorescence at about 700 nm and a blue fluorescence at about 460 (430) nm [4, 15]. Also, the polarization spectrum of the red fluorescence has been recorded depending on the excitation wavelength [10]. In contrast to other polymethine dyes, no evidence of photo-

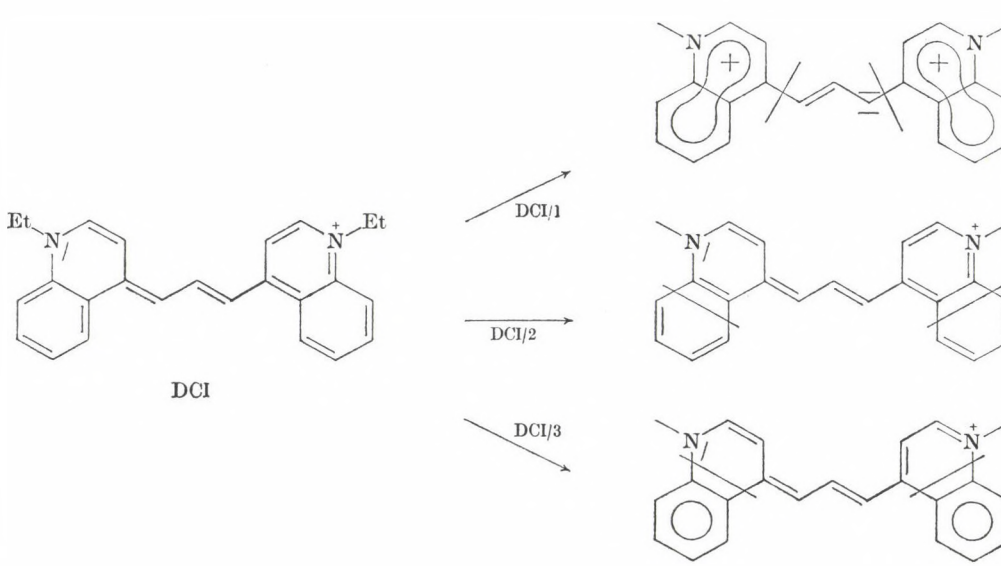

isomerization of DCI has been obtained [21], but an unusual two-component fluorescence decay curve has been found recently [25].

The results of standard type PPP calculations of DCI will be discussed first. In contrast to former PPP calculations [10, 26—28], all singly excited $\pi\pi^*$ configurations have been taken into account. In order to assess the degree of delocalization of the $\pi \rightarrow \pi^*$ transitions, the results of the PPP calculation have been subjected to the OHTA—KURODA—KUNII analysis [29]. The transitions are discussed in terms of heterocyclic localization (fragmentation mode DCI/1) or in terms of polymethinic delocalization (fragmentation modes DCI/2 and DCI/3).

Moreover, the excited states are interpreted by the BABA—SUZUKI—TAKEMURA configuration analysis [30]. Projection of the wavefunctions of DCI onto the wavefunctions of the fragmented molecules DCI/2 and DCI/3 will reveal correlations between fluorescence states of DCI and those of the dye sub-structures involved.

Then, the configuration interaction (S—CI) has been extended, taking into account the lowest-energy two- and three-electron excitations (SD—CI and SDT—CI, respectively). In order to estimate the extent of molecular relaxation in the S_1 and S_2 excited state and the photochemical behaviour, π-molecular diagrams are examined.

Method

The standard PPP method has been described in detail elsewhere [31]. The molecular geometry assumed in the calculations of the cationic DCI and of the fragmented molecules consisted of two regular hexagons and all bond lengths equal to 1.40 Å. The resonance integrals are all equal to -2.318 eV. The one-center integrals are the same as employed in former papers [32]: $U_C = -11.42$ eV; $U_{NCH_3} = -21.95$ eV; $\gamma_{CC} = 10.84$ eV and $\gamma_{NN} = 12.98$ eV. The two-center electron repulsion integrals are evaluated by the MATAGA—NISHIMOTO equation [33]. Because of the C_{2v} symmetry of planar *trans*-DCI, the electronic states either belong to the A_1 or B_2 symmetry. For analyzing electronic states and electronic transitions, limited configuration interaction calculations were used. The 36 configurations considered were generated from the six highest occupied and six lowest unoccupied MO's. The analysis techniques are reviewed elsewhere [34].

PPP calculations with inclusion of multiply excited states were performed by a computer program kindly placed at our disposal by Dr. OLBRICH (Mülheim/Ruhr). The multiply excited states considered are depicted in Fig. 1. The doubly excited singlet state is of A_1 symmetry and the triply excited state of B_2 symmetry.

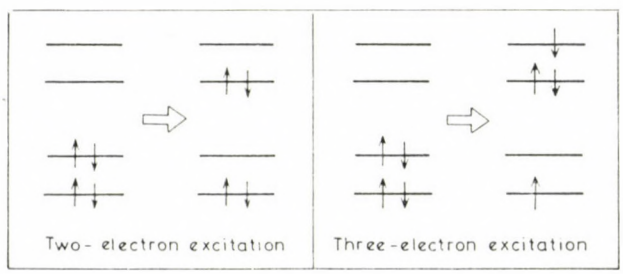

Fig. 1. Lowest-energy electronic configurations resulting from two-electron (left panel) and three-electron excitation (right panel)

Results and Discussion

The UV—VIS absorption spectrum of DCI and the results of the PPP calculations are presented in Fig. 2. The longest wavelength part of the spectrum displays three distinct absorption bands A, B and C.

The PPP calculation reflects the substantial feature of the experimental absorption spectrum. The theoretical results are illustrated in Fig. 2. Vertical lines indicate the theoretical wavenumbers and intensities ($\log f$). Weaker transitions are marked by wavy lines. According to the calculation, the B-band is an inherent part of the UV spectrum of DCI. Thus, in contrast to Ref. [15] the blue fluorescence might correspond to a weak electronic transition that causes B-band absorption in its long wave part. If the STOKES shift is calculated from the blue emission maximum and the longest-wavelength

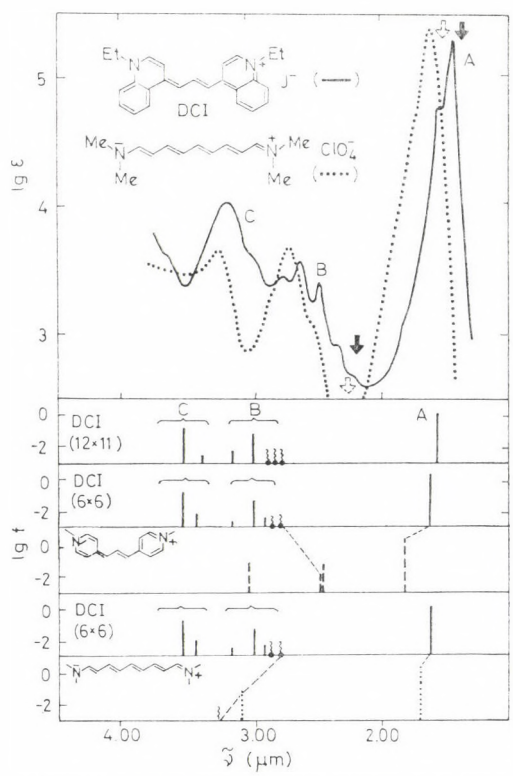

Fig. 2. Absorption spectrum of DCI in ethanol and of the parent dye streptopolymethine cyanine in dichloromethane [41] and maxima of fluorescence bands of their red and blue fluorescence [2, 4] (arrows). The vertical ($\lg f \geq -3$) and wavy lines ($\lg f \leq -3$) indicate the calculated absorption wavenumbers of DCI either by including all 132 singly excited states (12×11) or 36 singly excited states (6×6). For the latter case, the correlations are illustrated between excited states S_1 and S_2 of DCI and locally excited states of the polymethinic subunits in the fragmented molecules DCI/2 and DCI/3

absorption maximum of the B- band [10], a shift of about 1900 cm^{-1} is obtained. Hence, the STOKES shift of the blue emission is three times as large as that of the red emission. Strong differences in the STOKES shift of the two fluorescences seem to be a general characteristics of polymethine dyes [6].

Although all 132 singly excited $\pi\pi^*$ configurations of DCI have been taken into account, the transition energies in the ultraviolet region are obviously overestimated. Hypsochromicity of the calculated absorptions relative to the experiment is a well-known shortcoming of standard PPP calculations. In order to overcome this difficulty, a different kind of parameter adjustment has been proposed, such as drastic reduction of the ionization potential of the nitrogen atom [35], of the carbon nitrogen resonance integral [36] or of the electron repulsion integrals [10, 27]. However, as long as the deeper origin of the deficiency is unknown, reparametrization cannot be a proper remedy and efforts along these lines should be considered with caution.

Since our main interest is directed to the nature of the fluorescent states S_1 and S_2 only, numerical agreement between theoretical and experimental $S_0 \rightarrow S_1$ and $S_0 \rightarrow S_2$ transition energies is of minor importance. Fortunately, calculations on DCI in various parametrizations provide a consistent picture about the two lowest excited states. The S_1 excited state is of A_1 symmetry and the second excited state of B_2 symmetry. Consequently, the transition between the S_0 and S_1 states is polarized perpendicular to the twofold molecular axis (polarized along the trimethine chain). The transition between the S_0 and S_2 states, in contrast, is polarized along the twofold symmetry axis. In contrast to the $S_0 \rightarrow S_1$ transition, the $S_0 \rightarrow S_2$ transition is weak. Since this feature already results from limited configuration interaction PPP calculations in the standard parametrization, electronic transitions and electronic states of those calculations are analyzed and discussed in the following.

Analyses of the electronic transitions $S_0 \rightarrow S_1$ and $S_0 \rightarrow S_2$ (*cf.* Fig. 3) evaluate the degree of local excitation (LE) at the heterocyclic end groups to 48% in both cases (fragmentation mode DCI/1). Additional strong charge transfer (CT) contributions from the chain to the end groups indicate the delocalized nature of the electronic excitations. This conclusion is supported by analyses with regard to fragmentation mode DCI/2 and DCI/3. Local excitation in the polymethinic sub-structures dominates both the $S_0 \rightarrow S_1$ and $S_0 \rightarrow S_2$ electronic transition (*cf.* Fig. 3). Therefore, no theoretical support is found for the former assumption [5, 6] that the $S_0 \rightarrow S_2$ excitation, in contrast to the $S_0 \rightarrow S_1$ excitation, is localized on the end groups.

The same conclusion has been drawn from configuration analysis. This analysis provides definite correlations between the electronic states of DCI and the no-bond (NB), local excited (LE) and charge transfer (CT) configurations that are defined by the fragmented molecules. Only some correlations to local excited states of the dye sub-structures within the fragmentation

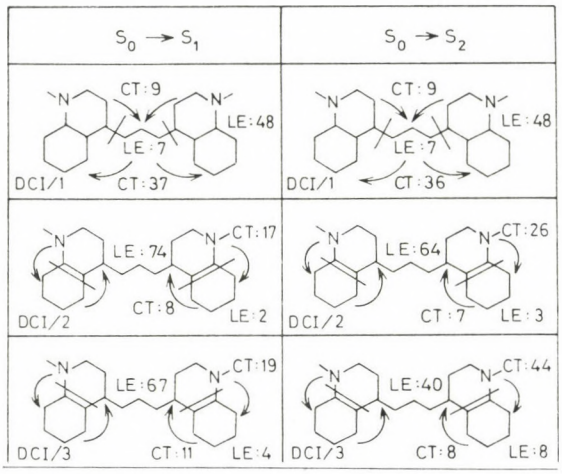

Fig. 3. Analyses of the electronic transitions $S_0 \rightarrow S_1$ and $S_0 \rightarrow S_2$ with respect to the fragmentation modes DCI/1 to DCI/3 (LE = local excitation, CT = charge transfer excitation)

modes DCI/2 and DCI/3 are illustrated in Fig. 2. Both the S_1 and S_2 excited state correlates definitely to excited states of the sub-structures. Interestingly, the S_2 state of DCI is not related to the S_2 states of the sub-structures but rather to the S_3 states. In other words, the delocalized S_2 states of the polymethine dyes are not necessarily electronically related.

Table I

Calculated and experimental excitation energies $\tilde{\nu}$ in μm^{-1} of DCI

		$S_0(A_1) \rightarrow S_1(B_2)$	$S_0(A_1) \rightarrow S_2(A_1)$
This paper[a]	S	1.62	2.82
	SD	1.69	2.22
	SDT	1.69	2.22
Literature[b]	S	1.45	2.52
Experiment[c]			
Absorption		1.41	2.36
Fluorescence		1.35	2.17

[a] 36 singly excited configurations (S), 36 singly excited configurations and the lowest-energy doubly excited configuration (SD), 36 singly excited configurations and both the lowest-energy doubly and triply excited configurations (SDT).

[b] PPP input parameters adjusted with the aid of the experimental spectrum [10].

[c] in methanol [10].

The nature of electronic states and electronic transitions is not essentially altered when multiply excited states are considered. The transition energies, however, are markedly affected (*cf.* Table I). This finding feeds the suspicion that the neglect of multiply excited states might be responsible for the above-mentioned shortcoming of the standard PPP method [37]. The lowest-energy excited configuration, which results from a twofold electron jump from the highest occupied MO to the lowest unoccupied MO, contributes 40% to the S_2 state and lowers considerably its energy relative to that of the S_0 state. Because of some ground state energy depression, the $S_0 \rightarrow S_1$ transition energy is now slightly increased. Mixing between the lowest triply excited configuration and the S_1 state is too weak to compensate for this effect, but decrease in $S_0 \rightarrow S_1$ excitation energy is to be expected with inclusion of doubly excited states of B_1 symmetry that are not considered in the present calculation. In order to judge the extent of the two-electron excitation, we have focussed attention to the lowest-energy doubly excited configuration only.

Obviously, the doubly excited configuration can no longer be viewed as a distinct electronic state accessible only by absorption of a second photon from the S_1 state as formerly assumed [15]. It represents rather an inherent part of the S_2 excited state. This state is reached by light absorption from the ground state.

Next, the question will be raised as to whether new deactivation channels are opened by the contribution of the multiply excited configurations to electronic state S_2. According to the molecular diagram (Fig. 4), there is no indication of enhanced reactivity towards nucleophilic solvent molecules in the S_2 state. In contrast, as to the electron densities along the chain, any inclination to nuclephilic attack should be higher in the S_1 than in the S_2 state. Consequently, formation of a localized heterocyclic structure by addition of the solvent molecule in the S_2 state is less probable. The bond orders along the trimethine chain, however, are more strongly alternating in the S_2 state than in the S_1 state. Thus, conjugation will counteract twisting of the terminal groups out of the plane less in S_2 than in S_1.

Calculations in the QCFF/Pi method (quantum chemical extension of the consistent force field to π-electron systems) of WARSHEL and LEVITT [38] have been performed in addition, in order to predict the equilibrium geometry by energy minimization with respect to the complete set of $3N$ cartesian coordinates. For computational reasons, only the dye sub-structures in DCI/2 and DCI/3 have been calculated so far [39]. In both cases the iterative calculations resulted in planar structures for S_2 states as found for the S_1 and S_0 states. Rotamers are energetically less favoured.

The calculation predicts, however, a considerable alteration of bond lengths upon electronic transitions from S_0 to S_2 and S_2 to S_0, respectively. This supports conclusions drawn from the π-bond orders. Due to the stronger

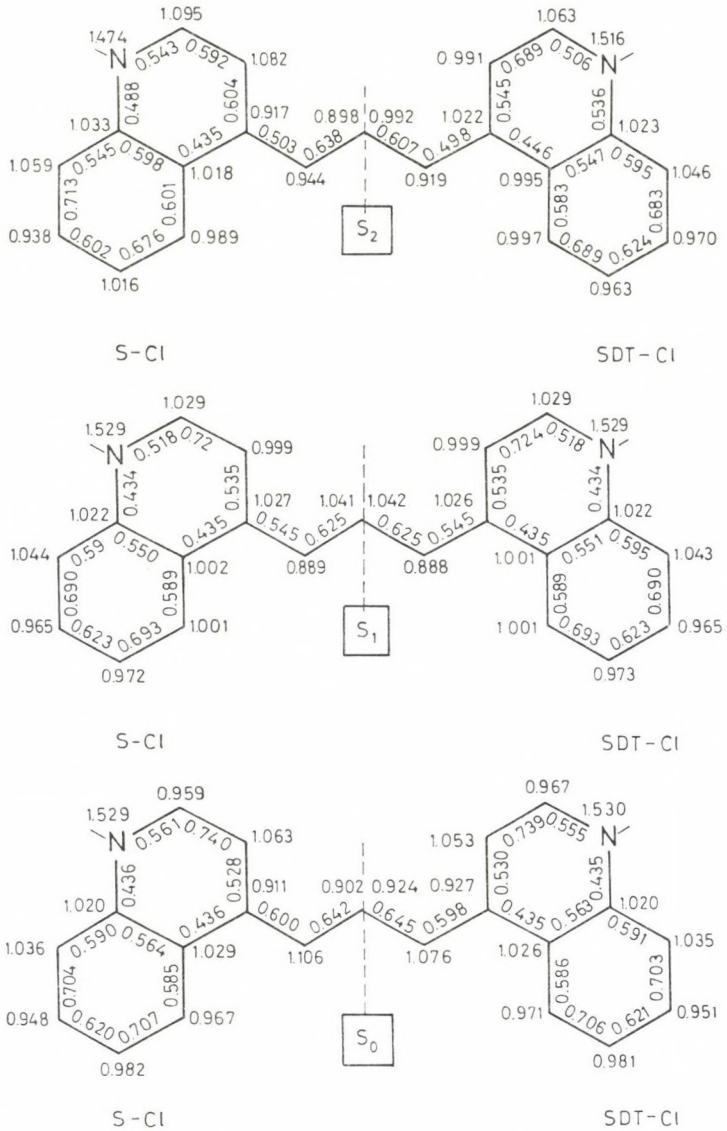

Fig. 4. π-Molecular diagrams of DCI in the ground state (S_0) and in the fluorescence states (S_1, S_2) without taking into account the lowest-energy doubly and triply excited configurations on the left and taking into account of those on the right. For abbreviations *cf.* Table I

molecular relaxation, the STOKES shift of the $S_0 \rightarrow S_2$ transition must considerably exceed that of the $S_0 \rightarrow S_1$ transition. In other words, formation of a rotamer must not be invoked in order to explain the difference in STOKES shift.

There is, however, an additional point worth of consideration. The QCFF/Pi calculations mentioned above refer to isolated molecules. Solvent effects are completely neglected. Formation of a rotamer by symmetric torsion of the heterocyclic groups out of the plane may create a more polar molecule. A molecule like that should be more stabilized by solvent effects than a less polar planar molecule, such as discussed for GRABOWSKI's TICT systems ("twisted internal charge transfer" [40]).

Preliminary calculations on the twisted second excited singlet state S_2' of DCI predict a low energy gap between the S_2' and the respective FRANCK—CONDON-state S_0'. Thus radiative deactivation from S_2' should result in a bathochromic rather than in a hypsochromic fluorescence in addition to the red fluorescence observed. Formation of a rotamer may be important, however, for the competitive radiationless deactivation process.

To sum up, there is no need to invoke any additional photochemical process in order to explain the emergence of the blue fluorescence of DCI and related compounds. The blue fluorescence is an upper-state fluorescence from the relaxed planar S_2 state. Polymethine dyes constitute an additional class of compounds which disobey KASHA's rule.

REFERENCES

[1] FABIAN, J.: J. Prakt. Chem. **323,** 561 (1981)
[2] MÜLLIER, A., PFLÜGER, E.: Chem. Phys. Lett., **2,** 155 (1968)
[3] DYADYUSHA, G. G., PRZHONSKAYA, O. V., TIKHONOV, E. A., SHPAK, M. T.: Zh. Eksp. Fiz., **14,** 330 (1971)
[4] KÖNIG, R., LEUPOLD, D., VOIGT, B., DÄHNE, S.: Lumin., **9,** 113 (1974)
[5] PRZHONSKAYA, O. V., TIKHONOV, E. A.: Izv. Akad. Nauk SSSR, Ser. Fiz., **39,** 2275 (1975)
[6] TIKHONOV, E. A., PRZHONSKAYA, O. V., SHPAK, M. T.: Kvant. Elektron., **10,** 92 (1976)
[7] VOIGT, B., SCHOLZ, M., LEUPOLD, D., KÖNIG, R., MORI, S.: Zh. Prikl. Spektr., **17,** 633 (1972)
[8] TASHIRO, H., YAJIMA, T.: Chem. Phys. Lett., **42,** 553 (1976)
[9] GALANIN, M. D., CHIZHIKOVA, Z. A.: Kaatk. Soobshch. Fiz., **1978,** 22; C. A., 201471g (1979)
[10] ŘEHÁK, V., NOVÁK, A., TITZ, M.: Chem. Phys. Lett., **52,** 39 (1977); TITZ, M., NOVÁK, A., ŘEHÁK, V.: Collect. Czechoslov. Chem. Commun., **45,** 307 (1980)
[11] KALITEEVSKAYA, E. N., RAZUMOVA, T. K.: Opt. Spektrosk., **48,** 290 (1980), and former papers
[12] MUENTER, A. A., COOPER, W.: Chem. Phys. Lett., **22,** 212 (1973)
[13] MÜLLER, A.: Int. Conf. Photochem., Bordeau 1971, taken from Ref. [4]
[14] DÄHNE, S., KLAGGE, H.-M.: unpublished results; KLAGGE, H.-M.: Thesis, Humboldt-University Berlin, 1973
[15] LEUPOLD, D., KÖNIG, R., VOIGT, B.: Acta Phys. Chem. Acta Univ. Szeged, **19,** 357 (1973)
[16] VOIGT, B., MENZEL, R., LEUPOLD, D., KÖNIG, R.: Opt. Commun., **9,** 274 (1973)
[17] SCHULTEN, K., OHMINE, I., KARPLUS, M.: J. Chem. Phys., **64,** 4422 (1976); TAVAN, P., SCHULTEN, K.: J. Chem. Phys., **70,** 5414 (1979)
[18] KOLC, J., DOWNING, J. W., MANZARA, A. P., MICHL, J.: J. Amer. Chem. Soc., **98,** 930 (1976)
[19] MENZEL, R.: Thesis, Humboldt-University Berlin, 1977; MENZEL, R., LEUPOLD, D.: Chem. Phys. Lett., **65,** 120 (1979); LEUPOLD, D., VOIGT, B., KÖNIG, R.: Lumin., **5,** 308 (1972)
[20] GALANIN, M. D., CHIZHIKOVA, Z. A.: Opt. Spektrosk., **34,** 197 (1973)
[21] DEMPSTER, D. N., MORROW, T., RANKIN, R., THOMPSON, G. F.: Chem. Phys. Lett., **18,** 488 (1973)

[22] FOUASSIER, J. P., LOUGNOT, D. J., FEURE, J.: Chem. Phys. Lett., **30,** 448 (1975)
[23] MÜLLER, A., SCHULZ-HENNIG, J., TASHIRO, H.: Z. phys. Chem. Frankfurt, **101,** 361 (1976)
[24] ESKE, T., RAZI NAQVI, R.: Chem. Phys. Lett., **63,** 128 (1979)
[25] TREDWELL, C. J., KEARY, C. M.: Chem. Phys., **43,** 307 (1979)
[26] FERRÉ, Y., LARIVÉ, H., VINCENT, E.-J.: Photogr. Sci. Eng., **18,** 457 (1974)
[27] FABIAN, J., ZAHRADNÍK, R.: Wiss. Z. Techn. Univ. Dresden, **26,** 315 (1977)
[28] ABRAMENKO, P. I., KOSOBUTSKII, V. A.: Khim. Geterotsikl. Soed., **1978,** 626
[29] OHTA, T., KURODA, H., KUNII, T. L.: Theor. Chim. Acta, **19,** 167 (1970)
[30] BABA, H., SUZUKI, S., TAKEMURA, T.: J. Chem. Phys., **50,** 2078 (1969)
[31] PARR, R. G.: Quantum Theory of Molecular Electronic Structure. Benjamin, New York 1964
[32] HARTMANN, H., FABIAN, J.: Ber. Bunsenges. physik. Chem., **73,** 107 (1969)
[33] MATAGA, N., NISHIMOTO, K.: Z. Physik. Chem. N. F., **13,** 140 (1957)
[34] FABIAN, J., MEHLHORN, A., FRATEV, F.: Int. J. Quant. Chem., **17,** 235 (1980); FABIAN, J.: Z. Chem., **20,** 197 (1980); J. Signal AM, **6,** 307 (1978); **7,** 67 (1979)
[35] DIETZ, F.: Tetrahedron, **28,** 1403 (1972)
[36] HONIG, B., GREENBERG, A. D., DINUR, U., EBREY, TH. G.: Biochemistry, **21,** 4593 (1976)
[37] DIETZ, F., FABIAN, J., KANEV, I., OLBRICH, G., TYUTYULKOV, N. N.: unpublished results, 1979; DINUR, U., HONIG, B., SCHULTEN, K.: Chem. Phys. Lett., **72,** 493 (1980)
[38] *cf.* WARSHEL, A.: in Modern Theoretical Chemistry, Vol. **7,** Part A (Ed. G. A. SEGAL), Chapt. **5,** Plenum Press, New York 1977
[39] FABIAN, J.: unpublished results, 1980
[40] GRABOWSKI, Z. R., ROTKIEWICZ, K., SIEMIARZUK, A., COWLEY, D. J., BAUMANN, W.: Nouv. J. Chim., **3,** 443 (1979)
[41] DMS UV Atlas of Organic Compounds. Verlag Chemie, Weinheim, 1966

Jürgen FABIAN — Sektion Chemie der Technischen Universität, Dresden, DDR-8027 Dresden, Mommsenstr. 13.

Fritz DIETZ — Sektion Chemie der Karl-Marx-Universität Leipzig, DDR-7010 Leipzig, Liebigstr. 18

Nikolai TYUTYULKOV — Institut für Organische Chemie der Bulgarischen Akademie der Wissenschaften, Sofia 13, Bulgarien

Acta Chimica Academiae Scientiarum Hungaricae, Tomus 109 (4), pp. 399—406 (1982)

STEROIDAL HYDROXYLACTAMS

J. W. MORZYCKI* and W. J. RODEWALD

(Department of Chemistry, University, 02093 Warszawa, Poland)

Received February 9, 1981
Accepted for publication April 29, 1981

The properties of the hydroxylactams **2a**, **2b**, **3a** and **3b**, obtained by reduction of the lactamoester **1** with $LiAlH_4$ or $LiAlH(O\text{-}t\text{-}Bu)_3$, have been investigated. It has been found that acids, bases and other catalysts effect mutual epimerization of the hydroxylactams. It has been established that reactions of the hydroxylactams **2** and **3**, unsaturated lactams **5** and **6**, as well as the dihydroxylactam **7**, proceed in acid medium *via* the respective α-acylimmonium ions.

In the course of our research on azasteroid synthesis, a reductive N-cyclization of lactamoesters has been observed. A number of lactamoesters, under the conditions of $LiAlH_4$ reduction, undergo transformation to the corresponding tertiary amines in good yields. It has been previously established that the reaction proceeds *via* hydroxylactams as the intermediates[1]. The growing synthetic potential of compounds of this type in the synthesis of polyheterocycles has been recently demonstrated [2—4]. It should be added that cyclic hydroxylactams have been found to constitute a new class of precursors of the highly reactive α-acylimmonium ion, and therefore serve for a variety of applications. One of the most important is the biomimetic heterocyclization of olefins [5—8] in which the cyclic acylimmonium species has been shown to behave as a highly reactive initiating centre for cationic olefin cyclization.

A common method of hydroxylactams synthesis is $NaBH_4/H^+$ reduction [9—11] of cyclic imides, *i.e.* substituted succinimide or glutarimide, proceeding according to a simple experimental procedure [12]. However, in our case the $NaBH_4$ reduction has not been useful for lack of N-cyclization of the lactamoester **1** under these conditions. Nevertheless, if the reduction of compound **1** was carried out with $LiAlH_4$ at —70 °C, two pairs of epimeric hydroxylactams (**2a** and **2b**, as well as **3a** and **3b**) were isolated. In further experiments we have established that these hydroxylactams are also formed as a result of reduction of the lactamoester **1** with lithium tri-*t*-butoxy-aluminium hydride at room temperature. On the other hand, we have also stated that the reduction of imide **4** with the latter hydride afforded almost the same mixture of hydroxylactams. This fact strongly supported our suggestion [1]

* To whom correspondence should be addressed.

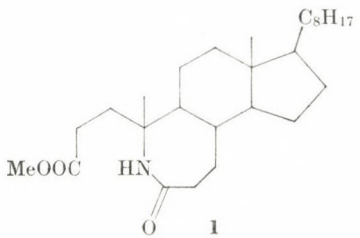

1

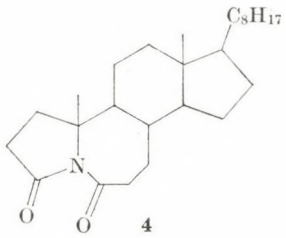

4

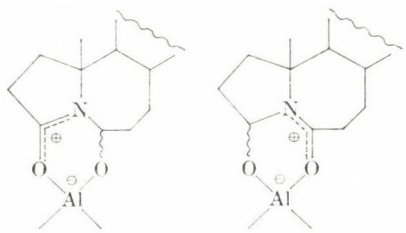

A *B*

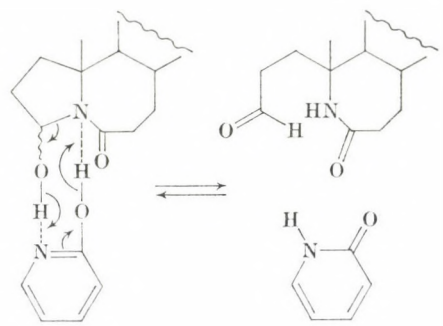

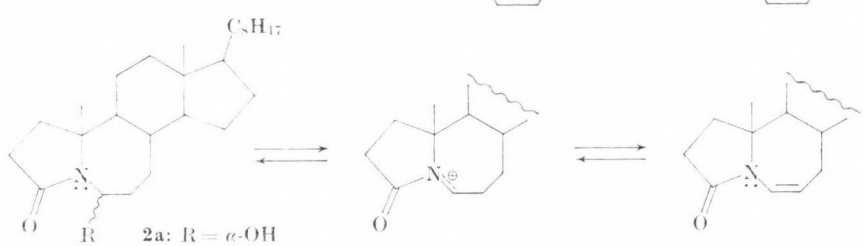

2a: R = α-OH
2b: R = β-OH
2c: R = β-OMe

5

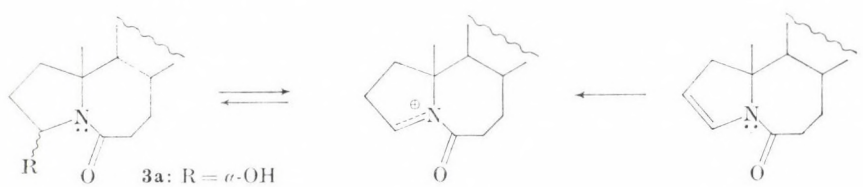

3a: R = α-OH
3b: R = β-OH
3c: R = α-OMe

6

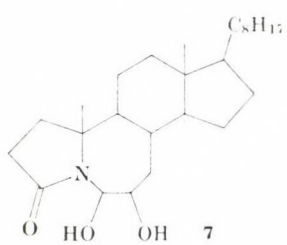

7

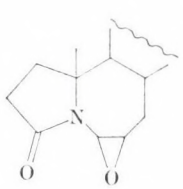

8

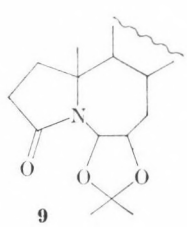

9

that the formation of imide **4** from the starting lactamoester **1** takes place as the first step of the reaction, preceding the subsequent reduction of **4** to hydroxylactams **2a**, **2b**, **3a** and **3b**, which are the final products. The discussed process is not highly regioselective; the susceptibility of both carbonyl groups in imide **4** to reduction was found to be approximately the same.

The observed resistance of hydroxylactams to further reduction under the described conditions is probably connected with the formation of quasi-six-membered cyclic complexes *A* or *B* [13]. It should be added that the ratio of the two epimers (α : β) in both pairs of hydroxylactams corresponds closely to their thermodynamic equilibration. This was evidenced by mutual isomerizations of the epimers (**2a** $\rightleftarrows$ **2b** and **3a** $\rightleftarrows$ **3b**) under the conditions of $LiAlH(O\text{-}t\text{-}Bu)_3$ reduction at room temperature (in the equilibrium state hydroxylactams **2b** and **3a**, respectively, predominated). Contrary to that reduction, the $NaBH_4/H^+$ method did not cause any equilibration of the hydroxylactams [11] and therefore under these conditions the stereochemical course of the reaction determined the product composition.

Similar isomerizations of the hydroxylactams **2a**, **2b**, **3a** and **3b** were also observed under other conditions, using bifunctional catalysts, as well as both acid and basic agents. For instance, each hydroxylactam in benzene solution underwent anomerization catalyzed by 2-hydroxypyridine as a bifunctional, tautomeric catalyst. It has also been found experimentally that pyridine, *p*-cresol, as well as 3-hydroxypyridine exhibit no catalytic activity for this isomerization. It is very probable that the mechanism of the above epimerization of hydroxylactams could be similar to that proposed for tetramethylglucose mutarotation [14] and other reactions [15] requiring bifunctional catalysts (see respective formulas). This concerted exchange of two protons gives the open-chain aldehyde form, which is immediately transformed into the corresponding epimer of hydroxylactam.

It seems that strong bases, such as NaOH, caused epimerization also *via seco*-lactamoaldehyde [16].

Compounds **2a** and **2b** in THF solution, treated separately with a drop of 60% $HClO_4$ at room temperature (0.5 h), afforded the same mixture consisting of the unsaturated lactam **5** (m.p. 133—135 °C, $[\alpha]_D^{24}$ + 154.6°; 65%), as well as hydroxylactams **2a** (5%) and **2b** (15%). The mixture composition was not significantly altered upon prolonging the reaction time to 3 h. It should be added that the obtained lactam **5**, when treated with a drop of 60% $HClO_4$ in dry THF, gave an identical equilibrium mixture of the substrate and hydroxylactams **2a** and **2b**.

In the case of the reaction of the hydroxylactam **3a** or **3b** with perchloric acid, the corresponding dehydrated product **6** was not formed, but only epimerization of the hydroxylactams **3a** $\rightleftarrows$ **3b** (70% and 18%, respectively) was observed. It is likely, therefore, that dehydration of these hydroxylactams

is not a favoured process due to a comparative high strain of the unsaturated five-membered ring system. However, the unsaturated lactam **6** (m.p. 126—128 °C, $[\alpha]_D^{24}$ + 97.6°) was prepared by dehydration of hydroxylactam **3a** or **3b** upon long heating in boiling pyridine. Under the same conditions hydroxylactam **2a** or **2b** also underwent almost quantitative dehydration to give compound **5**. The unsaturated lactam **6** in THF solution under acid conditions ($HClO_4$) immediately transformed into a mixture of hydroxylactams **3a** and **3b**, the ratio being 4 : 1.

Previous studies [17] on a similar hydroxylactam [18], 4-aza-5ξ-hydroxycholestan-3-one, have shown that this compound also readily undergoes dehydration on heating above 100 °C or in the presence of acid catalysts at 25 °C. We suppose that all reactions of hydroxylactams with an acid agent occur *via* stabilized α-acylimmonium ion, which may lose a proton, or to which a molecule of water may be added. This has been supported by methylation experiments of hydroxylactams with methanol in the presence of small amounts of pyridine hydrochloride (as an acid) at room temperature. Under these conditions both hydroxylactams **3a** and **3b** gave the same product, the α-methyl ether **3c** (m.p. 115—117 °C, $[\alpha]_D^{25}$ + 67.0°). Hydroxylactams **2a** and **2b**, rather unexpectedly, afforded the 6β-methoxysteroid **2c** ($[\alpha]_D^{25}$ + 96.0°) as the main product*. In return, also the transformation OMe → OH proved to be possible. Upon treatment of **3c** in THF with $HClO_4$ at room temperature a mixture of the hydroxylactams **3a** and **3b** was obtained in almost quantitative yield. Under the same conditions the methoxylactam **2c** afforded the unsaturated lactam **5** (65%) and hydroxylactams **2a** and **2b**. It seems that the transformations involve reactions occurring *via* an acylimmonium intermediate. Reactions of the lactamodiol **7** provided further evidence for the α-acylimmonium ion formation in acid medium. Compound **7** (m.p. 144—145 °C, $[\alpha]_D^{25}$ + 33.3°) was obtained from the unsaturated lactam **5** by oxidation with osmium tetroxide. The configuration of hydroxyl groups in the lactamodiol **7** was established on the basis of the 1H-NMR spectrum and analysis of the steric course of the reaction. The most indicative in the 1H-NMR spectrum was the chemical shift of the 19-H protons (δ 1.49) which were strongly deshielded by the two β-substituents at C-6 and C-7. Inspection of Dreiding stereomodels of the unsaturated lactam **5** showed that in the most privileged, flattened conformation (the absorption band at 237 nm confirms that the lactam group and double bond lie in the same plane) a steric hidrance for OsO_4 attack from the α-side of the steroid molecule (particularly 9α-H) is much higher

* Configurations of the methoxyl groups at C-4 or C-6 in compounds **2c** or **3c** were established on the basis of their 1H-NMR spectra. Comparison of the signal of the 4-H or 6-H proton in the spectra of the methyl ethers **2c** or **3c** with an analogous signal in the spectra of the hydroxylactams (after shaking the samples with D_2O) indicated β-substitution for **2c** and α-substitution for **3c**. In compound **2c**, the 6β-methoxyl group occupies a *pseudo-equatorial* position (6α-H appeared as dd, $J1$ = 9.5 Hz, $J2$ = 7.5 Hz at δ 5.19).

than from the β-side (C-19 methyl group). Treatment of **7** with perchloric acid in THF solution afforded a single, crystalline product, the epoxylactam **8** (m.p. 193—195 °C, $[\alpha]_D^{17} + 75.7°$). A similar reaction of the lactamodiol **7** effected in acetone solution resulted in formation of compound **9** (m.p. 89—90 °C, $[\alpha]_D^{17} + 45.1°$) possessing an additional dioxolane ring. Compound **9** was also formed from the epoxylactam **8** under acid conditions in acetone solution. The configurations of the oxygen substituents in compounds **8** and **9** were the same as in the starting lactamodiol **7**. During the reactions with perchloric acid the C(7)—O bond remained intact, and this simultaneously determined the β-position of oxygen at C-6. This assignment was confirmed by the strong chemical shift of the C-19 protons in the 1H-NMR spectra of compounds **7**, **8** and **9**. All these rather unusual reactions are promoted by participation of the neighbouring lactam group. The free electrons of nitrogen stabilize the intermediate α-acylimmonium cation, which undergoes an oxirane ring closure in the intramolecular process or reacts with the solvent (acetone) to give a dioxolane ring.

Experimental

M.p.'s were determined on a Boetius micro melting point apparatus and are uncorrected. Optical rotations were measured on a Perkin-Elmer 241 polarimeter in $CHCl_3$. IR spectra were recorded on UR-20 and Unicam SP 1100 spectrophotometers in $CHCl_3$ or in KBr. UV spectra were taken on a Specord UV-VIS spectrophotometer in ethanolic solutions. 1H-NMR spectra were obtained on a Jeol-100 apparatus in $CDCl_3$ solutions with TMS ($\delta = 0$ ppm) as internal standard. The methyl ester of 6-oxo-B-homo-A-nor-A-*seco*-5-azacholestan-3-oic acid (**1**), m.p. 155.5—156.5 °C, $[\alpha]_D^{25} + 53.6°$, was synthesized according to the known method [19].

Reduction of lactamoester 1 with $LiAlH(O\text{-}t\text{-}Bu)_3$

The lactamoester **1** (1 g) was dissolved in dry THF (100 mL) and $LiAlH(O\text{-}t\text{-}Bu)_3$ (4 g) was added in portions at room temperature. The mixture was allowed to stand for 3 h. The excess of hydride was decomposed with moist THF. The solvent was evaporated under reduced pressure. The residue was dissolved in benzene and washed with a solution of sodium tartrate. The organic layer was separated, washed with water, dried (anhydrous $MgSO_4$) and evaporated. The remaining oily residue was chromatographed on silica gel (> 230 mesh). Elution with benzene—ether (7 : 3) mixture yielded the hydroxylactam **3b** (65 mg). With benzene—ether (6 : 4) the chromatographically unseparable hydroxylactams **2a** and **3a** (325 mg) were eluted. Further elution with benzene—ether (1 : 1) mixture afforded the pure hydroxylactam **2b** (250 mg).

Crystallization of the mixture of compounds **2a** and **3a** from *n*-heptane* yielded the pure hydroxylactam **3a** (170 mg). Pure hydroxylactam **2a** was obtained by chromatographic separation of the equilibrium mixture of compounds **2a** and **2b** which formed on heating a solution of the hydroxylactam **2b** in *n*-heptane for 15 min.

The spectral data and physical constants of all these hydroxylactams were published in our preliminary communication [1].

Reduction of the imide **4** with the same hydride was carried out analogously as in the case of lactamoester **1**. The resulting mixture of products was almost identical with that described above.

* Under these conditions compound **2a** partially isomerized to **2b**.

Dehydration of the hydroxylactams 2 and 3

(a) Hydroxylactam **2** (**a** and/or **b**; 500 mg) in dry pyridine (150 mL) was refluxed for 8 h. After evaporation of the pyridine, the crude product was dissolved in a benzene—ether (1 : 1) mixture and filtered through silica gel. The unsaturated lactam **5** crystallized from heptane in the form of colorless needles (360 mg), m.p. 133—135 °C, $[\alpha]_D^{24}$ +154.6° (c = 0.5).

IR, ν_{max}^{KBr}: 1706 (C=O), 1677 cm^{-1} (w, C=C).

1H-NMR, δ: 6.25 (bd, J = 12 Hz, 1H, —CO—N—CH=C—), 5.03 (m, 1H, —CO—N—C=CH—), 1.21 (s, 3H, 19-CH_3), 0.63 (s, 3H, 18-CH_3).

UV, λ max. 237 nm (ε = 11600).

$C_{26}H_{43}NO$ (385.64). Calcd. C 80.98; H 11.24; N 3.63. Found C 80.79; H 11.19; N 3.59%.

(b) Dehydration of the hydroxylactam **3** (**a** and/or **b**) was carried out in the same manner as described above. The unsaturated lactam **6** crystallized from acetone, m.p. 126—128 °C, $[\alpha]_D^{24}$ +97.6° (c = 0.5). Yield 70%.

IR, ν_{max}^{KBr}: 1639 cm^{-1} (C=O).

1H-NMR, δ: 6.83 (m, 1H, —CO—N—CH=C—), 4.88 (m, 1H, —CO—N—C=CH—), 1.27 (s, 3H, 19-CH_3), 0.69 (s, 3H, 18-CH_3).

UV, λ max. 251 nm (ε = 10780).

$C_{26}H_{43}NO$ (385.64). Calcd. C 80.98; H 11.24; N 3.63. Found C 80.77; H 11.27; N 3.52%

Reactions of compounds 2, 3, 5 and 6 with perchloric acid

(a) To a sample (300 mg) of the hydroxylactam **2** (**a** or **b**), or the unsaturated lactam **5** dissolved in freshly distilled THF (20 mL), a drop of $HClO_4$ (60%) was added and the mixture was allowed to stand for 30 min. The resulting equilibrium mixture was poured into water and extracted with carbon tetrachloride. The extract was dried (anhydrous $MgSO_4$), evaporated and the remaining oily residue was chromatographed on silica gel (70—270 mesh). Elution with a benzene—ether (85 : 15) mixture afforded the unsaturated lactam **5** (200 mg). With benzene—ether (65 : 35) the hydroxylactam **2a** (17 mg) was eluted. Further elution with benzene—ether (55 : 45) yielded the most polar hydroxylactam **2b** (45 mg).

(b) The products of the reaction of the hydroxylactam **3** (**a** or **b**) or the unsaturated lactam **6** (sample of 300 mg) with perchloric acid were separated chromatographically on silica gel (70—270 mesh). A benzene—ether mixture (75 : 25) eluted the hydroxylactam **3b** (55 mg). Elution with benzene—ether (65 : 35) afforded the hydroxylactam **3a** (205 mg).

Isomerizations of the hydroxylactams by means of hydrides, NaOH or 2-hydroxypyridine were carried out by the standard method. The products were separated in an analogous manner as described above.

Methylation of hydroxylactams 2 and 3 with methanol

(a) To a solution of the hydroxylactam **2** (**a** and/or **b**; 300 mg) in methanol (30 mL) pyridine hydrochloride (30 mg) was added, and the mixture was allowed to stand for 30 min. After the usual work-up the product was filtered through a layer of silica gel (70—270 mesh) in a benzene—ether mixture (8 : 2). Pure 6β-methoxy-4-oxo-B-homo-A-nor-5-azacholestane (**2c**; 240 mg) crystallized in a mass, but it did not crystallize after having been dissolved in ordinary solvents; $[\alpha]_D^{25}$ +96.0° (c = 0.44).

IR, $\nu_{max}^{CHCl_3}$: 1680 (C=O), 1089 cm^{-1} (C—O—C).

1H-NMR, δ: 5.19 (dd, $J1$ = 9.5 Hz, $J2$ = 7.5 Hz, 1H, 6α-H), 3.07 (s, 3H, —O—CH_3), 1.31 (s, 3H, 19-CH_3), 0.69 (s, 3H, 18-CH_3).

$C_{27}H_{47}NO_2$ (417.68). Calcd. C 77.64; H 11.34; N 3.35. Found C 77.49; H 11.25; N 3.33%.

(b) Methylation of the hydroxylactam **3** (**a** and/or **b**) was carried out analogously. The crude product **3c** (yield 75%) crystallized from hexane, m.p. 115—117 °C, $[\alpha]_D^{25}$ +67.0° (c = 0.52).

IR, $\nu_{max}^{CHCl_3}$: 1630 (C=O), 1072 cm^{-1} (C—O—C).

1H-NMR, δ: 5.35 (m, $\frac{w}{2}$ = 6 Hz, 1H, 4β-H), 3.17 (s, 3H, —O—CH_3), 1.28 (s, 3H, 19-CH_3), 0.71 (s, 3H, 18-CH_3).

$C_{27}H_{47}NO_2$ (417.68). Calcd. C 77.64; H 11.34; N 3.35. Found C 77.43; H 11.33; N 3.32%.

Demethylation of compounds **2c** and **3c** was effected in the same manner as the other reactions with perchloric acid. The products of demethylation of compounds **2c** or **3c** were also identical with those there described.

Oxidation of 4-oxo-B-homo-A-nor-5-azacholest-6-ene (5) by osmium tetroxide

To a solution of the unsaturated lactam **5** (2.05 g) in dry pyridine (35 mL) osmium tetroxide (1.5 g) was added. The reaction mixture was allowed to stand for 1.5 h at room temperature, and the resulting osmium ester was decomposed with a solution of $Na_2S_2O_5$ (3 g) in water (30 mL) and pyridine (20 mL). The mixture was stirred vigorously for 30 min, poured into water and extracted with carbon tetrachloride. The solvent was evaporated from the dried (anhydrous $MgSO_4$) extract and the oily residue was crystallized from acetone to give the lactamodiol **7** in the form of colourless crystals (1.6 g), m.p. 144—145 °C, $[\alpha]_D^{25}$ +33.3° (c = 1.0).

IR, $\nu_{max}^{CHCl_3}$: 1672 (C=O), 3445 and 3613 cm^{-1} (O—H).

1H-NMR, δ: 5.57 (d, J = 5 Hz, 1H, 6α-H), 4.21 (m, 1H, 7α-H), 3.65 (bs, 2H, —O—H), 1.49 (s, 3H, 19-CH_3), 0.74 (s, 3H, 18-CH_3).

$C_{26}H_{45}NO_3$ (419.65). Calcd. C 74.42; H 10.81; N 3.34. Found C 74.21; H 10.72; N 3.35%.

Reactions of lactamoester 7 in acid medium

(a) The reaction, carried out analogously to the other reactions with perchloric acid, resulted in formation of an oily product which was purified chromatographically on silica gel (70—270 mesh). Elution with a benzene—ether mixture (8 : 2) afforded the epoxylactam **8** (yield 70%), m.p. 193—195 °C (from acetone), $[\alpha]_D^{17}$ +75.7° (c = 0.975).

IR, ν_{max}^{KBr}: 1708 (C=O), 1103 cm^{-1} (C—O—C).

1H-NMR, δ: 5.71 (d, J = 7.6 Hz, 1H, 6α-H), 3.85 (m, 1H, 7α-H), 1.52 (s, 3H, 19-CH_3), 0.68 (s, 3H, 18-CH_3).

$C_{26}H_{43}NO_2$ (401.64). Calcd. C 77.75; H 10.79; N 3.49. Found C 77.51; H 10.85; N 3.61%.

(b) To a solution of the lactamodiol **7** or epoxylactam **8** (300 mg) in acetone (20 mL) a drop of $HClO_4$ (60%) was added and the mixture was let to stand for 30 min. After the usual work-up product **9** was isolated in a pure state by silica gel (70—270 mesh) column chromatography. Elution with a benzene—ether mixture (85 : 15) afforded the acetonide **9** (205 mg), m.p. 89—90 °C (from moist acetone); $[\alpha]_D^{17}$ +45.1° (c = 0.81).

IR, ν_{max}^{KBr}: 1689 cm^{-1} (C=O).

1H-NMR, δ: 6.29 (d, J = 7 Hz, 1H, 6α-H), 4.52 (m, 1H, 7α-H), 1.35, 1.44 and 1.55 (3s, 9H, —O—C(CH_3)$_2$—O— and 19-CH_3), 0.72 (s, 3H, 18-CH_3).

$C_{29}H_{49}NO_3$ (459.72). Calcd. C 75.77; H 10.74; N 3.05. Found C 75.39; H 10.73; N 3.15%.

REFERENCES

[1] Rodewald, W. J., Morzycki, J. W.: Tetrahedron Lett. **1978,** 1077

[2] de Boer, J. J. J., Speckamp, W. N.: 11th International Symposium on Chemistry of Natural Products, IUPAC, Symposium Papers, p. 129, Golden Sands, Bulgaria, September 17—23, 1978

[3] Wijnberg, J. B. P. A., Speckamp, W. N.: Tetrahedron Lett., **1975,** 4035

[4] Wijnberg, J. B. P. A., Speckamp, W. N., de Boer, J. J. J.: Tetrahedron Lett., **1974,** 4077

[5] Dijkink, J., Schoemaker, H. E., Speckamp, W. N.: Tetrahedron Lett., **1975,** 4043

[6] Dijkink, J., Speckamp, W. N.: Tetrahedron Lett., **1975,** 4047

[7] Schoemaker, H. E., Dijkink, J., Speckamp, W. N.: Tetrahedron, **34,** 163 (1978)

[8] Dijkink, J., Speckamp, W. N.: Tetrahedron, **34,** 173 (1978)

[9] Wijnberg, J. B. P. A., Speckamp, W. N., Schoemaker, H. E.: Tetrahedron Lett., **1974,** 4073

[10] Hubert, J. C., Wijnberg, J. B. P. A., Speckamp, W. N.: Tetrahedron, **31,** 1437 (1975)

[11] Wijnberg, J. B. P. A., Schoemaker, H. E., Speckamp, W. N.: Tetrahedron, **34,** 179 (1978)

[12] Hubert, J. C., Steege, W., Speckamp, W. N., Huisman, H. O.: Synth. Commun., **1,** 103 (1971)

[13] YOON, N. M., BROWN, H. C.: J. Am. Chem. Soc., **90,** 2927 (1968)
[14] SWAIN, C. G., BROWN, J. F.: J. Am. Chem. Soc., **74,** 2538 (1952)
[15] RONY, P. R.: J. Am. Chem. Soc., **91,** 6090 (1969)
[16] DE BOER, J. J. J., SPECKAMP, W. N.: Tetrahedron Lett., **1975,** 4039
[17] For a review, see VALTER, R. E.: Usp. Khim., **42,** 1060 (1973)
[18] DOORENBOS, N. J., HUANG, C. L., TAMORRIA, C. R., WU, M. T.: J. Org. Chem., **26,** 2546 (1961)
[19] RODEWALD, W. J., WICHA, J.: Roczniki Chem., **40,** 837 (1966)

Jacek W. MORZYCKI
Władysław J. RODEWALD
Department of Chemistry University of Warsaw, 02093 Warsaw, Poland

Acta Chimica Academiae Scientiarum Hungaricae, Tomus 109 (4), pp. 407—414 (1982)

DER EINFLUSS VON THERMOCHEMISCHEN REAGENZIEN AUF DIE ANREGUNG IN DER ATOMEMISSIONSSPEKTRALANALYSE

R. RAUTSCHKE*, A. UDELNOW und C. KOWALSKI

(Martin-Luther-Universität, Sektion Chemie, Halle/Saale, DDR)

Eingegangen am 16. Februar 1981
Zur Veröffentlichung angenommen am 6. Mai 1981

In der Atomemissionsspektralanalyse mit dem Gleichstrombogen kann durch Zusätze von thermochemischen Reagenzien eine Veränderung des Verdampfungs- und Anregungsverhaltens der Analysenelemente erzielt werden. Die Beeinflussung der verschiedenen Parameter in den Matrizes C, C/SiO_2 und SiC wurde untersucht mit den thermochemischen Reagenzien LiF, BaF_2, CdF_2, PbF_2, CuF_2, AgCl, GeO_2 und Ga_2O_3. Weitere vergleichende Untersuchungen dienten dem Studium der Wirkung von Ga_2O_3, In_2O_3, Tl_2O_3, ZnO, CdO und HgO in einer C-Matrix auf das Analysenelement Titan. Es gelang, sowohl die stattfindenden thermochemischen Reaktionen in der Elektrode als auch den Einfluß der verdampfenden Substanzen auf die Plasmaparameter zu identifizieren.

Einleitung

Die Nachweisbarkeit vieler Elemente wird bei der Emissionsspektralanalyse mit Gleichstrombogenanregung erschwert sowohl durch chemische Reaktionen in der Elektrode, die zu schwerflüchtigen Verbindungen der zu analysierenden Elemente führen, als auch durch die Bildung relativ stabiler Moleküle im Plasma, die nur teilweise dissoziieren, so daß die Zahl der angeregten Teilchen der Elementkonzentration in der Probe nicht proportional ist. In vielen Fällen hat sich deshalb der Zusatz thermochemischer Reagenzien bewährt, die durch Halogenierung, Oxydation, Reduktion oder die Bildung binärer Verbindungen die vollständige Verdampfung der zu untersuchenden Elemente begünstigen [1, 2, 3, 4]. Vergleichende Untersuchungen mit den thermochemischen Reagenzien LiF, BaF_2, CdF_2, PbF_2, CuF_2, AgCl, GeO_2 und Ga_2O_3 sollten dem Studium des Einflusses dieser Reagenzien auf das Verdampfungs- und Anregungsverhalten von Titan in den Matrizes C, C/SiO_2 (5 : 1) und SiC im Gleichstrombogen von 9 A dienen. In weiteren Untersuchungen wurde die Möglichkeit geprüft, Ga_2O_3, In_2O_3, Tl_2O_3, ZnO, CdO und HgO als thermochemische Reagenzien einzusetzen, um die Verdampfungs- und Anregungsvorgänge in einer C-Matrix zu beeinflussen.

* Korrespondenz bitte an diesen Autor richten.

Experimenteller Teil

Einfluß thermochemischer Reagenzien in verschiedenen Matrizes

Probenzusammensetzung: TiO_2 *p. a.*, Spektralkohlenpulver EK 1 (VEB Elektrokohle Lichtenberg), SiO_2 *p. a.*, SiC *p. a.*. Die Matrizes C, SiO_2/C (1 : 5) und SiC enthielten 1% Titan als TiO_2. Die Konzentration der thermochemischen Reagenzien LiF, BaF_2, CdF_2, PbF_2, CuF_2, AgCl, GeO_2 und Ga_2O_3 betrug jeweils 5% bezogen auf die Gesamteinwaage der Probe.

Anregungs- und Aufnahmebedingungen

Spektrograph:	mittlerer Quarzspektrograph Q 24 (VEB Carl Zeiss Jena)
Anregungsgerät:	ABR 3 (VEB Carl Zeiss Jena)
Anregung:	Gleichstrombogen 9 A, 220 V
Arbeitsatmosphäre:	Luft
Elektrodenabstand:	3 mm
Elektrode:	Anode (Trägerelektrode) VEB Elektrokohle Lichtenberg *T* 1/107 Katode (Gegenelektrode) VEB Elektrokohle Lichtenberg *T* 1/102
Zwischenblende:	5 mm
Kamerablende:	1 : 11
Filter:	30% *D* bzw. 3% *D*
Spaltbreite:	0,03 mm
Platten:	ORWO WU 3 blau, extra hart
Belichtungszeit:	180 s
Analysenlinien:	Ti I 260,5 nm (4,78 eV) Ti II 252,5 nm (5,06 eV)

Die verdampfte Substanzmenge wurde bestimmt durch Einwwaage der zu untersuchenden Substanz und Auswaage des Rückstandes ohne Elektrode nach dem Abbrand.

Einfluß der thermochemischen Reagenzien Ga_2O_3, In_2O_3, Tl_2O_3, ZnO, CdO und HgO in der C-Matrix

Probenzusammensetzung: TiO_2 *p. a.*, Spektralkohlepulver EK 1 (VEB Elektrokohle Lichtenberg).

Thermochemische Reagenzien: Ga_2O_3, In_2O_3, Tl_2O_3, ZnO, CdO, HgO. Jede Probe enthielt 0,1% Titan als Analysenelement in der C-Matrix. Die Konzentration der thermochemischen Reagenzien variierte von 0,05 bis 10%.

Anregungs- und Aufnahmebedingungen

Spektrograph:	mittlerer Quarzspektrograph Q 24 (VEB Carl Zeiss Jena)
Anregungsgerät:	UBI 1 (VEB Carl Zeiss Jena)
Anregung:	Gleichstrombogen 9 A, 220 V
Arbeitsatmosphäre:	Luft
Elektroden:	Anode (Trägerelektrode) VEB Elektrokohle Lichtenberg, *T* 1/107 Katode (Gegenelektrode) VEB Elektrokohle Lichtenberg, *T* 1/102
Elektrodenabstand:	3 mm
Zwischenblende:	5 mm
Kamerablende:	1 : 11
Filter:	10% *D*
Spaltbreite:	0,02 mm
Platten:	ORWO WU 3 blau, extra hart
Belichtungszeit:	210 s
Analysenlinien:	Ti I 319,2 nm (3,91 eV) Ti II 319,1 nm (4,97 eV)

Mit den genannten Proben wurden unter den angegebenen Anregungs- und Aufnahmebedingungen die spektralanalytischen Untersuchungen durchgeführt. Die Auswertung der erhaltenen Ergebnisse erfolgte mit statistischen Prüfverfahren, um signifikante Intensitätsunterschiede zu erkennen.

Diskussion und Ergebnisse

Sowohl die Bestimmung der aus den jeweiligen Proben verdampften Substanz als auch die Messung der Linienintensitäten des Titans erlaubten Rückschlüsse auf den Einfluß der verschiedenen thermochemischen Reagenzien in den untersuchten Matrizes.

Aus dem Verhältnis der aus den Elektroden verdampften Substanzmengen mit und ohne Zusatz thermochemischer Reagenzien ist zu entnehmen, daß die Verdampfung in der C-Matrix vor allem durch CuF_2, AgCl und GeO_2 zunimmt, in der SiC-Matrix dagegen durch BaF_2, PbF_2 und AgCl verstärkt wird (Abb. 1).

Die untersuchten thermochemischen Reagenzien üben jedoch keinen Einfluß aus auf die Verdampfung der C/SiO_2-Matrix. Dieses unterschiedliche Verhalten der Matrizes deutet auf Elektrodenreaktionen hin, die durch einige thermochemische Reagenzien entscheidend beeinflußt werden. In der C-Matrix erfolgt eine verstärkte Verdampfung der Matrix nur dann, wenn die Elektrodentemperatur nur wenig durch die thermochemischen Reagenzien erniedrigt wird. In der SiC-Matrix wirken vor allem einige halogenierende Reagenzien auf die Verdampfung der Matrix. Dagegen ist in der SiO_2/C-Matrix zunächst die Bildung einer Schmelze zu beobachten, in der langsam eine Reaktion zum SiC eintritt. Dieser Verdampfungsvorgang in der Elektrode kann, wie die Ergebnisse zeigen, durch die eingesetzten thermochemischen Reagenzien nicht beeinflußt werden.

In den folgenden spektralanalytischen Untersuchungen der Intensitäten von Atom- und Ionenlinien sollte geprüft werden, welchen Einfluß die angegebenen thermochemischen Reagenzien auf das Anregungsverhalten des Titans nehmen. Dazu wurden die Ti-Linienintensitäten in der verschiedenen

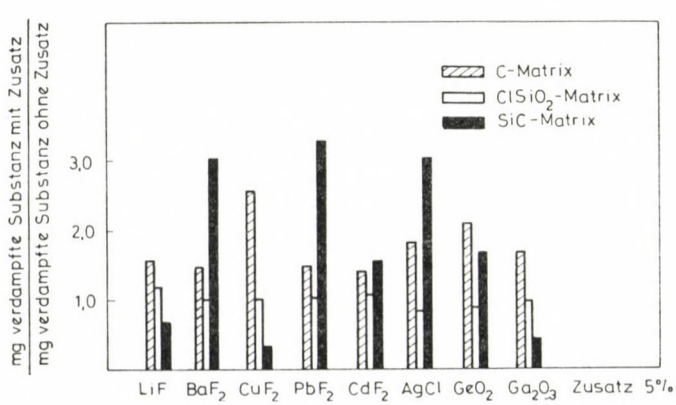

Abb. 1. Verdampfungsverhalten der C-, C/SiO_2- und SiC-Matrix bei Zusatz verschiedener thermochemischer Reagenzien. Anregung: 9 A Gleichstrombogen, Belichtung: 60 s

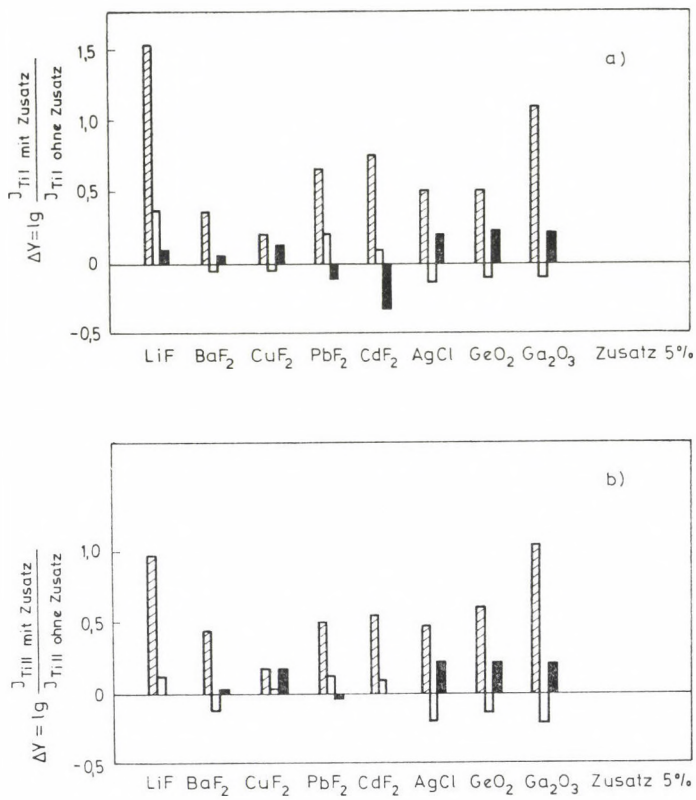

Abb. 2. a) Logarithmen des Verhältnisses der Linienintensitäten von Ti I 260,5 nm in der C-, C/SiO_2- und SiC-Matrix bei Zusatz verschiedener thermochemischer Reagenzien zur Titan-Linienintensität in der gleichen Matrix ohne Zusätze. $\Delta Y = \lg \frac{I_{\text{Ti I mit Zusatz}}}{I_{\text{Ti I ohne Zusatz}}}$. Anregung: 9 A Gleichstrombogen, Belichtung: 180 s
b) Logarithmen des Verhältnisses der Linienintensitäten von Ti II 252,5 nm in der C-, C/SiO_2- und SiC-Matrix bei Zusatz verschiedener thermochemischer Reagenzien zur Titan-Linienintensität in der gleichen Matrix ohne Zusätze. $\Delta Y = \lg \frac{I_{\text{Ti II mit Zusatz}}}{I_{\text{Ti II ohne Zusatz}}}$. Anregung: 9 A Gleichstrombogen, Belichtung: 180 s

Matrizes mit den Zusätzen der thermochemischen Reagenzien verglichen mit den Ti-Linienintensitäten der Proben ohne Zusätze (Abb. 2).

LiF, PbF_2, CdF_2, AgCl, GeO_2 und Ga_2O_3 bewirken in einer C-Matrix als thermochemischen Reagenzien eine wesentliche Erhöhung der Ti I-Intensität, während der Einfluß von allen untersuchten thermochemischen Reagenzien in den Matrizes SiO_2/C und SiC gering ist oder überhaupt nicht auftritt. Die Ti II-Intensität wird nur in der C-Matrix von LiF-, PbF_2-, CdF_2, GeO_2 und Ga_2O_3-Zusätzen etwas erhöht, nicht aber in den anderen Matrizes. Diese Ergebnisse lassen darauf schließen, daß durch den Zusatz eines thermochemi-

schen Reagenzes die Temperatur des Plasmas gesenkt wird und demzufolge die Zahl der Atome gegenüber der Zahl der Ionen zunimmt.

Ein Vergleich der Ergebnisse der Verdampfungsuntersuchungen mit den spektralanalytischen Ergebnissen läßt erkennen, daß zwischen der Menge der aus der Elektrode verdampfenden Substanz und der Erhöhung der Linienintensität kein unmittelbarer Zusammenhang besteht. Eine Erhöhung der Linienintensität kann nur mit jenen thermochemischen Reagenzien erzielt werden, die den Verdampfungs- ebenso wie den Anregungsprozeß des untersuchten Analysenelements begünstigen.

Zum Studium dieser Prozesse dienten die folgenden Messungen. Die spektralanalytischen Untersuchungen der thermochemischen Reagenzien Ga_2O_3, In_2O_3, Tl_2O_3, ZnO, CdO und HgO in einer C-Matrix ergaben, daß die

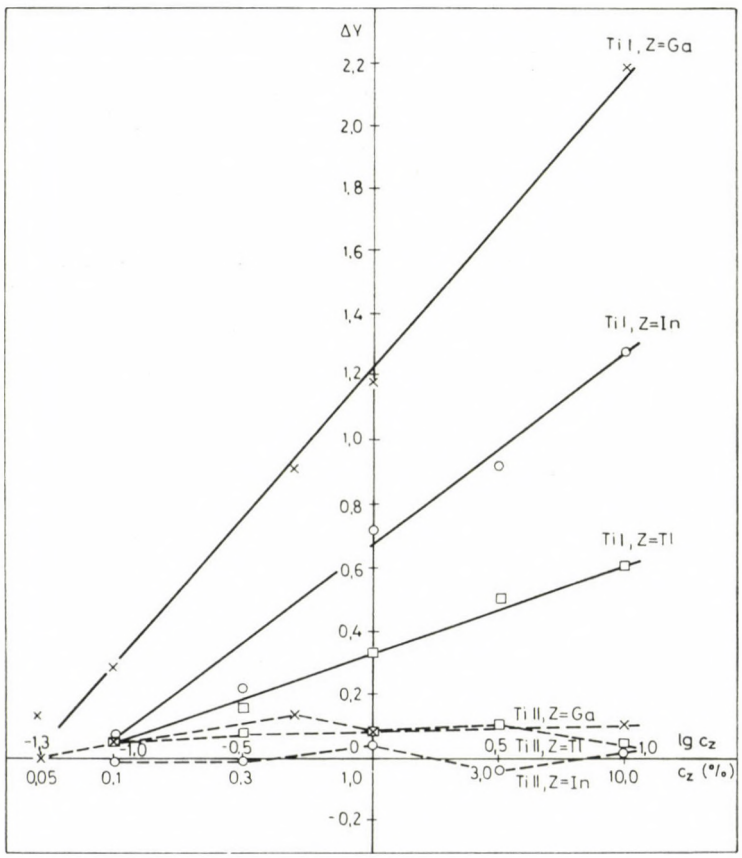

Abb. 3. Abhängigkeit der Ti I-Intensität und Ti II-Intensität von der Konzentration der thermochemischen Reagenzien Ga_2O_3, In_2O_3, Tl_2O_3. $\Delta Y = \lg \frac{I_{\text{Ti I, II mit Zusatz}}}{I_{\text{Ti I, II ohne Zusatz}}}$. Anregung: 9 A Gleichstrombogen, Belichtung: 210 s

Linienintensitätserhöhung des Titans sowohl abhängig ist von der Konzentration des Zusatzes als auch vom Ionisierungspotential der entsprechenden Metalle (Tab. I).

Schon bei niedrigen Konzentrationen von Ga_2O_3-, In_2O_3- und Tl_2O_3-Zusätzen kann eine signifikante Intensitätserhöhung beobachtet werden, die bis 10% Zusatz eine monotone Zunahme erfährt (Abb. 3). Die Wirkung dieser thermochemischen Reagenzien erstreckt sich vor allem auf die Atomlinien. Die Intensität der Ionenlinien wird kaum verändert.

Nur einen geringen Einfluß auf die Linienintensität üben die Zusätze von ZnO, CdO und HgO aus (Abb. 4).

Diese Unterschiede zwischen den beiden Gruppen der thermochemischen Reagenzien sind zu deuten mit den hohen Ionisierungspotentialen von Zn, Cd und Hg.

Tabelle I

Element	Ionisierungspotential (eV)	Atomgewicht	Schmelzpunkt des Metalls (K)	Schmelzpunkt des Oxids (K)
Ga	6,00	69,7	303,2	2068
In	5,78	114,8	430,2	988,2
Tl	6,11	204,4	575,7	990,2
Zn	9,39	65,4	692,7	2248
Cd	8,99	112,4	594,0	—
Hg	10,43	200,6	234,3	—

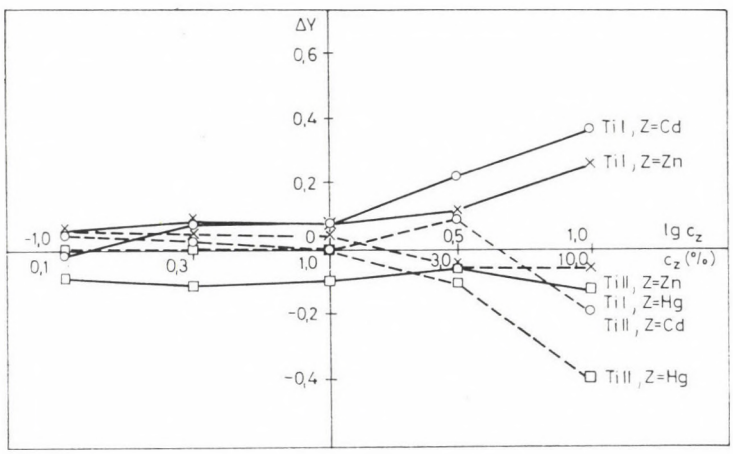

Abb. 4. Abhängigkeit der Ti I-Intensität und Ti II-Intensität von der Konzentration der thermochemischen Reagenzien ZnO, CdO und HgO. $\Delta Y = \lg \frac{I_{\text{Ti I, II mit Zusatz}}}{I_{\text{Ti I, II ohne Zusatz}}}$. Anregung: 9 A Gleichstrombogen, Belichtung: 210 s

Thermochemische Reagenzien mit niedrigem Ionisierungspotential verlängern nicht nur die Verweilzeit der verdampften Substanzen im Plasma, sondern verändern auch die Elektronendichte im Plasma, die Feldstärke, Temperatur und die Temperaturverteilung. Nach BOUMANS [5, 6, 7] besteht zwischen dem Transportparameter ψ im Bogen und der mittleren Verweilzeit τ die Beziehung

$$\tau = \frac{V}{\psi}$$

wobei mit V das Bogenvolumen bezeichnet wird. Sowohl der Transportparameter als auch die mittlere Verweilzeit der Teilchen sind eine Funktion des Ionisierungsgrades des untersuchten Elements, wobei der Transportparameter mit wachsendem Ionisationsgrad zunimmt. Die Teilchendichte im Plasma und die Spektrallinienintensität sind einander proportional. Die Teilchendichte n hängt ab von der Verdampfungsrate Q und dem Transportparameter der jeweiligen Bogenanordnung

$$n = \frac{Q}{\psi} .$$

Die Anwesenheit von Substanzen mit niedrigem Ionisierungspotential bewirkt eine Temperaturerniedrigung und damit auch eine Erniedrigung des Ionisierungsgrades der Elemente im Plasma. Entsprechend verändert sich auch der Transportparameter und führt zu einer größeren Teilchendichte, die wiederum eine Erhöhung der Spektrallinienintensität zur Folge hat.

Der Effekt der thermochemischen Reagenzien beruht nach NICKEL und SCHAEPS [8, 9] hauptsächlich auf folgenden Zusammenhängen. Die leicht ionisierbaren Substanzen erhöhen die Zahl der geladenen Teilchen im Plasma und entsprechend die elektrische Leitfähigkeit. Da die Ionisierungsgleichgewichte aller Teilchenarten von der Elektronendichte abhängen, führt eine Erhöhung der Elektronenkonzentration zu einer wesentlichen Beeinflussung der Ionisierungsgleichgewichte aller beteiligten Reaktionspartner. Diese durch Zusatz leicht ionisierbarer Substanzen erzeugten Elektronen bewirken höhere Atomkonzentrationen im Plasma und demzufolge eine Erhöhung der Atomlinienintensitäten.

Die Wirkung der thermochemischen Reagenzien wird außerdem dann verstärkt, wenn in der Elektrode durch Zusatz dieser Substanzen keine Bildung schwerflüchtiger Reaktionsprodukte wie z. B. Carbide erfolgt. Röntgenographische Untersuchungen zeigten, daß bei geringem Kohlenstoffgehalt der Titanprobe zunächst die Bildung von Galliumtitanat stattfindet, während bei höheren Kohlenstoffgehalten bevorzugt $TiGa_2$ entsteht.

Eine Linienintensitätserhöhung kann demzufolge nur dann erwartet werden, wenn die zugesetzten thermochemischen Reagenzien sowohl die Bil-

dung schwerflüchtiger Reaktionsprodukte in der Elektrode verhindern als auch durch ihr niedriges Ionisierungspotential einen günstigen Einfluß auf die Anregungsparameter im Plasma ausüben.

LITERATUR

[1] SCHROLL, E.: Z. Anal. Chem., **198,** 40 (1963)
[2] SCHROLL, E.: XIV. Coll. Spectr. Int. Debrecen, **1967,** 397
[3] RAUTSCHKE, R.: Wiss. Zeitschr. Karl-Marx-Universität Leipzig, **4,** 415 (1979)
[4] RAUTSCHKE, R., MICHAEL, P., ZANDER, U.: Spectrochim. Acta, **33B,** 359 (1978)
[5] BOUMANS, P. W. J. M.: XVI. Coll. Spectr. Int. Heidelberg, 1971, Plenary Lectures and Reports, S. 268
[6] BOUMANS, P. W. J. M., MAESSEN, F. J. M. J.: Spectrochim. Acta, **24B,** 585 (1969)
[7] BOUMANS, P. W. J. M.: Theory of Spectrochemical Excitation, Hilger & Watts Ltd., London 1966
[8] NICKEL, H., SCHAEPS, R.: Z. Anal. Chem., **281,** 193 (1976)
[9] NICKEL, H., SCHAEPS, R.: Z. Anal. Chem. **281,** 273 (1976)

Ruth RAUTSCHKE
A. UDELNOW
C. KOWALSKI

Martin-Luther-Universität, Sektion Chemie,
DDR-4020 Halle/S., Weinbergweg 16.

Acta Chimica Academiae Scientiarum Hungaricae, Tomus 109 (4), pp. 415—428 (1982)

EXPERIMENTAL STUDIES ON THE STATISTICAL THERMODYNAMIC THEORY OF SWELLING ON CHEMICALLY CROSS-LINKED POLYMER GELS, I

DETERMINATION OF THE COMPONENTS OF OVERALL CHEMICAL POTENTIAL CHANGE FOR POLY(VINYL ALCOHOL) HYDROGELS

F. HORKAY[1]* and M. NAGY[2]

([1]National Institute of Occupational Health, Budapest,
[2]Department of Colloid Science, Loránd Eötvös University, Budapest)

Received December 12, 1980
In revised form March 16, 1981
Accepted for publication May 14, 1981

Accurate mechanical and equilibrium deswelling measurements were carried out on chemically cross-linked poly(vinyl alcohol) (PVA) hydrogels. The overall chemical potential change *vs.* composition function accompanied by swelling, and its elastic and mixing components were determined through independent experimental methods.

It has been found that the character of the overall chemical potential change *vs.* composition functions is independent of the conditions of gel preparation (initial concentration of the polymer solution, degree of cross-linking, chemical nature of the cross-linking agent, medium of cross-linking).

Moreover, it has been established that for PVA—water systems the cross-linking component of the overall chemical potential change has a different character from that predicted theoretically.

Introduction

In recent years, interest in a deeper knowledge of the mechanical and other physico-chemical properties of swollen gels considerably increased, as indicated by the increased number of papers published on this subject.

FLORY and TATARA have shown by high-precision mechanical and vapour pressure measurements carried out on poly(dimethylsiloxane) networks, cross-linked by electron irradiation, that the change in free energy accompanied by swelling, is within the experimental error equal to the sum of free energy changes, produced by the deformation of the network, and by the mixing and interaction of the chains with the solvent molecules [1]. However, a generalization of this finding is limited by the fact that swelling investigations were carried out at relatively low diluent activity values, where the mixing component of the overall free energy change plays already a decisive role, so that an unequivocal decision on the question of additivity becomes difficult.

* To whom correspondence should be addressed.

Several publications of French scientists deal with the mechanical properties of gels, prepared by the anionic block polymerization of virtually monodisperse polystyrene and poly(dimethylsiloxane) chains, which, according to our present knowledge, approximate best the ideal model system [2, 3, 4, 5]. These authors investigated the effects of some important structural parameters (functionality of the junction points, relative molecular mass of the network chains) on mechanical properties. However, no swelling investigations were carried out, which might have given the most information on the gel structure and on the validity of theoretical relationships in that solvent activity region, where the mixing and elastic components of the total free energy change (or chemical potential change) are commensurable.

So far, complex investigations were carried out only rarely, on a few system [1, 6, 7, 8], but these investigations did not make possible a satisfactory elucidation of theoretical problems, thus *e.g.* the effect of gel structure on chemical potential functions playing a role during swelling, or the effect of cross-linking on the interaction of polymer and solvent. This is due partly to the limited solvent activity range studied and the uncertainty of the experimental data arising from the measuring techniques used, and partly to the lack of systematic investigations relevant to various types of systems.

Neither were investigations carried out in systems, where specific interactions are to be expected, thus *e.g.* the dipole interaction in polar polymer-solvent systems, or electrostatic interactions in gels containing ionizable groups.

The equilibrium swelling degree decreasing method developed by us and described in detail earlier, permits in a wide polymer concentration range the accurate measurement of the chemical potential change occurring during the swelling process [9]. We attempted the determination of the overall chemical potential change accompanying the change in degree of swelling, and independently from one another its components with the fewest arbitrary assumptions according to our present knowledge. The effect of the steric structure of the gel on the course of the functions was studied, and for unchanged steric structure of the gel the influence of the change in interaction conditions of the polymer-solvent system was investigated.

Theoretical

From thermodynamic point of view a network in swelling equilibrium with a diluent can be considered as a semi-open system: the change in the state characteristics (*e.g.* changes in temperature, deformation state) are accompanied by a change in composition (degree of swelling), in which only the quantity of the so-called diffusible components (not bound to the network)

do change within the gel. In the case of equilibrium the activity of the solvent is determined only by the interaction conditions of the polymer-solvent system and by the accessory elastic component arising from the deformation of the gel, caused by swelling. The elastic component has to be in close relationship with the structure of the network.

Thus, the relationship representing the change in Helmholtz energy during swelling must as a minimum contain a term depending on the structural characteristics and on the deformation state of the network (ΔA_{net}), and another term, taking into account the thermodynamics of the interaction of polymer-solvent system (ΔA_{mix}).

The change in Helmholtz energy depending on the network can be given on the basis of the statistical thermodynamic theory of rubber elasticity [10, 11] in the following form

$$\Delta A_{net} = \Delta A_{el} + \Delta A_{cr} = \frac{kTK_1 \nu_{el}}{2} (\lambda_x^2 + \lambda_y^2 + \lambda_z^2 - 3) - \\ - kTK_2 \nu_{el} \ln (\lambda_x \lambda_y \lambda_z), \tag{1}$$

where K_1 and K_2 are constants being in connection with the structure of the gel, ν_{el} is the number of the elastically active network chains, λ_x, λ_y and λ_z are the principal deformation ratios, k is Boltzmann's constant and T is the temperature.The principal deformation ratios λ_x, λ_y and λ_z relate to the deformation referred to volume V_0, belonging to the unperturbed (theta) state of the chains forming the network. The first term of Eq. (1), (ΔA_{el}), takes into consideration the change in conformation possibilities of the network chains, due to deformation. The second term, (ΔA_{cr}), reflects the effect of the cross-linking of the chains on the change in entropy accompanied by the deformation of the network.

For the component in conjunction with mixing (ΔA_{mix}), applying the theoretical relationship pertinent to irregular solutions to polymer-solvent mixtures, the following equation is obtained:

$$\Delta A_{mix} = kT(n_1 \ln v_1 + \chi n_1 v_2), \tag{2}$$

where n_1 is the number of the solvent molecules, v_1 and v_2 are the volume fractions of the components, and χ is Huggins' interaction parameter.

Equations (1) and (2) give for the total Helmholtz energy change

$$\Delta A_{tot} = \Delta A_{net} + \Delta A_{mix} = \frac{kTK_1 \nu_{el}}{2} (\lambda_x^2 + \lambda_y^2 + \lambda_z^2 - 3) - \\ - kTK_2 \nu_{el} \ln (\lambda_x \lambda_y \lambda_z) + kT(n_1 \ln v_1 + \chi n_1 v_2). \tag{3}$$

On the basis of general thermodynamic considerations, for two-phase systems in which each phase (or part of space being in connection with each other)

separately is homogeneous [superscript (1) solution phase, superscript (2) gel phase]:

$$\Delta A_{\text{tot}} = \Delta\mu_1^{(1)}(T, V)\, n_1^{(1)} + \Delta\mu_1^{(2)}(T, V)\, n_1^{(2)}, \tag{4}$$

where $\Delta\mu_1 = \mu_1 - \mu_1^0$ and μ_1^0 is the chemical potential of the pure solvent.

Since the number of particles in the system does not change during swelling, it follows from the condition of equilibrium ($d\Delta A_{\text{tot}} = 0$) that:

$$\mu_1^{(1)}(T, V) = \mu_1^{(2)}(T, V) \tag{5}$$

i.e. the chemical potential of the solvent is the same in the gel phase and in the solution (or vapour) phase.

For a gel in swelling equilibrium with the solvent of activity a_1

$$(\Delta\mu_1)_{\text{tot}} = \left(\frac{\partial \Delta A_{\text{tot}}}{\partial n_1}\right)_{T,V} = \left(\frac{\partial \Delta A_{\text{net}}}{\partial n_1}\right)_{T,V} + \left(\frac{\partial \Delta A_{\text{mix}}}{\partial n_1}\right)_{T,V} = RT \ln a_1 \tag{6}$$

Taking into consideration that in the case of isotropic swelling $\lambda_x = \lambda_y = \lambda_z$, and $\lambda_x \lambda_y \lambda_z = V/V_0$ (V is the volume of the swollen gel), the equation

$$\begin{aligned}(\Delta\mu_1)_{\text{net}} = \left(\frac{\partial \Delta A_{\text{net}}}{\partial n_1}\right)_{T,V} = (\Delta\mu_1)_{\text{el}} + (\Delta\mu_1)_{\text{cr}} = \\ = RTK_1 \nu_{\text{el}}^* q_0^{-2/3} q_i^{-1/3} \overline{V}_1 - RTK_2 \nu_{\text{el}}^* q_i^{-1} \overline{V}_1\end{aligned} \tag{7}$$

is obtained, where ν_{el}^* is the concentration of the elastically active chains in the dry ntwork $\nu_{\text{el}}^* = \nu_{\text{el}}/(N_A V_d)$, q_i is the swelling degree of the gel ($q_i = V/V_d$, V_d is the volume of the dry gel), q_0 is the so-called reference swelling degree ($q_0 = V_0/V_d$), $\overline{V}_1$ is the partial molar volume of the swelling agent, and R is the gas constant.

For the mixing part of the overall chemical potential change the following relationship can be written:

$$(\Delta\mu_1)_{\text{mix}} = \left(\frac{\partial \Delta A_{\text{mix}}}{\partial n_1}\right)_{T,V} = RT \ln [(1 - q_i^{-1}) + q_i^{-1} + \chi q_i^{-2}] \tag{8}$$

Taking into account Eqs (7) and (8), for a gel in swelling equilibrium with a diluent of activity a_1 we get:

$$\begin{aligned}RT \ln a_1 = (\Delta\mu_1)_{\text{el}} + (\Delta\mu_1)_{\text{cr}} + (\Delta\mu_1)_{\text{mix}} = RTK_1 \nu_{\text{el}}^* q_0^{-2/3} q_i^{-1/3} \overline{V}_1 - \\ - RTK_2 \nu_{\text{el}}^* q_i^{-1} \overline{V}_1 + RT [\ln (1 - q_i^{-1}) + q_i^{-1} + \chi q_i^{-2}]\end{aligned} \tag{9}$$

Experimental

Materials

For gel preparation poly(vinyl alcohol) (PVA) (Kuraray Poval 420 Japan) was used. The commercial product containing 18—20 mol% of acetate groups was subjected to alkaline hydrolysis in methanol-water mixture, then fractionated with *n*-propanol (Reanal, a.g.). Characteristics of the fractionated sample: $d_{PVA} = 1.27$ g cm^{-3}, $\overline{M}_w = 110\,000$, $\overline{M}_n = 100\,000$, acetate content 1—2 mol%.

For cross-linking, glutaric aldehyde (GDA, Merck, GFR) or succinic aldehyde (SDA) was used. SDA was prepared from 2,5-dimethoxytetrahydrofurane by hydrolysis with hydrochloric acid. The hydrolysate was neutralized with $NaHCO_3$, SDA was extracted with diethyl ether and purified by vacuum distillation repeated twice.

Investigations were carried out on gels prepared at four different polymer concentrations (c^0_{PVA}: 3, 6, 9 and 12 wt.%). The degree of cross-linking of the gels was 50, 100, 200 and 400, respectively (dc: ratio of the quantity in mol of the monomer of the polymer and of the cross-linking agent).

The gels were prepared in distilled water or in a mixture of 90 wt.% dimethyl sulfoxide and 10 wt.% water (DMSO, a.g. Reanal).

A gel pouring frame suitable for the preparation of cylindrical specimens of 1 cm height and 1 cm diameter was used. Cross-links were intoduced at 298 ± 0.1 K [12]. After the proceeding of the chemical reaction the medium of the gels was exchanged in each case for distilled water.

Methods

For the mechanical measurements, the apparatus described in an earlier communication [12] was used, which makes possible at unidirectional compression the accurate determination of the force *vs.* deformation relationship (±0.0001 N and ±6 μm) in a wide range of force and deformation (from 0.0001 N to 2.0 N and from 6 μm to 3.333 mm).

The equilibrium deswelling investigations were carried out by the method developed by us [9]. This method permits the determination of the activity of water in the gel or in the liquid phase in equilibrium with the gel in such a wide polymer concentration range which could be achieved so far only by swelling pressure measurements. For the adjustment of water activity poly(vinylpyrrolidone) (PVP K 30, Fluka, Switzerland) was used. To remove the fraction of low relative molecular mass, PVP solutions were dialized before use against distilled water. Dialysis was continued until PVP could not be detected with an interferometer in the equilibrium liquid phase. Characteristics of the PVP sample prepared in this way: $d_{PVP} = 1.275$ g cm^{-3}, $[\eta]_{298} = 26$ cm^3/g, $\overline{M}_n = 33\,000$.

All the investigations were carried out at 298 ± 0.1 K. The reproducibility of gel preparation and mechanical mesurements was found within 2—3%, that of equilibrium deswelling investigations within 1—2%. In each case, the arithmetic mean of at least 3 parallel measurements was used for evaluation.

Results and Discussion

Determination of the $\frac{(\Delta\mu_1)_{tot}}{RT}$ *vs.* q_i^{-1} functions

For the determination of the change of overall chemical potential *vs.* composition functions, the gels were brought into swelling equilibrium with PVP solutions of various concentrations through a dialyzing membrane. The polymer concentration-water activity functions of the PVP solutions were calculated from accurate (±0.1%) osmotic pressure data [13] relevant to

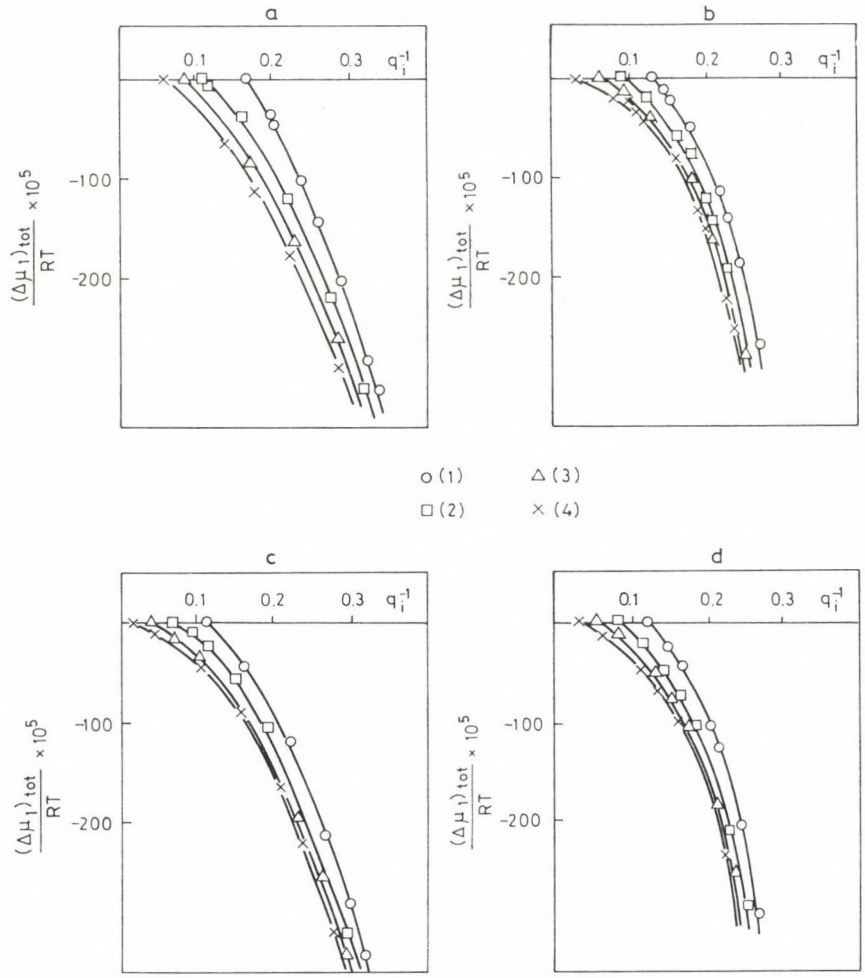

Fig. 1. $\frac{(\Delta\mu_1)_{tot}}{RT}$ *vs.* q_i^{-1} functions. a) 12/GDA/water, b) 9/GDA/water, c) 6/GDA/water, d) 9/SDA/water; dc: (1) 50, (2) 100, (3) 200, (4) 400

a sample of identical trade mark and prepared in the same way, as the PVP used by us. Data in the literature were checked in a limited concentration range also by osmotic pressure measurements (Knauer membrane osmometer, GFR), and a good agreement within 1—2% was found. The $\frac{(\Delta\mu_1)_{tot}}{RT}$ *vs.* q_i^{-1} functions for various systems are shown in Figs 1 and 2. It can be seen that the character of the curves is the same, independently of the initial polymer concentration, the degree of cross-linking, the chemical nature of the cross-linking agent and the medium of cross-linking.

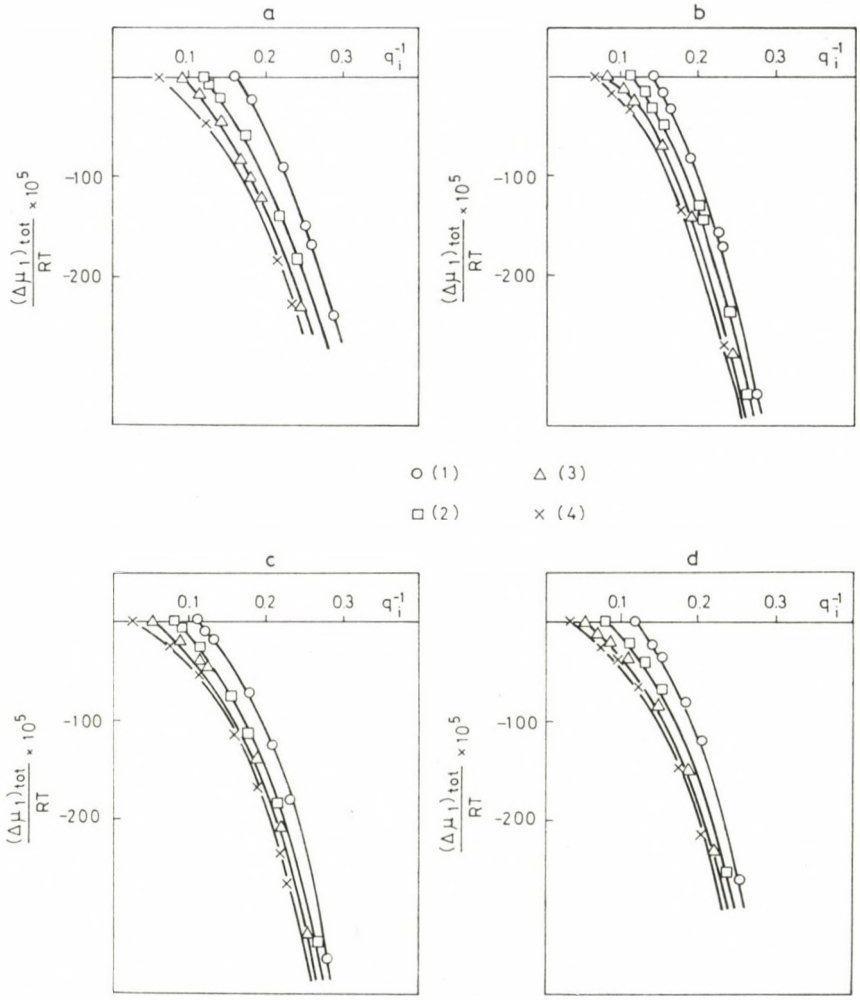

Fig. 2. $\frac{(\Delta\mu_1)_{tot}}{RT}$ *vs.* q_i^{-1} functions. a) 12/GDA/DMSO, b) 9/GDA/DMSO, c) 6/GDA/DMSO, d) 9/SDA/DMSO; dc: (1) 50, (2) 100, (3) 200, (4) 400

Determination of the $\frac{(\Delta\mu_1)_{el}}{RT}$ *vs.* q_i^{-1} functions

The product $K_1 \nu_{el}^* q_0^{-2/3}$ can be determined from unidirectional compression measurements at constant volume [14]:

$$K_1 \nu_{el}^* q_0^{-2/3} = \frac{f L_{Vx}}{V_d RT q_i^{2/3} (\Lambda_x - \Lambda_x^{-2})}$$

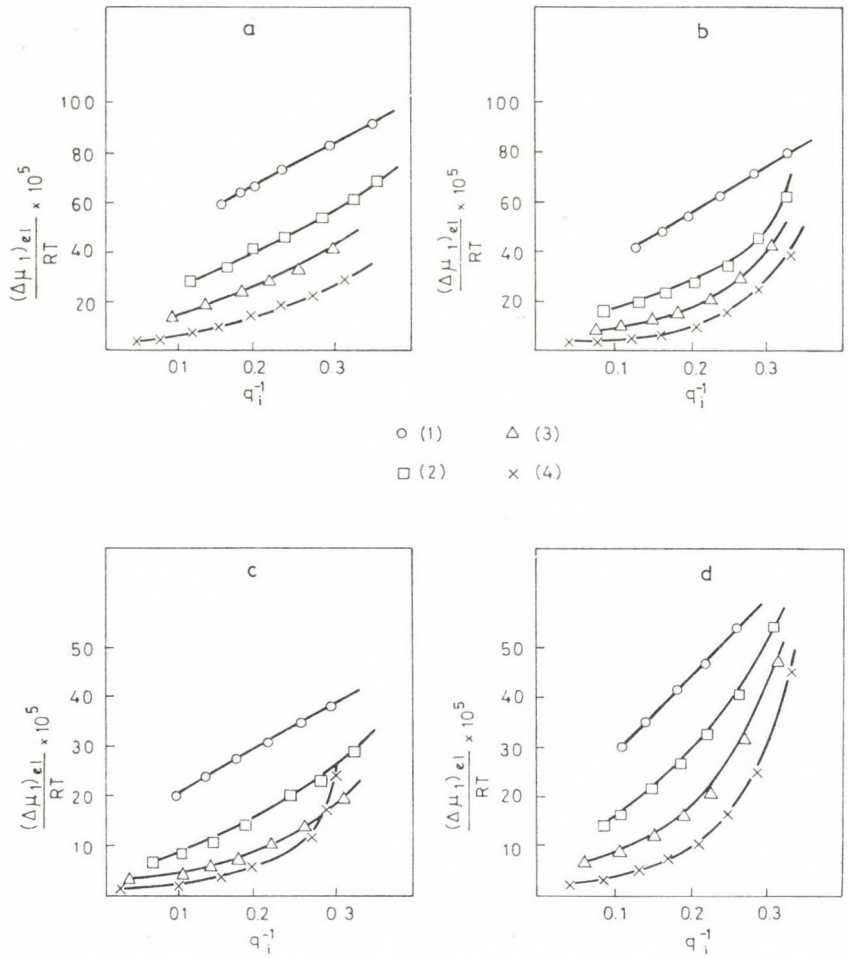

Fig. 3. $\frac{(\Delta\mu_1)_{el}}{RT}$ *vs.* q_i^{-1} functions. a) 12/GDA/water, b) 9/GDA/water, c) 6/GDA/water, d) 9/SDA/water; dc: (1) 50, (2) 100, (3) 200, (4) 400

where f is the force, L_{Vx} the length of the undeformed sample, Λ_x the macroscopic deformation ratio ($\Lambda_x = L_x/L_{Vx}$, L_x is the length of the deformed sample measured in the direction of the x axis).

It was found in earlier investigations that, contrary to the theory, for PVA gels the product $K_1 v_{el}^* q_0^{-2/3}$ is not constant, but increases with decreasing degree of swelling [14]. The functions $K_1 v_{el}^* q_0^{-2/3}$ *vs.* q_i^{-1} were obtained for the various systems from the force *vs.* deformation relationships determined for the same gel samples as a function of the degree of swelling. Functions $\frac{(\Delta\mu_1)_{el}}{RT}$ *vs.* q_i^{-1} are shown for a few systems in Figs 3 and 4.

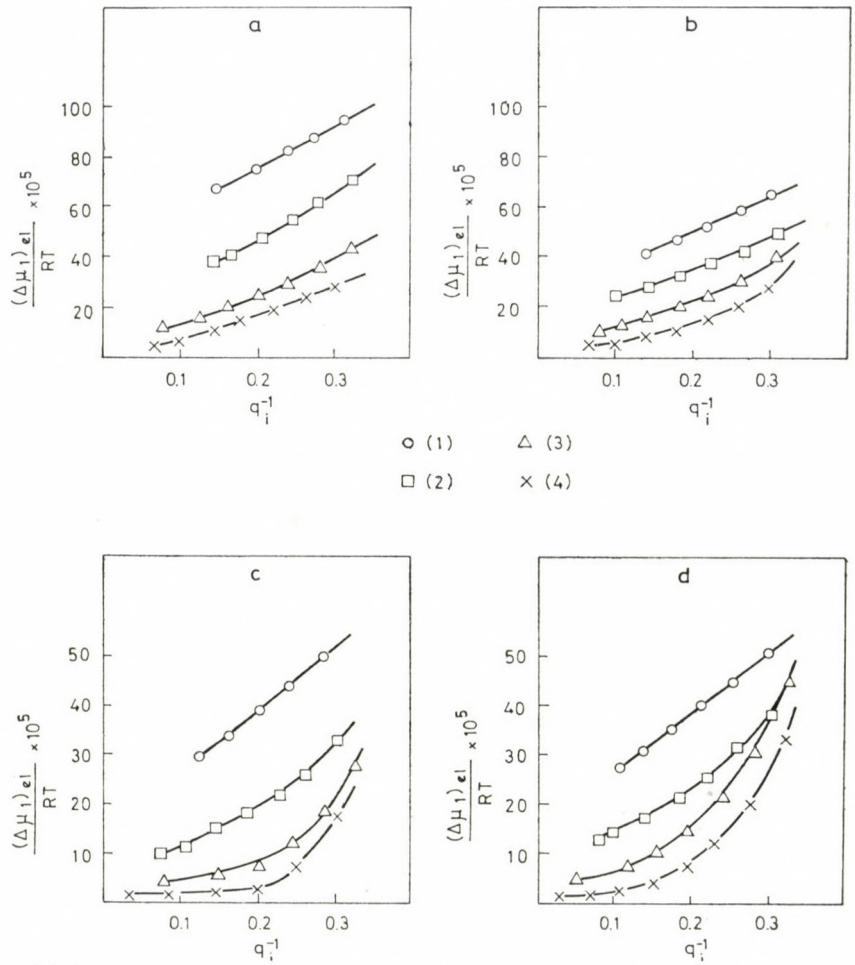

Fig. 4. $\frac{(\Delta\mu_1)_{el}}{RS}$ *vs.* q_i^{-1} functions. a) 12/GDA/DMSO, b) 9/GDA/DMSO, c) 6/GDA/DMSO, d) /SDA/DMSO; dc: (1) 50, (2) 100, (3) 200, (4) 400

Determination of the $\frac{(\Delta\mu_1)_{mix}}{RT}$ *vs.* q_i^{-1} functions

The crucial point in the determination of the $\frac{(\Delta\mu_1)_{mix}}{RT}$ *vs.* q_i^{-1} function is the exact knowledge of the parameter χ in Eq. (8).

Experimental data (vapour pressure, osmotic pressure, freezing point depression measurements) have been reported in the literature for PVA-water systems, from which χ can be calculated [15, 16, 17, 18]. However, these investigations were generally carried out in a considerably narrower concentration range as studied by us, moreover, χ values given in the literature differ

also from one another. All this indicates that χ may depend to a substantial extent on the individual properties (*e.g.* tacticity) of the polymer sample used, so that χ and its dependence on the concentration had to be determined for the polymer used in our experiments by an independent method.

For this purpose gel samples, for which the $\frac{(\Delta\mu_1)_{tot}}{RT}$ *vs.* q_i^{-1} functions were already known from equilibrium deswelling experiments with PVP solu-

Table I

Value of the parameter χ for PVA — *water system*

Volume fraction of the polymer v_2	χ (this work)	χ Refs.	
		[17]	[16]
0.04	0.495±0.005	0.52	0.494
0.08	0.508±0.005	0.54	0.494
0.12	0.520±0.005	0.56	0.494
0.16	0.526±0.005	0.58	—
0.20	0.532±0.005	0.60	—

tions, were equilibrated with uncross-linked PVA solutions of different concentrations. The change of the degree of swelling of the gels was measured as a function of the concentration of PVA solution. Since in the case of equilibrium $\Delta\mu_1^{(1)} = \Delta\mu_1^{(2)}$, from the polymer concentration *vs.* water activity function pertinent to the gel the activity of water in the equilibrium liquid phase can be determined. In Fig. 5 the values obtained experimentally for water activities are plotted as a function of the concentration of the PVA solution. Using the FLORY—HUGGINS equation, the value of χ was calculated from the curve in knowledge of the degree of polymerization of the uncross-linked polymer. χ values found by us and those reported in the literature are contained in Table I.

Knowing parameter χ, the function $\frac{(\Delta\mu_1)_{mix}}{RT}$ *vs.* q_i^{-1} was calculated using Eq. (8) (Fig. 5).

Determination of the $\frac{(\Delta\mu_1)_{cr}}{RT}$ *vs.* q_i^{-1} functions

The $\frac{(\Delta\mu_1)_{cr}}{RT}$ *vs.* q_i^{-1} relationship cannot be directly measured. For its determination, the sum of the function values $\frac{(\Delta\mu_1)_{el}}{RT}$ *vs.* q_i^{-1} and $\frac{(\Delta\mu_1)_{mix}}{RT}$

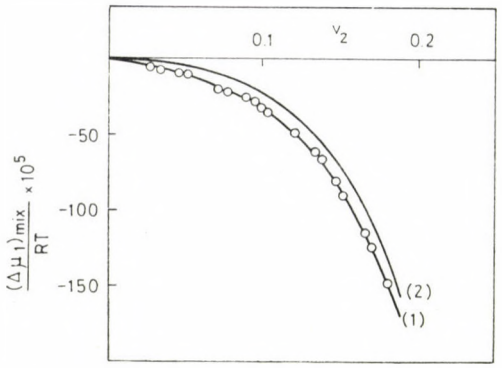

Fig. 5. $\frac{(\Delta\mu_1)_{mix}}{RT}$ *vs.* v_2 function determined experimentally and calculated with Eq. (8) for PVA solutions
(1) experimental points, (2) calculated function

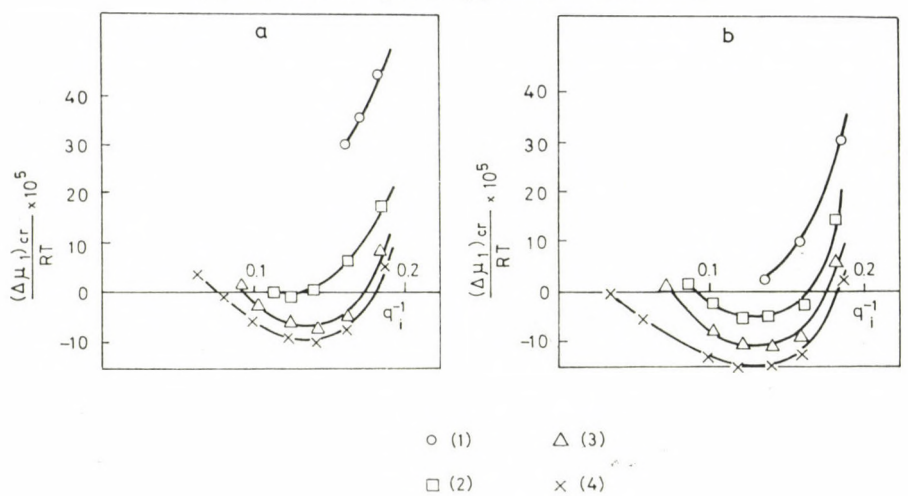

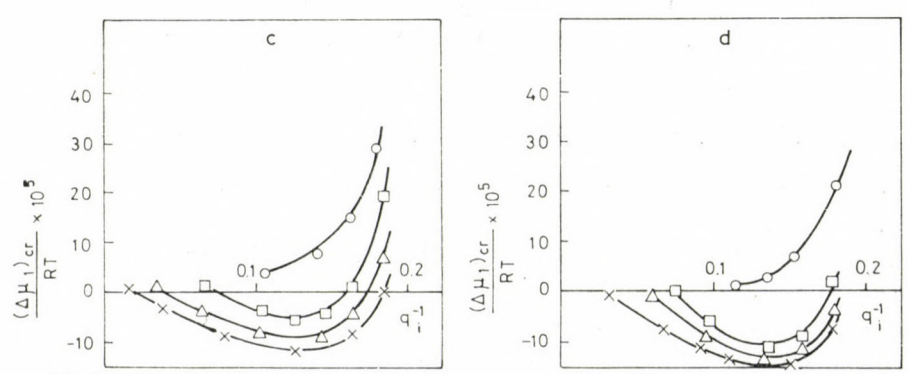

Fig. 6. $\frac{(\Delta\mu_1)_{cr}}{RT}$ *vs.* q_i^{-1} functions. a) 12/GDA/water, b) 9/GDA/water, c) 6/GDA/water, d) 9/SDA/water; dc: (1) 50, (2) 100, (3) 200, (4) 400

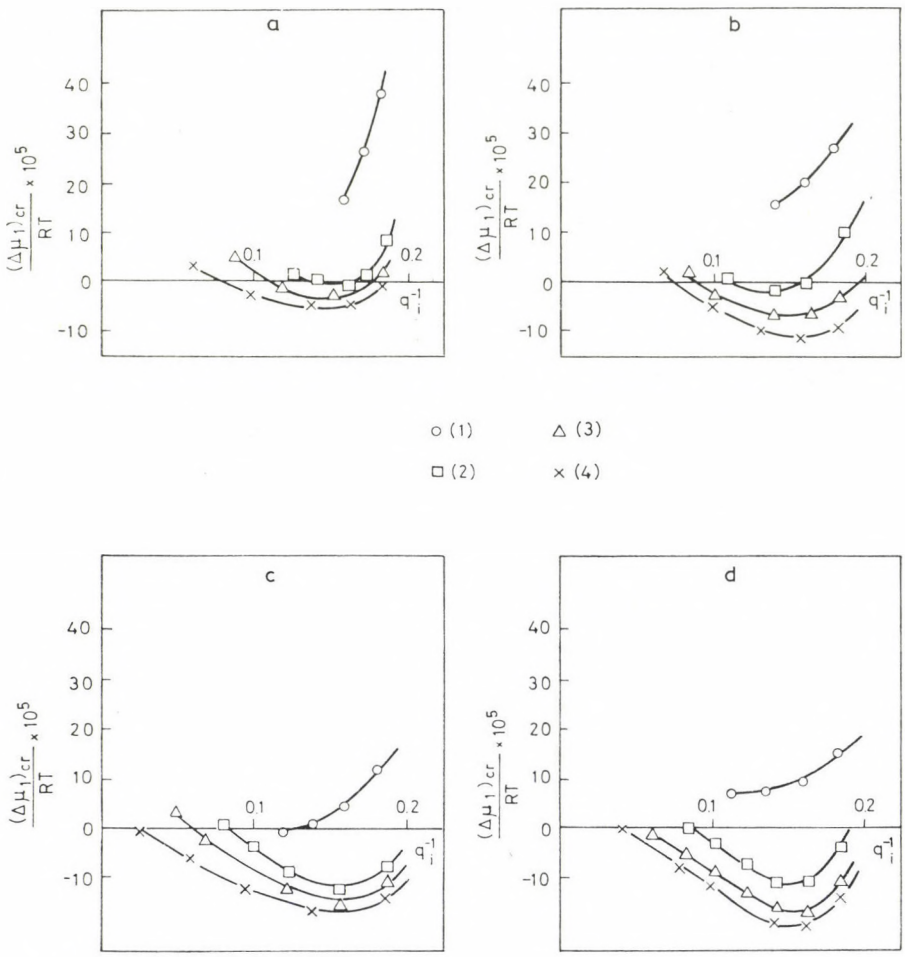

Fig. 7. $\frac{(\Delta\mu_1)_{cr}}{RT}$ *vs.* q_i^{-1} functions. a) 12/GDA/DMSO, b) 9/GDA/DMSO, c) 6/GDA/DMSO, d) 9/SDA/DMSO; dc: (1) 50, (2) 100, (3) 200, (4) 400

vs. q_i^{-1} belonging to the actual q_i^{-1} was substracted from the $\frac{(\Delta\mu_1)_{tot}}{RT}$ *vs.* q_i^{-1}, total chemical potential change *vs.* composition functions (Figs 6 and 7). It can be seen from the figures that the course of the functions is similar for all the system: they pass in the range $q_i^{-1} \approx 0.10 - 0.14$ through a minimum. The value of this minimum is the lowest for the least cross-linked gels, increases with increasing cross-linking density, and finally disappears.

The character of the curves differs fundamentally from that of the theoretical curve. According to theory, $\frac{(\Delta\mu_1)_{cr}}{RT} = -K_2 \nu_{el}^* \overline{V}_1 q_i^{-1}$, that is, the

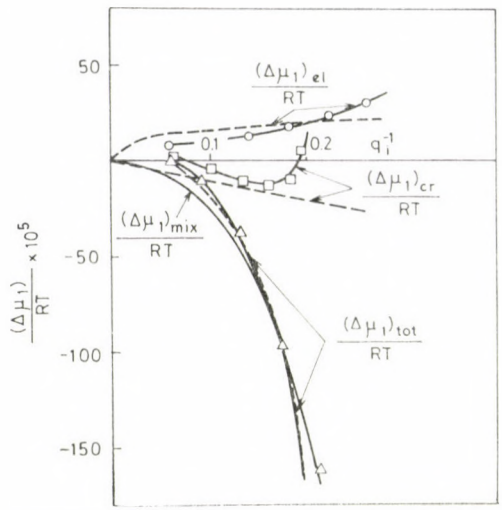

Fig. 8. Chemical potential functions calculated theoretically and determined experimentally (symbol of the system: 9/200/GDA/water)

function is a straight line of negative slope, starting from the origin. According to our experimental results, $-K_2 v_{el}^* \overline{V}_1$ considerably increases with increasing polymer concentration.

Comparison of experimental results with theory

Figure 8 shows for the 9/200/GDA/water system the theoretically calculated and the experimentally determined functions. For the calculation we used the following theoretical values: $K_1 = 1$, $K_2 = 0.5$, $q_0 = q_c$ and $v_{el}^* = v^* \left(1 - \frac{2d_2}{v^* \overline{M}_n}\right)$, where v^* is the concentration of the chains in the dry gel, d_2 is the density of the polymer and $\overline{M}_n$ is the number average molecular mass of the primary chains [19]. It is remarkable that though the components of the total chemical potential change *vs.* composition function determined experimentally considerably differ from the theoretical ones, the difference is scarcely reflected in the overall function.

The deviation of the components from the theoretical functions may have several reasons. It is uncertain how closely real systems are approximated by the use of Eq. (1), valid for ideal networks. The clearing of the physical meaning of the second term, (ΔA_{cr}), is particularly problematic. Neither is it unambiguously clarified, whether the value of χ determined for the solution of the uncross-linked polymer can be substituted for the network polymer.

In our following work a great number of experimental results referring to systems of various types will be evaluated according to uniform points of view, to obtain thereby further information on the main poperties of chemical potential functions, playing a role during swelling.

*

We wish to thank Dr. János KABAI for his advices and for reading of the manuscript.

REFERENCES

[1] FLORY, P. J., TATARA, Y.: J. Polymer Sci. A-2, **13,** 683 (1975)
[2] RIETSCH, F., FROELICH, D.: Polymer, **16,** 873 (1975)
[3] RIETSCH, F., BRAULT, A., FROELICH, D.: Polymer, **19,** 1043 (1978)
[4] BELKEBIR-MRANI, A., HERZ, J. E., REMPP, P.: Macromol. Chem., **178,** 485 (1977)
[5] BELKEBIR-MRANI, A., BEINERT, G., HERZ, J. E., REMPP, P.: Europ. Polym. J., **13,** 277 (1977)
[6] DUŠEK, K.: Collect. Czech. Chem. Commun., **32,** 1554 (1967)
[7] van de KRAATS, E. J., WINKELERS, M. A. M., POTTERS, J. M., PRINS, W.: Rec. Trav. Chim., **88,** 449 (1969)
[8] FROELICH, D., CRAWFORD, D., ROZEK, T., PRINS, W.: Macromolecules, **5,** 100 (1972)
[9] NAGY, M., HORKAY, F.: Magy. Kém. Folyóirat, **85,** 513 (1979)
[10] FLORY, P. J.: J. Chem. Phys., **18,** 108 (1950)
[11] WALL, F. T., FLORY, P. J.: J. Chem. Phys., **19,** 1435 (1951)
[12] HORKAY, F., NAGY, M., ZRINYI, M.: Magy. Kém. Folyóirat, **85,** 567 (1979)
[13] VINK, H.: Europ. Polym. J., **7,** 1411 (1971)
[14] HORKAY, F., NAGY, M.: Acta Chim. Acad. Sci. Hung. **107,** 321 (1981)
[15] SAKURADA, I., NAKAJIMA, A., FUJIWARA, H.: J. Polym. Sci., **35,** 497 (1959)
[16] NAKAJIMA, A., FURUTACHI, K.: J. Soc. High Polymers (Japan), **6,** 460 (1949)
[17] YANO, Y.: J. Chem. Soc. Japan, **76,** 668 (1955)
[18] KAWAI, T.: J. Polym. Sci., **32,** 425 (1958)
[19] DUŠEK, K., PRINS, W.: Fortschr. Hochpolym. Forschung, **6,** 1 (1969)

Ferenc HORKAY H-1096 Budapest, Nagyvárad tér 2.
Miklós NAGY H-1088 Budapest, Puskin utca 11—13.

Acta Chimica Academiae Scientiarum Hungaricae, Tomus 109 (4), pp. 429—448 (1982)

CATALYSIS FROM THE STANDPOINT OF COORDINATION CHEMISTRY

H. NOLLER

(Institut für Physikalische Chemie Technische Universität Wien)

Received January 9, 1981
Accepted for publication May 14, 1981

The coordination chemical approach to catalysis starts from the assumption (postulate) that all bonds between the catalyst and the reactant are EPD—EPA bonds and at least two such bonds are needed which may be called complementary. An essential point of catalysis is the weakening of bonds adjacent to the (EPD—EPA) bonds between the catalyst and the reactant. This bond weakening increases with the interaction strength, which, for a given reactant, in turn, depends upon the site strength of the catalyst. For reactions of the type of elimination, there is a good correlation between the EPA site strength and activity, whereas reactions in which only hydrogen is involved as leaving species, like H/D exchange or (de)hydrogenation, as well as oxidations are favoured by high basicity (high EPD site strength). The mechanistic results in elimination reactions are best accounted for by taking into consideration the cooperation of both EPA and EPD sites. High EPA strength favours E1, high EPD strength E1CB mechanism, whereas a balanced strength favours E2 mechanism. An important question for discussing mixed catalysts is the variation of site strength as a function of the composition. In addition to the strength, the number of sites should be taken into account (but was not considered in this paper).

It is my opinion that our world is becoming more and more complicated and, furthermore, that this increase of complexity is rapidly becoming faster and faster so that the extent of complexity will soon be too great for being mastered by men. In science, also in the science of catalysis, we are accumulating data much more rapidly than reviewing them and finding relationships between them. The danger of going down in this ocean of data is great.

Some may think that it is the task of theory to act against this tendency (trend), however, theory itself has so high a degree of complexity that it is difficult to manage. For all these reasons I consider it convenient to try to find a description of catalysis relatively easy to handle, which of course must be a qualitative description and, first of all, a chemical description. I do not try to find what is usually called the truth or a correct theory, but I do try to find a model which enables me to describe experimental results as congruent and consistent as possible.

Everybody agrees that catalysis can be considered a kinetic phenomenon. I would like to stress the coordination chemical aspect of catalysis [1] rather than the kinetic, hoping that this may bring a remarkable simplification of the description of catalysis and may at the same time be a useful approach, especially for chemists.

Catalysis is brought about by intermolecular interactions, *i.e.* the interaction between the catalyst and the reactant. Intermolecular interactions, however, are part of the huge field of coordination chemistry. This approach immediately leads to asking the question about the bonds between the catalyst and the reactant [2].

For brevity, things will be presented in the form of postulates or statements without reasoning.

Starting postulate: All bonds between the reactant and the catalyst are of the coordinate type, *i.e.* bonds between an electron pair donor (EPD) and an electron pair acceptor (EPA) (this of course is not assumed to be so without any exception, but say in 95 or even 99% of the cases to be considered).

Prototype of a coordinate (EPD—EPA) bond: $H_3N \rightarrow BF_3$. The bond is symbolized with an arrow. This however does not mean that it is a special type of bond, it may be considered to be a normal covalent bond. Instead of EPD and EPA, the terms (Lewis) base and acid respectively are also used.

Our next question is what are the EPD and EPA sites on the catalyst and on the reactant? Note that we speak of sites rather than active sites. It is our purpose to find relationships between chemical properties and catalytic behaviour rather than localize these sites on planes, edges, corners, *etc.* On polar catalysts — the paper will only deal with polar catalysts — EPA sites are obviously cations, EPD sites anions. Anions probably are always present on polar catalysts, because they usually are larger than cations. On the side of the reactants, (electronegative) groups with free electron pairs are EPD, whereas the EPA function can be assumed by C—H-groups, mainly those neighbouring to electronegative groups. (When referring to the catalyst, we use the term site, whereas when referring to the reactant, we prefer the term function.)

Of course, in the interaction between the reactant and the catalyst, we always have to do with interactions between an EPA and an EPD. For a reactant with an electronegative group, *e.g.* an alcohol, the following interaction structure is likely.

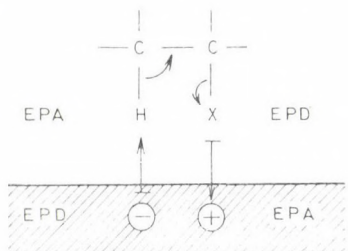

Fig. 1. Interaction structure

It is our opinion that at least these two interactions are necessary for bringing about the catalytic effect.

Effect of coordinate interaction

A crucial point for the catalytic effect is the weakening of adjacent bonds brought about by coordinate bonding. It is GUTMANN [3] who has drawn attention to this important effect.

In the formation of the adducts indicated in Table I the B—F bonds are lengthened (and weakened). The N—B distance is taken as a measure of the EPD strength of the molecule with the free electron pair. The lengthening

Table I

Bond distances in BF_3 *and* BF_3 *adducts*

	BF_3	$CH_3CN\vert\rightarrow BF_3$	$H_3N\vert\rightarrow BF_3$	$Me_3N\vert\rightarrow BF_3$
N|→ B distance (Å)	—	1.63	1.60	1.58
B|→ F distances (Å)	1.30	1.33	1.38	1.39

(and weakening) of the B—F bonds increases with the EPD strength of the other molecule.

A necessary condition for the lengthening and weakening of the adjacent bonds is that their polarity is increased when the coordinate bond is formed. On the other hand, when the polarity is decreased, the bond is strengthened. This may be seen from the variation of bond lengths in the adduct between $SbCl_5$ and tetrachloroethylene carbonate (Fig. 2) [3].

It may however be mentioned that in most cases (in catalysis) the polarity is increased and hence the bond weakened.

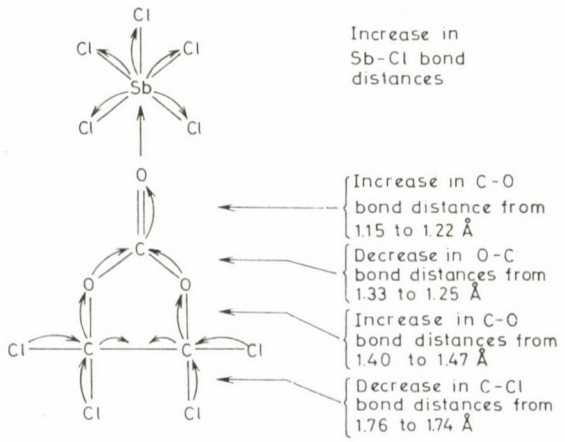

Fig. 2. Variation of bond length in adduct formation

Since for a given substrate, interaction strength and bond weakening depend upon the strength of the surface sites, it would be of utmost importance to have criteria of site strength. For cations, the magnitude e/r (formal charge over radius) may give an orientation. We further propose the electronegativity, either in the form put forward by PAULING [4] or according to the suggestion of SANDERSON [5]. The usefulness of SANDERSON's concept consists mainly in that he proposed an equation to estimate the electronegativity of the compound itself (not only the atoms) — which he called intermediate electronegativity S_{int}.

$$S_{\text{int}} = (S_{\text{P}}^{p} S_{\text{Q}}^{q} S_{\text{R}}^{r})^{\frac{1}{p+q+r}}$$

is the electronegativity of the compound $\text{P}_p\,\text{Q}_q\,\text{R}_r$.

We would suggest to further use the average $\bar{E}_{\text{Ion}}$ of the ionization energies of the valence electrons.

Example: the energies of the successive ionization of the three valence electrons of alumina are [6]:

$$5.98 + 18.82 + 28.44 = 53.24 \text{ eV}$$

$$\bar{E}_{\text{Ion}} = 53.24 : 3 = 17.75 \text{ eV}.$$

At present, we would propose to make use of all these criteria for estimating site strength. As far as we can see, they tell us the same thing in many, perhaps in most cases.

Activity of catalysts

The following results can be interpreted considering the effect of the EPA site only (although the participation of the EPD site should not be forgotten). The activation energy was used as a measure of catalytic activity in the results represented in Table II [1].

The same fundamental activity pattern has frequently been found in zeolite catalysis. In the dehydration of butan-1-ol [7], the following order of activity was observed: LiNaX > NaX > KNaX > RbNaX. With pentan-1-ol SHARF *et. al.* [8] found a similar sequence: HNaY > ZnNaY > MgNaY > > ZnNaX > MgNaX > NaY > NaX. For the cracking of hexane [9], a corresponding order of activity was found NaX ≈ NaY < BaY < MgX < SrY < < CaY < MgY, and similarly for the cracking of cumene [9]: NaY < BaY < < SrY < CaY ≈ MgY ≈ BeY.

Table II

Activation energies of dehydrochlorination on alkali metal and alkaline earth metal chlorides and sulfates

Reactant	Catalyst	E_a (kcal/mol)	Temperature (°C)
2-Chloropropane	LiCl	20	242–271
	NaCl	25	362–393
	KCl	46	295–315
	$CaCl_2$	18	116–189
	$SrCl_2$	20	128–171
	$BaCl_2$	28	82–142
	$CaSO_4$	17	72–132
2-Chlorobutane	$MgSO_4$	13	150–300
	$CaSO_4$	16	180–320
	$BaSO_4$	22	250–400

The cations of the first groups of the periodic table exhibit the general activity pattern shown in Fig. 3, in agreement with our criteria of EPA strength discussed above.

The numerical values are indicated in Table III for comparison. e/r is the charge in elementary units divided by the radius (in Å) of the cation in its usual valence state. The electronegativity S is the Sanderson value of the metal atom. Of course, in a series of compounds (polar catalysts) with the same anion the sequence of the intermediate electronegativity S_{int} should be the same as that of the atoms. The average of the ionization energy ($\overline{E}_{Ion}$, in eV) is the energy required for transforming the atom into a cation, divided by the number of valence electrons.

The activity (interaction) pattern (Fig. 3) is not limited to catalysis, it is general in chemistry and found for example in hydration enthalpies, which are also indicated in Table III. The values are those per "mol" of the

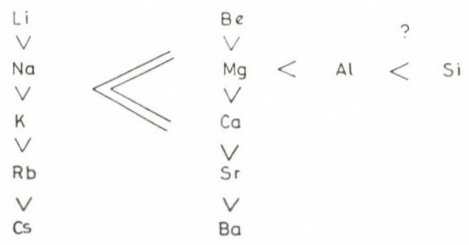

Fig. 3. Regular activity pattern

Table III

Properties for characterizing EPA strength (r, e/r, S, $\overline{E}_{Ion}$) and hydration enthalpy ($-\Delta H_{Hydr}$) of the ion

	r Å	e/r	S (eV)	$\overline{E}_{Ion}$ (eV)	$-\Delta H_{Hydr}$ (kcal/mol)
Li^+	0.68	1.47	0.74	5.39	132
Na^+	0.97	1.03	0.70	5.1	106
K^+	1.33	0.75	0.42	4.3	86
Rb^+	1.47	0.63	0.36	4.2	80
Cs^+	1.67	0.60	0.28	3.9	72
Be^{2+}	0.35	5.71	2.39	13.8	612
Mg^{2+}	0.66	3.03	1.56	11.3	477
Ca^{2+}	0.99	2.02	1.22	9.0	399
Sr^{2+}	1.12	1.78	1.06	8.3	363
Ba^{2+}	1.34	1.49	0.78	7.6	329
Al^{3+}	0.51	5.88	2.22	17.75	1141
Si^{4+}	0.42	9.52	2.84	25.8	—

ion, not per mol of water. The hydration enthalpies were calculated from a compilation [11] of conventional enthalpies of hydration using a value of −269.7 kcal/gram ion for the hydration enthalpy of the proton.

The generality of this interaction pattern can further be seen from the frequency of a determined band of pyridine adsorbed on zeolites with different group 1A and 2A cations [13] (Fig. 4). (It is not important to discuss the assignation of that band, provided it is always the same band.)

According to these criteria, Si^{4+} is expected to be an extremely strong EPA. The catalytic activity of silica, however, is very poor. This riddle of silica (therefore the question mark in Fig. 3) will not be discussed here. I am sure that the EPA strength of a Si surface site is really extremely high [10].

Table IV gives further values of hydration enthalpies, in particular of higher valent cations [12]. For divalent ions, *e.g.* Ca^{2+}, the values resulting per water molecule are of the order of magnitude of 100 kcal, with trivalent ions, values of more than 150 kcal. Note that the bond energy of H_2 is 104 kcal/mol. This means that the bond between a divalent cation and one water molecule of the first hydration shell is as strong as the strongest chemical single bonds, with trivalent ions, these (cation—water) bonds ar much stronger. As far as I can see, most chemists have not realized the strength of these (coordinate) bonds, and therefore doubt the catalytic effect of (surface) cations. I personally believe that the interaction between a surface cation and a donor molecule, *e.g.* an alcohol, is of similar strength (as the interaction in hydration bonds) and hence cations are catalytically important EPA sites.

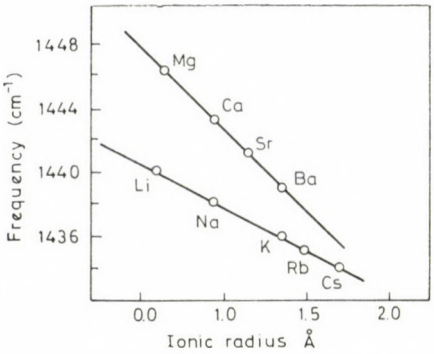

Fig. 4. Correlation between frequency of an absorption band of coordinatively bound pyridine and ionic radius (EPA strength)

Table IV

Hydration enthalpies of cations of different valency

Cation	$\Delta H_{hydr.}$ (kcal/mol of ion)	N*	$\Delta H_{hydr.}/N$ (kcal)
K^+	−84	4	−21
Cu^+	−145	4	−36
Ca^{+2}	−389	4	−97
Cr^{+2}	−449	4 (6)	−112 (−75)
Fe^{+2}	−467	4 (6)	−117 (−78)
Cu^{+2}	−508	4	−127
Cr^{+3}	−960	6	−176
Fe^{+3}	−1055	6	−176

* N = Probable number of ligands in the first coordination sphere.

As a last example, the retention of water in zeolites, treated at 500 °C in air [9], is mentioned. In Table V, the weight loss is indicated which is observed when those samples are heated to 1000 °C.

Mechanisms

In the above discussion (about activity), it is only the EPA sites which are taken into account to interpret the results. Now, for discussing the mechanisms, the EPD sites must also be included in order to achieve a consistent description. Only the timing of the bond rupture is meant by mechanism here. Three possibilities of timing can be predicted, even without knowing details.

Table V

Retention of water in zeolites

Catalyst	Wt % loss on heating from 500 to 1000° C
NaX	0.27
MgX	1.04
NaY	0.14
MgY	0.88
CaY	0.88
SrY	0.45
BaY	0.25

1. The C—X bond is broken in the first step and the carbonium ion intermediate formed, which loses a proton in the second step.
2. The C—H bond is broken in the first step and the carbanion intermediate loses the group X^- in the second step.
3. Both bonds are broken in one step, which would be a concerted reaction without intermediate.

These three possibilities are depicted in the following scheme (Fig. 5) and the notations E1, E2, E1cB, usual in liquid phase chemistry, are indicated.

We have not used kinetics for determining the mechanisms. One of our methods is to study the product distribution. Fig. 6 represents in an idealized manner how this can be done with butan-1-ol and -2-ol.

Three patterns of butene distribution are observed, which are reasonably assigned to the three mechanisms according to the following considerations.

An E1 mechanism is expected over catalysts of high EPA strength (very acidic catalysts). As the carbonium ion, which is the intermediate of the E1 mechanism isomerizes readily, the primary carbonium ion formed from butan-1-ol in the first step is rapidly converted to the secondary carbonium ion, which is more stable. From butan-2-ol the secondary carbonium ion is formed directly. So from both reactants, the same intermediate, *i.e.* the 2-butyl cation, is obtained and consequently the same distribution of butenes. For formation of isobutene, very acidic catalysts, like silica-alumina are required.

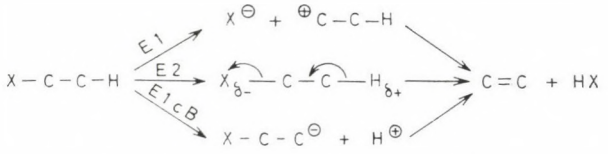

Fig. 5. Elimination mechanisms (timing)

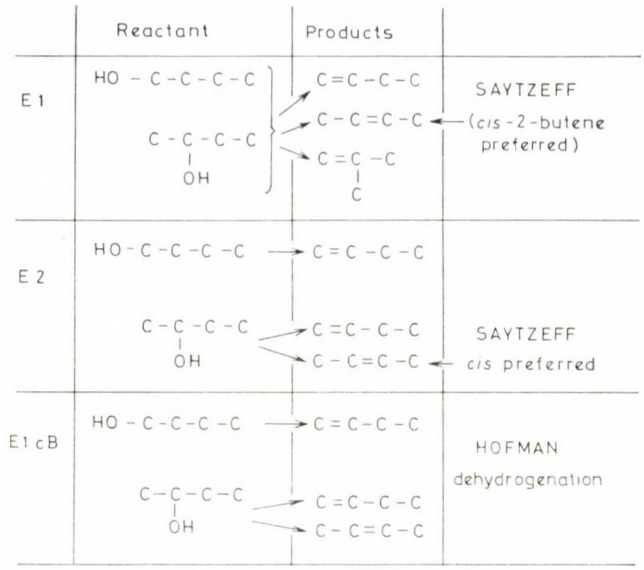

Fig. 6. Determination of dehydration mechanism from product distribution

An E1cB mechanism is expected over catalysts with high EPD strength, as in this case the C—H bond is most affected (see Fig. 1) and therefore separated first. Thus, the most acidic hydrogen is abstracted preferably and this is why formation of terminal olefins from alkan-2-ol is so much favoured. With butan-1-ol, of course, there is no other possibility than the formation of but-1-ene. With catalysts of medium acidity (balanced EPA and EPD strength), both bonds are roughly equally affected and hence separated in one step.

Table VI gives representative product distributions over catalysts of very different acidity. These results are characteristic for a rather broad temperature range around 300 °C. Indeed, with BPO_4 [14], which is the most acidic catalyst, *i.e.* that of highest EPA and (consequently) lowest EPD strength, the product distribution obtained with butan-1-ol is equal to that obtained with butan-2-ol and this is indicative of an E1 mechanism.

Over Al_2O_3, a catalyst of medium (moderate) acidity and (consequently) also medium basicity, the two essential interactions (Fig. 1) are of comparable strength (balanced interaction strength). Thus the weakening of the C—O and the C—H bond takes place to a similar extent. The two bonds are broken in a concerted process (approximately simultaneously) without intermediate. This mechanism is termed E2 [15].

Over ThO_2 [16], the most basic catalyst, *i.e.* that of highest EPD and (consequently) lowest EPA strength, it is the interaction with the C—H group, which is most pronounced. C—H bond breaking precedes C—O bond

Table VI

Representative butene distributions over catalysts of very different acidity

Cat. mech.	React.	C=C–C–C	C–C=C–C
BPO_4	COH–C–C–C	30	70
E1	C–COH–C–C	30	70
Al_2O_3	COH–C–C–C	85	15
E2	C–COH–C–C	20	80
ThO_2	COH–C–C–C	95	5
E1cB	C–COH–C–C	90	10

breaking. C–H bond breaking however is easiest with the most acidic H, which is the terminal and this is why but-1-ene is the predominant product, not only from butan-1-ol, but also from butan-2-ol.

Secondary isomerization of the olefins formed in dehydration can be ruled out for Al_2O_3 and ThO_2, as the olefin distribution is far from equilibrium (on Al_2O_3 with butan-1-ol). Furthermore, double bond shift is low on these catalysts under the conditions used.

Ether formation was also low under the conditions of these studies. Moreover, the butene distribution does not vary appreciably even at higher temperatures, where practically no ether is formed. Hence, butene distribution, which is considered to be indicative of mechanism, is not affected by ether formation.

Over BPO_4, on the other hand, double bond shift is rapid. However, there is evidence which leads us to assume, that, similarly to other E1 systems, most part of the final butene distribution comes out from the carbonium ion formed in the first step of dehydration [1, 17]. For example, in several cases, the butene distribution obtained in the elimination reaction is closer to equilibrium than that observed in a direct isomerization of butenes.

Table VII gives experimental results for systems which cover mainly the range of E1 and E2 mechanisms (for SO_4 catalysts see [17]; for PO_4 catalysts see [14]). Always, the more acidic catalyst has a higher tendency toward E1, *i.e.* gives less but-1-ene from butan-2-ol because isomerization to but-2-ene takes place (but-1-ene + but-2-ene = 100%). Of course, the mechanism does not only depend on the catalysts but also on the reactant. The C—Cl bond is easier to break than the C—O bond and this is why the tendency toward E1 is greater with chloroalkanes than alcohols or esters.

Table VII

Product distributions (mechanisms) as a function of leaving group and catalyst

Catal.	Temp. (°C)	X	X–C–C–C–C ↙ C=C–C–C	X–C–C–C–C ↘ C–C=C–C
$MgSO_4$	240	Cl	10	90
$BaSO_4$	245	Cl	21	79
Li_2SO_4	390	Cl	100	—
$MgSO_4$		CH_3COO	45	55
$BaSO_4$		CH_3COO	100	—
$Mg_3(PO_4)_2$	280	OH	50	50
$Ca_3(PO_4)_2$	340	OH	92	8
BPO_4	260	OH	26	74
$AlPO_4$	320	OH	89	11

With 2,3-dichlorobutane, an E1 mechanism is observed over $CaCl_2$, but an E2 mechanism over K_3PO_4 [18] (Fig. 7). Clearly, $CaCl_2$ is the stronger EPA (and weaker EPD) of these two catalysts.

The tendency outlined here, E1 mechanism over (very) acidic, E1cB over (very) basic catalysts, is generally observed. The three mechanistic patterns, E1, E2, and E1cB are not only obtained when the olefin distribution in dehydration of alcohols is determined, but also when the H/D exchange in dehydration of alcohols is studied [19].

Table VIII gives olefin distributions obtained in dehydration of alcohols over a series of catalysts of different acidity. All the basic catalysts are selective for the formation of terminal olefins from alkan-2-ols [10a]. Note that (low) values, around 530 eV, of the XPS O 1s binding energy are indicative of high basicity. For a broader discussion of the use of XPS in catalysis see VINEK *et al.* [10a].

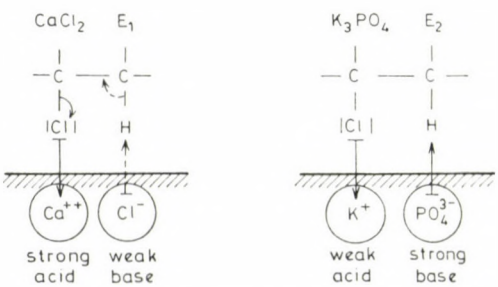

Fig. 7. Mechanism and site strength

Table VIII

Selectivity to terminal olefin from 4-methyl-pentan-2-ol

Oxide	Temp. (°C)	Olefin products (%)		
		Alk-1-ene	Alk-2-ene	O 1s (eV)
ThO_2	399	97.5	2.5	530.2
Y_2O_3	412	96	4	529.5
La_2O_3	414	96	4	529.0
CeO_2	350	86	14	529.4
Sm_2O_3	415	94	6	529.2
Dy_2O_3	404	97	3	529.4
Al_2O_3*	270	25	75	531.8
SiO_2*	400	28	72	533.1

* Reactant: Butan-2-ol.

Dehydrogenation

Whenever the E1cB mechanism is observed, dehydrogenation occurs besides dehydration [15]. This means that dehydrogenation obviously needs basic sites. The reason probably is that in dehydrogenation an α-H must be abstracted in the form of a hydride. Abstraction of a hydride from a carbon atom, to which an oxygen atom is attached, is difficult. The electron population of that H must be high in the transition state. This in turn is facilitated by a high input of negative charge into the molecule. The structure depicted in Fig. 8, which describes interaction rather than steric arrangement in the transition state, is to give an idea of how this input of negative charge may be achieved by coordinative interaction.

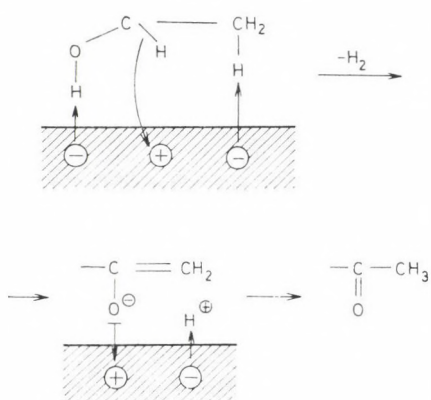

Fig. 8. Dehydrogenation of alcohols — structure of interaction

Table IX

Selectivity for the dehydrogenation correlated with intermediate electronegativity, S_{int} and mean ionization energy, $\overline{E}_{Ion}$ of the cation

Selectivity for dehydrogenation	S_{int}	$\overline{E}_{Ion}$ (eV)
CaO	2.5	9
∨		
MgO	2.8	11
∨		
ZnO	3.9	14
∨		
$FeO.Fe_2O_3$	* *	12 } 16
∨		18 }
Cr_2O_3	* *	18
∨		
TiO_2	3.4	23*
∨		
Al_2O_3	3.7	18
∨		
SiO_2	4.3	26
∨		
WO_3	* *	* *

* Ti^{3+} : $\overline{E}_{Ion} = 16$ eV; part of Ti may be trivalent.

** data not available.

Szabó *et al.* [20] have reported the variation of selectivity in a series of oxides shown in Table IX. As far as data are available these agree approximately with our criteria of EPA strength.

Metals are hydrogenation (and dehydrogenation) catalysts par excellence. In our opinion, metals must have high EPD strength (high basicity) and we would like to draw attention to this important aspect, which has probably not been given sufficient attention. This does not mean, of course, that metals do not need EPA capacities for having dehydrogenation activity, as both functions are always needed. The fact that only transition metals with unfilled d-orbitals are good hydrogenation catalysts has probably to do with the necessity of EPA capacity.

Oxidation

A further conclusion may be drawn concerning oxidation. In elementary chemistry we are taught that a hydrogenation may be considered to be a reduction, whereas a dehydrogenation is equivalent to an oxidation. Hydrogenations and dehydrogenations thus are part of the great field of redox reactions. As basic catalysts are useful for hydrogenation and dehydrogenation, we may ask the question if basicity is not a necessary conditions for all redox reactions and hence also for oxidations, *i.e.* introduction of oxygen.

Let us consider the oxidation of CO. Provided oxygen is transferred in the form of O^{2-}, a high electron population would increase the donor strength of oxygen and so facilitate the transfer. In order to maintain electroneutrality of the product, two electrons should be transferred from CO (or CO_2) to the catalyst, as depicted in the following scheme (Fig. 9). Interestingly, according to ERTL [21], in CO oxidation over Pd, the surface is not completely covered with oxygen (it is simply not possible to have a complete monolayer formed with oxygen) so that CO can come into contact with the surface. On the other hand, when CO is preadsorbed, it covers the surface completely, inhibiting the access of oxygen to the surface. In this case no oxidation is observed when oxygen is admitted.

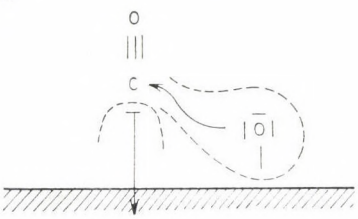

Fig. 9. Interaction and electron transfer for oxidation of CO

It is my impression that there is much evidence in the literature that it is not the catalyst of highest oxygen coverage (highest oxidation state) that has the highest activity but the catalyst of some intermediate oxidation state.

Provided this description of oxidation catalysis is useful (correct), this would mean that the features of redox reactions (redox catalysis) are more similar to those of acid-base reactions (acid-base catalysis) than usually assumed. The coordination chemical approach would also be useful for describing redox catalysis. An essential difference would be that in oxidation reactions with oxygen (for example), electrons must be transferred from the reactant to the catalyst in order to compensate the electronic charge transferred with oxygen to the reactant.

Direct evidence of interaction (catalyst) EPD—H

IR studies of acetone adsorbed on oxides show that the C—H frequency is shifted downward [22]. This is attributed to the interaction structure depicted in Fig. 10. Note that the downward shift with MgO is 50 cm^{-1}, *i.e.* greater than with Al_2O_3, where only 30 cm^{-1} is observed. Since MgO is more basic, *i.e.* a stronger EPD, the shift is reasonably assigned to (short range) interaction with the EPD site (of the catalyst). If it were due to (long range) interaction between the CO group and the EPA site, the shift should be greater with the stronger EPA, *i.e.* Al_2O_3. We consider this to be evidence of the steep

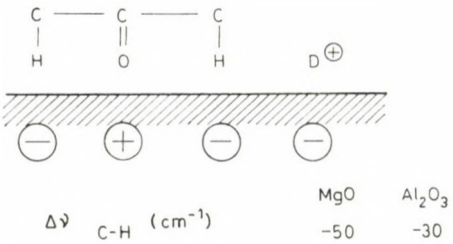

Fig. 10. Interaction between C—H groups and EPD sites of oxides

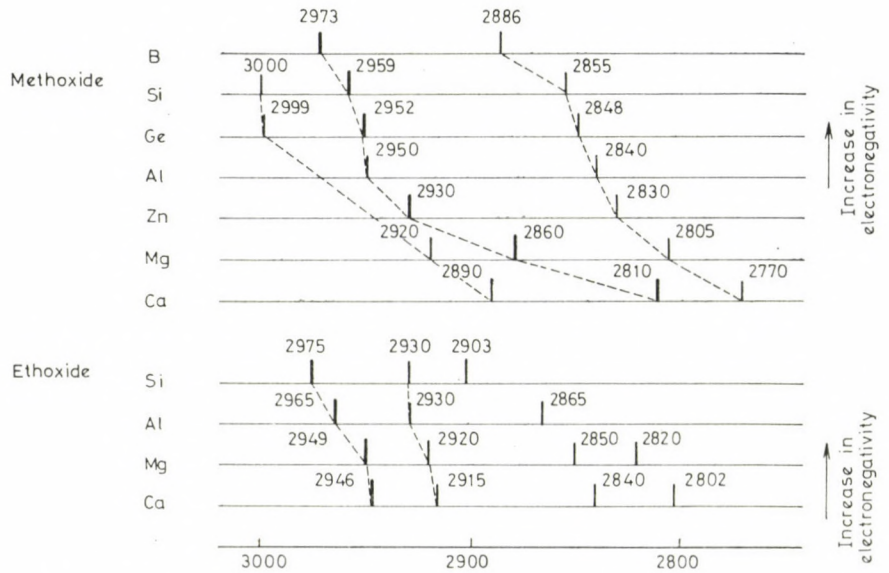

Fig. 11. C—H stretching frequency shift of surface alcoholates as a function of basicity (electronegativity)

decay with the distance of the effect of interaction between the molecule and the catalyst. I would suppose that much more than half of the effect is localized upon the bond adjacent to the interaction.

A similar trend can be clearly seen in the studies [23] of the C—H frequency of methoxide and ethoxide groups upon a series of oxides, which is represented in Fig. 11. Obviously, the shift increases with the basicity of the oxide.

The interaction between the EPD site of the catalyst and the C—H group leads to a H/D exchange (indicated in Fig. 10), which increases with the basicity of the oxide. This correlation is so good that we use the rate of the H/D exchange with acetone-d_6 for determining the basicity of a catalyst [24].

UTIYAMA *et al.* [25] have found that the CH_4-D_2 exchange similarly increases with the basicity of the catalyst, as shown in Fig. 12.

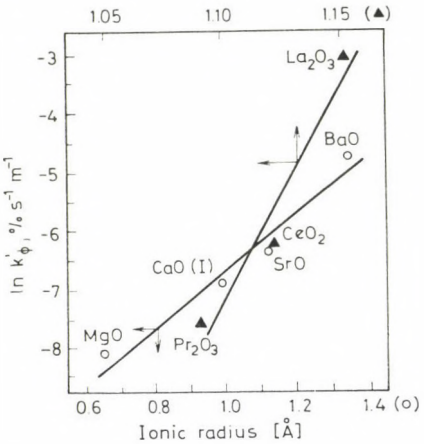

Fig. 12. Rate of CH_4-D_2 exchange as a function of ionic radius, *i.e.* basicity

Additives, mixed catalysts

The field of mixed catalysts, the effect of additives, sometimes called promoters, is one of the most fascinating problems in catalysis. The essential question within our model is: How do the number and the strength of the surface sites vary as a function of composition? Here only the variation of the strength will be discussed.

One of the governing principles is what we call our mixing rule [10], which states that site strength in a mixture must be between that of the components. In other words, mixing can never create EPA sites of higher strength than those of the more (most) acidic component, nor EPD sites stronger than those of the more (most) basic component. This rule would be in agreement with the concept of electronegativity and SANDERSON's equation [5].

As a first example, mixtures of alumina with oxides of divalent cations are considered. Mixtures with spinel structure are obtained. The divalent oxides added are more basic than alumina. As example, our numerical criteria of basicity are given for magnesia as an additive in Table X. Consequently, the EPA sites of the spinel $MgAl_2O_4$ should be weaker, and the EPD sites stronger than those of alumina.

In our opinion, Al^{3+} should be considered to be the main EPA site rather than Mg^{2+}. Of course, the charges indicated are not effective charges. It is an unsolved problem of terminology, if the elements of a polar compound should be called ions or atoms.

Table X

Criteria of basicity

	MgO	Al_2O_3
e/r^*_{cation}	3.03	5.88
S_{Int}	2.85	3.70
$\overline{E}_{Ion}$	11.3	17.75
XPS O 1s (eV)**	530	532

* r in Å.

** round values.

Table XI shows some catalytic results obtained in the dehydration of butan-1-ol [26]. Indeed the spinel is less active, the reaction begins at a higher temperature than on alumina. Furthermore, the percentage of but-2-ene is lower over the spinel and this means that the mechanism is more E2 and less E1 than over alumina.

When the percentage of magnesia added is continuously varied, the EPA strength decreases continuously and this is why the yield of *iso*-butene obtained from 1- and 2-chlorobutane decreases [10a, 27] continuously as shown in Fig. 13. The curve has the shape of a poisoning curve. There is no principal difference between MgO and other oxides like NiO, CoO and ZnO. All diminish the EPA strength of alumina. The only difference is probably due to the dif-

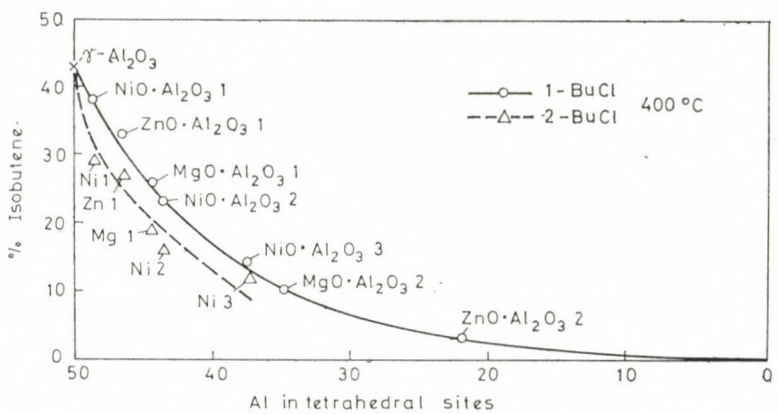

Fig. 13. Variation of the yield of isobutene with the amount of divalent oxide. Composition of the catalyst (x means x.Me/100 Al):

	$NiO.Al_2O_3$			$ZnO.Al_2O_3$		$MgO.Al_2O_3$	
	Ni 1	Ni 2	Ni 3	Zn 1	Zn 2	Mg 1	Mg 2
x	6	30	53	4	28	6	15

ferent preference of divalent cations for the tetrahedral and octahedral sites in the crystal lattice and probably also in the surface.

At the Amsterdam Catalysis Congress, SCHWAB and KRAL [28] presented results concerning the cracking activity of alumina with several additives. The results indicated in Table XII were just opposite to what was expected according to the so-called electronic theory of catalysis. Now with our approach, it is obvious that Li_2O diminishes the EPA strength of alumina and hence the cracking activity, whereas oxides of higher valency increase the EPA strength and hence the cracking activity.

Table XI

Activity and selectivity over alumina and spinel

React.	Cat.	T (°C)	% C=C–C–C*
C–C–C–C | OH	$CoAl_2O_4$	280	begin of the reaction
		390	70
	γ-Al_2O_3	240	begin of the reaction
		350	42

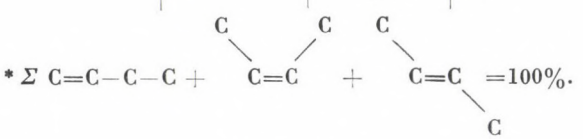

Table XII

Cumene cracking over alumina with additives

Character	Dope	at. %	Activation energy (kcal/mol)
—	—	0	54
p	Li_2O	2	57
p	Li_2O	6	62
n	GeO_2	3	48
n	V_2O_5	1	42
n	WO_3	0.25	41
n	WO_3	0.5	31
n	WO_3	1	26
n	WO_3	2	17.5
n	WO_3	2.5	17
n	WO_3	3	17.5
n	WO_3	4	22

SCHWAB and BLOCK [29] found that small aditives of Li_2O increase the catalytic activity of NiO for the oxidation of CO and explained this result with the increase of p-semiconductivity. It can also be explained with our idea of oxidation catalysts needing basicity. Li_2O, of course, increases the basicity (EPD strength) of NiO.

The regularity of this criterion of EPD strength is really surprising. AI [30] (Tokyo Congress) has found a direct correlation of oxidation activity and basicity for the oxidation of hexane (Fig. 14) as well as CO. PÄTOW and

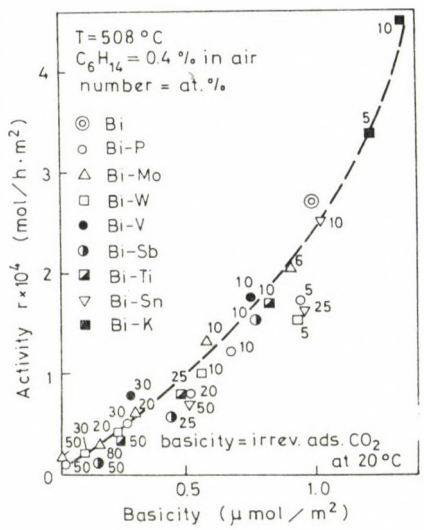

Fig. 14. Increase of activity in oxidation of n-hexane to CO_2 with basicity

RIEKERT [31] found the activity for oxidation to decrease in the following order: $CuO > CuAl_2O_4 > CuY$. This should correlate with the order of acidity. AI [32] found that the activity of Co_3O_4 for CO oxidation was increased by the addition of K_2O, but decreased by the addition of P_2O_5.

Finally MASSON *et al.* [33] studied the effect of addition of alkali oxides to a chromia/alumina catalyst for CO oxidation. Here the inverse order was found relative to that for the activity of these cations in elimination reactions, namely $Cs > Rb > K > Na > Li$.

REFERENCES

[1] NOLLER, H., KLADNIG, W.: Catal. Rev. — Sci. Eng., **13,** 149 (1976)
[2] HEINEMANN, H.: Actes 2ème Congrès International de Catalyse, Technip, Paris 1961, p. 129
[3] *a:* GUTMANN, V.: Coord. Chem. Rev., **15,** 207 (1975); *b:* GUTMANN, V.: The Donor-Acceptor Approach to Molecular Interactions. Plenum Press, New York, 1978
[4] PAULING, L.: The Nature of the Chemical Bond. Cornell University Press, Ithaka, New York, 1960 — Die Natur der chemischen Bindung. Verlag Chemie GmbH, Weinheim/ Bergstr. 1964

[5] SANNERSON, R. T.: Chemical Bonds and Bond Energy, 2nd ed. Academic Press, New York 1976
[6] CRC Handbook of Chemistry and Physics, 58th ed., CRC Press, Inc. 1977—1978
[7] GALICH, P. N., GOLUBSHENKO, I. T., GUTYRYA, V. S., IL'IN, V. G., NEIMARK, I. E.: Dokl. Akad. Nauk SSSR, Ser. Khim., **161,** 627 (1965)
[8] SHARF, V. Z. FREIDLIN, L. KH., SAMOKHVALOV, G. I., NEIMARK, I. E., GERMAN, E. N., PIONTKOVSKAYA, M. A., NEKRASOV, A. S., KRUTII, V. N., Izv. Akad. Nauk SSSR, Ser. Khim., **1968,** 780
[9] PICKERT, P. E., RABO, J. A., DEMPSEY, E., SCHOMAKER, V.: Proc. Third Internat. Congress on Catalysis, Amsterdam, 1964, North Holland, Amsterdam, 1965, p. 714.
[10] *a:* VINEK, H., NOLLER, H., EBEL, M., SCHWARZ, K.: J. Chem. Soc., Faraday Transactions I, **73,** 734 (1977); *b:* NOLLER, H., VINEK, H., LERCHER, J.: Proc. 7° Simposio Ibero-Americano de Catálisis. La Plata 1980 (In press)
[11] ROSSEINSKY, D. R.: Chem. Rev., **65,** 467 (1965)
[12] PIMENTEL, G. C., SPRATLEY, R. D.: Understanding Chemistry. Holden-Day Inc., 1971
[13] WARD, J. W.: J. Catal., **10,** 34 (1968)
[14] THOMKE, K., NOLLER, H.: Proc. Fifth Internat. Congress on Catalysis, Miami Beach, Fla., 1972, North-Holland Publ. Comp., 1973, p. 1183
[15] NOLLER, H., THOMKE, K.: J. Mol. Catal., **6,** 375 (1979)
[16] THOMKE, K.: Proc. Sixth Internat. Congress on Catalysis, London, 1976, The Chem. Society, Burlington House, London, 1977, p. 303
[17] NOLLER, H., ANDRÉU, P., HUNGER, M.: Angew, Chem. Internat. Edit., **10,** 172 (1971)
[18] NOLLER, H., ANDRÉU, P., SCHMITZ, E., SERAIN, S., NEUFANG, O., GIRÓN, J.: Proc. Fourth Internat. Congress on Catalysis, Moscow, 1968, Akadémiai Kiadó, Budapest 1971, p. 420
[19] THOMKE, K.: Z. Phys. Chem. Neue Folge, **106,** 295 (1977)
[20] BATTA, I., BÖRCSÖK, S., SOLYMOSI, F., SZABÓ, Z. G.: Proc. Third Internat. Congress on Catalysis, Amsterdam, 1964, North-Holland Publ. Comp., Amsterdam, 1965, p. 1340
[21] ERTL, G.: Proc. Seventh Internat. Congress on Catalysis, Tokyo, 1980, P2 (In press)
[22] LERCHER, J.: to be published
[23] TAKEZAWA, N., KOBAYASHI, H.: J. Catal., **28,** 335 (1973)
[24] LATZEL, J., KOUBOWETZ, F., VINEK, H.: Z. Phys. Chem. Neue Folge, **105,** 327 (1977)
[25] UTIYAMA, M., HATTORI, H., TANABE, K.: J. Catal., **53,** 237 (1978)
[26] FORSTER, G., NOLLER, H., VINEK, H.: Proc. Fifth Ibero-American Symp. on Catalysis, Lisbon, 1976, Edited in 1979 in Lisbon, p. 138.
[27] VINEK, H., NOLLER, H.: Z. Phys. Chem. Neue Folge, **102,** 247 (1976)
[28] SCHWAB, G.-M., KRAL, H.: Proc. Third Internat. Congress on Catalysis, Amsterdam, 1964, North-Holland Publ. Comp. Amsterdam, 1965, p. 433
[29] SCHWAB, G.-M., BLOCK, J.: Z. Phys. Chem. Neue Folge, **1,** 42 (1954)
[30] AI, M.: Proc. Seventh Internat. Congress on Catalysis, Tokyo, 1980, B28 (In press)
[31] PÄTOW, H., RIEKERT, L.: Ber. Bunsenges. Phys. Chem., **83,** 807 (1979)
[32] AI, M.: J. Catal., **54,** 223 (1978)
[33] MASSON, J., BONNIER, J., DUVIGNEAUD, P. H., DELMON, B.: J. Chem. Soc. Faraday Transactions I, **73,** 1471 (1977)

Heinrich NOLLER A-1060 Wien 6., Getreidemarkt 9., Austria

INDEX

PHYSICAL AND INORGANIC CHEMISTRY

ORGANIC CHEMISTRY

ANALYTICAL CHEMISTRY

PRINTED IN HUNGARY

Akadémiai Nyomda, Budapest

Les Acta Chimica paraissent en français, allemand, anglais et russe et publient des mémoires du domaine des sciences chimiques.

Les Acta Chimica sont publiés sous forme de fascicules. Quatre fascicules seront réunis en un volume (3 volumes par an).

On est prié d'envoyer les manuscrits destinés à la rédaction à l'adresse suivante:

Acta Chimica
Budapest, P.O. Box 67, H-1450, Hongrie

Toute correspondance doit être envoyée à cette même adresse.

La rédaction ne rend pas de manuscript.

Abonnement en Hongrie à l'Akadémiai Kiadó (1363 Budapest, P. O. B. 24, C. C. B. 215 11488), à l'étranger à l'Entreprise du Commerce Extérieur «Kultura» (H-1389 Budapest 62, P.O.B. 149 Compte-courant No. 218 10990) ou chez représentants à l'étranger.

Die Acta Chimica veröffentlichen Abhandlungen aus dem Bereich der chemischen Wissenschaften in deutscher, englischer, französischer und russischer Sprache.

Die Acta Chimica erscheinen in Heften wechselnden Umfanges. Vier Hefte bilden einen Band. Jährlich erscheinen 3 Bände.

Die zur Veröffentlichung bestimmten Manuskripte sind an folgende Adresse zu senden

Acta Chimica
Budapest, Postfach 67, H-1450, Ungarn

An die gleiche Anschrift ist jede für die Redaktion bestimmte Korrespondenz zu richten.

Manuskripte werden nicht zurückerstattet.

Bestellbar für das Inland bei Akadémiai Kiadó (1363 Budapest, Postfach 24, Bankkonto Nr. 215 11488), für das Ausland bei »Kultura« Außenhandelsunternehmen (H-1389 Budapest 62, P.O.B. 149. Bankkonto Nr. 218 10990) oder seinen Auslandsvertretungen.

«Acta Chimica» издают статьи по химии на русском, английском, французском и немецком языках.

«Acta Chimica» выходит отдельными выпусками разного объема, 4 выпуска составляют один том и за год выходят 3 тома.

Предназначенные для публикации рукописи следует направлять по адресу:

Acta Chimica
Budapest, P.O. Box 67, H-1450, ВНР

Всякую корреспонденцию в редакцию направляйте по этому же адресу.

Редакция рукописей не возвращает.

Отечественные подписчики направляйте свои заявки по адресу Издательства Академии Наук (1363 Budapest, P.O.B. 24, Текущий счет 215 11488), а иностранные подписчики через организацию по внешней торговле **«Kultura» (H-1389 Budapest 62, P.O.B. 149.** Текущий счет 218 10990) или через ее заграничные представительства и уполномоченных.

Reviews of the Hungarian Academy of Sciences are obtainable at the following addresses:

AUSTRALIA
C.B.D. LIBRARY AND SUBSCRIPTION SERVICE, Box 4886, G.P.O., *Sydney N.S.W. 2001*
COSMOS BOOKSHOP, 145 Ackland Street, *St. Kilda (Melbourne), Victoria 3182*

AUSTRIA
GLOBUS, Höchstädtplatz 4, *1200 Wien XX*

BELGIUM
OFFICE INTERNATIONAL DE LIBRAIRIE, 30 Avenue Marnix, *1050 Bruxelles*
LIBRAIRIE DU MONDE ENTIER, 162 Rue du Midi, *1000 Bruxelles*

BULGARIA
HEMUS, Bulvar Ruszki 6, *Sofia*

CANADA
PANNONIA BOOKS, P.O. Box 1017, Postal Station "B", *Toronto, Ontario M5T 2T8*

CHINA
CNPICOR, Periodical Department, P.O. Box 50, *Peking*

CZECHOSLOVAKIA
MAD'ARSKÁ KULTURA, Národní třida 22, *115 66 Praha*
PNS DOVOZ TISKU, Vinohradská 46, *Praha 2*
PNS DOVOZ TLAČE, *Bratislava 2*

DENMARK
EJNAR MUNKSGAARD Norregade 6, *1165 Copenhagen*

FINLAND
AKATEEMINEN KIRJAKAUPPA, P.O. Box 128, *SF-00101 Helsinki 10*

FRANCE
EUROPERIODIQUES S. A., 31 Avenue de Versailles, *78170 La Celle St.-Cloud*
LIBRAIRIE LAVOISIER, 11 rue Lavoisier, *75008 Paris*
OFFICE INTERNATIONAL DE DOCUMENTATION ET LIBRAIRIE, 48 rue Gay-Lussac, *75240 Paris Cedex 05*

GERMAN DEMOCRATIC REPUBLIC
HAUS DER UNGARISCHEN KULTUR, Karl-Liebknecht-Strasse 9, *DDR-102 Berlin*
DEUTSCHE POST ZEITUNGSVERTRIEBSAMT, Strasse der Pariser Kommüne 3—4, *DDR-104 Berlin*

GERMAN FEDERAL REPUBLIC
KUNST UND WISSEN ERICH BIEBER, Postfach 46, *7000 Stuttgart 1*

GREAT BRITAIN
BLACKWELL'S PERIODICALS DIVISION, Hythe Bridge Street, *Oxford OX1 2ET*
BUMPUS, HALDANE AND MAXWELL LTD., Cowper Works, *Olney, Bucks MK46 4BN*
COLLET'S HOLDINGS LTD., Denington Estate, *Wellingborough, Northants NN8 2QT*
W.M. DAWSON AND SONS LTD., Cannon House, *Folkestone, Kent CT19 5EE*
H. K. LEWIS AND CO., 136 Gower Street, *London WC1E 6BS*

GREECE
KOSTARAKIS BROTHERS, International Booksellers, 2 Hippokratous Street, *Athens-143*

HOLLAND
MEULENHOFF-BRUNA B.V., Beulingstraat 2, *Amsterdam*
MARTINUS NIJHOFF B.V., Lange Voorhout 9—11, *Den Haag*
SWETS SUBSCRIPTION SERVICE, 347b Heereweg, *Lisse*

INDIA
ALLIED PUBLISHING PRIVATE LTD., 13/14 Asat Ali Road, *New Delhi 110001*
150 B-6 Mount Road, *Madras 600002*
INTERNATIONAL BOOK HOUSE PVT. LTD., Madame Cama Road, *Bombay 400039*
THE STATE TRADING CORPORATION OF INDIA LTD., Books Import Division, Chandralok, 36 Janpath, *New Delhi 110001*

ITALY
EUGENIO CARLUCCI, P.O. Box 252, *70100 Bari*
INTERSCIENTIA, Via Mazzé 28, *10149 Torino*
LIBRERIA COMMISSIONARIA SANSONI, Via Lamarmora 45, *50121 Firenze*
SANTO VANASIA, Via M. Macchi 58, *20124 Milano*
D. E. A., Via Lima 28, *00198 Roma*

JAPAN
KINOKUNIYA BOOK-STORE CO. LTD., 17-7, Shinjuku-ku 3 chome, Shinjuku-ku, *Tokyo 160-91*
MARUZEN COMPANY LTD., Book Department P.O. Box 5056 Tokyo International, *Tokyo 100-31*
NAUKA LTD., IMPORT DEPARTMENT, 2-30-19 Minami Ikebukuro, Toshima-ku, *Tokyo 171*

KOREA
CHULPANMUL, *Phenjan*

NORWAY
TANUM-CAMMERMEYER, Karl Johansgatan 41—43, *1000 Oslo*

POLAND
WĘGIERSKI INSTYTUT KULTURY, Marszałkowska 80, *Warszawa*
CKP I W ul. Towarowa 28 *00-958 Warsawa*

ROMANIA
D. E. P., *Bucureşti*
ROMLIBRI, Str. Biserica Amzei 7, *Bucureşti*

SOVIET UNION
SOJUZPETCHATJ — IMPORT, *Moscow*
and the post offices in each town
MEZHDUNARODNAYA KNIGA, *Moscow G-200*

SPAIN
DIAZ DE SANTOS, Lagasca 95, *Madrid 6*

SWEDEN
ALMQVIST AND WIKSELL, Gamla Brogatan 26, *101 20 Stockholm*
GUMPERTS UNIVERSITETSBOKHANDEL AB, Box 346, *401 25 Göteborg 1*

SWITZERLAND
KARGER LIBRI AG, Petersgraben 31, *4011 Base*

USA
EBSCO SUBSCRIPTION SERVICES, P.O. Box 1943, *Birmingham, Alabama 35201*
F. W. FAXON COMPANY, INC., 15 Southwest Park, *Westwood, Mass, 02090*
THE MOORE-COTTRELL SUBSCRIPTION AGENCIES, *North Cohocton, N. Y. 14868*
READ-MORE PUBLICATIONS, INC., 140 Cedar Street, *New York, N. Y. 10006*
STECHERT-MACMILLAN, INC., 7250 Westfield Avenue, *Pennsauken N. J. 08110*

VIETNAM
XUNHASABA, 32, Hai Ba Trung, *Hanoi*

YUGOSLAVIA
JUGOSLAVENSKA KNJIGA, Terazije 27, *Beograd*
FORUM, Vojvode Mišića 1, *21000 Novi Sad*

HU ISSN 0001—5407 Index: 26.007